

High-Resolution Geochemical Analysis of Controls on Organic Matter Accumulation in the
Middle-Upper Devonian Horn River Group

by

Haolin Zhou

A thesis submitted in partial fulfillment of the requirements for the degree of

Master of Science

Department of Earth and Atmospheric Sciences
University of Alberta

© Haolin Zhou, 2020

ABSTRACT

Organic carbon-rich mudstones, or ‘black shales’, record highly anomalous perturbations of local or earth systems at critical times in earth history. Paleoenvironmental parameters, including primary productivity, redox conditions, and sedimentation rate, have been widely recognized as the controls for organic matter (OM) accumulation in shales. However, immediate triggers for organic carbon deposition in these formations are commonly difficult to identify because of feedback loops that cause geochemical proxies for these controls to vary apparently synchronously when sampled at decimeter to meter spacing. This thesis examines a set of 133 samples from a long, continuous core in the Middle and Upper Devonian Horn River Group in the northwestern Western Canadian Sedimentary Basin, a black shale and important shale gas reservoir. We compare a geochemical data set comprised of bulk geochemical analyses of 133 7-12 cm-long slabs to a novel set of millimeter-resolution geochemical profiles of the same slabs, based on energy dispersive X-ray fluorescence (EDXRF) and hyperspectral imagery (infrared scan) analyses.

Proxies applied in this high-resolution analysis identify multiple patterns of controls (bioproductivity, redox conditions, and dilution by terrestrial or carbonate input) on organic richness and feedback loops between bioproductivity and redox conditions at different intervals. In these profiles, proxies for bioproduction and redox conditions, biogenic Si and S/Fe, show separate trends when compared to apparently synchronous variation between them observed in more coarsely sampled profiles. Bioproductivity and dilution are identified as the primary controls on OM accumulation in the Horn River Group based on the high-resolution profiles, while redox conditions are the less common trigger for organic matter accumulation in this shale.

Comparison of geochemical profiles reveals bioproductivity-redox feedback loops developed on time scales of decades to centuries.

Geochemical datasets do not always provide unambiguous constraints on interpretations of paleoenvironments, because different sources and processes can contribute minerals of similar geochemical composition. Through petrographic analysis, different biogenic inputs can be distinguished from detrital inputs and diagenetic mineralization, for example, carbonate bioclasts from carbonate detritus and authigenic carbonate minerals, and syndeposition from authigenic pyrite.

Because sea-level change can influence bioproductivity, redox states, and dilution and therefore organic matter accumulation, this study compares both millimeter-scale and meter-scale geochemical analysis with second- and third-order sequence stratigraphy to develop the connection between relative sea level and OM accumulation. Results of meter-scale analysis show that sea-level changes can influence bioproductivity, redox conditions, terrestrial input, and carbonate input, but we cannot identify the immediate controls on organic richness because of the synchronous variations in proxies. Regression analysis based on the meter-scale dataset suggests that redox conditions are the primary control on organic richness. Results of millimeter-scale analysis show varying immediate triggers for organic matter accumulation during third-order sea-level changes, but may not effectively identify long-term, for example, timescale of hundreds of thousands of years, paleoredox variations that are effectively indicated by meter-scale analysis.

PREFACE

This thesis is an original work by Haolin Zhou. The shale core slabs in this study were collected from the EOG TATTOO D-A28-F/094-O-10 well of the distal Horn River Group, northeastern British Columbia. The study presented in this thesis is part of the research that is undertaken to examine the sedimentology, geochemistry, and stratigraphy of the Middle-Upper Devonian Horn River Group, northwest of Western Canada Sedimentary Basin. This thesis extends previous work by Dr. Tian Dong who was PhD student and a post-doctoral research fellow in the SURGe research group.

Chapter 2 of this thesis has been in review as H. Zhou, N.B. Harris, J. Feng, T. Dong, B. Rivard, K. Ayranci, P. Hackley, and J. Hatcherian ‘New insights into organic matter accumulation from high-resolution geochemical analysis of a black shale: Middle and Upper Devonian Horn River Group, Canada,’ *Geology*. I was responsible for EDXRF data collection and all data analysis as well as manuscript. N.B. Harris supervised the research and provided primary editorial input for this paper. J. Feng and B. Rivard provided assistance on the hyperpynal imagery data collection. T. Dong provided whole-rock data. K. Ayranci was involved in the analysis of sea level change. P. Hackley, and J. Hatcherian provided assistance on organic petrographic analysis.

Chapter 3 is in preparation for submission as H. Zhou, N.B. Harris, T. Dong, P. Hackley, J. Hatcherian, J. Feng, B. Rivard, and K. Ayranci, ‘Physical sedimentological, oceanographic, and diagenetic influences on shale geochemistry from high resolution geochemical and petrographic profiles, Horn River Group, Middle-Upper Devonian, British Columbia,’ *Journal of Sedimentary Research or Sedimentary Geology*. Authors’ contributions are the same with the Chapter 2.

Chapter 4 will be submitted as H. Zhou, N.B. Harris, J. Feng, T. Dong, B. Rivard, and K. Ayranci, 'Sea-level change and organic matter burial in the Middle-Upper Devonian Horn River shale through high-resolution geochemical analysis and third-order sequence stratigraphy,' *GSA Bulletin or Sedimentary Geology*. Authors' contributions are the same with the Chapter 2.

ACKNOWLEDGEMENTS

I would like to thank my supervisor, Dr. Nicholas Harris, for his support through my master's study. His office is always open to any academic questions. He shows me how to think in a scientific way, how to develop network in academia, and how to find new topics during research.

I am also grateful to the help of my colleagues of SURGe research group. I would like to thank Tian for his contribution to my research and his suggestions on my future development. I greatly appreciate the support from Noga on my research and lab works. She is busy but is always willing to help me. I would like to thank Randy for his technique support. I very much appreciate the help of Dan, Evan, Chris, Elaine, Martin, Stephany, Victoria, and Hui. Our group is the best group. I would like to thank Drs. Korhan Ayranic and Al Moghadam for their assistance in my thesis.

I would like to thank Mr. Peng Li, and Drs. Nancy Zhang and Min Zhang for the collaboration of XRF training and analysis. I am grateful to Drs. Jilu Feng and Benoit Rivard for their assistance of hyperspectral imagery analysis. I greatly appreciate Dr. Karlis Muehlenbachs for his class 'Stable Isotope Geochemistry' and advice on my future academic career. I would like to thank all faculties and staff in EAS for their assistance in my master's study and my officemates for the help of my work and life.

TABLE OF CONTENTS

ABSTRACT.....	ii
PREFACE.....	iv
ACKNOWLEDGEMENTS.....	vi
CHAPTER 1 INTRODUCTION.....	1
1.1 OVERVIEW.....	1
1.2 ORGANAZATION OF THE THESIS.....	4
1.3 REFERENCES CITED.....	4
CHAPTER 2 NEW INSIGHTS INTO ORGANIC MATTER ACCUMULATION FROM HIGH-RESOLUTION GEOCHEMICAL ANALYSIS OF A BLACK SHALE: MIDDLE AND UPPER DEVONIAN HORN RIVER GROUP, CANADA.....	9
ABSTRACT.....	9
2.1 INTRODUCTION.....	10
2.2 GEOLOGICAL SETTING.....	11
2.3 METHODS.....	14
2.3.1 Proxies.....	15
2.4 RESULTS AND INTERPRETATIONS.....	16
2.4.1 Bioproductivity trigger for OM burial.....	18
2.4.2 Preservation trigger for OM burial.....	19
2.4.3 Dilution as the trigger for OM burial.....	19
2.4.4 Bioproductivity-lead-redox-lag feedback.....	19
2.4.5 Redox-lead-bioproductivity-lag feedback.....	20
2.4.6 Terrestrial flux influences bioproductivity.....	20
2.5 FREQUENCY OF CONTROLS AND TIME SCALES IN ORGANIC MATTER ACCUMULATION.....	21

2.6 ACKNOWLEDGMENTS	23
2.7 REFERENCES CITED.....	23
CHAPTER 3 PHYSICAL SEDIMENTOLOGICAL, OCEANOGRAPHIC, AND DIAGENETIC INFLUENCES ON SHALE GEOCHEMISTRY FROM HIGH RESOLUTION GEOCHEMICAL AND PETROGRAPHIC PROFILES, HORN RIVER GROUP, MIDDLE-UPPER DEVONIAN, BRITISH COLUMBIA	30
ABSTRACT.....	30
3.1 INTRODUCTION	31
3.2 GEOLOGICAL BACKGROUNDS	33
3.2.1 Geological Setting.....	33
3.3 METHODOLOGY	37
3.3.1 Meter-Scale Whole-Rock Geochemical Analysis.....	37
3.3.2 Millimeter-Scale Geochemical Analysis.....	38
3.3.3 Geochemical Proxies.....	39
3.3.4 Petrographic Analysis	39
3.4 RESULTS	40
3.4.1 Laminated Clay-, Silt- and Microcrystalline Silica-Bearing Mudstone.....	42
3.4.2 Laminated Sand-Bearing, Clay-Rich Mudstone	45
3.4.3 Carbonate Silt-Bearing Mudstone and Carbonate Mesoplankton-Bearing Mudstone.....	47
3.4.4 Diagenetic Mineral-Bearing Mudstone.....	51
3.5 DISCUSSION	55
3.5.1 Bioproductivity Control on Petrography.....	55
3.5.2 Physical Sedimentological Controls	55
3.5.3 Diagenetic Controls.....	56
3.6 CONCLUSION	57
3.7 ACKNOWLEDGMENTS	58
3.8 REFERENCES CITED.....	58

CHAPTER 4 SEA-LEVEL CHANGE AND ORGANIC MATTER BURIAL IN THE MIDDLE-UPPER DEVONIAN HORN RIVER SHALE THROUGH HIGH-RESOLUTION GEOCHEMICAL ANALYSIS AND THIRD-ORDER SEQUENCE

STRATIGRAPHY	67
ABSTRACT	67
4.1 INTRODUCTION	68
4.2 GEOLOGICAL BACKGROUNDS	69
4.2.1 Geological Setting.....	69
4.2.2 Organic Matter Enrichment Patterns.....	74
4.3 METHODOLOGY	76
4.3.1 Samples	76
4.3.2 Methods.....	76
4.3.3 Proxies.....	77
4.4 RESULTS	78
4.4.1 Sequence Stratigraphy.....	78
4.4.2 Formation-Scale Geochemical Profiles from Whole-Slab Analysis.....	79
4.4.3 Frequency of Different Patterns	82
4.5 DISCUSSION	85
4.5.1 Sea Level and Organic Matter Accumulation	85
4.5.1.1 Meter-Scale Geochemistry and Sea-Level Controls.....	86
4.5.1.2 Millimeter-Scale Geochemistry and Sea-Level Controls	88
4.5.2 Effects of Varying Sample Spacing of Meter and Millimeter Scale and Analytical Methods ..	90
4.6 CONCLUSION	98
4.7 ACKNOWLEDGMENTS	98
4.8 REFERENCES CITED.....	99
CHAPTER 5 CONCLUSIONS.....	104
5.1 PROCESSES OF ORGANIC MATTER ACCUMULATION.....	104
5.2 PETROGRAPHIC VALIDATION ON GEOCHEMICAL FEATURES.....	105

5.3 SEA LEVEL CONTROL ON ORGANIC MATTER ACCUMULATION	105
5.4 EFFECTS OF DIFFERENT SAMPLING SCALES AND ANALYTICAL METHODS	105
REFERENCES CITED.....	107
APPENDICES	121
APPENDIX A: CORE DESCRIPTION AND PETROGRAPHY MICROGRAPHS.....	121
APPENDIX B: HIGH-RESOLUTION DATASET	133
APPENDIX C: WHOLE-ROCK GEOCHEMICAL DATA	437
APPENDIX D: COMPLEMENTARY TABLES AND PLOTS BASED ON GEOCHEMICAL ANALYSIS FOR CHAPTER 2.....	443
APPENDIX E: ORGANIC PETROGRAPHIC ANALYSIS	448

LIST OF TABLES

Chapter 4	67
Table 4.1. Distributions of samples exhibiting different organic matter accumulation patterns in third-order sequence stratigraphic units.....	84
Table 4.2. Distributions of samples exhibiting different feedback patterns in third-order sequence stratigraphic units.....	85

LIST OF FIGURES

Chapter 2	9
Figure 2.1 Location of the Horn River Basin and the studied well.....	13
Figure 2.2 Gamma-ray log, geochemical profiles, and sequence stratigraphy of the Horn River Group.....	15
Figure 2.3 Classification of triggers for OM burial and redox-bioproduction feedbacks.....	17
Figure 2.4 Frequencies of organic matter enrichment patterns and feedback patterns in different sequence stratigraphic units.....	23
Chapter 3	30
Figure 3.1 Geological maps of the study area.....	35
Figure 3.2 Stratigraphy of the Horn River Group in the Horn River Basin.....	36
Figure 3.3 Gamma-ray log, whole-rock geochemical profiles, and 3 rd sequence stratigraphy of the long-drill core of this study	37
Figure 3.4 Ternary diagram of major geochemical compositions (SiO ₂ , Al ₂ O ₃ , and CaO).....	41
Figure 3.5 Millimeter-resolution geochemical profiles and thin section scan of laminated silt- and siliceous nannoplankton-bearing, clay-rich mudstone.	43
Figure 3.6 Micrographs of laminated silt- and siliceous nannoplankton-bearing, clay-rich mudstone	44
Figure 3.7 Millimeter-resolution geochemical profiles and thin section scan of laminated silt-bearing, clay-rich mudstone	46
Figure 3.8 Micrographs of laminated sand-bearing, clay-rich mudstone.....	47
Figure 3.9 Millimeter-resolution geochemical profiles and thin section scan of laminated calcite silt-bearing, clay-rich mudstone.....	49
Figure 3.10 Micrographs of calcareous mudstones in the Otter Park Member and lower Muskwa Formation	50

Figure 3.11 Millimeter-resolution geochemical profiles and thin section scan of the representative sample from TST1 of calcareous mesoplankton- and dolomite cement-bearing, clay-rich mudstone.	52
Figure 3.12 Millimeter-resolution geochemical profiles and thin section scan of laminated silt- and siliceous nannoplankton-bearing, clay-rich mudstone.	53
Figure 3.13 Micrographs of mudstones with large amounts of diagenetic minerals in the Horn River Group.	54
Chapter 4	67
Figure 4.1 Location of the study area and the well	71
Figure 4.2 Stratigraphy of the Horn River Group in the Horn River Basin	72
Figure 4.3 Different controls on organic matter accumulation and feedback loops between redox condition, bioproductivity, and terrestrial input.....	75
Figure 4.4 Gamma-ray log, whole-rock geochemical profiles, and third-order sequence stratigraphy of the long-drill core of this study	81
Figure 4.5 Gamma-ray log, 3 rd sequence stratigraphy, and distribution of organic matter accumulation processes of the long-drill core in this study.	83
Figure 4.6 Relationships between total organic carbon (TOC) and redox, bioproductivity, and dilution proxies in the entire shale	92
Figure 4.7 Relationships between total organic carbon (TOC) and redox, bioproductivity, and dilution proxies in the Evie Member, Otter Park Member, and the Muskwa Formation.....	96

CHAPTER 1 INTRODUCTION

1.1 OVERVIEW

Organic-rich “black” shales are significant components of the sedimentary rock record, both because of their importance to petroleum systems as source rocks or unconventional hydrocarbon reservoirs and because they record important disturbances to earth systems. The origin of organic matter enrichment is the primary topic in this project. This thesis presents three studies of the Horn River Group, a Middle to Upper Devonian organic-rich shale in the Western Canada Sedimentary Basin in an investigation of organic matter enrichment patterns and connection to sea level fluctuations.

Models for organic matter accumulation in marine black shales have been presented since the 1920s (Tyson, 2005). Primary productivity, preservation, and dilution were documented as primary controls on organic carbon accumulation in marine sediments in both theoretical and empirical terms (e.g., Algeo et al., 2011; Arthur and Sageman, 2005; Hee et al., 2001; Ingall et al., 1993; Jenkyns and Weedon, 2013; Raven et al., 2018; Sepúlveda et al., 2009; Zhou et al., 2015). Bioproductivity, usually considered to be primarily a function of nutrient supply, provides organic flux to the seafloor and is positively related to organic matter concentration in sediments (Pedersen and Calvert, 1990; Schieber et al., 2000; Schoepfer et al., 2015). Redox conditions can influence organic matter preservation during deposition (Aller, 1994; Ocubalidet et al., 2018; Rimmer et al., 2004). For example, oxygen deficiency limits organic matter decomposition by oxidants. Clay minerals, which possess very large mineral surface areas, can also enhance organic matter preservation by absorbing organic matter in the interlayer space (Kennedy et al., 2002 and 2014). Finally, dilution by detrital sediments (carbonate or clastic) or biogenic sediments such as silica also influence marine organic matter concentration, but at the same time,

can elevate burial efficiency of organic matter by decreasing exposure time to an oxic water column (Torres et al., 2017; Tyson, 2005). Sedimentation rate can be positively related to organic carbon concentration in some formations when the sedimentation rate is less than 5 cm/kyr (Tyson, 2001), in which increased clay input is also related with increased mineral surface areas that enhance organic matter preservation (Kennedy et al., 2014).

Although these processes have been recognized in many formations, the immediate control on organic richness is still not yet well understood, because data from commonly-used meter-scale sampling in geochemical studies generally show apparently synchronous variations in geochemical proxies, especially between redox and bioproductivity proxies (e.g., Tribovillard et al., 2006; Ocubalidet et al., 2018). Based on this widely observed phenomenon and global-scale environmental studies, e.g. upwelling and oxygen minimum zone, researchers have proposed that redox and bioproductivity controls may be linked through feedback loops (Ingall and Jahnke, 1994; Little et al., 2015; Rowe et al., 1975); however, this hypothesis lacks direct basin-scale evidence in ancient mudstones. The Middle and Upper Devonian Horn River Group in the northwestern Western Canadian Sedimentary Basin has been well-studied in recent years in geochemical, sedimentological, geomechanical, and stratigraphic aspects. The availability of well-preserved long cores provides an opportunity to extend that work to better understand organic matter accumulation processes. In this research, we apply a novel combination of technologies to develop high-resolution geochemical profiles (hyperspectral imagery scan and energy dispersive X-ray fluorescence line scan) to improve meter-resolution data to millimeter-resolution, effectively improving the temporal resolution between two samples from tens of thousands of years to decades or centuries, much closer to the timescales of redox-bioproductivity feedback loops observed in the modern environments.

Because geochemical features cannot always constrain paleoenvironmental interpretations, for example where high calcium content in a geochemical profile may be related to either biogenic carbonate input, carbonate detrital input, or diagenetic carbonate, petrographic study is required to validate these geochemical features and interpretations. However, the conventional geochemical analysis based on powder and solution (e.g. ICP-MS), typically at a meter-scale resolution cannot capture millimeter- to centimeter-scale variability evident in petrographic sample. The new techniques of hyperspectral imagery scan and energy dispersive X-ray fluorescence line scan are both non-destructive and can provide millimeter-scale geochemical data. We therefore can correlate petrographic data to high-resolution geochemical data to complement interpretations on paleoenvironment.

Organic matter accumulation is also related to sea level change. Many studies have documented the control of sea-level change on bioproductivity, redox conditions, siliciclastic/carbonate inputs, and consequently organic richness (Arthur and Sageman, 2005; Dong et al., 2018) by: (1) limiting open ocean nutrient-rich inflow to a restricted basin to influence primary productivity; (2) influencing the position of the redox chemocline; (3) trapping terrestrial flux; (4) controlling the development of carbonate platforms and carbonate shedding to basinal areas. However, the same limitation in meter-scale geochemical data occurs when we study how sea-level changes influenced organic matter accumulation. High-resolution geochemical analysis may bring some new insights on this topic.

This thesis presents a geochemical study based on the novel combination of techniques of hyperspectral imagery scan and energy dispersive X-ray fluorescence line scan, and third-order sequence stratigraphy, to identify the immediate controls on organic richness in the Horn River shale. In addition, this study complements a petrographic analysis to distinguish

sedimentological and diagenetic contributions on the geochemical signals and mineral compositions.

1.2 ORGANAZATION OF THE THESIS

This thesis comprises five chapters. Chapters 1 and 5 provide an introduction and conclusion, respectively. Chapter 2 introduces the high-resolution geochemical data and identifies different primary controls on organic matter accumulation in the Horn River Group. Chapter 3 reports a petrographic study of representative samples to validate geochemical features and interpretations of Chapter 2. Chapter 4 identifies the relationship between third-order sea-level changes and processes of organic matter accumulation in the Horn River Group. In addition, this chapter also compares the results between meter-scale and millimeter-scale geochemical analyses to indicate how different observation scales and analytical methods influence interpretations.

1.3 REFERENCES CITED

- Algeo, T.J., Kuwahara, K., Sano, H., Bates, S., Lyons, T., Elswick, E., Hinnov, L., Ellwood, B., Moser, J., and Maynard, J.B., 2011, Spatial variation in sediment fluxes, redox conditions, and productivity in the Permian-Triassic Panthalassic Ocean: *Palaeogeography, Palaeoclimatology, Palaeoecology*, v. 308, p. 65–83, doi:10.1016/j.palaeo.2010.07.007.
- Aller, R.C., 1994, Bioturbation and remineralization of sedimentary organic matter: effects of redox oscillation: *Chemical Geology*, v. 114, p. 331–345, doi:10.1016/0009-2541(94)90062-0.

- Arthur, M.A., and Sageman, B.B., 1994, Marine Black Shales: Depositional Mechanisms and Environments of Ancient Deposits: *Annual Review of Earth and Planetary Sciences*, v. 22, p. 499–551, doi:10.1146/annurev.ea.22.050194.002435.
- Dong, T., Harris, N.B., and Ayranci, K., 2018, Relative sea-level cycles and organic matter accumulation in shales of the Middle and Upper Devonian Horn River Group, northeastern British Columbia, Canada: Insights into sediment flux, redox conditions, and bioproductivity: *Bulletin of the Geological Society of America*, v. 130, p. 859–880, doi:10.1130/B31851.1.
- Hee, C.A., Pease, T.K., Alperin, M.J., Martens, C.S., 2001, Dissolved organic carbon production and consumption in anoxic marine sediments: A pulsed-tracer experiment: *Limnology and Oceanography*, v. 46, p. 1908–1920, doi:10.4319/lo.2001.46.8.1908.
- Ingall, E.D., Bustin, R.M., and Van Cappellen, P., 1993, Influence of water column anoxia on the burial and preservation of carbon and phosphorus in marine shales: *Geochimica et Cosmochimica Acta*, v. 57, p. 303–316, doi:10.1016/0016-7037(93)90433-W.
- Ingall, E., and Jahnke, R., 1994, Evidence for enhanced phosphorus regeneration from marine sediments overlain by oxygen depleted waters: *Geochimica et Cosmochimica Acta*, v. 58, p. 2571–2575, doi:10.1016/0016-7037(94)90033-7.
- Jenkyns, H.C., and Weedon, G.P., 2013, Chemostratigraphy (CaCO_3 , TOC, $\delta^{13}\text{C}_{\text{org}}$) of Sinemurian (Lower Jurassic) black shales from the Wessex Basin, Dorset and palaeoenvironmental implications: *Newsletters on Stratigraphy*, v. 46, p. 1–21, doi:10.1127/0078-0421/2013/0029.
- Kennedy, M.J., Löhr, S.C., Fraser, S.A., and Baruch, E.T., 2014, Direct evidence for organic carbon preservation as clay-organic nanocomposites in a Devonian black shale; from

- deposition to diagenesis: *Earth and Planetary Science Letters*, v. 388, p. 59–70,
doi:10.1016/j.epsl.2013.11.044.
- Kennedy, M.J., Pevear, D.R., and Hill, R.J., 2002, Mineral Surface Control of Organic Carbon in Black Shale: *Science*, v. 295, p. 657–660, doi:10.1126/science.1066611.
- Little, S.H., Vance, D., Lyons, T.W., and McManus, J., 2015, Controls on trace metal authigenic enrichment in reducing sediments: Insights from modern oxygen-deficient settings: *American Journal of Science*, v. 315, p.77–119, doi:10.2475/02.2015.01.
- Ocubalidet, S.G., Rimmer, S.M., and Conder, J.A., 2018, Redox conditions associated with organic carbon accumulation in the Late Devonian New Albany Shale, west-central Kentucky, Illinois Basin: *International Journal of Coal Geology*, v. 190, p. 42–55,
doi:10.1016/j.coal.2017.11.017.
- Pedersen, T.F., and Calvert, S.E., 1990, Anoxia vs. Productivity: What controls the formation of organic-carbon-rich sediments and sedimentary rocks?: Discussion (1): *AAPG Bulletin*, v. 74, p. 454–466, doi:10.1306/0c9b2821-1710-11d7-8645000102c1865d.
- Rimmer, S.M., Thompson, J.A., Goodnight, S.A., and Robl, T.L., 2004, Multiple controls on the preservation of organic matter in Devonian–Mississippian marine black shales: geochemical and petrographic evidence: *Palaeogeography, Palaeoclimatology, Palaeoecology*, v. 215, p. 125–154, doi:10.1016/j.palaeo.2004.09.001.
- Raven, M.R., Fike, D.A., Gomes, M.L., Webb, S.M., Bradley, A.S., and McClelland, M.O., 2018, Organic carbon burial during OAE2 driven by changes in the locus of organic matter sulfurization: *Nature Communications*, doi:10.1038/s41467-018-05943-6.

- Rowe, G.T., Clifford, C.H., Smith Jr, K.L., and Hamilton, P.L., 1975, Benthic nutrient regeneration and its coupling to primary productivity in coastal waters: *Nature*, v. 225, p. 215–217, doi:10.1038/255215a0.
- Schieber, J., Krinsley, D., and Riciputi, L., 2000, Diagenetic origin of quartz silt in mudstones and implications for silica cycling: *Nature*, v. 406, p. 981–985, doi:10.1038/35023143.
- Schoepfer, S.D., Shen, J., Wei, H., Tyson, R.V., Ingall, E., and Algeo, T.J., 2015, Total organic carbon, organic phosphorus, and biogenic barium fluxes as proxies for paleomarine productivity: *Earth-Science Reviews*, v. 149, p. 23–52, doi:10.1016/j.earscirev.2014.08.017.
- Sepúlveda, J., Wendler, J.E., Summons, R.E., and Hinrichs, K., 2009, Rapid resurgence of marine productivity after the Cretaceous-Paleogene mass extinction: *Science*, v. 326, p. 129–132, doi:10.1126/science.1176233.
- Torres, M.A., Limaye, A.B., Ganti, V., Lamb, M.P., West, A.J., and Fischer, W.W., 2017, Model predictions of long-lived storage of organic carbon in river deposits: *Earth Surface Dynamics*, v. 5, p. 711–730, doi:10.5194/esurf-5-711-2017.
- Tribovillard, N., Algeo, T. J., Lyons, T., and Riboulleau, A., 2006, Trace metals as paleoredox and paleoproductivity proxies: An update: *Chemical Geology*, v. 232, p. 12–32, doi:10.1016/j.chemgeo.2006.02.012.
- Tyson, R.V., 2001, Sedimentation rate, dilution, preservation and total organic carbon: some results of a modelling study: *Organic Geochemistry*, v. 32, p. 333–339, doi:10.1016/S0146-6380(00)00161-3.
- Tyson, R.V., 2005, The "productivity versus preservation" controversy: cause, flaws, and resolution, *in* Harris, N.B., ed., *The Deposition of Organic-Carbon-Rich Sediments: Models,*

Mechanisms, and Consequences: Society for Sedimentary Geology, Tulsa, Oklahoma,
Special Publication 82, p. 17–33.

Zhou, L., Algeo, T.J., Shen, J., Hu, Z., Gong, H., Xie, S., Huang, J., and Gao, S., 2015, Changes
in marine productivity and redox conditions during the Late Ordovician Hirnantian
glaciation: *Palaeogeography, Palaeoclimatology, Palaeoecology*, v. 420, p. 223–234,
doi:10.1016/j.palaeo.2014.12.012.

**CHAPTER 2 NEW INSIGHTS INTO ORGANIC MATTER
ACCUMULATION FROM HIGH-RESOLUTION GEOCHEMICAL
ANALYSIS OF A BLACK SHALE: MIDDLE AND UPPER DEVONIAN
HORN RIVER GROUP, CANADA**

Haolin Zhou¹, Nicholas B. Harris¹, Jilu Feng¹, Benoit Rivard¹, Tian Dong², Korhan Ayranci³, Paul Hackley⁴, and Javin Hatcherian⁴

¹ Department of Earth and Atmospheric Sciences, University of Alberta, Edmonton, AB, T6G2E3, Canada

² Key Laboratory of Tectonics and Petroleum Resources of Ministry of Education, China University of Geosciences, Wuhan, 430074, China

³ College of Petroleum Engineering & Geosciences, King Fahd University of Petroleum & Minerals, Dhahran 31261, Saudi Arabia

⁴ U.S. Geological Survey, Reston, VA, 20192, USA

ABSTRACT

Organic carbon-rich mudstones, or ‘black shales’, record highly anomalous perturbations of local or earth systems at critical times in earth history. In these rocks, organic matter (OM) accumulation is controlled by bioproductivity, preservation, and dilution. However, immediate triggers for organic carbon deposition in these formations are commonly difficult to identify because of feedback loops that cause geochemical proxies for these controls to vary apparently synchronously when sampled at decimeter to meter spacing. We built a geochemical dataset based on energy dispersive X-ray fluorescence (EDXRF) and infrared imagery analyses, applying geochemical proxies in millimeter-resolution profiles to the Middle and Upper Devonian Horn River shale in the Western Canadian Sedimentary Basin. In these profiles,

bioproductivity and redox proxies, biogenic Si and S/Fe, show different trends in contrast to the synchronous variation between them observed in more coarsely sampled profiles.

Bioproductivity and dilution by siliciclastic or carbonate input are identified as the primary controls on OM burial, while redox is the less common trigger in this formation. Comparison of geochemical profiles reveals bioproductivity-redox feedback loops developed on time scales of decades to centuries.

2.1 INTRODUCTION

Bioproductivity, preservation, and dilution are widely recognized as primary controls for organic matter (OM) accumulation in sedimentary rocks (e.g., Algeo et al., 2004). Redox states control OM accumulation because labile OM degrades in the presence of oxidants (e.g., Katz, 2005), typically through biological processes. High primary productivity, generally resulting from high nutrient delivery, triggers OM accumulation by increasing organic flux through the water column (e.g., Pedersen and Calvert, 1990), locally exceeding organic consumption by oxidation reactions even where the water column is oxygenated. Low mineral sedimentation rates concentrate OM by limiting dilution (Loutit et al., 1988), although this may be offset by enhanced burial efficiency of OM at low to moderate rates (Tyson, 2001). In addition, clays with greater mineral surface area than quartz or carbonate silt, can preserve OM in interlayer space (Kennedy et al. 2014). Although clay preservation that enhanced organic enrichment is subtle in some Devonian formations, e.g., Cleveland shales (Rimmer et al., 2004), this mechanism is observed in certain shales, e.g., Woodford Formation (Kennedy et al., 2014).

These controls are commonly linked through feedback loops, especially between anoxia and bioproductivity. Anoxia stimulates productivity by stripping phosphorus (P) from sinking OM, which recirculates to surface water (Ingall and Jahnke, 1994). Similarly, high

bioproductivity stimulates high fluxes of OM to the seafloor, consuming oxygen as OM settles through the water column (Katz, 2005). The time required for basin-scale feedback loops that are related with nutrient cycling to develop (e.g., the time lag between increased bioproductivity and decreased oxygen levels) is effectively unknown but may be estimated at the magnitude of $10^4 - 10^5$ yr or less, from an analysis of global marine phosphorus (P) cycle that was studied based on systematic quantitative modeling of P input fluxes, sinks, and removal out of oceans (Froelich et al., 1982; Ruttenberg, 2003). The timescale of global marine P cycle, $10^4 - 10^5$ yr, is equivalent to tens of centimeters of stratigraphic section at common mudstone sedimentation rates (Harris et al., 2013). Thus, apparently synchronous shifts in proxies for bioproductivity and redox conditions may result from insufficient sampling resolution to distinguish the time in which feedback loops develop.

Our analysis of the Horn River Group (Middle-Upper Devonian of British Columbia, Canada) applies geochemical proxies for redox states, biogenic inputs, and detrital contributions. Dong et al. (2018) examined samples spaced at ~ 1 m from 5 long cores and identified apparently synchronous shifts in bioproductivity and redox states associated with changes in TOC. We investigate the same shale section at a much denser sample spacing.

2.2 GEOLOGICAL SETTING

The Horn River Basin, part of the Western Canada Sedimentary Basin, is surrounded by carbonate platforms and reefs to the south and east and is separated from the Liard Basin by the Bovie Fault to the west (Fig. 2.1). The fault was post-depositional without influences on sedimentation of the Horn River Group. The Horn River shale was deposited from the late Givetian to the early Frasnian Stage (Ross and Bustin, 2009) and includes the Evie Member, Otter Park Member, and Muskwa Formation, representing three third-order sea level cycles

superimposed on a partial second order cycle (Ayranci et al., 2018b) (Fig. 2.2). The Evie Member is a dark grey to black, organic-rich, and calcareous mudstone (Fig. 2.2); total organic carbon (TOC) content is the highest of the entire Horn River Group (Fig. 2.2). The Otter Park Member is a grey to dark grey, organic-lean, argillaceous, and calcareous mudstone (Fig. 2.2). TOC content is typically the lowest in the entire shale (Fig. 2.2). The Muskwa Formation is a dark grey to black, organic-rich, and siliceous mudstone (Fig. 2.2). TOC concentration in this formation is less than the Evie Member but more than the Otter Park Member (Fig. 2.2). The Horn River shale is within the dry gas window; thermal maturities range from 1.6% to 2.5% R_o (vitrinite reflectance; Ross and Bustin, 2009), so the thermal loss of organic matter is likely similar in this mudrock given the predominant Type II kerogen in the entire shale.

A delta near the southeastern corner of the basin introduced siliciclastic silt and mud that were deposited through suspension settling, sediment gravity flows, and bottom currents (Ayranci et al., 2018a). Carbonate sediment was shed from surrounding platforms. Original OM is identified as Type II (Appendix E), consistent with previous studies (Feinstein et al., 1991; Stasiuk and Fowler, 2004) and with nearby coeval Duvernay mudrock in the Alberta Basin (Harris et al., 2018) east of the Horn River Basin.

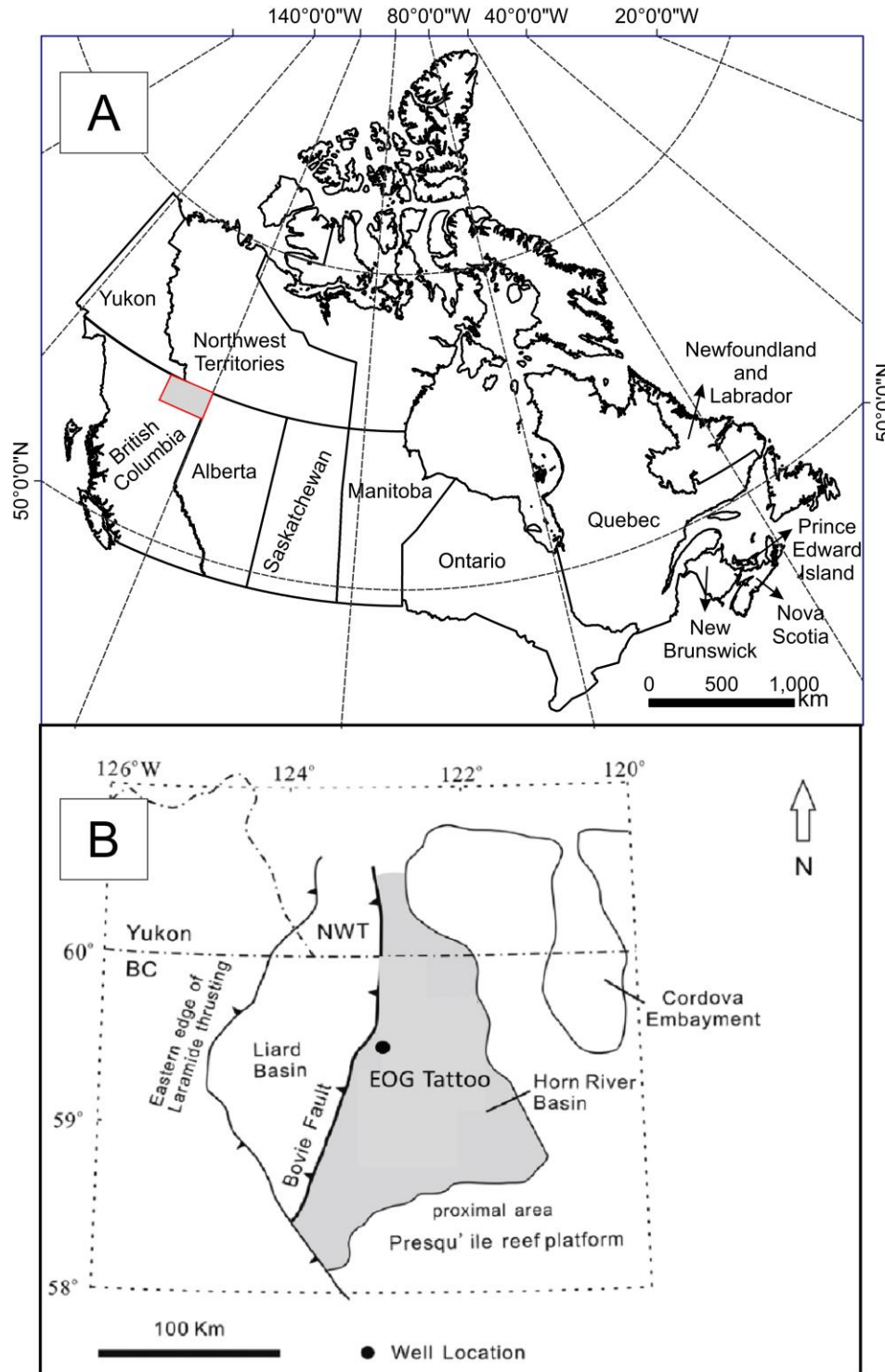


Figure 2.1. Location of the Horn River Basin and the well location. A: Canada Map. The location of the Horn River Basin is indicated by the red square. B: Map of the Horn River Basin (Moghadam et al., 2019). BC – British Columbia; NWT – the Northwest Territories.

2.3 METHODS

We analyzed 133 core slabs of the Horn River shale from the vertical EOG TATTOO D-A28-F/094-O-10 well in the distal Horn River Basin (Fig. 2.1B), obtained at ~ 1 m spacing, each representing a 7 – 12 cm section. Bulk major, minor, and trace element compositions of each slab were analyzed by ICP-MS and LECO analysis (Appendix C), following Dong et al. (2018).

Samples were scanned in transects perpendicular to visible bedding by the benchtop Orbis PC Micro-EDXRF Elemental Analyzer at the nanoFAB facility, University of Alberta. Scan points were separated vertically by ~ 1 – 2 mm, 30 s/scan. Diameter of the detector window is 2 mm. The detection limit is 0.01%. We selected elements with effective peaks above noise, including Si, Al, K, Ca, Mg, Fe, S, Ba, and Ti (wt.%). Total organic carbon (TOC) and Si contents were analyzed at a ~ 0.8 – 1.5 mm vertical resolution by hyperspectral (infrared) imaging of core slabs using a SisuROCK system at the University of Alberta Spectral Imaging Facility, obtaining measurements in the spectral range of 970 – 2510 nm and 7400 – 12100 nm for quantification of TOC and SiO₂, respectively (Rivard et al., 2018). Silica data, obtained from both methods, were used to register the two datasets (Appendix B). TOC data from hyperspectral imaging were calibrated to a shale model based on the Horn River Group (Rivard et al., 2018). Averages of values from XRF scans of slabs were compared to whole-rock data from ICP-MS analysis for calibration (Appendix D).

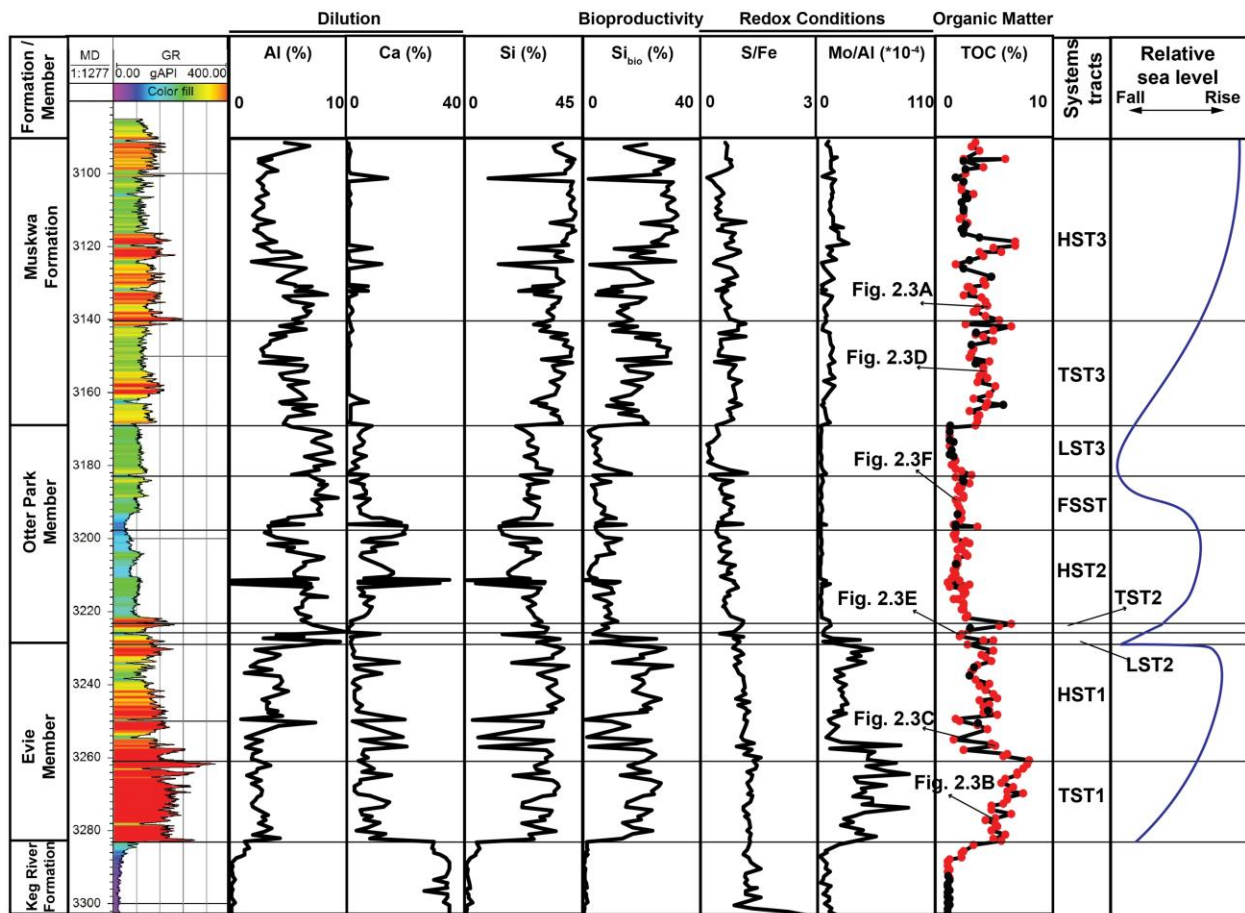


Figure 2.2. Core log of the Horn River shale in this study, including stratigraphic units, gamma ray log, geochemical analyses, and systems tracts (based on Ayranci et al., 2018b). Locations of examples in Figure 2.3 are indicated. Red spots in TOC profile are the samples analyzed by EDXRF and hyperspectral imagery. HST – highstand systems tract; TST – transgressive systems tract; LST – lowstand systems tract; FSST – falling stage systems tract; Si_{bio} – biogenic silica.

2.3.1 Proxies

We applied elemental concentrations and ratios as proxies for redox conditions, bioproductivity, siliciclastic and carbonate input, and OM accumulation. Al concentration was used for clastic input (Tribovillard et al., 2006), which is closely correlated with Ti concentration ($R^2 = 0.96$, Appendix D). Ca concentration was used for carbonate input derived from platform

shedding, calcareous planktic sources (Obermajer et al, 1999), or early diagenetic processes. Limitations of the XRF scanning system precluded the application of trace element ratios as proxies; thus, we applied S/Fe ratios (DOP_T), described by Algeo and Liu (2020) as a relatively strong proxy for redox conditions, although less reliable than trace metal enrichment factors (EFs), in part due to local diagenetic effects. $S/Fe < 0.4$ is considered to indicate oxic conditions, and $0.72 < S/Fe < 1.15$, anoxic conditions ($S/Fe = 1.15$ is the ratio for pyrite) (Arthur and Sageman, 1994; Ocubalidet et al., 2018). Dong et al. (2018) and Harris et al. (2018) compared S/Fe to Mo/Al for this shale and coeval Duvernay Formation, respectively, validating S/Fe ratios as a redox proxy. TOC is an appropriate measure of OM enrichment, but bitumen migration, referring here to the early product of kerogen cracking, merits discussion in high-resolution analysis. Biogenic silica (Si_{bio}), a proxy for bioproduction (Schieber et al. 2000), was calculated after Ross and Bustin (2009):

$$Si_{bio} = Si_{sample} - [Al_{sample} \times (Si/Al)_{background}]. \quad (1)$$

The background Si/Al ratio used is 3.1 (Wedepohl, 1971), consistent with previous studies of the Horn River shale (Dong et al., 2018), where this ratio effectively distinguished biogenic and detrital Si.

2.4 RESULTS AND INTERPRETATIONS

We show representative patterns for geochemical proxies in 6 stratigraphic profiles (Fig. 2.3) and interpret them in the context of mechanisms for OM accumulation. Bulk elemental concentrations vary in different intervals and are therefore displayed at different scales in the profiles. Excursions in TOC range from less than 0.4 % (slab 3218.55 m) to 7.2 % (slab 3251.48 m).

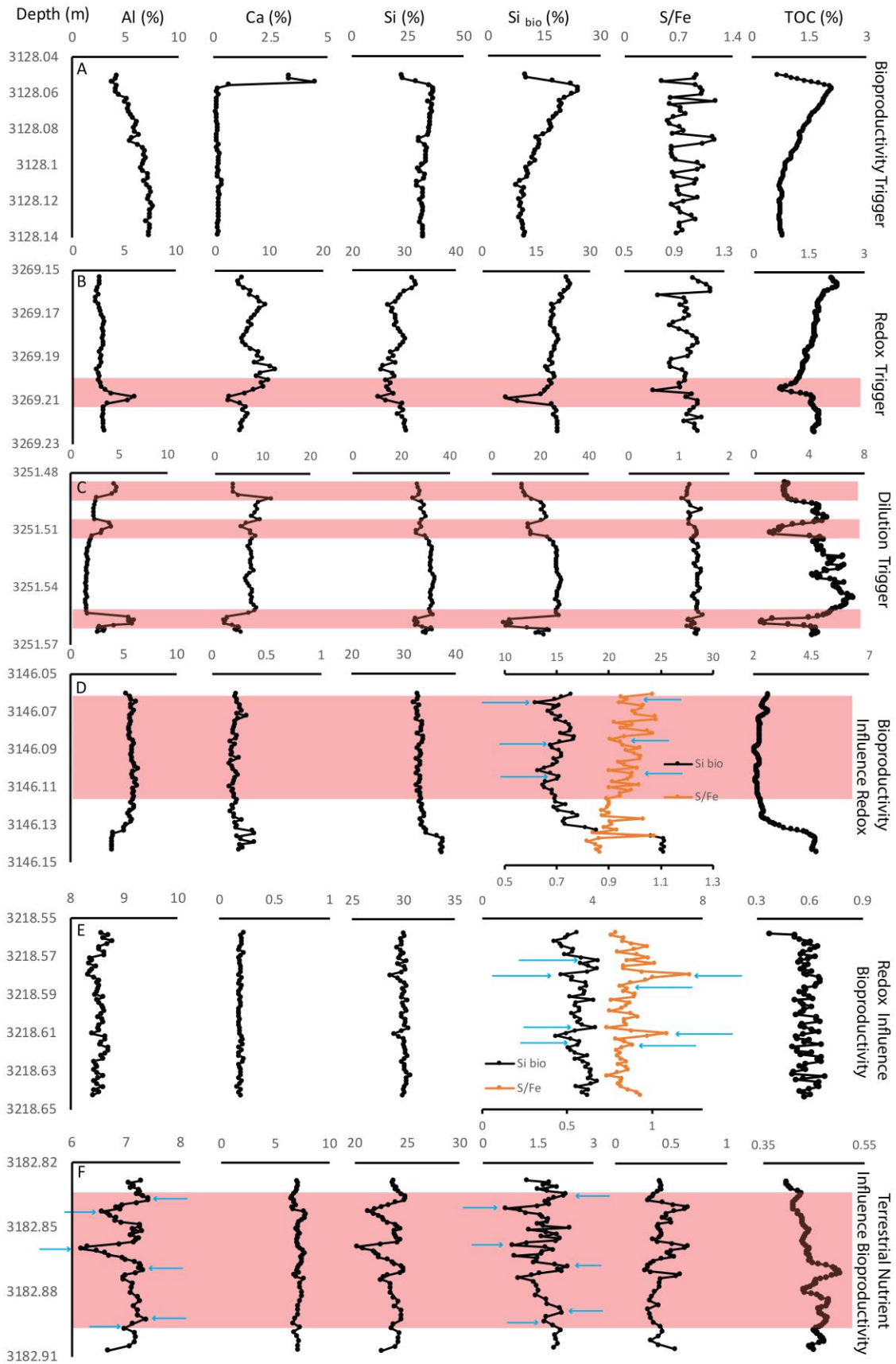


Figure 2.3. Classification of triggers for OM burial and redox-bioproduction feedbacks. A: Bioproductivity triggers OM accumulation. B: Redox conditions trigger OM accumulation in the red interval. C: Dilution controls OM accumulation in red intervals. D: Bioproductivity-induced redox feedback. E: Redox-induced bioproductivity feedback. F: Continental nutrients influence bioproductivity. Marker peaks are indicated by blue arrows.

2.4.1 Bioproductivity trigger for OM burial

In many samples, Si_{bio} correlates positively to %TOC in the absence of systematic relationships between TOC and other proxies. In Fig. 2.3A, Si_{bio} profile precisely tracks TOC profile ($R^2 = 0.96$, Appendix D). Varying the assumed detrital Si/Al ratio in equation 1 has little impact on the shape of the Si_{bio} curve or its correlation to TOC, indicating a robust relationship (Appendix D). The combined concentrations of carbonate and siliciclastic minerals, indicated by Al and Ca, respectively, also track TOC negatively; the shift from siliciclastic to carbonate-enriched sediment near the top of the profile may reflect early diagenetic carbonate cement (Lash and Blood, 2004). S/Fe ratios almost everywhere exceed 0.4, variable on 5 mm scale but uncorrelated to TOC.

Stable Si_{bio}/TOC of 11 to 12 and the absence of correlation between S/Fe and TOC indicate that OM accumulation was influenced by bioproductivity and unrelated to redox conditions. Dilution may have affected both Si_{bio} and OM accumulation but that did not influence OM burial efficiency nor introduce significant terrestrial OM based on organic petrography analysis (Appendix D).

2.4.2 Preservation trigger for OM burial

In the highlighted interval of Fig. 2.3B, TOC parallels the S/Fe profile. Changes in other parameters, increased Al content and decreased Ca and Si_{bio} contents, occur 3.1 mm below decreases in S/Fe and TOC.

The coincidence of reduced TOC and S/Fe in the absence of other direct relationships indicates that oxygenation influenced OM preservation, possibly related to short-term deepwater ventilation (Dahl et al. 2019) by sediment gravity flows to nearby areas, without affecting Si_{bio} or clay (Al) contents. Stable Si_{bio} content indicates that observed variation in S/Fe ratios was not related to OM loading.

2.4.3 Dilution as the trigger for OM burial

Fig. 2.3C highlights three intervals of lower TOC associated with elevated Al and decreased Ca and Si_{bio}. No systematic relationship to S/Fe is evident.

In the bottom interval, decreases in Si_{bio} and TOC are associated with nearly constant Si_{bio}/Ca ratio (3 – 5), suggesting that dilution by detrital clastics controlled OM accumulation. In contrast to Fig. 2.3A, Si_{bio}/TOC increases from 5 to 15, demonstrating that bioproductivity was decoupled from OM accumulation, related to poorer preservation. TOC distribution was probably not significantly affected by bitumen migration, which could have redistributed organic matter to open primary pores during initial kerogen cracking (Dong et al., 2020). However, no increase in TOC was observed in intervals with high Ti/Al (Appendix D), which are expected to be the coarsest grained (Murphy et al., 2000) and have had highest primary porosity.

2.4.4 Bioproductivity-lead-redox-lag feedback

Two redox-bioproductivity feedback patterns are shown in our profiles. In Fig. 2.3D, TOC is positively correlated to Si_{bio} and inversely correlated to Al, indicating that nutrient

delivery or dilution was the primary control on OM accumulation. At the notable upward increase in Al at 3146.13 m, the ratio of Si_{bio}/TOC increases from 5 to 8, reflecting possible slightly enhanced degradation of OM. Burial efficiency remained stable during deposition of the red interval (Si_{bio}/TOC ratio varies within a narrow range). The overall upward increase in S/Fe in the highlighted interval may represent (1) depletion of components such as Mn and Fe that function as electron acceptors based on the slightly decreased terrestrial input (decreased Al concentrations in general); (2) a possible increasing sulfide supply by more buried organic matter reflected by slightly increased TOC content, i.e., overall increasing bioproductivity ($\%Si_{bio}$) led to progressively reducing conditions.

Smaller scale relationships between Si_{bio} and S/Fe are present in the highlighted section, where peaks in Si_{bio} are offset from peaks in S/Fe profile by ~ 3 mm, shown as arrows in Fig. 2.3D. These offsets are attributed to lag in the development of a feedback loop as oxygen was consumed through OM degradation. S/Fe spikes at 3146.125 m and 3146.134 m correspond to observed diagenetic pyrite (former) and likely to microscopic diagenetic pyrite (latter).

2.4.5 Redox-lead-bioproductivity-lag feedback

A less common pattern is shown in Fig. 2.3E, where all elemental proxies show limited variation on a 5 mm scale. Si_{bio} peaks occur stratigraphically above (thus lag behind) peaks in the S/Fe profile by $\sim 1.5 - 3$ mm, which we attribute to changes in bioproductivity related to P release from sinking OM in variable redox conditions.

2.4.6 Terrestrial flux influences bioproductivity

In Fig. 2.3F, TOC is low and weakly correlated with Al and Si_{bio} . Al is correlated positively with Si_{bio} and negatively with S/Fe. Peaks in Al occur stratigraphically ~ 1 mm below peaks in Si_{bio} profile in the red interval.

The observed negative correlation between S/Fe and Al suggests variation in river discharge and sediment delivery controlled deepwater redox states or temporary increased delivery of oxidants by increased clay input. Increased river discharge resulted in increased continental flux (Al) and likely turbulent mixing of oxygen, i.e., lower S/Fe, although water balance and density variations also control oxygen penetration. The positive correlation of Si_{bio} and Al, combined with deposition in oxic conditions that limited marine P recycling during low sea level (Ayranci et al., 2018a) suggest that nutrient supply in this interval was largely continental. Al-Si_{bio} offsets reflect delays between the initial input of terrestrial-derived nutrients and subsequent changes in bioproduction.

2.5 FREQUENCY OF CONTROLS AND TIME SCALES IN ORGANIC MATTER ACCUMULATION

Dense sampling of the Horn River section identifies a suite of short-term triggers for OM accumulation. Dilution (59% of samples) and bioproductivity (35%) are most common, although a redox control is also evident (7%) (Fig. 2.4).

Stratigraphic lags noted between bioproductivity and redox proxies can be used to estimate time lags. The shale was deposited during a time span of ~ 6 – 8 m.y. (Morrow, 2018; Mossop and Shetesn, 1994) equivalent to an average sedimentation rate of ~ 0.02 – 0.03 mm/yr, although the clastic-rich Otter Park Member, deposited during a second order lowstand (Ayranci et al., 2018b), was probably deposited more rapidly than other units. Possible erosion events or deposition hiatus also influence the consistency of sedimentation and sedimentation rates. Our dataset improves temporal resolution from an average of ~ 30 – 40 kyr (1 m spacing) to a few decades (1 – 2 mm spacing). The estimate of timescales represented by sample spacings assumes the linear relationship between depth and time. Although this averaged sedimentation rate cannot

accurately illustrate the actual sedimentation processes, it describes how the resolution of geochemical analysis is improved.

Redox-bioproductivity feedback lags are indicated by $\text{Si}_{\text{bio}}\text{-S/Fe}$ offsets of $\sim 1.5 - 3$ mm (Figs. 3D and 3E), indicating that changes in redox conditions induced changes in bioproductivity and vice versa over decades to centuries. An Al- Si_{bio} lag of ~ 1 mm reflects that the biotic response to increased continental nutrient was less than 50 yr. Research in modern environments shows, however, that increases in C/P ratio lag anoxic events by less than a few years (Emeis et al, 2000) and that biological responses to nutrient level change are on the order of weeks (Cottingham et al., 1997). Differences between modern systems and our interpretation of time lags in the Horn River shale may result from averaged sedimentation rate, or intermediate timescale feedback loops that are not evident in studies of modern environments.

Dense sampling of the Horn River section identified controls for OM accumulation, primarily dilution and bioproductivity, that differ from the single primary control on OM burial (redox conditions) identified by coarser sampling in our previous work (Dong et al., 2018). This suggests that variability in OM concentrations over decades to centuries may be controlled by different processes than those operating over hundreds of thousands of years.

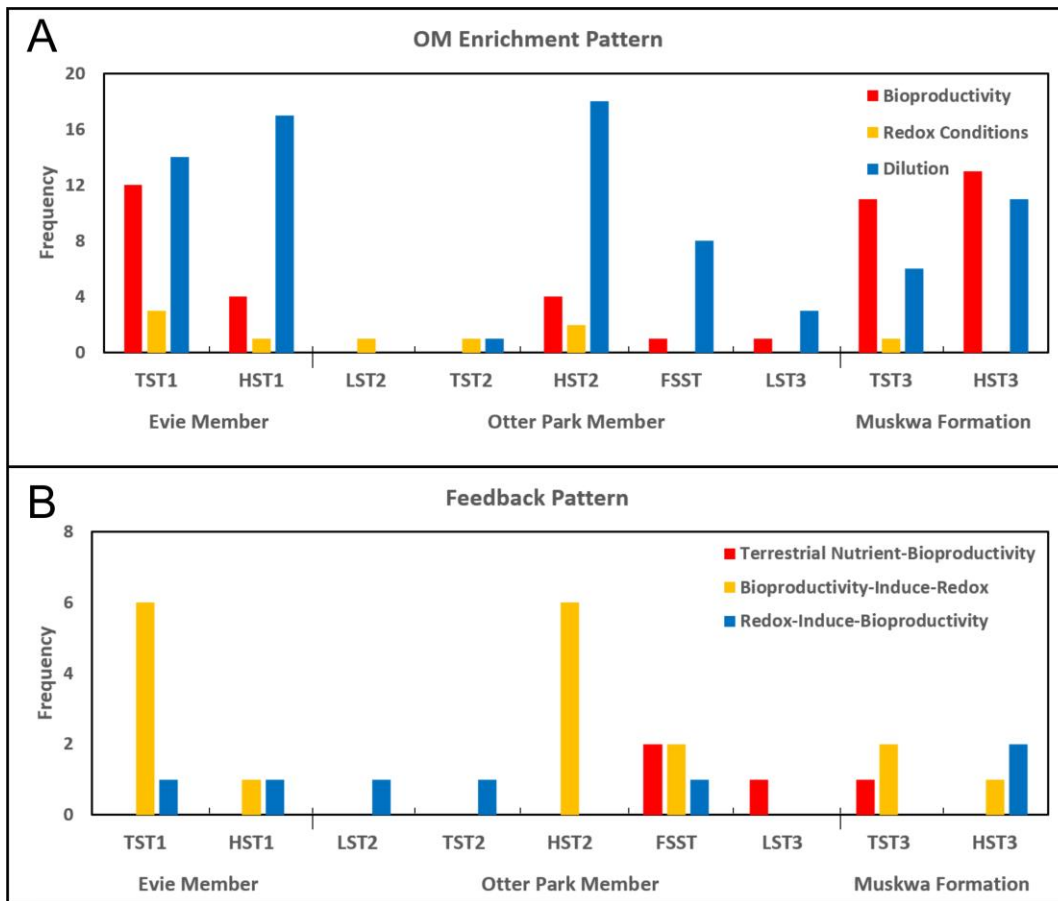


Figure 2.4. A: Frequencies of OM enrichment patterns. B: Frequencies of feedback patterns among terrestrial input, bioproductivity, and redox conditions. 3rd order sequence stratigraphy is following Ayarnci et al. (2018b).

2.6 ACKNOWLEDGMENTS

We thank Dr. Nancy Zhang and Mr. Peng Li for assistance with EDXRF analysis. We are grateful to Dr. Rob Creaser and Dr. Mike Arthur for their comments on the manuscript, reviewer Dr. Eric Sperling and two anonymous reviewers for their inciteful reviews.

2.7 REFERENCES CITED

Algeo, T.J., and Liu, J., 2020, A re-assessment of elemental proxies for paleoredox analysis:

Chemical Geology, in press, doi:10.1016/j.chemgeo.2020.119549.

- Algeo, T.J., Schwark, L., and Hower, J.C., 2004, High-resolution geochemistry and sequence stratigraphy of the Hushpuckney Shale (Swope Formation, eastern Kansas): Implications for climato-environmental dynamics of the Late Pennsylvanian Midcontinent Seaway: *Chemical Geology*, v. 206, p. 259–288, doi:10.1016/j.chemgeo.2003.12.028.
- Arthur, M.A., and Sageman, B.B., 1994, Marine Black Shales: Depositional Mechanisms and Environments of Ancient Deposits: *Annual Review of Earth and Planetary Sciences*, v. 22, p. 499–551, doi:10.1146/annurev.ea.22.050194.002435.
- Ayranci, K., Harris, N.B., and Dong, T., 2018a, Sedimentological and Ichnological Characterization of the Middle to Upper Devonian Horn River Group, British Columbia, Canada: Insights into Mudstone Depositional Conditions and Processes Below Storm Wave Base: *Journal of Sedimentary Research*, v. 88, p. 1–23, doi:10.2110/jsr.2017.76.
- Ayranci, K., Harris, N.B., and Dong, T., 2018b, High resolution sequence stratigraphic reconstruction of mud-dominated systems below storm wave base: A case study from the Middle to Upper Devonian Horn River Group, British Columbia, Canada: *Sedimentary Geology*, v. 373, p. 239–253, doi:10.1016/j.sedgeo.2018.06.009.
- Cottingham, K.L., Knight, S.E., Carpenter, S.R., Cole, J.J., Pace, M.L., and Wagner, A.E., 1997, Response of phytoplankton and bacteria to nutrients and zooplankton: a mesocosm experiment: *Journal of Plankton Research*, v. 19, p. 995–1010, doi:10.1093/plankt/19.8.995.
- Dahl, T.W., Siggaard-Andersen, M., Schovsbo, N.H., Persson, D.O., Husted, S., Hougård, I.W., Dickson, A.J., Kjær, K., and Nielsen, A.T., 2019, Brief oxygenation events in locally anoxic oceans during the Cambrian solves the animal breathing paradox: *Scientific Reports*, doi:10.1038/s41598-019-48123-2.

- Dong, T., and Harris, N.B., 2020, The effect of thermal maturity on porosity development in the Upper Devonian-Lower Mississippian Woodford Shale, Permian Basin, US: Insights into the role of silica nanospheres and microcrystalline quartz on porosity preservation: *International Journal of Coal Geology*, v. 217, p. 1–14, doi:10.1016/j.coal.2019.103346.
- Dong, T., Harris, N.B., and Ayranci, K., 2018, Relative sea-level cycles and organic matter accumulation in shales of the Middle and Upper Devonian Horn River Group, northeastern British Columbia, Canada: Insights into sediment flux, redox conditions, and bioproductivity: *Bulletin of the Geological Society of America*, v. 130, p. 859–880, doi:10.1130/B31851.1.
- Emeis, K.-C., Struck, U., Leipe, T., Pollehne, F., Kunzendorf, H., and Christiansen, C., 2000, Changes in the C, N, P burial rates in some Baltic Sea sediments over the last 150 years—relevance to P regeneration rates and the phosphorus cycle: *Marine Geology*, v. 167, p. 43–59, doi:10.1016/S0025-3227(00)00015-3.
- Feinstein, S., Williams, G.K., Snowdon, L.R., Brooks, P.W., Fowler, M.G., Goodarzi, F., and Gentzis, T., 1991, Organic geochemical characterization and hydrocarbon generation potential of mid-Late Devonian Horn River bituminous shales, southern Northwest Territories: *Bulletin of Canadian Petroleum Geology*, v. 39, p. 192–202.
- Froelich, P.N., Bender, M.L., Luedtke, N.A., Heath, G.R., and DeVries, T., 1982, The marine phosphorus cycle: *American Journal of Science*, v. 282, p. 475–511, doi:10.2475/ajs.282.4.474.
- Harris, N.B., McMillan, J.M., Knapp, L.J., and Mastalerz, M., 2018, Organic matter accumulation in the Upper Devonian Duvernay Formation, Western Canada Sedimentary

- Basin, from sequence stratigraphic analysis and geochemical proxies: *Sedimentary Geology*, v. 376, p. 185–203, doi:10.1016/j.sedgeo.2018.09.004.
- Harris, N.B., Mnich, C.A., Selby, D., and Korn, D., 2013, Minor and trace element and Re–Os chemistry of the Upper Devonian Woodford Shale, Permian Basin, west Texas: Insights into metal abundance and basin processes: *Chemical Geology*, v. 356, p. 76–93, doi:10.1016/j.chemgeo.2013.07.018.
- Ingall, E., and Jahnke, R., 1994, Evidence for enhanced phosphorus regeneration from marine sediments overlain by oxygen depleted waters: *Geochimica et Cosmochimica Acta*, v. 58, p. 2571–2575, doi:10.1016/0016-7037(94)90033-7.
- Katz, B.J., 2005, Controlling factors on source rock development—a review of productivity, preservation, and sedimentation rate, *in* Harris, N.B., ed, *The Deposition of Organic-Carbon-Rich Sediments: Models, Mechanisms, and Consequences*: Society for Sedimentary Geology, Tulsa, Oklahoma, Special Publication 82, p. 7–16.
- Kennedy, M.J., Löhr, S.C., Fraser, S.A., and Baruch, E.T., 2014, Direct evidence for organic carbon preservation as clay-organic nanocomposites in a Devonian black shale; from deposition to diagenesis: *Earth and Planetary Science Letters*, v. 388, p. 59–70, doi:10.1016/j.epsl.2013.11.044.
- Lash, G.G., and Blood, D., 2004, Geochemical and textural evidence for early (shallow) diagenetic growth of stratigraphically confined carbonate concretions, Upper Devonian Rhinestreet black shale, western New York: *Chemical Geology*, v. 206, p. 407–424, doi:10.1016/j.chemgeo.2003.12.017.
- Loutit, T., Hardenbol, J., Vail, P., and Baum, G., 1988, Condensed sections: the key to age determination and correlation of continental margin sequences, *in* Wilgus, C.K., Hastings,

- B.S., Ross, C.A., Posamentier, H., Wagoner, J., Van, and Kendall, C.G.St.C., eds, *Sea-Level Changes: An Integrated Approach*: Society for Sedimentary Geology, Tulsa, Oklahoma, Special Publication 42, p. 183–213.
- Moghadam, A., Harris, N.B., Ayranci, K., Gomez, J.S., Angulo, N.A., and Chalaturnyk, R., 2019, Brittleness in the Devonian Horn River shale, British Columbia, Canada: *Journal of Natural Gas Science and Engineering*, v. 62, p. 247–258, doi:10.1016/j.jngse.2018.12.012.
- Morrow, D.W., 2018, Devonian of the Northern Canadian Mainland Sedimentary Basin: A Review: *Bulletin of Canadian Petroleum Geology*, v. 66, p. 623–694.
- Mossop, G.D., and Shetsen, I., 1994, *Geological Atlas of the Western Canada Sedimentary Basin*: Calgary, Alberta, Canadian Society of Petroleum Geologists and Alberta Research Council, 510 p: http://www.ags.gov.ab.ca/publications/wcsb_atlas/atlas.html.
- Murphy, A.E., Sageman, B.B., Hollander, D.J., Lyons, T.W., and Brett, C.E., 2000, Black shale deposition and faunal overturn in the Devonian Appalachian Basin: Clastic starvation, seasonal water – column mixing, and efficient biolimiting nutrient recycling: *Paleoceanography and Paleoclimatology*, v. 15, p. 280–291, doi:10.1029/1999PA000445.
- Obermajer, M., Stasiuk, L.D., Fowler, M.G., and Osadetz, K.G., 1999, Application of acritarch fluorescence in thermal maturity studies: *International Journal of Coal Geology*, v. 39, p. 185–204, doi:10.1016/S0166-5162(98)00045-7.
- Ocubalidet, S.G., Rimmer, S.M., and Conder, J.A., 2018, Redox conditions associated with organic carbon accumulation in the Late Devonian New Albany Shale, west-central Kentucky, Illinois Basin: *International Journal of Coal Geology*, v. 190, p. 42–55, doi:10.1016/j.coal.2017.11.017.

- Pedersen, T.F., and Calvert, S.E., 1990, Anoxia vs. Productivity: What controls the formation of organic-carbon-rich sediments and sedimentary rocks?: Discussion (1): AAPG Bulletin, v. 74, p. 454–466, doi:10.1306/0c9b2821-1710-11d7-8645000102c1865d.
- Rivard, B., Harris, N.B., Feng, J., and Dong, T., 2018, Inferring total organic carbon and major element geochemical and mineralogical characteristics of shale core from hyperspectral imagery: AAPG Bulletin, v. 102, p. 2101–2121, doi:10.1306/03291817217.
- Ross, D.J.K., and Bustin, R.M., 2009, Investigating the use of sedimentary geochemical proxies for paleoenvironment interpretation of thermally mature organic-rich strata: Examples from the Devonian-Mississippian shales, Western Canadian Sedimentary Basin: Chemical Geology, v. 260, p. 1–19, doi:10.1016/j.chemgeo.2008.10.027.
- Ruttenberg, K.C., 2003, The global phosphorus cycle: Treatise on Geochemistry, v. 8, p. 585–643, doi:10.1016/B0-08-043751-6/08153-6.
- Schieber, J., Krinsley, D., and Riciputi, L., 2000, Diagenetic origin of quartz silt in mudstones and implications for silica cycling: Nature, v. 406, p. 981–985, doi:10.1038/35023143.
- Stasiuk, L.D., and Fowler, M.G., 2004, Organic facies in Devonian and Mississippian strata of Western Canada Sedimentary Basin: relation to kerogen type, paleoenvironment, and paleogeography: Bulletin of Canadian Petroleum Geology, v. 52, p. 234–255, doi:10.2113/52.3.234.
- Tribovillard, N., Algeo, T. J., Lyons, T., and Riboulleau, A., 2006, Trace metals as paleoredox and paleoproductivity proxies: An update: Chemical Geology, v. 232, p. 12–32, doi:10.1016/j.chemgeo.2006.02.012.

Tyson, R.V., 2001, Sedimentation rate, dilution, preservation and total organic carbon: some results of a modelling study: *Organic Geochemistry*, v. 32, p. 333–339, doi:10.1016/S0146-6380(00)00161-3.

Wedepohl, K.H., 1971, Environmental influences on the chemical composition of shales and clays: *Physics and Chemistry of the Earth*, v. 8, p. 307–333, doi:10.1016/0079-1946(71)90020-6.

**CHAPTER 3 PHYSICAL SEDIMENTOLOGICAL, OCEANOGRAPHIC,
AND DIAGENETIC INFLUENCES ON SHALE GEOCHEMISTRY FROM
HIGH RESOLUTION GEOCHEMICAL AND PETROGRAPHIC
PROFILES, HORN RIVER GROUP, MIDDLE-UPPER DEVONIAN,
BRITISH COLUMBIA**

Haolin Zhou¹, Nicholas B. Harris¹, Tian Dong², Paul Hackley³, Javin Hatcherian³, Jilu Feng¹, Benoit Rivard¹, and Korhan Ayranci⁴

¹ Department of Earth and Atmospheric Sciences, University of Alberta, Edmonton, AB, T6G2E3, Canada

² Key Laboratory of Tectonics and Petroleum Resources of Ministry of Education, China University of Geosciences, Wuhan, 430074, China

³ U.S. Geological Survey, Reston, VA, 20192, USA

⁴ College of Petroleum Engineering & Geosciences, King Fahd University of Petroleum & Minerals, Dhahran 31261, Saudi Arabia

ABSTRACT

In our prior study (Chapter 2), we examined processes and paleoenvironmental parameters (bioproductivity, redox conditions, and siliciclastic and carbonate input) related to organic matter accumulation in the Middle-Upper Devonian Horn River Group, British Columbia, based on millimeter-scale geochemical analysis. However, in some cases geochemical proxies cannot effectively distinguish sedimentological from diagenetic effects on rock composition. For example, calcium concentration may indicate carbonate mineral concentrations related to input of detrital carbonate, biogenic carbonate, or carbonate diagenesis. In this chapter, we complement previous geochemical profiles and a petrographic analysis of representative

samples that display different processes of organic matter accumulation in this Horn River Group to test evidence for sedimentological or diagenetic processes. In this study, we identify the controls of biogenic input, terrestrial detrital input, carbonate detrital input, and diagenesis on the shale petrography, which provide evidence for our previous interpretation based on the geochemical dataset.

3.1 INTRODUCTION

We documented different controls on organic matter accumulation in marine black shales through variations in geochemical compositions, including siliciclastic and carbonate dilution, bioproductivity, and redox conditions (Chapter 2). These controls can also affect inorganic rock compositions in shales through (1) siliciclastic detrital input, (2) carbonate detrital input, (3) biogenic input, (4) other chemical sediments, and (5) diagenetic products (e.g., Algeo et al., 2011; Boulesteix et al., 2019; Ghadeer and Macquaker, 2011; Macquaker et al., 2010; Schieber, 2000; Yawar and Schieber, 2017).

The composition of detrital sediment, whether clastic or carbonate, is predominantly determined by parent sources (Day-Stirrat et al., 2010; Dong et al., 2017; Schieber, 2016). Biogenic input is directly related to primary productivity, for example, forming biogenic silica, carbonate bioclasts, and organic matter, which may be preserved in sediments (e.g., Zhou et al., 2015; Obermajer et al., 1999; Schieber et al., 2000; Schoepfer et al., 2015). Chemical sediments also include syndepositional framboidal pyrite, whose formation is related to seawater euxinia (Algeo et al., 2010; Rimmer et al., 2018). Framboids, when formed at the redox interface separating oxic and euxinic waters, have relatively uniform small sizes ($\sim 5 \mu\text{m}$, e.g., Wilkin and Barnes, 1997; Wignall and Newton, 1998). Finally, some chemical components are highly mobile during early diagenesis and consequently influence rock compositions through mineral

precipitation and dissolution, for example, diagenetic pyrite and carbonate precipitation in the zone of anaerobic methane oxidation, and barite dissolution under anoxic, sulfate-depleted conditions within sediments (e.g., Algeo et al., 2007; Lash and Blood, 2004; Taylor and Macquaker, 2000; Tribovillard et al., 2006).

Temporal variation in bioproductivity, redox conditions, and terrestrial/carbonate input during the deposition of shales has been inferred in many formations based on geochemical proxies (e.g., Algeo et al., 2013; Berner and Raiswell, 1983; Betts and Holland, 1991; Dahl et al., 2019; Meyers, 1994; Percival et al., 2019; Tyson, 2001). However, geochemical compositions cannot always constrain paleoenvironmental interpretations. For example, substantial recycled shale lithics in the sediments can keep information of parent mudstones and may overprint the geochemical signals at deposition (Schieber et al., 2016), and sulfate and barium remobilized by barite dissolution may obscure a record of original biogenic input (Lash and Blood, 2014), we argue that geochemical features need petrographic validation to identify whether these features are predominantly represented original depositional processes. Few studies, however, have applied petrography to complement the geochemical interpretations (e.g., Harazim et al., 2015; Lash and Blood, 2014; Raven et al., 2018; Sperling et al., 2018). One of the obstacles to petrographic analysis for geochemical results comes from conventional geochemical analytical methods that, based on powder and solution (e.g. ICP-MS), typically at a meter-scale resolution cannot capture millimeter- to centimeter-scale variability evident in petrographic sample. Therefore, we apply new techniques of hyperspectral imagery scan and energy dispersive X-ray fluorescence line scan that are both non-destructive to samples and can provide millimeter-scale geochemical data (Appendix B), and have built millimeter-resolution geochemical profiles for the core slabs from the Middle-Upper Devonian Horn River Group, the northwestern Western

Canada Sedimentary Basin (Chapter 2). We report here a study that applies optical and scanning electron microscope (SEM) analysis to the selected slabs with microgeochemical analysis (Chapter 2) in order to correlate petrographic data to geochemical data to complement interpretations on the paleoenvironment.

3.2 GEOLOGICAL BACKGROUNDS

3.2.1 Geological Setting

The Horn River Basin occupies approximately 12,000 km² in the northwestern part of the Western Canada Sedimentary Basin (Fig. 3.1). The basin is bounded on the east and south by carbonate reefs and on the west by the Bovie Fault zone which is a post-depositional structure that separates the basin from the Liard Basin (Ross and Bustin, 2008). The carbonate platforms located south and east of the basin is considered as the primary source of carbonate minerals influx (Ayranci et al., 2018a). Siliciclastic mud and silt were sourced from a delta system located at the southeastern corner of the Horn River Basin, transported through suspension settling, hyperpycnal flows, and bottom currents, deposited below storm wave base through (Ayranci et al., 2018a). Organic matter is predominantly from marine primary producers (Type II; Chapter 2) (Feinstein et al., 1991; Stasiuk and Fowler, 2004). Vitrinite reflectance (R_o) in the Horn River shale ranges from 1.6% to 2.5% (within dry gas window; Ross and Bustin, 2009).

The Horn River Group is subdivided into the Evie Member and Otter Park Member of the Horn River Formation, and overlying Muskwa Formation (Morrow, 2018; Mossop and Shetesn, 1994), and ranges in age from the Givetian Stage to the early Frasnian Stage (Oldale and Munday, 1994) (Fig. 3.2). The Evie Member unconformably overlies shallow marine carbonates of the lower Keg River Formation and is a dark grey to black, organic-rich, calcareous mudstone (Fig. 3.3), with a total organic carbon (TOC) content that is the highest of the entire Horn River

Group (Fig. 3.3). The Otter Park Member consists of grey to dark grey (Dong et al., 2018), organic-lean, calcareous, and argillaceous mudstone (Fig. 3.3). It contains typically the lowest TOC content of the Horn River shale (Fig. 3.3). The Muskwa Formation overlies the Horn River Formation and is composed of dark grey to black (Dong et al., 2017), organic-rich, and siliceous mudstone (Fig. 3.3) and is in turn overlain by the Fort Simpson Formation. TOC content in the Muskwa Formation is higher than in the Otter Park Member but lower than in the Evie Member.

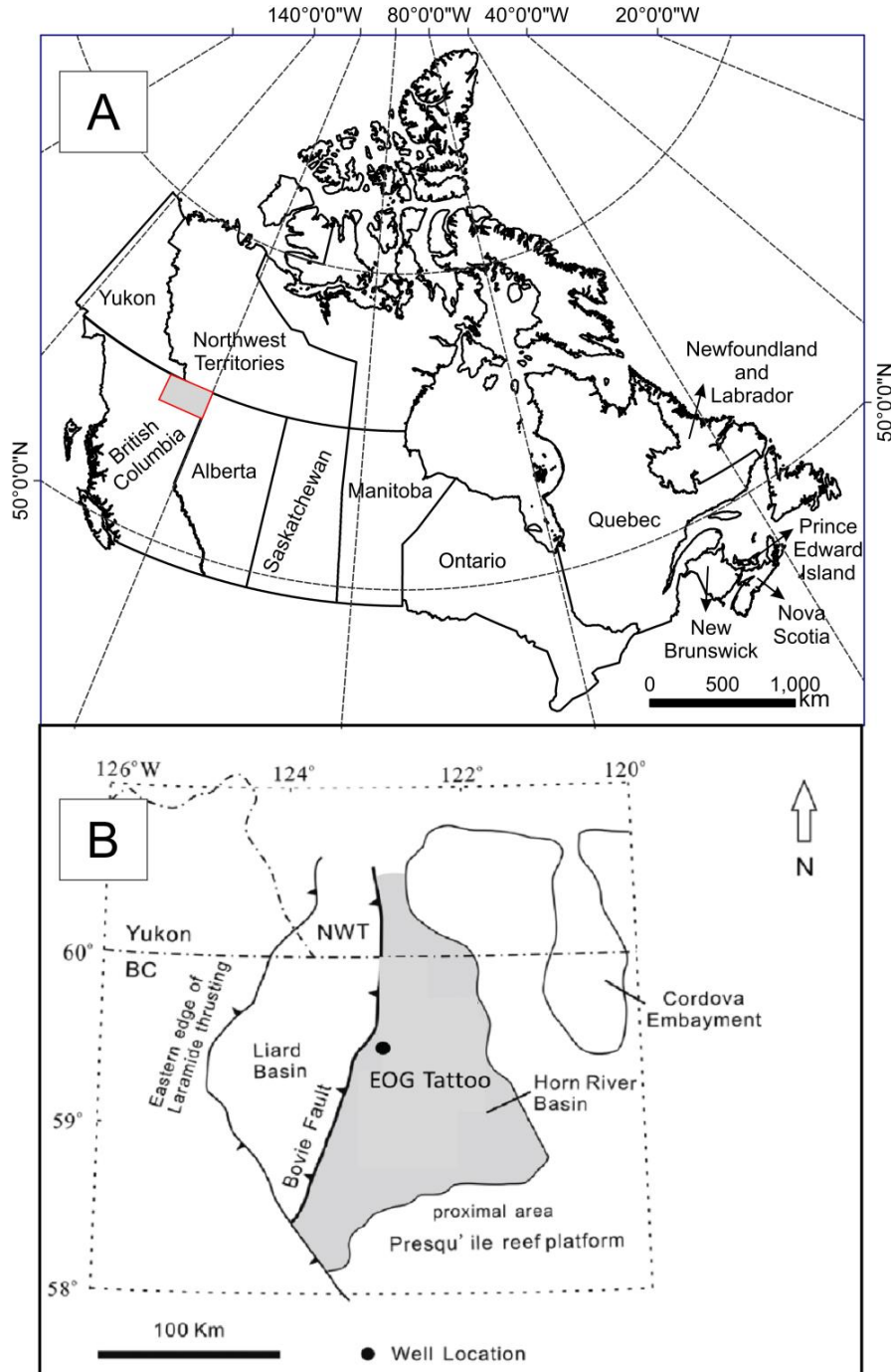


Figure 3.1. Geological maps of the study area. A: Canada map with the Horn River Basin location, highlighted as grey area. B: Geological map of the Horn River Basin and the location of the well in this work (Moghadam et al., 2019). BC – British Columbia; NWT – the Northwest Territories.

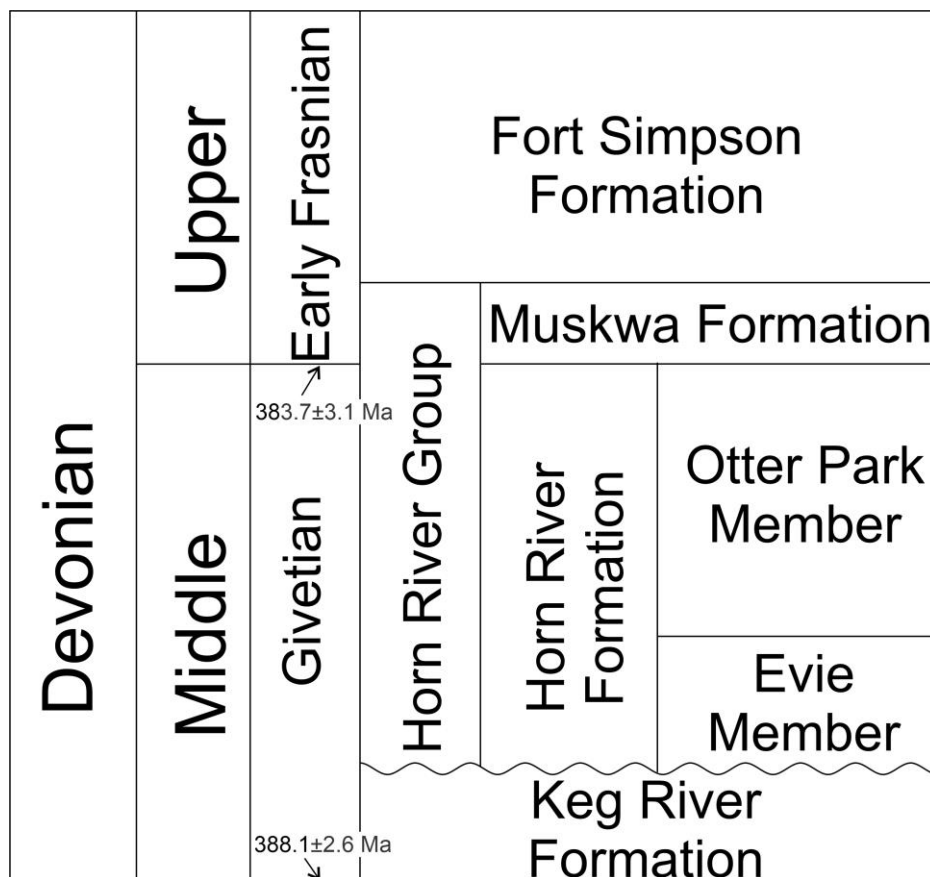


Figure 3.2. Stratigraphy of the Horn River Group in the Horn River Basin (modified after Morrow, 2012; Dong et al., 2018). Wavy line between the Keg River Formation and Horn River Group represents an unconformable contact. Ages of strata follow the U-Pb ID-TIMS age and conodont zones by Kaufmann (2006).

The Horn River shale is interpreted to have been deposited during three third-order sea-level cycles, superimposed on a partial second-order order sea-level cycle (Ayranci et al., 2018b). The Evie Member consists of a third-order transgressive systems tract and overlying highstand systems tract (TST1 and HST1, Fig. 3.3); the Otter Park Member, superimposed on second-order lowstand, includes a full third-order depositional cycle (LST2, TST2, HST2, and

FSST) and an overlying lowstand systems tract (LST3); the Muskwa Formation is composed of a third-order transgressive systems tract and highstand systems tract (TST3 and HST3).

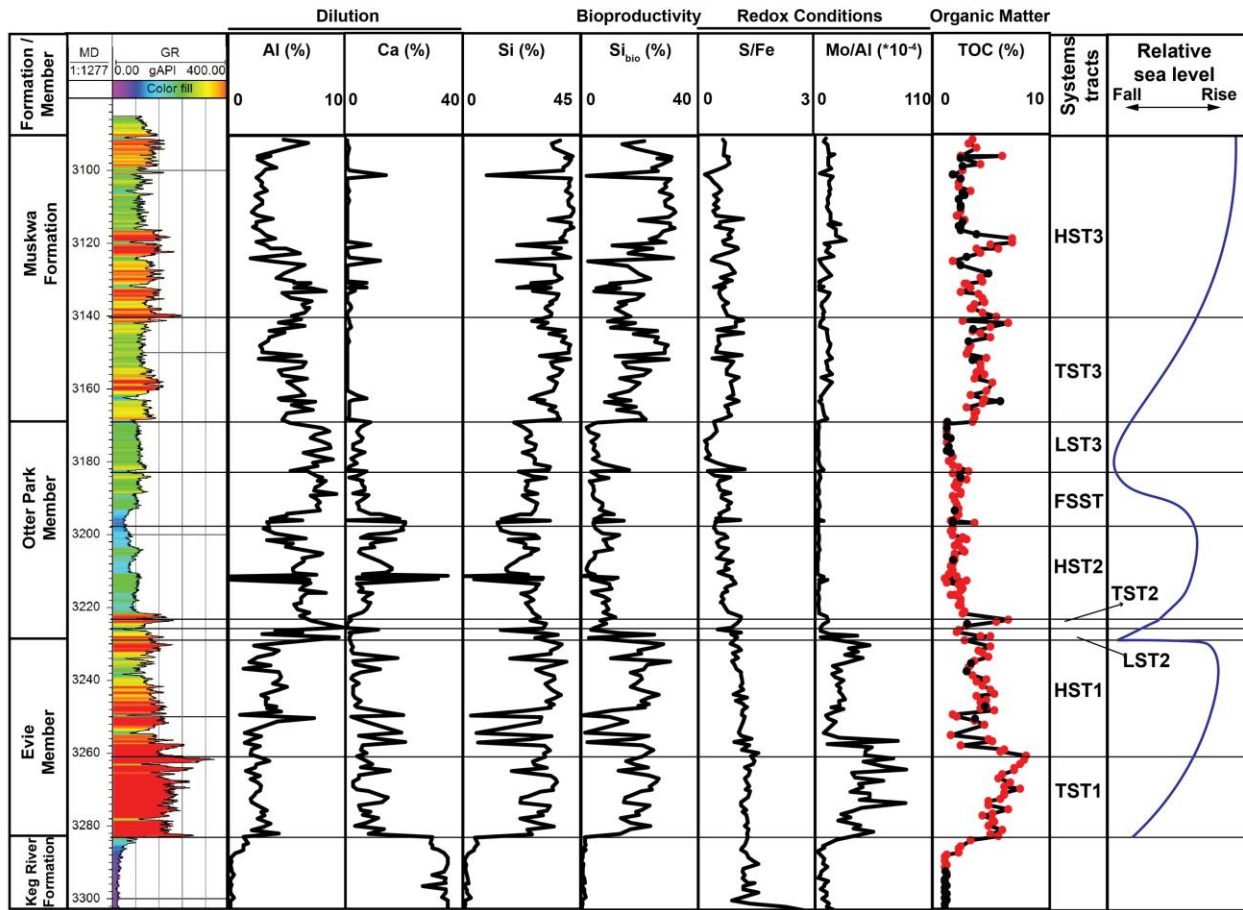


Figure 3.3. Gamma-ray log, whole-rock geochemical profiles, and 3rd sequence stratigraphy of the long-drill core of this study. The red spots in the TOC profile represent the core slabs processed by high-resolution geochemical analysis. Si_{bio} – biogenic silica.

3.3 METHODOLOGY

3.3.1 Meter-Scale Whole-Rock Geochemical Analysis

A total of 212 core slabs were collected for whole-rock geochemical analysis from the vertical long-drill core EOG HZ TATTOO D-A028-F/094-O-10 from the distal part of the Horn River Basin (Fig. 3.1). The core was sampled at intervals of ~ 1 m. Each core slab represents ~

10 cm of stratigraphic section. The analytical methods were following the work by Dong et al. (2015 and 2018). Two splits were cut vertically from the side of each hand sample for TOC content and whole-rock geochemical data, respectively. Samples for the analysis of TOC content was through LECO combustion at GeoMark Research Laboratories, Houston. TOC measurements represent present-day TOC concentration given the loss of organic carbon during thermal maturation. Samples for whole-rock inorganic data were pulverized, combined with lithium borate and digested by nitric acid digestion, and then were analyzed by Inductively Coupled Plasma Mass Spectrometry (ICP-MS) at Bureau Veritas Commodities Laboratories, Canada.

3.3.2 Millimeter-Scale Geochemical Analysis

A total of 133 core slabs after meter-scale organic and inorganic geochemical analysis were selected for millimeter-scale analysis. These core slabs were scanned by benchtop Orbis PC Micro-EDXRF (energy dispersive X-ray fluorescence) Elemental Analyzer in a direction perpendicular to lamination under vacuum at the nanoFAB of the University of Alberta to obtain inorganic geochemical data with 1 – 2 mm vertical resolution. TOC and SiO₂ data were measured by hyperspectral imagery analysis (infrared scan) under 970 – 2510 nm and 7400 – 12100 nm spectral range, respectively, using SisuROCK system with ~ 0.8 – 1.5 mm vertical resolution at the University of Alberta Spectral Imaging Facility. Silica data by both methods were used to register these two high-resolution datasets. TOC data were calibrated to the shale model of hyperspectral imaging developed for the same formation (Rivard et al., 2018). Averages of values from EDXRF scans were calibrated by bulk elemental compositions by ICP-MS analysis.

3.3.3 Geochemical Proxies

We apply major and some minor elements as paleoenvironmental proxies. Al and Ca concentrations are used to represent terrestrial and carbonate input, respectively (Tribovillard et al., 2006; Ross and Bustin, 2009). We apply S/Fe ratios to indicate redox conditions, which has been validated as redox proxy by comparison to Mo/Al ratios by Dong et al. (2018) and Harris et al., (2018) in the Horn River Group and nearby coeval Duvernay Formation. When the ratio is more than 0.72, it is considered to indicate anoxic conditions; when less than 0.4, it indicates oxic conditions (Ocupalidet et al., 2018; Rimmer et al., 2004). We apply TOC to represent organic matter accumulation (Chapter 2) and biogenic Si (Si_{bio}), represented by excess Si, to indicate primary productivity (Schieber et al., 2000). Excess Si (biogenic Si) is calculated after Ross and Bustin (2009):

$$Si_{excess} = Si_{sample} - [Al_{sample} \times (Si/Al)_{background}]. \quad (1)$$

The background Si/Al ratio is 3.1 (Wedepohl, 1971), consistent with Dong et al.'s (2018) study of the Horn River Group.

3.3.4 Petrographic Analysis

In this study, 15 samples from a set of 133 core slabs that had been studied under high-resolution geochemical analysis from the same TATTOO core (Chapter 2) were selected for petrographic analysis as well characterized examples of different controls on organic matter accumulation (Chapter 2). Thin sections were 20 μm thick and were examined with Axio Zeiss Scope.A1 optical microscope in the SURGe research laboratory at the University of Alberta. Four of these samples were mechanically polished to expose a surface of approximately 0.5 – 1 cm^2 at the university of Alberta and were ion-milled for 2 – 3 hours at 5 kV accelerating voltage on each sample with a Fischione Model 1060 SEM Mill using argon gas in the SURGe research

laboratory, University of Alberta. These four ion-milled samples were applied for scanning electron microscopy (SEM) and energy dispersive x-ray spectroscopy (EDS) analysis with a Zeiss EVO M10 SEM, using an accelerating voltage of 20 kV at the nanoFAB at the University of Alberta, and with a Zeiss Sigma 300 VP-FESEM, using an accelerating voltage of 10 kV at the EAS-SEM facility at the University of Alberta. Five of these 15 samples that were analyzed under optical microscopy were selected for organic petrographic analysis (one from the Evie Member, two from the Otter Park Member, and two from the Muskwa Formation) at U.S. Geological Survey, Virginia. These samples were examined under reflected white light (200× and 500×; whole-rock particulate pellets; oil immersion) by SEM with a Smith illuminator.

3.4 RESULTS

We report here on five mudstone types based on the petrographic compositions under optical and scanning electron microscopic analysis, following the inclusive nomenclature for mudstones by Macquaker and Adams (2003). They are (1) laminated clay-, silt- and microcrystalline silica-bearing mudstone, (2) laminated sand-bearing, clay-rich mudstone, (3) laminated calcite silt-bearing, clay-rich mudstone, (4) calcareous mesoplankton- and dolomite cement-bearing, clay-rich mudstone, and (5) laminated pyrite-bearing, clay-rich mudstone.

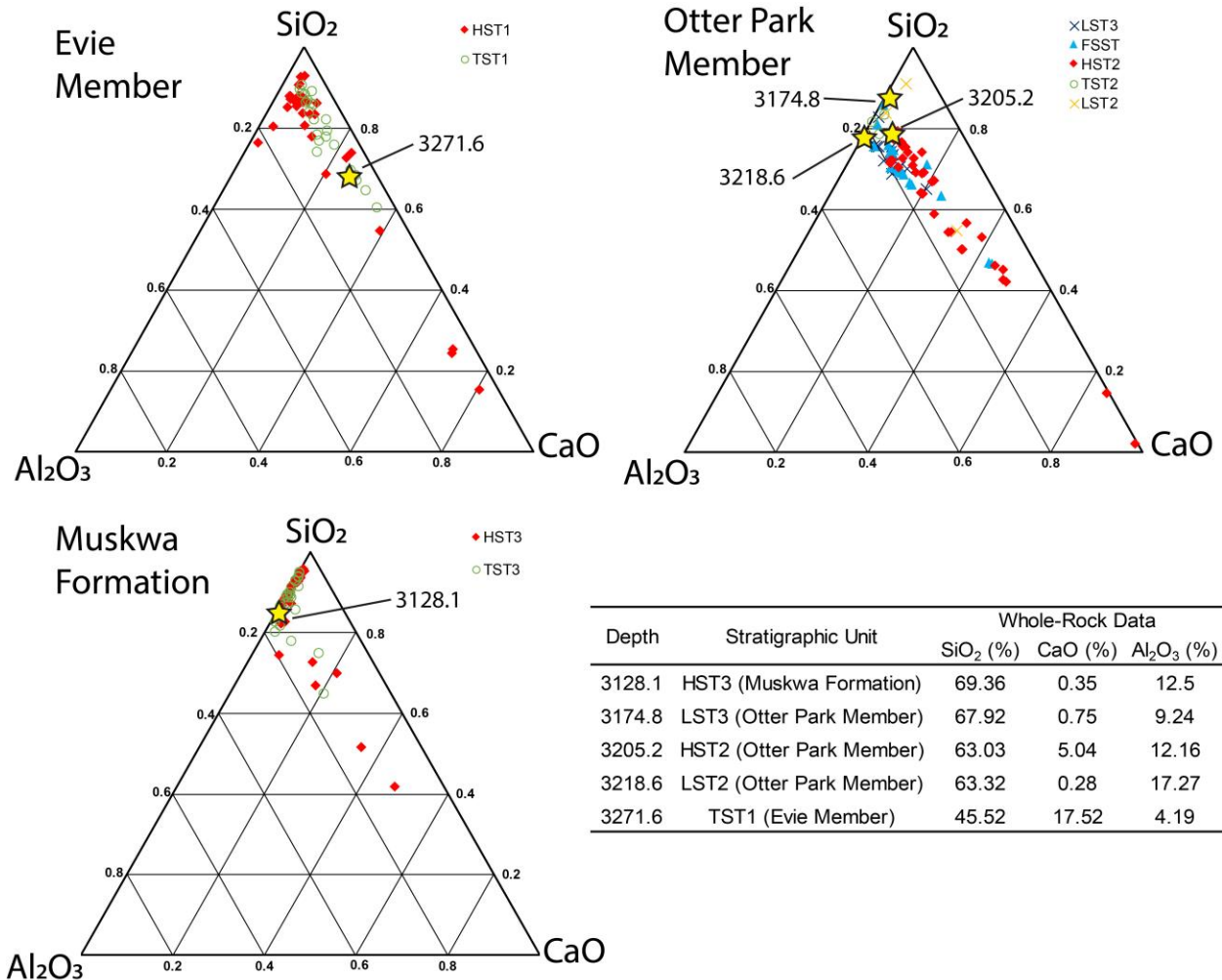


Figure 3.4. Ternary diagram of the shale major oxides, SiO₂, Al₂O₃, and CaO, which represent quartz, clays (and feldspars), and carbonate minerals. Samples from TSTs are represented by hollow circles, from HSTs are represented by diamonds, from LSTs are represented by crosses, and from FSST are represented by triangles. Asterisks represent the representative samples in this study.

In Figure 3.4, we plot whole-rock data for the core slabs that have been classified into third-order sequence stratigraphic units onto a ternary diagram for major components (SiO₂, Al₂O₃, and CaO), which represent quartz, clay (and feldspar), and carbonate, based on ICP-MS

whole-rock data (Appendix C). In the Evie Member (HST1 and TST1), Al_2O_3 concentrations are generally low (less than 5 %), and SiO_2 contents are relatively enriched (generally more than 60%). CaO concentration is quite variable, generally ranging from 0 to 40%. In the Otter Park Member (LST2, TST2, HST2, FSST, and LST3), Al_2O_3 and CaO are enriched in most samples, typically ranging from 10% to 20% and from 5% to 50%, respectively, and SiO_2 is less abundant than in other formations. The Muskwa Formation (TST3 and HST3) has the highest values in the SiO_2 content (more than 80%), low Al_2O_3 (5% – 20%), and negligible %CaO.

3.4.1 Laminated Clay-, Silt- and Microcrystalline Silica-Bearing Mudstone

Samples exhibiting a bioproductivity control on organic matter enrichment come primarily from the Evie Member and Muskwa Formation (Chapter 4). Typical geochemical compositions are characterized by enriched total Si and biogenic Si (Si_{bio}) contents (Si_{bio} max. 35%), enriched total organic carbon (TOC) content (max. 8.8%), and low Al contents (less than 4%) (Figs. 3.3, 3.4). A representative sample demonstrating this type of control from 3128 m (Fig. 3.5) in geochemistry shows increasing Si_{bio} and TOC contents upward before 3128.06 m with decreasing Al content; the ratio between Si_{bio} and TOC is relatively stable in the entire slab, 11 – 12. This sample is composed mainly of clay-sized materials, organized into millimeter-thick laminae (Fig. 3.5). Silt-sized detritus is scattered through the sample, composed of fine-grained quartz grains and deformed clay-aggregates (Figs. 3.6A-B), which are embedded by fine-grained quartz grains (Fig. 3.6B). A small fraction of bioclasts is preserved, including phosphorous fossils and agglutinated foraminifera (Fig. 3.6A). Pyrite in this sample is generally present as framboids (Figs. 3.6C-D), with diameters generally $\sim 5 - 6 \mu\text{m}$, consistent with the description of framboids in Ayranci et al. (2018a). This mudstone exhibits a matrix composed mainly of

microcrystalline silica (Figs. 3.6E-F), with speckled to wispy distributed organic matter and subordinate feldspar and mica (Fig. 3.6E).

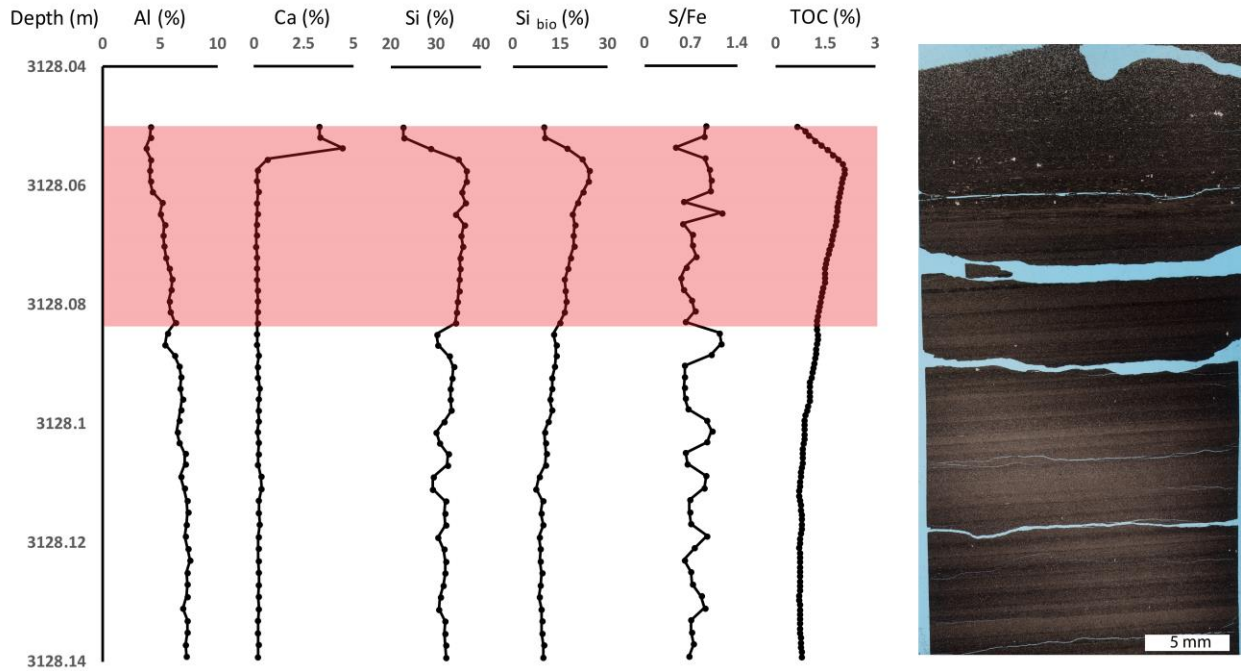


Figure 3.5. Millimeter-resolution geochemical profiles and thin section scan of the representative sample from HST3 of laminated clay-, silt- and microcrystalline silica-bearing mudstone. Red colored interval in profiles is the sample analyzed under optical microscopy.

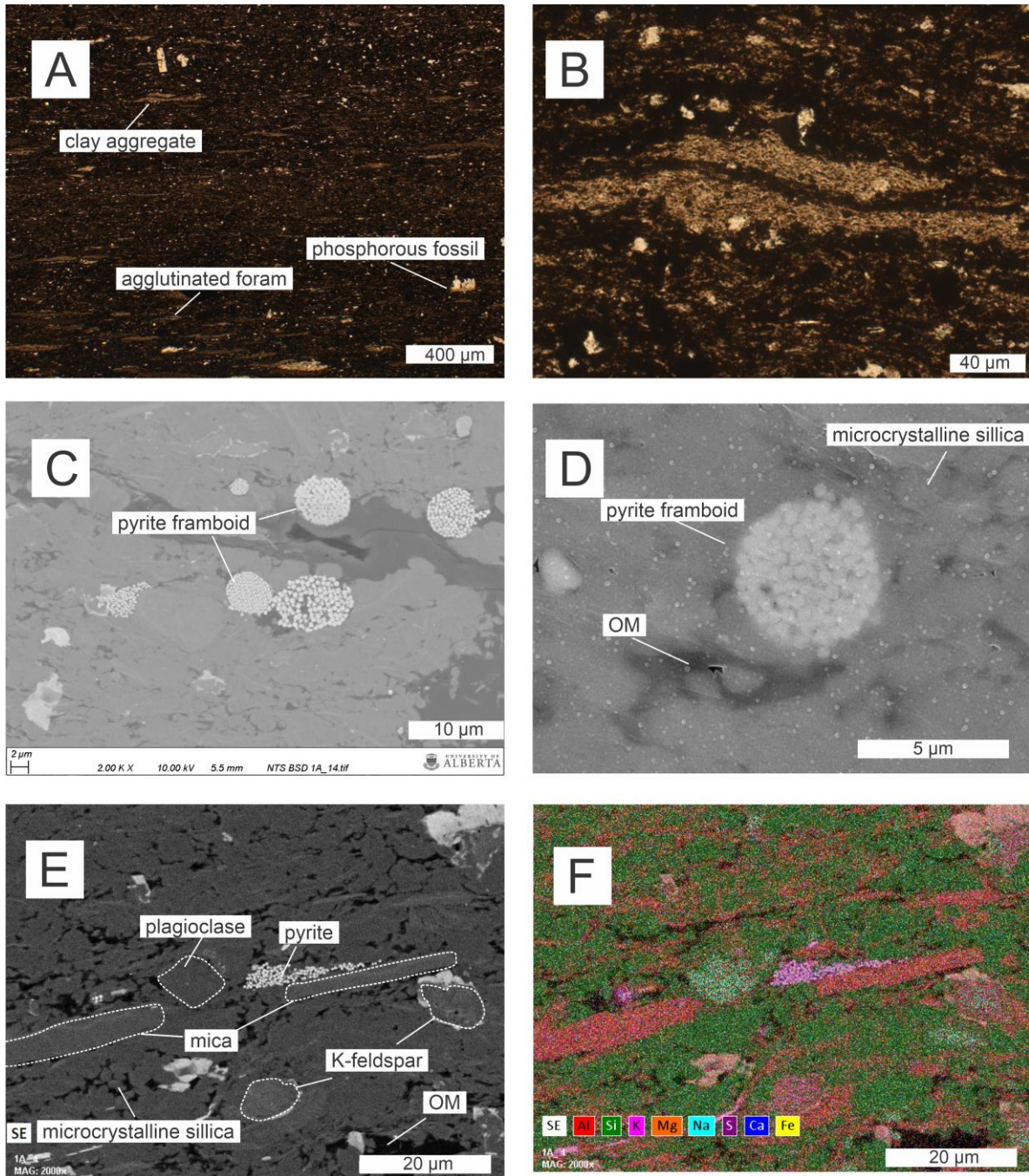


Figure 3.6. Laminated clay-, silt- and microcrystalline silica-bearing mudstone from the Muskwa Formation. (A) Optical micrograph of clay aggregates and agglutinate foraminifera. (B) Representative micrograph of deformed clay aggregate. (C) and (D) Backscattered and In-Lens micrographs of pyrite framboids. (E) and (F) Backscattered and EDS electron micrographs. Microcrystalline silica is rich in this sample.

3.4.2 Laminated Sand-Bearing, Clay-Rich Mudstone

Although samples exhibiting a terrestrial dilution control on organic accumulation are present throughout the Horn River shale section in the TATTOO core (Chapter 4), samples from the Otter Park Member are notably enriched in %Al, with relatively low biogenic Si and TOC concentrations (Fig. 3.4). A representative sample from 3183 m (LST2) show high Al and Si concentrations (~ 8% and 30%, respectively) with low Si_{bio} and TOC contents (~ 5% and 0.5%, respectively, Fig. 3.7). A large fraction of detritus in this mudstone is composed of sand-sized deformed clay aggregates, varying in size from 100 µm to 600 µm, with subordinate pyrite (Fig. 3.8A). The majority of pyrite occurs as framboids, diameters of which range from 3 µm to 8 µm, with a little fraction of euhedral and cemented pyrite (Figs. 3.8B-C). Thin laminae (thickness of 0.4 – 10 mm) are distinguished by varied contents of clay aggregates with sharp changes at contacts (Fig. 3.8A). Pyrite is also variably distributed in relatively rich and lean laminae (Figs. 3.8C-D). This mudstone comprises an argillaceous framework (Fig. 3.8D).

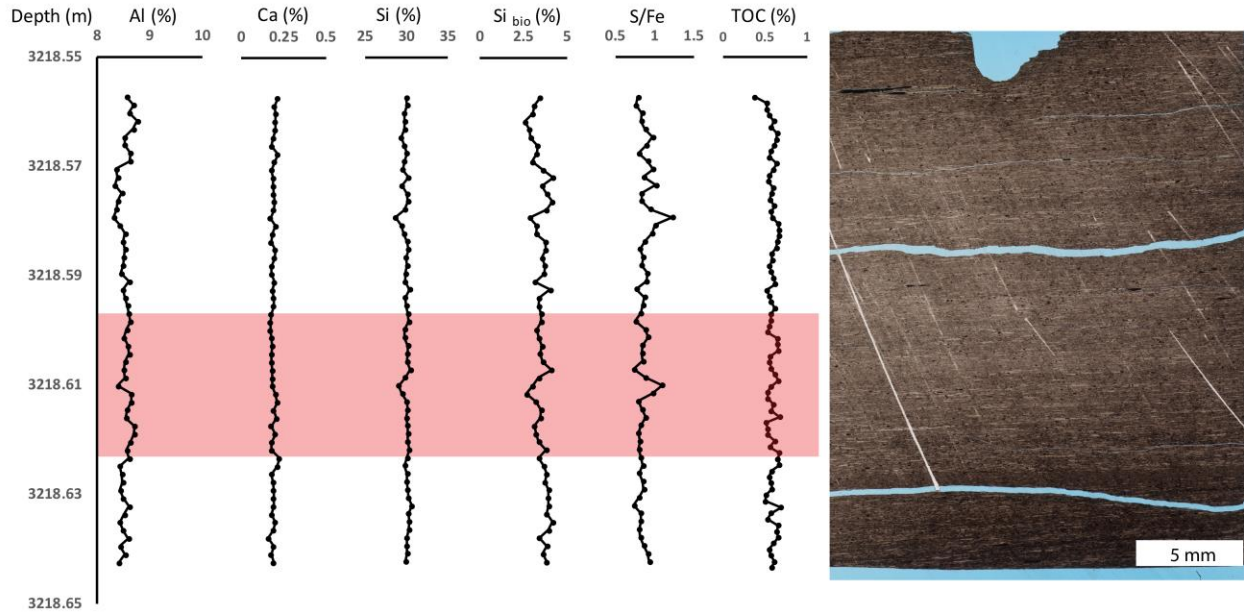


Figure 3.7. Millimeter-resolution geochemical profiles and thin section scan of the representative sample from LST2 of laminated sand-bearing, clay-rich mudstone. Red colored interval in profiles is the sample analyzed under optical microscopy.

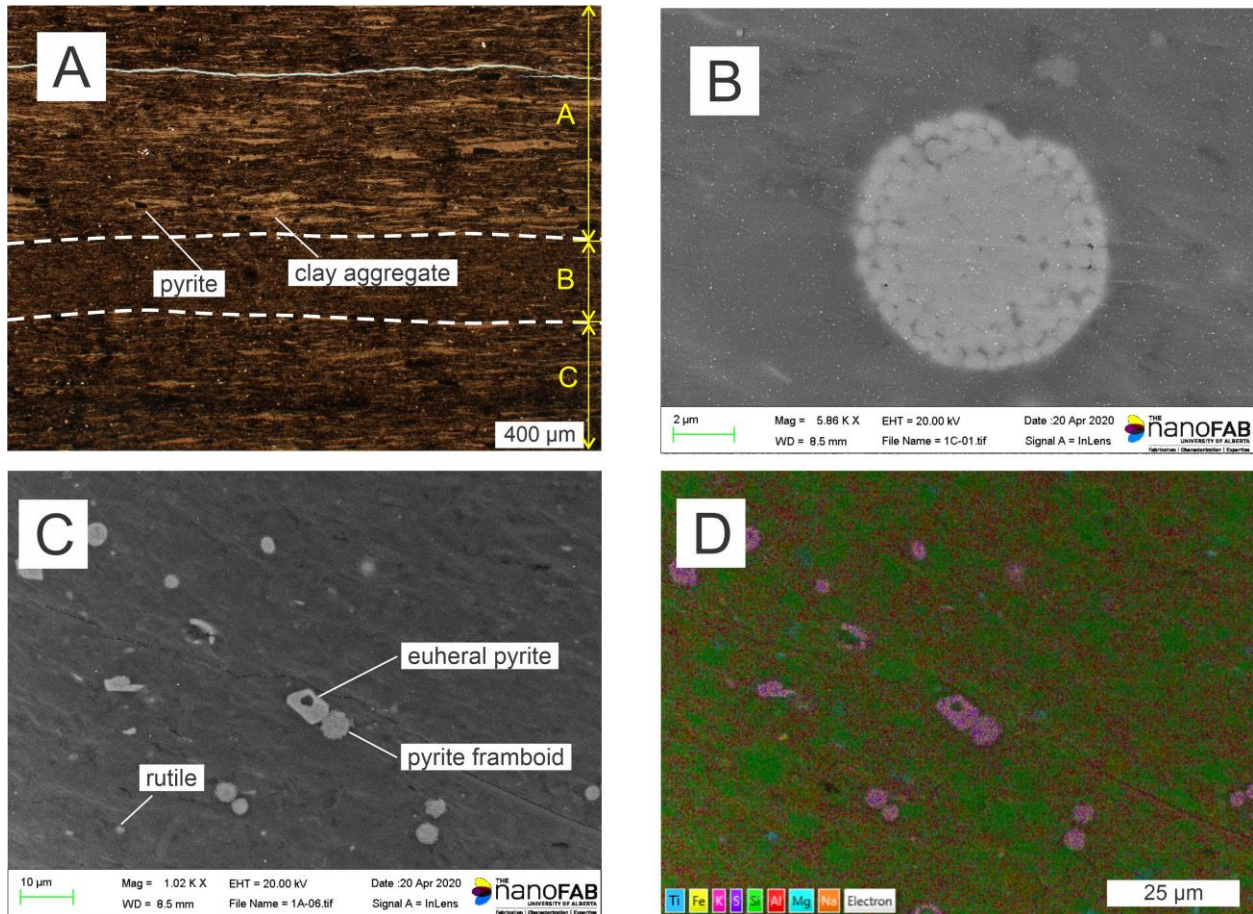


Figure 3.8. Laminated sand-bearing, clay-rich mudstone in the Otter Park Member. (A) Optical micrograph of laminae (labeled A-C) distinguished by varying clay aggregates. (B) In-Lens SEM micrograph of center-cement pyrite framboid. (C) and (D) In-Lens and EDS electron micrographs of framboid and euhedral pyrite. EDS electron micrograph shows an argillaceous framework.

3.4.3 Carbonate Silt-Bearing Mudstone and Carbonate Mesoplankton-Bearing Mudstone

HST2 of the Otter Park Member and TST1 of the Evie Member contain carbonate-bearing mudstones (Figs. 3.3, 3.4), in which Ca concentration can reach approximately 10% – 20%. A representative sample from 3205 m in HST2 exhibiting an important carbonate signal is characterized by varying calcium content with an inverse trend in Al, Si, and Si_{bio} profiles (Fig.

3.9), which is interpreted as carbonate dilution effect (Chapter 2). The varying %Ca and %Al in geochemical profiles coincide with calcareous and argillaceous units in petrography in Fig. 3.9. This mudstone contains abundant calcite detritus (Figs. 3.10A-B) with sparse recognizable bioclasts (Fig. 3.10B). It is organized into alternating calcareous and argillaceous laminae, typically 2 – 5 mm thick, with clear planar or minor deformed contacts (Figs. 3.9, 3.10A). Calcareous laminae show normally graded structures (Fig. 3.10A) with silt lags at the bases (dominant calcite and secondary quartz; Fig. 3.10B).

Another representative Ca-rich sample is from 3271 m in TST1 (Fig. 3.11). Similarly, it exhibits a relatively high Ca concentration, ~ 20% in the highlighted interval (Fig. 3.11). However, the petrography of this mudstone is different from laminated calcite silt-bearing, clay-rich mudstone in HST2. The high Ca concentrations in the lower part of the highlighted profile, 3271.63 m – 3271.64 m (Fig. 3.11), are related to the more enriched carbonate bioclasts at the lower section of the thin section (Fig. 3.11). This calcareous mesoplankton- and dolomite cement-bearing, clay-rich mudstone consists of abundant carbonate bioclasts (Fig. 3.10C), including *Tentaculites* and *Styliolina* (Fig. 10D). Most fossils are collapsed, with dolomite cements developed on the inner walls of the bioclasts (Fig. 3.10D). Dolomite cements are also present in the matrix as small masses (Figs. 3.10C-D).

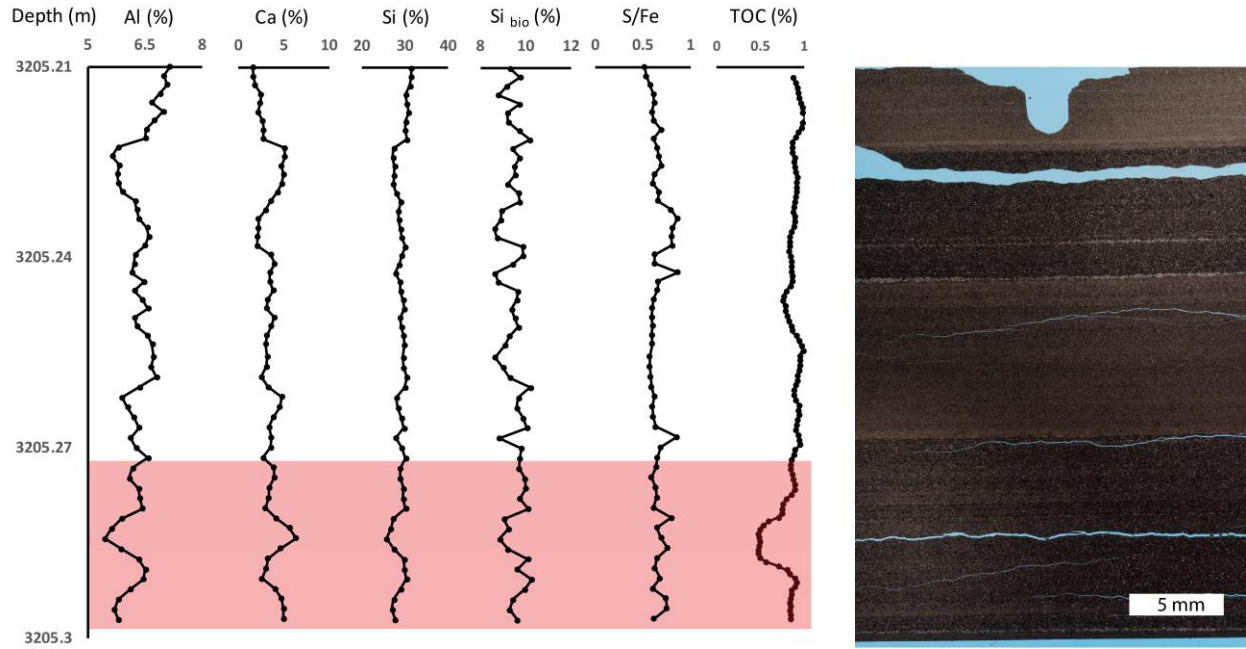


Figure 3.9. Millimeter-resolution geochemical profiles and thin section scan of the representative sample from HST2 of laminated calcite silt-bearing, clay-rich mudstone. Red colored interval in profiles is the sample analyzed under optical microscopy.

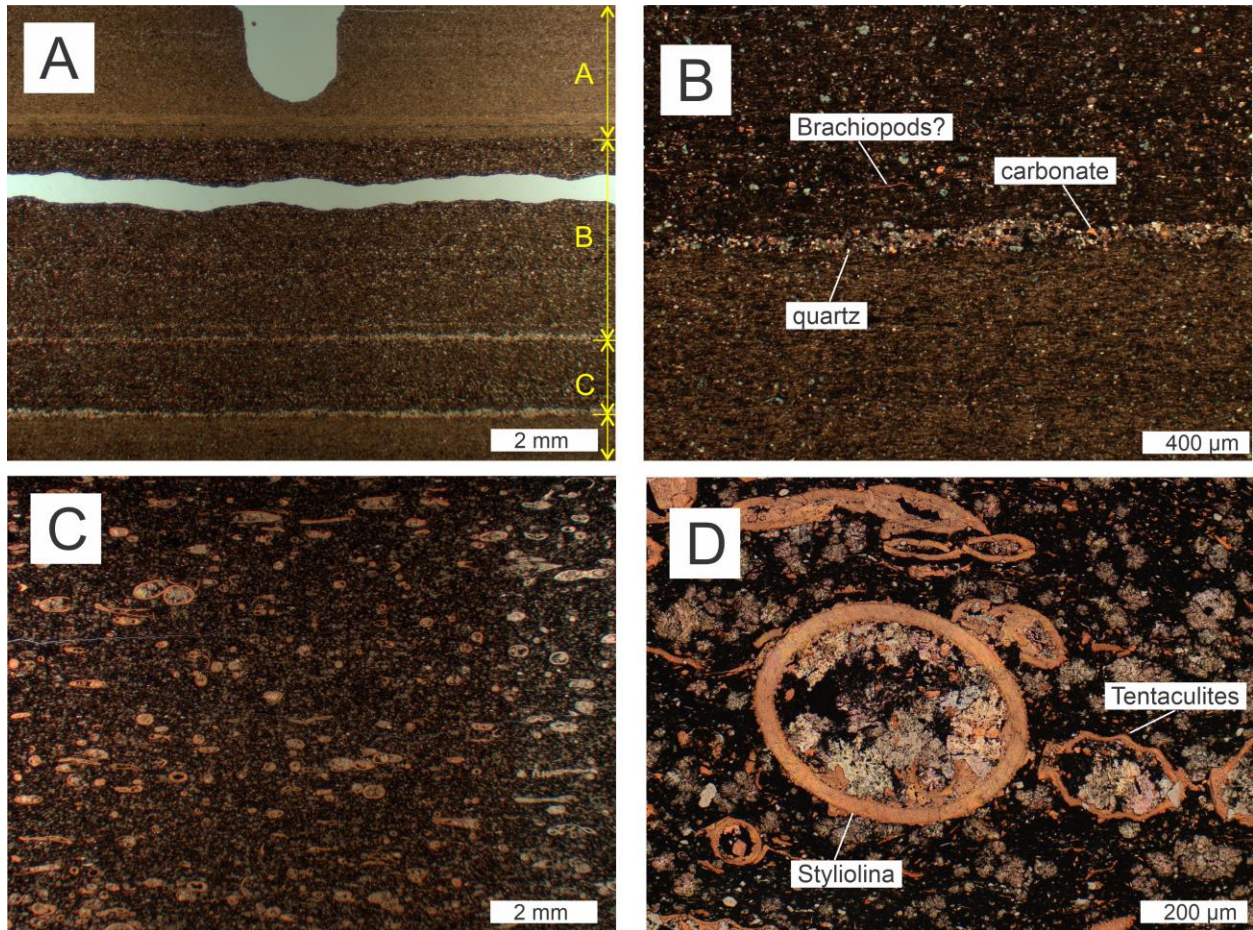


Figure 3.10. Calcareous mudstones in the Otter Park Member and lower Muskwa Formation.

(A) and (B) Representative optical micrographs of laminated calcite silt-bearing, clay-rich mudstone in the HST2 of the Muskwa Formation. (C) and (D) Representative optical micrograph of calcareous mesoplankton- and dolomite cement-bearing, clay-rich mudstone in the TST1 of the Evie Member. Calcareous fossils are mainly *Tentaculites* and *Styliolina*.

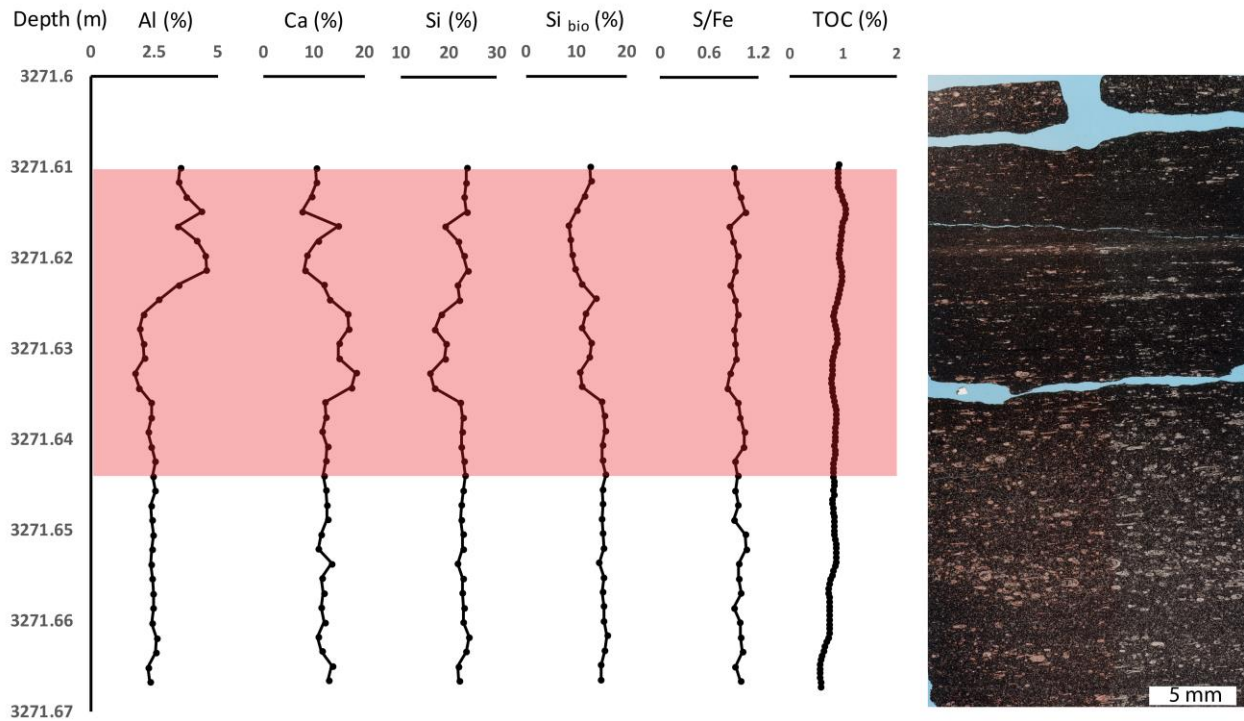


Figure 3.11. Millimeter-resolution geochemical profiles and thin section scan of the representative sample from TST1 of calcareous mesoplankton- and dolomite cement-bearing, clay-rich mudstone. Red colored interval in profiles is the sample analyzed under optical microscopy.

3.4.4 Diagenetic Mineral-Bearing Mudstone

A small number of samples (less than 15 in our dataset of 133 samples) show anomalous geochemical features that cannot be interpreted by models that invoke paleoenvironmental perturbations (redox conditions, bioproductivity or sedimentary input). In these samples, we identify abundant diagenetic pyrite or carbonate minerals (Figs. 3.12, 3.13).

A laminated pyrite-bearing, clay-rich mudstone from the Otter Park Member exhibits high S/Fe ratios, ~ 1.1 (Fig. 3.12). S/Fe ratios first increase upward and then decrease, with an inverse trend in Al, Ca, Si, and TOC concentrations in geochemical profiles (Fig. 3.12). The

micrograph of highlighted interval in Fig. 3.12 shows a related distribution of pyrite to the S/Fe ratio profile; pyrite is highly enriched at the middle section with less abundance upward and downward. Pyritic laminae in this mudstone are less than 1 mm thick (Figs. 3.13A). Most pyrite is authigenic diagenetic pyrite, sizes of which varies in a range from 3 μm to 200 μm . The morphology of pyrite is euhedral, subhedral, and round or elliptical; many pyrite occurrences are replacements of bioclasts, for example, radiolarian (Fig. 3.13B) and brachiopod (Fig. 3.13C). A little fraction of deformed clay aggregates and ferroan dolomite grains is also present (Figs. 3.13A, D).

The presence of diagenetic carbonate minerals is observed in the laminated clay-, silt- and microcrystalline silica-bearing mudstone from 3128 m in the Muskwa Formation (Fig. 3.5). Near the top of this mudstone, the geochemical profiles exhibit a sharply increased Ca concentration with a sharp decrease in TOC, Si, and Si_{bio} contents (Fig. 3.5), which is interpreted as carbonate dilution effect (Chapter 2). In micrographs of this interval, ferroan dolomite that was stained as turquoise, occurs as replacement of quartz silt in this section (Figs. 3.13E-F).

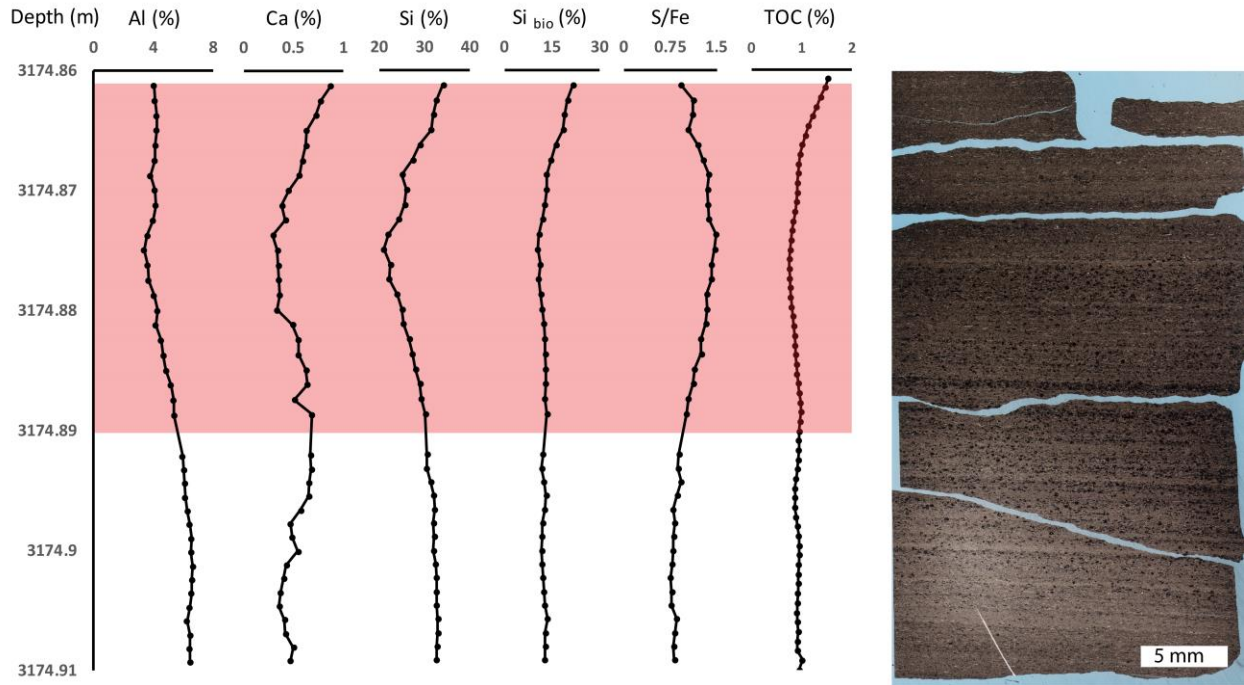


Figure 3.12. Millimeter-resolution geochemical profiles and thin section scan of the representative sample from FSST of laminated pyrite-bearing, clay-rich mudstone. Red colored interval in profiles is the sample analyzed under optical microscopy.

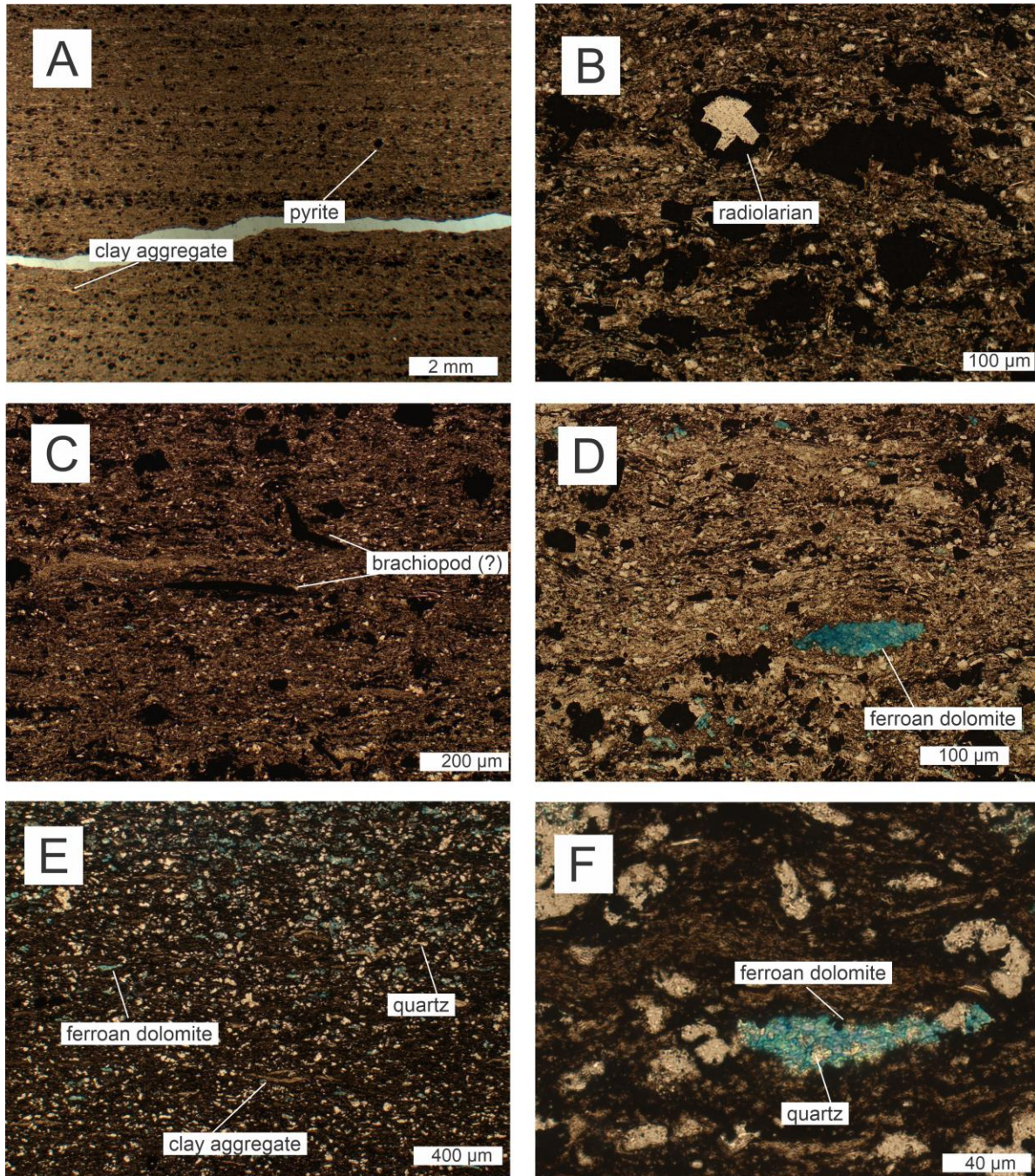


Figure 3.13. Mudstones with large amounts of diagenetic minerals. (A) Micrograph of mudstone with enriched diagenetic pyrite in the Otter Park Member. (B) and (C) Micrographs of pyrite replacements of bioclasts, including radiolarian and possible brachiopod. (D) Representative micrograph of ferroan dolomite grain. (E) and (F) Representative micrographs of ferroan dolomite replacement in the sample of Fig. 3.5 from the Muskwa Formation.

3.5 DISCUSSION

Our results document comparisons between small scale geochemical variability of a marine shale and petrographic features in the same samples. The petrographic data identify different mineral compositions in the samples that have similar SiO₂, Al₂O₃, and CaO concentrations (Fig. 3.4), and distinguish the contributions by sedimentological and diagenetic processes that cannot be indicated by geochemical profiles.

3.5.1 Bioproductivity Control on Petrography

Marine biogenic processes are a primary source of sediment to the seabed, especially in the Evie Member and Muskwa Formation (Ayranci et al., 2018a; Dong et al., 2018). In these samples, we observe a microcrystalline siliceous matrix (Fig. 3.6E), interpreted as reprecipitation of dissolved siliceous bioclasts, e.g., diatoms and radiolarian, in prior studies (Al Rajaibi et al. 2015; Milliken and Olson, 2017). Organic matter (present as kerogen and solid bitumen) in these samples is identified as marine Type II (Chapter 2), indicating that the organic input to the sediments were sourced from primary producers. These petrographic features indicate a relatively high biogenic input in these samples, which support the interpretation of high bioproductivity based on high excess Si (biogenic Si) content in geochemical analysis (Fig. 3.5; Chapter 2).

3.5.2 Physical Sedimentological Controls

Siliciclastic silt and mud in the Horn River shale was primarily sourced from a delta system located in the southeast corner of the basin (Ayranci et al., 2018a); aeolian input may have also contributed terrestrial input. A representative sample from a third-order lowstand systems tract in the Otter Park Member exhibits argillaceous matrix (Fig. 3.8A). Abundant clay

aggregates, interpreted as mud intraclasts, occur as flattened to deformed morphology that were compacted during deposition, different from either shale lithics that resist compaction (Schieber, 2016) or ovoid-shape aggregates of marine snow with diffuse to wispy edges observed in the nearby Duvernay Formation (Knapp et al, 2017). The predominant deformed clay aggregates indicate that the enriched Al content observed from geochemistry was primarily sourced from clay clasts that were produced from erosion of surficial muds (Schieber, 2016).

Detrital carbonate input also influences rock compositions. We observe different expressions of detrital carbonate compositions in the Ca-rich middle Otter Park Member (HST2) and lower Evie Member (TST1). The sample from HST2 exhibit normally graded calcite laminae with calcite silt lags at the bases and sharp contacts with underlying argillaceous laminae (Fig. 3.10A), consistent with carbonate delivered by hyperpycnal flow to the seabed. We suggest that these beds represent highstand shedding from a carbonate platform during the deposition of HST2. The petrographic character of these beds differs from a carbonate sample from TST1, in which the dominant carbonate compositions are carbonate bioclasts (Fig. 3.10C). Both samples exhibit high Ca content in geochemistry (Figs. 3.9, 3.11), yet represent very different types of input and processes.

3.5.3 Diagenetic Controls

Diagenetic effects on rock compositions have been observed in many formations (e.g., Lash and Blood, 2004; Raiswell et al., 2008), partially or totally overprinting depositional signals. In the Horn River shale, we observe isolated analyses extremely high S/Fe ratios (anoxic conditions) in a sample deposited during a sea-level lowstand (Fig. 3.12), and isolated analyses with high Ca content (high carbonate input) in the Muskwa Formation (Fig. 3.5) where Ca

content is generally negligible from formation-scale profile (Fig. 3.3). In both cases, we require petrographic data to distinguish between sedimentological and diagenetic contributions.

In the sample from the FSST (Figs. 3.13A-C) with high S/Fe ratios (Fig. 3.12), we observe abundant diagenetic pyrite occurred with varying morphology and size, including replacement of bioclasts. Diagenetic pyrite does not reflect deepwater redox conditions, in contrast to pyrite framboids precipitated from a euxinic water mass, and its presence can blur or overprint S/Fe ratios, leading to misinterpretation of the paleoredox signal.

Ferroan dolomite represent another type of common diagenetic minerals in the Horn River shale. A representative sample exhibits diagenetic ferroan dolomite in petrographic analysis (Figs. 3.13E-F). The formation of diagenetic carbonate is probably related to underlying TOC-rich interval (Fig. 3.5) by either anerobic methane oxidation zone which enables carbonate precipitation (Lash and Blood, 2004), adipocere breakdown that removes hydrocarbon portion and forms CaCO_3 concretion (Berner, 1968), or temporary increased pH through ammonia reduction that favors CaCO_3 formation (Berner, 1968). In the geochemical profile, we observe a sharply higher Ca content with low TOC and biogenic Si contents near the top of Fig. 3.5. Petrographic analysis is required to discriminate sedimentary and diagenetic contributions to the shale, where addition of carbonate dilutes both organic carbon and biogenic silica.

3.6 CONCLUSION

In this study, we apply petrographic analysis to interpretations of biogenic input, terrestrial detrital input, carbonate detrital input in the Horn River shale based on prior high-resolution geochemical profiles and show that petrography can effectively identify bioclasts and detritus to characterize different types of biogenic and detrital input. Petrographic analysis can

also identify the contribution of diagenesis to rock compositions, which are not effectively identified through geochemical analysis alone.

3.7 ACKNOWLEDGMENTS

We thank Drs. Noga Vaisblat, Nathan Gerein, and Guibin Ma for their assistance with SEM analysis.

3.8 REFERENCES CITED

- Algeo, T.J., Henderson, C.M., Tong, J., Feng, Q., Yin., H., and Tyson, R.V., 2013, Plankton and productivity during the Permian–Triassic boundary crisis: An analysis of organic carbon fluxes: *Global and Planetary Change*, v. 105, p. 52–67, doi:10.1016/j.gloplacha.2012.02.008.
- Algeo, T.J., Kuwahara, K., Sano, H., Bates, S., Lyons, T., Elswick, E., Hinnov, L., Ellwood, B., Moser, J., and Maynard, J.B., 2011, Spatial variation in sediment fluxes, redox conditions, and productivity in the Permian-Triassic Panthalassic Ocean: *Palaeogeography, Palaeoclimatology, Palaeoecology*, v. 308, p. 65–83, doi:10.1016/j.palaeo.2010.07.007.
- Algeo, T.J., and Liu, J., 2020, A re-assessment of elemental proxies for paleoredox analysis: *Chemical Geology*, in press, doi:10.1016/j.chemgeo.2020.119549.
- Algeo, T.J., Lyons, T.W., Blakey, R.C., and Over, D.J., 2007, Hydrographic conditions of the Devonian–Carboniferous North American Seaway inferred from sedimentary Mo–TOC relationships: *Palaeogeography, Palaeoclimatology, Palaeoecology*, v. 256, p. 204–230, doi:10.1016/j.palaeo.2007.02.035.
- Al Rajaibi, I.M., Hollis, C., Macquaker, J.H., 2015, Origin and variability of a terminal Proterozoic primary silica precipitate, Athel Silicilyte, South Oman Salt Basin, Sultanate of Oman: *Sedimentology*, v. 62, p. 793–825, doi:10.1111/sed.12173.

- Ayranci, K., Harris, N.B., and Dong, T., 2018a, Sedimentological and Ichnological Characterization of the Middle to Upper Devonian Horn River Group, British Columbia, Canada: Insights into Mudstone Depositional Conditions and Processes Below Storm Wave Base: *Journal of Sedimentary Research*, v. 88, p. 1–23, doi:10.2110/jsr.2017.76.
- Ayranci, K., Harris, N.B., and Dong, T., 2018b, High resolution sequence stratigraphic reconstruction of mud-dominated systems below storm wave base: A case study from the Middle to Upper Devonian Horn River Group, British Columbia, Canada: *Sedimentary Geology*, v. 373, p. 239–253, doi:10.1016/j.sedgeo.2018.06.009.
- Betts, J.N., and Holland, H.D., 1991, The oxygen content of ocean bottom waters, the burial efficiency of organic carbon, and the regulation of atmospheric oxygen: *Palaeogeography, Palaeoclimatology, Palaeoecology*, v. 97, p. 5–18, doi:10.1016/0031-0182(91)90178-T.
- Berner, R.A., 1968, Calcium carbonate concretions formed by the decomposition of organic matter: *Science*, v. 159, p. 195–197, doi:10.1126/science.159.3811.195.
- Berner, R.A., and Raiswell, R., 1983, Burial of organic carbon and pyrite sulfur in sediments over phanerozoic time: a new theory: *Geochimica et Cosmochimica Acta*, v. 47, p. 855–862, doi:10.1016/0016-7037(83)90151-5.
- Bohacs, K.M., Jr., Grabowski, G.J., Carroll, A.R., Mankiewicz, P.J., Miskell-Gerhardt, K.J., Schwalbach, J.R., Wegner, M.B., and Simo, J.A., 2005, Production, destruction, and dilution—the many paths to source-rock development, *in* Harris, N.B., ed, *The Deposition of Organic-Carbon-Rich Sediments: Models, Mechanisms, and Consequences*: Society for Sedimentary Geology, Tulsa, Oklahoma, Special Publication 82, p. 61–101.

- Boulestex, K., Poyatos-Moré, M., Flint, S.S., Taylor, K.G., Hodgson, D.M., and Hasiotis, S.T., 2019, Transport and deposition of mud in deep-water environments: Processes and stratigraphic implications: *Sedimentology*, v. 66, p. 2894–2925, doi:10.1111/sed.12614.
- Dahl, T.W., Siggaard-Andersen, M., Schovsbo, N.H., Persson, D.O., Husted, S., Hougård, I.W., Dickson, A.J., Kjær, K., and Nielsen, A.T., 2019, Brief oxygenation events in locally anoxic oceans during the Cambrian solves the animal breathing paradox: *Scientific Reports*, doi:10.1038/s41598-019-48123-2.
- Day-Stirrat, J.R., Milliken, K.L., Dutton, S.P., Loucks, R.G., Hillier, S., Aplin, A.C., AND Schleicher, A.M., 2010, Open-system chemical behavior in deep Wilcox Group mudstones, Texas Gulf Coast, USA: *Marine and Petroleum Geology*, v. 27, p. 1804–1818, doi:10.1016/j.marpetgeo.2010.08.006.
- Dong, T., Harris, N.B., and Ayranci, K., 2018, Relative sea-level cycles and organic matter accumulation in shales of the Middle and Upper Devonian Horn River Group, northeastern British Columbia, Canada: Insights into sediment flux, redox conditions, and bioproductivity: *Bulletin of the Geological Society of America*, v. 130, p. 859–880, doi:10.1130/B31851.1.
- Dong, T., Harris, N.B., Ayranci, K., and Yang, S., 2017, The impact of rock composition on geomechanical properties of a shale formation: Middle and Upper Devonian Horn River Group shale, Northeast British Columbia, Canada: *AAPG Bulletin*, v. 101, p. 177–204, doi:10.1306/07251615199.
- Feinstein, S., Williams, G.K., Snowdon, L.R., Brooks, P.W., Fowler, M.G., Goodarzi, F., and Gentzis, T., 1991, Organic geochemical characterization and hydrocarbon generation

- potential of mid-Late Devonian Horn River bituminous shales, southern Northwest Territories: *Bulletin of Canadian Petroleum Geology*, v. 39, p. 192–202.
- Froelich, P.N., Bender, M.L., Luedtke, N.A., Heath, G.R., and DeVries, T., 1982, The marine phosphorus cycle: *American Journal of Science*, v. 282, p. 475–511.
- Ghadeer, S.G., and Macquaker, J.H.S., 2011, Sediment transport processes in an ancient mud-dominated succession: a comparison of processes operating in marine offshore settings and anoxic basinal environments: *Journal of the Geological Society, London*, v. 168, p. 1121–1132, doi:10.1144/0016-76492010-016.
- Harazim, D., McIlroy, D., Edwards, N.P., Wogelius, R.A., Manning, P.L., Poduska, K.M., Layne, G.D., Sokaras, D., Alonso-Mori, R., and Bergmann, U., 2015, Bioturbating animals control the mobility of redox-sensitive trace elements in organic-rich mudstone: *Geology*, v. 43, p. 1007–1010, doi:10.1130/G37025.1.
- Harris, N.B., McMillan, J.M., Knapp, L.J., and Mastalerz, M., 2018, Organic matter accumulation in the Upper Devonian Duvernay Formation, Western Canada Sedimentary Basin, from sequence stratigraphic analysis and geochemical proxies: *Sedimentary Geology*, v. 376, p. 185–203, doi:10.1016/j.sedgeo.2018.09.004.
- Katz, B.J., 2005, Controlling factors on source rock development—a review of productivity, preservation, and sedimentation rate, *in* Harris, N.B., ed, *The Deposition of Organic-Carbon-Rich Sediments: Models, Mechanisms, and Consequences*: Society for Sedimentary Geology, Tulsa, Oklahoma, Special Publication 82, p. 7–16.
- Kaufmann, B., 2006, Calibrating the Devonian Time Scale: A synthesis of U–Pb ID–TIMS ages and conodont stratigraphy: *Earth-Science Reviews*, v. 76, p. 175–190, doi:10.1016/j.earscirev.2006.01.001.

- Knapp, L.J., McMillan, J.M., and Harris, N.B., 2017, A depositional model for organic-rich Duvernay Formation mudstones: *Sedimentary Geology*, v. 347, p. 160–182, doi:10.1016/j.sedgeo.2016.11.012.
- Lash, G.G., and Blood, D., 2004, Geochemical and textural evidence for early (shallow) diagenetic growth of stratigraphically confined carbonate concretions, Upper Devonian Rhinestreet black shale, western New York: *Chemical Geology*, v. 206, p. 407–424, doi:10.1016/j.chemgeo.2003.12.017.
- Lash, G.G., and Blood, D.R., 2014, Organic matter accumulation, redox, and diagenetic history of the Marcellus Formation, southwestern Pennsylvania, Appalachian basin: *Marine and Petroleum Geology*, v. 57, p.244–263, doi:10.1016/j.marpetgeo.2014.06.001.
- Macquaker, J.H.S., and Adams, A.E., 2003, Maximizing Information from Fine-Grained Sedimentary Rocks: An Inclusive Nomenclature for Mudstones: *Journal of Sedimentary Research*, v. 73, p. 735–744, doi:10.1306/012203730735.
- Macquaker, J.H.S., Keller, M.A., and Davies, S.J., 2010, Algal blooms and ‘marine snow’: Mechanisms that enhance preservation of organic carbon in ancient fine-grained sediments: *Journal of Sedimentary Research*, v. 80, p. 934–942, doi:10.2110/jsr.2010.085.
- Meyers, P.A., 1994, Preservation of elemental and isotopic source identification of sedimentary organic matter: *Chemical Geology*, v. 114, p. 289–302, doi:10.1016/0009-2541(94)90059-0.
- Milliken, K.L., and Olson, T., 2017, Silica Diagenesis, Porosity Evolution, and Mechanical Behavior in Siliceous Mudstones, Mowry Shale (Cretaceous), Rocky Mountains, U.S.A.: *Journal of Sedimentary Research*, v. 87, p. 366–387, doi:10.2110/jsr.2017.24.

- Moghadam, A., Harris, N.B., Ayranci, K., Gomez, J.S., Angulo, N.A., and Chalaturnyk, R., 2019, Brittleness in the Devonian Horn River shale, British Columbia, Canada: *Journal of Natural Gas Science and Engineering*, v. 62, p. 247–258, doi:10.1016/j.jngse.2018.12.012.
- Morrow, D.W., 2018, Devonian of the Northern Canadian Mainland Sedimentary Basin: A Review: *Bulletin of Canadian Petroleum Geology*, v. 66, p. 623–694.
- Mossop, G.D., and Shetsen, I., 1994, Geological Atlas of the Western Canada Sedimentary Basin: Calgary, Alberta, Canadian Society of Petroleum Geologists and Alberta Research Council, 510 p: http://www.ags.gov.ab.ca/publications/wcsb_atlas/atlas.html.
- Oldale, H.S., and Munday, R.J., 1994, Devonian Beaverhill Lake Group of the Western Canada Sedimentary Basin, *in* Mossop, G., et al., *Atlas of the Western Canada Sedimentary Basin: Canada's Energy Geoscientists*, Calgary, p. 148–163.
- Obermajer, M., Stasiuk, L.D., Fowler, M.G., and Osadetz, K.G., 1999, Application of acritarch fluorescence in thermal maturity studies: *International Journal of Coal Geology*, v. 39, p. 185–204, doi:10.1016/S0166-5162(98)00045-7.
- Ocubalidet, S.G., Rimmer, S.M., and Conder, J.A., 2018, Redox conditions associated with organic carbon accumulation in the Late Devonian New Albany Shale, west-central Kentucky, Illinois Basin: *International Journal of Coal Geology*, v. 190, p. 42–55, doi:10.1016/j.coal.2017.11.017.
- Percival, L.M.E., Selby, D., Bond, D.P.G., Rakociński, M., Racki, G., Marynowski, L., Adatte, T., Spangenberg, J.E., and Föllmi, K.B., 2019, Pulses of enhanced continental weathering associated with multiple Late Devonian climate perturbations: Evidence from osmium-isotope compositions: *Palaeogeography, Palaeoclimatology, Palaeoecology*, v. 524, p. 240–249, doi:10.1016/j.palaeo.2019.03.036.

- Potma, K., Jonk, R., Matthew, D., Austin, N., 2012. A mudstone lithofacies classification of the Horn River Group: integrated stratigraphic analysis and inversion from wireline log and seismic data: Sixth BC Unconventional Gas Technical Forum.
- Raiswell, R., Newton, R., Bottrell, S.H., Coburn, P.M., Briggs, D.E.G., Bond, D.P.G., and Poulton, S.W., 2008, Turbidite depositional influences on the diagenesis of Beecher's Trilobite Bed and the Hunsrück Slate; sites of soft tissue pyritization: *American Journal of Science*, v. 308, p. 105–129, doi:10.2475/02.2008.01.
- Raven, M.R., Fike, D.A., Gomes, M.L., Webb, S.M., Bradley, A.S., and McClelland, M.O., 2018, Organic carbon burial during OAE2 driven by changes in the locus of organic matter sulfurization: *Nature Communications*, doi:10.1038/s41467-018-05943-6.
- Rimmer, S.M., Thompson, J.A., Goodnight, S.A., and Robl, T.L., 2004, Multiple controls on the preservation of organic matter in Devonian–Mississippian marine black shales: geochemical and petrographic evidence: *Palaeogeography, Palaeoclimatology, Palaeoecology*, v. 215, p. 125–154, doi:10.1016/j.palaeo.2004.09.001.
- Rivard, B., Harris, N.B., Feng, J., and Dong, T., 2018, Inferring total organic carbon and major element geochemical and mineralogical characteristics of shale core from hyperspectral imagery: *AAPG Bulletin*, v. 102, p. 2101–2121, doi:10.1306/03291817217.
- Ross, D.J.K., and Bustin, R.M., 2008, Characterizing the shale gas resource potential of Devonian–Mississippian strata in the Western Canada sedimentary basin: Application of an integrated formation evaluation: *AAPG Bulletin*, v. 92, p. 87–125, doi:10.1306/09040707048.
- Ross, D.J.K., and Bustin, R.M., 2009, Investigating the use of sedimentary geochemical proxies for paleoenvironment interpretation of thermally mature organic-rich strata: Examples from

- the Devonian-Mississippian shales, Western Canadian Sedimentary Basin: *Chemical Geology*, v. 260, p. 1–19, doi:10.1016/j.chemgeo.2008.10.027.
- Schieber, J., Krinsley, D., and Riciputi, L., 2000, Diagenetic origin of quartz silt in mudstones and implications for silica cycling: *Nature*, v. 406, p. 981–985, doi:10.1038/35023143.
- Schieber, J.K., 2016, Experimental testing of the transport-durability of shale lithics and its implications for interpreting the rock record: *Sedimentary Geology*, v. 331, p. 162–169, doi:10.1016/j.sedgeo.2015.11.006.
- Schoepfer, S.D., Shen, J., Wei, H., Tyson, R.V., Ingall, E., and Algeo, T.J., 2015, Total organic carbon, organic phosphorus, and biogenic barium fluxes as proxies for paleomarine productivity: *Earth-Science Reviews*, v. 149, p. 23–52, doi:10.1016/j.earscirev.2014.08.017.
- Sperling, E.A., Balthasar, U., and Skovsted, C.B., 2018, On the edge of exceptional preservation: insights into the role of redox state in Burgess Shale-type taphonomic windows from the Mural Formation, Alberta, Canada: *Emerging Topics in Life Sciences*, v. 2, p. 311–323, doi:10.1042/ETLS20170163.
- Stasiuk, L.D., and Fowler, M.G., 2004, Organic facies in Devonian and Mississippian strata of Western Canada Sedimentary Basin: relation to kerogen type, paleoenvironment, and paleogeography: *Bulletin of Canadian Petroleum Geology*, v. 52, p. 234–255, doi:10.2113/52.3.234.
- Taylor, K.G., and Macquaker, J.H.S., 2000, Early diagenetic pyrite morphology in a mudstone-dominated succession: the Lower Jurassic Cleveland Ironstone Formation, eastern England: *Sedimentary Geology*, v. 131, p. 77–86, doi:10.1016/S0037-0738(00)00002-6.

- Torres, M.A., Kemeny, P.C., Lamb, M.P., Cole, T.L., and Fischer, W.W., 2019, Long-Term Storage and Age-Biased Export of Fluvial Organic Carbon: Field Evidence From West Iceland: *Geochemistry, Geophysics, Geosystems*, v.21, doi:10.1029/2019GC008632.
- Tribovillard, N., Algeo, T. J., Lyons, T., and Riboulleau, A., 2006, Trace metals as paleoredox and paleoproductivity proxies: An update: *Chemical Geology*, v. 232, p. 12–32, doi:10.1016/j.chemgeo.2006.02.012.
- Tyson, R.V., 2001, Sedimentation rate, dilution, preservation and total organic carbon: some results of a modelling study: *Organic Geochemistry*, v. 32, p. 333–339, doi:10.1016/S0146-6380(00)00161-3.
- Wedepohl, K.H., 1971, Environmental influences on the chemical composition of shales and clays: *Physics and Chemistry of the Earth*, v. 8, p. 307–333, doi:10.1016/0079-1946(71)90020-6.
- Wignall, P.B., and Newton, R.J., 1998, Pyrite framboid diameter as a measure of oxygen deficiency in ancient mudrocks: *American Journal of Science*, v. 298, p. 537–552, doi:10.2475/ajs.298.7.537.
- Wilkin, R.T., and Barnes, H.L., 1997, Formation processes of framboidal pyrite: *Geochimica et Cosmochimica Acta*, v. 61, p. 323–339, doi:10.1016/S0016-7037(96)00320-1.
- Yawar, Z., and Schieber, J., 2017, On the origin of silt laminae in laminated shales: *Sedimentary Geology*, v. 360, p. 22–34, doi:10.1016/j.sedgeo.2017.09.001.
- Zhou, L., Algeo, T.J., Shen, J., Hu, Z., Gong, H., Xie, S., Huang, J., and Gao, S., 2015, Changes in marine productivity and redox conditions during the Late Ordovician Hirnantian glaciation: *Palaeogeography, Palaeoclimatology, Palaeoecology*, v. 420, p. 223–234, doi:10.1016/j.palaeo.2014.12.012.

CHAPTER 4 SEA-LEVEL CHANGE AND ORGANIC MATTER BURIAL IN THE MIDDLE-UPPER DEVONIAN HORN RIVER SHALE THROUGH HIGH-RESOLUTION GEOCHEMICAL ANALYSIS AND THIRD-ORDER SEQUENCE STRATIGRAPHY

Haolin Zhou¹, Nicholas B. Harris¹, Tian Dong², Korhan Ayranci³, Jilu Feng¹, and Benoit Rivard¹

¹ Department of Earth and Atmospheric Sciences, University of Alberta, Edmonton, AB, T6G2E3, Canada

² Key Laboratory of Tectonics and Petroleum Resources of Ministry of Education, China University of Geosciences, Wuhan, 430074, China

³ College of Petroleum Engineering & Geosciences, King Fahd University of Petroleum & Minerals, Dhahran 31261, Saudi Arabia

ABSTRACT

In our millimeter-resolution analysis (Chapter 2), we identified different controls (redox conditions, bioproductivity, and dilution) on organic matter (OM) accumulation in the Middle-Upper Devonian Horn River Group in the Western Canada Sedimentary Basin, based on small-scale relationships between geochemical proxies and organic matter concentration. This study examines relationships between these controls, relative sea level, and OM accumulation in the Horn River Group (includes the Evie Member, Otter Park Member, and Muskwa Formation), based on a comparison of 133 ~10 cm core slabs analyzed for major elements and organic carbon content at high-resolution (mm-scale) and a core- and log-based sequence stratigraphic analysis. The dominance of different controls on organic matter accumulation varies with sequence

stratigraphic position: (1) bioproductivity and terrestrial dilution are significant controls on organic matter accumulation in the third-order transgressive and highstand systems tracts that were superimposed on second-order sea-level highstands (TST1 and HST1 in the Evie Member and TST3 and HST3 in the Muskwa Formation); (2) terrestrial dilution is the most common control during a third-order lowstand sea level that was superimposed on a second-order lowstand (FSST and LST3 in the upper Otter Park Member); (3) carbonate dilution is the predominant control in the third-order highstand systems tract that was deposited during a second-order lowstand (HST2 in the middle Otter Park Member); (4) redox conditions are a secondary control on organic richness in the third-order transgressive systems tract, superimposed on a second-order sea-level highstand (TST1 in the Evie Member).

We also compare our interpretations of millimeter-scale analysis to the interpretations based on meter-scale sampling to examine the effects by different observation scales and analytical methods. Meter-scale dataset compared to high-resolution analysis may obscure millimeter- to centimeter-scale variation in organic carbon accumulation processes but can illustrate long-term paleoenvironmental perturbations. Regression analysis of data from core slab composite samples weakens the effect of stratigraphic units with few samples in the study of the entire formation.

4.1 INTRODUCTION

The millimeter-resolution geochemical analysis in Chapter 2 provided new insights into the multiple processes that control organic matter (OM) accumulation, each operating over centuries to millennia. These processes, or triggers for organic carbon deposition and accumulation, which include primary productivity, preservation, and dilution, have been identified in the Horn River shale (Chapter 2). Conclusions based on high-resolution

geochemical profiles differ from those derived from meter-resolution datasets (Dong et al., 2018). In contrast to redox as the primary control on the organic matter accumulation concluded from meter-scale sampling, millimeter-scale analysis in Chapter 2 indicates that dilution and bioproductivity are the predominant pathways for organic carbon storage in this formation.

Organic matter accumulation can be related to variations in relative sea level because of the close relationships between relative sea level and the three controls on OM accumulation, bioproductivity, preservation, and dilution, widely documented in many formations based on decimeter/meter-resolution datasets (e.g., Bohacs et al., 2005; Jones et al., 2018; Sageman et al., 2003). Relative sea-level fluctuations influence bioproductivity, redox states, detrital/carbonate input, and consequently organic richness by (1) limiting nutrient inflow from open oceans for bioproductivity, (2) influencing redox chemocline position, (3) trapping terrestrial clastic input, (4) controlling carbonate platform growth and shedding (Arthur and Sageman, 2005; Dong et al., 2018; Kendall and Schlager, 1981). Here, we report a study, based on a dataset that includes the millimeter-resolution geochemical profiles of 133 core slabs of the Middle-Upper Devonian Horn River Group in the northwestern Western Canada Sedimentary Basin, that examines the role of relative sea level in organic richness through correlating the processes of organic matter accumulation (Chapter 2) to the third-order sea-level cycles (Ayranci et al., 2018a, b). We compare our results to the previous meter-resolution analysis for this mudstone (Dong et al., 2018) to illustrate the effects of different observation scales and analytical methods.

4.2 GEOLOGICAL BACKGROUNDS

4.2.1 Geological Setting

The Horn River Basin is located in the northwestern part of the Western Canada Sedimentary Basin, covering an area of approximately 12,000 km² (Fig. 4.1). It is surrounded by

reefs to the south and east and is bordered by the post-depositional Bovie Fault to the west that separates it from the Liard Basin (Oldale and Munday, 1994). The Horn River Group was deposited from the Givetian Stage to the early Frasnian Stage, spanning 6 to 8 m.y., and includes, in ascending order, the Evie Member and Otter Park Member of the Horn River Formation, and Muskwa Formation (Morrow, 2012; Mossop and Shetsen, 1994) (Fig. 4.2). The Evie Member unconformably overlies carbonates of the Keg River Formation (Fig. 4.2). It comprises dark grey to black, calcareous mudstone and becomes more argillaceous upward (Dong et al., 2018); total organic carbon (TOC) in this unit is the most enriched in the entire Horn River Group (Fig. 4.4). The middle unit is the Otter Park Member, composed of grey to dark grey, organic-lean, calcareous, and argillaceous mudstone. TOC content in this unit is the lowest in the Horn River Group (Fig. 4.4). The Muskwa Formation consists of dark grey to black, organic-rich, and siliceous mudstone (Dong et al., 2018, Fig. 4.2) and is in turn overlain by the Fort Simpson Formation (Fig. 4.2). TOC in the Muskwa Formation is relatively enriched, more than the underlying Otter Park Member but less than the Evie Member (Fig. 4.2).

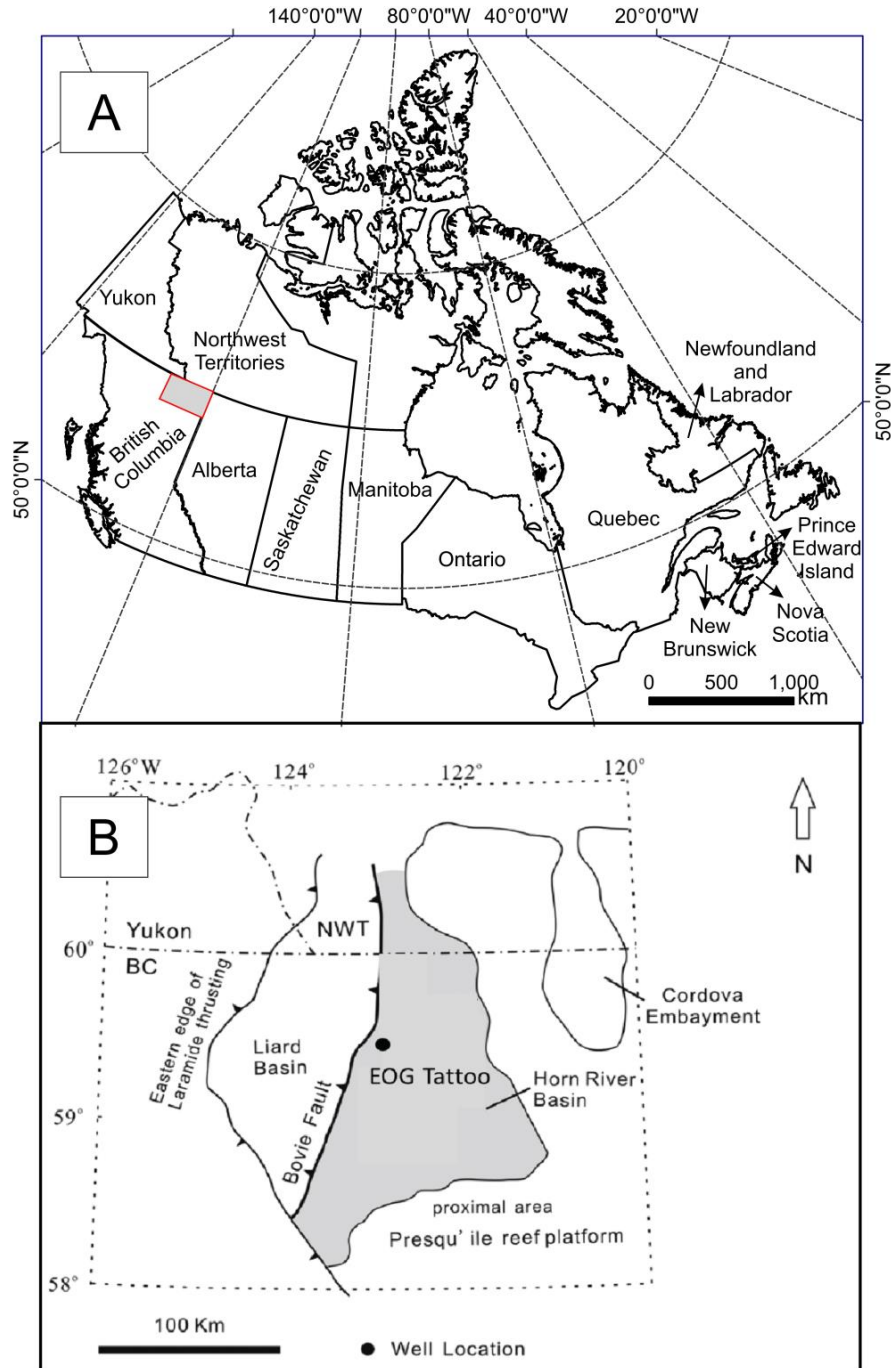


Figure 4.1. Geological maps of the study area. A: Canada map with the Horn River Basin location, highlighted as grey area. B: Geological map of the Horn River Basin and the location of the well in this work (Moghadam et al., 2019). BC – British Columbia; NWT – the Northwest Territories.

Sediments in the Horn River Group were largely deposited below storm wave base through a combination of suspension settling, hyperpycnal flows, and bottom currents. Sources of sediment included a delta system located in the southeastern part of the basin that introduced siliciclastic mud and silt into the basin (Ayranci et al., 2018a), nearby reefs that shed carbonate sediments (Ayranci et al., 2018a), and biogenic processes that introduced silica and possibly calcareous bioclasts (Dong et al., 2018). Type II organic matter is predominant in this shale (Chapter 2), consistent with previous research (Feinstein et al., 1991; Stasiuk and Fowler, 2004). Thermal maturities range from 1.6% to 2.5% R_o (vitrinite reflectance; Ross and Bustin, 2009).

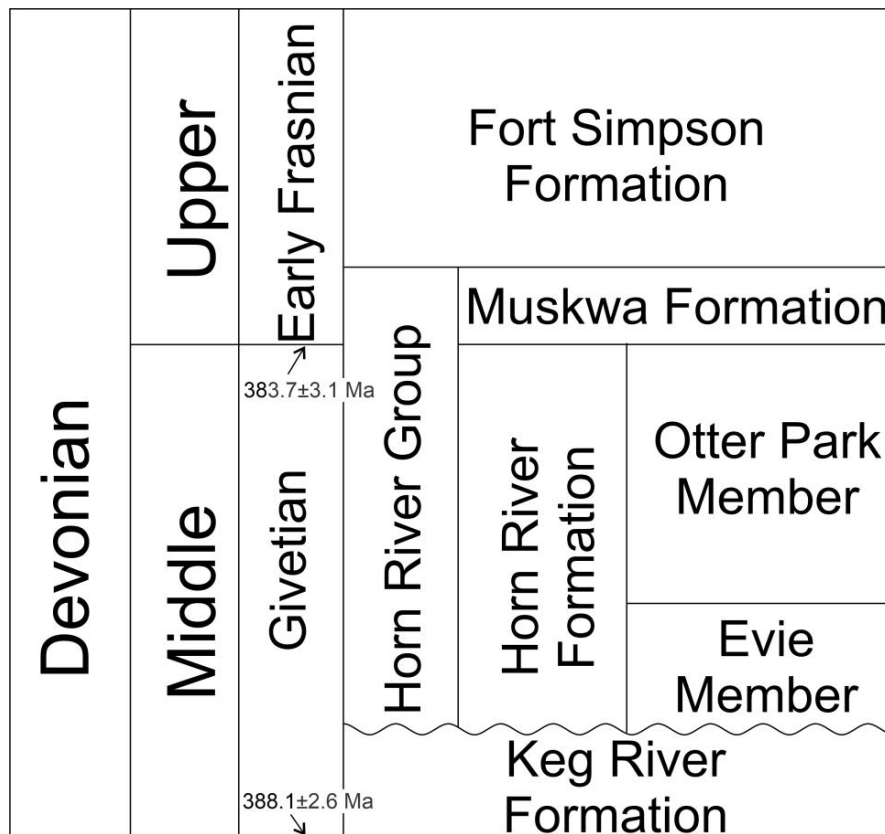


Figure 4.2. Stratigraphy of the Horn River Group in the Horn River Basin (modified after Morrow, 2012; Dong et al., 2018). Wavy line between the Keg River Formation and Horn River Group represents an unconformable contact. Ages of strata follow the U-Pb ID-TIMS age and conodont zones by Kaufmann (2006).

The Horn River shale is interpreted to have been deposited during three third-order sea-level cycles, superimposed on a partial second-order eustatic cycle that reached a lowstand during the deposition of the Otter Park Member (Ayranci et al., 2018b). Classification of lithofacies follows the depositional model of the Horn River Group in the distal basin (long-drill cores C3 and C4) by Ayranci et al. (2018 a, b). The Evie Member contains predominantly massive mudstone and pyritic mudstone with minor moderately bioturbated mudstone, reflecting deposition under low-energy, anoxic conditions during a third-order sea-level rise (TST1 and HST1). Depositional processes during this time were largely suspension settling and short-duration hyperpycnal flows. The Otter Park Member experienced a full third-order eustatic cycle and consists of three units: (1) a basal unit is dominated by intensely bioturbated pinstripe mudstone at the bottom and massive and pyritic mudstone upward, deposited as a lowstand systems tract (LST2) under relatively oxygenated conditions; (2) a middle unit composed of alternating massive and pyritic mudstones, deposited as TST2 under less oxygenated and possibly anoxic conditions during a time of rising sea level, and alternating heterolithic calcareous siltstone and massive mudstone, faintly laminated mudstone, and moderately bioturbated mudstone, deposited as HST2 under relatively oxic and energetic conditions within a progradational package during rising sea level ; (3) an upper unit is dominated by interlaminated calcareous-siliceous mudstone, heterolithic calcareous siltstone and massive mudstone, and faintly laminated mudstone, comprising FSST and LST3, deposited under oxygenated and energetic conditions during a relative low sea level. The Muskwa Formation represents a third-order sea-level rise and is composed of massive mudstone and pyritic mudstone, deposited under

relatively less oxygenated and possibly anoxic conditions, with sedimentation dominated by suspension settling.

4.2.2 Organic Matter Enrichment Patterns

We have identified different controls on organic matter accumulation (Fig. 4.3) during the deposition of the Horn River Group in Chapter 2: (1) Bioproductivity primarily controlled organic matter accumulation, based on a robust correlation between biogenic Si (bioproductivity proxy) and TOC (OM proxy) in high-resolution profiles (e.g., Si_{bio}/TOC ratio is 21 – 23 in slab 3131.82 m, Fig. 4.3A). (2) Redox conditions controlled OM accumulation, based on synchronous variation between S/Fe ratio (redox proxy) and TOC in high-resolution profiles (the red colored section in Fig. 4.3B). (3) Carbonate or siliciclastic minerals diluted organic matter concentration, based on negative correlations between Ca or Al contents and TOC in high-resolution profiles (the red colored section in Fig. 4.3C).

Bioproductivity, redox conditions, and terrestrial input are also linked through feedbacks (Chapter 2). Bioproductivity-redox feedbacks are recognized based on the 1 – 3 mm offsets shown by blue arrows between profiles of bioproductivity and redox proxies, % Si_{bio} and S/Fe ratios (Figs. 4.3D-E). We also demonstrate a link between terrestrial nutrient supply and marine bioproduction, illustrated by millimeter-scale offsets between Al (clay proxy) and Si_{bio} profiles (Fig. 4.3F).

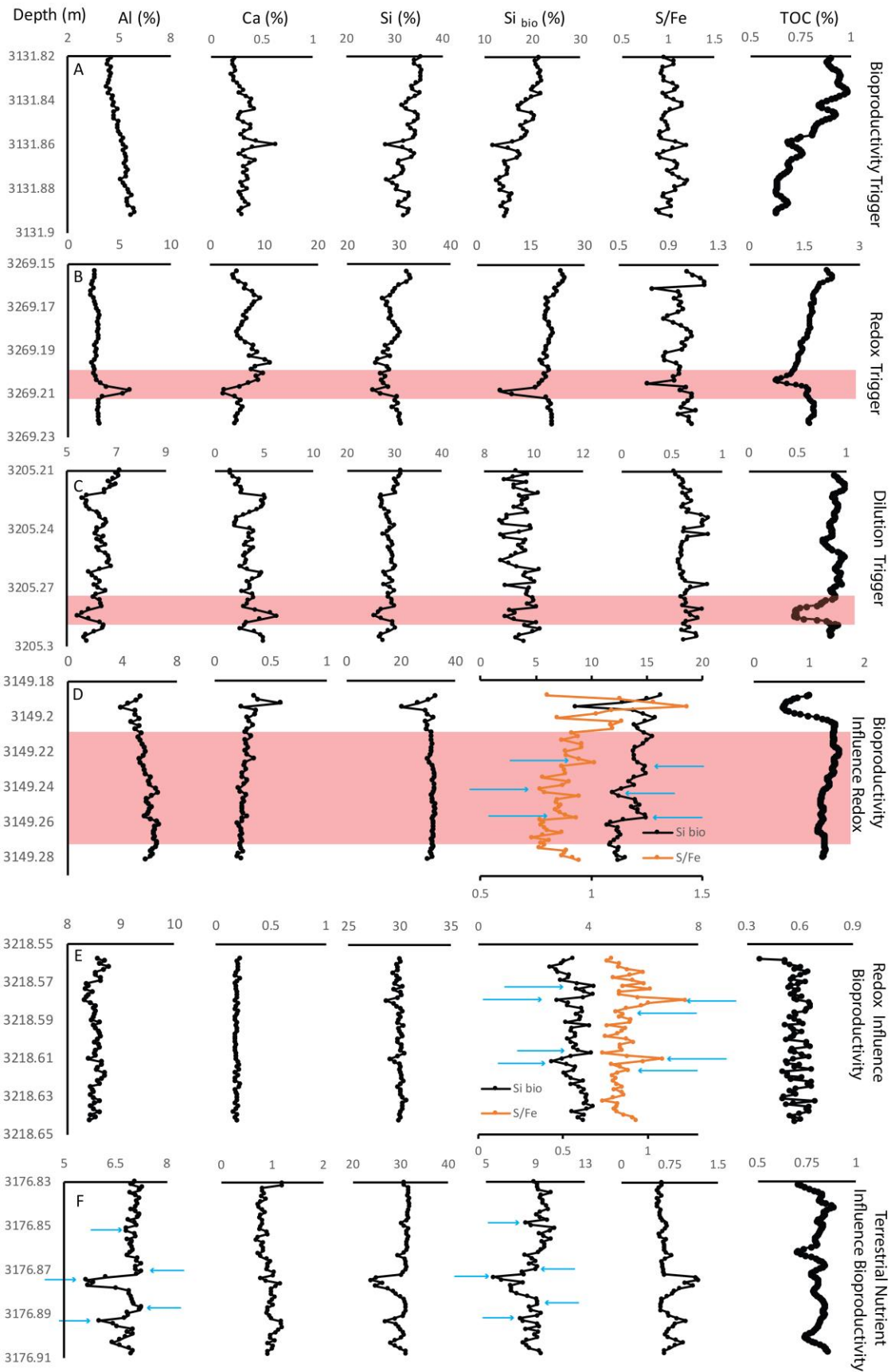


Figure 4.3. Different controls on organic matter accumulation and feedback loops between redox condition, bioproductivity, and terrestrial input. A: Bioproductivity primarily controlled OM accumulation. B: Redox controlled OM accumulation in the red colored section. C: Carbonate input diluted OM concentration. D: Feedback of bioproductivity influencing redox conditions. The offsets between biogenic Si (Si_{bio}) and S/Fe ratios are shown by arrows. E: Feedback of redox conditions influencing bioproductivity. The offsets between biogenic Si (Si_{bio}) and S/Fe ratios are shown by arrows. F: Feedback of terrestrial nutrient influencing bioproductivity. The offsets between biogenic Si (Si_{bio}) and Al are shown by arrows.

4.3 METHODOLOGY

4.3.1 Samples

In this study, we analyzed 133 core slabs, collected at ~ 1 m intervals from the vertical long-drill core EOG HZ TATTOO D-A028-F/094-O-10 from the distal part of the Horn River Basin (Fig. 4.1). Each core slab represents 7 cm – 12 cm of stratigraphic section.

4.3.2 Methods

We performed X-ray fluorescence scanning for a total of 133 core slabs through the benchtop Orbis PC Micro-EDXRF Elemental Analyzer at the nanoFAB of the University of Alberta. The scan was in a direction perpendicular to horizontal bedding and was set under vacuum for 30 seconds on each scanning spot with 2 mm diameter detector window. Based on the length of core slabs, there are 48 – 128 scanning points vertically on each core slab, so the vertical resolution is 1 – 2 mm. We applied certain major and minor elements that displayed effective peaks above noise (detection limit is 0.01 wt.%), including Si, Al, K, Ca, Mg, Fe, S, Ba, and Ti, for this study. We applied hyperspectral imagery analysis for total organic carbon (TOC)

and silica contents with $\sim 0.8 - 1.5$ mm vertical resolution for the entire core via SisuROCK system at the University of Alberta Spectral Imaging Facility. TOC was measured in the 970 – 2510 nm spectral range, and SiO₂ was analyzed in the 7400 – 12100 nm spectral range. Silica data from both methods were used to register these two datasets. TOC data were calibrated to the shale model of hyperspectral imagery developed for the same formation (Rivard et al., 2018). We need to note that TOC measurements represent present-day TOC content because of the loss of organic carbon during thermal maturation, and that the thermal loss was probably similar in the entire shale because the Horn River shale is within dry gas window and has predominantly the same Type II organic matter.

Whole-rock geochemical data were obtained on the same core slabs as the microgeochemical profiles. Vertical slices (perpendicular to bedding) were cut from the slab, ensuring that identical stratigraphic intervals were analyzed for major, minor and trace elements by inductively coupled plasma-mass spectrometry (ICP-MS) and for total organic carbon LECO combustion analyses following Dong et al. (2018). The bulk elemental compositions by ICP-MS analysis were used as standards to calibrate the averages of values from EDXRF scans. The millimeter- and meter-scale datasets are reported in Appendices B and C.

4.3.3 Proxies

Elemental concentrations and ratios are applied as proxies for carbonate and terrestrial inputs, redox conditions, bioproductivity, and OM accumulation. Al concentration is an effective proxy for clastic input (Tribovillard et al., 2006), and Ca concentration is used for carbonate input. Detection limits for trace metals in EDXRF precludes the use of some standard ratios for assessing redox conditions, such as trace metal enrichment factors (EFs) and bimetal proxies, e.g., V/Cr; thus, we applied major elemental redox proxy, S/Fe ratio, which was described as a

relatively strong proxy in shales by Algeo and Liu (2020). Dong et al. (2018) and Harris et al. (2018) validated this redox proxy through a comparison to Mo/Al ratios (similar to Mo_{EF}) in the Horn River and nearby coeval Duvernay shales. $S/Fe < 0.4$ is considered to indicate oxic conditions, and $0.72 < S/Fe < 1.15$ is for anoxic conditions ($S/Fe = 1.15$ is the ratio for pyrite) (Arthur and Sageman, 1994; Ross and Bustin, 2009; Ocubalidet et al., 2018; Rimmer et al., 2004). TOC is an appropriate measure of OM enrichment (Chapter 2). Because euxinic conditions were inferred for deposition of the Evie Member (Dong et al., 2018), we select biogenic Si (Si_{bio}) to represent bioproduction (Schieber et al. 2000), instead of the redox-sensitive biological proxy barium (Tribovillard et al, 2006), calculated after Ross and Bustin (2009):

$$Si_{bio} = Si_{sample} - [Al_{sample} \times (Si/Al)_{background}]. \quad (1)$$

The background Si/Al ratio is 3.1 (Wedepohl, 1971), consistent with Dong et al.'s (2018) study of the Horn River shale, in which it can effectively distinguish detrital and biogenic Si.

4.4 RESULTS

4.4.1 Sequence Stratigraphy

We correlate the Horn River shale section in the TATTOO well to other wells in the distal Horn River Basin based on well log and geochemical profiles (Fig. 4.4), following the stratigraphic model of the Horn River shale (Ayranci et al., 2018b) to identify stratigraphic units. The Evie Member is identified by high gamma-ray values in well log, and high Si and TOC contents, high values of S/Fe and Mo/Al ratios, and low Al concentrations in meter-scale geochemical profiles. The Otter Park Member in this study is correlated by low gamma-ray values to the wells in the study by Ayranci et al. (2018b), with low %Si, S/Fe ratios, Mo/Al ratios, %TOC, but high Al and Ca contents in geochemical profiles. The Muskwa Formation

shows sharp increases in gamma-ray values and Si and TOC contents compared to the underlying Otter Park Member.

Third-order stratigraphic sequences in the TATTOO core are also identified based on correlations to documented sequences in nearby wells (Ayranci et al., 2018b). These include a third-order regressive and highstand systems tract (TST1 and HST1) in the Evie Member, a full third-order eustatic cycle (LST2, TST2, HST2, FSST, and LST3) in the Otter Park Member, and a third-order regressive systems tract and overlying highstand systems tract (TST3 and HST3) in the Muskwa Formation. Potma et al. (2012) documented two second-order transgressive and regressive cycles for the Horn River Group, including a second-order sequence boundary between the Evie Member and Otter Park Member, and a second-order maximum flooding surface within the Evie Member and the Muskwa Formation; the latter coincides with the third-order maximum flooding surfaces. Based on the gamma-ray profile (Fig. 4.4), we recognize a second-order sea-level lowstand in the Otter Park Member and a second-order sea-level highstand in the Evie Member and Muskwa Formation.

4.4.2 Formation-Scale Geochemical Profiles from Whole-Slab Analysis

Organic carbon (OC). In this and the following three sections, we describe the results of analyses of the ~10 cm core slab composites. TOC is relatively enriched in the Evie Member and Muskwa Formation and depleted in the Otter Park Member. OC concentration increases upward throughout TST1 in the lower Evie Member and reaches the highest values at the maximum flooding surface between TST1 and HST1 (max. 9.5 wt.%). OC decreases to 1.5% through the upper Evie Member, HST1, and the basal unit of the Otter Park Member, LST2. The middle and upper Otter Park Member (HST2, FSST2, and LST3) display low organic carbon contents (min. 0.3%). There is a sharp increase in OC content at the maximum regressive surface between LST3

and TST3. In the Muskwa Formation, TOC values average 4.2 wt.% (2.7% – 6.1%) in TST3 and decrease slightly through HST3 (aver. 3.2%).

Bioproductivity proxy. Biogenic Si (Si_{bio}) content is relatively stable in the Evie Member (TST1 and HST1), generally in the range of 15% – 30%. % Si_{bio} is the lowest in the Otter Park Member (min. less than 1%), but it sharply increases to ~ 25% at the maximum regressive surface between LST3 and TST3. In the Muskwa Formation, Si_{bio} increases upward generally throughout TST3 to ~ 30%. In the upper Muskwa Formation (HST3), biogenic Si first decreases to 10% in the lower HST3 and then increases to 35% throughout the rest of HST3, which is the highest of the entire Horn River Group.

Paleoredox proxies. Mo/Al and S/Fe ratios are applied to reflect redox conditions in our whole core slab dataset. S/Fe ratios increase slightly upward in the TST1 of the Evie Member from 1.1 to 1.3, which are the highest values in this shale. S/Fe ratios then show a steady decline from 1.3 to 0.2 in the rest of the Evie Member (HST1) to the top of the Otter Park Member (LST3). In the Muskwa Formation (TST3 and HST3), S/Fe ratios increase to 1.0 at the maximum flooding surface of TST3 with slightly lower values (~ 0.8) in the HST3.

Values of Mo/Al ratios (ppm/%) are the highest in the Evie Member TST1 and lower HST1 (max. 80), then decrease sharply in the lower HST1 and gradually increase to approximately 48 throughout the rest of HST1. Mo/Al ratios are low in the middle and upper Otter Park Member (HST2, FSST, and LST3), generally less than 2. In the Muskwa Formation, Mo/Al ratios slightly increase to ~ 13 in TST3 and have higher values in HST3 (max. 26).

Dilution proxies. Al concentration is relatively low in the TST1 of the Evie Member and increases upward to 4% in HST1. In the Otter Park Member, %Al decreases through TST2 and HST2 and sharply increases to 9% in FSST and LST3. In the Muskwa Formation, %Al varies

inversely with %Si_{bio}; it declines in lower TST3, then increases to 7% through the upper TST3 and lower HST3, and decreases in the rest of HST3.

Calcium content fluctuates at the range from 3% to 20% with a generally diminishing trend upward through the Evie Member. In the Otter Park Member, Ca varies inversely with Al, first increasing to approximately 23% in HST2 and then decreasing to 5% in FSST and LST3. Within the TST3 and HST3 in the Muskwa Formation, calcium concentrations are low, mostly less than 1%.

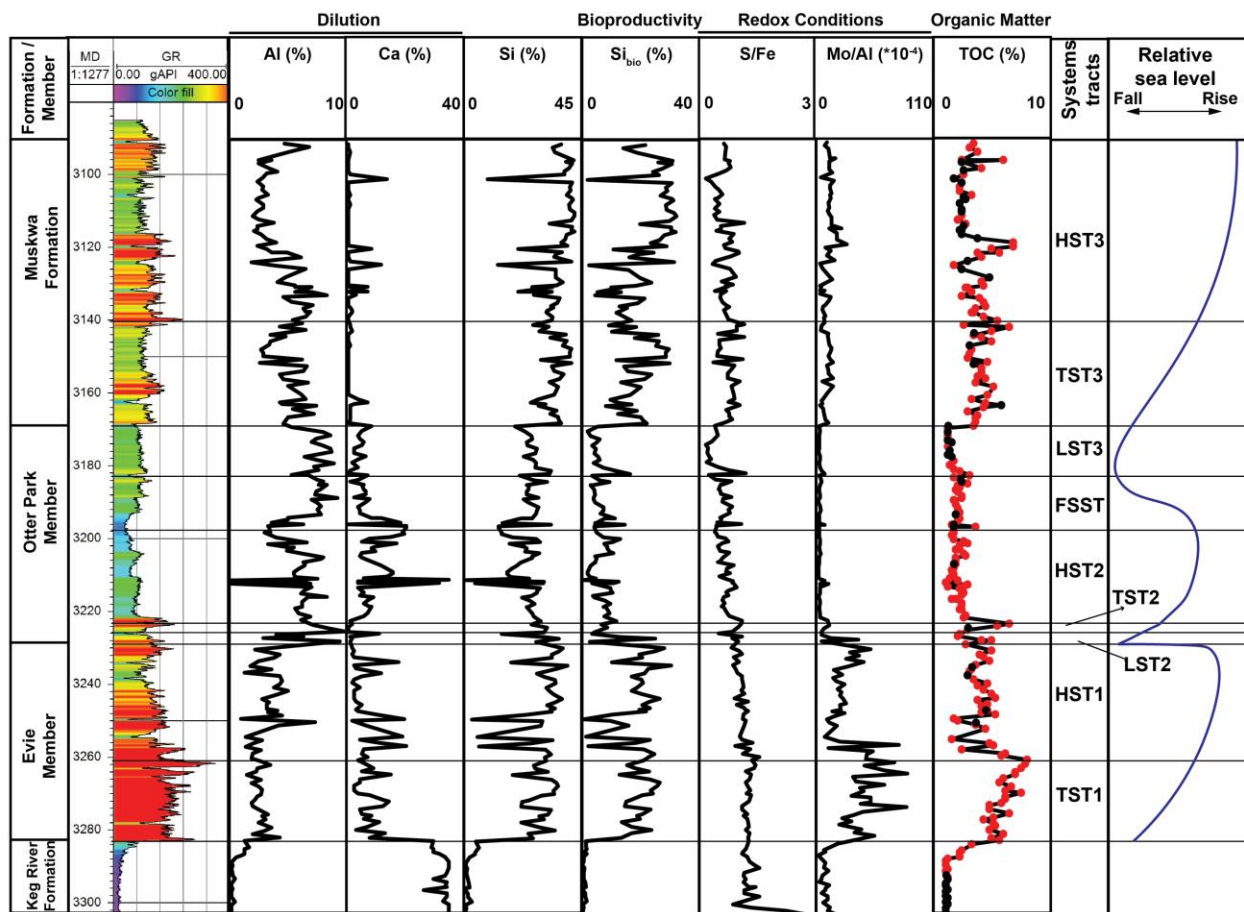


Figure 4.4. Gamma-ray log, whole-rock geochemical profiles, and third-order sequence stratigraphy of the long-drill core of this study. The red spots in the TOC profile are the core slabs analyzed by both EDXRF and hyperspectral imagery. Si_{bio} – biogenic Si.

4.4.3 Frequency of Different Patterns

Microsampled geochemical profiles for 133 core slabs from our Horn River shale core were described in Chapter 2 and classified into three patterns of OM enrichment and three patterns of feedback loops (Fig. 4.3). These patterns, described in the Geological Backgrounds section, are

- 1) Bioproductivity-driven organic enrichment, in which elevated organic carbon (OC) content coincides with elevated biogenic Si content.
- 2) Redox-driven organic accumulation, in which increased OC content coincides with increased S/Fe ratios.
- 3) Dilution-driven organic accumulation, in which decreased OC content is associated with increased Ca or Al contents.
- 4) Feedback where increased bioproductivity induces a redox response, shown by a peak in biogenic Si profile that leads a peak in S/Fe ratios by 1 – 3 mm.
- 5) Feedback where decreased oxygen levels (redox conditions) trigger enhanced bioproductivity, shown by a peak in S/Fe ratios that leads a peak in biogenic Si profile by 1 – 3 mm.
- 6) Feedback where increased terrestrial input enhances bioproductivity, shown by a peak in Al that leads a peak in biogenic Si profile by 1 mm.

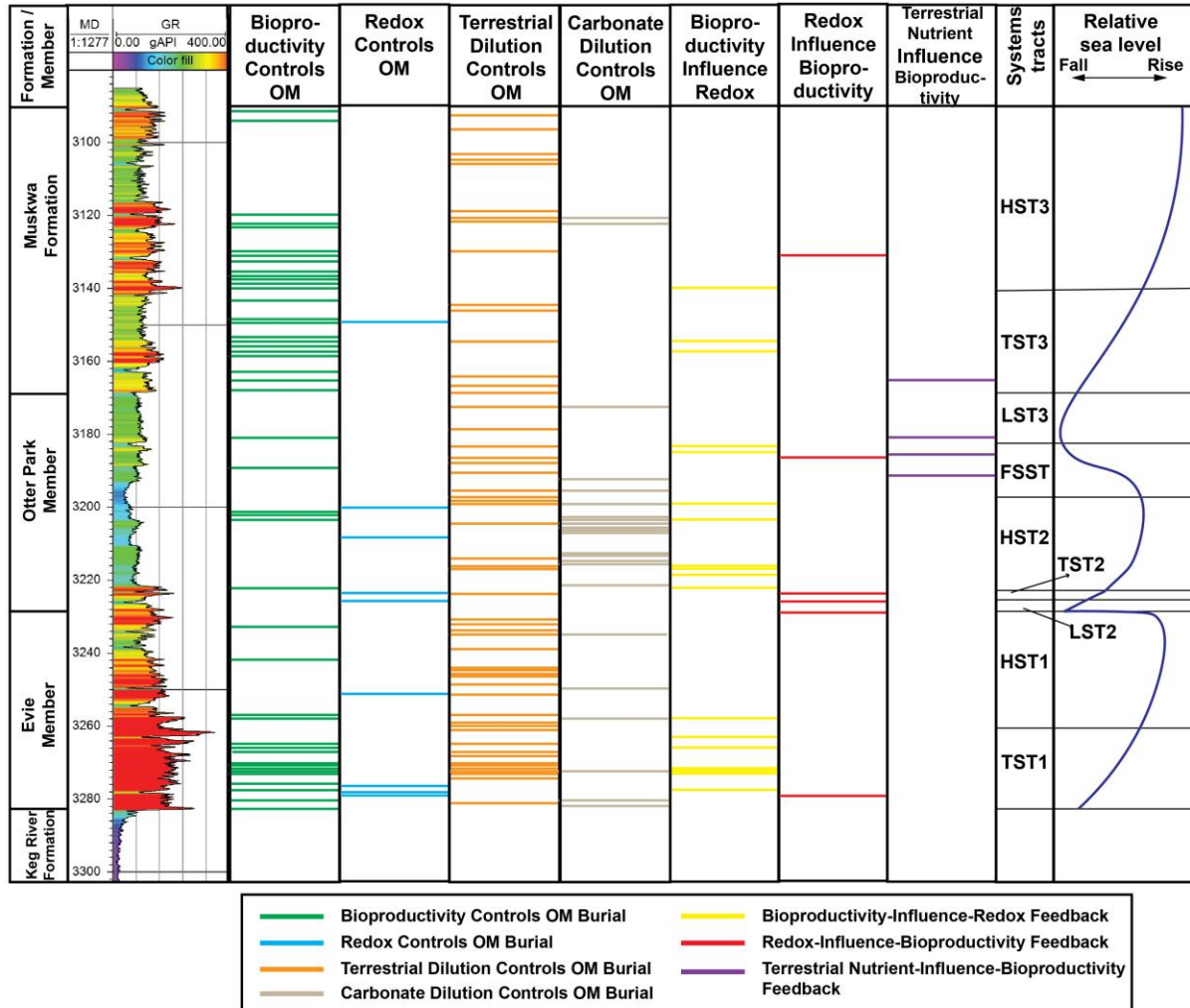


Figure 4.5. Gamma-ray log, 3rd sequence stratigraphy, and distribution of organic matter accumulation processes of the long-drill core of this study. Occurrences of different organic matter enrichment pattern and feedbacks in the shale are highlighted in the seven columns, represented by different color bars.

Results of the classification of our samples is presented in Figure 4.5. Given the limited number of samples in LST2 and TST2, the data in these two stratigraphic intervals are too few for a meaningful analysis.

At the scale of second-order sea level cycles, samples exhibiting a bioproductivity control are most common in the Evie Member and Muskwa Formation, both deposited during a second-order sea-level highstand (Potma et al., 2012). Samples exhibiting a redox control are rare in the entire Horn River Group. Carbonate dilution as a control on organic matter enrichment is relatively common in the middle Otter Park Member, deposited during the second-order sea-level lowstand (Potma et al., 2012). Samples exhibiting a terrestrial dilution control are common in the entire section (Fig. 4.5).

At the scale of the third-order sea level cycles, samples exhibiting a bioproductivity control are highly distributed in the units deposited during high relative sea level, including TST1, HST1, TST3, and HST3. Samples that display terrestrial dilution controls are present everywhere in the section but are more common in units deposited during a low relative sea level (FSST and LST3) (Fig. 4.5). Carbonate dilution controls are relatively common in samples of HSTs, especially HST2 (43%) (Table 4.1). Samples exhibiting redox controls are sparsely distributed, less than 15% in each unit (Table 4.1).

Table 4.1. Distribution of om accumulation patterns of the core in this work.

Formation	Systems Tracts	Total Samples	Bioproductivity Controls OM	Redox Conditions Control OM	Terrestrial Dilution Controls OM	Carbonate Dilution Controls OM
Muskwa Formation	HST3	26	50%	0	35%	8%
	TST3	18	61%	6%	33%	0
Otter Park Member	LST3	5	20%	0	40%	20%
	FSST	16	6%	0	38%	13%
	HST2	28	14%	7%	21%	43%
	TST2	1	0	100%	100%	0
	LST2	1	0	100%	0	0
Evie Member	HST1	19	21%	5%	74%	16%
	TST1	21	57%	14%	52%	14%

The distribution of feedback patterns is also shown in Figure 4.5. At the scale of second-order sea level, all feedback patterns are represented both in units deposited during the lowstand (the Otter Park Member) and in highstand (the Evie Member and Muskwa Formation). In the third-order systems tracts, however, samples exhibiting feedback where bioproductivity triggers a redox response are relatively common during third-order high sea level (TSTs and HSTs), and samples exhibiting feedback where terrestrial nutrient triggers a bioproductivity response are primarily distributed in FSST, LST3, and lower TST3 (Fig. 4.5 and Table 4.2). Samples showing feedback in which anoxia (redox) triggers a bioproductivity response are rare in this section (Fig. 4.5).

Table 4.2. Distribution of feedback patterns of the core in this work.

Formation	Systems Tracts	Total Samples	Terrestrial Nutrient-Bioproductivity Feedback	Bioproductivity-Lead-Redox Feedback	Redox-Lead-Bioproductivity Feedback
Muskwa Formation	HST3	26	-	1	2
	TST3	18	1	2	-
Otter Park Member	LST3	5	1	-	-
	FSST	16	2	2	1
	HST2	28	-	6	-
	TST2	1	-	-	1
	LST2	1	-	-	1
Evie Member	HST1	19	-	1	1
	TST1	21	-	6	1

4.5 DISCUSSION

4.5.1 Sea Level and Organic Matter Accumulation

Relationships between sea-level changes and organic matter accumulation have been identified in many black shales (e.g., Algeo et al., 2004; Erlich et al., 1999; Harris et al., 2018; Li et al., 2017). Relative sea-level fluctuations can influence bioproductivity, redox states, detrital/carbonate input, and consequently organic richness by (1) limiting nutrient inflow from

open oceans for bioproductivity, (2) influencing position of a chemocline and oxygenation of bottom waters, (3) trapping clastic sediment flux, (4) controlling carbonate platform growth and shedding (Arthur and Sageman, 2005; Dong et al., 2018; Kendall and Schlager, 1981). In this study, we compare distributions of proxies for different organic matter enrichment processes (bioproductivity, redox, and dilution as controls on OM accumulation), based on both macroscale and microscale geochemical profiles to sequence stratigraphic units of the Horn River Group (Figs. 4.4, 4.5), in order to characterize the role and possible influences of sea-level changes on OM accumulation.

4.5.1.1 Meter-Scale Geochemistry and Sea-Level Controls

Elemental concentrations and ratios as proxies for bioproductivity, redox conditions, terrestrial and carbonate inputs, and organic enrichment vary systematically in different sequence stratigraphic units, based on formation-scale profiles in Figure. 4.4.

Enriched biogenic Si (Si_{bio}) and total organic carbon (TOC) contents (Fig. 4.4) indicate high bioproductivity in the HST1 and TST1 of the Evie Member and in TST3 and HST3 of the Muskwa Formation, in both cases superimposed on second-order sea-level highstands. Elevated Si_{bio} coincides with relatively high values of S/Fe ratios and Mo/Al ratios in these stratigraphic units (Fig. 4.4), indicating that high bioproductivity coincides with relatively reducing conditions. We should note that values of Si_{bio} content are the highest in HST3, but TOC content is intermediate compared to other units, which indicates a possible autodilution effect by biogenic Si for organic richness (Bohacs et al., 2005). Low terrestrial input is indicated by low Al content in both the Evie Member and Muskwa Formation, consistent with high relative sea level. Carbonate content is relatively enriched with decreased %TOC in the middle part of the Evie Member, suggesting that highstand shedding was an important mechanism for contributing

sediment in the earlier part of the sea-level highstand (HST1) but decreased later, possibly related to increasing water depth above the platform. Based on meter-scale sampled 10-cm core composite, we conclude that the rising relative sea level during the deposition of the Evie Member (TST1 and HST1) and Muskwa Formation (TST3 and HST3) favored organic richness through increased bioproductivity, limiting clastic dilution, and the development of oxygen deficiency in the deep water. Autodilution by high bioproductivity in HST3 and carbonate shedding in the lower part of HST1 limited organic richness.

A third-order TST and HST are also present in the Otter Park Member (TST2 and HST2); however, these units are characterized by lower S/Fe and Mo/Al ratios, lower values of %Si_{bio}, generally higher values of % Ca and %Al, and generally lower values of %TOC than the TST/HST pairs in the Evie Member and Muskwa Formation. Thus, in contrast to the Evie and Muskwa units that were deposited during relative highstands, the Otter Park Member TST and HST experienced less reducing conditions, lower bioproductivity, and greater detrital sediment input, as a result of their position in a second-order lowstand. The high Ca content is related to the position of the carbonate platform of the basin; the platform growth was closer to the sea surface during the deposition of this third-order HST that was superimposed on the second-order sea-level lowstand (Potma et al., 2012), so carbonate dilution by platform shedding became more significant than in HST1.

The Otter Park Member contains the only FSST and LSTs present in the Horn River Group. Because of the small number of samples in LST2, we here mainly discuss the sea-level controls on organic matter accumulation in FSST and LST3, both of which are superimposed on a second-order sea-level lowstand. These two units are characterized by high Al content with low TOC and Si_{bio} contents (Fig. 4.4) that indicate a high terrestrial input and low biogenic input

during a relative low third-order sea level. Low values of S/Fe ratios and Mo/Al ratios (Fig. 4.4) reflect an oxygenated condition, which coincides with the low bioproductivity in these units indicated by low %Si_{bio}. Low Ca content in FSST and LST3 reflect a limiting carbonate influx, because of the insufficient carbonate production related to exposed carbonate platform during this period of sea-level lowstand (Potma et al., 2012). Therefore, the relative low sea level during the deposition of the upper Otter Park Member (FSST and LST3) limited organic matter accumulation through increasing terrestrial detrital input, decreasing bioproductivity, and the development of oxic conditions.

4.5.1.2 Millimeter-Scale Geochemistry and Sea-Level Controls

Interpretations based on geochemical profiles of analyses of 10 cm slabs at meter-scale sampling (Fig. 4.4) identifies the connections between sea level and organic richness (previous section), but the immediate control on organic enrichment is unclear because of synchronous variations in geochemical proxies, most notably proxies for redox conditions and bioproductivity. In order to deconvolve these relationships, we apply millimeter-resolution geochemical analysis (Fig. 4.5) to identify the immediate controls on organic matter accumulation during relative sea-level changes and classify interpretation of these high-resolution profiles based on whether they indicate a redox, bioproductivity, or a dilution control and whether feedback develops between these controls.

More than half of the samples of TST1 and TST3, both deposited during third-order highstand, exhibit the pattern of bioproductivity-driven OC accumulation (Table 4.1, Fig. 4.5). Some of these bioproductivity-control samples also exhibit the feedback of bioproductivity influencing redox (Fig. 4.5), indicating the organic flux by bioproductivity consumed free oxygen in the bottom water, leading to anoxic conditions. Thus, at least at a lamina scale,

bioproductivity was the trigger for organic enrichment. Anoxia was of secondary importance and, in some case, a consequence of elevated bioproductivity. In TST1, a large number of samples also show organic accumulation controlled by terrestrial dilution, which present as millimeter-scale beds with sharply increased Al% that may be related to temporary changes in fluvial or aeolian discharge (Chapter 2). A significant fraction of the samples exhibiting a redox control in the entire shale are in TST1 (Fig. 4.5, Table 4.1), demonstrating redox as a secondary control on organic richness in TST1. In TST3, the fraction of the samples exhibiting a terrestrial dilution control is smaller than those of the samples exhibiting a bioproductivity control (Table 4.1), so the terrestrial dilution during this third-order sea-level rising is a secondary control on organic matter accumulation.

In HST1 and HST3, samples exhibiting bioproductivity and terrestrial dilution controls are abundant (Fig. 4.5, Table 4.1), indicating that, similar to TSTs, bioproductivity and dilution are the primary controls on organic richness in these two units. HST2 exhibits a significant control by carbonate dilution (Fig. 4.5, Table 4.1). HST2 was superimposed on a second-order lowstand; thus, the relative sea level was lower than during the deposition of HST1 and HST3, which were both superimposed on second-order sea-level highstands. Prior work (Potma et al., 2012) proposed that the carbonate platform was developed during the deposition of the Evie Member and Otter Park Member, i.e., HST1 and HST2, in which carbonate shedding process was the main source of carbonate input (Ayranci et al., 2018a), so the difference between carbonate input contributions in HST1 and HST2 is likely related to second-order sea level, where the platform was shallowly submerged in HST2 and more deeply submerged in HST1. The geochemical interpretation of a higher carbonate input by highstand platform shedding during the deposition in HST2 is supported by lithofacies analysis (Ayranci et al., 2018a), which

found that massive mudstone was dominant in HST1, and heterolithic calcareous siltstone and massive mudstone were dominant in HST2. The second-order sea-level highstand in the Muskwa was so profound that, even during the deposition of HST3 (upper Muskwa Formation), the carbonate platform remained drowned, shutting off carbonate production (Potma et al., 2012), supported by the rare occurrence of samples exhibiting carbonate dilution control.

LST3 and FSST in the Otter Park Member (a negligible number of samples were analyzed from LST1) have a large fraction of samples exhibiting control by terrestrial dilution (Fig. 4.5, Table 4.1), with additional samples indicating control by carbonate dilution (Fig. 4.5). This suggests that during the deposition of FSST and LST3, the carbonate platform shed sediment as it did during deposition of HST2. Many more samples in FSST and LST3 show a terrestrial dilution control (Fig. 4.5, Table 4.1), indicating active clastic transport during this sea-level lowstand, where the sea level was below carbonate platform edge (Potma et al., 2012), so the carbonate production was ceased. These few samples exhibiting a carbonate control represent times of short-lived sea level above the platform surface and therefore carbonate shedding. The main fraction of the samples exhibiting a feedback of terrestrial nutrient influencing bioproductivity are observed within FSST and LST3 (Fig. 4.5, Table 4.2), also related to the sea-level lowstand. The high clastic transport to the distal area may have contributed terrestrial nutrients to drive primary productivity during the sea-level lowstand.

4.5.2 Effects of Varying Sample Spacing of Meter and Millimeter Scale and Analytical Methods

The meter-scale analysis presented here compared a set of proxies for bioproductivity, redox conditions, and sediment flux to organic matter profiles and concluded that all three parameters collectively controlled OM accumulation in the Horn River shale, based on their

apparently synchronous variations in stratigraphic profiles (Fig. 4.2), similar to the results of Dong et al. (2018). Recognizing interactions between the different controls, Dong et al. (2018) concluded that redox states exerted the primary control for OM accumulation, based on the strength of correlation between individual proxies and TOC.

Our analysis of the same geochemical proxies for the TATTOO core as in the Dong et al. (2018) study (Fig. 4.6) yielded similar results. Th/U ratios, where 0.6 is the threshold of anoxic and dysoxic conditions (Adams and Weaver, 1958; Dong et al., 2018; Lash and Blood, 2014), effectively differentiate high from low TOC values, although a wide range of TOC values characterize samples with Th/U ratios of less than 0.6 (indicating anoxic conditions). Proxies for bioproductivity (biogenic Si), clays (Al), and carbonates (Ca) show weak or no correlations to TOC (Figs. 4.6B-D). A comparison of correlation strength between different proxies and TOC suggests that redox conditions are the primary control on OM accumulation, bioproductivity is secondary, and dilution has unclear influence in OM accumulation, consistent with Dong et al.'s (2018) results.

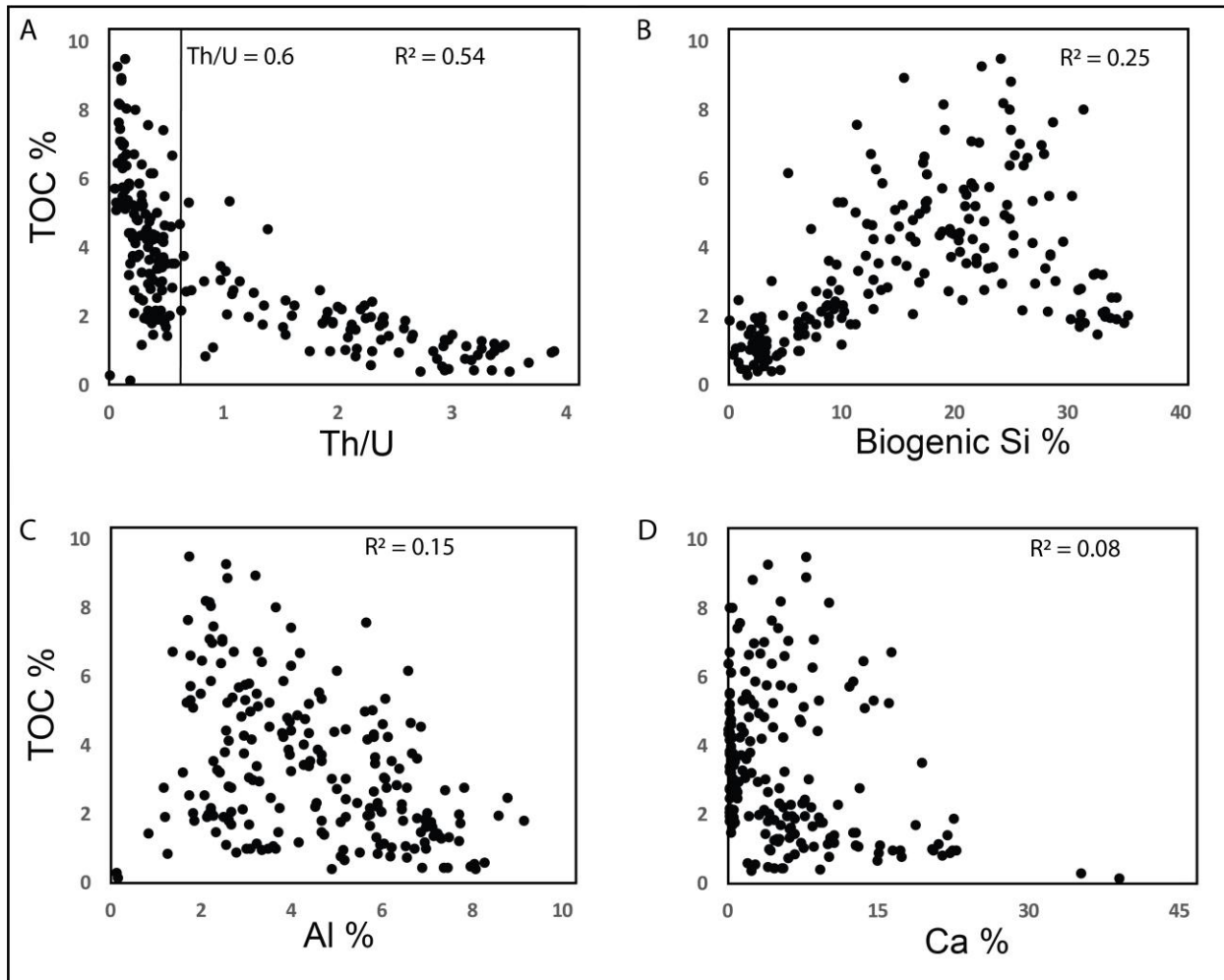


Figure 4.6. Relationships between total organic carbon (TOC) and redox, bioproductivity, and dilution proxies. (A) TOC vs. redox proxy, Th/U, cross plot. Th/U < 0.6 is considered to indicate anoxic conditions; Th/U > 0.6 is for dysoxic/oxic conditions. (B) TOC vs. bioproductivity proxy, biogenic Si, cross plot. They have weak relationship. (C) TOC vs. terrestrial dilution proxy, Al, cross plot. No correlation is identified. (D) TOC vs. carbonate dilution proxy, Ca, cross plot. No correlation is identified.

A bivariate regression analysis can be problematic when comparing data from all stratigraphic units, because it may weaken the influence of certain formations that have fewer

samples and thereby obscure the influences by sea-level changes that are varied between formations. Thus, we extend our examination of correlations between TOC and environmental proxies into different stratigraphic units in Figure 4.7. We organized the plots following second-order relative sea level, i.e., a sea-level highstand in the Evie Member and Muskwa Formation, and a sea-level lowstand in the Otter Park Member. In the Muskwa Formation and Evie Member, proxies for bioproductivity and dilution show weak correlations with TOC (Fig. 4.7). In the Muskwa Formation, a relatively strong correlation between Th/U and %TOC (Fig. 4.7A) suggests that redox control was important for organic richness in the Muskwa Formation; however, the range of variation in %TOC at the similar Th/U ratio is large, for example, samples a, b, and c, which represent a range of TOC values at similar Th/U ratio (Th/U ~ 0.5). In these three samples, TOC content decreases with increasing biogenic Si content (Fig. 4.7A), indicating an autodilution control by biogenic Si, consistent with what we discussed in Section 4.5.1.1 based on the meter-scale profile. Thus, the very weak correlation between biogenic Si and TOC contents in the Muskwa Formation (Fig. 4.7A) indicates an offset of the positive correlation between bioproductivity and organic richness and the negative correlation between autodilution and organic richness. In contrast, samples in the Evie Member that exhibit similar redox conditions, for example, samples d, e, and f (Th/U ~ 0.2), do not show a negative correlation between TOC and biogenic Si contents (Fig. 4.7C), so here the autodilution effect is less significant. In addition, although we observe a strong relationship between Th/U and %TOC in the Evie Member (Fig. 4.7C), because of a limited number of samples (one sample) with Th/U ratios more than 0.6 (indicating oxic conditions), it is difficult to evaluate the actual importance of redox control on organic richness.

Regression analysis of the Otter Park Member shows a negative correlation between TOC and dilution proxies and a positive correlation between TOC and the bioproductivity proxy (Fig. 4.7B). Thus, dilution and bioproductivity both influenced organic matter accumulation in the Otter Park Member. We apply an Al and Ca combination to represent dilution is because of both high siliciclastic and carbonate input in this formation (Fig. 4.4). A weaker correlation between Th/U ratios and %TOC in the Otter Park Member (Fig. 4.7B), indicating a less important redox control on organic matter accumulation in this formation. The negative correlation between %Si_{bio} and Th/U ratios (Fig. 4.7B) suggests a possible feedback loop between redox conditions and bioproductivity. Based on the similar R-squared values between %TOC and %(Al + Ca), and between %TOC and %Si_{bio} (Fig. 4.7B), it is difficult to identify a more significant control between dilution and bioproductivity on organic richness. However, the interpretation based on millimeter-scale analysis suggests that dilution is the most common control on organic matter accumulation in the Otter Park Member.

We propose three factors that may develop a positive Si_{bio}-TOC correlation in the regression analysis of the Otter Park Member. First, bioproductivity can inherently influence organic richness by directly providing organic flux to the sediments. Second, the oxic conditions (indicated by high Th/U ratios) that generally characterized Otter Park Member deposition should have had a negative effect on phosphorus remineralization, i.e., limiting nutrients supply, and therefore influenced bioproductivity, indicated by the negative correlation between Th/U and biogenic Si (Fig. 4.7B). Redox conditions thus influenced both organic matter preservation and bioproductivity and therefore developed a positive correlation between biogenic Si and TOC. Finally, because the sum of the total elemental concentrations is 1, when the fractions of dilution-related components, such as Al, Ca, and Ti, are high, other elemental concentration are

diluted, which can force a positive correlation between those diluted elements, e.g., TOC and Si_{bio} . In sum, an analysis of whole core slabs leads to the following conclusions: (1) autodilution, bioproductivity, and redox conditions collectively influenced organic matter accumulation in the Muskwa Formation, but the primary control is unclear; (2) controls on organic richness are unclear in the Evie Member because of almost no redox difference in this formation and very weak correlation between TOC and other proxies; (3) bioproductivity, dilution, and redox conditions influenced organic matter accumulation in the Otter Park Member, but the predominant control is unclear because the strength of correlations between TOC and bioproductivity and dilution proxies is similar.

Given the autodilution effect by biogenic silica in the upper HST3 of the Muskwa Formation (Figs. 4.4 and 4.7A), we plot biogenic Si and TOC contents of the samples from upper HST3 and the rest of the Horn River Group (Fig. 4.7D). The negative correlation between HST3 validate the interpretation of autodilution on organic carbon concentration, and the stronger correlation between biogenic Si and TOC contents in the rest shale (Fig. 4.7D) compared to the correlation in the entire Horn River Group (Fig. 4.6) indicates the bioproductivity is another significant control on organic richness during the deposition of the Horn River shale except for upper HST3.

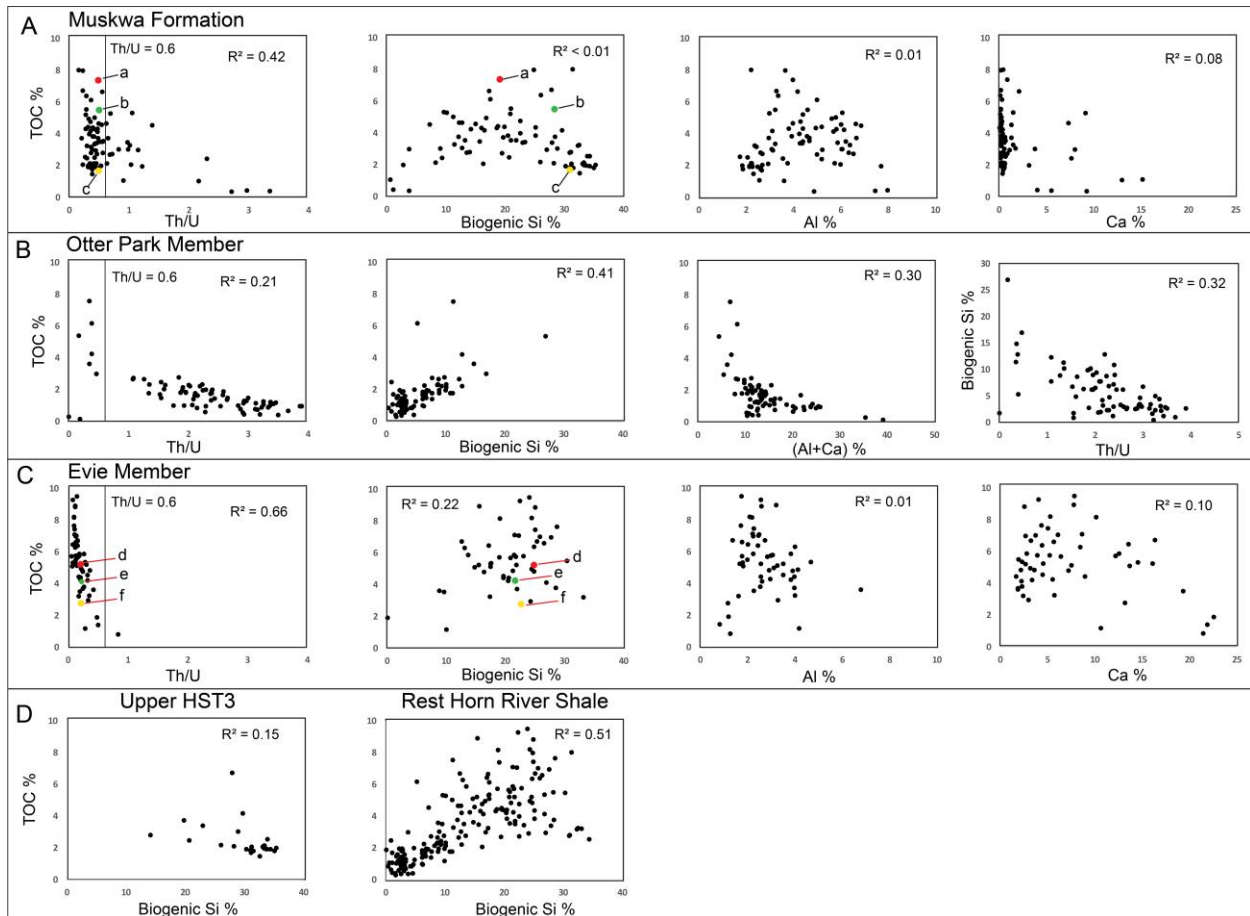


Figure 4.7. Relationships between total organic carbon (TOC) and redox, bioproductivity, and dilution proxies in the Evie Member, Otter Park Member, and the Muskwa Formation. (A) Relationships between proxies and TOC in the Muskwa Formation. Red, green, and yellow colored samples (a, b, and c) in the plots of Th/U vs. TOC and biogenic Si vs. TOC are the same. (B) Relationships between proxies and TOC, and between Th/U and biogenic Si in the Otter Park Member. (C) Relationships between proxies and TOC in the Evie Member. Red, green, and yellow colored samples (d, e, and f) in the plots of Th/U vs. TOC and biogenic Si vs. TOC are the same. (D) Relationships between biogenic Si and TOC in the upper HST3 of the Muskwa Formation and the rest Horn River shale.

In contrast, analysis of millimeter-scale geochemical profiles in this study identifies bioproductivity and clastic dilution as the most common controls on OM accumulation in this shale, with the exception of carbonate dilution as the primary control on OM accumulation in HST2 (Fig. 4.5). Because the cores in the Dong et al. (2018) and our studies are located in close proximity in a distal part of the basin (ConocoPhillips McAdam C-87-K/094-O-7 core and EOG TATTOO D-A28-F/094-O-10 core), differences in local environmental influences on OM accumulation were minimal, and different observation scales (meter- and millimeter-scale) and analytical methods are likely the reasons of the apparent contradictions between the whole slab data set and the high-resolution profiles.

Interpretations from Dong et al.'s (2018) study and our meter-scale sample analysis are based on core slabs that averaged ~ 10 cm of stratigraphic section. Based on an average sedimentation rate of ~ 0.02 – 0.03 mm/yr during the deposition of the Horn River Group (Chapter 2), a meter-scale spacing is approximately equivalent to tens of thousands of years, and each ~ 10-cm-long core slab represents timescale of a few thousand years. The meter-scale geochemical data therefore represent long-term depositional conditions and processes. However, these conditions may not represent for actual events responsible for organic carbon deposition. In contrast, millimeter-resolution profiles emphasize small-scale variations (Chapter 2) and thus the immediate triggers for OC accumulation, but may underestimate the role of relative long-term conditions on OM accumulation, for example, deepwater redox conditions that may vary with relative sea-level change. Thus, long-term conditions necessary for OM accumulation are effectively illustrated by meter-scale profiles (Fig. 4.4) based on composite analysis of 10 cm slabs, while the millimeter-resolution profiles effectively identifies the actual triggers for OM

accumulation (Fig. 4.3; Chapter 2), which are highly variable over time scales of centuries to millennia.

4.6 CONCLUSION

This high-resolution analysis of a long-drill core of the Middle-Upper Devonian Horn River Group at the distal Horn River Basin provides evidence of the sea-level control on OM accumulation at multiple time scales: (1) bioproductivity is significant for OM accumulation during the third-order highstand, including Evie Member (TST1 and HST1) and Muskwa Formation (TST3 and HST3); (2) terrestrial dilution is important for OM accumulation during the deposition of the Evie Member (TST1 and HST1), Otter Park Member (LST2, TST2, HST2, FSST, and LST3), and upper Muskwa Formation (HST3); (3) carbonate platform shedding significantly diluted OM concentration in HST2; (4) redox conditions are the secondary control during the deposition of lower Evie Member (TST1).

Comparisons between millimeter- and meter-resolution datasets and between distribution of samples with different organic matter accumulation processes analysis and regression analysis demonstrate the effects of observation scales and analytical methods on the results. Long-term changes in paleoredox conditions are illustrated by meter-scale sampling, and microsampling effectively reflects short-lived organic carbon accumulation events. Regression analysis may obscure characteristics of few samples in the study of the whole formation.

4.7 ACKNOWLEDGMENTS

We thank Dr. Nancy Zhang and Mr. Peng Li for their assistance with EDXRF analysis.

4.8 REFERENCES CITED

- Adams, J.A.S., Weaver, C.E., 1958. Thorium to uranium ratios as indicators of sedimentary processes: Examples of the concept of geochemical facies: AAPG Bulletin, v. 42, p. 387–430. doi:10.1306/0BDA5A89-16BD-11D7-8645000102C1865D.
- Algeo, T.J., and Liu, J., 2020, A re-assessment of elemental proxies for paleoredox analysis: Chemical Geology, v. 540, doi:10.1016/j.chemgeo.2020.119549.
- Algeo, T.J., Schwark, L., and Hower, J.C., 2004, High-resolution geochemistry and sequence stratigraphy of the Hushpuckney Shale (Swope Formation, eastern Kansas): Implications for climato-environmental dynamics of the Late Pennsylvanian Midcontinent Seaway: Chemical Geology, v. 206, p. 259–288, doi:10.1016/j.chemgeo.2003.12.028.
- Arthur, M.A., and Sageman, B.B., 1994, Marine Black Shales: Depositional Mechanisms and Environments of Ancient Deposits: Annual Review of Earth and Planetary Sciences, v. 22, p. 499–551, doi:10.1146/annurev.ea.22.050194.002435.
- Arthur, M.A., and Sageman, B.B., 2005, Sea-level control on source-rock development: Perspectives from the Holocene Black Sea, the Mid-Cretaceous Western Interior Basin of North America, and the Late Devonian Appalachian Basin, *in* Harris, N.B., ed, The Deposition of Organic-Carbon-Rich Sediments: Models, Mechanisms, and Consequences: Society for Sedimentary Geology, Tulsa, Oklahoma, Special Publication 82, p. 35–59.
- Ayranci, K., Harris, N.B., and Dong, T., 2018a, Sedimentological and Ichnological Characterization of the Middle to Upper Devonian Horn River Group, British Columbia, Canada: Insights into Mudstone Depositional Conditions and Processes Below Storm Wave Base: Journal of Sedimentary Research, v. 88, p. 1–23, doi:10.2110/jsr.2017.76.

- Ayranci, K., Harris, N.B., and Dong, T., 2018b, High resolution sequence stratigraphic reconstruction of mud-dominated systems below storm wave base: A case study from the Middle to Upper Devonian Horn River Group, British Columbia, Canada: *Sedimentary Geology*, v. 373, p. 239–253, doi:10.1016/j.sedgeo.2018.06.009.
- Bohacs, K.M., Jr., Grabowski, G.J., Carroll, A.R., Mankiewicz, P.J., Miskell-Gerhardt, K.J., Schwalbach, J.R., Wegner, M.B., and Simo, J.A., 2005, Production, destruction, and dilution—the many paths to source-rock development, *in* Harris, N.B., ed, *The Deposition of Organic-Carbon-Rich Sediments: Models, Mechanisms, and Consequences*: Society for Sedimentary Geology, Tulsa, Oklahoma, Special Publication 82, p. 61–101.
- Dong, T., Harris, N.B., and Ayranci, K., 2018, Relative sea-level cycles and organic matter accumulation in shales of the Middle and Upper Devonian Horn River Group, northeastern British Columbia, Canada: Insights into sediment flux, redox conditions, and bioproductivity: *Bulletin of the Geological Society of America*, v. 130, p. 859–880, doi:10.1130/B31851.1.
- Erlich, R.N., Macsotay, O., Nederbragt, A.J., and Lorente, M.A., 1999, Palaeoecology, palaeogeography and depositional environments of Upper Cretaceous rocks of western Venezuela: *Palaeogeography, Palaeoclimatology, Palaeoecology*, v. 153, p. 203–238, doi:10.1016/S0031-0182(99)00072-3.
- Feinstein, S., Williams, G.K., Snowdon, L.R., Brooks, P.W., Fowler, M.G., Goodarzi, F., and Gentzis, T., 1991, Organic geochemical characterization and hydrocarbon generation potential of mid-Late Devonian Horn River bituminous shales, southern Northwest Territories: *Bulletin of Canadian Petroleum Geology*, v. 39, p. 192–202.

- Harris, N.B., McMillan, J.M., Knapp, L.J., and Mastalerz, M., 2018, Organic matter accumulation in the Upper Devonian Duvernay Formation, Western Canada Sedimentary Basin, from sequence stratigraphic analysis and geochemical proxies: *Sedimentary Geology*, v. 376, p. 185–203, doi:10.1016/j.sedgeo.2018.09.004.
- Jones, M.M., Sageman, B.B., and Meyers, S.R., 2018, Turonian sea level and paleoclimatic events in astronomically tuned records from the Tropical North Atlantic and Western Interior Seaway: *Paleoceanography and Paleoclimatology*, v. 33, p. 470–492, doi:10.1029/2017PA003158.
- Kaufmann, B., 2006, Calibrating the Devonian Time Scale: A synthesis of U–Pb ID–TIMS ages and conodont stratigraphy: *Earth-Science Reviews*, v. 76, p. 175–190, doi:10.1016/j.earscirev.2006.01.001.
- Kendall, C.G.St.C., and Schlager, W., 1981, Carbonates and relative changes in sea level: *Marine Geology*, v. 44, p. 181–212, doi:10.1016/0025-3227(81)90118-3.
- Lash, G.G., and Blood, D.R., 2014, Organic matter accumulation, redox, and diagenetic history of the Marcellus Formation, southwestern Pennsylvania, Appalachian basin: *Marine and Petroleum Geology*, v. 57, p.244–263, doi:10.1016/j.marpetgeo.2014.06.001.
- Li, Y., Zhang, T., Ellis, G.S., and Shao, D., 2017, Depositional environment and organic matter accumulation of Upper Ordovician–Lower Silurian marine shale in the Upper Yangtze Platform, South China: *Palaeogeography, Palaeoclimatology, Palaeoecology*, v. 466, p. 252–264, doi:10.1016/j.palaeo.2016.11.037.
- Moghadam, A., Harris, N.B., Ayranci, K., Gomez, J.S., Angulo, N.A., and Chalaturnyk, R., 2019, Brittleness in the Devonian Horn River shale, British Columbia, Canada: *Journal of Natural Gas Science and Engineering*, v. 62, p. 247–258, doi:10.1016/j.jngse.2018.12.012.

- Morrow, D.W., 2012, Devonian of the Northern Canadian Mainland Sedimentary Basin (a Contribution to the Geological Atlas of the Northern Canadian Mainland Sedimentary Basin): Calgary, Alberta, Geological Survey of Canada, doi:10.4095/290970.
- Mossop, G.D., and Shetsen, I., 1994, Geological Atlas of the Western Canada Sedimentary Basin: Calgary, Alberta, Canadian Society of Petroleum Geologists and Alberta Research Council, 510 p: http://www.ags.gov.ab.ca/publications/wcsb_atlas/atlas.html.
- Oldale, H.S., and Munday, R.J., 1994, Devonian Beaverhill Lake Group of the Western Canada Sedimentary Basin, *in* Mossop, G., et al., Atlas of the Western Canada Sedimentary Basin: Canada's Energy Geoscientists, Calgary, p. 148–163.
- Obermajer, M., Stasiuk, L.D., Fowler, M.G., and Osadetz, K.G., 1999, Application of acritarch fluorescence in thermal maturity studies: *International Journal of Coal Geology*, v. 39, p. 185–204, doi:10.1016/S0166-5162(98)00045-7.
- Ocubalidet, S.G., Rimmer, S.M., and Conder, J.A., 2018, Redox conditions associated with organic carbon accumulation in the Late Devonian New Albany Shale, west-central Kentucky, Illinois Basin: *International Journal of Coal Geology*, v. 190, p. 42–55, doi:10.1016/j.coal.2017.11.017.
- Potma, K., Jonk, R., Matthew, D., Austin, N., 2012. A mudstone lithofacies classification of the Horn River Group: integrated stratigraphic analysis and inversion from wireline log and seismic data: Sixth BC Unconventional Gas Technical Forum.
- Rimmer, S.M., Thompson, J.A., Goodnight, S.A., and Robl, T.L., 2004, Multiple controls on the preservation of organic matter in Devonian–Mississippian marine black shales: geochemical and petrographic evidence: *Palaeogeography, Palaeoclimatology, Palaeoecology*, v. 215, p. 125–154, doi:10.1016/j.palaeo.2004.09.001.

- Rivard, B., Harris, N.B., Feng, J., and Dong, T., 2018, Inferring total organic carbon and major element geochemical and mineralogical characteristics of shale core from hyperspectral imagery: *AAPG Bulletin*, v. 102, p. 2101–2121, doi:10.1306/03291817217.
- Ross, D.J.K., and Bustin, R.M., 2009, Investigating the use of sedimentary geochemical proxies for paleoenvironment interpretation of thermally mature organic-rich strata: Examples from the Devonian-Mississippian shales, Western Canadian Sedimentary Basin: *Chemical Geology*, v. 260, p. 1–19, doi:10.1016/j.chemgeo.2008.10.027.
- Sageman, B.B., Murphy, A.E., Werne, J.P., Ver Straeten, C.A., Hollander, D.J., and Lyons, T.W., 2003, A tale of shales: the relative roles of production, decomposition, and dilution in the accumulation of organic-rich strata, Middle–Upper Devonian, Appalachian basin: *Chemical Geology*, v. 195, p. 229–273, doi:10.1016/S0009-2541(02)00397-2.
- Schieber, J., Krinsley, D., and Riciputi, L., 2000, Diagenetic origin of quartz silt in mudstones and implications for silica cycling: *Nature*, v. 406, p. 981–985, doi:10.1038/35023143.
- Stasiuk, L.D., and Fowler, M.G., 2004, Organic facies in Devonian and Mississippian strata of Western Canada Sedimentary Basin: relation to kerogen type, paleoenvironment, and paleogeography: *Bulletin of Canadian Petroleum Geology*, v. 52, p. 234–255, doi:10.2113/52.3.234.
- Tribovillard, N., Algeo, T. J., Lyons, T., and Riboulleau, A., 2006, Trace metals as paleoredox and paleoproductivity proxies: An update: *Chemical Geology*, v. 232, p. 12–32, doi:10.1016/j.chemgeo.2006.02.012.
- Wedepohl, K.H., 1971, Environmental influences on the chemical composition of shales and clays: *Physics and Chemistry of the Earth*, v. 8, p. 307–333, doi:10.1016/0079-1946(71)90020-6.

CHAPTER 5 CONCLUSIONS

This thesis describes and interprets geochemical, petrological, and stratigraphic analyses of core samples from the Middle-Upper Devonian Horn River Group, in the northwestern Western Canada Sedimentary Basin. The objectives of this study are to investigate immediate triggers for organic matter accumulation and to relate organic matter (OM) accumulation processes to sea level change.

5.1 PROCESSES OF ORGANIC MATTER ACCUMULATION

Chapter 2 introduces and applies millimeter-resolution geochemical analysis of shale core samples through Energy Dispersive X-ray Fluorescence (EDXRF) scan and hyperspectral imagery scan on 133 ~ 10 cm core slabs from TATTOO core of the Horn River shale in the distal part of the Horn River Basin. This chapter applies proxies for redox conditions, bioproductivity, and mineral flux in the context of organic matter accumulation and identifies three different controls on the OM burial in different intervals of the Horn River shale based on the strong correlation between geochemical proxies and TOC content in geochemical profiles. Bioproductivity and dilution by siliciclastic or carbonate input are the most common controls on organic richness, while redox controls are less common in the entire Horn River Group. Two redox-bioproductivity feedbacks, are identified based on the 1 – 3 mm offset between Si_{bio} -S/Fe profiles, in which (1) phosphorus released from sediments favored by deepwater anoxia recirculated to stimulated bioproductivity, and (2) organic flux from bioproductivity were oxidized and therefore consumed free oxygen in the water column, leading to less oxic conditions. A feedback that terrestrial nutrients influenced marine bioproductivity is observed based on ~ 1 mm offsets between Al and Si_{bio} profiles. These offsets indicate the time required for feedbacks to develop is on the scale of decades to centuries.

5.2 PETROGRAPHIC VALIDATION ON GEOCHEMICAL FEATURES

We compare geochemical profiles based on high resolution analysis to petrographic features observed in thin section and SEM analysis. Petrographic analysis observes biogenic microcrystalline silica and carbonate bioclasts, corresponding to geochemically observed biogenic input of silica and carbonate input. Calcite silt grains associated with hyperpycnal flow-related sedimentary structures, and abundant carbonate bioclasts are observed separately in mudstones, demonstrating different processes related to carbonate dilution that cannot be distinguished from geochemical profiles alone. This chapter also identifies authigenic pyrite and diagenetic ferroan dolomite in the samples exhibiting high S/Fe ratios and high Ca signal; such high contribution by diagenetic minerals overprinted the deposition signals in geochemistry.

5.3 SEA LEVEL CONTROL ON ORGANIC MATTER ACCUMULATION

Chapter 4 documents the distribution of OM enrichment patterns in a sequence stratigraphic framework, most strongly associated with the 3rd order sea-level change. Millimeter-scale geochemical analysis identifies that (1) bioproductivity is significant for organic richness during the deposition of the Evie Member (TST1 and HST1) and Muskwa Formation (TST3 and HST3), (2) terrestrial detrital dilution is the predominant control on organic matter accumulation during the deposition of the Evie Member (TST1 and HST1), Otter Park Member (LST2, TST2, HST2, FSST, and LST3), and upper Muskwa Formation (HST3), (3) carbonate dilution is a common control during the deposition of the middle Otter Park Member (HST2).

5.4 EFFECTS OF DIFFERENT SAMPLING SCALES AND ANALYTICAL METHODS

Chapter 4 applies both meter-scale and millimeter-scale geochemical datasets to identify the sea-level control on organic matter accumulation. However, two datasets yield different interpretations: meter-scale data identify redox is the primary control, and in contrast, millimeter-

scale data suggest bioproductivity and terrestrial input are significant for organic richness. The contradictory results are considered to come from the different sample spacings. Long-term conditions required for OM accumulation are effectively illustrated by meter-scale profiles, in which meter-scale spacing between two analytical spots represents tens of thousands of years, while the millimeter-resolution profiles effectively identify the actual triggers for OM accumulation, which are highly variable over time scales of centuries to millennia.

This thesis provides an insight into the short-term controls on organic matter accumulation and shows the necessity of millimeter-resolution dataset to illustrate actual organic enrichment events. For further research, a high-resolution sedimentation rate study is required in order to be accurate about time period estimates of feedback loops. High-resolution measurements of trace elements to indicate redox conditions, bioproduction, and terrestrial input are also needed to complement the interpretations of paleoenvironmental perturbations in this thesis. A study of the distances of bitumen migration within this shale can directly illustrate the influences of thermal maturation and hydrocarbon expulsion on the use of TOC to represent original organic richness in this study based on millimeter-scale analysis.

REFERENCES CITED

- Adams, J.A.S., Weaver, C.E., 1958. Thorium to uranium ratios as indicators of sedimentary processes: Examples of the concept of geochemical facies: AAPG Bulletin, v. 42, p. 387–430. doi:10.1306/0BDA5A89-16BD-11D7-8645000102C1865D.
- Algeo, T.J., Henderson, C.M., Tong, J., Feng, Q., Yin., H., and Tyson, R.V., 2013, Plankton and productivity during the Permian–Triassic boundary crisis: An analysis of organic carbon fluxes: *Global and Planetary Change*, v. 105, p. 52–67, doi:10.1016/j.gloplacha.2012.02.008.
- Algeo, T.J., Kuwahara, K., Sano, H., Bates, S., Lyons, T., Elswick, E., Hinnov, L., Ellwood, B., Moser, J., and Maynard, J.B., 2011, Spatial variation in sediment fluxes, redox conditions, and productivity in the Permian-Triassic Panthalassic Ocean: *Palaeogeography, Palaeoclimatology, Palaeoecology*, v. 308, p. 65–83, doi:10.1016/j.palaeo.2010.07.007.
- Algeo, T.J., and Liu, J., 2020, A re-assessment of elemental proxies for paleoredox analysis: *Chemical Geology*, v. 540, doi:10.1016/j.chemgeo.2020.119549.
- Algeo, T.J., Lyons, T.W., Blakey, R.C., and Over, D.J., 2007, Hydrographic conditions of the Devonian–Carboniferous North American Seaway inferred from sedimentary Mo–TOC relationships: *Palaeogeography, Palaeoclimatology, Palaeoecology*, v. 256, p. 204–230, doi:10.1016/j.palaeo.2007.02.035.
- Algeo, T.J., Schwark, L., and Hower, J.C., 2004, High-resolution geochemistry and sequence stratigraphy of the Hushpuckney Shale (Swope Formation, eastern Kansas): Implications for climato-environmental dynamics of the Late Pennsylvanian Midcontinent Seaway: *Chemical Geology*, v. 206, p. 259–288, doi:10.1016/j.chemgeo.2003.12.028.

- Aller, R.C., 1994, Bioturbation and remineralization of sedimentary organic matter: effects of redox oscillation: *Chemical Geology*, v. 114, p. 331–345, doi:10.1016/0009-2541(94)90062-0.
- Al Rajaibi, I.M., Hollis, C., Macquaker, J.H., 2015, Origin and variability of a terminal Proterozoic primary silica precipitate, Athel Silicilyte, South Oman Salt Basin, Sultanate of Oman: *Sedimentology*, v. 62, p. 793–825, doi:10.1111/sed.12173.
- Arthur, M.A., and Sageman, B.B., 1994, Marine Black Shales: Depositional Mechanisms and Environments of Ancient Deposits: *Annual Review of Earth and Planetary Sciences*, v. 22, p. 499–551, doi:10.1146/annurev.earth.22.050194.002435.
- Arthur, M.A., and Sageman, B.B., 2005, Sea-level control on source-rock development: Perspectives from the Holocene Black Sea, the Mid-Cretaceous Western Interior Basin of North America, and the Late Devonian Appalachian Basin, *in* Harris, N.B., ed, *The Deposition of Organic-Carbon-Rich Sediments: Models, Mechanisms, and Consequences*: Society for Sedimentary Geology, Tulsa, Oklahoma, Special Publication 82, p. 35–59.
- Ayranci, K., Harris, N.B., and Dong, T., 2018a, Sedimentological and Ichnological Characterization of the Middle to Upper Devonian Horn River Group, British Columbia, Canada: Insights into Mudstone Depositional Conditions and Processes Below Storm Wave Base: *Journal of Sedimentary Research*, v. 88, p. 1–23, doi:10.2110/jsr.2017.76.
- Ayranci, K., Harris, N.B., and Dong, T., 2018b, High resolution sequence stratigraphic reconstruction of mud-dominated systems below storm wave base: A case study from the Middle to Upper Devonian Horn River Group, British Columbia, Canada: *Sedimentary Geology*, v. 373, p. 239–253, doi:10.1016/j.sedgeo.2018.06.009.

- Betts, J.N., and Holland, H.D., 1991, The oxygen content of ocean bottom waters, the burial efficiency of organic carbon, and the regulation of atmospheric oxygen: *Palaeogeography, Palaeoclimatology, Palaeoecology*, v. 97, p. 5–18, doi:10.1016/0031-0182(91)90178-T.
- Berner, R.A., 1968, Calcium carbonate concretions formed by the decomposition of organic matter: *Science*, v. 159, p. 195–197, doi:10.1126/science.159.3811.195.
- Berner, R.A., and Raiswell, R., 1983, Burial of organic carbon and pyrite sulfur in sediments over phanerozoic time: a new theory: *Geochimica et Cosmochimica Acta*, v. 47, p. 855–862, doi:10.1016/0016-7037(83)90151-5.
- Bohacs, K.M., Jr., Grabowski, G.J., Carroll, A.R., Mankiewicz, P.J., Miskell-Gerhardt, K.J., Schwalbach, J.R., Wegner, M.B., and Simo, J.A., 2005, Production, destruction, and dilution—the many paths to source-rock development, *in* Harris, N.B., ed, *The Deposition of Organic-Carbon-Rich Sediments: Models, Mechanisms, and Consequences*: Society for Sedimentary Geology, Tulsa, Oklahoma, Special Publication 82, p. 61–101.
- Boulestex, K., Poyatos-Moré, M., Flint, S.S., Taylor, K.G., Hodgson, D.M., and Hasiotis, S.T., 2019, Transport and deposition of mud in deep-water environments: Processes and stratigraphic implications: *Sedimentology*, v. 66, p. 2894–2925, doi:10.1111/sed.12614.
- Cottingham, K.L., Knight, S.E., Carpenter, S.R., Cole, J.J., Pace, M.L., and Wagner, A.E., 1997, Response of phytoplankton and bacteria to nutrients and zooplankton: a mesocosm experiment: *Journal of Plankton Research*, v. 19, p. 995–1010, doi:10.1093/plankt/19.8.995.
- Dahl, T.W., Siggaard-Andersen, M., Schovsbo, N.H., Persson, D.O., Husted, S., Hougård, I.W., Dickson, A.J., Kjær, K., and Nielsen, A.T., 2019, Brief oxygenation events in locally anoxic oceans during the Cambrian solves the animal breathing paradox: *Scientific Reports*, doi:10.1038/s41598-019-48123-2.

- Day-Stirrat, J.R., Milliken, K.L., Dutton, S.P., Loucks, R.G., Hillier, S., Aplin, A.C., AND Schleicher, A.M., 2010, Open-system chemical behavior in deep Wilcox Group mudstones, Texas Gulf Coast, USA: *Marine and Petroleum Geology*, v. 27, p. 1804–1818, doi:10.1016/j.marpetgeo.2010.08.006.
- Dong, T., and Harris, N.B., 2020, The effect of thermal maturity on porosity development in the Upper Devonian-Lower Mississippian Woodford Shale, Permian Basin, US: Insights into the role of silica nanospheres and microcrystalline quartz on porosity preservation: *International Journal of Coal Geology*, v. 217, p. 1–14, doi:10.1016/j.coal.2019.103346.
- Dong, T., Harris, N.B., and Ayranci, K., 2018, Relative sea-level cycles and organic matter accumulation in shales of the Middle and Upper Devonian Horn River Group, northeastern British Columbia, Canada: Insights into sediment flux, redox conditions, and bioproductivity: *Bulletin of the Geological Society of America*, v. 130, p. 859–880, doi:10.1130/B31851.1.
- Emeis, K.-C., Struck, U., Leipe, T., Pollehne, F., Kunzendorf, H., and Christiansen, C., 2000, Changes in the C, N, P burial rates in some Baltic Sea sediments over the last 150 years—relevance to P regeneration rates and the phosphorus cycle: *Marine Geology*, v. 167, p. 43–59, doi:10.1016/S0025-3227(00)00015-3.
- Erlich, R.N., Macsotay, O., Nederbragt, A.J., and Lorente, M.A., 1999, Palaeoecology, palaeogeography and depositional environments of Upper Cretaceous rocks of western Venezuela: *Palaeogeography, Palaeoclimatology, Palaeoecology*, v. 153, p. 203–238, doi:10.1016/S0031-0182(99)00072-3.
- Feinstein, S., Williams, G.K., Snowdon, L.R., Brooks, P.W., Fowler, M.G., Goodarzi, F., and Gentzis, T., 1991, Organic geochemical characterization and hydrocarbon generation

- potential of mid-Late Devonian Horn River bituminous shales, southern Northwest Territories: *Bulletin of Canadian Petroleum Geology*, v. 39, p. 192–202.
- Froelich, P.N., Bender, M.L., Luedtke, N.A., Heath, G.R., and DeVries, T., 1982, The marine phosphorus cycle: *American Journal of Science*, v. 282, p. 475–511, doi:10.2475/ajs.282.4.474.
- Ghadeer, S.G., and Macquaker, J.H.S., 2011, Sediment transport processes in an ancient mud-dominated succession: a comparison of processes operating in marine offshore settings and anoxic basinal environments: *Journal of the Geological Society, London*, v. 168, p. 1121–1132, doi:10.1144/0016-76492010-016.
- Harazim, D., McIlroy, D., Edwards, N.P., Wogelius, R.A., Manning, P.L., Poduska, K.M., Layne, G.D., Sokaras, D., Alonso-Mori, R., and Bergmann, U., 2015, Bioturbating animals control the mobility of redox-sensitive trace elements in organic-rich mudstone: *Geology*, v. 43, p. 1007–1010, doi:10.1130/G37025.1.
- Harris, N.B., McMillan, J.M., Knapp, L.J., and Mastalerz, M., 2018, Organic matter accumulation in the Upper Devonian Duvernay Formation, Western Canada Sedimentary Basin, from sequence stratigraphic analysis and geochemical proxies: *Sedimentary Geology*, v. 376, p. 185–203, doi:10.1016/j.sedgeo.2018.09.004.
- Harris, N.B., Mnich, C.A., Selby, D., and Korn, D., 2013, Minor and trace element and Re–Os chemistry of the Upper Devonian Woodford Shale, Permian Basin, west Texas: Insights into metal abundance and basin processes: *Chemical Geology*, v. 356, p. 76–93, doi:10.1016/j.chemgeo.2013.07.018.

- Hee, C.A., Pease, T.K., Alperin, M.J., Martens, C.S., 2001, Dissolved organic carbon production and consumption in anoxic marine sediments: A pulsed-tracer experiment: *Limnology and Oceanography*, v. 46, p. 1908–1920, doi:10.4319/lo.2001.46.8.1908.
- Ingall, E.D., Bustin, R.M., and Van Cappellen, P., 1993, Influence of water column anoxia on the burial and preservation of carbon and phosphorus in marine shales: *Geochimica et Cosmochimica Acta*, v. 57, p. 303–316, doi:10.1016/0016-7037(93)90433-W.
- Ingall, E., and Jahnke, R., 1994, Evidence for enhanced phosphorus regeneration from marine sediments overlain by oxygen depleted waters: *Geochimica et Cosmochimica Acta*, v. 58, p. 2571–2575, doi:10.1016/0016-7037(94)90033-7.
- Jenkyns, H.C., and Weedon, G.P., 2013, Chemostratigraphy (CaCO_3 , TOC, $\delta^{13}\text{C}_{\text{org}}$) of Sinemurian (Lower Jurassic) black shales from the Wessex Basin, Dorset and palaeoenvironmental implications: *Newsletters on Stratigraphy*, v. 46, p. 1–21, doi:10.1127/0078-0421/2013/0029.
- Jones, M.M., Sageman, B.B., and Meyers, S.R., 2018, Turonian sea level and paleoclimatic events in astronomically tuned records from the Tropical North Atlantic and Western Interior Seaway: *Paleoceanography and Paleoclimatology*, v. 33, p. 470–492, doi:10.1029/2017PA003158.
- Katz, B.J., 2005, Controlling factors on source rock development—a review of productivity, preservation, and sedimentation rate, *in* Harris, N.B., ed, *The Deposition of Organic-Carbon-Rich Sediments: Models, Mechanisms, and Consequences*: Society for Sedimentary Geology, Tulsa, Oklahoma, Special Publication 82, p. 7–16.

- Kaufmann, B., 2006, Calibrating the Devonian Time Scale: A synthesis of U–Pb ID–TIMS ages and conodont stratigraphy: *Earth-Science Reviews*, v. 76, p. 175–190, doi:10.1016/j.earscirev.2006.01.001.
- Kendall, C.G.St.C., and Schlager, W., 1981, Carbonates and relative changes in sea level: *Marine Geology*, v. 44, p. 181–212, doi:10.1016/0025-3227(81)90118-3.
- Kennedy, M.J., Löhr, S.C., Fraser, S.A., and Baruch, E.T., 2014, Direct evidence for organic carbon preservation as clay-organic nanocomposites in a Devonian black shale; from deposition to diagenesis: *Earth and Planetary Science Letters*, v. 388, p. 59–70, doi:10.1016/j.epsl.2013.11.044.
- Kennedy, M.J., Pevear, D.R., and Hill, R.J., 2002, Mineral Surface Control of Organic Carbon in Black Shale: *Science*, v. 295, p. 657–660, doi:10.1126/science.1066611.
- Knapp, L.J., McMillan, J.M., and Harris, N.B., 2017, A depositional model for organic-rich Duvernay Formation mudstones: *Sedimentary Geology*, v. 347, p. 160–182, doi:10.1016/j.sedgeo.2016.11.012.
- Lash, G.G., and Blood, D., 2004, Geochemical and textural evidence for early (shallow) diagenetic growth of stratigraphically confined carbonate concretions, Upper Devonian Rhinestreet black shale, western New York: *Chemical Geology*, v. 206, p. 407–424, doi:10.1016/j.chemgeo.2003.12.017.
- Lash, G.G., and Blood, D.R., 2014, Organic matter accumulation, redox, and diagenetic history of the Marcellus Formation, southwestern Pennsylvania, Appalachian basin: *Marine and Petroleum Geology*, v. 57, p.244–263, doi:10.1016/j.marpetgeo.2014.06.001.
- Li, Y., Zhang, T., Ellis, G.S., and Shao, D., 2017, Depositional environment and organic matter accumulation of Upper Ordovician–Lower Silurian marine shale in the Upper Yangtze

- Platform, South China: *Palaeogeography, Palaeoclimatology, Palaeoecology*, v. 466, p. 252–264, doi:10.1016/j.palaeo.2016.11.037.
- Little, S.H., Vance, D., Lyons, T.W., and McManus, J., 2015, Controls on trace metal authigenic enrichment in reducing sediments: Insights from modern oxygen-deficient settings: *American Journal of Science*, v. 315, p.77–119, doi:10.2475/02.2015.01.
- Loutit, T., Hardenbol, J., Vail, P., and Baum, G., 1988, Condensed sections: the key to age determination and correlation of continental margin sequences, *in* Wilgus, C.K., Hastings, B.S., Ross, C.A., Posamentier, H., Wagoner, J., Van, and Kendall, C.G.St.C., eds, *Sea-Level Changes: An Integrated Approach*: Society for Sedimentary Geology, Tulsa, Oklahoma, Special Publication 42, p. 183–213.
- Macquaker, J.H.S., and Adams, A.E., 2003, Maximizing Information from Fine-Grained Sedimentary Rocks: An Inclusive Nomenclature for Mudstones: *Journal of Sedimentary Research*, v. 73, p. 735–744, doi:10.1306/012203730735.
- Macquaker, J.H.S., Keller, M.A., and Davies, S.J., 2010, Algal blooms and ‘marine snow’: Mechanisms that enhance preservation of organic carbon in ancient fine-grained sediments: *Journal of Sedimentary Research*, v. 80, p. 934–942, doi:10.2110/jsr.2010.085.
- Meyers, P.A., 1994, Preservation of elemental and isotopic source identification of sedimentary organic matter: *Chemical Geology*, v. 114, p. 289–302, doi:10.1016/0009-2541(94)90059-0.
- Milliken, K.L., and Olson, T., 2017, Silica Diagenesis, Porosity Evolution, and Mechanical Behavior in Siliceous Mudstones, Mowry Shale (Cretaceous), Rocky Mountains, U.S.A.: *Journal of Sedimentary Research*, v. 87, p. 366–387, doi:10.2110/jsr.2017.24.

- Moghadam, A., Harris, N.B., Ayranci, K., Gomez, J.S., Angulo, N.A., and Chalaturnyk, R., 2019, Brittleness in the Devonian Horn River shale, British Columbia, Canada: *Journal of Natural Gas Science and Engineering*, v. 62, p. 247–258, doi:10.1016/j.jngse.2018.12.012.
- Morrow, D.W., 2012, Devonian of the Northern Canadian Mainland Sedimentary Basin (a Contribution to the Geological Atlas of the Northern Canadian Mainland Sedimentary Basin): Calgary, Alberta, Geological Survey of Canada, doi:10.4095/290970.
- Mossop, G.D., and Shetsen, I., 1994, Geological Atlas of the Western Canada Sedimentary Basin: Calgary, Alberta, Canadian Society of Petroleum Geologists and Alberta Research Council, 510 p: http://www.ags.gov.ab.ca/publications/wcsb_atlas/atlas.html.
- Murphy, A.E., Sageman, B.B., Hollander, D.J., Lyons, T.W., and Brett, C.E., 2000, Black shale deposition and faunal overturn in the Devonian Appalachian Basin: Clastic starvation, seasonal water – column mixing, and efficient biolimiting nutrient recycling: *Paleoceanography and Paleoclimatology*, v. 15, p. 280–291, doi:10.1029/1999PA000445.
- Oldale, H.S., and Munday, R.J., 1994, Devonian Beaverhill Lake Group of the Western Canada Sedimentary Basin, *in* Mossop, G., et al., *Atlas of the Western Canada Sedimentary Basin: Canada's Energy Geoscientists*, Calgary, p. 148–163.
- Obermajer, M., Stasiuk, L.D., Fowler, M.G., and Osadetz, K.G., 1999, Application of acritarch fluorescence in thermal maturity studies: *International Journal of Coal Geology*, v. 39, p. 185–204, doi:10.1016/S0166-5162(98)00045-7.
- Ocubalidet, S.G., Rimmer, S.M., and Conder, J.A., 2018, Redox conditions associated with organic carbon accumulation in the Late Devonian New Albany Shale, west-central Kentucky, Illinois Basin: *International Journal of Coal Geology*, v. 190, p. 42–55, doi:10.1016/j.coal.2017.11.017.

- Percival, L.M.E., Selby, D., Bond, D.P.G., Rakocińskie, M., Racki, G., Marynowski, L., Adatte, T., Spangenberg, J.E., and Föllmi, K.B., 2019, Pulses of enhanced continental weathering associated with multiple Late Devonian climate perturbations: Evidence from osmium-isotope compositions: *Palaeogeography, Palaeoclimatology, Palaeoecology*, v. 524, p. 240–249, doi:10.1016/j.palaeo.2019.03.036.
- Potma, K., Jonk, R., Matthew, D., Austin, N., 2012. A mudstone lithofacies classification of the Horn River Group: integrated stratigraphic analysis and inversion from wireline log and seismic data: Sixth BC Unconventional Gas Technical Forum.
- Pedersen, T.F., and Calvert, S.E., 1990, Anoxia vs. Productivity: What controls the formation of organic-carbon-rich sediments and sedimentary rocks?: Discussion (1): *AAPG Bulletin*, v. 74, p. 454–466, doi:10.1306/0c9b2821-1710-11d7-8645000102c1865d.
- Raiswell, R., Newton, R., Bottrell, S.H., Coburn, P.M., Briggs, D.E.G., Bond, D.P.G., and Poulton, S.W., 2008, Turbidite depositional influences on the diagenesis of Beecher's Trilobite Bed and the Hunsrück Slate; sites of soft tissue pyritization: *American Journal of Science*, v. 308, p. 105–129, doi:10.2475/02.2008.01.
- Raven, M.R., Fike, D.A., Gomes, M.L., Webb, S.M., Bradley, A.S., and McClelland, M.O., 2018, Organic carbon burial during OAE2 driven by changes in the locus of organic matter sulfurization: *Nature Communications*, doi:10.1038/s41467-018-05943-6.
- Rimmer, S.M., Thompson, J.A., Goodnight, S.A., and Robl, T.L., 2004, Multiple controls on the preservation of organic matter in Devonian–Mississippian marine black shales: geochemical and petrographic evidence: *Palaeogeography, Palaeoclimatology, Palaeoecology*, v. 215, p. 125–154, doi:10.1016/j.palaeo.2004.09.001.

- Rivard, B., Harris, N.B., Feng, J., and Dong, T., 2018, Inferring total organic carbon and major element geochemical and mineralogical characteristics of shale core from hyperspectral imagery: *AAPG Bulletin*, v. 102, p. 2101–2121, doi:10.1306/03291817217.
- Ross, D.J.K., and Bustin, R.M., 2008, Characterizing the shale gas resource potential of Devonian–Mississippian strata in the Western Canada sedimentary basin: Application of an integrated formation evaluation: *AAPG Bulletin*, v. 92, p. 87–125, doi:10.1306/09040707048.
- Ross, D.J.K., and Bustin, R.M., 2009, Investigating the use of sedimentary geochemical proxies for paleoenvironment interpretation of thermally mature organic-rich strata: Examples from the Devonian-Mississippian shales, Western Canadian Sedimentary Basin: *Chemical Geology*, v. 260, p. 1–19, doi:10.1016/j.chemgeo.2008.10.027.
- Rowe, G.T., Clifford, C.H., Smith Jr, K.L., and Hamilton, P.L., 1975, Benthic nutrient regeneration and its coupling to primary productivity in coastal waters: *Nature*, v. 225, p. 215–217, doi:10.1038/255215a0.
- Ruttenberg, K.C., 2003, The global phosphorus cycle: *Treatise on Geochemistry*, v. 8, p. 585–643, doi:10.1016/B0-08-043751-6/08153-6.
- Sageman, B.B., Murphy, A.E., Werne, J.P., Ver Straeten, C.A., Hollander, D.J., and Lyons, T.W., 2003, A tale of shales: the relative roles of production, decomposition, and dilution in the accumulation of organic-rich strata, Middle–Upper Devonian, Appalachian basin: *Chemical Geology*, v. 195, p. 229–273, doi:10.1016/S0009-2541(02)00397-2.
- Schieber, J.K., 2016, Experimental testing of the transport-durability of shale lithics and its implications for interpreting the rock record: *Sedimentary Geology*, v. 331, p. 162–169, doi:10.1016/j.sedgeo.2015.11.006.

- Schieber, J., Krinsley, D., and Riciputi, L., 2000, Diagenetic origin of quartz silt in mudstones and implications for silica cycling: *Nature*, v. 406, p. 981–985, doi:10.1038/35023143.
- Schoepfer, S.D., Shen, J., Wei, H., Tyson, R.V., Ingall, E., and Algeo, T.J., 2015, Total organic carbon, organic phosphorus, and biogenic barium fluxes as proxies for paleomarine productivity: *Earth-Science Reviews*, v. 149, p. 23–52, doi:10.1016/j.earscirev.2014.08.017.
- Sepúlveda, J., Wendler, J.E., Summons, R.E., and Hinrichs, K., 2009, Rapid resurgence of marine productivity after the Cretaceous-Paleogene mass extinction: *Science*, v. 326, p. 129–132, doi:10.1126/science.1176233.
- Sperling, E.A., Balthasar, U., and Skovsted, C.B., 2018, On the edge of exceptional preservation: insights into the role of redox state in Burgess Shale-type taphonomic windows from the Mural Formation, Alberta, Canada: *Emerging Topics in Life Sciences*, v. 2, p. 311–323, doi:10.1042/ETLS20170163.
- Stasiuk, L.D., and Fowler, M.G., 2004, Organic facies in Devonian and Mississippian strata of Western Canada Sedimentary Basin: relation to kerogen type, paleoenvironment, and paleogeography: *Bulletin of Canadian Petroleum Geology*, v. 52, p. 234–255, doi:10.2113/52.3.234.
- Torres, M.A., Kemeny, P.C., Lamb, M.P., Cole, T.L., and Fischer, W.W., 2019, Long-Term Storage and Age-Biased Export of Fluvial Organic Carbon: Field Evidence From West Iceland: *Geochemistry, Geophysics, Geosystems*, v.21, doi:10.1029/2019GC008632.
- Torres, M.A., Limaye, A.B., Ganti, V., Lamb, M.P., West, A.J., and Fischer, W.W., 2017, Model predictions of long-lived storage of organic carbon in river deposits: *Earth Surface Dynamics*, v. 5, p. 711–730, doi:10.5194/esurf-5-711-2017.

- Tribovillard, N., Algeo, T. J., Lyons, T., and Riboulleau, A., 2006, Trace metals as paleoredox and paleoproductivity proxies: An update: *Chemical Geology*, v. 232, p. 12–32, doi:10.1016/j.chemgeo.2006.02.012.
- Tyson, R.V., 2001, Sedimentation rate, dilution, preservation and total organic carbon: some results of a modelling study: *Organic Geochemistry*, v. 32, p. 333–339, doi:10.1016/S0146-6380(00)00161-3.
- Tyson, R.V., 2005, The "productivity versus preservation" controversy: cause, flaws, and resolution, *in* Harris, N.B., ed., *The Deposition of Organic-Carbon-Rich Sediments: Models, Mechanisms, and Consequences*: Society for Sedimentary Geology, Tulsa, Oklahoma, Special Publication 82, p. 17–33.
- Tribovillard, N., Algeo, T. J., Lyons, T., and Riboulleau, A., 2006, Trace metals as paleoredox and paleoproductivity proxies: An update: *Chemical Geology*, v. 232, p. 12–32, doi:10.1016/j.chemgeo.2006.02.012.
- Wedepohl, K.H., 1971, Environmental influences on the chemical composition of shales and clays: *Physics and Chemistry of the Earth*, v. 8, p. 307–333, doi:10.1016/0079-1946(71)90020-6.
- Wignall, P.B., and Newton, R.J., 1998, Pyrite framboid diameter as a measure of oxygen deficiency in ancient mudrocks: *American Journal of Science*, v. 298, p. 537–552, doi:10.2475/ajs.298.7.537.
- Wilkin, R.T., and Barnes, H.L., 1997, Formation processes of framboidal pyrite: *Geochimica et Cosmochimica Acta*, v. 61, p. 323–339, doi:10.1016/S0016-7037(96)00320-1.
- Yawar, Z., and Schieber, J., 2017, On the origin of silt laminae in laminated shales: *Sedimentary Geology*, v. 360, p. 22–34, doi:10.1016/j.sedgeo.2017.09.001.

Zhou, L., Algeo, T.J., Shen, J., Hu, Z., Gong, H., Xie, S., Huang, J., and Gao, S., 2015, Changes in marine productivity and redox conditions during the Late Ordovician Hirnantian glaciation: *Palaeogeography, Palaeoclimatology, Palaeoecology*, v. 420, p. 223–234, doi:10.1016/j.palaeo.2014.12.012.

APPENDICES

APPENDIX A: CORE DESCRIPTION AND PETROGRAPHY MICROGRAPHS

Appendix A contains core description of the TATTOO core and micrographs of the samples that are not shown in the Chapter 3. The descriptions of the slabs are in the figure captions.

The core description of TATTOO core follows the work by Moghadam et al. (2019) of the same long-drill core from the Horn River Group. Lithofacies in this core description is based on the sedimentological analysis of the Horn River Group by Ayranci et al. (2018a, b).

The Muskwa Formation mainly contains pyritic mudstone and to a lesser extend massive mudstone, composed of enriched quartz and low clay contents. In the middle Muskwa Formation, there is a thick interval of clay-rich laminated mudstone where clay compositions are relatively enriched with less abundant quartz. The Otter Park Member is composed of laminated mudstone and interbedded carbonate-rich layers. Clay contents are the most enriched in this formation (max. 60%) compared to rest Horn River Group, with less abundant quartz in this formation than the Muskwa Formation. TOC content is the lowest in the entire shale. The upper Evie Member is dominated by pyritic mudstone, and the lower Evie Member is largely composed of massive mudstone. TOC content in this formation is the highest in the entire Horn River Group and is the most enriched in the lower Evie Member.

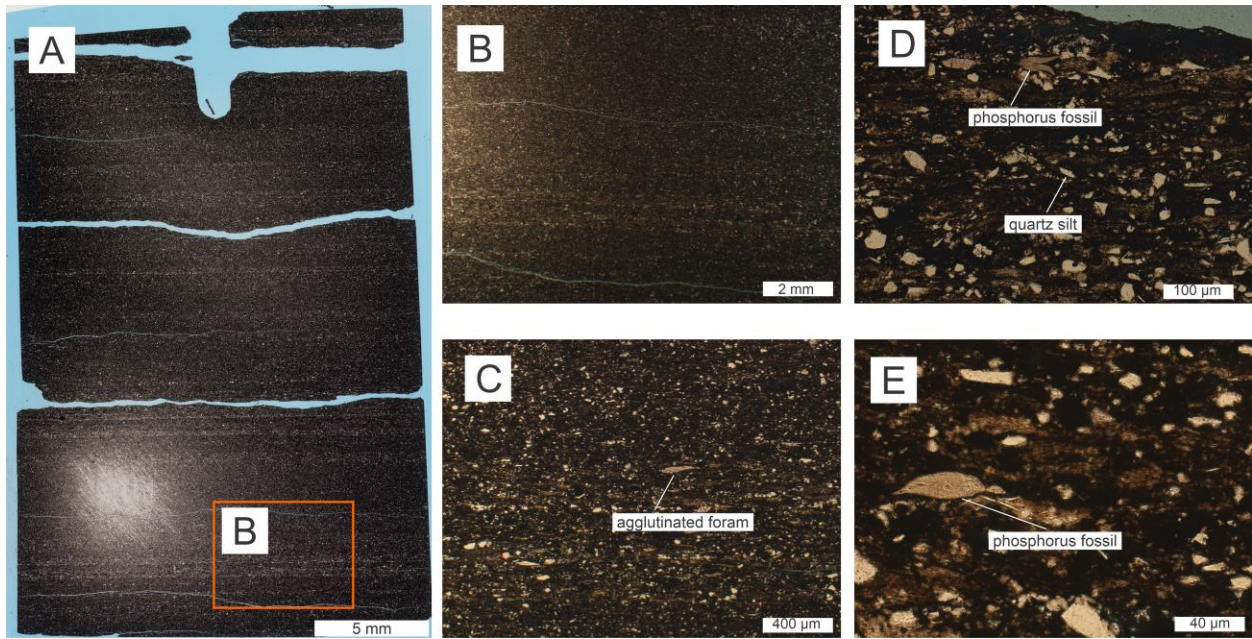


Figure A.1. Representative photographs of the slab 3131.8 m, which is laminated silt- and bioclasts-bearing, clay-rich mudstone. This mudstone contains abundant quartz silts with the presence of siliceous and phosphorous bioclasts. In geochemistry, Al and Ca concentrations are low (less than 5% and 1%, respectively), with relatively enriched Si_{bio} , ranging from 13% to 22%. Si_{bio} and TOC contents show similar trends in profiles, with stable Si_{bio}/TOC ratios, approximately 22 in the whole section. A: Whole-section view. B: Representative micrograph of beddings with quartz silts and bioclasts. C: Zoomed photograph of silts enriched layer in Figure A.1.B. D and E: Representative phosphorus fossils in this slab.

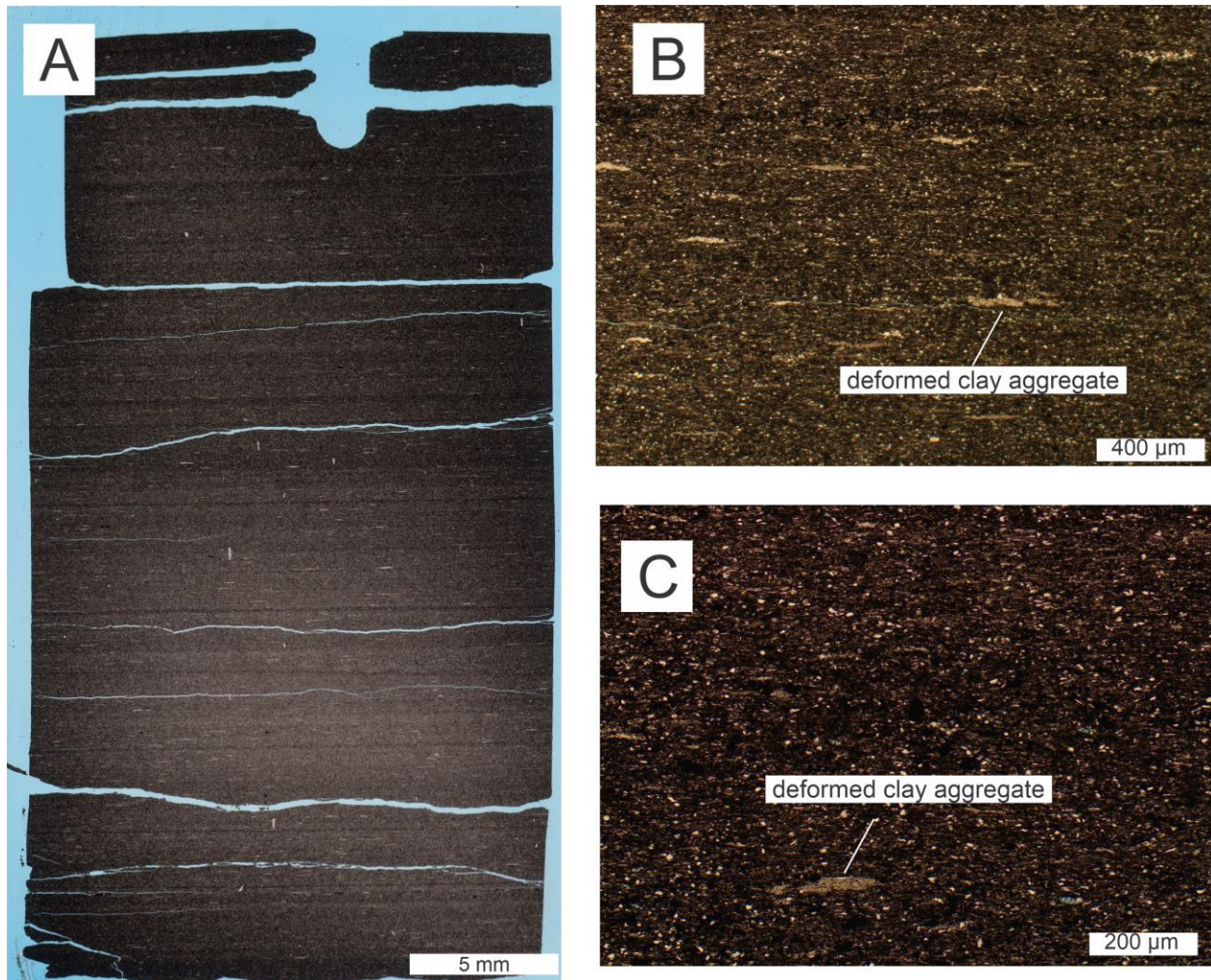


Figure A.2. Representative photographs of the slab 3146.05 m (organic petrography in Appendix E), which is laminated sand- and silt- bearing, clay-rich mudstone. Deformed clay aggregates are present in this slab, sizes varying from 200 to 400 μm . Description of geochemistry is in Chapter 2. A: Whole-section view. B: Representative micrograph of millimeter-scale laminae. C: Zoomed photograph of interlamination in Figure A.2.B. Deformed clay aggregates are present in laminae.

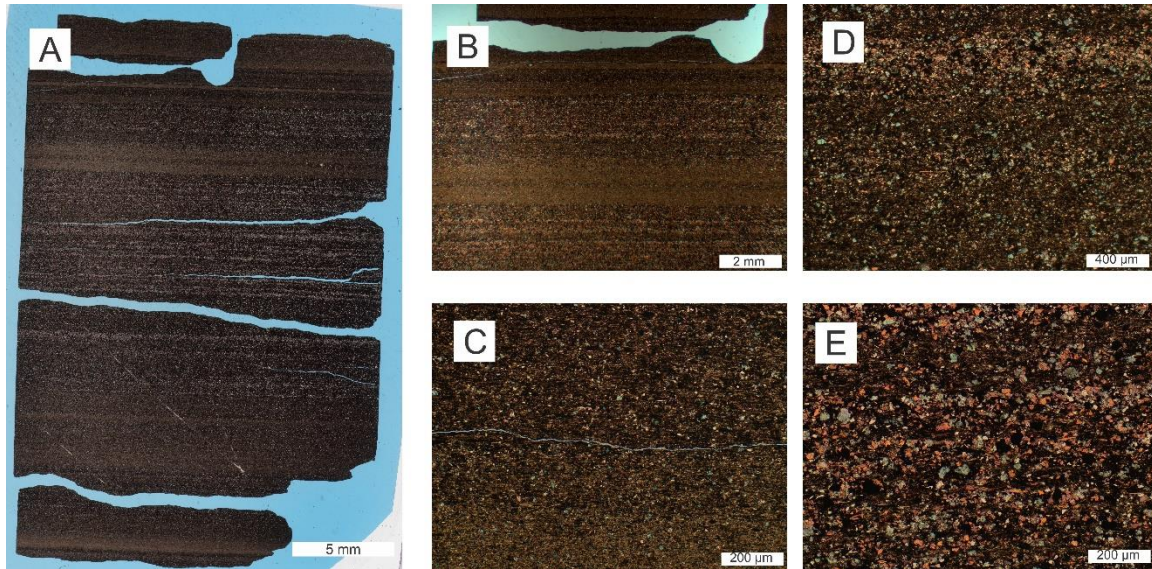


Figure A.3. Representative photographs of the slab 3207.2 m, which is laminated calcite silt-bearing, clay-rich mudstone. Petrography of this slab is similar to the slab from HST2 in Chapter 3. There are abundant calcite grains, organized into normally graded calcareous beddings. In geochemistry, Ca content ranges from 4% to 10%. Al, TOC, and Si_{bio} contents are less than 6%, 1%, and 10%, respectively, profiles of which show a negative correlation to the Ca content profile. A: Whole-section scan. B: Representative micrograph of interlaminated calcareous and argillaceous laminae, thickness of 2 – 5 mm. C: Iron-carbonate (possible ferroan dolomite) present in calcareous laminae. D and E: Representative calcareous laminae, in which a large fraction of detritus is calcite.

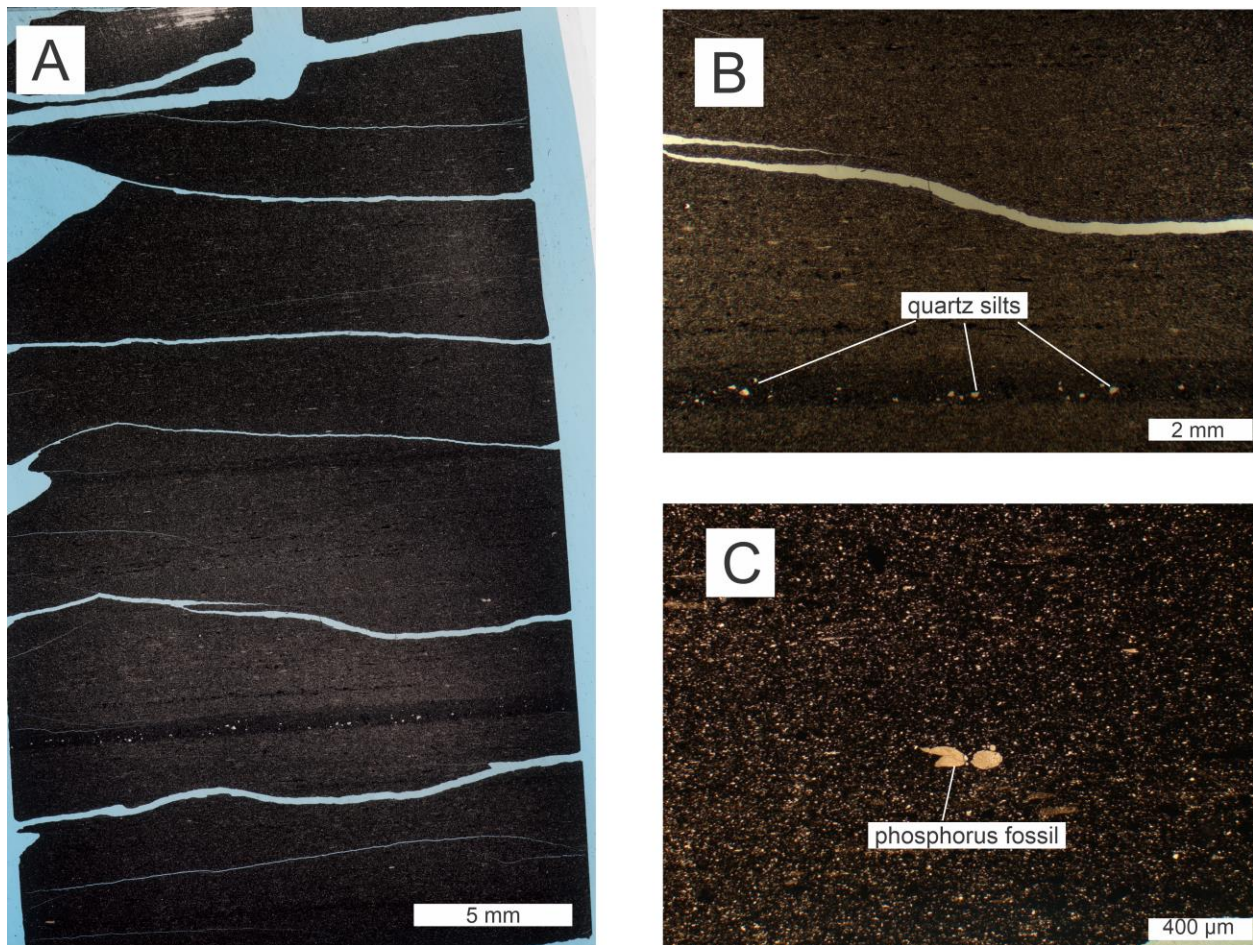


Figure A.4. Representative photographs of the slab 3215.45 m, which is laminated silt-bearing, clay-rich mudstone. In geochemistry, there are limited variations in major elemental concentrations. Al content ranges from 5% to 6%; %Ca and %Si_{bio} are ~ 1.5% and 12% in most section. TOC content decreases in general from 1.2% to 0.8%. A: Whole-section scan. B: Representative micrograph of the lamina with quartz silts. C: Representative phosphorus fossils in this slab.

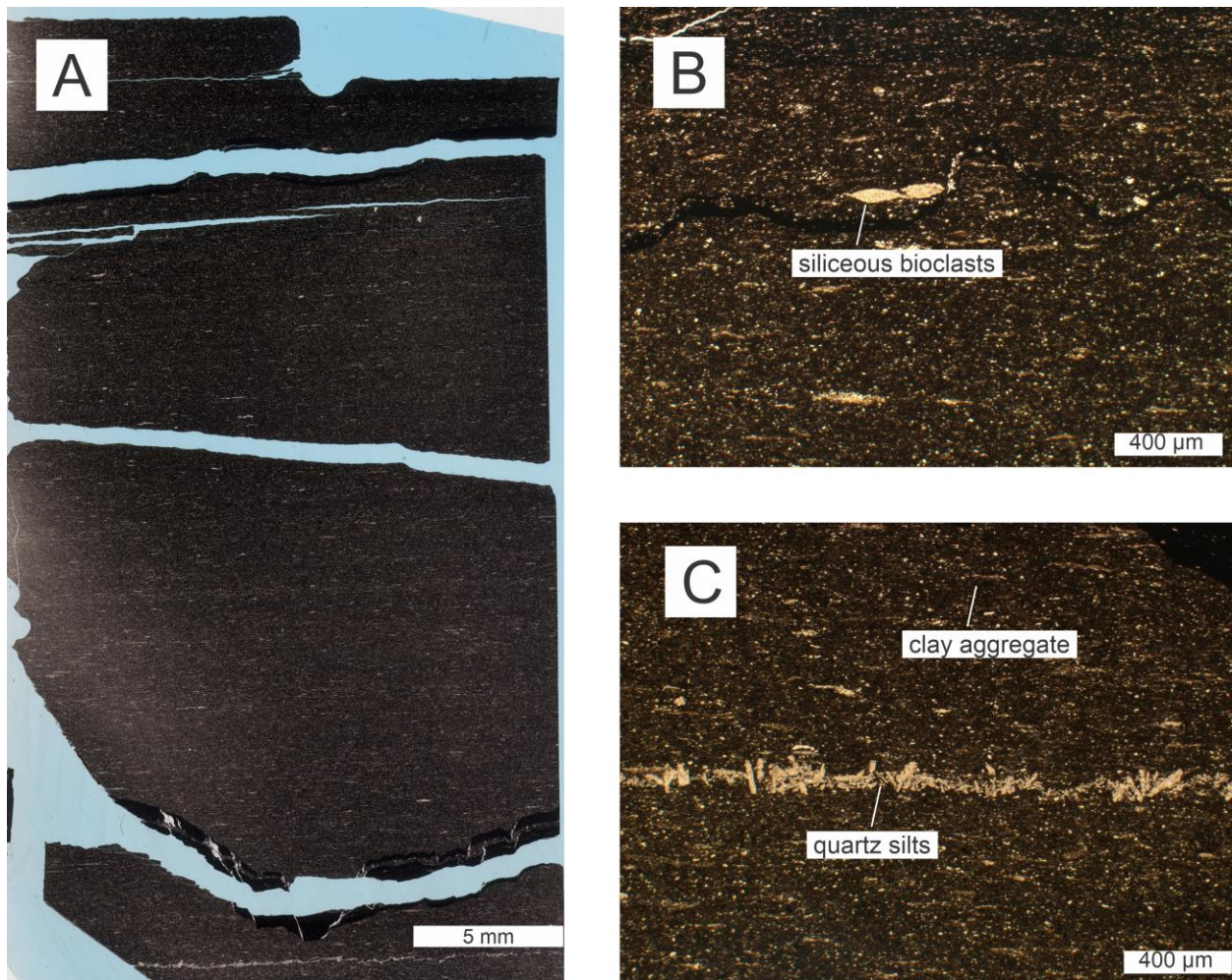


Figure A.5. Representative photographs of the slab 3223.28 m, which is laminated silt-bearing, clay-rich mudstone. In the lower section, there is a quartz silt enriched layer, and the long axis of quartz grains is oblique to perpendicular to the direction of lamination. In geochemistry, the relationships between proxies are similar to the sample of dilution effect in Chapter 2. There are two peaks in Al content, increasing from 2% to 4%, which correlates with decreases in Ca (from 1.5% to 1%), Si_{bio} (from 30% to 20%), and TOC contents (from 3% to 1%). A: Whole-section view. B: Photograph of siliceous bioclasts. C: Photograph of the zone with enriched silt-sized quartz grains.

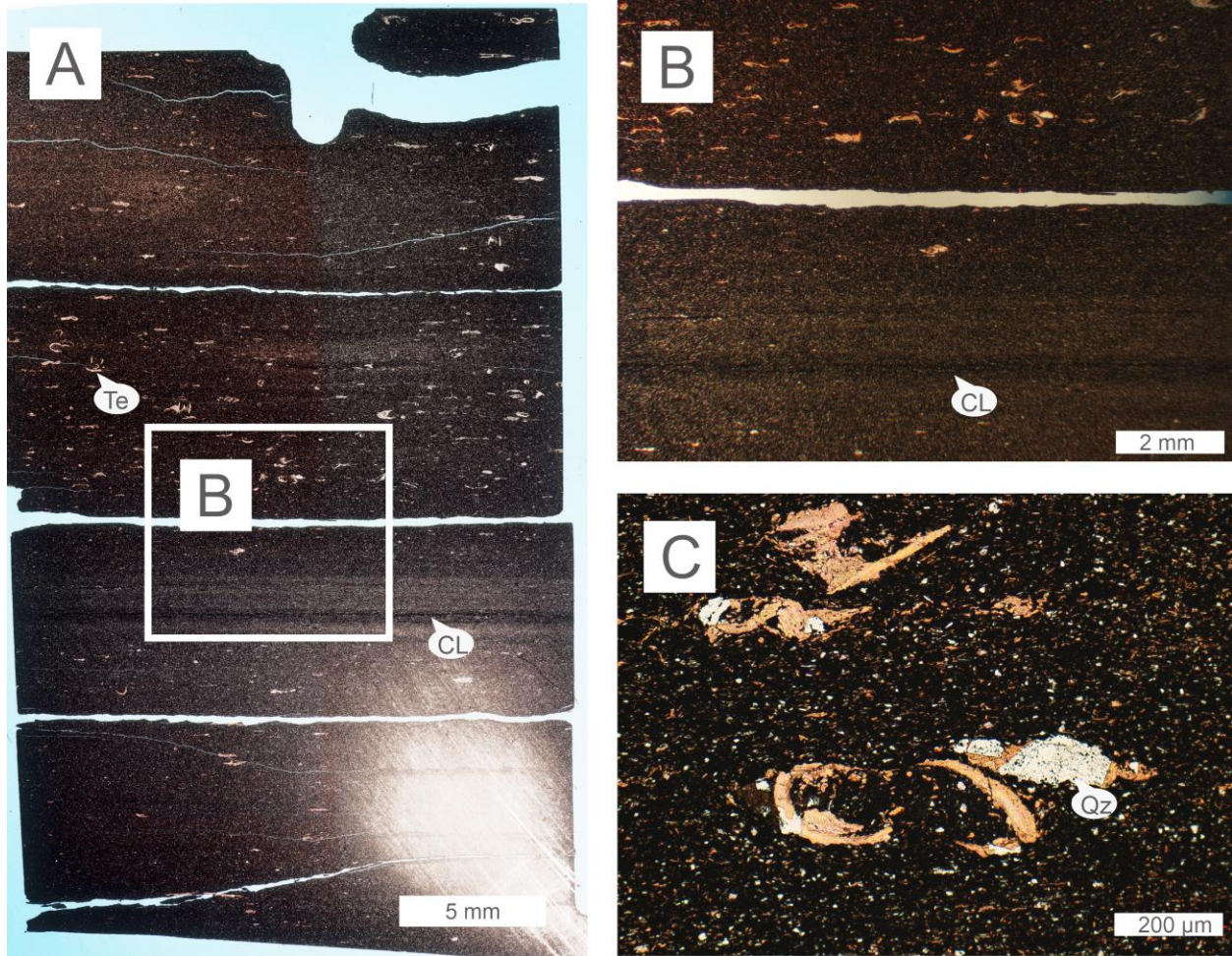


Figure A.6. Representative photographs of the slab 3269.15 m (SEM micrographs are Figure A.11), which is calcareous mesoplankton-bearing, clay-rich mudstone. In the lower and upper sections, there are abundant calcareous bioclasts, e.g., *Tentaculites* and *Styliolina*. The middle section is a laminated clay-rich interval. In geochemistry, Al content is relatively low, ranging from 2% to 4%. Ca content is ~ 6% - 10%; %Si_{bio} varies in the range from 10% to 20%; TOC content changes from 0.8% to 2.2%. Detailed description is in Chapter 2. A: Whole-section view. B: Photograph of upper calcareous bioclast-rich interval and middle clay-rich interval. C: Photograph of typical calcareous fossils. CL – clay-rich layer; Te – *Tentaculites*; Qz – quartz.

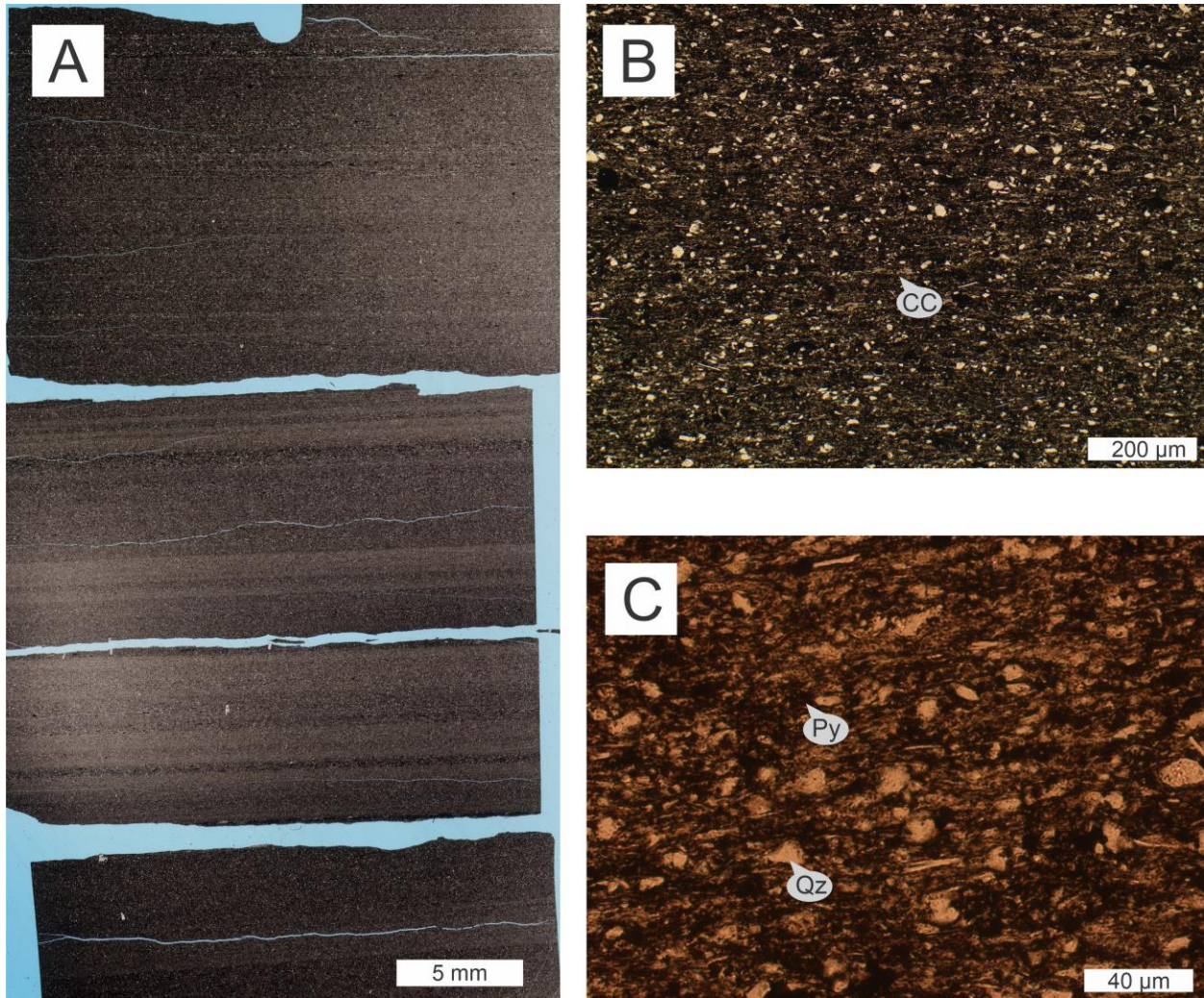


Figure A.7. Representative photographs of the slab 3149.18 m (SEM micrographs are Figure A.10), which is laminated silt-bearing, clay-rich mudstone. The sample is largely composed of clays, with subordinate quartz silts, pyrite, and clay aggregates. In geochemistry, Al content relatively ranges from 4% to 6%. Ca content is less abundant, less than 1%. %Si_{bio} varies in the range from 10% to 15%, and TOC content changes from 0.5% to 1.5%. A: Whole-section view. B: Photograph of quartz silts and deformed clay clasts. C: Photograph of pyrite and quartz silts. CC – clay clast; Py – pyrite; Qz – quartz.

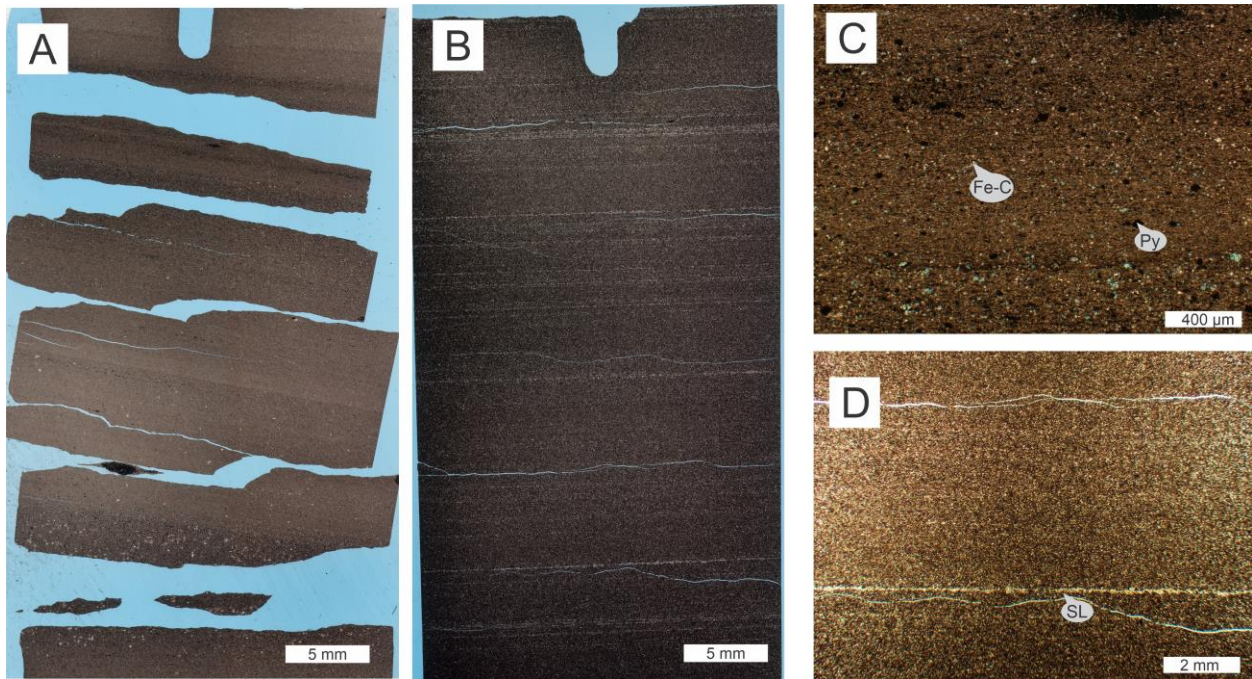


Figure A.8. Representative photographs of the slab 3182.81 m (organic petrography in Appendix E), which is laminated calcite silt-bearing, clay-rich mudstone, and the slab 3153.93 m, which is laminated silt-bearing, clay-rich mudstone. In the slab 3182.81m, there is the presence of pyrite and iron-carbonate. In geochemistry, there are limited variations in each proxy. Al and Ca contents are approximately 7%. %Si_{bio} and %TOC are lower, ~ 2% and 0.5%, respectively. The slab 3153.93 m is organized into clay-rich and silt-rich laminae. The geochemical characteristic of this sample is similar to the slab 3182.81 m; elemental concentrations are varied in limited ranges. Al, Ca, Si_{bio}, and TOC contents are approximately 6%, 4%, 8%, and 0.75%, respectively. A: Whole-section view of the slab 3182.81 m. B: Whole-section view of the slab 3153.93 m. C: Photograph of pyrite and iron-carbonate in the slab 3182.81 m. D: Photograph of silt-rich lamina in the slab 3153.93 m. SL – silt-rich layer; Py – pyrite; Fe-C – iron-carbonate.

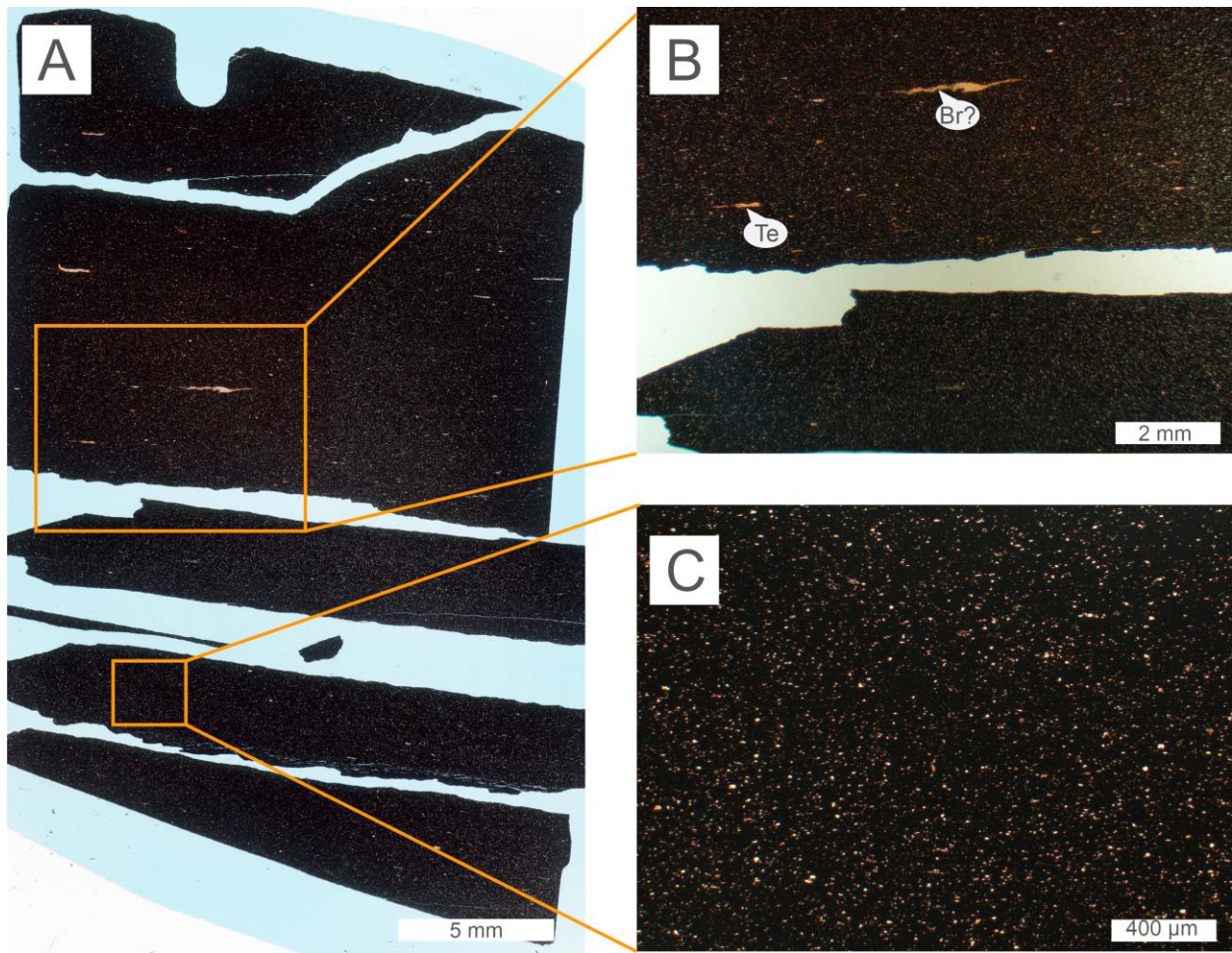


Figure A.9. Representative photographs of the slab 3251.48 m (organic petrography in Appendix E), which is silt-bearing, clay-rich mudstone. The sample is largely composed of clays, with subordinate silts and calcareous bioclasts. Sizes of bioclasts are 1 – 2 mm. No lamination is observed. Detailed description of geochemistry is in Chapter 2. A: Whole-section view. B: Representative photograph of calcareous bioclasts. C: Photograph of massive mudstone in the lower section. Te – *Tentaculites*; Br - *Brachiopod*.

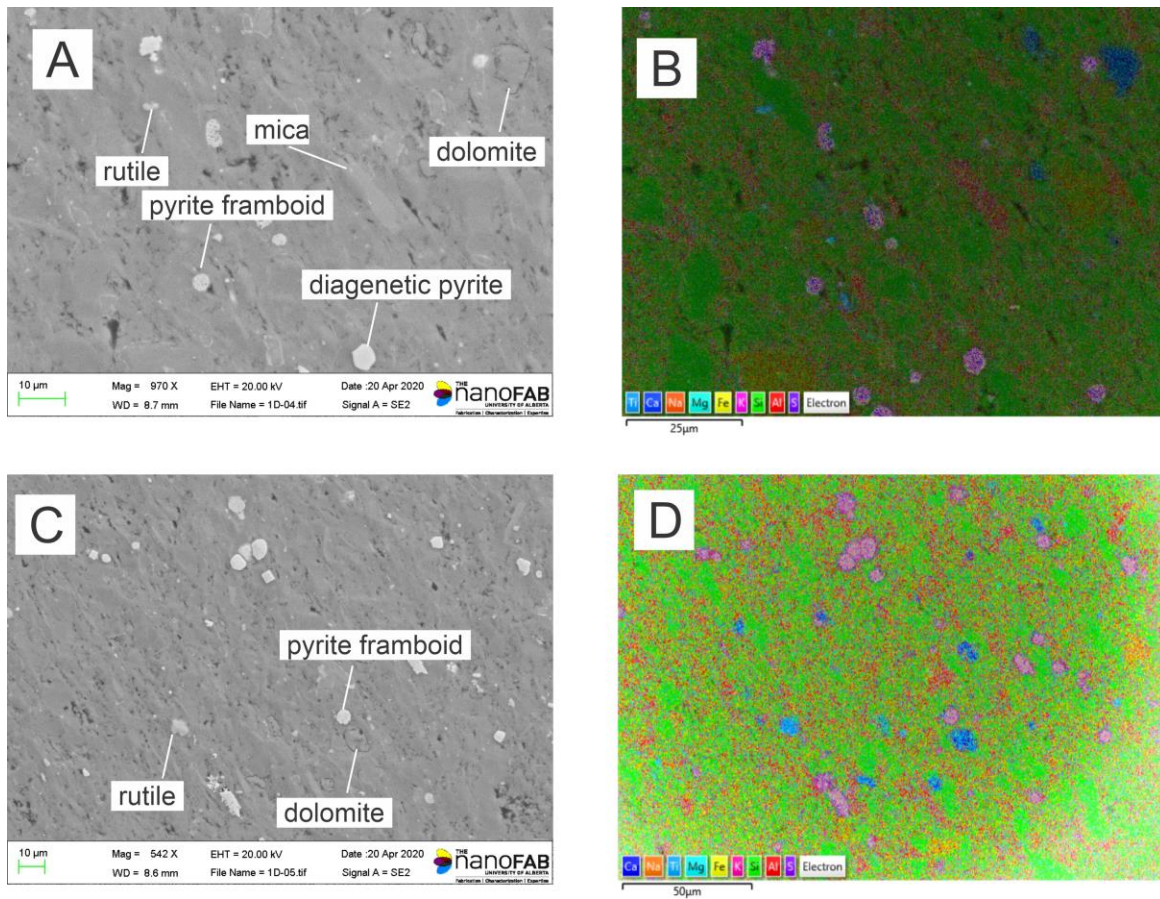


Figure A.10. SEM photographs of the slab 3149.18 m. A and B: Backscattered and EDS representative micrographs of pyrite-rich layer. C and D: Backscattered and EDS representative micrographs of pyrite framboid and euhedral pyrite, sizes of which are approximately 5 μm . Dolomite and rutile are also present.

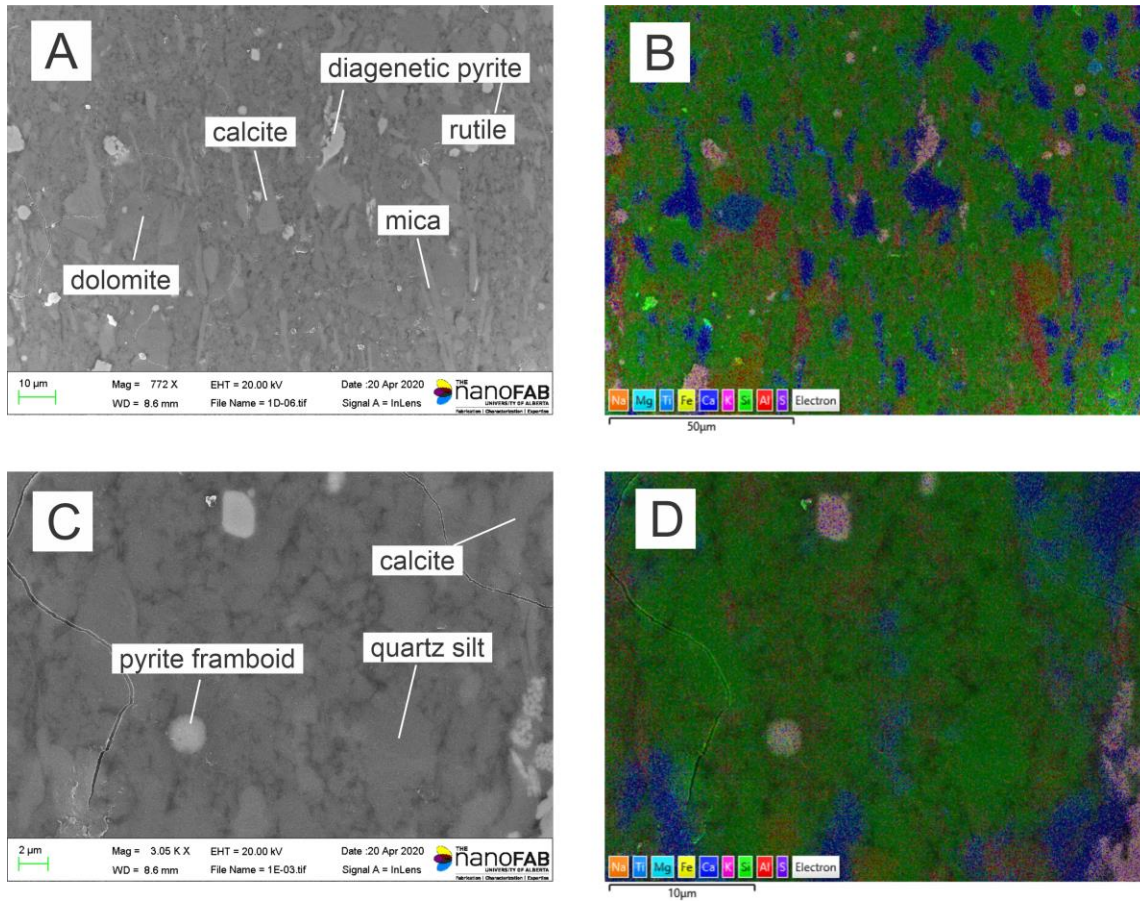


Figure A.11. SEM photographs of the slab 3269.15 m. A and B: Backscattered and EDS representative micrographs of enriched calcite and dolomite grains, with the presence of mica and euhedral pyrite. C and D: Backscattered and EDS representative micrographs of microcrystalline silica matrix and pyrite framboid.

APPENDIX B: HIGH-RESOLUTION DATASET

Appendix B presents the millimeter-scale dataset based on EDXRF and hyperspectral imagery scans of 133 core slabs.

EDXRF													Hyperspectral Imagery	
Mg %	Al %	Si %	S %	K %	Ca %	Ti %	Fe %	K/Al	Ti/Al	Si bio %	S/Fe	Depth m	TOC %	Depth m
0.535	4.031	37.164	1.129	1.330	0.267	0.184	1.694	0.330	0.046	24.667	0.666	3083.19544	1.452	3083.17948
0.495	4.014	37.322	1.123	1.273	0.231	0.167	1.690	0.317	0.042	24.878	0.664	3083.19740	1.442	3083.18076
													1.431	3083.18205
													1.419	3083.18333
													1.406	3083.18462
													1.395	3083.18591
													1.384	3083.18719
													1.377	3083.18848
													1.376	3083.18976
													1.384	3083.19105
													1.398	3083.19233
													1.412	3083.19362
													1.423	3083.19490
													1.424	3083.19619
													1.412	3083.19748

EDXRF													Hyperspectral Imagery	
Mg %	Al %	Si %	S %	K %	Ca %	Ti %	Fe %	K/Al	Ti/Al	Si bio %	S/Fe	Depth m	TOC %	Depth m
0.666	7.524	31.286	1.780	2.537	0.148	0.319	2.205	0.337	0.042	7.961	0.808	3084.18857	0.615	3084.14852
0.741	7.380	31.105	1.943	2.579	0.152	0.340	2.244	0.349	0.046	8.228	0.866	3084.19000	0.619	3084.14930
													0.620	3084.15009
													0.619	3084.15087
													0.619	3084.15165
													0.617	3084.15243
													0.610	3084.15322
													0.599	3084.15400
													0.592	3084.15478
													0.592	3084.15556
													0.600	3084.15635
													0.611	3084.15713
													0.619	3084.15791
													0.622	3084.15870
													0.619	3084.15948
													0.611	3084.16026
													0.602	3084.16104
													0.594	3084.16183
													0.590	3084.16261
													0.589	3084.16339
													0.594	3084.16417
													0.601	3084.16496
													0.604	3084.16574
													0.602	3084.16652
													0.603	3084.16730
													0.611	3084.16809
													0.626	3084.16887
													0.642	3084.16965
													0.654	3084.17043
													0.664	3084.17122
													0.671	3084.17200
													0.676	3084.17278
													0.676	3084.17356
													0.673	3084.17435
													0.670	3084.17513
													0.670	3084.17591
													0.675	3084.17669
													0.685	3084.17748
													0.699	3084.17826
													0.713	3084.17904
													0.726	3084.17983
													0.733	3084.18061
													0.737	3084.18139
													0.746	3084.18217
													0.765	3084.18296
													0.794	3084.18374
													0.823	3084.18452
													0.845	3084.18530
													0.861	3084.18609
													0.879	3084.18687
													0.899	3084.18765
													0.914	3084.18843
													0.918	3084.18922
													0.912	3084.19000
													0.615	3084.14852

EDXRF													Hyperspectral Imagery	
Mg %	Al %	Si %	S %	K %	Ca %	Ti %	Fe %	K/Al	Ti/Al	Si bio %	S/Fe	Depth m	TOC %	Depth m
0.899	5.444	31.639	1.940	1.828	1.279	0.375	2.139	0.336	0.069	14.763	0.907	3085.23986	1.414	3085.21408
0.745	5.004	33.164	1.883	1.682	1.004	0.310	2.104	0.336	0.062	17.650	0.895	3085.24095	1.380	3085.21479
0.658	4.515	34.920	1.445	1.560	0.949	0.275	1.777	0.345	0.061	20.923	0.813	3085.24203	1.348	3085.21549
													1.323	3085.21620
													1.303	3085.21690
													1.287	3085.21761
													1.273	3085.21831
													1.270	3085.21902
													1.279	3085.21972
													1.299	3085.22043
													1.323	3085.22113
													1.345	3085.22184
													1.360	3085.22255
													1.365	3085.22325
													1.359	3085.22396
													1.346	3085.22466
													1.331	3085.22537
													1.316	3085.22607
													1.301	3085.22678
													1.286	3085.22748
													1.272	3085.22819
													1.260	3085.22889
													1.243	3085.22960
													1.215	3085.23030
													1.177	3085.23101
													1.141	3085.23171
													1.122	3085.23242
													1.130	3085.23312
													1.167	3085.23383
													1.218	3085.23453
													1.266	3085.23524
													1.298	3085.23594
													1.310	3085.23665
													1.305	3085.23735
													1.283	3085.23806
													1.246	3085.23877
													1.198	3085.23947
													1.146	3085.24018
													1.104	3085.24088
													1.091	3085.24159

EDXRF												Hyperspectral Imagery		
Mg	Al	Si	S	K	Ca	Ti	Fe	K/Al	Ti/Al	Si bio	S/Fe	Depth	TOC	Depth
%	%	%	%	%	%	%	%			%		m	%	m
													1.018	3087.84546
													1.492	3087.84619
													1.945	3087.84692
													2.048	3087.84765
													2.107	3087.84838
													2.134	3087.84910
													2.134	3087.84983
													2.118	3087.85056
													2.104	3087.85129
													2.106	3087.85202
													2.119	3087.85275
													2.138	3087.85348
													2.164	3087.85421
													2.206	3087.85493
													2.258	3087.85566
													2.294	3087.85639
													2.292	3087.85712
													2.261	3087.85785
													2.219	3087.85858
													2.180	3087.85931
													2.147	3087.86003
													2.126	3087.86076
													2.122	3087.86149
													2.135	3087.86222
													2.161	3087.86295
													2.200	3087.86368
													2.241	3087.86441
													2.278	3087.86513
													2.316	3087.86586
													2.369	3087.86659
													2.436	3087.86732
													2.509	3087.86805
													2.578	3087.86878
													2.639	3087.86951
													2.686	3087.87023
													2.713	3087.87096
													2.725	3087.87169
													2.740	3087.87242
													2.762	3087.87315
													2.786	3087.87388
													2.800	3087.87461
													2.797	3087.87534
													2.766	3087.87606
													2.713	3087.87679
													2.649	3087.87752

EDXRF													Hyperspectral Imagery	
Mg %	Al %	Si %	S %	K %	Ca %	Ti %	Fe %	K/Al	Ti/Al	Si bio %	S/Fe	Depth m	TOC %	Depth m
													3.612	3094.95504
													3.736	3094.95583
													3.782	3094.95662
													3.783	3094.95741
													3.800	3094.95820
													3.854	3094.95899
													3.915	3094.95978
													3.958	3094.96056
													3.993	3094.96135
													4.055	3094.96214
													4.137	3094.96293
													4.203	3094.96372
													4.245	3094.96451
													4.280	3094.96530
													4.329	3094.96609
													4.390	3094.96688
													4.438	3094.96767
													4.476	3094.96846
													4.520	3094.96925
													4.576	3094.97003
													4.629	3094.97082
													4.669	3094.97161
													4.703	3094.97240
													4.739	3094.97319
													4.759	3094.97398
													4.731	3094.97477
													4.655	3094.97556
													4.584	3094.97635
													4.573	3094.97714
													4.614	3094.97793
													4.644	3094.97871
													4.620	3094.97950
													4.555	3094.98029
													4.504	3094.98108
													4.510	3094.98187
													4.576	3094.98266
													4.679	3094.98345
													4.779	3094.98424
													4.849	3094.98503
													4.881	3094.98582
													4.875	3094.98661
													4.830	3094.98739
													4.769	3094.98818
													4.728	3094.98897
													4.730	3094.98976
													4.757	3094.99055
													4.783	3094.99134
													4.793	3094.99213
													4.793	3094.99292
													4.797	3094.99371
													4.807	3094.99450
													4.828	3094.99529
													4.872	3094.99607
													4.946	3094.99686
													5.044	3094.99765
													5.126	3094.99844
													5.157	3094.99923
													5.139	3095.00002
													5.091	3095.00081
													5.026	3095.00160
													4.962	3095.00239
													4.908	3095.00318
													4.882	3095.00397
													4.888	3095.00475
													4.912	3095.00554
													4.929	3095.00633
													4.927	3095.00712
													4.917	3095.00791

EDXRF													Hyperspectral Imagery	
Mg	Al	Si	S	K	Ca	Ti	Fe	K/Al	Ti/Al	Si bio	S/Fe	Depth	TOC	Depth
%	%	%	%	%	%	%	%			%		m	%	m
													4.760	3095.00870
													4.747	3095.00949
													4.758	3095.01028
													4.822	3095.01107
													4.939	3095.01186
													5.058	3095.01265
													5.132	3095.01343
													5.171	3095.01422

EDXRF													Hyperspectral Imagery		
Mg %	Al %	Si %	S %	K %	Ca %	Ti %	Fe %	K/Al	Ti/Al	Si bio %	S/Fe	Depth m	TOC %	Depth m	
0.281	2.284	40.268	1.056	0.658	0.387	0.084	1.136	0.288	0.037	33.186	0.929	3096.10950	2.935	3096.05313	
0.272	2.212	40.327	1.056	0.701	0.367	0.089	1.119	0.317	0.040	33.469	0.944	3096.11060	3.172	3096.05371	
													3.271	3096.05428	
													3.294	3096.05486	
													3.299	3096.05543	
													3.314	3096.05601	
													3.349	3096.05658	
													3.396	3096.05715	
													3.454	3096.05773	
													3.537	3096.05830	
													3.653	3096.05888	
													3.789	3096.05945	
													3.925	3096.06002	
													4.057	3096.06060	
													4.210	3096.06117	
													4.389	3096.06175	
													4.602	3096.06232	
													4.837	3096.06289	
													5.063	3096.06347	
													5.231	3096.06404	
													5.337	3096.06462	
													5.433	3096.06519	
													5.572	3096.06576	
													5.729	3096.06634	
													5.838	3096.06691	
													5.856	3096.06749	
													5.813	3096.06806	
													5.759	3096.06864	
													5.717	3096.06921	
													5.707	3096.06978	
													5.737	3096.07036	
													5.781	3096.07093	
													5.828	3096.07151	
													5.888	3096.07208	
													5.969	3096.07265	
													6.065	3096.07323	
													6.158	3096.07380	
													6.222	3096.07438	
													6.216	3096.07495	
													6.124	3096.07552	
													5.986	3096.07610	
													5.864	3096.07667	
													5.787	3096.07725	
													5.730	3096.07782	
													5.700	3096.07840	
													5.360	3096.07897	
													5.371	3096.07954	
													5.415	3096.08012	
													5.469	3096.08069	
													5.420	3096.08127	
													5.355	3096.08184	
													5.325	3096.08241	
													5.333	3096.08299	
													5.331	3096.08356	
													5.297	3096.08414	
													5.261	3096.08471	
													5.240	3096.08528	
													5.214	3096.08586	
													5.182	3096.08643	
													5.160	3096.08701	
													5.167	3096.08758	
													5.187	3096.08815	
													5.213	3096.08873	
													5.230	3096.08930	
													5.261	3096.08988	
													5.320	3096.09045	
													5.411	3096.09103	
													5.510	3096.09160	

EDXRF												Hyperspectral Imagery		
Mg %	Al %	Si %	S %	K %	Ca %	Ti %	Fe %	K/Al	Ti/Al	Si bio %	S/Fe	Depth m	TOC %	Depth m
													5.580	3096.09217
													5.575	3096.09275
													5.520	3096.09332
													5.461	3096.09390
													5.407	3096.09447
													5.355	3096.09504
													5.312	3096.09562
													5.310	3096.09619
													5.383	3096.09677
													5.515	3096.09734
													5.642	3096.09791
													5.710	3096.09849
													5.715	3096.09906
													5.675	3096.09964
													5.624	3096.10021
													5.616	3096.10078
													5.653	3096.10136
													5.674	3096.10193
													5.628	3096.10251
													5.522	3096.10308
													5.409	3096.10366
													5.324	3096.10423
													5.287	3096.10480
													5.319	3096.10538
													5.426	3096.10595
													5.562	3096.10653
													5.660	3096.10710
													5.691	3096.10767
													5.681	3096.10825
													5.666	3096.10882
													5.634	3096.10940
													5.554	3096.10997
													5.453	3096.11054

EDXRF													Hyperspectral Imagery	
Mg %	Al %	Si %	S %	K %	Ca %	Ti %	Fe %	K/Al	Ti/Al	Si bio %	S/Fe	Depth m	TOC %	Depth m
0.561	2.980	34.856	2.189	0.879	1.857	0.332	1.830	0.295	0.111	25.619	1.197	3097.19782	4.646	3097.17567
0.377	2.935	34.969	2.252	0.926	1.797	0.327	1.847	0.315	0.112	25.870	1.219	3097.20012	4.517	3097.17716
0.382	2.841	38.186	1.634	0.865	0.494	0.110	1.485	0.304	0.039	29.380	1.100	3097.20127	4.417	3097.17790
0.438	2.941	39.209	0.930	0.898	0.550	0.089	1.145	0.305	0.030	30.092	0.812	3097.20242	4.332	3097.17864
0.500	2.880	39.127	0.943	0.856	0.610	0.093	1.167	0.297	0.032	30.201	0.808	3097.20357	4.276	3097.17939
0.443	2.880	38.209	1.408	0.879	0.650	0.110	1.463	0.305	0.038	29.282	0.962	3097.19897	4.601	3097.17642
0.390	2.924	38.521	1.196	0.912	0.722	0.097	1.346	0.312	0.033	29.456	0.889	3097.20472	4.244	3097.18013
0.386	2.952	39.132	0.923	0.903	0.618	0.093	1.193	0.306	0.032	29.981	0.774	3097.20586	4.218	3097.18087
0.469	2.807	37.928	1.661	0.837	0.586	0.093	1.511	0.298	0.033	29.226	1.099	3097.20701	4.176	3097.18161
0.443	2.763	37.734	1.837	0.837	0.574	0.089	1.529	0.303	0.032	29.169	1.202	3097.20816	4.106	3097.18236
0.399	2.941	38.888	1.123	0.865	0.618	0.102	1.197	0.294	0.035	29.771	0.937	3097.20931	4.029	3097.18310
0.447	3.035	38.892	1.010	0.921	0.610	0.093	1.180	0.304	0.031	29.482	0.856	3097.21046	3.989	3097.18384
0.421	2.818	39.204	0.960	0.870	0.622	0.093	1.180	0.309	0.033	30.467	0.813	3097.21161	3.712	3097.18458
0.329	2.919	38.490	1.382	0.879	0.538	0.089	1.428	0.301	0.030	29.442	0.967	3097.21276	3.702	3097.18532
													3.682	3097.18607
													3.644	3097.18681
													3.533	3097.18755
													3.265	3097.18829
													2.662	3097.18904
													1.618	3097.18978
													1.912	3097.19052
													2.693	3097.19126
													3.070	3097.19200
													3.379	3097.19275
													3.522	3097.19349
													3.527	3097.19423
													3.470	3097.19497
													3.429	3097.19572
													3.413	3097.19646
													3.406	3097.19720
													3.395	3097.19794
													3.367	3097.19868
													3.316	3097.19943
													3.224	3097.20017
													3.116	3097.20091
													3.088	3097.20165
													3.068	3097.20240
													3.095	3097.20314
													3.023	3097.20388
													2.988	3097.20462
													2.925	3097.20537
													2.882	3097.20611
													2.892	3097.20685
													2.893	3097.20759
													2.867	3097.20833
													2.756	3097.20908
													2.660	3097.20982
													2.571	3097.21056
													2.531	3097.21130
													2.498	3097.21205
													2.460	3097.21279

EDXRF											Hyperspectral Imagery			
Mg %	Al %	Si %	S %	K %	Ca %	Ti %	Fe %	K/Al	Ti/Al	Si bio %	S/Fe	Depth m	TOC %	Depth m
0.386	6.134	27.038	4.721	2.006	0.088	0.336	3.914	0.327	0.055	8.023	1.206	3110.37839	5.987	3110.34886
0.583	6.962	25.644	4.688	2.302	0.076	0.388	4.088	0.331	0.056	4.061	1.147	3110.37952	5.798	3110.34958
0.570	7.435	24.866	4.745	2.471	0.084	0.410	4.202	0.332	0.055	1.817	1.129	3110.38064	5.594	3110.35031
0.579	7.686	25.336	4.366	2.480	0.108	0.418	3.901	0.323	0.054	1.511	1.119	3110.38177	5.459	3110.35104
0.544	7.686	25.137	4.472	2.546	0.120	0.418	3.905	0.331	0.054	1.312	1.145	3110.38290	5.376	3110.35177
0.679	7.847	25.160	4.246	2.574	0.116	0.431	3.892	0.328	0.055	0.835	1.091	3110.38403	5.282	3110.35250
0.627	8.448	24.965	4.080	2.678	0.128	0.401	3.661	0.317	0.047	-1.222	1.114	3110.38516	5.155	3110.35323
0.627	8.398	25.486	3.721	2.814	0.080	0.475	3.626	0.335	0.057	-0.547	1.026	3110.38629	5.033	3110.35396
0.605	7.836	26.775	3.465	2.579	0.076	0.392	3.404	0.329	0.050	2.484	1.018	3110.38742	4.956	3110.35469
0.548	6.017	23.545	6.164	1.912	0.060	0.288	5.462	0.318	0.048	4.892	1.129	3110.38854	4.931	3110.35542
0.561	5.956	22.893	6.921	1.879	0.096	0.310	5.152	0.316	0.052	4.431	1.343	3110.38967	4.931	3110.35614
0.719	7.969	25.680	3.824	2.706	0.112	0.483	3.718	0.340	0.061	0.976	1.029	3110.39080	4.916	3110.35687
													4.841	3110.35760
													4.653	3110.35833
													4.343	3110.35906
													3.974	3110.35979
													3.667	3110.36052
													3.501	3110.36125
													3.442	3110.36198
													3.427	3110.36270
													3.385	3110.36343
													3.264	3110.36416
													3.069	3110.36489
													2.860	3110.36562
													2.690	3110.36635
													2.573	3110.36708
													2.496	3110.36781
													2.446	3110.36854
													2.402	3110.36926
													2.348	3110.36999
													2.263	3110.37072
													2.126	3110.37145
													1.916	3110.37218
													1.644	3110.37291
													1.404	3110.37364
													1.285	3110.37437
													1.233	3110.37510
													1.162	3110.37582
													1.041	3110.37655
													0.896	3110.37728
													0.755	3110.37801
													0.640	3110.37874
													0.575	3110.37947
													0.545	3110.38020
													0.530	3110.38093
													0.516	3110.38166
													0.486	3110.38238
													0.452	3110.38311
													0.443	3110.38384
													0.474	3110.38457
													0.543	3110.38530
													0.611	3110.38603
													0.613	3110.38676
													0.560	3110.38749
													0.487	3110.38822
													0.436	3110.38894
													0.536	3110.38967
													0.673	3110.39040
													1.483	3110.39113

EDXRF													Hyperspectral Imagery	
Mg	Al	Si	S	K	Ca	Ti	Fe	K/Al	Ti/Al	Si bio	S/Fe	Depth	TOC	Depth
%	%	%	%	%	%	%	%			%		m	%	m
													5.919	3111.40195
													5.989	3111.40264
													6.089	3111.40333
													6.182	3111.40403
													5.783	3111.40056
													5.856	3111.40126
													6.190	3111.40472
													6.071	3111.40541
													5.877	3111.40610
													5.706	3111.40680
													5.607	3111.40749
													5.579	3111.40818
													5.596	3111.40887
													5.632	3111.40957
													5.657	3111.41026
													5.653	3111.41095
													5.626	3111.41164
													5.604	3111.41234
													5.600	3111.41303
													5.602	3111.41372
													5.594	3111.41442
													5.569	3111.41511
													5.529	3111.41580
													5.473	3111.41649
													5.405	3111.41719
													5.361	3111.41788
													5.372	3111.41857
													5.430	3111.41926
													5.479	3111.41996
													5.493	3111.42065
													5.504	3111.42134
													5.543	3111.42203
													5.600	3111.42273
													5.637	3111.42342
													5.639	3111.42411
													5.611	3111.42480
													5.560	3111.42550
													5.505	3111.42619
													5.472	3111.42688
													5.456	3111.42758
													5.438	3111.42827
													5.420	3111.42896
													5.423	3111.42965
													5.443	3111.43035
													5.461	3111.43104
													5.474	3111.43173
													5.479	3111.43242
													5.474	3111.43312
													5.442	3111.43381
													5.380	3111.43450
													5.314	3111.43519
													5.270	3111.43589
													5.256	3111.43658
													5.413	3111.43727
													5.457	3111.43796
													5.533	3111.43866
													5.580	3111.43935
													5.567	3111.44004
													5.512	3111.44074
													5.439	3111.44143
													5.334	3111.44212

EDXRF													Hyperspectral Imagery	
Mg	Al	Si	S	K	Ca	Ti	Fe	K/Al	Ti/Al	Si bio	S/Fe	Depth	TOC	Depth
%	%	%	%	%	%	%	%			%		m	%	m
													5.160	3111.44281
													4.927	3111.44351
													4.696	3111.44420
													4.523	3111.44489
													4.423	3111.44558
													4.384	3111.44628
													4.389	3111.44697
													4.411	3111.44766

EDXRF												Hyperspectral Imagery		
Mg	Al	Si	S	K	Ca	Ti	Fe	K/Al	Ti/Al	Si bio	S/Fe	Depth	TOC	Depth
%	%	%	%	%	%	%	%			%		m	%	m
													0.783	3112.33889
													0.776	3112.33968
													0.773	3112.34046
													0.765	3112.34124
													0.756	3112.34203
													0.750	3112.34281
													0.747	3112.34359
													0.744	3112.34438
													0.735	3112.34516
													0.726	3112.34594
													0.716	3112.34673
													0.700	3112.34751
													0.676	3112.34829
													0.646	3112.34907
													0.612	3112.34986
													0.579	3112.35064
													0.553	3112.35142
													0.537	3112.35221
													0.531	3112.35299
													0.528	3112.35377
													0.528	3112.35456
													0.529	3112.35534
													0.529	3112.35612
													0.525	3112.35690
													0.515	3112.35769
													0.502	3112.35847
													0.489	3112.35925
													0.480	3112.36004
													0.475	3112.36082
													0.473	3112.36160
													0.469	3112.36239
													0.463	3112.36317
													0.454	3112.36395
													0.446	3112.36473
													0.439	3112.36552
													0.435	3112.36630
													0.433	3112.36708
													0.432	3112.36787
													0.447	3112.36865
													0.451	3112.36943
													0.460	3112.37022
													0.475	3112.37100
													0.496	3112.37178
													0.523	3112.37256
													0.556	3112.37335
													0.593	3112.37413
													0.629	3112.37491
													0.658	3112.37570
													0.683	3112.37648
													0.701	3112.37726
													0.705	3112.37805
													0.698	3112.37883
													0.686	3112.37961
													0.674	3112.38039

EDXRF												Hyperspectral Imagery		
Mg %	Al %	Si %	S %	K %	Ca %	Ti %	Fe %	K/Al	Ti/Al	Si bio %	S/Fe	Depth m	TOC %	Depth m
0.307	2.702	39.060	1.299	0.738	0.120	0.145	1.189	0.273	0.054	30.684	1.093	3113.22006	5.143	3113.18916
0.307	2.741	38.820	1.432	0.752	0.100	0.110	1.193	0.274	0.040	30.324	1.200	3113.22138	5.312	3113.18992
0.281	2.579	37.476	2.335	0.649	0.132	0.123	1.677	0.252	0.048	29.480	1.393	3113.22271	5.449	3113.19068
0.263	2.852	37.137	2.116	0.785	0.160	0.123	1.742	0.275	0.043	28.296	1.214	3113.22403	5.490	3113.19144
0.250	3.002	37.707	1.744	0.865	0.152	0.162	1.516	0.288	0.054	28.400	1.151	3113.22535	5.483	3113.19220
0.219	3.002	36.150	2.595	0.846	0.112	0.119	1.947	0.282	0.040	26.844	1.332	3113.22667	5.519	3113.19296
0.294	3.002	37.847	1.584	0.903	0.128	0.145	1.472	0.301	0.048	28.541	1.076	3113.22800	5.628	3113.19372
0.268	2.996	35.929	2.571	0.865	0.172	0.158	2.056	0.289	0.053	26.640	1.250	3113.22932	5.740	3113.19448
0.355	3.191	36.254	2.252	0.888	0.156	0.154	1.860	0.278	0.048	26.362	1.211	3113.23064	5.789	3113.19524
0.250	3.325	36.327	2.119	0.978	0.140	0.171	1.808	0.294	0.051	26.020	1.172	3113.23197	5.784	3113.19600
0.281	3.480	35.671	2.365	0.992	0.108	0.158	1.965	0.285	0.045	24.881	1.204	3113.23329	5.774	3113.19676
0.250	3.391	34.969	2.814	0.954	0.108	0.145	2.196	0.281	0.043	24.456	1.281	3113.23461	5.769	3113.19752
0.180	3.102	32.268	4.685	0.884	0.080	0.136	2.885	0.285	0.044	22.651	1.624	3113.23593	5.746	3113.19828
0.141	1.317	12.016	16.462	0.287	0.024	0.071	9.695	0.218	0.054	7.934	1.698	3113.23726	5.686	3113.19904
0.101	0.849	8.405	18.170	0.175	0.024	0.071	11.479	0.206	0.084	5.772	1.583	3113.23858	5.597	3113.19980
0.189	1.895	18.151	13.152	0.452	0.044	0.102	7.293	0.238	0.054	12.276	1.803	3113.23990	5.511	3113.20056
													5.471	3113.20132
													5.504	3113.20209
													5.593	3113.20285
													5.665	3113.20361
													5.636	3113.20437
													5.498	3113.20513
													5.345	3113.20589
													5.252	3113.20665
													5.204	3113.20741
													5.137	3113.20817
													5.001	3113.20893
													4.817	3113.20969
													4.652	3113.21045
													4.558	3113.21121
													4.540	3113.21197
													4.539	3113.21273
													4.524	3113.21349
													4.514	3113.21425
													4.526	3113.21501
													4.547	3113.21577
													4.555	3113.21653
													4.554	3113.21729
													4.549	3113.21805
													4.523	3113.21881
													4.462	3113.21957
													4.390	3113.22033
													4.330	3113.22109
													4.299	3113.22185
													4.289	3113.22261
													4.284	3113.22337
													4.280	3113.22413
													3.801	3113.22489
													3.753	3113.22565
													3.650	3113.22641
													3.542	3113.22717
													3.450	3113.22793
													3.379	3113.22869
													3.298	3113.22946
													3.180	3113.23022
													3.040	3113.23098
													2.913	3113.23174
													2.817	3113.23250
													2.723	3113.23326
													2.541	3113.23402
													2.183	3113.23478
													1.538	3113.23554
													1.026	3113.23630
													0.579	3113.23706
													0.512	3113.23782

EDXRF												Hyperspectral Imagery		
Mg %	Al %	Si %	S %	K %	Ca %	Ti %	Fe %	K/Al	Ti/Al	Si bio %	S/Fe	Depth m	TOC %	Depth m
													0.503	3113.23858
													0.525	3113.23934
													1.039	3113.24238
													0.574	3113.24010
													0.664	3113.24086
													0.818	3113.24162

Slab 3113.42 m

EDXRF												Hyperspectral Imagery		
Mg %	Al %	Si %	S %	K %	Ca %	Ti %	Fe %	K/Al	Ti/Al	Si bio %	S/Fe	Depth m	TOC %	Depth m
0.474	4.788	34.381	1.840	1.508	0.351	0.215	1.917	0.315	0.045	19.540	0.960	3113.43233	1.430	3113.43357
0.535	4.559	34.797	1.754	1.532	0.311	0.249	1.786	0.336	0.055	20.663	0.982	3113.43387	1.481	3113.43418
0.548	4.559	35.539	1.418	1.475	0.327	0.254	1.607	0.324	0.056	21.405	0.882	3113.43541	1.556	3113.43480
0.644	4.576	35.472	1.365	1.499	0.315	0.258	1.594	0.328	0.056	21.285	0.856	3113.43695	1.659	3113.43541
0.526	4.626	35.291	1.515	1.527	0.319	0.258	1.708	0.330	0.056	20.949	0.887	3113.43850	1.745	3113.43603
0.513	4.654	35.137	1.581	1.536	0.287	0.228	1.747	0.330	0.049	20.709	0.905	3113.44004	1.803	3113.43665
0.592	4.660	35.200	1.581	1.485	0.275	0.267	1.721	0.319	0.057	20.755	0.919	3113.44158	1.833	3113.43726
0.465	4.231	35.598	1.551	1.414	0.395	0.206	1.642	0.334	0.049	22.481	0.945	3113.44312	1.859	3113.43788
0.566	4.487	35.589	1.325	1.489	0.399	0.223	1.555	0.332	0.050	21.679	0.852	3113.44466	1.899	3113.43850
0.504	4.571	35.603	1.352	1.536	0.319	0.258	1.577	0.336	0.056	21.434	0.857	3113.44620	1.949	3113.43911
0.443	4.376	35.503	1.564	1.428	0.363	0.267	1.699	0.326	0.061	21.938	0.921	3113.44774	1.999	3113.43973
0.478	4.443	35.282	1.638	1.475	0.319	0.245	1.729	0.332	0.055	21.509	0.947	3113.44928	2.042	3113.44035
0.474	4.493	35.128	1.744	1.475	0.267	0.258	1.769	0.328	0.057	21.200	0.986	3113.45083	2.079	3113.44096
0.425	4.465	35.458	1.674	1.419	0.259	0.254	1.738	0.318	0.057	21.617	0.963	3113.45237	2.107	3113.44158
0.460	4.626	35.313	1.608	1.499	0.279	0.258	1.694	0.324	0.056	20.972	0.949	3113.45391	2.122	3113.44220
0.566	4.404	35.752	1.478	1.438	0.247	0.228	1.660	0.327	0.052	22.100	0.891	3113.45545	2.122	3113.44281
0.456	4.381	35.594	1.644	1.419	0.279	0.241	1.677	0.324	0.055	22.011	0.980	3113.45699	2.117	3113.44343
0.570	4.326	35.675	1.501	1.391	0.319	0.228	1.664	0.322	0.053	22.265	0.902	3113.45853	2.114	3113.44404
0.421	4.359	35.662	1.594	1.419	0.275	0.258	1.747	0.326	0.059	22.148	0.913	3113.46007	2.116	3113.44466
0.460	4.292	35.386	1.704	1.480	0.263	0.193	1.786	0.345	0.045	22.079	0.954	3113.46161	2.116	3113.44528
0.377	4.359	35.019	1.847	1.396	0.363	0.223	1.869	0.320	0.051	21.505	0.988	3113.46316	2.112	3113.44589
0.368	3.647	29.771	4.681	1.095	0.662	0.180	3.434	0.300	0.049	18.464	1.363	3113.46470	2.110	3113.44651
0.233	3.720	28.124	5.682	1.133	0.463	0.206	4.358	0.304	0.055	16.593	1.304	3113.46624	2.117	3113.44713
0.289	3.886	31.259	4.063	1.217	0.371	0.175	3.316	0.313	0.045	19.211	1.225	3113.46778	2.139	3113.44774
0.425	4.109	33.155	3.050	1.241	0.331	0.215	2.545	0.302	0.052	20.417	1.199	3113.46932	2.172	3113.44836
0.412	4.048	34.553	2.212	1.273	0.371	0.206	2.100	0.315	0.051	22.005	1.054	3113.47086	2.202	3113.44898
0.386	4.142	35.567	1.614	1.367	0.407	0.228	1.681	0.330	0.055	22.725	0.960	3113.47240	2.215	3113.44959
0.390	4.009	36.345	1.322	1.349	0.367	0.219	1.503	0.336	0.055	23.918	0.880	3113.47394	2.211	3113.45021
0.561	4.170	36.521	1.156	1.386	0.351	0.232	1.407	0.332	0.056	23.594	0.822	3113.47549	2.207	3113.45083
0.430	4.187	36.612	1.199	1.386	0.291	0.254	1.433	0.331	0.061	23.633	0.837	3113.47703	2.155	3113.45144
0.408	4.142	35.422	1.508	1.358	0.395	0.228	2.013	0.328	0.055	22.581	0.749	3113.47857	2.160	3113.45206
0.500	4.198	34.680	1.591	1.480	0.319	0.245	2.436	0.353	0.058	21.666	0.653	3113.48011	2.174	3113.45268
0.408	4.331	35.734	1.574	1.424	0.283	0.228	1.655	0.329	0.053	22.307	0.951	3113.48165	2.198	3113.45329
0.482	4.521	34.929	1.797	1.461	0.275	0.258	1.891	0.323	0.057	20.915	0.951	3113.48319	2.228	3113.45391
0.412	4.437	35.028	1.747	1.504	0.331	0.262	1.838	0.339	0.059	21.273	0.950	3113.48473	2.252	3113.45452
0.474	4.470	35.096	1.834	1.461	0.283	0.254	1.795	0.327	0.057	21.238	1.022	3113.48627	2.266	3113.45514
0.469	4.209	35.562	1.661	1.386	0.343	0.215	1.694	0.329	0.051	22.514	0.980	3113.48782	2.275	3113.45576
0.417	4.120	35.910	1.518	1.372	0.375	0.219	1.651	0.333	0.053	23.138	0.920	3113.48936	2.285	3113.45637
0.425	4.109	36.277	1.232	1.372	0.451	0.223	1.463	0.334	0.054	23.539	0.842	3113.49090	2.291	3113.45699
0.333	4.287	36.345	1.312	1.414	0.279	0.245	1.511	0.330	0.057	23.055	0.868	3113.49244	2.292	3113.45761
0.456	4.220	35.879	1.511	1.353	0.343	0.228	1.581	0.321	0.054	22.796	0.956	3113.49398	2.297	3113.45822
0.487	4.192	36.010	1.438	1.405	0.319	0.232	1.551	0.335	0.055	23.014	0.928	3113.49552	2.321	3113.45884
0.500	4.126	36.033	1.531	1.325	0.283	0.210	1.633	0.321	0.051	23.243	0.937	3113.49706	2.349	3113.45946
0.395	4.142	35.775	1.611	1.367	0.315	0.241	1.751	0.330	0.058	22.934	0.920	3113.49860	2.354	3113.46007
0.487	3.981	36.051	1.531	1.292	0.351	0.202	1.668	0.325	0.051	23.710	0.918	3113.50015	2.335	3113.46069
0.465	4.053	36.164	1.495	1.269	0.347	0.197	1.625	0.313	0.049	23.599	0.920	3113.50169	2.319	3113.46131
0.460	4.198	35.956	1.505	1.311	0.315	0.228	1.612	0.312	0.054	22.942	0.934	3113.50323	2.320	3113.46192
0.482	4.081	35.951	1.601	1.339	0.311	0.228	1.690	0.328	0.056	23.300	0.947	3113.50477	2.319	3113.46254
0.373	4.126	35.978	1.571	1.386	0.323	0.223	1.673	0.336	0.054	23.189	0.939	3113.50631	2.268	3113.46316
0.495	4.076	35.929	1.535	1.372	0.367	0.232	1.625	0.337	0.057	23.294	0.945	3113.50785	2.124	3113.46377
													1.880	3113.46439
													1.492	3113.46500
													1.323	3113.46562
													1.289	3113.46624
													1.389	3113.46685
													1.757	3113.46747
													1.996	3113.46809
													2.181	3113.46870
													2.278	3113.46932
													2.317	3113.46994
													2.335	3113.47055

EDXRF													Hyperspectral Imagery	
Mg %	Al %	Si %	S %	K %	Ca %	Ti %	Fe %	K/Al	Ti/Al	Si bio %	S/Fe	Depth m	TOC %	Depth m
													2.365	3113.47117
													2.474	3113.47240
													2.525	3113.47302
													2.561	3113.47364
													2.574	3113.47425
													2.415	3113.47179
													2.563	3113.47487
													2.533	3113.47548
													2.499	3113.47610
													2.465	3113.47672
													2.421	3113.47733
													2.361	3113.47795
													2.303	3113.47857
													2.264	3113.47918
													2.242	3113.47980
													2.228	3113.48042
													2.221	3113.48103
													2.231	3113.48165
													2.257	3113.48227
													2.285	3113.48288
													2.309	3113.48350
													2.335	3113.48411
													2.367	3113.48473
													2.401	3113.48535
													2.428	3113.48596
													2.446	3113.48658
													2.454	3113.48720
													2.449	3113.48781
													2.434	3113.48843
													2.418	3113.48905
													2.417	3113.48966
													2.421	3113.49028
													2.421	3113.49090
													2.410	3113.49151
													2.398	3113.49213
													2.391	3113.49275
													2.407	3113.49336
													2.446	3113.49398
													2.498	3113.49459
													2.531	3113.49521
													2.532	3113.49583
													2.503	3113.49644
													2.452	3113.49706
													2.390	3113.49768
													2.340	3113.49829
													2.318	3113.49891
													2.329	3113.49953
													2.363	3113.50014
													2.402	3113.50076
													2.434	3113.50138
													2.458	3113.50199
													2.475	3113.50261
													2.477	3113.50323
													2.468	3113.50384
													2.455	3113.50446
													2.437	3113.50507
													2.402	3113.50569
													2.358	3113.50631
													2.327	3113.50692
													2.324	3113.50754

EDXRF												Hyperspectral Imagery		
Mg	Al	Si	S	K	Ca	Ti	Fe	K/Al	Ti/Al	Si bio	S/Fe	Depth	TOC	Depth
%	%	%	%	%	%	%	%			%		m	%	m
													1.604	3114.46474
													1.599	3114.46543
													1.617	3114.46612
													1.658	3114.46680
													1.611	3114.46405
													1.702	3114.46749
													1.732	3114.46818
													1.744	3114.46887
													1.751	3114.46956
													1.759	3114.47025
													1.756	3114.47093
													1.733	3114.47162
													1.696	3114.47231
													1.652	3114.47300
													1.613	3114.47369
													1.592	3114.47438
													1.593	3114.47506
													1.601	3114.47575
													1.598	3114.47644
													1.590	3114.47713
													1.588	3114.47782
													1.597	3114.47851
													1.621	3114.47919
													1.652	3114.47988
													1.679	3114.48057
													1.692	3114.48126
													1.689	3114.48195
													1.672	3114.48264
													1.654	3114.48332
													1.645	3114.48401
													1.650	3114.48470
													1.667	3114.48539
													1.692	3114.48608
													1.722	3114.48677
													1.747	3114.48745
													1.762	3114.48814
													1.765	3114.48883
													1.768	3114.48952
													1.774	3114.49021
													1.779	3114.49089
													1.774	3114.49158
													1.751	3114.49227
													1.709	3114.49296
													1.655	3114.49365
													1.614	3114.49434
													1.603	3114.49502
													1.618	3114.49571
													1.640	3114.49640
													1.658	3114.49709
													1.672	3114.49778
													1.682	3114.49847
													1.688	3114.49915
													1.694	3114.49984
													1.699	3114.50053
													1.701	3114.50122
													1.692	3114.50191
													1.665	3114.50260
													1.623	3114.50328
													1.572	3114.50397
													1.512	3114.50466
													1.459	3114.50535
													1.431	3114.50604

Slab 3116.78 m

EDXRF													Hyperspectral Imagery		
Mg %	Al %	Si %	S %	K %	Ca %	Ti %	Fe %	K/Al	Ti/Al	Si bio %	S/Fe	Depth m	TOC %	Depth m	
5.118	5.077	16.237	1.039	1.147	11.747	0.232	3.404	0.226	0.046	0.499	0.305	3116.78000	0.324	3116.77935	
5.249	5.077	16.142	1.006	1.128	11.743	0.206	3.369	0.222	0.041	0.404	0.299	3116.78189	0.323	3116.78009	
6.082	4.042	14.251	1.242	0.809	12.982	0.132	4.023	0.200	0.033	1.720	0.309	3116.78377	0.318	3116.78083	
6.507	4.042	14.337	0.930	0.846	13.134	0.145	3.665	0.209	0.036	1.806	0.254	3116.78566	0.319	3116.78156	
6.516	4.359	14.613	0.681	0.959	13.245	0.171	3.290	0.220	0.039	1.099	0.207	3116.78755	0.332	3116.78230	
6.524	4.398	14.989	0.647	0.964	12.986	0.180	3.238	0.219	0.041	1.354	0.200	3116.78944	0.345	3116.78304	
7.063	3.931	13.771	0.717	0.743	13.568	0.132	3.691	0.189	0.034	1.586	0.194	3116.79132	0.346	3116.78377	
6.643	3.759	13.767	1.076	0.738	13.432	0.119	3.936	0.196	0.032	2.116	0.273	3116.79321	0.346	3116.78451	
6.524	4.142	14.667	0.644	0.837	13.468	0.184	3.408	0.202	0.044	1.826	0.189	3116.79510	0.347	3116.78525	
6.638	4.254	14.604	0.784	0.917	13.130	0.141	3.347	0.215	0.033	1.418	0.234	3116.79698	0.350	3116.78599	
6.573	4.265	14.726	0.541	0.888	13.393	0.180	3.308	0.208	0.042	1.506	0.164	3116.79887	0.353	3116.78672	
6.481	4.381	14.518	0.734	0.860	13.297	0.158	3.373	0.196	0.036	0.935	0.218	3116.80076	0.353	3116.78746	
6.419	4.532	14.568	0.674	0.926	13.381	0.154	3.190	0.204	0.034	0.520	0.211	3116.80265	0.352	3116.78820	
6.928	4.315	14.233	0.730	0.860	13.265	0.145	3.299	0.199	0.034	0.857	0.221	3116.80453	0.350	3116.78893	
6.226	4.587	15.215	0.720	0.921	12.815	0.154	3.234	0.201	0.034	0.994	0.223	3116.80642	0.350	3116.78967	
6.191	4.381	14.839	0.734	0.893	13.225	0.180	3.404	0.204	0.041	1.257	0.216	3116.80831	0.350	3116.79041	
6.340	4.265	14.568	1.003	0.884	13.054	0.171	3.478	0.207	0.040	1.347	0.288	3116.81019	0.351	3116.79114	
6.029	4.826	15.260	0.770	0.996	12.671	0.210	3.255	0.206	0.044	0.298	0.237	3116.81208	0.351	3116.79188	
6.209	4.760	15.088	0.644	0.954	12.914	0.154	3.181	0.200	0.032	0.333	0.202	3116.81397	0.350	3116.79262	
6.297	4.782	14.518	1.023	1.020	12.807	0.202	3.234	0.213	0.042	-0.306	0.316	3116.81585	0.349	3116.79336	
6.919	4.565	13.993	0.524	0.949	13.616	0.175	3.064	0.208	0.038	-0.159	0.171	3116.81774	0.347	3116.79409	
5.990	5.327	15.418	0.627	1.137	12.552	0.219	2.876	0.213	0.041	-1.096	0.218	3116.81963	0.343	3116.79483	
5.981	5.238	15.432	0.697	1.114	12.440	0.223	2.972	0.213	0.043	-0.806	0.235	3116.82152	0.339	3116.79557	
6.152	4.938	14.844	0.627	1.039	13.106	0.189	3.077	0.210	0.038	-0.463	0.204	3116.82340	0.337	3116.79630	
6.595	4.832	14.690	0.604	1.015	13.074	0.180	3.002	0.210	0.037	-0.289	0.201	3116.82529	0.337	3116.79704	
5.872	4.993	15.260	0.534	1.095	12.994	0.202	3.033	0.219	0.040	-0.219	0.176	3116.82718	0.338	3116.79778	
6.038	5.138	15.084	0.591	1.057	13.010	0.171	2.920	0.206	0.033	-0.844	0.202	3116.82906	0.339	3116.79851	
6.678	4.610	13.880	0.817	0.945	13.484	0.189	3.203	0.205	0.041	-0.410	0.255	3116.83095	0.340	3116.79925	
6.892	4.648	13.599	0.528	0.893	14.034	0.149	3.120	0.192	0.032	-0.811	0.169	3116.83284	0.339	3116.79999	
7.015	4.309	13.201	0.624	0.846	14.269	0.145	3.308	0.196	0.034	-0.157	0.189	3116.83473	0.335	3116.80073	
7.024	4.237	13.581	0.538	0.837	14.074	0.154	3.334	0.197	0.036	0.447	0.161	3116.83661	0.330	3116.80146	
6.581	3.998	13.862	0.883	0.757	13.520	0.132	3.840	0.189	0.033	1.469	0.230	3116.83850	0.327	3116.80220	
5.530	5.110	15.771	0.926	1.137	12.118	0.314	3.229	0.223	0.062	-0.070	0.287	3116.84200	0.326	3116.80294	
5.429	5.244	15.726	0.910	1.123	12.034	0.236	3.247	0.214	0.045	-0.529	0.280	3116.84393	0.328	3116.80367	
6.546	4.326	14.563	0.903	0.926	12.950	0.154	3.421	0.214	0.036	1.153	0.264	3116.84587	0.330	3116.80441	
6.415	4.265	14.468	1.275	0.917	12.508	0.154	3.735	0.215	0.036	1.248	0.341	3116.84780	0.331	3116.80515	
6.170	4.537	15.102	1.046	0.964	12.412	0.197	3.504	0.212	0.043	1.036	0.299	3116.84973	0.331	3116.80589	
6.283	4.832	15.156	0.641	1.025	12.859	0.197	3.077	0.212	0.041	0.177	0.208	3116.85167	0.329	3116.80662	
6.095	4.743	14.518	1.345	1.029	12.456	0.219	3.526	0.217	0.046	-0.185	0.382	3116.85360	0.327	3116.80736	
6.476	4.443	14.835	0.667	0.973	13.134	0.167	3.212	0.219	0.038	1.062	0.208	3116.85553	0.326	3116.80810	
6.529	4.493	14.903	0.727	0.954	12.895	0.189	3.225	0.212	0.042	0.975	0.225	3116.85747	0.324	3116.80883	
													0.323	3116.80957	
													0.322	3116.81031	
													0.323	3116.81104	
													0.323	3116.81178	
													0.321	3116.81252	
													0.319	3116.81326	
													0.317	3116.81399	
													0.314	3116.81473	
													0.312	3116.81547	
													0.310	3116.81620	
													0.309	3116.81694	
													0.310	3116.81768	
													0.309	3116.81841	
													0.307	3116.81915	
													0.303	3116.81989	
													0.299	3116.82063	
													0.298	3116.82136	
													0.298	3116.82210	
													0.298	3116.82284	
													0.297	3116.82357	
													0.296	3116.82431	

EDXRF												Hyperspectral Imagery		
Mg	Al	Si	S	K	Ca	Ti	Fe	K/Al	Ti/Al	Si bio	S/Fe	Depth	TOC	Depth
%	%	%	%	%	%	%	%			%		m	%	m
													0.295	3116.82505
													0.295	3116.82579
													0.295	3116.82652
													0.293	3116.82726
													0.292	3116.82800
													0.289	3116.82873
													0.287	3116.82947
													0.286	3116.83021
													0.287	3116.83094
													0.290	3116.83168
													0.296	3116.83242
													0.302	3116.83316
													0.308	3116.83389
													0.312	3116.83463
													0.314	3116.83537
													0.316	3116.83610
													0.316	3116.83684
													0.316	3116.83758
													0.314	3116.83831
													0.313	3116.83905
													0.314	3116.83979
													0.317	3116.84053
													0.322	3116.84126
													0.325	3116.84200
													0.325	3116.84274
													0.322	3116.84347
													0.320	3116.84421
													0.318	3116.84495
													0.314	3116.84569
													0.307	3116.84642
													0.301	3116.84716
													0.298	3116.84790
													0.304	3116.84863
													0.303	3116.84937
													0.302	3116.85011
													0.303	3116.85084
													0.308	3116.85158
													0.315	3116.85232
													0.321	3116.85306
													0.323	3116.85379
													0.324	3116.85453
													0.325	3116.85527
													0.325	3116.85600
													0.326	3116.85674
													0.327	3116.85748

Slab 3121.25 m

EDXRF													Hyperspectral Imagery	
Mg %	Al %	Si %	S %	K %	Ca %	Ti %	Fe %	K/Al	Ti/Al	Si bio %	S/Fe	Depth m	TOC %	Depth m
0.412	4.320	36.372	1.325	1.433	0.096	0.197	1.367	0.332	0.046	22.979	0.969	3121.25000	2.230	3121.25006
0.430	4.248	36.453	1.299	1.410	0.112	0.184	1.363	0.332	0.043	23.285	0.953	3121.25205	2.265	3121.25072
0.346	4.771	36.046	1.312	1.560	0.056	0.228	1.455	0.327	0.048	21.257	0.902	3121.25411	1.672	3121.25138
0.460	4.765	35.539	1.521	1.532	0.052	0.219	1.572	0.321	0.046	20.767	0.968	3121.25616	2.126	3121.25204
0.303	5.160	33.978	1.930	1.771	0.152	0.258	1.869	0.343	0.050	17.982	1.033	3121.25821	2.185	3121.25270
0.386	5.249	34.408	1.724	1.748	0.068	0.280	1.782	0.333	0.053	18.136	0.968	3121.26027	2.243	3121.25335
0.526	5.661	33.051	2.023	1.893	0.064	0.288	2.021	0.334	0.051	15.502	1.001	3121.26232	2.257	3121.25401
0.552	6.979	30.553	2.302	2.283	0.076	0.358	2.370	0.327	0.051	8.918	0.971	3121.26437	2.197	3121.25467
0.574	7.474	30.689	1.903	2.476	0.076	0.431	2.157	0.331	0.058	7.519	0.883	3121.26643	2.069	3121.25533
0.675	7.402	29.961	2.153	2.480	0.172	0.410	2.300	0.335	0.055	7.015	0.936	3121.26848	1.918	3121.25598
0.530	5.600	31.988	1.555	1.762	0.921	0.284	1.943	0.315	0.051	14.629	0.800	3121.27053	1.793	3121.25664
0.561	6.768	31.363	1.947	2.316	0.076	0.384	2.170	0.342	0.057	10.383	0.897	3121.27259	1.704	3121.25730
0.438	6.729	30.780	2.458	2.292	0.088	0.340	2.401	0.341	0.051	9.920	1.024	3121.27464	1.639	3121.25796
0.438	5.516	34.164	1.604	1.945	0.072	0.284	1.777	0.353	0.051	17.064	0.903	3121.27669	1.570	3121.25861
0.408	5.678	32.476	2.428	1.931	0.068	0.301	2.152	0.340	0.053	14.876	1.128	3121.27875	1.475	3121.25927
0.434	4.810	35.562	1.468	1.583	0.072	0.258	1.533	0.329	0.054	20.652	0.958	3121.28080	1.354	3121.25993
0.377	4.159	36.499	1.491	1.433	0.092	0.162	1.324	0.345	0.039	23.606	1.127	3121.28280	1.239	3121.26059
0.408	4.203	36.462	1.468	1.428	0.108	0.202	1.328	0.340	0.048	23.432	1.105	3121.28384	1.170	3121.26125
0.338	3.197	39.241	0.870	0.996	0.032	0.115	0.949	0.312	0.036	29.331	0.917	3121.28488	1.147	3121.26190
0.351	3.097	39.367	0.877	0.898	0.036	0.115	0.927	0.290	0.037	29.768	0.946	3121.28592	1.165	3121.26256
0.320	2.907	39.539	0.807	0.898	0.036	0.123	0.910	0.309	0.042	30.526	0.887	3121.28696	1.263	3121.26322
0.360	2.835	39.363	0.880	0.888	0.036	0.089	0.940	0.313	0.031	30.574	0.936	3121.28800	1.358	3121.26388
0.390	2.863	39.435	0.890	0.870	0.036	0.115	0.931	0.304	0.040	30.560	0.955	3121.28904	1.306	3121.26453
0.268	2.818	39.942	0.777	0.870	0.036	0.097	0.897	0.309	0.035	31.205	0.867	3121.29008	1.199	3121.26519
0.241	2.774	40.041	0.770	0.851	0.028	0.097	0.892	0.307	0.035	31.442	0.863	3121.29112	1.083	3121.26585
0.320	2.807	39.897	0.850	0.870	0.028	0.102	0.936	0.310	0.036	31.194	0.908	3121.29216	1.007	3121.26651
0.395	3.380	38.173	1.142	1.250	0.052	0.154	1.202	0.370	0.046	27.694	0.951	3121.29320	0.981	3121.26716
0.360	3.764	37.449	1.282	1.367	0.040	0.215	1.350	0.363	0.057	25.780	0.950	3121.29424	0.989	3121.26782
0.320	3.136	39.037	0.983	1.072	0.032	0.123	1.110	0.342	0.039	29.317	0.885	3121.29528	1.024	3121.26848
													1.100	3121.26914
													1.233	3121.26980
													1.405	3121.27045
													1.573	3121.27111
													1.714	3121.27177
													1.809	3121.27243
													1.855	3121.27308
													1.868	3121.27374
													1.885	3121.27440
													1.936	3121.27506
													2.017	3121.27571
													2.093	3121.27637
													2.145	3121.27703
													2.187	3121.27769
													2.237	3121.27835
													2.298	3121.27900
													2.352	3121.27966
													2.386	3121.28032
													2.290	3121.28098
													3.763	3121.28163
													4.055	3121.28229
													4.407	3121.28295
													4.783	3121.28361
													5.183	3121.28426
													5.634	3121.28492
													6.085	3121.28558
													6.543	3121.28624
													7.009	3121.28690
													7.402	3121.28755
													7.622	3121.28821
													7.671	3121.28887
													7.640	3121.28953
													7.590	3121.29018

EDXRF												Hyperspectral Imagery		
Mg	Al	Si	S	K	Ca	Ti	Fe	K/Al	Ti/Al	Si bio	S/Fe	Depth	TOC	Depth
%	%	%	%	%	%	%	%			%		m	%	m
													7.521	3121.29084
													7.424	3121.29150
													7.366	3121.29216
													6.940	3121.29281
													6.951	3121.29347
													6.934	3121.29413
													6.834	3121.29479

Slab 3122.23 m

EDXRF													Hyperspectral Imagery		
Mg %	Al %	Si %	S %	K %	Ca %	Ti %	Fe %	K/Al	Ti/Al	Si bio %	S/Fe	Depth m	TOC %	Depth m	
0.583	4.910	34.168	2.093	1.710	0.060	0.228	2.104	0.348	0.046	18.948	0.995	3122.24929	1.319	3122.25057	
0.539	4.732	34.933	1.910	1.659	0.040	0.223	1.921	0.350	0.047	20.264	0.994	3122.25122	1.362	3122.25114	
0.491	4.671	35.865	1.478	1.649	0.056	0.258	1.638	0.353	0.055	21.386	0.903	3122.25315	1.404	3122.25171	
0.579	4.799	35.888	1.362	1.663	0.044	0.228	1.572	0.347	0.047	21.012	0.866	3122.25508	1.430	3122.25228	
0.395	4.676	35.856	1.481	1.626	0.056	0.232	1.686	0.348	0.050	21.360	0.879	3122.25701	1.430	3122.25285	
0.522	4.676	35.725	1.545	1.588	0.056	0.228	1.681	0.340	0.049	21.228	0.919	3122.25894	1.420	3122.25341	
0.443	4.532	35.739	1.631	1.583	0.060	0.197	1.738	0.349	0.044	21.690	0.938	3122.26086	1.422	3122.25398	
0.438	4.687	35.865	1.491	1.616	0.048	0.215	1.655	0.345	0.046	21.334	0.901	3122.26279	1.445	3122.25455	
0.430	4.660	35.684	1.468	1.626	0.132	0.219	1.668	0.349	0.047	21.239	0.880	3122.26472	1.484	3122.25512	
0.395	4.788	35.598	1.584	1.663	0.072	0.223	1.708	0.347	0.047	20.757	0.928	3122.26665	1.535	3122.25569	
0.382	4.776	35.567	1.591	1.616	0.064	0.223	1.777	0.338	0.047	20.760	0.895	3122.26858	1.591	3122.25626	
0.552	4.660	35.562	1.631	1.649	0.052	0.228	1.699	0.354	0.049	21.117	0.960	3122.27051	1.634	3122.25683	
0.513	4.826	35.607	1.531	1.654	0.048	0.223	1.703	0.343	0.046	20.645	0.899	3122.27244	1.664	3122.25739	
0.355	4.854	35.716	1.448	1.701	0.116	0.236	1.646	0.350	0.049	20.668	0.880	3122.27437	1.699	3122.25796	
0.421	4.726	34.725	2.090	1.588	0.076	0.254	2.008	0.336	0.054	20.073	1.040	3122.27630	1.751	3122.25853	
0.539	4.893	35.693	1.425	1.691	0.048	0.254	1.646	0.346	0.052	20.524	0.865	3122.27823	1.810	3122.25910	
0.474	4.788	35.404	1.584	1.767	0.056	0.228	1.734	0.369	0.048	20.562	0.914	3122.28015	1.855	3122.25967	
0.570	4.938	35.006	1.724	1.673	0.064	0.232	1.834	0.339	0.047	19.699	0.940	3122.28208	1.872	3122.26024	
0.544	5.049	34.644	1.827	1.738	0.080	0.254	1.939	0.344	0.050	18.992	0.942	3122.28401	1.863	3122.26081	
0.338	4.899	33.671	1.787	1.701	0.582	0.241	2.000	0.347	0.049	18.485	0.894	3122.28594	1.839	3122.26137	
0.509	4.938	33.626	2.448	1.588	0.112	0.258	2.335	0.322	0.052	18.319	1.048	3122.28787	1.816	3122.26194	
0.509	4.893	33.019	2.711	1.593	0.080	0.215	2.444	0.326	0.044	17.850	1.109	3122.28980	1.804	3122.26251	
0.587	4.927	34.490	1.854	1.781	0.092	0.236	1.943	0.361	0.048	19.217	0.954	3122.29180	1.798	3122.26308	
0.548	4.999	34.530	1.814	1.738	0.104	0.215	1.947	0.348	0.043	19.034	0.931	3122.29313	1.795	3122.26365	
0.417	4.671	33.802	2.571	1.588	0.120	0.228	2.266	0.340	0.049	19.323	1.135	3122.29447	1.794	3122.26422	
0.460	4.810	35.313	1.588	1.663	0.144	0.241	1.751	0.346	0.050	20.403	0.907	3122.29580	1.803	3122.26479	
0.399	4.938	35.426	1.545	1.757	0.052	0.271	1.808	0.356	0.055	20.119	0.854	3122.29713	1.829	3122.26535	
0.530	4.860	35.168	1.701	1.720	0.056	0.245	1.860	0.354	0.050	20.103	0.914	3122.29847	1.863	3122.26592	
0.408	4.810	35.119	1.790	1.720	0.068	0.258	1.934	0.358	0.054	20.208	0.926	3122.29980	1.887	3122.26649	
0.474	4.899	34.820	1.864	1.748	0.056	0.258	1.934	0.357	0.053	19.634	0.963	3122.30113	1.899	3122.26706	
0.574	4.860	34.933	1.754	1.720	0.060	0.241	1.904	0.354	0.049	19.868	0.921	3122.30247	1.898	3122.26763	
0.447	4.977	35.431	1.485	1.762	0.064	0.232	1.725	0.354	0.047	20.003	0.861	3122.30380	1.878	3122.26820	
0.539	4.943	35.250	1.601	1.720	0.060	0.241	1.760	0.348	0.049	19.926	0.910	3122.30513	1.839	3122.26876	
0.395	5.027	35.639	1.408	1.795	0.068	0.271	1.694	0.357	0.054	20.056	0.831	3122.30647	1.797	3122.26933	
0.509	4.999	35.331	1.535	1.771	0.068	0.254	1.708	0.354	0.051	19.835	0.899	3122.30780	1.772	3122.26990	
0.430	4.799	34.666	2.083	1.663	0.060	0.223	2.013	0.347	0.047	19.790	1.035	3122.30913	1.766	3122.27047	
0.539	4.793	34.829	1.947	1.668	0.060	0.241	1.912	0.348	0.050	19.970	1.018	3122.31047	1.774	3122.27104	
0.430	5.021	35.648	1.388	1.710	0.112	0.254	1.638	0.341	0.050	20.082	0.848	3122.31180	1.782	3122.27161	
0.535	4.993	35.232	1.375	1.893	0.092	0.280	1.795	0.379	0.056	19.752	0.766	3122.31380	1.778	3122.27218	
0.596	5.099	35.123	1.365	1.823	0.084	0.236	1.782	0.357	0.046	19.316	0.766	3122.31558	1.758	3122.27274	
0.552	4.915	34.698	1.578	1.743	0.100	0.249	2.257	0.355	0.051	19.460	0.699	3122.31736	1.734	3122.27331	
0.526	5.110	35.512	1.352	1.781	0.084	0.210	1.655	0.348	0.041	19.671	0.817	3122.31914	1.722	3122.27388	
0.513	4.954	35.634	1.358	1.785	0.060	0.215	1.646	0.360	0.043	20.276	0.825	3122.32092	1.729	3122.27445	
0.421	4.910	35.802	1.375	1.743	0.068	0.236	1.633	0.355	0.048	20.581	0.842	3122.32270	1.755	3122.27502	
0.570	4.654	33.924	2.432	1.565	0.092	0.197	2.222	0.336	0.042	19.497	1.094	3122.32448	1.793	3122.27559	
0.452	4.993	34.530	1.970	1.729	0.064	0.215	1.973	0.346	0.043	19.051	0.998	3122.32626	1.826	3122.27616	
0.495	5.032	35.236	1.478	1.818	0.128	0.288	1.694	0.361	0.057	19.636	0.872	3122.32804	1.839	3122.27672	
0.522	5.199	35.363	1.398	1.809	0.100	0.232	1.594	0.348	0.045	19.246	0.877	3122.32982	1.825	3122.27729	
0.495	5.088	35.576	1.275	1.790	0.108	0.258	1.612	0.352	0.051	19.803	0.791	3122.33160	1.798	3122.27786	
0.478	5.060	35.585	1.372	1.743	0.112	0.223	1.633	0.344	0.044	19.898	0.840	3122.33338	1.767	3122.27843	
													1.737	3122.27900	
													1.707	3122.27957	
													1.683	3122.28014	
													1.674	3122.28070	
													1.645	3122.28127	
													1.625	3122.28184	
													1.589	3122.28241	
													1.553	3122.28298	
													1.521	3122.28355	
													1.489	3122.28411	
													1.459	3122.28468	

EDXRF												Hyperspectral Imagery		
Mg	Al	Si	S	K	Ca	Ti	Fe	K/Al	Ti/Al	Si bio	S/Fe	Depth	TOC	Depth
%	%	%	%	%	%	%	%			%		m	%	m
													1.416	3122.28639
													1.394	3122.28696
													1.358	3122.28753
													1.319	3122.28809
													1.438	3122.28525
													1.427	3122.28582
													1.283	3122.28866
													1.270	3122.28923
													1.291	3122.28980
													1.355	3122.29037
													1.433	3122.29094
													1.493	3122.29151
													1.524	3122.29207
													1.535	3122.29264
													1.538	3122.29321
													1.542	3122.29378
													1.552	3122.29435
													1.576	3122.29492
													1.601	3122.29549
													1.626	3122.29605
													1.652	3122.29662
													1.672	3122.29719
													1.686	3122.29776
													1.698	3122.29833
													1.706	3122.29890
													1.687	3122.29946
													1.651	3122.30003
													1.617	3122.30060
													1.605	3122.30117
													1.607	3122.30174
													1.614	3122.30231
													1.641	3122.30288
													1.687	3122.30344
													1.723	3122.30401
													1.724	3122.30458
													1.707	3122.30515
													1.715	3122.30572
													1.747	3122.30629
													1.788	3122.30686
													1.811	3122.30742
													1.797	3122.30799
													1.760	3122.30856
													1.725	3122.30913
													1.705	3122.30970
													1.706	3122.31027
													1.719	3122.31084
													1.737	3122.31140
													1.757	3122.31197
													1.764	3122.31254
													1.759	3122.31311
													1.740	3122.31368
													1.715	3122.31425
													1.709	3122.31481
													1.729	3122.31538
													1.767	3122.31595
													1.796	3122.31652
													1.785	3122.31709
													1.733	3122.31766
													1.708	3122.31823
													1.725	3122.31879
													1.710	3122.31936

EDXRF												Hyperspectral Imagery		
Mg	Al	Si	S	K	Ca	Ti	Fe	K/Al	Ti/Al	Si bio	S/Fe	Depth	TOC	Depth
%	%	%	%	%	%	%	%			%		m	%	m
													1.756	3122.31993
													1.750	3122.32050
													1.685	3122.32107
													1.603	3122.32164
													1.486	3122.32221
													1.278	3122.32448
													1.272	3122.32505
													1.234	3122.32562
													1.386	3122.32619
													1.494	3122.32277
													1.450	3122.32334
													1.339	3122.32391
													1.435	3122.32675
													1.374	3122.32732
													1.407	3122.32789
													1.408	3122.32846
													1.459	3122.32903
													1.498	3122.32960
													1.532	3122.33016
													1.538	3122.33073
													1.604	3122.33130
													1.587	3122.33187
													1.517	3122.33244
													1.497	3122.33301
													1.492	3122.33358
													1.525	3122.33414

Slab 3122.95 m

EDXRF												Hyperspectral Imagery			
Mg %	Al %	Si %	S %	K %	Ca %	Ti %	Fe %	K/Al	Ti/Al	Si bio %	S/Fe	Depth m	TOC %	Depth m	
0.693	6.328	32.657	1.807	2.255	0.204	0.327	1.987	0.356	0.052	13.039	0.910	3122.97357	0.808	3122.97267	
0.732	6.890	33.137	1.199	2.438	0.148	0.336	1.721	0.354	0.049	11.777	0.697	3122.97514	0.832	3122.97335	
0.693	6.479	32.879	1.624	2.325	0.196	0.349	1.899	0.359	0.054	12.796	0.855	3122.97671	0.844	3122.97402	
0.653	6.245	32.793	1.790	2.227	0.227	0.310	2.000	0.357	0.050	13.434	0.895	3122.97829	0.849	3122.97469	
0.557	6.328	32.603	1.883	2.199	0.279	0.345	1.973	0.347	0.054	12.985	0.954	3122.97986	0.851	3122.97537	
0.802	6.456	32.607	1.707	2.283	0.184	0.314	1.982	0.354	0.049	12.593	0.861	3122.98143	0.851	3122.97604	
0.609	6.284	31.888	2.345	2.241	0.235	0.340	2.196	0.357	0.054	12.408	1.068	3122.98300	0.848	3122.97671	
0.513	6.428	32.626	1.827	2.260	0.176	0.336	2.130	0.351	0.052	12.697	0.858	3122.98457	0.845	3122.97739	
0.671	6.490	31.956	2.066	2.316	0.212	0.327	2.165	0.357	0.050	11.838	0.954	3122.98614	0.844	3122.97806	
0.653	6.473	32.798	1.747	2.241	0.176	0.345	1.978	0.354	0.053	12.731	0.883	3122.98771	0.842	3122.97873	
0.741	6.512	32.598	1.774	2.283	0.200	0.340	1.939	0.351	0.052	12.412	0.915	3122.98929	0.835	3122.97941	
0.706	6.339	32.621	1.880	2.246	0.204	0.306	1.991	0.354	0.048	12.969	0.944	3122.99086	0.826	3122.98008	
0.640	6.250	32.662	1.910	2.175	0.227	0.314	2.043	0.348	0.050	13.285	0.935	3122.99243	0.822	3122.98075	
0.583	6.317	32.046	2.212	2.227	0.267	0.319	2.148	0.352	0.050	12.463	1.030	3122.99400	0.827	3122.98143	
0.631	6.301	32.119	2.123	2.184	0.212	0.319	2.222	0.347	0.051	12.587	0.955	3122.99557	0.838	3122.98210	
0.706	6.384	32.436	1.874	2.250	0.184	0.323	2.122	0.352	0.051	12.645	0.883	3122.99714	0.853	3122.98278	
0.697	6.523	32.883	1.634	2.288	0.176	0.332	1.895	0.351	0.051	12.662	0.862	3122.99871	0.863	3122.98345	
0.609	6.200	32.933	1.751	2.227	0.196	0.306	2.056	0.359	0.049	13.712	0.851	3123.00029	0.869	3122.98412	
0.609	6.212	32.648	1.930	2.170	0.215	0.301	2.096	0.349	0.049	13.392	0.921	3123.00186	0.876	3122.98480	
0.684	6.423	31.825	2.259	2.189	0.200	0.345	2.253	0.341	0.054	11.914	1.003	3123.00343	0.889	3122.98547	
0.662	6.072	30.476	3.126	2.044	0.255	0.301	2.819	0.337	0.050	11.652	1.109	3123.00500	0.907	3122.98614	
0.741	6.384	32.870	1.668	2.283	0.208	0.323	1.899	0.358	0.051	13.080	0.878	3123.00657	0.923	3122.98682	
0.771	6.384	32.585	1.800	2.316	0.239	0.332	1.891	0.363	0.052	12.795	0.952	3123.00814	0.930	3122.98749	
0.636	6.072	32.033	2.379	2.109	0.291	0.332	2.209	0.347	0.055	13.208	1.077	3123.00971	0.922	3122.98816	
0.741	6.317	31.748	2.103	2.213	0.335	0.301	2.314	0.350	0.048	12.164	0.909	3123.01129	0.899	3122.98884	
0.662	6.045	32.055	2.342	2.142	0.271	0.336	2.218	0.354	0.056	13.317	1.056	3123.01286	0.869	3122.98951	
0.688	6.256	31.218	2.605	2.227	0.263	0.327	2.427	0.356	0.052	11.825	1.073	3123.01443	0.843	3122.99018	
0.566	6.061	32.146	2.229	2.086	0.323	0.314	2.248	0.344	0.052	13.356	0.992	3123.01600	0.832	3122.99086	
0.622	6.212	32.458	2.020	2.175	0.215	0.310	2.165	0.350	0.050	13.202	0.933	3123.01757	0.840	3122.99153	
0.697	5.989	31.675	2.525	2.067	0.184	0.310	2.580	0.345	0.052	13.109	0.979	3123.01914	0.860	3122.99220	
0.675	6.301	32.698	1.824	2.180	0.188	0.319	2.104	0.346	0.051	13.166	0.867	3123.02071	0.879	3122.99288	
0.640	5.945	32.399	2.129	2.123	0.156	0.327	2.379	0.357	0.055	13.971	0.895	3123.02229	0.887	3122.99355	
0.688	6.161	32.399	2.006	2.156	0.124	0.301	2.327	0.350	0.049	13.299	0.862	3123.02386	0.886	3122.99422	
0.671	6.100	32.544	1.953	2.189	0.132	0.301	2.296	0.359	0.049	13.633	0.851	3123.02543	0.881	3122.99490	
0.728	6.223	32.558	1.937	2.231	0.208	0.332	2.087	0.359	0.053	13.268	0.928	3123.02700	0.876	3122.99557	
0.592	5.956	32.549	2.179	2.048	0.251	0.301	2.196	0.344	0.051	14.086	0.992	3123.02857	0.874	3122.99624	
0.666	6.178	32.218	2.136	2.076	0.259	0.319	2.170	0.336	0.052	13.066	0.984	3123.03014	0.882	3122.99692	
0.679	6.095	31.653	2.512	2.147	0.263	0.349	2.340	0.352	0.057	12.759	1.073	3123.03171	0.899	3122.99759	
0.706	6.150	32.322	2.206	2.170	0.223	0.332	2.021	0.353	0.054	13.256	1.091	3123.03329	0.909	3122.99827	
0.644	6.484	32.612	1.830	2.250	0.180	0.314	2.000	0.347	0.048	12.511	0.915	3123.03486	0.879	3122.99894	
0.618	6.440	31.861	2.219	2.278	0.196	0.353	2.244	0.354	0.055	11.898	0.989	3123.03643	0.880	3122.99961	
0.644	6.339	32.246	1.967	2.231	0.215	0.332	2.191	0.352	0.052	12.593	0.897	3123.03800	0.885	3123.00029	
0.649	6.217	32.372	1.960	2.222	0.208	0.323	2.183	0.357	0.052	13.099	0.898	3123.03957	0.895	3123.00096	
0.693	6.273	32.693	1.857	2.213	0.223	0.345	1.991	0.353	0.055	13.248	0.933	3123.04114	0.902	3123.00163	
0.649	6.050	32.046	2.382	2.058	0.184	0.284	2.327	0.340	0.047	13.291	1.024	3123.04271	0.901	3123.00231	
0.679	6.195	32.635	1.910	2.166	0.168	0.306	2.148	0.350	0.049	13.431	0.889	3123.04429	0.889	3123.00298	
0.618	6.223	31.865	2.359	2.114	0.255	0.306	2.248	0.340	0.049	12.575	1.049	3123.04586	0.875	3123.00365	
0.679	6.417	30.938	2.751	2.194	0.259	0.319	2.405	0.342	0.050	11.044	1.144	3123.04743	0.866	3123.00433	
0.754	6.312	32.318	2.026	2.227	0.196	0.349	2.104	0.353	0.055	12.752	0.963	3123.04900	0.863	3123.00500	
													0.863	3123.00567	
													0.858	3123.00635	
													0.848	3123.00702	
													0.841	3123.00769	
													0.843	3123.00837	
													0.859	3123.00904	
													0.881	3123.00971	
													0.896	3123.01039	
													0.898	3123.01106	
													0.887	3123.01173	
													0.872	3123.01241	
													0.862	3123.01308	
													0.858	3123.01376	
													0.857	3123.01443	
													0.856	3123.01510	
													0.857	3123.01578	

EDXRF												Hyperspectral Imagery		
Mg %	Al %	Si %	S %	K %	Ca %	Ti %	Fe %	K/Al	Ti/Al	Si bio %	S/Fe	Depth m	TOC %	Depth m
													0.861	3123.01645
													0.867	3123.01712
													0.874	3123.01780
													0.875	3123.01847
													0.866	3123.01914
													0.850	3123.01982
													0.837	3123.02049
													0.830	3123.02116
													0.826	3123.02184
													0.818	3123.02251
													0.808	3123.02318
													0.801	3123.02386
													0.804	3123.02453
													0.816	3123.02520
													0.827	3123.02588
													0.831	3123.02655
													0.829	3123.02722
													0.827	3123.02790
													0.829	3123.02857
													0.831	3123.02925
													0.831	3123.02992
													0.829	3123.03059
													0.828	3123.03127
													0.825	3123.03194
													0.813	3123.03261
													0.792	3123.03329
													0.772	3123.03396
													0.756	3123.03463
													0.742	3123.03531
													0.731	3123.03598
													0.730	3123.03665
													0.734	3123.03733
													0.735	3123.03800
													0.726	3123.03867
													0.727	3123.03935
													0.741	3123.04002
													0.778	3123.04069
													0.812	3123.04137
													0.830	3123.04204
													0.832	3123.04271
													0.821	3123.04339
													0.801	3123.04406
													0.767	3123.04474
													0.761	3123.04541
													0.763	3123.04608
													0.772	3123.04676
													0.770	3123.04743
													0.765	3123.04810
													0.754	3123.04878
													0.740	3123.04945

EDXRF												Hyperspectral Imagery		
Mg %	Al %	Si %	S %	K %	Ca %	Ti %	Fe %	K/Al	Ti/Al	Si bio %	S/Fe	Depth m	TOC %	Depth m
5.118	5.177	18.228	0.568	1.189	10.922	0.197	3.295	0.230	0.038	2.180	0.172	3124.24479	0.382	3124.19721
5.368	4.888	17.712	0.634	1.109	11.257	0.223	3.482	0.227	0.046	2.561	0.182	3124.24670	0.378	3124.19797
													0.373	3124.19873
													0.370	3124.19949
													0.372	3124.20025
													0.378	3124.20102
													0.385	3124.20178
													0.390	3124.20254
													0.390	3124.20330
													0.386	3124.20406
													0.382	3124.20482
													0.380	3124.20558
													0.380	3124.20635
													0.381	3124.20711
													0.384	3124.20787
													0.388	3124.20863
													0.391	3124.20939
													0.393	3124.21015
													0.393	3124.21091
													0.396	3124.21168
													0.399	3124.21244
													0.401	3124.21320
													0.401	3124.21396
													0.400	3124.21472
													0.399	3124.21548
													0.399	3124.21624
													0.401	3124.21700
													0.403	3124.21777
													0.409	3124.21853
													0.417	3124.21929
													0.425	3124.22005
													0.430	3124.22081
													0.431	3124.22157
													0.425	3124.22233
													0.414	3124.22310
													0.400	3124.22386
													0.388	3124.22462
													0.381	3124.22538
													0.380	3124.22614
													0.387	3124.22690
													0.397	3124.22766
													0.405	3124.22843
													0.407	3124.22919
													0.404	3124.22995
													0.398	3124.23071
													0.393	3124.23147
													0.391	3124.23223
													0.391	3124.23299
													0.392	3124.23376
													0.393	3124.23452
													0.394	3124.23528
													0.393	3124.23604
													0.390	3124.23680
													0.386	3124.23756
													0.382	3124.23832
													0.379	3124.23909
													0.377	3124.23985
													0.378	3124.24061
													0.380	3124.24137
													0.382	3124.24213
													0.382	3124.24289
													0.381	3124.24365

EDXRF												Hyperspectral Imagery		
Mg	Al	Si	S	K	Ca	Ti	Fe	K/Al	Ti/Al	Si bio	S/Fe	Depth	TOC	Depth
%	%	%	%	%	%	%	%			%		m	%	m
													0.378	3124.24442
													0.376	3124.24518
													0.375	3124.24594
													0.377	3124.24670

EDXRF												Hyperspectral Imagery		
Mg	Al	Si	S	K	Ca	Ti	Fe	K/Al	Ti/Al	Si bio	S/Fe	Depth	TOC	Depth
%	%	%	%	%	%	%	%			%		m	%	m
													2.873	3125.84197
													2.805	3125.84263
													2.770	3125.84329
													2.776	3125.84395
													2.811	3125.84460
													2.852	3125.84526
													2.882	3125.84592
													2.900	3125.84658
													2.904	3125.84724
													2.888	3125.84790
													2.857	3125.84856
													2.832	3125.84922
													2.837	3125.84988

EDXRF													Hyperspectral Imagery	
Mg %	Al %	Si %	S %	K %	Ca %	Ti %	Fe %	K/Al	Ti/Al	Si bio %	S/Fe	Depth m	TOC %	Depth m
0.377	4.765	35.490	1.199	1.729	0.144	0.215	2.039	0.363	0.045	20.717	0.588	3127.02789	2.171	3126.99958
0.469	4.865	35.829	1.149	1.738	0.104	0.210	1.747	0.357	0.043	20.746	0.658	3127.02899	2.144	3127.00031
0.530	4.977	35.680	1.146	1.799	0.092	0.254	1.686	0.362	0.051	20.252	0.680	3127.03008	2.125	3127.00105
0.653	5.004	35.539	1.179	1.710	0.088	0.215	1.716	0.342	0.043	20.026	0.687	3127.03117	2.111	3127.00179
0.495	5.043	35.607	1.166	1.795	0.092	0.249	1.725	0.356	0.049	19.973	0.676	3127.03227	2.094	3127.00253
0.517	5.027	35.390	1.176	1.795	0.124	0.262	1.817	0.357	0.052	19.807	0.647	3127.03336	2.060	3127.00327
0.474	4.971	35.589	1.176	1.781	0.108	0.249	1.790	0.358	0.050	20.179	0.657	3127.03445	2.008	3127.00401
0.408	5.004	35.657	1.189	1.771	0.120	0.245	1.795	0.354	0.049	20.143	0.662	3127.03554	2.000	3127.00475
0.561	4.832	35.739	1.212	1.696	0.120	0.232	1.712	0.351	0.048	20.759	0.708	3127.03664	2.037	3127.00549
0.482	4.771	35.720	1.252	1.682	0.112	0.215	1.803	0.353	0.045	20.931	0.694	3127.03773	2.087	3127.00622
													2.135	3127.00696
													2.174	3127.00770
													2.190	3127.00844
													2.166	3127.00918
													2.162	3127.00992
													2.154	3127.01066
													2.172	3127.01140
													2.211	3127.01213
													2.244	3127.01287
													2.270	3127.01361
													2.291	3127.01435
													2.279	3127.01509
													2.223	3127.01583
													2.143	3127.01657
													2.085	3127.01731
													2.059	3127.01804
													2.046	3127.01878
													2.037	3127.01952
													2.031	3127.02026
													2.039	3127.02100
													2.056	3127.02174
													2.080	3127.02248
													2.116	3127.02322
													2.171	3127.02395
													2.232	3127.02469
													2.268	3127.02543
													2.272	3127.02617
													2.244	3127.02691
													2.199	3127.02765
													2.157	3127.02839
													2.115	3127.02913
													2.095	3127.02986
													2.104	3127.03060
													2.133	3127.03134
													2.149	3127.03208
													2.133	3127.03282
													2.084	3127.03356
													2.030	3127.03430
													1.995	3127.03504
													1.988	3127.03577
													2.005	3127.03651
													2.025	3127.03725
													2.039	3127.03799

Slab 3128.05 m

EDXRF													Hyperspectral Imagery		
Mg %	Al %	Si %	S %	K %	Ca %	Ti %	Fe %	K/Al	Ti/Al	Si bio %	S/Fe	Depth m	TOC %	Depth m	
1.188	4.153	22.730	4.844	0.968	3.276	0.184	5.248	0.233	0.044	9.855	0.923	3128.05000	0.653	3128.05000	
1.210	4.115	22.857	4.781	0.893	3.308	0.275	5.292	0.217	0.067	10.102	0.904	3128.05183	0.903	3128.05080	
1.626	3.742	28.743	1.422	0.809	4.443	0.097	3.037	0.216	0.026	17.144	0.468	3128.05366	1.016	3128.05159	
0.373	4.181	34.978	1.202	1.198	0.686	0.175	1.324	0.287	0.042	22.017	0.908	3128.05550	1.194	3128.05239	
0.289	4.087	36.761	1.209	1.264	0.176	0.171	1.241	0.309	0.042	24.092	0.974	3128.05733	1.381	3128.05318	
0.342	4.115	36.775	1.332	1.325	0.148	0.206	1.328	0.322	0.050	24.020	1.003	3128.05916	1.558	3128.05398	
0.382	4.343	35.671	1.581	1.630	0.227	0.210	1.590	0.375	0.048	22.209	0.995	3128.06099	1.735	3128.05477	
0.500	5.182	36.508	0.727	1.889	0.148	0.288	1.228	0.364	0.056	20.442	0.592	3128.06283	1.902	3128.05557	
0.601	4.971	34.372	1.990	1.767	0.164	0.254	1.708	0.355	0.051	18.962	1.165	3128.06466	2.025	3128.05636	
0.583	5.355	36.250	0.701	1.917	0.128	0.254	1.210	0.358	0.047	19.650	0.579	3128.06649	2.082	3128.05716	
0.557	5.271	35.530	0.996	2.025	0.124	0.284	1.381	0.384	0.054	19.189	0.722	3128.06832	2.077	3128.05796	
0.500	5.338	35.906	0.907	1.907	0.112	0.262	1.258	0.357	0.049	19.357	0.720	3128.07015	2.037	3128.05875	
0.596	5.483	35.250	1.099	1.950	0.152	0.284	1.402	0.356	0.052	18.253	0.784	3128.07199	1.997	3128.05955	
0.592	5.744	35.336	0.823	2.142	0.148	0.284	1.319	0.373	0.049	17.529	0.624	3128.07382	1.971	3128.06034	
0.701	6.039	35.137	0.701	2.250	0.140	0.314	1.280	0.373	0.052	16.416	0.547	3128.07565	1.954	3128.06114	
0.618	5.956	35.087	0.777	2.170	0.172	0.301	1.333	0.364	0.051	16.624	0.583	3128.07748	1.928	3128.06193	
0.644	5.767	34.816	0.986	2.133	0.192	0.301	1.385	0.370	0.052	16.939	0.712	3128.07932	1.896	3128.06273	
0.557	5.872	34.530	1.129	2.156	0.180	0.297	1.481	0.367	0.051	16.327	0.763	3128.08115	1.871	3128.06352	
0.649	6.295	34.295	0.913	2.349	0.164	0.345	1.472	0.373	0.055	14.781	0.620	3128.08298	1.858	3128.06432	
0.561	5.589	30.128	3.605	1.917	0.152	0.280	3.177	0.343	0.050	12.804	1.135	3128.08481	1.850	3128.06512	
0.526	5.422	30.440	3.542	1.865	0.140	0.236	3.059	0.344	0.044	13.633	1.158	3128.08665	1.835	3128.06591	
0.596	6.206	32.933	1.751	2.297	0.231	0.319	1.742	0.370	0.051	13.695	1.005	3128.08848	1.802	3128.06671	
0.697	6.645	33.847	0.863	2.447	0.164	0.349	1.428	0.368	0.053	13.247	0.604	3128.09031	1.763	3128.06750	
0.763	6.823	33.612	0.893	2.424	0.188	0.336	1.472	0.355	0.049	12.459	0.607	3128.09214	1.731	3128.06830	
0.771	6.723	33.209	0.926	2.480	0.275	0.358	1.542	0.369	0.053	12.367	0.601	3128.09397	1.707	3128.06909	
0.653	6.940	33.182	0.933	2.565	0.247	0.336	1.520	0.370	0.048	11.668	0.614	3128.09581	1.673	3128.06989	
0.649	6.751	33.345	1.036	2.457	0.219	0.336	1.572	0.364	0.050	12.417	0.659	3128.09764	1.628	3128.07068	
0.666	6.612	31.798	1.927	2.368	0.243	0.319	2.061	0.358	0.048	11.300	0.935	3128.09947	1.584	3128.07148	
0.614	6.456	29.992	2.954	2.236	0.184	0.310	2.911	0.346	0.048	9.978	1.015	3128.10130	1.548	3128.07228	
0.622	6.645	30.852	2.322	2.358	0.231	0.319	2.466	0.355	0.048	10.251	0.942	3128.10314	1.516	3128.07307	
0.802	7.140	32.730	1.020	2.579	0.208	0.384	1.642	0.361	0.054	10.594	0.621	3128.10497	1.498	3128.07387	
0.719	7.152	32.535	1.103	2.635	0.196	0.397	1.712	0.368	0.055	10.365	0.644	3128.10680	1.496	3128.07466	
0.723	6.773	29.345	2.787	2.358	0.363	0.353	2.994	0.348	0.052	8.348	0.931	3128.10880	1.494	3128.07546	
0.868	7.063	29.237	2.678	2.302	0.375	0.375	2.968	0.326	0.053	7.343	0.902	3128.11082	1.479	3128.07625	
0.758	7.302	32.105	1.249	2.602	0.231	0.392	1.838	0.356	0.054	9.470	0.679	3128.11284	1.448	3128.07705	
0.842	7.407	31.906	1.216	2.640	0.247	0.401	1.790	0.356	0.054	8.943	0.679	3128.11486	1.407	3128.07784	
0.636	7.268	32.123	1.302	2.588	0.283	0.423	1.851	0.356	0.058	9.591	0.703	3128.11688	1.372	3128.07864	
0.719	7.146	30.458	2.252	2.494	0.219	0.366	2.388	0.349	0.051	8.306	0.943	3128.11890	1.351	3128.07943	
0.706	7.396	31.748	1.432	2.602	0.227	0.423	1.891	0.352	0.057	8.819	0.757	3128.12092	1.333	3128.08023	
0.798	7.602	32.137	1.010	2.790	0.219	0.453	1.681	0.367	0.060	8.570	0.600	3128.12294	1.305	3128.08103	
0.688	7.330	31.970	1.272	2.668	0.239	0.410	1.821	0.364	0.056	9.248	0.699	3128.12496	1.270	3128.08182	
0.842	7.363	31.644	1.385	2.649	0.231	0.384	1.912	0.360	0.052	8.819	0.724	3128.12698	1.246	3128.08262	
0.745	7.296	30.924	1.940	2.546	0.219	0.397	2.261	0.349	0.054	8.306	0.858	3128.12900	1.244	3128.08341	
0.771	6.962	30.599	2.222	2.443	0.239	0.358	2.449	0.351	0.051	9.015	0.908	3128.13102	1.256	3128.08421	
0.750	7.363	32.015	1.299	2.663	0.188	0.379	1.847	0.362	0.052	9.190	0.703	3128.13304	1.264	3128.08500	
0.723	7.346	31.956	1.329	2.593	0.196	0.405	1.886	0.353	0.055	9.183	0.704	3128.13506	1.261	3128.08580	
0.728	7.196	32.101	1.358	2.574	0.219	0.388	1.838	0.358	0.054	9.793	0.739	3128.13708	1.248	3128.08659	
0.679	7.257	32.164	1.236	2.659	0.204	0.388	1.834	0.366	0.053	9.667	0.674	3128.13910	1.232	3128.08739	
													1.216	3128.08819	
													1.197	3128.08898	
													1.175	3128.08978	
													1.152	3128.09057	
													1.121	3128.09137	
													1.081	3128.09216	
													1.043	3128.09296	
													1.021	3128.09375	
													1.018	3128.09455	
													1.025	3128.09535	
													1.021	3128.09614	
													0.991	3128.09694	
													0.942	3128.09773	
													0.899	3128.09853	

EDXRF												Hyperspectral Imagery		
Mg	Al	Si	S	K	Ca	Ti	Fe	K/Al	Ti/Al	Si bio	S/Fe	Depth	TOC	Depth
%	%	%	%	%	%	%	%			%		m	%	m
													0.878	3128.09932
													0.877	3128.10012
													0.883	3128.10091
													0.879	3128.10171
													0.862	3128.10251
													0.842	3128.10330
													0.830	3128.10410
													0.822	3128.10489
													0.810	3128.10569
													0.808	3128.10648
													0.783	3128.10728
													0.773	3128.10807
													0.756	3128.10887
													0.740	3128.10967
													0.727	3128.11046
													0.718	3128.11126
													0.718	3128.11205
													0.730	3128.11285
													0.753	3128.11364
													0.776	3128.11444
													0.792	3128.11523
													0.800	3128.11603
													0.799	3128.11683
													0.789	3128.11762
													0.768	3128.11842
													0.745	3128.11921
													0.725	3128.12001
													0.719	3128.12080
													0.730	3128.12160
													0.743	3128.12239
													0.744	3128.12319
													0.734	3128.12399
													0.730	3128.12478
													0.735	3128.12558
													0.739	3128.12637
													0.733	3128.12717
													0.722	3128.12796
													0.714	3128.12876
													0.716	3128.12955
													0.723	3128.13035
													0.728	3128.13115
													0.727	3128.13194
													0.727	3128.13274
													0.733	3128.13353
													0.742	3128.13433
													0.747	3128.13512
													0.752	3128.13592
													0.762	3128.13671
													0.774	3128.13751
													0.784	3128.13830
													0.782	3128.13910

EDXRF												Hyperspectral Imagery		
Mg %	Al %	Si %	S %	K %	Ca %	Ti %	Fe %	K/Al	Ti/Al	Si bio %	S/Fe	Depth m	TOC %	Depth m
0.714	5.894	33.377	1.408	1.959	0.590	0.297	1.895	0.332	0.050	15.104	0.743	3128.64517	1.244	3128.60086
0.693	5.716	32.997	1.677	1.917	0.598	0.310	2.048	0.335	0.054	15.276	0.819	3128.64670	1.239	3128.60168
													1.227	3128.60249
													1.214	3128.60331
													1.209	3128.60413
													1.218	3128.60495
													1.237	3128.60577
													1.253	3128.60659
													1.256	3128.60741
													1.249	3128.60822
													1.234	3128.60904
													1.216	3128.60986
													1.198	3128.61068
													1.184	3128.61150
													1.181	3128.61232
													1.196	3128.61314
													1.232	3128.61395
													1.271	3128.61477
													1.294	3128.61559
													1.295	3128.61641
													1.289	3128.61723
													1.290	3128.61805
													1.296	3128.61887
													1.302	3128.61969
													1.299	3128.62050
													1.284	3128.62132
													1.265	3128.62214
													1.256	3128.62296
													1.265	3128.62378
													1.283	3128.62460
													1.293	3128.62542
													1.285	3128.62623
													1.255	3128.62705
													1.222	3128.62787
													1.210	3128.62869
													1.223	3128.62951
													1.240	3128.63033
													1.242	3128.63115
													1.219	3128.63196
													1.188	3128.63278
													1.161	3128.63360
													1.149	3128.63442
													1.147	3128.63524
													1.147	3128.63606
													1.142	3128.63688
													1.133	3128.63770
													1.127	3128.63851
													1.143	3128.63933
													1.146	3128.64015
													1.152	3128.64097
													1.155	3128.64179
													1.156	3128.64261
													1.160	3128.64343
													1.168	3128.64424
													1.176	3128.64506
													1.179	3128.64588
													1.177	3128.64670
													1.165	3128.64752
													1.141	3128.64834
													1.118	3128.64916
													1.090	3128.64997
													1.091	3128.65079

EDXRF												Hyperspectral Imagery		
Mg	Al	Si	S	K	Ca	Ti	Fe	K/Al	Ti/Al	Si bio	S/Fe	Depth	TOC	Depth
%	%	%	%	%	%	%	%			%		m	%	m
													1.097	3128.65161

EDXRF												Hyperspectral Imagery		
Mg %	Al %	Si %	S %	K %	Ca %	Ti %	Fe %	K/Al	Ti/Al	Si bio %	S/Fe	Depth m	TOC %	Depth m
0.991	5.967	31.436	1.305	2.011	1.813	0.349	2.187	0.337	0.058	12.939	0.597	3129.63763	1.022	3129.59301
0.942	6.134	31.336	1.794	2.044	1.140	0.345	2.296	0.333	0.056	12.322	0.781	3129.63920	1.024	3129.59386
													1.034	3129.59472
													1.050	3129.59557
													1.062	3129.59642
													1.060	3129.59728
													1.047	3129.59813
													1.031	3129.59898
													1.018	3129.59984
													1.010	3129.60069
													1.005	3129.60154
													1.001	3129.60239
													0.999	3129.60325
													0.998	3129.60410
													0.996	3129.60495
													0.992	3129.60581
													0.986	3129.60666
													0.983	3129.60751
													0.984	3129.60836
													0.990	3129.60922
													0.999	3129.61007
													1.015	3129.61092
													1.030	3129.61178
													1.031	3129.61263
													1.014	3129.61348
													0.993	3129.61433
													0.992	3129.61519
													1.010	3129.61604
													1.030	3129.61689
													1.039	3129.61775
													1.033	3129.61860
													1.024	3129.61945
													1.020	3129.62031
													1.021	3129.62116
													1.021	3129.62201
													1.016	3129.62286
													1.009	3129.62372
													1.003	3129.62457
													0.998	3129.62542
													0.994	3129.62628
													0.994	3129.62713
													0.995	3129.62798
													0.989	3129.62883
													0.991	3129.62969
													0.990	3129.63054
													0.981	3129.63139
													0.965	3129.63225
													0.954	3129.63310
													0.955	3129.63395
													0.963	3129.63480
													0.968	3129.63566
													0.966	3129.63651
													0.964	3129.63736

Slab 3129.85 m

EDXRF														Hyperspectral Imagery	
Mg %	Al %	Si %	S %	K %	Ca %	Ti %	Fe %	K/Al	Ti/Al	Si bio %	S/Fe	Depth m	TOC %	Depth m	
0.995	6.056	28.929	2.605	1.950	1.694	0.371	3.002	0.322	0.061	10.156	0.867	3129.85000	0.958	3129.85046	
1.047	6.078	28.798	2.615	1.898	1.710	0.340	3.002	0.312	0.056	9.956	0.871	3129.85119	0.984	3129.85125	
0.982	6.295	31.128	1.551	2.053	1.459	0.353	2.226	0.326	0.056	11.614	0.697	3129.85239	0.989	3129.85203	
0.938	6.145	30.856	1.611	1.987	1.650	0.323	2.287	0.323	0.053	11.808	0.704	3129.85358	0.978	3129.85282	
0.938	6.479	31.454	1.465	2.166	1.279	0.375	2.039	0.334	0.058	11.370	0.718	3129.85477	0.968	3129.85361	
0.868	6.723	31.811	1.305	2.269	1.012	0.388	1.930	0.337	0.058	10.969	0.676	3129.85597	0.968	3129.85439	
0.890	6.740	31.648	1.236	2.269	1.200	0.379	1.973	0.337	0.056	10.754	0.626	3129.85716	0.966	3129.85518	
1.069	6.428	30.915	1.348	2.095	1.702	0.349	2.178	0.326	0.054	10.987	0.619	3129.85835	0.956	3129.85597	
1.052	6.573	30.956	1.348	2.100	1.562	0.349	2.196	0.319	0.053	10.579	0.614	3129.85955	0.938	3129.85675	
0.938	6.356	30.182	1.943	2.081	1.499	0.340	2.549	0.327	0.054	10.478	0.762	3129.86074	0.922	3129.85754	
1.021	6.301	29.730	2.103	1.978	1.614	0.340	2.719	0.314	0.054	10.198	0.773	3129.86194	0.906	3129.85833	
1.017	6.456	30.675	1.638	2.086	1.538	0.349	2.287	0.323	0.054	10.661	0.716	3129.86313	0.889	3129.85911	
1.039	6.428	31.481	1.305	2.081	1.439	0.358	2.043	0.324	0.056	11.553	0.639	3129.86432	0.870	3129.85990	
1.065	6.629	31.639	1.166	2.236	1.267	0.405	1.917	0.337	0.061	11.090	0.608	3129.86552	0.851	3129.86069	
0.855	6.467	31.580	1.345	2.194	1.251	0.379	2.061	0.339	0.059	11.531	0.653	3129.86671	0.835	3129.86148	
0.872	6.440	30.983	1.664	2.142	1.323	0.379	2.257	0.333	0.059	11.020	0.737	3129.86790	0.831	3129.86226	
0.776	6.773	31.847	1.412	2.358	0.773	0.362	1.895	0.348	0.053	10.850	0.745	3129.86910	0.844	3129.86305	
0.736	6.896	32.051	1.302	2.429	0.630	0.401	1.899	0.352	0.058	10.674	0.685	3129.87029	0.871	3129.86384	
0.732	6.312	31.255	1.727	2.142	1.132	0.301	2.266	0.339	0.048	11.689	0.762	3129.87148	0.897	3129.86462	
0.846	6.150	30.205	1.970	2.001	1.706	0.340	2.514	0.325	0.055	11.139	0.784	3129.87268	0.906	3129.86541	
1.065	6.095	29.644	2.222	1.940	1.746	0.340	2.675	0.318	0.056	10.750	0.831	3129.87387	0.900	3129.86620	
1.201	5.711	28.866	2.345	1.781	2.264	0.284	2.959	0.312	0.050	11.162	0.793	3129.87506	0.883	3129.86698	
1.201	5.800	29.015	2.362	1.813	2.017	0.349	3.020	0.313	0.060	11.035	0.782	3129.87626	0.862	3129.86777	
1.240	5.733	28.594	2.342	1.799	2.343	0.288	3.020	0.314	0.050	10.821	0.776	3129.87745	0.843	3129.86856	
1.047	5.894	28.988	2.272	1.828	2.216	0.306	2.933	0.310	0.052	10.715	0.775	3129.87864	0.831	3129.86934	
1.126	6.017	30.047	1.764	2.062	1.865	0.323	2.523	0.343	0.054	11.394	0.699	3129.87984	0.830	3129.87013	
1.161	6.089	29.549	1.907	1.879	2.112	0.288	2.649	0.309	0.047	10.672	0.720	3129.88103	0.842	3129.87092	
1.034	6.200	30.241	1.638	1.987	2.021	0.323	2.423	0.321	0.052	11.020	0.676	3129.88222	0.864	3129.87170	
1.078	6.178	29.838	1.687	1.954	2.252	0.362	2.523	0.316	0.059	10.686	0.669	3129.88342	0.886	3129.87249	
1.205	6.200	29.929	1.641	1.968	2.084	0.358	2.440	0.317	0.058	10.708	0.673	3129.88461	0.903	3129.87328	
1.118	6.306	30.395	1.564	2.030	1.873	0.336	2.279	0.322	0.053	10.846	0.687	3129.88581	0.912	3129.87406	
1.135	5.917	28.372	2.618	1.856	2.160	0.301	3.007	0.314	0.051	10.031	0.871	3129.88700	0.912	3129.87485	
1.179	6.239	29.010	2.153	1.983	1.837	0.327	2.898	0.318	0.052	9.668	0.743	3129.88900	0.903	3129.87564	
1.157	6.167	29.124	2.103	1.983	1.857	0.323	2.915	0.321	0.052	10.006	0.721	3129.89084	0.887	3129.87642	
1.004	6.289	29.666	1.867	2.058	1.933	0.336	2.593	0.327	0.053	10.169	0.720	3129.89268	0.869	3129.87721	
1.328	5.950	27.875	2.684	1.781	2.216	0.319	3.129	0.299	0.054	9.429	0.858	3129.89452	0.855	3129.87800	
1.087	6.618	31.205	1.212	2.316	1.375	0.401	2.078	0.350	0.061	10.690	0.583	3129.89636	0.851	3129.87878	
1.065	6.673	31.404	1.179	2.302	1.299	0.392	2.008	0.345	0.059	10.717	0.587	3129.89820	0.857	3129.87957	
0.925	6.907	31.644	1.016	2.400	1.236	0.405	1.899	0.348	0.059	10.233	0.535	3129.90004	0.870	3129.88036	
1.104	6.584	31.327	1.226	2.264	1.367	0.371	2.017	0.344	0.056	10.916	0.608	3129.90188	0.886	3129.88114	
0.973	6.651	31.227	1.312	2.236	1.399	0.366	2.104	0.336	0.055	10.610	0.623	3129.90372	0.904	3129.88193	
1.012	6.022	29.581	2.359	1.917	1.738	0.345	2.758	0.318	0.057	10.911	0.855	3129.90556	0.913	3129.88272	
0.964	6.184	29.345	2.419	1.968	1.634	0.306	2.893	0.318	0.049	10.176	0.836	3129.90740	0.909	3129.88351	
1.122	6.512	31.056	1.269	2.161	1.542	0.366	2.135	0.332	0.056	10.869	0.594	3129.90924	0.895	3129.88429	
0.899	6.612	31.295	1.335	2.288	1.291	0.340	2.122	0.346	0.051	10.798	0.629	3129.91108	0.885	3129.88508	
0.899	6.523	31.160	1.415	2.213	1.423	0.345	2.183	0.339	0.053	10.938	0.648	3129.91292	0.883	3129.88587	
0.877	6.618	31.074	1.561	2.283	1.156	0.375	2.257	0.345	0.057	10.559	0.692	3129.91476	0.882	3129.88665	
1.170	6.117	30.078	1.830	1.992	1.809	0.323	2.475	0.326	0.053	11.116	0.740	3129.91660	0.876	3129.88744	
0.925	6.562	31.522	1.172	2.208	1.463	0.401	2.013	0.336	0.061	11.180	0.582	3129.91844	0.863	3129.88823	
1.069	6.684	31.499	1.079	2.274	1.403	0.366	1.956	0.340	0.055	10.778	0.552	3129.92028	0.852	3129.88901	
0.916	6.590	31.164	1.099	2.161	1.789	0.362	2.113	0.328	0.055	10.736	0.520	3129.92212	0.843	3129.88980	
1.026	6.440	30.906	1.299	2.231	1.738	0.384	2.218	0.347	0.060	10.944	0.586	3129.92396	0.835	3129.89059	
1.069	6.378	30.345	1.651	2.058	1.762	0.319	2.401	0.323	0.050	10.572	0.688	3129.92580	0.828	3129.89137	
0.942	6.056	27.391	3.911	1.936	1.267	0.310	3.386	0.320	0.051	8.618	1.155	3129.92764	0.821	3129.89216	
1.118	6.556	31.033	1.152	2.189	1.754	0.388	2.109	0.334	0.059	10.708	0.547	3129.92948	0.810	3129.89295	
1.039	6.634	31.241	1.073	2.283	1.658	0.401	2.039	0.344	0.060	10.675	0.526	3129.93132	0.796	3129.89373	
1.179	6.490	30.318	1.388	2.138	1.881	0.353	2.331	0.329	0.054	10.200	0.596	3129.93316	0.787	3129.89452	
1.179	6.501	30.639	1.096	2.128	2.092	0.340	2.196	0.327	0.052	10.487	0.499	3129.93500	0.792	3129.89531	
1.056	6.818	30.780	1.362	2.307	1.451	0.401	2.144	0.338	0.059	9.644	0.635	3129.93684	0.812	3129.89609	
1.083	6.718	30.526	1.329	2.241	1.742	0.384	2.218	0.334	0.057	9.701	0.599	3129.93868	0.842	3129.89688	
1.179	6.490	29.630	1.860	2.086	1.734	0.340	2.654	0.321	0.052	9.512	0.701	3129.94052	0.869	3129.89767	
													0.888	3129.89845	

EDXRF												Hyperspectral Imagery		
Mg	Al	Si	S	K	Ca	Ti	Fe	K/Al	Ti/Al	Si bio	S/Fe	Depth	TOC	Depth
%	%	%	%	%	%	%	%			%		m	%	m
													0.897	3129.89924
													0.902	3129.90003
													0.906	3129.90081
													0.913	3129.90160
													0.923	3129.90239
													0.928	3129.90317
													0.921	3129.90396
													0.904	3129.90475
													0.890	3129.90553
													0.880	3129.90632
													0.873	3129.90711
													0.868	3129.90790
													0.866	3129.90868
													0.864	3129.90947
													0.858	3129.91026
													0.850	3129.91104
													0.841	3129.91183
													0.831	3129.91262
													0.825	3129.91340
													0.829	3129.91419
													0.846	3129.91498
													0.874	3129.91576
													0.898	3129.91655
													0.905	3129.91734
													0.896	3129.91812
													0.879	3129.91891
													0.867	3129.91970
													0.869	3129.92048
													0.878	3129.92127
													0.885	3129.92206
													0.885	3129.92284
													0.869	3129.92363
													0.846	3129.92442
													0.830	3129.92520
													0.823	3129.92599
													0.822	3129.92678
													0.828	3129.92756
													0.840	3129.92835
													0.856	3129.92914
													0.865	3129.92993
													0.862	3129.93071
													0.854	3129.93150
													0.845	3129.93229
													0.836	3129.93307
													0.824	3129.93386
													0.809	3129.93465
													0.788	3129.93543
													0.765	3129.93622
													0.748	3129.93701
													0.743	3129.93779
													0.742	3129.93858
													0.738	3129.93937
													0.730	3129.94015
													0.724	3129.94094

EDXRF												Hyperspectral Imagery		
Mg	Al	Si	S	K	Ca	Ti	Fe	K/Al	Ti/Al	Si bio	S/Fe	Depth	TOC	Depth
%	%	%	%	%	%	%	%			%		m	%	m
													1.033	3131.11900
													1.054	3131.12006
													1.077	3131.12111
													1.099	3131.12217
													1.117	3131.12323
													1.133	3131.12429
													1.147	3131.12535
													1.158	3131.12641
													1.167	3131.12747
													1.173	3131.12853
													1.171	3131.12959
													1.164	3131.13065
													1.161	3131.13171
													1.169	3131.13277
													1.189	3131.13383
													1.215	3131.13489
													1.239	3131.13595
													1.256	3131.13701
													1.265	3131.13807
													1.266	3131.13913

Slab 3131.8 m

EDXRF														Hyperspectral Imagery	
Mg %	Al %	Si %	S %	K %	Ca %	Ti %	Fe %	K/Al	Ti/Al	Si bio %	S/Fe	Depth m	TOC %	Depth m	
0.373	4.509	35.390	1.641	1.527	0.231	0.258	1.712	0.339	0.057	21.411	0.959	3131.82040	0.907	3131.81993	
0.351	4.359	34.069	2.442	1.485	0.212	0.228	2.300	0.341	0.052	20.555	1.061	3131.82186	0.899	3131.82072	
0.535	4.304	34.083	2.359	1.433	0.215	0.210	2.222	0.333	0.049	20.741	1.062	3131.82331	0.887	3131.82150	
0.403	4.554	35.377	1.614	1.546	0.227	0.215	1.712	0.339	0.047	21.259	0.943	3131.82477	0.879	3131.82229	
0.412	4.448	35.603	1.541	1.560	0.235	0.267	1.651	0.351	0.060	21.813	0.934	3131.82623	0.880	3131.82307	
0.434	4.526	35.508	1.551	1.583	0.196	0.232	1.673	0.350	0.051	21.477	0.927	3131.82768	0.888	3131.82386	
0.443	4.465	35.517	1.568	1.555	0.223	0.219	1.646	0.348	0.049	21.676	0.952	3131.82914	0.897	3131.82464	
0.443	4.415	35.558	1.561	1.518	0.219	0.223	1.638	0.344	0.051	21.871	0.953	3131.83060	0.908	3131.82543	
0.346	4.343	34.585	2.146	1.438	0.259	0.223	2.030	0.331	0.051	21.123	1.057	3131.83206	0.923	3131.82622	
0.469	4.276	33.589	2.598	1.353	0.283	0.193	2.366	0.317	0.045	20.334	1.098	3131.83351	0.936	3131.82700	
0.421	4.493	33.770	2.322	1.494	0.315	0.228	2.165	0.333	0.051	19.843	1.072	3131.83497	0.942	3131.82779	
0.500	4.354	35.336	1.591	1.565	0.275	0.275	1.686	0.359	0.063	21.839	0.944	3131.83643	0.943	3131.82857	
0.482	4.665	34.327	1.930	1.513	0.347	0.254	1.965	0.324	0.054	19.865	0.982	3131.83788	0.941	3131.82936	
0.465	4.576	33.001	2.548	1.527	0.395	0.245	2.401	0.334	0.054	18.815	1.061	3131.83934	0.939	3131.83014	
0.412	4.687	32.422	2.914	1.560	0.379	0.267	2.532	0.333	0.057	17.891	1.151	3131.84080	0.935	3131.83093	
0.517	4.648	31.576	3.269	1.565	0.391	0.232	2.846	0.337	0.050	17.166	1.149	3131.84226	0.932	3131.83171	
0.631	4.904	32.404	2.581	1.607	0.423	0.258	2.514	0.328	0.053	17.200	1.027	3131.84371	0.934	3131.83250	
0.601	4.699	34.408	1.797	1.673	0.295	0.275	1.851	0.356	0.059	19.843	0.971	3131.84517	0.943	3131.83328	
0.399	4.693	34.942	1.684	1.659	0.271	0.258	1.764	0.353	0.055	20.394	0.955	3131.84663	0.959	3131.83407	
0.438	4.721	34.938	1.638	1.574	0.263	0.245	1.755	0.333	0.052	20.303	0.933	3131.84808	0.974	3131.83486	
0.421	4.960	34.092	1.920	1.715	0.315	0.288	1.969	0.346	0.058	18.716	0.975	3131.84954	0.982	3131.83564	
0.539	4.899	32.820	2.415	1.644	0.387	0.262	2.440	0.336	0.054	17.634	0.990	3131.85100	0.978	3131.83643	
0.561	4.893	33.422	2.173	1.654	0.391	0.284	2.170	0.338	0.058	18.253	1.001	3131.85246	0.963	3131.83721	
0.539	4.993	34.359	1.677	1.696	0.323	0.275	1.830	0.340	0.055	18.879	0.917	3131.85391	0.942	3131.83800	
0.579	5.066	34.359	1.634	1.720	0.291	0.267	1.812	0.339	0.053	18.655	0.902	3131.85537	0.921	3131.83878	
0.495	5.221	33.951	1.767	1.771	0.323	0.275	1.912	0.339	0.053	17.765	0.924	3131.85683	0.899	3131.83957	
0.622	5.110	31.816	2.728	1.710	0.443	0.288	2.523	0.335	0.056	15.974	1.081	3131.85828	0.876	3131.84035	
0.771	5.266	28.105	4.303	1.762	0.630	0.280	3.604	0.335	0.053	11.781	1.194	3131.85974	0.854	3131.84114	
0.548	5.399	31.798	2.641	1.842	0.403	0.306	2.505	0.341	0.057	15.059	1.054	3131.86120	0.838	3131.84193	
0.583	5.271	33.322	1.960	1.837	0.319	0.306	2.048	0.348	0.058	16.981	0.957	3131.86266	0.837	3131.84271	
0.552	5.338	34.073	1.591	1.846	0.275	0.297	1.799	0.346	0.056	17.525	0.884	3131.86411	0.855	3131.84350	
0.517	5.416	33.657	1.727	1.870	0.335	0.306	1.882	0.345	0.056	16.867	0.918	3131.86557	0.881	3131.84428	
0.566	5.416	31.010	2.967	1.832	0.435	0.336	2.763	0.338	0.062	14.220	1.074	3131.86703	0.904	3131.84507	
0.666	5.283	30.825	3.153	1.776	0.375	0.288	2.859	0.336	0.055	14.449	1.103	3131.86848	0.917	3131.84585	
0.495	5.394	31.671	2.764	1.846	0.319	0.288	2.540	0.342	0.053	14.950	1.088	3131.86994	0.919	3131.84664	
0.557	5.527	31.920	2.485	1.837	0.351	0.284	2.510	0.332	0.051	14.785	0.990	3131.87140	0.909	3131.84742	
0.566	5.388	31.598	2.741	1.865	0.319	0.297	2.606	0.346	0.055	14.895	1.052	3131.87285	0.892	3131.84821	
0.605	5.399	30.047	3.505	1.790	0.351	0.293	3.133	0.332	0.054	13.308	1.119	3131.87431	0.872	3131.84899	
0.526	5.077	28.345	4.638	1.612	0.359	0.254	3.853	0.317	0.050	12.607	1.204	3131.87577	0.852	3131.84978	
0.552	5.271	29.730	3.877	1.771	0.291	0.293	3.286	0.336	0.056	13.388	1.180	3131.87723	0.834	3131.85057	
0.579	5.377	30.648	3.183	1.884	0.311	0.306	2.981	0.350	0.057	13.979	1.068	3131.87868	0.823	3131.85135	
0.478	5.500	30.327	3.299	1.898	0.355	0.280	3.046	0.345	0.051	13.279	1.083	3131.88014	0.818	3131.85214	
0.535	5.577	33.001	1.940	1.997	0.271	0.293	2.026	0.358	0.052	15.711	0.958	3131.88160	0.815	3131.85292	
0.535	5.728	32.983	1.933	1.978	0.287	0.345	2.043	0.345	0.060	15.227	0.946	3131.88305	0.812	3131.85371	
0.622	5.461	32.359	2.322	1.903	0.311	0.284	2.253	0.348	0.052	15.431	1.031	3131.88451	0.808	3131.85449	
0.561	5.483	31.046	2.887	1.893	0.335	0.327	2.876	0.345	0.060	14.050	1.004	3131.88597	0.806	3131.85528	
0.544	5.527	30.698	3.043	1.912	0.367	0.323	2.937	0.346	0.058	13.563	1.036	3131.88743	0.804	3131.85606	
0.618	5.872	32.997	1.717	2.048	0.303	0.349	1.956	0.349	0.059	14.793	0.878	3131.88888	0.744	3131.85685	
0.530	5.900	32.906	1.840	2.011	0.275	0.314	2.021	0.341	0.053	14.616	0.910	3131.89034	0.729	3131.85764	
0.579	5.694	31.906	2.419	2.011	0.299	0.323	2.348	0.353	0.057	14.254	1.030	3131.89180	0.702	3131.85842	
													0.684	3131.85921	
													0.687	3131.85974	
													0.705	3131.86068	
													0.726	3131.86163	
													0.741	3131.86257	
													0.751	3131.86351	
													0.753	3131.86446	
													0.745	3131.86540	
													0.726	3131.86634	
													0.703	3131.86728	
													0.686	3131.86823	
													0.682	3131.86917	

EDXRF												Hyperspectral Imagery		
Mg	Al	Si	S	K	Ca	Ti	Fe	K/Al	Ti/Al	Si bio	S/Fe	Depth	TOC	Depth
%	%	%	%	%	%	%	%			%		m	%	m
													0.686	3131.87011
													0.691	3131.87105
													0.689	3131.87200
													0.678	3131.87294
													0.664	3131.87388
													0.650	3131.87483
													0.639	3131.87577
													0.631	3131.87671
													0.629	3131.87765
													0.630	3131.87860
													0.630	3131.87954
													0.627	3131.88048
													0.623	3131.88143
													0.623	3131.88237
													0.631	3131.88331
													0.646	3131.88425
													0.663	3131.88520
													0.677	3131.88614
													0.681	3131.88708
													0.673	3131.88803
													0.655	3131.88897
													0.636	3131.88991
													0.623	3131.89085
													0.622	3131.89180

EDXRF													Hyperspectral Imagery		
Mg %	Al %	Si %	S %	K %	Ca %	Ti %	Fe %	K/Al	Ti/Al	Si bio %	S/Fe	Depth m	TOC %	Depth m	
0.395	3.608	34.797	2.422	1.175	0.530	0.241	2.183	0.326	0.067	23.612	1.110	3133.94504	0.921	3133.90870	
0.412	3.770	34.766	2.325	1.203	0.562	0.245	2.170	0.319	0.065	23.080	1.072	3133.94790	0.792	3133.91015	
0.491	3.642	35.589	2.033	1.245	0.502	0.219	1.908	0.342	0.060	24.300	1.065	3133.94933	0.746	3133.91088	
0.377	3.775	34.336	2.618	1.208	0.522	0.241	2.366	0.320	0.064	22.633	1.107	3133.95075	0.731	3133.91160	
0.443	3.814	33.960	2.708	1.194	0.586	0.249	2.466	0.313	0.065	22.137	1.098	3133.95218	0.755	3133.91232	
0.360	4.081	32.246	2.728	1.311	0.586	0.262	3.696	0.321	0.064	19.594	0.738	3133.94647	0.856	3133.90943	
0.434	3.998	32.236	3.316	1.273	0.570	0.258	3.077	0.319	0.065	19.844	1.078	3133.95361	0.828	3133.91305	
0.360	4.270	32.037	3.382	1.339	0.530	0.262	2.968	0.314	0.061	18.800	1.140	3133.95504	0.936	3133.91377	
0.307	3.725	24.318	7.968	0.964	0.367	0.180	5.693	0.259	0.048	12.770	1.400	3133.95647	1.037	3133.91449	
0.513	3.792	29.662	5.170	1.104	0.375	0.206	3.735	0.291	0.054	17.907	1.384	3133.95790	1.097	3133.91522	
													1.117	3133.91594	
													1.117	3133.91667	
													1.114	3133.91739	
													1.112	3133.91811	
													1.113	3133.91884	
													1.114	3133.91956	
													1.114	3133.92028	
													1.115	3133.92101	
													1.114	3133.92173	
													1.110	3133.92246	
													1.106	3133.92318	
													1.109	3133.92390	
													1.123	3133.92463	
													1.136	3133.92535	
													1.134	3133.92607	
													1.116	3133.92680	
													1.092	3133.92752	
													1.076	3133.92824	
													1.073	3133.92897	
													1.076	3133.92969	
													1.081	3133.93042	
													1.086	3133.93114	
													1.093	3133.93186	
													1.101	3133.93259	
													1.104	3133.93331	
													1.106	3133.93403	
													1.110	3133.93476	
													1.113	3133.93548	
													1.104	3133.93621	
													1.082	3133.93693	
													1.054	3133.93765	
													1.031	3133.93838	
													1.023	3133.93910	
													1.031	3133.93982	
													1.049	3133.94055	
													1.063	3133.94127	
													1.066	3133.94199	
													1.062	3133.94272	
													1.055	3133.94344	
													1.044	3133.94417	
													1.022	3133.94489	
													0.989	3133.94561	
													0.955	3133.94634	
													0.926	3133.94706	
													0.898	3133.94778	
													0.865	3133.94851	
													0.827	3133.94923	
													0.780	3133.94996	
													0.728	3133.95068	
													0.691	3133.95140	
													0.686	3133.95213	

EDXRF												Hyperspectral Imagery		
Mg	Al	Si	S	K	Ca	Ti	Fe	K/Al	Ti/Al	Si bio	S/Fe	Depth	TOC	Depth
%	%	%	%	%	%	%	%			%		m	%	m
													0.703	3133.95285
													0.710	3133.95357
													0.681	3133.95430
													0.628	3133.95502
													0.585	3133.95575
													0.736	3133.95864
													0.792	3133.95936
													0.826	3133.96009
													0.578	3133.95647
													0.610	3133.95719
													0.672	3133.95792

Slab 3134.95 m

EDXRF														Hyperspectral Imagery			
Mg	Al	Si	S	K	Ca	Ti	Fe	K/Al	Ti/Al	Si bio	S/Fe	Depth	TOC	Depth			
%	%	%	%	%	%	%	%			%		m	%	m			
1.411	5.155	27.282	3.150	1.612	2.471	0.336	3.534	0.313	0.065	11.303	0.891	3134.95000	1.424	3134.95053			
1.354	5.155	27.350	3.156	1.597	2.475	0.327	3.552	0.310	0.063	11.370	0.889	3134.95147	1.418	3134.95133			
1.236	5.188	27.572	3.199	1.644	2.419	0.314	3.412	0.317	0.061	11.489	0.938	3134.95294	1.413	3134.95213			
1.332	5.016	27.042	3.572	1.494	2.459	0.271	3.595	0.298	0.054	11.494	0.993	3134.95441	1.405	3134.95294			
1.389	5.166	27.006	3.535	1.513	2.447	0.284	3.513	0.293	0.055	10.992	1.006	3134.95588	1.392	3134.95374			
1.315	5.216	27.391	3.332	1.555	2.355	0.301	3.443	0.298	0.058	11.221	0.968	3134.95735	1.377	3134.95454			
1.214	5.277	27.228	3.508	1.569	2.331	0.301	3.504	0.297	0.057	10.869	1.001	3134.95882	1.363	3134.95534			
1.271	5.305	27.151	3.572	1.579	2.224	0.327	3.521	0.298	0.062	10.706	1.014	3134.96029	1.354	3134.95614			
1.218	5.155	26.897	3.914	1.546	2.144	0.301	3.656	0.300	0.058	10.918	1.070	3134.96176	1.348	3134.95694			
1.345	5.438	26.992	3.555	1.588	2.128	0.284	3.574	0.292	0.052	10.134	0.995	3134.96323	1.342	3134.95775			
1.218	5.461	27.861	3.289	1.593	2.084	0.314	3.273	0.292	0.058	10.933	1.005	3134.96470	1.334	3134.95855			
1.324	5.477	27.893	3.050	1.649	2.200	0.319	3.173	0.301	0.058	10.913	0.961	3134.96617	1.328	3134.95935			
1.245	5.488	28.056	3.076	1.612	2.096	0.293	3.190	0.294	0.053	11.042	0.964	3134.96764	1.326	3134.96015			
1.324	5.477	27.617	3.286	1.659	2.092	0.310	3.229	0.303	0.057	10.637	1.018	3134.96911	1.327	3134.96095			
1.376	5.538	27.875	3.160	1.649	2.009	0.275	3.203	0.298	0.050	10.705	0.986	3134.97058	1.330	3134.96176			
1.096	5.444	28.092	3.279	1.654	1.925	0.336	3.255	0.304	0.062	11.216	1.007	3134.97205	1.337	3134.96256			
1.262	5.427	28.042	3.093	1.663	2.044	0.327	3.203	0.306	0.060	11.218	0.966	3134.97352	1.348	3134.96336			
1.210	5.522	27.915	3.163	1.682	2.048	0.319	3.207	0.305	0.058	10.798	0.986	3134.97499	1.360	3134.96416			
1.271	5.672	27.413	3.183	1.762	2.017	0.327	3.391	0.311	0.058	9.830	0.939	3134.97646	1.371	3134.96496			
1.258	5.644	27.648	3.199	1.673	1.985	0.323	3.356	0.296	0.057	10.152	0.953	3134.97793	1.376	3134.96576			
1.210	5.544	27.653	3.366	1.644	1.989	0.336	3.364	0.297	0.061	10.467	1.000	3134.97940	1.341	3134.96657			
1.240	5.555	27.540	3.339	1.663	2.028	0.319	3.377	0.299	0.057	10.319	0.989	3134.98087	1.338	3134.96737			
1.240	5.733	27.621	3.319	1.691	1.821	0.332	3.351	0.295	0.058	9.849	0.990	3134.98234	1.333	3134.96817			
0.999	5.639	27.771	3.409	1.720	1.849	0.349	3.430	0.305	0.062	10.291	0.994	3134.98381	1.329	3134.96897			
1.214	5.694	27.626	3.422	1.705	1.750	0.336	3.386	0.300	0.059	9.974	1.011	3134.98528	1.327	3134.96977			
1.113	5.772	27.567	3.329	1.748	1.769	0.349	3.460	0.303	0.060	9.674	0.962	3134.98675	1.325	3134.97058			
1.104	5.817	27.866	3.309	1.757	1.598	0.332	3.382	0.302	0.057	9.834	0.978	3134.98822	1.324	3134.97138			
1.122	5.833	27.667	3.356	1.771	1.690	0.345	3.373	0.304	0.059	9.583	0.995	3134.98969	1.324	3134.97218			
1.052	5.906	27.857	3.239	1.795	1.654	0.336	3.382	0.304	0.057	9.549	0.958	3134.99116	1.322	3134.97298			
1.109	5.856	28.381	3.206	1.738	1.431	0.362	3.216	0.297	0.062	10.229	0.997	3134.99263	1.316	3134.97378			
0.938	5.794	28.404	3.336	1.734	1.439	0.345	3.260	0.299	0.059	10.442	1.023	3134.99410	1.306	3134.97458			
1.030	5.928	28.268	3.263	1.818	1.439	0.319	3.234	0.307	0.054	9.892	1.009	3134.99557	1.293	3134.97539			
1.065	5.872	28.024	3.395	1.724	1.431	0.353	3.347	0.294	0.060	9.820	1.015	3134.99703	1.278	3134.97619			
1.061	5.856	27.866	3.449	1.762	1.419	0.340	3.425	0.301	0.058	9.714	1.007	3134.99850	1.262	3134.97699			
0.982	5.850	28.368	3.316	1.818	1.279	0.327	3.282	0.311	0.056	10.233	1.010	3134.99997	1.248	3134.97779			
0.855	5.511	25.680	5.160	1.626	1.200	0.314	4.245	0.295	0.057	8.597	1.216	3135.00144	1.240	3134.97859			
0.872	5.555	26.146	4.755	1.649	1.232	0.327	4.184	0.297	0.059	8.925	1.136	3135.00291	1.240	3134.97940			
0.837	5.271	24.640	5.924	1.522	1.028	0.297	4.712	0.289	0.056	8.298	1.257	3135.00438	1.244	3134.98020			
0.877	5.294	23.110	6.439	1.541	1.068	0.284	5.274	0.291	0.054	6.700	1.221	3135.00585	1.248	3134.98100			
0.995	6.061	27.567	3.605	1.856	1.315	0.353	3.434	0.306	0.058	8.777	1.050	3135.00732	1.249	3134.98180			
0.942	6.150	28.327	3.376	1.813	1.156	0.366	3.264	0.295	0.060	9.261	1.034	3135.00879	1.245	3134.98260			
0.815	6.084	28.639	3.362	1.884	1.084	0.358	3.216	0.310	0.059	9.780	1.045	3135.01026	1.236	3134.98340			
0.881	6.100	28.707	3.206	1.851	1.152	0.358	3.125	0.303	0.059	9.796	1.026	3135.01173	1.223	3134.98421			
0.903	6.117	28.440	3.349	1.889	1.104	0.362	3.212	0.309	0.059	9.478	1.043	3135.01320	1.214	3134.98501			
0.815	6.262	28.300	3.352	1.936	1.016	0.384	3.290	0.309	0.061	8.889	1.019	3135.01467	1.215	3134.98581			
0.776	6.228	28.644	3.153	1.968	1.012	0.362	3.277	0.316	0.058	9.336	0.962	3135.01614	1.225	3134.98661			
0.885	6.100	28.567	3.289	1.912	0.992	0.345	3.255	0.313	0.056	9.656	1.010	3135.01761	1.236	3134.98741			
0.863	6.161	28.572	3.336	1.865	0.977	0.345	3.234	0.303	0.056	9.471	1.032	3135.01908	1.239	3134.98821			
0.815	6.239	28.354	3.356	1.968	0.961	0.375	3.316	0.315	0.060	9.012	1.012	3135.02055	1.237	3134.98902			
0.863	6.317	28.250	3.395	1.922	0.937	0.358	3.312	0.304	0.057	8.667	1.025	3135.02202	1.235	3134.98982			
0.837	6.262	28.531	3.349	1.912	0.937	0.314	3.186	0.305	0.050	9.120	1.051	3135.02349	1.238	3134.99062			
0.763	6.034	28.499	3.545	1.870	0.917	0.332	3.303	0.310	0.055	9.795	1.073	3135.02496	1.242	3134.99142			
0.732	6.234	28.852	3.256	1.931	0.897	0.366	3.234	0.310	0.059	9.527	1.007	3135.02643	1.241	3134.99222			
0.877	6.328	28.608	3.269	1.945	0.877	0.358	3.199	0.307	0.057	8.990	1.022	3135.02790	1.233	3134.99303			
0.855	6.184	28.531	3.412	1.973	0.853	0.366	3.203	0.319	0.059	9.361	1.065	3135.02937	1.218	3134.99383			
0.719	6.206	28.499	3.399	1.964	0.869	0.353	3.343	0.316	0.057	9.261	1.017	3135.03084	1.201	3134.99463			
													1.188	3134.99543			
													1.181	3134.99623			
													1.179	3134.99703			
													1.180	3134.99784			
													1.183	3134.99864			
													1.182	3134.99944			

EDXRF												Hyperspectral Imagery		
Mg	Al	Si	S	K	Ca	Ti	Fe	K/Al	Ti/Al	Si bio	S/Fe	Depth	TOC	Depth
%	%	%	%	%	%	%	%			%		m	%	m
													1.168	3135.00024
													1.139	3135.00104
													1.103	3135.00185
													1.076	3135.00265
													1.061	3135.00345
													1.049	3135.00425
													1.040	3135.00505
													1.039	3135.00585
													1.051	3135.00666
													1.072	3135.00746
													1.096	3135.00826
													1.116	3135.00906
													1.128	3135.00986
													1.135	3135.01067
													1.140	3135.01147
													1.143	3135.01227
													1.141	3135.01307
													1.132	3135.01387
													1.124	3135.01467
													1.124	3135.01548
													1.129	3135.01628
													1.131	3135.01708
													1.123	3135.01788
													1.108	3135.01868
													1.095	3135.01949
													1.085	3135.02029
													1.079	3135.02109
													1.074	3135.02189
													1.072	3135.02269
													1.073	3135.02349
													1.076	3135.02430
													1.079	3135.02510
													1.083	3135.02590
													1.087	3135.02670
													1.091	3135.02750
													1.091	3135.02830
													1.084	3135.02911
													1.071	3135.02991
													1.058	3135.03071
													1.048	3135.03151

EDXRF												Hyperspectral Imagery		
Mg %	Al %	Si %	S %	K %	Ca %	Ti %	Fe %	K/Al	Ti/Al	Si bio %	S/Fe	Depth m	TOC %	Depth m
0.114	0.994	4.491	19.755	0.212	0.020	0.058	13.013	0.214	0.059	1.410	1.518	3136.76840	1.444	3136.71304
0.123	0.660	2.682	20.798	0.132	0.024	0.037	13.715	0.201	0.056	0.635	1.516	3136.77040	1.413	3136.71376
0.154	0.899	2.596	20.668	0.170	0.032	0.037	13.680	0.189	0.041	-0.193	1.511	3136.77240	1.354	3136.71448
0.105	0.955	2.700	20.502	0.203	0.036	0.041	13.781	0.212	0.043	-0.261	1.488	3136.77440	1.277	3136.71521
0.119	0.911	2.962	20.359	0.203	0.020	0.045	13.728	0.223	0.050	0.139	1.483	3136.77640	1.214	3136.71593
													1.199	3136.71665
													1.236	3136.71738
													1.301	3136.71810
													1.362	3136.71882
													1.403	3136.71955
													1.425	3136.72027
													1.435	3136.72099
													1.439	3136.72172
													1.440	3136.72244
													1.444	3136.72316
													1.447	3136.72389
													1.443	3136.72461
													1.425	3136.72533
													1.397	3136.72606
													1.369	3136.72678
													1.347	3136.72750
													1.333	3136.72823
													1.322	3136.72895
													1.313	3136.72967
													1.303	3136.73040
													1.284	3136.73112
													1.232	3136.73185
													1.130	3136.73257
													1.000	3136.73329
													0.902	3136.73402
													0.868	3136.73474
													0.899	3136.73546
													0.990	3136.73619
													1.118	3136.73691
													1.228	3136.73763
													1.295	3136.73836
													1.316	3136.73908
													1.316	3136.73980
													1.329	3136.74053
													1.374	3136.74125
													1.438	3136.74197
													1.486	3136.74270
													1.511	3136.74342
													1.520	3136.74414
													1.517	3136.74487
													1.507	3136.74559
													1.498	3136.74631
													1.498	3136.74704
													1.511	3136.74776
													1.531	3136.74848
													1.547	3136.74921
													1.549	3136.74993
													1.536	3136.75065
													1.518	3136.75138
													1.507	3136.75210
													1.502	3136.75282
													1.501	3136.75355
													1.502	3136.75427
													1.497	3136.75499
													1.478	3136.75572
													1.443	3136.75644
													1.402	3136.75716
													1.364	3136.75789
													1.341	3136.75861
													1.337	3136.75933

EDXRF												Hyperspectral Imagery		
Mg	Al	Si	S	K	Ca	Ti	Fe	K/Al	Ti/Al	Si bio	S/Fe	Depth	TOC	Depth
%	%	%	%	%	%	%	%			%		m	%	m
													1.347	3136.76006
													1.359	3136.76078
													1.365	3136.76150
													1.368	3136.76223
													1.376	3136.76295
													1.387	3136.76367
													1.394	3136.76440
													1.120	3136.76512
													1.033	3136.76584
													0.851	3136.76657
													0.686	3136.76729
													0.569	3136.76802
													0.489	3136.76874
													0.435	3136.76946
													0.396	3136.77019
													0.369	3136.77091
													0.351	3136.77163
													0.341	3136.77236
													0.339	3136.77308
													0.345	3136.77380
													0.361	3136.77453
													0.386	3136.77525
													0.421	3136.77597
													0.485	3136.77670

EDXRF												Hyperspectral Imagery		
Mg %	Al %	Si %	S %	K %	Ca %	Ti %	Fe %	K/Al	Ti/Al	Si bio %	S/Fe	Depth m	TOC %	Depth m
													1.730	3137.80755
													1.704	3137.80832
													1.696	3137.80909
													1.709	3137.80987
													1.732	3137.81064
													1.753	3137.81141
													1.762	3137.81219
													1.763	3137.81296
													1.760	3137.81373
													1.756	3137.81450
													1.747	3137.81528
													1.726	3137.81605
													1.702	3137.81682
													1.688	3137.81760
													1.685	3137.81837
													1.683	3137.81914
													1.676	3137.81992
													1.664	3137.82069
													1.649	3137.82146
													1.634	3137.82223
													1.621	3137.82301
													1.603	3137.82378
													1.580	3137.82455
													1.556	3137.82533
													1.538	3137.82610
													1.523	3137.82687
													1.511	3137.82764
													1.505	3137.82842
													1.504	3137.82919
													1.513	3137.82996
													1.505	3137.83074
													1.489	3137.83151
													1.473	3137.83228

EDXRF													Hyperspectral Imagery	
Mg %	Al %	Si %	S %	K %	Ca %	Ti %	Fe %	K/Al	Ti/Al	Si bio %	S/Fe	Depth m	TOC %	Depth m
													3.548	3140.05362
													3.546	3140.05446
													3.535	3140.05530
													3.531	3140.05614
													3.502	3140.05194
													3.527	3140.05278
													3.534	3140.05698
													3.538	3140.05782
													3.548	3140.05866
													3.575	3140.05950
													3.614	3140.06034
													3.641	3140.06118
													3.644	3140.06202
													3.629	3140.06286
													3.612	3140.06370
													3.601	3140.06454
													3.591	3140.06538
													3.583	3140.06622
													3.591	3140.06706
													3.613	3140.06790
													3.632	3140.06874
													3.636	3140.06958
													3.630	3140.07042
													3.611	3140.07126
													3.561	3140.07210
													3.461	3140.07294
													3.322	3140.07378
													3.166	3140.07462
													3.024	3140.07546
													2.922	3140.07630
													2.931	3140.07714
													3.006	3140.07798
													3.089	3140.07882
													3.149	3140.07966
													3.186	3140.08050
													3.229	3140.08134
													3.270	3140.08218
													3.279	3140.08302
													3.244	3140.08386
													3.191	3140.08470
													3.151	3140.08554
													3.131	3140.08638
													3.118	3140.08722
													3.107	3140.08806
													3.098	3140.08890
													3.088	3140.08974
													3.071	3140.09058
													3.044	3140.09142

EDXRF												Hyperspectral Imagery		
Mg %	Al %	Si %	S %	K %	Ca %	Ti %	Fe %	K/Al	Ti/Al	Si bio %	S/Fe	Depth m	TOC %	Depth m
													2.428	3141.04967
													2.434	3141.05047
													2.438	3141.05127
													2.426	3141.05206
													2.390	3141.05286
													2.343	3141.05366
													2.300	3141.05446
													2.267	3141.05525
													2.244	3141.05605
													2.237	3141.05685
													2.199	3141.05765
													2.220	3141.05844
													2.259	3141.05924
													2.300	3141.06004
													2.332	3141.06084
													2.358	3141.06163
													2.382	3141.06243
													2.409	3141.06323
													2.429	3141.06403
													2.427	3141.06482
													2.401	3141.06562
													2.365	3141.06642
													2.319	3141.06722
													2.266	3141.06801
													2.229	3141.06881
													2.213	3141.06961
													2.212	3141.07041
													2.213	3141.07120
													2.207	3141.07200
													2.214	3141.07280
													2.253	3141.07360
													2.315	3141.07439
													2.381	3141.07519
													2.420	3141.07599
													2.432	3141.07679
													2.417	3141.07758
													2.374	3141.07838
													2.322	3141.07918
													2.274	3141.07998
													2.212	3141.08077
													2.137	3141.08157
													2.055	3141.08237
													2.009	3141.08317
													2.024	3141.08396
													2.087	3141.08476
													2.158	3141.08556
													2.162	3141.08636

Slab 3144.9 m

EDXRF													Hyperspectral Imagery		
Mg %	Al %	Si %	S %	K %	Ca %	Ti %	Fe %	K/Al	Ti/Al	Si bio %	S/Fe	Depth m	TOC %	Depth m	
0.517	4.726	34.340	1.794	1.607	0.447	0.210	1.886	0.340	0.044	19.689	0.951	3144.90000	2.432	3144.90007	
0.596	4.665	34.273	1.837	1.621	0.463	0.228	1.860	0.347	0.049	19.811	0.988	3144.90107	2.366	3144.90057	
0.552	4.398	35.132	1.754	1.457	0.435	0.197	1.777	0.331	0.045	21.498	0.987	3144.90214	2.274	3144.90107	
0.469	4.615	34.730	1.684	1.607	0.518	0.189	1.777	0.348	0.041	20.423	0.948	3144.90320	2.175	3144.90157	
0.570	5.088	33.924	1.820	1.696	0.474	0.236	1.860	0.333	0.046	18.152	0.979	3144.90427	2.077	3144.90206	
0.522	5.066	33.648	2.006	1.823	0.427	0.275	1.991	0.360	0.054	17.945	1.008	3144.90534	1.984	3144.90256	
0.609	5.427	32.920	2.086	1.860	0.463	0.271	2.096	0.343	0.050	16.095	0.996	3144.90641	1.924	3144.90306	
0.605	5.856	32.580	1.940	2.109	0.391	0.284	2.043	0.360	0.048	14.428	0.949	3144.90747	1.915	3144.90356	
0.601	5.811	31.725	2.026	2.011	0.686	0.314	2.191	0.346	0.054	13.711	0.925	3144.90854	1.945	3144.90406	
0.438	5.555	31.775	2.173	1.987	0.737	0.288	2.244	0.358	0.052	14.554	0.968	3144.90961	1.986	3144.90456	
0.579	5.894	32.087	2.256	2.114	0.323	0.327	2.248	0.359	0.056	13.814	1.003	3144.91068	2.018	3144.90505	
0.522	6.050	31.834	2.315	2.114	0.367	0.306	2.218	0.349	0.051	13.078	1.044	3144.91174	2.046	3144.90555	
0.530	5.783	31.983	2.498	1.992	0.331	0.284	2.309	0.344	0.049	14.055	1.082	3144.91281	2.096	3144.90605	
0.574	5.555	32.440	2.299	1.940	0.407	0.284	2.187	0.349	0.051	15.219	1.051	3144.91388	2.156	3144.90655	
0.417	5.383	32.345	1.950	1.954	0.773	0.219	2.039	0.363	0.041	15.659	0.956	3144.91495	2.193	3144.90705	
0.495	5.427	33.236	1.897	1.837	0.558	0.245	1.912	0.338	0.045	16.412	0.992	3144.91602	2.286	3144.90755	
0.570	5.277	33.236	2.149	1.799	0.387	0.232	2.008	0.341	0.044	16.878	1.070	3144.91708	2.275	3144.90804	
0.487	5.483	32.879	2.276	1.889	0.395	0.267	2.039	0.344	0.049	15.882	1.116	3144.91815	2.249	3144.90854	
0.548	5.600	32.748	2.119	2.006	0.435	0.245	1.978	0.358	0.044	15.389	1.072	3144.91922	2.227	3144.90904	
0.583	5.605	32.517	2.183	1.973	0.459	0.284	2.117	0.352	0.051	15.141	1.031	3144.92029	2.233	3144.90954	
0.622	5.494	32.268	2.359	1.954	0.427	0.262	2.235	0.356	0.048	15.237	1.055	3144.92135	2.265	3144.91004	
0.539	5.616	32.829	2.073	1.898	0.443	0.275	2.122	0.338	0.049	15.419	0.977	3144.92242	2.286	3144.91053	
0.552	5.500	33.417	1.737	1.954	0.459	0.241	1.991	0.355	0.044	16.369	0.873	3144.92349	2.276	3144.91103	
0.500	5.438	33.404	1.867	1.912	0.399	0.258	2.043	0.352	0.047	16.545	0.914	3144.92456	2.247	3144.91153	
0.609	5.316	33.132	2.040	1.813	0.474	0.249	2.117	0.341	0.047	16.653	0.963	3144.92562	2.225	3144.91203	
0.574	5.433	32.725	2.212	1.898	0.427	0.228	2.148	0.349	0.042	15.883	1.030	3144.92669	2.227	3144.91253	
0.609	5.594	33.196	1.880	1.922	0.379	0.254	1.982	0.343	0.045	15.854	0.949	3144.92776	2.243	3144.91303	
0.587	5.483	33.101	2.006	1.879	0.415	0.275	2.013	0.343	0.050	16.104	0.997	3144.92883	2.259	3144.91352	
0.609	5.828	32.811	1.933	2.006	0.379	0.267	1.982	0.344	0.046	14.745	0.975	3144.92990	2.272	3144.91402	
0.557	5.844	32.485	2.060	2.119	0.367	0.284	2.069	0.363	0.049	14.368	0.995	3144.93096	2.284	3144.91452	
0.535	5.767	32.042	2.412	2.076	0.363	0.258	2.170	0.360	0.045	14.166	1.112	3144.93203	2.293	3144.91502	
0.579	5.783	32.291	2.269	1.983	0.395	0.258	2.117	0.343	0.045	14.363	1.072	3144.93310	2.279	3144.91552	
0.583	5.483	32.286	2.468	1.903	0.427	0.267	2.213	0.347	0.049	15.289	1.115	3144.93510	2.222	3144.91602	
0.552	5.633	32.214	2.478	1.889	0.427	0.249	2.196	0.335	0.044	14.751	1.129	3144.93687	2.137	3144.91651	
0.671	5.388	33.490	1.824	1.856	0.478	0.245	1.864	0.344	0.045	16.786	0.978	3144.93863	2.076	3144.91701	
0.526	5.310	33.386	1.957	1.813	0.538	0.241	2.004	0.341	0.045	16.923	0.976	3144.94040	2.062	3144.91751	
													2.076	3144.91801	
													2.088	3144.91851	
													2.085	3144.91901	
													2.074	3144.91950	
													2.066	3144.92000	
													2.061	3144.92050	
													2.040	3144.92100	
													1.986	3144.92150	
													1.935	3144.92200	
													1.901	3144.92249	
													1.887	3144.92299	
													1.897	3144.92349	
													1.901	3144.92399	
													1.903	3144.92449	
													1.914	3144.92499	
													1.933	3144.92548	
													1.942	3144.92598	
													1.930	3144.92648	
													1.910	3144.92698	
													1.899	3144.92748	
													1.900	3144.92798	
													1.906	3144.92847	
													1.910	3144.92897	
													1.903	3144.92947	
													1.884	3144.92997	
													1.856	3144.93047	

EDXRF												Hyperspectral Imagery		
Mg	Al	Si	S	K	Ca	Ti	Fe	K/Al	Ti/Al	Si bio	S/Fe	Depth	TOC	Depth
%	%	%	%	%	%	%	%			%		m	%	m
													1.804	3144.93146
													1.777	3144.93196
													1.757	3144.93246
													1.743	3144.93296
													1.830	3144.93097
													1.737	3144.93346
													1.745	3144.93396
													1.769	3144.93445
													1.799	3144.93495
													1.827	3144.93545
													1.861	3144.93595
													1.910	3144.93645
													1.970	3144.93694
													2.021	3144.93744
													2.039	3144.93794
													2.016	3144.93844
													1.967	3144.93894
													1.922	3144.93944

EDXRF												Hyperspectral Imagery		
Mg	Al	Si	S	K	Ca	Ti	Fe	K/A	Ti/Al	Si bio	S/Fe	Depth	TOC	Depth
%	%	%	%	%	%	%	%			%		m	%	m
													2.162	3146.10772
													2.183	3146.10846
													2.188	3146.10920
													2.160	3146.10994
													2.126	3146.10698
													2.162	3146.11068
													2.168	3146.11142
													2.176	3146.11216
													2.187	3146.11290
													2.207	3146.11364
													2.238	3146.11438
													2.273	3146.11512
													2.301	3146.11586
													2.315	3146.11660
													2.322	3146.11734
													2.332	3146.11808
													2.350	3146.11882
													2.375	3146.11956
													2.400	3146.12030
													2.422	3146.12104
													2.433	3146.12178
													2.426	3146.12252
													2.402	3146.12326
													2.375	3146.12400
													2.371	3146.12474
													2.413	3146.12548
													2.500	3146.12622
													2.610	3146.12696
													2.726	3146.12770
													2.839	3146.12844
													2.955	3146.12918
													3.104	3146.12992
													3.323	3146.13066
													3.613	3146.13140
													3.911	3146.13214
													4.152	3146.13288
													4.324	3146.13362
													4.450	3146.13436
													4.554	3146.13510
													4.636	3146.13584
													4.682	3146.13658
													4.683	3146.13732
													4.658	3146.13806
													4.631	3146.13880
													4.610	3146.13954
													4.589	3146.14028
													4.568	3146.14102
													4.543	3146.14176
													4.548	3146.14250
													4.701	3146.14324

EDXRF													Hyperspectral Imagery	
Mg %	Al %	Si %	S %	K %	Ca %	Ti %	Fe %	K/Al	Ti/Al	Si bio %	S/Fe	Depth m	TOC %	Depth m
0.438	3.608	37.956	1.149	1.259	0.208	0.119	1.306	0.349	0.033	26.770	0.880	3147.23240	4.308	3147.20019
0.460	3.647	37.802	1.226	1.250	0.192	0.136	1.333	0.343	0.037	26.495	0.920	3147.23375	4.400	3147.20101
0.368	3.736	37.684	1.212	1.358	0.208	0.158	1.350	0.363	0.042	26.102	0.898	3147.23510	4.471	3147.20183
													4.519	3147.20265
													4.524	3147.20346
													4.482	3147.20428
													4.430	3147.20510
													4.411	3147.20592
													4.436	3147.20673
													4.472	3147.20755
													4.473	3147.20837
													4.425	3147.20919
													4.351	3147.21000
													4.287	3147.21082
													4.246	3147.21164
													4.221	3147.21246
													4.201	3147.21328
													4.185	3147.21409
													4.184	3147.21491
													4.199	3147.21573
													4.205	3147.21655
													4.272	3147.21736
													4.313	3147.21818
													4.324	3147.21900
													4.309	3147.21982
													4.291	3147.22063
													4.289	3147.22145
													4.288	3147.22227
													4.277	3147.22309
													4.266	3147.22390
													4.285	3147.22472
													4.340	3147.22554
													4.397	3147.22636
													4.428	3147.22717
													4.431	3147.22799
													4.414	3147.22881
													4.395	3147.22963
													4.392	3147.23044
													4.417	3147.23126
													4.452	3147.23208
													4.482	3147.23290
													4.509	3147.23372
													4.534	3147.23453
													4.545	3147.23535

EDXRF												Hyperspectral Imagery		
Mg	Al	Si	S	K	Ca	Ti	Fe	K/Al	Ti/Al	Si bio	S/Fe	Depth	TOC	Depth
%	%	%	%	%	%	%	%			%		m	%	m
													1.343	3149.23799
													1.356	3149.23880
													1.349	3149.23962
													1.324	3149.24044
													1.291	3149.24125
													1.258	3149.24207
													1.237	3149.24289
													1.231	3149.24370
													1.224	3149.24452
													1.214	3149.24534
													1.211	3149.24615
													1.207	3149.24697
													1.197	3149.24779
													1.191	3149.24860
													1.186	3149.24942
													1.187	3149.25024
													1.193	3149.25105
													1.214	3149.25187
													1.239	3149.25269
													1.248	3149.25350
													1.239	3149.25432
													1.222	3149.25514
													1.207	3149.25595
													1.201	3149.25677
													1.204	3149.25759
													1.221	3149.25840
													1.237	3149.25922
													1.235	3149.26004
													1.213	3149.26085
													1.187	3149.26167
													1.169	3149.26249
													1.160	3149.26330
													1.150	3149.26412
													1.136	3149.26494
													1.132	3149.26575
													1.146	3149.26657
													1.186	3149.26739
													1.223	3149.26820
													1.258	3149.26902
													1.268	3149.26984
													1.268	3149.27065
													1.267	3149.27147
													1.259	3149.27229
													1.255	3149.27310
													1.260	3149.27392
													1.261	3149.27474
													1.261	3149.27555
													1.286	3149.27637
													1.274	3149.27719
													1.261	3149.27800
													1.249	3149.27882
													1.245	3149.27964
													1.245	3149.28045
													1.235	3149.28127

EDXRF												Hyperspectral Imagery		
Mg %	Al %	Si %	S %	K %	Ca %	Ti %	Fe %	K/Al	Ti/Al	Si bio %	S/Fe	Depth m	TOC %	Depth m
0.307	3.391	38.273	1.146	1.240	0.144	0.162	1.280	0.366	0.048	27.761	0.895	3150.49950	2.723	3150.45559
0.377	3.407	38.292	1.056	1.170	0.152	0.145	1.267	0.343	0.043	27.729	0.833	3150.49796	2.730	3150.45473
													2.728	3150.45645
													2.714	3150.45731
													2.681	3150.45818
													2.658	3150.45904
													2.647	3150.45990
													2.639	3150.46076
													2.651	3150.46162
													2.675	3150.46248
													2.698	3150.46335
													2.703	3150.46421
													2.669	3150.46507
													2.590	3150.46593
													2.449	3150.46679
													2.233	3150.46765
													1.952	3150.46852
													1.593	3150.46938
													1.306	3150.47024
													1.228	3150.47110
													1.359	3150.47196
													1.547	3150.47282
													1.743	3150.47369
													1.902	3150.47455
													1.988	3150.47541
													2.019	3150.47627
													2.029	3150.47713
													2.029	3150.47799
													2.021	3150.47885
													2.027	3150.47972
													2.061	3150.48058
													2.127	3150.48144
													2.223	3150.48230
													2.328	3150.48316
													2.408	3150.48402
													2.465	3150.48489
													2.506	3150.48575
													2.524	3150.48661
													2.514	3150.48747
													2.483	3150.48833
													2.441	3150.48919
													2.415	3150.49006
													2.448	3150.49092
													2.580	3150.49178
													2.801	3150.49264
													3.040	3150.49350
													3.214	3150.49436
													3.301	3150.49523
													3.337	3150.49609
													3.364	3150.49695
													3.392	3150.49781
													3.410	3150.49867
													3.426	3150.49953
													3.474	3150.50039
													3.575	3150.50126
													3.709	3150.50212
													3.824	3150.50298
													3.869	3150.50384
													3.829	3150.50470
													3.706	3150.50556
													3.517	3150.50643
													3.291	3150.50729

EDXRF												Hyperspectral Imagery		
Mg	Al	Si	S	K	Ca	Ti	Fe	K/Al	Ti/Al	Si bio	S/Fe	Depth	TOC	Depth
%	%	%	%	%	%	%	%			%		m	%	m
													3.078	3150.50815

EDXRF													Hyperspectral Imagery	
Mg %	Al %	Si %	S %	K %	Ca %	Ti %	Fe %	K/Al	Ti/Al	Si bio %	S/Fe	Depth m	TOC %	Depth m
1.241	6.213	26.803	2.087	1.875	3.763	0.332	2.768	0.302	0.053	7.543	0.754	3154.02672	0.743	3153.98256
1.100	6.195	27.099	1.983	1.908	3.686	0.362	2.732	0.308	0.058	7.893	0.726	3154.02830	0.729	3153.98341
													0.728	3153.98426
													0.737	3153.98510
													0.748	3153.98595
													0.757	3153.98680
													0.766	3153.98765
													0.774	3153.98850
													0.775	3153.98935
													0.770	3153.99020
													0.764	3153.99105
													0.759	3153.99190
													0.753	3153.99274
													0.747	3153.99359
													0.742	3153.99444
													0.742	3153.99529
													0.739	3153.99614
													0.732	3153.99699
													0.721	3153.99784
													0.710	3153.99869
													0.706	3153.99953
													0.709	3154.00038
													0.717	3154.00123
													0.723	3154.00208
													0.723	3154.00293
													0.718	3154.00378
													0.715	3154.00463
													0.715	3154.00548
													0.718	3154.00633
													0.718	3154.00717
													0.710	3154.00802
													0.699	3154.00887
													0.695	3154.00972
													0.701	3154.01057
													0.716	3154.01142
													0.732	3154.01227
													0.738	3154.01312
													0.728	3154.01396
													0.713	3154.01481
													0.706	3154.01566
													0.713	3154.01651
													0.727	3154.01736
													0.737	3154.01821
													0.736	3154.01906
													0.725	3154.01991
													0.717	3154.02075
													0.715	3154.02160
													0.717	3154.02245
													0.723	3154.02330
													0.732	3154.02415
													0.744	3154.02500
													0.754	3154.02585
													0.755	3154.02670
													0.749	3154.02755
													0.740	3154.02839
													0.735	3154.02924
													0.729	3154.03009
													0.719	3154.03094

EDXRF													Hyperspectral Imagery	
Mg %	Al %	Si %	S %	K %	Ca %	Ti %	Fe %	K/Al	Ti/Al	Si bio %	S/Fe	Depth m	TOC %	Depth m
													1.105	3154.74048
													1.060	3154.74111
													1.020	3154.74175
													1.028	3154.74238
													1.138	3154.73984
													1.044	3154.74302
													1.057	3154.74365
													1.032	3154.74429
													1.006	3154.74493
													0.994	3154.74556
													0.987	3154.74620
													0.978	3154.74683
													0.965	3154.74747
													0.969	3154.74811
													0.970	3154.74874
													0.971	3154.74938
													0.966	3154.75001
													0.943	3154.75065
													0.924	3154.75129
													0.888	3154.75192
													0.861	3154.75256
													0.812	3154.75319
													0.770	3154.75383
													0.748	3154.75446
													0.753	3154.75510
													0.774	3154.75574
													0.806	3154.75637
													0.858	3154.75701
													0.886	3154.75764
													0.888	3154.75828
													0.886	3154.75892
													0.876	3154.75955
													0.868	3154.76019
													0.868	3154.76082
													0.892	3154.76146
													0.908	3154.76209
													0.913	3154.76273
													0.901	3154.76337
													0.882	3154.76400
													0.884	3154.76464
													0.887	3154.76527
													0.897	3154.76591
													0.890	3154.76655
													0.900	3154.76718
													0.908	3154.76782
													0.927	3154.76845
													0.939	3154.76909
													0.934	3154.76972
													0.918	3154.77036
													0.901	3154.77100
													0.900	3154.77163
													0.921	3154.77227
													0.946	3154.77290
													0.958	3154.77354
													0.960	3154.77418
													0.961	3154.77481
													0.938	3154.77545
													0.940	3154.77608
													0.939	3154.77672
													0.942	3154.77735
													0.922	3154.77799
													0.900	3154.77863

EDXRF												Hyperspectral Imagery		
Mg %	Al %	Si %	S %	K %	Ca %	Ti %	Fe %	K/Al	Ti/Al	Si bio %	S/Fe	Depth m	TOC %	Depth m
													0.877	3154.77926
													0.844	3154.77990
													0.828	3154.78053
													0.792	3154.78308
													0.781	3154.78371
													0.788	3154.78435
													0.794	3154.78498
													0.825	3154.78117
													0.811	3154.78181
													0.806	3154.78244
													0.798	3154.78562
													0.790	3154.78626
													0.772	3154.78689
													0.772	3154.78753
													0.766	3154.78816
													0.773	3154.78880
													0.786	3154.78944
													0.793	3154.79007
													0.728	3154.79071
													0.740	3154.79134
													0.755	3154.79198
													0.760	3154.79261
													0.755	3154.79325
													0.756	3154.79389
													0.764	3154.79452
													0.791	3154.79516
													0.819	3154.79579
													0.843	3154.79643
													0.846	3154.79707
													0.822	3154.79770
													0.796	3154.79834
													0.780	3154.79897
													0.765	3154.79961
													0.761	3154.80024
													0.758	3154.80088
													0.745	3154.80152
													0.738	3154.80215
													0.719	3154.80279

EDXRF												Hyperspectral Imagery		
Mg %	Al %	Si %	S %	K %	Ca %	Ti %	Fe %	K/Al	Ti/Al	Si bio %	S/Fe	Depth m	TOC %	Depth m
													0.664	3155.96230
													0.661	3155.96293
													0.660	3155.96355
													0.654	3155.96418
													0.652	3155.96481
													0.651	3155.96543
													0.652	3155.96606
													0.654	3155.96669
													0.642	3155.96731
													0.644	3155.96794
													0.638	3155.96857
													0.648	3155.96919
													0.653	3155.96982
													0.670	3155.97045
													0.660	3155.97107
													0.655	3155.97170
													0.658	3155.97232
													0.679	3155.97295
													0.682	3155.97358
													0.670	3155.97420
													0.698	3155.97483
													0.695	3155.97546
													0.683	3155.97608
													0.683	3155.97671
													0.677	3155.97734
													0.673	3155.97796
													0.656	3155.97859
													0.645	3155.97922
													0.648	3155.97984
													0.622	3155.98047
													0.621	3155.98110
													0.608	3155.98172
													0.578	3155.98235
													0.575	3155.98297
													0.559	3155.98360
													0.525	3155.98423
													0.532	3155.98485
													0.483	3155.98548
													0.483	3155.98611
													0.494	3155.98673
													0.500	3155.98736
													0.515	3155.98799
													0.507	3155.98861
													0.484	3155.98924
													0.458	3155.98987
													0.442	3155.99049
													0.435	3155.99112
													0.389	3155.99174
													0.371	3155.99237
													0.323	3155.99300
													0.270	3155.99362
													0.202	3155.99425
													0.212	3155.99488
													0.221	3155.99550
													0.229	3155.99613
													0.233	3155.99676
													0.228	3155.99738
													0.208	3155.99801
													0.165	3155.99864
													0.223	3155.99926
													0.250	3155.99989
													0.297	3156.00051
													0.331	3156.00114
													0.348	3156.00177
													0.473	3156.00239

EDXRF												Hyperspectral Imagery		
Mg	Al	Si	S	K	Ca	Ti	Fe	K/Al	Ti/Al	Si bio	S/Fe	Depth	TOC	Depth
%	%	%	%	%	%	%	%			%		m	%	m
													0.479	3156.00365
													0.479	3156.00427
													0.472	3156.00490
													0.471	3156.00553
													0.475	3156.00302
													0.482	3156.00615
													0.495	3156.00678
													0.518	3156.00741
													0.528	3156.00803
													0.529	3156.00866
													0.532	3156.00928
													0.544	3156.00991
													0.566	3156.01054
													0.584	3156.01116
													0.595	3156.01179
													0.595	3156.01242

EDXRF													Hyperspectral Imagery	
Mg	Al	Si	S	K	Ca	Ti	Fe	K/Al	Ti/Al	Si bio	S/Fe	Depth	TOC	Depth
%	%	%	%	%	%	%	%			%		m	%	m
													2.064	3158.82122
													2.104	3158.82216
													2.123	3158.82309
													2.113	3158.82403
													2.082	3158.82496
													2.046	3158.82589
													2.011	3158.82683
													1.996	3158.82776
													2.001	3158.82869
													2.027	3158.82963
													2.061	3158.83056
													2.073	3158.83150
													2.055	3158.83243
													2.024	3158.83336
													1.994	3158.83430
													1.960	3158.83523
													1.918	3158.83616
													1.890	3158.83710
													1.880	3158.83803
													1.872	3158.83897
													1.850	3158.83990
													1.821	3158.84083
													1.797	3158.84177
													1.789	3158.84270
													1.798	3158.84363
													1.809	3158.84457
													1.830	3158.84550
													1.867	3158.84644
													1.907	3158.84737
													1.945	3158.84830
													1.979	3158.84924
													2.002	3158.85017
													2.002	3158.85110
													1.990	3158.85204
													2.026	3158.85297
													2.190	3158.85391
													2.515	3158.85484
													2.705	3158.85577
													2.635	3158.85671
													2.328	3158.85764
													2.019	3158.85858
													1.772	3158.85951
													1.359	3158.86044
													0.627	3158.86138
													0.904	3158.86231
													0.832	3158.86324
													1.134	3158.86418
													1.298	3158.86511
													1.357	3158.86605
													1.424	3158.86698
													1.499	3158.86791
													1.530	3158.86885
													1.549	3158.86978
													1.478	3158.87071
													1.449	3158.87165
													1.410	3158.87258
													1.385	3158.87352

EDXRF												Hyperspectral Imagery		
Mg %	Al %	Si %	S %	K %	Ca %	Ti %	Fe %	K/Al	Ti/Al	Si bio %	S/Fe	Depth m	TOC %	Depth m
0.587	4.543	34.662	1.465	1.527	1.056	0.210	2.087	0.336	0.046	20.579	0.702	3156.98486	1.658	3156.95652
0.583	4.498	34.901	1.438	1.466	1.024	0.202	2.030	0.326	0.045	20.957	0.708	3156.98597	1.634	3156.95716
0.609	4.482	35.236	1.388	1.513	0.829	0.206	1.921	0.338	0.046	21.343	0.723	3156.98708	1.616	3156.95780
0.609	4.437	35.612	1.186	1.489	0.941	0.210	1.821	0.336	0.047	21.857	0.651	3156.98819	1.611	3156.95845
0.509	4.509	35.666	1.126	1.513	0.925	0.210	1.847	0.336	0.047	21.687	0.610	3156.98930	1.618	3156.95909
													1.630	3156.95973
													1.632	3156.96038
													1.621	3156.96102
													1.623	3156.96166
													1.651	3156.96231
													1.684	3156.96295
													1.697	3156.96359
													1.684	3156.96424
													1.680	3156.96488
													1.579	3156.96552
													1.591	3156.96617
													1.611	3156.96681
													1.642	3156.96745
													1.682	3156.96810
													1.729	3156.96874
													1.782	3156.96938
													1.832	3156.97003
													1.866	3156.97067
													1.879	3156.97131
													1.872	3156.97196
													1.863	3156.97260
													1.857	3156.97324
													1.854	3156.97388
													1.848	3156.97453
													1.833	3156.97517
													1.817	3156.97581
													1.814	3156.97646
													1.826	3156.97710
													1.836	3156.97774
													1.835	3156.97839
													1.844	3156.97903
													1.869	3156.97967
													1.893	3156.98032
													1.903	3156.98096
													1.908	3156.98160
													1.917	3156.98225
													1.928	3156.98289
													1.929	3156.98353
													1.918	3156.98418
													1.906	3156.98482
													1.911	3156.98546
													1.940	3156.98611
													1.978	3156.98675
													1.999	3156.98739
													1.992	3156.98804
													1.969	3156.98868
													1.932	3156.98932
													1.871	3156.98996

EDXRF												Hyperspectral Imagery		
Mg	Al	Si	S	K	Ca	Ti	Fe	K/Al	Ti/Al	Si bio	S/Fe	Depth	TOC	Depth
%	%	%	%	%	%	%	%			%		m	%	m
													2.728	3159.81699
													2.737	3159.81773
													2.735	3159.81847
													2.708	3159.81921
													2.724	3159.81625
													2.639	3159.81995
													2.533	3159.82069
													2.428	3159.82143
													2.358	3159.82217
													2.322	3159.82291
													2.302	3159.82365
													2.290	3159.82439
													2.293	3159.82513
													2.306	3159.82588
													2.315	3159.82662
													2.306	3159.82736
													2.279	3159.82810
													2.250	3159.82884
													2.241	3159.82958
													2.267	3159.83032
													2.328	3159.83106
													2.406	3159.83180
													2.483	3159.83254
													2.548	3159.83328
													2.597	3159.83402
													2.638	3159.83476
													2.680	3159.83551
													2.721	3159.83625
													2.747	3159.83699
													2.753	3159.83773
													2.754	3159.83847
													2.745	3159.83921
													2.720	3159.83995
													2.689	3159.84069
													2.670	3159.84143
													2.681	3159.84217
													2.730	3159.84291
													2.800	3159.84365
													2.853	3159.84440
													2.873	3159.84514
													2.878	3159.84588
													2.921	3159.84662
													3.009	3159.84736
													3.091	3159.84810
													3.142	3159.84884
													3.171	3159.84958
													3.201	3159.85032
													3.235	3159.85106
													3.287	3159.85180
													3.338	3159.85254
													3.304	3159.85328
													3.184	3159.85403
													3.036	3159.85477
													2.939	3159.85551
													2.900	3159.85625
													2.900	3159.85699
													2.956	3159.85773
													3.034	3159.85847
													3.091	3159.85921
													3.104	3159.85995
													3.098	3159.86069
													3.142	3159.86143

EDXRF												Hyperspectral Imagery		
Mg %	Al %	Si %	S %	K %	Ca %	Ti %	Fe %	K/Al	Ti/Al	Si bio %	S/Fe	Depth m	TOC %	Depth m
													3.249	3159.86217
													3.355	3159.86291
													3.367	3159.86366
													3.295	3159.86662
													3.197	3159.86736
													3.210	3159.86810
													3.302	3159.86884
													3.364	3159.86440
													3.264	3159.86514
													3.210	3159.86588
													3.153	3159.86958

EDXRF													Hyperspectral Imagery	
Mg	Al	Si	S	K	Ca	Ti	Fe	K/Al	Ti/Al	Si bio	S/Fe	Depth	TOC	Depth
%	%	%	%	%	%	%	%			%		m	%	m
													2.910	3160.84858
													2.920	3160.84936
													2.851	3160.85014
													2.772	3160.85092
													2.669	3160.85170
													2.549	3160.85248
													2.423	3160.85326
													2.306	3160.85404
													2.243	3160.85482
													2.269	3160.85560
													2.377	3160.85638
													2.512	3160.85716
													2.614	3160.85794
													2.645	3160.85872
													2.631	3160.85950
													2.603	3160.86028
													2.558	3160.86106
													2.468	3160.86184
													2.333	3160.86262
													2.208	3160.86340
													2.123	3160.86418
													2.069	3160.86496
													2.014	3160.86574
													1.958	3160.86652
													1.918	3160.86730
													1.907	3160.86808
													1.928	3160.86886
													1.948	3160.86964
													1.967	3160.87042
													1.986	3160.87120
													2.009	3160.87198
													2.044	3160.87276
													2.096	3160.87354
													2.160	3160.87432
													2.201	3160.87510
													2.201	3160.87588
													2.184	3160.87666
													2.195	3160.87744
													2.261	3160.87822
													2.339	3160.87900
													2.399	3160.87978
													2.414	3160.88056
													2.417	3160.88134
													2.440	3160.88212
													2.482	3160.88290
													2.520	3160.88368
													2.539	3160.88446
													2.539	3160.88524

EDXRF												Hyperspectral Imagery		
Mg	Al	Si	S	K	Ca	Ti	Fe	K/Al	Ti/Al	Si bio	S/Fe	Depth	TOC	Depth
%	%	%	%	%	%	%	%			%		m	%	m
													0.336	3164.04754
													0.343	3164.04833
													0.346	3164.04911
													0.344	3164.04989
													0.340	3164.05067
													0.338	3164.05145
													0.338	3164.05223
													0.339	3164.05301
													0.339	3164.05379
													0.339	3164.05458
													0.338	3164.05536
													0.334	3164.05614
													0.333	3164.05692
													0.335	3164.05770
													0.336	3164.05848
													0.335	3164.05926
													0.336	3164.06004
													0.343	3164.06082
													0.353	3164.06161
													0.362	3164.06239
													0.366	3164.06317
													0.369	3164.06395
													0.371	3164.06473
													0.375	3164.06551
													0.379	3164.06629
													0.381	3164.06707
													0.380	3164.06785
													0.376	3164.06864
													0.373	3164.06942
													0.369	3164.07020
													0.365	3164.07098
													0.361	3164.07176
													0.362	3164.07254
													0.366	3164.07332
													0.371	3164.07410
													0.376	3164.07488
													0.381	3164.07567
													0.384	3164.07645
													0.385	3164.07723
													0.385	3164.07801
													0.383	3164.07879
													0.379	3164.07957
													0.373	3164.08035
													0.368	3164.08113
													0.364	3164.08191
													0.361	3164.08270
													0.357	3164.08348

EDXRF												Hyperspectral Imagery		
Mg	Al	Si	S	K	Ca	Ti	Fe	K/Al	Ti/Al	Si bio	S/Fe	Depth	TOC	Depth
%	%	%	%	%	%	%	%			%		m	%	m
													0.386	3166.86792
													0.384	3166.86871
													0.381	3166.86950
													0.378	3166.87029
													0.375	3166.87108
													0.372	3166.87187
													0.368	3166.87266
													0.364	3166.87346
													0.358	3166.87425
													0.351	3166.87504
													0.349	3166.87583

EDXRF												Hyperspectral Imagery		
Mg	Al	Si	S	K	Ca	Ti	Fe	K/Al	Ti/Al	Si bio	S/Fe	Depth	TOC	Depth
%	%	%	%	%	%	%	%			%		m	%	m
													0.523	3170.82126
													0.529	3170.82201
													0.533	3170.82275
													0.532	3170.82350
													0.529	3170.82425
													0.529	3170.82499
													0.529	3170.82574
													0.524	3170.82649
													0.513	3170.82723
													0.500	3170.82798
													0.491	3170.82873
													0.486	3170.82947
													0.483	3170.83022
													0.480	3170.83097
													0.473	3170.83171
													0.464	3170.83246
													0.458	3170.83321
													0.461	3170.83395
													0.467	3170.83470
													0.471	3170.83545
													0.472	3170.83619
													0.474	3170.83694
													0.476	3170.83769
													0.475	3170.83843
													0.467	3170.83918
													0.453	3170.83993
													0.439	3170.84067
													0.432	3170.84142
													0.431	3170.84216
													0.435	3170.84291
													0.436	3170.84366
													0.439	3170.84440
													0.449	3170.84515
													0.481	3170.84590
													0.527	3170.84664
													0.556	3170.84739
													0.563	3170.84814
													0.562	3170.84888
													0.564	3170.84963
													0.566	3170.85038
													0.564	3170.85112
													0.559	3170.85187
													0.551	3170.85262
													0.566	3170.85336
													0.546	3170.85411
													0.510	3170.85486
													0.478	3170.85560
													0.459	3170.85635
													0.452	3170.85710
													0.451	3170.85784
													0.450	3170.85859
													0.448	3170.85934
													0.447	3170.86008
													0.448	3170.86083
													0.447	3170.86157
													0.448	3170.86232
													0.451	3170.86307
													0.456	3170.86381
													0.462	3170.86456
													0.470	3170.86531
													0.477	3170.86605

EDXRF													Hyperspectral Imagery	
Mg	Al	Si	S	K	Ca	Ti	Fe	K/Al	Ti/Al	Si bio	S/Fe	Depth	TOC	Depth
%	%	%	%	%	%	%	%			%		m	%	m
													0.478	3170.86680
													0.476	3170.86755
													0.473	3170.86829
													0.467	3170.86904
													0.464	3170.86979

EDXRF												Hyperspectral Imagery		
Mg %	Al %	Si %	S %	K %	Ca %	Ti %	Fe %	K/Al	Ti/Al	Si bio %	S/Fe	Depth m	TOC %	Depth m
1.074	7.474	29.019	0.747	2.508	2.407	0.397	2.776	0.336	0.053	5.849	0.269	3172.94368	0.777	3172.89818
0.526	7.502	29.476	0.747	2.574	2.395	0.384	2.706	0.343	0.051	6.220	0.276	3172.94502	0.762	3172.89897
1.008	7.797	29.666	0.584	2.570	2.204	0.397	2.523	0.330	0.051	5.496	0.232	3172.94636	0.751	3172.89976
													0.747	3172.90055
													0.744	3172.90134
													0.731	3172.90213
													0.700	3172.90292
													0.663	3172.90371
													0.643	3172.90450
													0.652	3172.90529
													0.683	3172.90608
													0.728	3172.90687
													0.776	3172.90766
													0.813	3172.90845
													0.823	3172.90924
													0.810	3172.91003
													0.783	3172.91082
													0.747	3172.91161
													0.734	3172.91240
													0.721	3172.91319
													0.717	3172.91398
													0.713	3172.91477
													0.697	3172.91556
													0.653	3172.91635
													0.585	3172.91714
													0.512	3172.91793
													0.470	3172.91872
													0.462	3172.91951
													0.486	3172.92030
													0.532	3172.92109
													0.571	3172.92188
													0.589	3172.92267
													0.596	3172.92346
													0.604	3172.92425
													0.614	3172.92504
													0.627	3172.92583
													0.641	3172.92662
													0.655	3172.92741
													0.668	3172.92820
													0.676	3172.92899
													0.687	3172.92978
													0.702	3172.93057
													0.705	3172.93136
													0.680	3172.93215
													0.634	3172.93294
													0.595	3172.93373
													0.578	3172.93452
													0.582	3172.93531
													0.592	3172.93610
													0.598	3172.93689
													0.606	3172.93768
													0.628	3172.93847
													0.663	3172.93926
													0.693	3172.94005
													0.703	3172.94084
													0.698	3172.94163
													0.686	3172.94242
													0.675	3172.94321
													0.664	3172.94400
													0.652	3172.94479
													0.638	3172.94558
													0.622	3172.94636

Slab 3174.81 m

EDXRF										Hyperspectral Imagery					
Mg %	Al %	Si %	S %	K %	Ca %	Ti %	Fe %	K/Al	Ti/Al	Si bio %	S/Fe	Depth m	TOC %	Depth m	
0.443	4.042	34.105	2.355	1.311	0.869	0.171	2.540	0.324	0.042	21.574	0.927	3174.86122	1.532	3174.86066	
0.500	4.092	32.639	3.216	1.288	0.773	0.154	2.876	0.315	0.038	19.953	1.118	3174.86247	1.463	3174.86145	
0.377	4.220	31.938	3.538	1.325	0.722	0.189	3.190	0.314	0.045	18.855	1.109	3174.86372	1.382	3174.86225	
0.403	4.198	31.445	3.675	1.339	0.630	0.184	3.539	0.319	0.044	18.431	1.038	3174.86497	1.296	3174.86304	
0.425	4.109	28.979	5.110	1.212	0.622	0.162	4.289	0.295	0.040	16.241	1.192	3174.86621	1.214	3174.86384	
0.469	4.087	27.413	5.994	1.212	0.586	0.141	4.685	0.297	0.034	14.744	1.279	3174.86746	1.135	3174.86463	
0.425	3.803	25.074	7.453	1.119	0.558	0.128	5.435	0.294	0.034	13.285	1.371	3174.86871	1.077	3174.86543	
0.289	4.092	25.997	6.905	1.259	0.451	0.162	5.121	0.308	0.040	13.311	1.348	3174.86996	1.013	3174.86622	
0.311	4.159	25.572	7.111	1.259	0.383	0.145	5.230	0.303	0.035	12.679	1.359	3174.87121	0.966	3174.86702	
0.233	3.975	24.336	7.878	1.165	0.419	0.141	5.754	0.293	0.035	12.013	1.369	3174.87246	0.941	3174.86781	
0.272	3.575	22.015	9.516	1.015	0.291	0.123	6.395	0.284	0.035	10.933	1.488	3174.87371	0.931	3174.86860	
0.320	3.369	20.943	10.048	0.954	0.339	0.102	6.861	0.283	0.030	10.499	1.464	3174.87496	0.918	3174.86940	
0.320	3.614	22.481	9.025	1.095	0.347	0.141	6.364	0.303	0.039	11.278	1.418	3174.87621	0.915	3174.87019	
0.237	3.670	22.137	9.241	1.039	0.351	0.128	6.534	0.283	0.035	10.762	1.414	3174.87746	0.895	3174.87099	
0.285	4.026	23.916	7.961	1.203	0.359	0.149	5.967	0.299	0.037	11.437	1.334	3174.87871	0.867	3174.87178	
0.421	4.259	25.024	7.290	1.278	0.331	0.149	5.440	0.300	0.035	11.821	1.340	3174.87996	0.839	3174.87258	
0.390	4.159	25.291	7.097	1.212	0.490	0.149	5.379	0.292	0.036	12.398	1.320	3174.88120	0.812	3174.87337	
0.465	4.498	26.621	6.070	1.381	0.546	0.162	4.890	0.307	0.036	12.677	1.241	3174.88245	0.790	3174.87416	
0.382	4.660	27.291	5.675	1.494	0.546	0.184	4.546	0.321	0.040	12.846	1.248	3174.88370	0.772	3174.87496	
0.399	4.838	28.015	5.004	1.551	0.622	0.171	4.393	0.321	0.035	13.018	1.139	3174.88495	0.759	3174.87575	
0.465	5.160	28.943	4.356	1.668	0.638	0.215	3.896	0.323	0.042	12.946	1.118	3174.88620	0.755	3174.87655	
0.530	5.349	29.246	4.020	1.729	0.506	0.223	3.861	0.323	0.042	12.663	1.041	3174.88745	0.761	3174.87734	
0.482	5.383	30.146	3.515	1.734	0.682	0.232	3.482	0.322	0.043	13.460	1.009	3174.88870	0.771	3174.87814	
0.596	5.956	30.594	2.628	2.222	0.670	0.306	2.959	0.373	0.051	12.132	0.888	3174.89210	0.785	3174.87893	
0.859	6.045	30.481	2.541	2.189	0.678	0.301	2.907	0.362	0.050	11.742	0.874	3174.89325	0.804	3174.87973	
0.627	6.095	31.332	2.438	2.100	0.654	0.262	2.645	0.345	0.043	12.438	0.922	3174.89439	0.825	3174.88052	
0.758	6.111	32.010	2.073	2.053	0.650	0.267	2.409	0.336	0.044	13.065	0.860	3174.89554	0.844	3174.88131	
0.631	6.278	32.214	1.903	2.142	0.570	0.262	2.388	0.341	0.042	12.751	0.797	3174.89669	0.858	3174.88211	
0.631	6.417	31.938	2.013	2.203	0.467	0.293	2.440	0.343	0.046	12.044	0.825	3174.89783	0.867	3174.88290	
0.522	6.534	32.092	1.907	2.217	0.486	0.275	2.375	0.339	0.042	11.836	0.803	3174.89898	0.878	3174.88370	
0.631	6.506	31.938	1.903	2.260	0.542	0.284	2.388	0.347	0.044	11.768	0.797	3174.90013	0.893	3174.88449	
0.552	6.645	32.395	1.707	2.372	0.427	0.314	2.191	0.357	0.047	11.794	0.779	3174.90127	0.906	3174.88529	
0.574	6.573	32.580	1.651	2.344	0.399	0.288	2.191	0.357	0.044	12.204	0.753	3174.90242	0.929	3174.88608	
0.579	6.534	32.621	1.684	2.325	0.367	0.301	2.174	0.356	0.046	12.365	0.775	3174.90357	0.951	3174.88688	
0.679	6.423	32.644	1.668	2.283	0.355	0.314	2.183	0.355	0.049	12.733	0.764	3174.90471	0.976	3174.88767	
0.526	6.256	32.938	1.771	2.208	0.407	0.306	2.074	0.353	0.049	13.544	0.854	3174.90586	0.983	3174.88846	
0.614	6.462	32.874	1.631	2.292	0.419	0.293	1.987	0.355	0.045	12.843	0.821	3174.90701	0.969	3174.88926	
0.583	6.428	32.707	1.681	2.255	0.498	0.336	2.091	0.351	0.052	12.779	0.804	3174.90815	0.953	3174.89005	
0.561	6.451	32.662	1.711	2.283	0.467	0.314	2.104	0.354	0.049	12.665	0.813	3174.90930	0.943	3174.89085	
													0.942	3174.89164	
													0.934	3174.89244	
													0.911	3174.89323	
													0.888	3174.89402	
													0.865	3174.89482	
													0.869	3174.89561	
													0.864	3174.89641	
													0.890	3174.89720	
													0.916	3174.89800	
													0.940	3174.89879	
													0.949	3174.89959	
													0.947	3174.90038	
													0.943	3174.90117	
													0.929	3174.90197	
													0.937	3174.90276	
													0.926	3174.90356	
													0.912	3174.90435	
													0.908	3174.90515	
													0.914	3174.90594	
													0.929	3174.90674	
													0.915	3174.90753	
													0.919	3174.90832	

EDXRF													Hyperspectral Imagery	
Mg	Al	Si	S	K	Ca	Ti	Fe	K/Al	Ti/Al	Si bio	S/Fe	Depth	TOC	Depth
%	%	%	%	%	%	%	%			%		m	%	m
													1.017	3174.90912
													0.951	3174.90991

EDXRF													Hyperspectral Imagery	
Mg	Al	Si	S	K	Ca	Ti	Fe	K/Al	Ti/Al	Si bio	S/Fe	Depth	TOC	Depth
%	%	%	%	%	%	%	%			%		m	%	m
													0.382	3175.24771
													0.380	3175.24850
													0.369	3175.24928
													0.348	3175.25006
													0.324	3175.25085
													0.306	3175.25163
													0.299	3175.25241
													0.296	3175.25320
													0.296	3175.25398
													0.303	3175.25476
													0.320	3175.25555
													0.339	3175.25633
													0.347	3175.25711
													0.341	3175.25790
													0.328	3175.25868
													0.315	3175.25946
													0.308	3175.26025
													0.310	3175.26103
													0.318	3175.26181
													0.325	3175.26260
													0.329	3175.26338
													0.327	3175.26416
													0.321	3175.26495
													0.319	3175.26573
													0.318	3175.26651
													0.317	3175.26730
													0.318	3175.26808
													0.319	3175.26886
													0.321	3175.26965
													0.315	3175.27043
													0.310	3175.27121
													0.310	3175.27200
													0.315	3175.27278
													0.318	3175.27356
													0.319	3175.27435
													0.314	3175.27513
													0.309	3175.27591
													0.307	3175.27670
													0.310	3175.27748
													0.320	3175.27826
													0.341	3175.27905
													0.371	3175.27983
													0.393	3175.28061
													0.392	3175.28140
													0.369	3175.28218
													0.340	3175.28296
													0.319	3175.28375
													0.310	3175.28453
													0.308	3175.28531
													0.311	3175.28610
													0.312	3175.28688
													0.308	3175.28766
													0.311	3175.28610
													0.312	3175.28688
													0.308	3175.28766
													0.303	3175.28845
													0.298	3175.28923
													0.300	3175.29001
													0.302	3175.29080

EDXRF													Hyperspectral Imagery		
Mg %	Al %	Si %	S %	K %	Ca %	Ti %	Fe %	K/Al	Ti/Al	Si bio %	S/Fe	Depth m	TOC %	Depth m	
1.179	7.524	27.784	1.113	2.386	3.100	0.327	3.020	0.317	0.043	4.459	0.368	3176.39753	0.473	3176.34770	
1.359	7.346	27.563	1.113	2.368	3.240	0.319	3.037	0.322	0.043	4.789	0.366	3176.39882	0.480	3176.34848	
1.341	7.101	26.798	1.202	2.208	3.845	0.332	3.347	0.311	0.047	4.783	0.359	3176.40010	0.487	3176.34927	
													0.487	3176.35005	
													0.480	3176.35083	
													0.467	3176.35161	
													0.452	3176.35239	
													0.442	3176.35318	
													0.443	3176.35396	
													0.454	3176.35474	
													0.471	3176.35552	
													0.481	3176.35630	
													0.480	3176.35709	
													0.470	3176.35787	
													0.457	3176.35865	
													0.452	3176.35943	
													0.430	3176.36021	
													0.425	3176.36100	
													0.417	3176.36178	
													0.413	3176.36256	
													0.409	3176.36334	
													0.409	3176.36412	
													0.411	3176.36491	
													0.416	3176.36569	
													0.420	3176.36647	
													0.427	3176.36725	
													0.434	3176.36803	
													0.440	3176.36882	
													0.440	3176.36960	
													0.435	3176.37038	
													0.435	3176.37116	
													0.441	3176.37194	
													0.451	3176.37273	
													0.459	3176.37351	
													0.461	3176.37429	
													0.462	3176.37507	
													0.463	3176.37585	
													0.464	3176.37664	
													0.458	3176.37742	
													0.462	3176.37820	
													0.462	3176.37898	
													0.461	3176.37976	
													0.463	3176.38055	
													0.467	3176.38133	
													0.473	3176.38211	
													0.473	3176.38289	
													0.473	3176.38367	
													0.470	3176.38446	
													0.463	3176.38524	
													0.453	3176.38602	
													0.448	3176.38680	
													0.455	3176.38758	
													0.470	3176.38837	
													0.482	3176.38915	
													0.494	3176.38993	
													0.509	3176.39071	
													0.523	3176.39149	
													0.530	3176.39228	
													0.528	3176.39306	
													0.523	3176.39384	
													0.519	3176.39462	

EDXRF													Hyperspectral Imagery	
Mg	Al	Si	S	K	Ca	Ti	Fe	K/Al	Ti/Al	Si bio	S/Fe	Depth	TOC	Depth
%	%	%	%	%	%	%	%			%		m	%	m
													0.520	3176.39540
													0.523	3176.39619
													0.520	3176.39697
													0.507	3176.39775
													0.491	3176.39853
													0.475	3176.39931
													0.485	3176.40010

EDXRF												Hyperspectral Imagery		
Mg %	Al %	Si %	S %	K %	Ca %	Ti %	Fe %	K/Al	Ti/Al	Si bio %	S/Fe	Depth m	TOC %	Depth m
0.802	6.896	29.847	2.199	2.302	0.996	0.323	2.911	0.334	0.047	8.471	0.755	3176.90543	0.804	3176.87682
0.745	7.024	31.096	1.641	2.400	0.905	0.314	2.453	0.342	0.045	9.323	0.669	3176.90666	0.808	3176.87759
0.719	6.962	31.001	1.658	2.447	0.913	0.327	2.475	0.352	0.047	9.418	0.670	3176.90790	0.803	3176.87836
													0.793	3176.87913
													0.784	3176.87989
													0.781	3176.88066
													0.785	3176.88143
													0.792	3176.88220
													0.802	3176.88297
													0.814	3176.88374
													0.824	3176.88451
													0.831	3176.88527
													0.836	3176.88604
													0.841	3176.88681
													0.842	3176.88758
													0.840	3176.88835
													0.835	3176.88912
													0.830	3176.88989
													0.832	3176.89066
													0.838	3176.89142
													0.838	3176.89219
													0.828	3176.89296
													0.822	3176.89373
													0.818	3176.89450
													0.814	3176.89527
													0.810	3176.89604
													0.808	3176.89680
													0.804	3176.89757
													0.795	3176.89834
													0.786	3176.89911
													0.777	3176.89988
													0.762	3176.90065
													0.745	3176.90142
													0.736	3176.90219
													0.741	3176.90295
													0.757	3176.90372
													0.775	3176.90449
													0.794	3176.90526
													0.815	3176.90603
													0.834	3176.90680
													0.845	3176.90757
													0.844	3176.90833
													0.857	3176.90910

Slab 3177.9 m

EDXRF												Hyperspectral Imagery		
Mg %	Al %	Si %	S %	K %	Ca %	Ti %	Fe %	K/Al	Ti/Al	Si bio %	S/Fe	Depth m	TOC %	Depth m
1.297	7.830	23.029	1.704	2.391	5.535	0.384	3.718	0.305	0.049	-1.245	0.458	3177.91097	0.329	3177.91113
1.306	8.103	23.920	1.362	2.462	5.140	0.397	3.360	0.304	0.049	-1.198	0.405	3177.91253	0.339	3177.91185
1.306	7.752	23.386	1.511	2.269	5.834	0.397	3.434	0.293	0.051	-0.646	0.440	3177.91410	0.353	3177.91258
1.503	7.213	22.133	1.654	2.020	6.806	0.371	3.936	0.280	0.051	-0.227	0.420	3177.91567	0.367	3177.91331
1.621	6.612	19.830	1.996	1.762	8.173	0.336	4.777	0.266	0.051	-0.667	0.418	3177.91723	0.373	3177.91404
1.315	7.502	22.762	1.591	2.194	6.208	0.384	3.774	0.292	0.051	-0.494	0.422	3177.91880	0.370	3177.91476
1.328	6.873	21.124	1.880	1.950	7.571	0.327	4.236	0.284	0.048	-0.184	0.444	3177.92037	0.359	3177.91549
1.600	6.328	19.305	2.179	1.588	8.810	0.297	4.768	0.251	0.047	-0.313	0.457	3177.92193	0.348	3177.91622
1.332	5.828	18.459	2.076	1.471	10.380	0.284	4.720	0.252	0.049	0.393	0.440	3177.92350	0.346	3177.91695
1.328	6.684	21.314	1.774	1.818	7.946	0.332	4.036	0.272	0.050	0.593	0.440	3177.92507	0.352	3177.91768
1.232	7.407	23.223	1.631	2.199	6.069	0.375	3.595	0.297	0.051	0.260	0.454	3177.92663	0.362	3177.91840
1.341	7.007	21.658	1.973	2.011	6.969	0.353	4.062	0.287	0.050	-0.064	0.486	3177.92820	0.371	3177.91913
1.196	7.101	21.581	1.933	2.062	6.934	0.332	4.271	0.290	0.047	-0.434	0.453	3177.92977	0.378	3177.91986
1.267	6.951	21.518	1.973	1.983	7.049	0.332	4.276	0.285	0.048	-0.031	0.462	3177.93133	0.384	3177.92059
1.337	7.274	21.866	1.907	2.053	6.499	0.336	4.210	0.282	0.046	-0.683	0.453	3177.93290	0.383	3177.92132
1.424	7.558	21.920	1.927	2.128	6.069	0.314	4.232	0.282	0.042	-1.508	0.455	3177.93447	0.380	3177.92204
1.424	8.092	24.300	1.362	2.560	4.718	0.410	3.295	0.316	0.051	-0.784	0.413	3177.93603	0.379	3177.92277
1.196	8.409	24.622	1.325	2.584	4.475	0.375	3.264	0.307	0.045	-1.445	0.406	3177.93760	0.385	3177.92350
1.157	8.214	24.848	1.169	2.593	4.626	0.392	3.277	0.316	0.048	-0.616	0.357	3177.93917	0.396	3177.92423
1.175	8.169	25.146	1.142	2.612	4.443	0.414	3.194	0.320	0.051	-0.179	0.358	3177.94073	0.402	3177.92496
1.416	8.353	25.092	1.013	2.574	4.443	0.392	3.029	0.308	0.047	-0.802	0.334	3177.94230	0.397	3177.92568
1.223	8.131	25.038	1.149	2.490	4.694	0.410	3.164	0.306	0.050	-0.167	0.363	3177.94387	0.386	3177.92641
1.245	7.919	24.205	1.358	2.485	5.001	0.423	3.530	0.314	0.053	-0.344	0.385	3177.94543	0.374	3177.92714
1.236	7.813	23.594	1.764	2.429	4.957	0.397	3.735	0.311	0.051	-0.627	0.472	3177.94700	0.365	3177.92787
1.188	8.025	24.106	1.382	2.499	5.129	0.423	3.395	0.311	0.053	-0.771	0.407	3177.94857	0.360	3177.92860
1.240	8.292	24.481	1.119	2.513	4.989	0.384	3.203	0.303	0.046	-1.223	0.349	3177.95013	0.360	3177.92932
1.324	8.281	24.477	1.152	2.537	4.858	0.418	3.181	0.306	0.051	-1.194	0.362	3177.95170	0.362	3177.93005
1.262	8.381	24.798	0.963	2.579	4.862	0.414	3.068	0.308	0.049	-1.183	0.314	3177.95327	0.361	3177.93078
1.249	8.203	24.486	1.285	2.570	4.766	0.440	3.264	0.313	0.054	-0.943	0.394	3177.95483	0.355	3177.93151
1.192	8.186	24.612	1.249	2.640	4.662	0.405	3.247	0.322	0.050	-0.765	0.385	3177.95640	0.344	3177.93224
1.288	8.475	24.938	0.960	2.626	4.642	0.405	3.059	0.310	0.048	-1.336	0.314	3177.95797	0.334	3177.93296
1.253	8.142	24.517	1.182	2.551	4.790	0.423	3.412	0.313	0.052	-0.722	0.346	3177.95953	0.326	3177.93369
1.297	8.453	25.305	0.913	2.673	4.415	0.418	3.011	0.316	0.049	-0.900	0.303	3177.96110	0.323	3177.93442
1.096	8.453	25.029	1.302	2.649	4.264	0.405	3.159	0.313	0.048	-1.176	0.412	3177.96267	0.326	3177.93515
1.302	8.375	24.802	1.199	2.640	4.495	0.423	3.085	0.315	0.050	-1.161	0.389	3177.96423	0.338	3177.93588
1.205	8.503	24.925	1.073	2.692	4.495	0.436	3.020	0.317	0.051	-1.435	0.355	3177.96580	0.350	3177.93660
1.249	8.342	24.486	1.199	2.588	4.774	0.405	3.207	0.310	0.049	-1.374	0.374	3177.96737	0.358	3177.93733
1.394	7.980	23.622	1.561	2.480	5.065	0.414	3.552	0.311	0.052	-1.118	0.440	3177.96893	0.359	3177.93806
1.288	7.880	23.214	1.933	2.405	5.041	0.384	3.700	0.305	0.049	-1.214	0.523	3177.97050	0.358	3177.93879
1.078	8.353	24.540	1.212	2.570	4.873	0.401	3.216	0.308	0.048	-1.354	0.377	3177.97207	0.357	3177.93952
1.227	8.147	24.033	1.242	2.490	5.224	0.379	3.329	0.306	0.047	-1.223	0.373	3177.97363	0.361	3177.94024
1.218	7.891	23.422	1.780	2.508	5.156	0.392	3.556	0.318	0.050	-1.041	0.501	3177.97520	0.366	3177.94097
1.297	8.214	24.400	1.242	2.527	4.921	0.479	3.247	0.308	0.058	-1.064	0.383	3177.97677	0.369	3177.94170
1.175	8.392	24.816	1.076	2.626	4.742	0.427	3.064	0.313	0.051	-1.199	0.351	3177.97833	0.370	3177.94243
1.205	8.231	24.540	1.099	2.593	5.093	0.431	3.103	0.315	0.052	-0.975	0.354	3177.97990	0.370	3177.94315
1.359	8.169	24.377	1.076	2.513	5.144	0.397	3.159	0.308	0.049	-0.948	0.341	3177.98147	0.369	3177.94388
1.271	8.208	24.128	1.342	2.518	4.969	0.397	3.334	0.307	0.048	-1.318	0.402	3177.98303	0.367	3177.94461
1.236	8.097	24.626	1.677	2.621	4.132	0.362	3.316	0.324	0.045	-0.475	0.506	3177.98460	0.362	3177.94534
1.245	8.025	23.857	1.850	2.555	4.503	0.397	3.513	0.318	0.049	-1.020	0.527	3177.98617	0.358	3177.94607
1.232	8.014	23.070	2.232	2.457	4.587	0.379	3.874	0.307	0.047	-1.773	0.576	3177.98773	0.357	3177.94679
1.161	8.181	23.581	2.103	2.447	4.300	0.366	3.787	0.299	0.045	-1.779	0.555	3177.98930	0.362	3177.94752
1.205	8.192	23.762	1.987	2.527	4.328	0.401	3.687	0.309	0.049	-1.633	0.539	3177.99087	0.370	3177.94825
1.034	8.487	24.983	1.329	2.616	4.300	0.366	3.177	0.308	0.043	-1.325	0.418	3177.99243	0.380	3177.94898
1.201	8.292	25.354	1.265	2.602	4.089	0.384	3.181	0.314	0.046	-0.350	0.398	3177.99400	0.387	3177.94971
1.232	8.598	26.097	0.840	2.673	3.861	0.349	2.876	0.311	0.041	-0.557	0.292	3177.99557	0.388	3177.95043
1.179	8.442	25.404	1.245	2.612	4.033	0.371	3.129	0.309	0.044	-0.766	0.398	3177.99713	0.385	3177.95116
1.288	8.275	24.920	1.146	2.602	4.599	0.388	3.103	0.314	0.047	-0.733	0.369	3177.99870	0.381	3177.95189
													0.380	3177.95262
													0.380	3177.95335
													0.378	3177.95407
													0.374	3177.95480

EDXRF												Hyperspectral Imagery		
Mg %	Al %	Si %	S %	K %	Ca %	Ti %	Fe %	K/Al	Ti/Al	Si bio %	S/Fe	Depth m	TOC %	Depth m
													0.361	3177.95626
													0.359	3177.95699
													0.360	3177.95771
													0.360	3177.95844
													0.361	3177.95917
													0.361	3177.95990
													0.361	3177.96063
													0.382	3177.96135
													0.382	3177.96208
													0.382	3177.96281
													0.380	3177.96354
													0.377	3177.96427
													0.376	3177.96499
													0.377	3177.96572
													0.379	3177.96645
													0.378	3177.96718
													0.372	3177.96791
													0.362	3177.96863
													0.352	3177.96936
													0.346	3177.97009
													0.344	3177.97082
													0.344	3177.97154
													0.348	3177.97227
													0.353	3177.97300
													0.358	3177.97373
													0.360	3177.97446
													0.358	3177.97518
													0.353	3177.97591
													0.348	3177.97664
													0.342	3177.97737
													0.340	3177.97810
													0.343	3177.97882
													0.351	3177.97955
													0.360	3177.98028
													0.370	3177.98101
													0.374	3177.98174
													0.375	3177.98246
													0.375	3177.98319
													0.377	3177.98392
													0.381	3177.98465
													0.383	3177.98538
													0.381	3177.98610
													0.377	3177.98683
													0.371	3177.98756
													0.368	3177.98829
													0.368	3177.98902
													0.370	3177.98974
													0.372	3177.99047
													0.374	3177.99120
													0.376	3177.99193
													0.379	3177.99266
													0.384	3177.99338
													0.388	3177.99411
													0.392	3177.99484
													0.394	3177.99557
													0.393	3177.99630
													0.385	3177.99702
													0.376	3177.99775
													0.370	3177.99848

EDXRF													Hyperspectral Imagery			
Mg %	Al %	Si %	S %	K %	Ca %	Ti %	Fe %	K/Al	Ti/Al	Si bio %	S/Fe	Depth m	TOC %	Depth m		
1.288	7.541	22.735	2.199	2.189	5.372	0.375	3.957	0.290	0.050	-0.642	0.556	3177.81254	0.368	3177.78602		
1.232	7.724	23.106	1.967	2.325	5.312	0.401	3.800	0.301	0.052	-0.840	0.517	3177.81370	0.363	3177.78672		
1.170	7.869	23.490	1.827	2.330	5.121	0.388	3.674	0.296	0.049	-0.904	0.497	3177.81486	0.363	3177.78741		
1.328	7.730	23.079	1.933	2.241	5.344	0.375	3.779	0.290	0.049	-0.885	0.512	3177.81602	0.369	3177.78811		
1.179	7.813	23.477	1.877	2.349	5.152	0.379	3.617	0.301	0.049	-0.745	0.519	3177.81719	0.380	3177.78881		
1.245	7.864	23.427	1.777	2.363	5.220	0.384	3.600	0.300	0.049	-0.950	0.494	3177.81835	0.391	3177.78951		
1.201	7.741	23.092	1.714	2.349	5.690	0.410	3.696	0.303	0.053	-0.905	0.464	3177.81951	0.397	3177.79020		
1.293	7.858	23.708	1.651	2.410	5.176	0.392	3.508	0.307	0.050	-0.652	0.471	3177.82068	0.395	3177.79090		
1.253	7.969	23.830	1.591	2.452	5.089	0.401	3.456	0.308	0.050	-0.875	0.460	3177.82184	0.388	3177.79160		
1.196	8.108	24.142	1.285	2.541	5.200	0.423	3.295	0.313	0.052	-0.994	0.390	3177.82300	0.381	3177.79230		
1.341	8.119	23.726	1.412	2.386	5.272	0.388	3.391	0.294	0.048	-1.445	0.416	3177.82416	0.380	3177.79300		
1.271	7.947	23.793	1.438	2.424	5.380	0.436	3.351	0.305	0.055	-0.842	0.429	3177.82533	0.386	3177.79369		
1.148	8.075	23.821	1.418	2.447	5.348	0.457	3.408	0.303	0.057	-1.212	0.416	3177.82649	0.389	3177.79439		
													0.386	3177.79509		
													0.383	3177.79579		
													0.385	3177.79649		
													0.384	3177.79718		
													0.378	3177.79788		
													0.371	3177.79858		
													0.370	3177.79928		
													0.377	3177.79997		
													0.395	3177.80067		
													0.419	3177.80137		
													0.441	3177.80207		
													0.451	3177.80277		
													0.442	3177.80346		
													0.415	3177.80416		
													0.385	3177.80486		
													0.364	3177.80556		
													0.353	3177.80625		
													0.350	3177.80695		
													0.350	3177.80765		
													0.353	3177.80835		
													0.356	3177.80905		
													0.357	3177.80974		
													0.354	3177.81044		
													0.347	3177.81114		
													0.341	3177.81184		
													0.339	3177.81253		
													0.344	3177.81323		
													0.352	3177.81393		
													0.359	3177.81463		
													0.362	3177.81533		
													0.363	3177.81602		
													0.367	3177.81672		
													0.367	3177.81742		
													0.363	3177.81812		
													0.364	3177.81881		
													0.375	3177.81951		
													0.383	3177.82021		
													0.378	3177.82091		
													0.379	3177.82161		
													0.369	3177.82230		
													0.357	3177.82300		
													0.360	3177.82370		
													0.349	3177.82440		
													0.344	3177.82509		
													0.339	3177.82579		
													0.334	3177.82649		

Slab 3178.9 m

EDXRF													Hyperspectral Imagery		
Mg %	Al %	Si %	S %	K %	Ca %	Ti %	Fe %	K/Al	Ti/Al	Si bio %	S/Fe	Depth m	TOC %	Depth m	
1.420	6.673	21.730	2.040	2.076	6.443	0.401	4.328	0.311	0.060	1.043	0.471	3178.90000	0.418	3178.90000	
1.227	6.751	21.816	2.113	2.142	6.459	0.436	4.311	0.317	0.065	0.888	0.490	3178.90193	0.424	3178.90072	
1.372	7.624	24.232	0.830	2.354	5.981	0.405	3.225	0.309	0.053	0.597	0.257	3178.90386	0.429	3178.90143	
1.389	7.802	23.735	1.079	2.297	5.913	0.384	3.308	0.294	0.049	-0.453	0.326	3178.90580	0.427	3178.90215	
1.218	8.003	24.549	0.817	2.485	5.619	0.427	3.090	0.311	0.053	-0.259	0.264	3178.90773	0.417	3178.90287	
1.284	7.941	24.870	0.737	2.438	5.543	0.423	3.029	0.307	0.053	0.252	0.243	3178.90966	0.403	3178.90358	
1.437	7.569	23.260	1.734	2.236	5.583	0.371	3.595	0.295	0.049	-0.204	0.482	3178.91159	0.389	3178.90430	
1.310	7.669	24.101	0.867	2.335	6.089	0.384	3.247	0.304	0.050	0.328	0.267	3178.91353	0.381	3178.90502	
1.385	7.841	24.341	0.877	2.288	5.770	0.397	3.151	0.292	0.051	0.033	0.278	3178.91546	0.379	3178.90573	
1.218	7.775	24.300	0.960	2.283	5.834	0.366	3.312	0.294	0.047	0.199	0.290	3178.91739	0.381	3178.90645	
1.551	7.602	24.807	0.990	2.325	5.085	0.371	3.360	0.306	0.049	1.240	0.295	3178.91932	0.386	3178.90717	
1.411	7.263	23.698	1.103	2.067	6.412	0.366	3.491	0.285	0.050	1.184	0.316	3178.92125	0.391	3178.90788	
1.332	7.057	23.468	1.049	2.044	6.878	0.401	3.469	0.290	0.057	1.591	0.303	3178.92319	0.392	3178.90860	
1.354	7.146	23.427	1.059	2.030	6.826	0.392	3.526	0.284	0.055	1.274	0.300	3178.92512	0.390	3178.90932	
1.595	6.962	22.898	1.066	2.030	7.133	0.340	3.574	0.291	0.049	1.314	0.298	3178.92705	0.388	3178.91003	
1.551	6.890	22.590	1.335	2.044	6.882	0.384	3.779	0.297	0.056	1.231	0.353	3178.92898	0.381	3178.91075	
1.170	6.668	22.341	1.890	1.931	6.790	0.384	4.258	0.290	0.058	1.671	0.444	3178.93092	0.372	3178.91147	
1.096	6.885	22.355	1.937	1.959	6.667	0.358	4.175	0.285	0.052	1.013	0.464	3178.93285	0.364	3178.91218	
1.350	5.750	18.382	3.605	1.541	7.970	0.267	5.462	0.268	0.046	0.558	0.660	3178.93478	0.359	3178.91290	
1.407	6.690	21.739	2.179	1.912	6.834	0.327	4.097	0.286	0.049	1.001	0.532	3178.93671	0.359	3178.91362	
1.319	7.808	24.866	0.720	2.349	5.643	0.410	3.068	0.301	0.052	0.661	0.235	3178.93865	0.364	3178.91433	
1.280	7.724	24.531	1.395	2.391	4.997	0.366	3.356	0.310	0.047	0.585	0.416	3178.94058	0.363	3178.91505	
1.385	7.563	24.825	0.774	2.302	5.814	0.418	3.042	0.304	0.055	1.379	0.254	3178.94251	0.366	3178.91577	
1.271	7.680	24.499	0.963	2.264	5.750	0.362	3.199	0.295	0.047	0.691	0.301	3178.94444	0.373	3178.91648	
1.337	7.597	24.011	1.063	2.325	5.838	0.388	3.277	0.306	0.051	0.461	0.324	3178.94637	0.380	3178.91720	
1.367	7.441	23.296	1.468	2.236	5.953	0.379	3.604	0.301	0.051	0.229	0.407	3178.94831	0.384	3178.91792	
1.324	7.324	22.472	2.050	2.123	5.870	0.366	4.005	0.290	0.050	-0.232	0.512	3178.95024	0.385	3178.91863	
1.315	7.847	24.214	0.917	2.288	5.830	0.384	3.242	0.292	0.049	-0.111	0.283	3178.95217	0.385	3178.91935	
1.302	7.763	24.237	0.917	2.349	5.902	0.392	3.181	0.303	0.051	0.170	0.288	3178.95410	0.386	3178.92007	
1.402	8.103	24.563	0.747	2.504	5.403	0.457	3.016	0.309	0.056	-0.556	0.248	3178.95604	0.394	3178.92078	
1.380	8.069	25.246	0.770	2.443	4.961	0.414	3.024	0.303	0.051	0.231	0.255	3178.95797	0.404	3178.92150	
1.328	7.747	24.635	0.807	2.344	5.682	0.444	3.164	0.303	0.057	0.620	0.255	3178.95990	0.412	3178.92222	
1.245	7.813	23.907	1.142	2.358	5.639	0.431	3.438	0.302	0.055	-0.315	0.332	3178.96190	0.419	3178.92293	
1.210	7.730	23.974	1.162	2.344	5.666	0.427	3.452	0.303	0.055	0.011	0.337	3178.96309	0.425	3178.92365	
1.183	7.813	24.169	1.056	2.396	5.583	0.392	3.369	0.307	0.050	-0.053	0.313	3178.96429	0.431	3178.92437	
1.424	7.658	24.033	1.029	2.269	5.762	0.410	3.391	0.296	0.054	0.294	0.304	3178.96548	0.432	3178.92508	
1.565	7.207	23.309	1.202	2.147	6.487	0.405	3.482	0.298	0.056	0.967	0.345	3178.96668	0.427	3178.92580	
1.332	7.224	22.671	1.445	2.086	6.647	0.375	3.831	0.289	0.052	0.277	0.377	3178.96787	0.418	3178.92652	
1.363	7.246	23.395	1.219	2.138	6.543	0.405	3.556	0.295	0.056	0.932	0.343	3178.96906	0.406	3178.92723	
1.424	7.024	22.834	1.269	1.997	7.117	0.375	3.670	0.284	0.053	1.061	0.346	3178.97026	0.395	3178.92795	
1.367	6.356	21.052	2.502	1.748	7.288	0.327	4.441	0.275	0.051	1.348	0.563	3178.97145	0.396	3178.92867	
1.332	6.601	21.988	1.993	1.940	6.846	0.323	4.267	0.294	0.049	1.525	0.467	3178.97265	0.405	3178.92938	
1.293	6.111	20.920	2.681	1.691	7.328	0.323	4.655	0.277	0.053	1.975	0.576	3178.97384	0.413	3178.93010	
1.179	6.178	20.780	2.492	1.715	7.639	0.345	4.707	0.278	0.056	1.628	0.529	3178.97503	0.414	3178.93082	
1.630	6.345	20.676	2.282	1.691	7.467	0.327	4.681	0.267	0.052	1.006	0.488	3178.97623	0.406	3178.93153	
1.429	6.479	21.694	1.771	1.846	7.551	0.336	4.228	0.285	0.052	1.611	0.419	3178.97742	0.393	3178.93225	
1.319	6.762	22.029	1.578	1.884	7.312	0.327	4.145	0.279	0.048	1.066	0.381	3178.97862	0.383	3178.93297	
1.359	6.640	22.214	1.624	1.922	7.320	0.349	4.001	0.289	0.053	1.631	0.406	3178.97981	0.378	3178.93368	
1.240	7.051	23.083	1.309	1.992	6.922	0.371	3.683	0.282	0.053	1.224	0.355	3178.98100	0.379	3178.93440	
													0.381	3178.93512	
													0.380	3178.93583	
													0.376	3178.93655	
													0.374	3178.93727	
													0.377	3178.93798	
													0.386	3178.93870	
													0.403	3178.93942	
													0.409	3178.94007	
													0.406	3178.94071	
													0.398	3178.94136	
													0.391	3178.94201	
													0.386	3178.94266	

EDXRF											Hyperspectral Imagery			
Mg %	Al %	Si %	S %	K %	Ca %	Ti %	Fe %	K/Al	Ti/Al	Si bio %	S/Fe	Depth m	TOC %	Depth m
													0.385	3178.94331
													0.372	3178.94395
													0.367	3178.94460
													0.359	3178.94525
													0.354	3178.94590
													0.351	3178.94655
													0.350	3178.94719
													0.349	3178.94784
													0.351	3178.94849
													0.357	3178.94914
													0.363	3178.94979
													0.371	3178.95044
													0.375	3178.95108
													0.375	3178.95173
													0.377	3178.95238
													0.380	3178.95303
													0.382	3178.95368
													0.383	3178.95432
													0.382	3178.95497
													0.383	3178.95562
													0.384	3178.95627
													0.381	3178.95692
													0.372	3178.95757
													0.364	3178.95821
													0.338	3178.95886
													0.310	3178.95951
													0.361	3178.96016
													0.363	3178.96081
													0.371	3178.96145
													0.382	3178.96210
													0.385	3178.96275
													0.379	3178.96340
													0.367	3178.96405
													0.358	3178.96469
													0.365	3178.96534
													0.373	3178.96599
													0.381	3178.96664
													0.382	3178.96729
													0.377	3178.96794
													0.372	3178.96858
													0.372	3178.96923
													0.375	3178.96988
													0.378	3178.97053
													0.382	3178.97118
													0.382	3178.97182
													0.382	3178.97247
													0.383	3178.97312
													0.379	3178.97377
													0.379	3178.97442
													0.376	3178.97507
													0.374	3178.97571
													0.371	3178.97636
													0.368	3178.97701
													0.365	3178.97766
													0.361	3178.97831
													0.353	3178.97895
													0.356	3178.97960
													0.358	3178.98025
													0.364	3178.98090

Slab 3179.45 m

EDXRF													Hyperspectral Imagery		
Mg %	Al %	Si %	S %	K %	Ca %	Ti %	Fe %	K/Al	Ti/Al	Si bio %	S/Fe	Depth m	TOC %	Depth m	
1.420	6.918	22.649	1.362	1.922	7.232	0.349	3.709	0.278	0.050	1.203	0.367	3179.45634	0.391	3179.45508	
1.394	6.762	22.581	1.365	1.846	7.491	0.332	3.748	0.273	0.049	1.618	0.364	3179.45792	0.398	3179.45584	
1.451	6.684	22.341	1.707	1.879	7.117	0.323	3.940	0.281	0.048	1.620	0.433	3179.45950	0.403	3179.45660	
1.284	6.634	22.590	1.697	1.875	7.113	0.345	3.874	0.283	0.052	2.024	0.438	3179.46109	0.407	3179.45737	
1.376	6.873	22.993	1.275	1.907	7.272	0.358	3.574	0.278	0.052	1.685	0.357	3179.46267	0.408	3179.45813	
1.359	7.046	23.264	1.043	1.997	7.204	0.349	3.460	0.283	0.050	1.422	0.301	3179.46426	0.408	3179.45889	
1.556	6.595	21.676	1.528	1.771	7.806	0.323	4.123	0.269	0.049	1.230	0.371	3179.46584	0.408	3179.45966	
1.411	6.840	21.776	1.538	1.828	7.651	0.345	4.092	0.267	0.050	0.571	0.376	3179.46742	0.411	3179.46042	
1.468	6.768	21.599	1.897	1.842	7.276	0.345	4.193	0.272	0.051	0.619	0.452	3179.46901	0.417	3179.46118	
1.271	7.224	22.717	1.508	2.044	6.794	0.366	3.787	0.283	0.051	0.323	0.398	3179.47059	0.419	3179.46195	
1.205	7.202	22.735	1.634	2.095	6.503	0.353	3.892	0.291	0.049	0.410	0.420	3179.47218	0.415	3179.46271	
1.332	7.491	23.404	1.066	2.222	6.623	0.392	3.386	0.297	0.052	0.183	0.315	3179.47376	0.407	3179.46347	
1.354	7.341	23.318	1.083	2.123	6.758	0.388	3.438	0.289	0.053	0.562	0.315	3179.47534	0.398	3179.46424	
1.293	7.229	22.178	1.950	2.039	6.555	0.358	3.944	0.282	0.049	-0.233	0.494	3179.47693	0.388	3179.46500	
1.253	7.736	24.056	0.887	2.325	6.220	0.401	3.177	0.301	0.052	0.076	0.279	3179.47851	0.373	3179.46576	
1.350	7.936	24.671	0.704	2.476	5.730	0.379	2.976	0.312	0.048	0.070	0.236	3179.48010	0.358	3179.46653	
1.319	8.047	24.703	0.780	2.541	5.515	0.397	2.963	0.316	0.049	-0.243	0.263	3179.48168	0.346	3179.46729	
1.376	6.907	22.486	1.674	1.950	6.874	0.349	3.652	0.282	0.051	1.075	0.458	3179.48326	0.342	3179.46805	
1.271	4.415	16.541	5.389	1.081	7.862	0.241	6.129	0.245	0.054	2.854	0.879	3179.48485	0.342	3179.46882	
1.267	6.712	22.658	1.654	1.945	7.085	0.362	3.792	0.290	0.054	1.850	0.436	3179.48643	0.344	3179.46958	
1.354	6.962	23.101	1.415	2.053	6.870	0.358	3.539	0.295	0.051	1.518	0.400	3179.48802	0.345	3179.47034	
1.319	7.213	23.748	0.917	2.166	6.850	0.366	3.207	0.300	0.051	1.389	0.286	3179.48960	0.347	3179.47111	
1.394	6.829	22.984	1.226	1.903	7.479	0.358	3.482	0.279	0.052	1.814	0.352	3179.49118	0.349	3179.47187	
1.455	6.723	22.739	1.372	1.912	7.312	0.371	3.648	0.284	0.055	1.897	0.376	3179.49277	0.348	3179.47263	
1.455	6.306	21.156	2.196	1.762	7.579	0.310	4.315	0.279	0.049	1.607	0.509	3179.49435	0.345	3179.47340	
1.380	6.645	21.807	1.864	1.799	7.487	0.314	3.983	0.271	0.047	1.206	0.468	3179.49594	0.341	3179.47416	
1.354	6.818	22.680	1.481	1.954	7.260	0.392	3.665	0.287	0.058	1.545	0.404	3179.49752	0.336	3179.47492	
1.354	7.135	23.332	1.066	2.109	7.053	0.379	3.408	0.296	0.053	1.214	0.313	3179.49910	0.334	3179.47569	
1.359	7.563	23.626	1.222	2.264	6.308	0.405	3.268	0.299	0.054	0.180	0.374	3179.50069	0.333	3179.47645	
1.389	7.519	23.993	0.900	2.339	6.340	0.384	3.142	0.311	0.051	0.685	0.286	3179.50227	0.334	3179.47721	
1.341	7.335	23.554	1.059	2.199	6.559	0.388	3.421	0.300	0.053	0.815	0.310	3179.50386	0.338	3179.47798	
1.543	7.202	22.463	1.442	2.025	6.734	0.345	3.853	0.281	0.048	0.138	0.374	3179.50544	0.342	3179.47874	
1.477	6.885	21.952	1.601	1.936	7.260	0.349	4.066	0.281	0.051	0.610	0.394	3179.50702	0.346	3179.47950	
1.565	7.107	22.468	1.435	2.067	6.910	0.362	3.800	0.291	0.051	0.436	0.378	3179.50861	0.347	3179.48027	
1.275	7.285	23.029	1.771	2.147	6.049	0.397	3.809	0.295	0.054	0.445	0.465	3179.51019	0.346	3179.48103	
1.350	7.268	22.662	1.960	2.109	6.049	0.392	3.901	0.290	0.054	0.130	0.502	3179.51178	0.348	3179.48179	
1.433	7.229	22.902	1.518	2.048	6.463	0.371	3.678	0.283	0.051	0.491	0.413	3179.51336	0.358	3179.48256	
1.350	7.508	23.260	1.452	2.264	6.117	0.375	3.521	0.302	0.050	-0.014	0.412	3179.51494	0.376	3179.48332	
1.389	7.457	23.377	1.329	2.297	6.188	0.405	3.465	0.308	0.054	0.259	0.383	3179.51653	0.398	3179.48409	
1.372	7.752	23.762	1.003	2.405	5.937	0.410	3.321	0.310	0.053	-0.270	0.302	3179.51811	0.416	3179.48485	
1.218	7.457	23.246	1.408	2.260	6.165	0.384	3.683	0.303	0.051	0.128	0.382	3179.51970	0.422	3179.48561	
1.437	7.819	23.974	0.986	2.396	5.957	0.366	3.116	0.306	0.047	-0.265	0.317	3179.52128	0.416	3179.48638	
1.240	7.635	24.287	1.033	2.339	5.953	0.375	3.173	0.306	0.049	0.617	0.326	3179.52286	0.405	3179.48714	
1.310	7.752	24.133	1.079	2.311	5.838	0.423	3.242	0.298	0.055	0.101	0.333	3179.52445	0.395	3179.48790	
1.297	8.003	24.635	0.857	2.480	5.575	0.418	2.972	0.310	0.052	-0.173	0.288	3179.52603	0.388	3179.48867	
1.170	8.108	24.929	0.797	2.546	5.344	0.418	2.946	0.314	0.052	-0.207	0.271	3179.52762	0.383	3179.48943	
1.288	7.775	24.250	1.408	2.396	5.308	0.392	3.238	0.308	0.050	0.149	0.435	3179.52920	0.384	3179.49019	
1.512	7.797	24.789	0.850	2.396	5.391	0.375	3.042	0.307	0.048	0.619	0.279	3179.53078	0.388	3179.49096	
1.376	7.196	23.481	1.405	2.105	6.125	0.345	3.674	0.292	0.048	1.174	0.382	3179.53237	0.392	3179.49172	
1.262	7.018	23.260	1.601	2.015	6.519	0.336	3.582	0.287	0.048	1.504	0.447	3179.53395	0.393	3179.49248	
1.332	7.063	23.305	1.458	2.123	6.543	0.358	3.465	0.301	0.051	1.411	0.421	3179.53554	0.392	3179.49325	
1.324	7.090	23.174	1.402	2.086	6.702	0.371	3.513	0.294	0.052	1.193	0.399	3179.53712	0.389	3179.49401	
1.363	7.496	23.852	1.043	2.231	6.352	0.384	3.212	0.298	0.051	0.613	0.325	3179.53870	0.386	3179.49477	
1.341	7.635	24.300	0.867	2.255	6.200	0.384	3.024	0.295	0.050	0.630	0.287	3179.54029	0.385	3179.49554	
1.148	7.930	25.228	0.694	2.485	5.595	0.423	2.798	0.313	0.053	0.644	0.248	3179.54187	0.384	3179.49630	
1.284	8.008	25.535	0.614	2.490	5.188	0.401	2.828	0.311	0.050	0.710	0.217	3179.54346	0.382	3179.49706	
1.319	7.413	24.092	0.764	2.222	6.615	0.379	3.138	0.300	0.051	1.112	0.243	3179.54504	0.383	3179.49783	
1.512	7.074	23.047	1.116	2.020	7.288	0.353	3.316	0.286	0.050	1.119	0.336	3179.54662	0.383	3179.49859	
1.148	5.155	18.445	4.236	1.396	7.854	0.236	5.597	0.271	0.046	2.466	0.757	3179.54821	0.379	3179.49935	
1.236	5.906	20.350	3.096	1.583	7.687	0.284	4.629	0.268	0.048	2.043	0.669	3179.54980	0.374	3179.50012	
													0.370	3179.50088	

EDXRF												Hyperspectral Imagery		
Mg	Al	Si	S	K	Ca	Ti	Fe	K/Al	Ti/Al	Si bio	S/Fe	Depth	TOC	Depth
%	%	%	%	%	%	%	%			%		m	%	m
													0.367	3179.50164
													0.364	3179.50241
													0.360	3179.50317
													0.353	3179.50393
													0.344	3179.50470
													0.339	3179.50546
													0.337	3179.50622
													0.340	3179.50699
													0.346	3179.50775
													0.353	3179.50851
													0.355	3179.50928
													0.351	3179.51004
													0.347	3179.51080
													0.344	3179.51157
													0.343	3179.51233
													0.339	3179.51309
													0.333	3179.51386
													0.328	3179.51462
													0.327	3179.51538
													0.329	3179.51615
													0.332	3179.51691
													0.335	3179.51767
													0.333	3179.51844
													0.334	3179.51920
													0.328	3179.51996
													0.333	3179.52073
													0.338	3179.52149
													0.341	3179.52225
													0.340	3179.52302
													0.338	3179.52378
													0.339	3179.52454
													0.341	3179.52531
													0.347	3179.52607
													0.352	3179.52683
													0.352	3179.52760
													0.348	3179.52836
													0.343	3179.52912
													0.344	3179.52989
													0.353	3179.53065
													0.363	3179.53141
													0.370	3179.53218
													0.373	3179.53294
													0.374	3179.53370
													0.372	3179.53447
													0.368	3179.53523
													0.362	3179.53599
													0.360	3179.53676
													0.361	3179.53752
													0.361	3179.53828
													0.358	3179.53905
													0.356	3179.53981
													0.357	3179.54057
													0.362	3179.54134
													0.369	3179.54210
													0.373	3179.54286
													0.383	3179.54363
													0.394	3179.54439
													0.397	3179.54515
													0.389	3179.54592
													0.373	3179.54668
													0.357	3179.54744

EDXRF												Hyperspectral Imagery		
Mg %	Al %	Si %	S %	K %	Ca %	Ti %	Fe %	K/Al	Ti/Al	Si bio %	S/Fe	Depth m	TOC %	Depth m
													0.356	3179.54821
													0.366	3179.54897
													0.385	3179.54973

EDXRF											Hyperspectral Imagery			
Mg	Al	Si	S	K	Ca	Ti	Fe	K/Al	Ti/Al	Si bio	S/Fe	Depth	TOC	Depth
%	%	%	%	%	%	%	%			%		m	%	m
													0.402	3180.50342
													0.408	3180.50427
													0.418	3180.50513
													0.424	3180.50598
													0.408	3180.50684
													0.406	3180.50769
													0.406	3180.50854
													0.410	3180.50940
													0.412	3180.51025
													0.407	3180.51110
													0.398	3180.51196
													0.390	3180.51281
													0.387	3180.51367
													0.389	3180.51452
													0.398	3180.51537
													0.407	3180.51623
													0.411	3180.51708
													0.408	3180.51794
													0.402	3180.51879
													0.396	3180.51964
													0.393	3180.52050
													0.390	3180.52135
													0.388	3180.52221
													0.387	3180.52306
													0.387	3180.52391
													0.389	3180.52477
													0.393	3180.52562
													0.399	3180.52648
													0.399	3180.52733
													0.395	3180.52818
													0.387	3180.52904
													0.380	3180.52989
													0.375	3180.53075
													0.376	3180.53160
													0.383	3180.53245
													0.392	3180.53331
													0.394	3180.53416
													0.392	3180.53502
													0.387	3180.53587
													0.383	3180.53672
													0.383	3180.53758
													0.380	3180.53843
													0.376	3180.53929
													0.372	3180.54014
													0.371	3180.54099
													0.371	3180.54185
													0.370	3180.54270
													0.367	3180.54356
													0.362	3180.54441
													0.360	3180.54526
													0.359	3180.54612
													0.360	3180.54697
													0.358	3180.54783
													0.354	3180.54868
													0.349	3180.54953
													0.347	3180.55039
													0.348	3180.55124
													0.351	3180.55210
													0.350	3180.55295
													0.352	3180.55380
													0.349	3180.55466
													0.347	3180.55551

EDXRF												Hyperspectral Imagery		
Mg	Al	Si	S	K	Ca	Ti	Fe	K/Al	Ti/Al	Si bio	S/Fe	Depth	TOC	Depth
%	%	%	%	%	%	%	%			%		m	%	m
													0.353	3180.55722
													0.356	3180.55807
													0.359	3180.55893
													0.363	3180.55978
													0.368	3180.56064

Slab 3181.18 m

EDXRF												Hyperspectral Imagery			
Mg %	Al %	Si %	S %	K %	Ca %	Ti %	Fe %	K/Al	Ti/Al	Si bio %	S/Fe	Depth m	TOC %	Depth m	
0.903	8.492	28.508	1.113	3.030	1.925	0.475	2.357	0.357	0.056	2.183	0.472	3181.18000	0.302	3181.17800	
0.855	8.798	28.314	1.129	3.016	1.881	0.379	2.353	0.343	0.043	1.040	0.480	3181.18148	0.312	3181.17888	
0.999	8.598	27.893	1.465	2.884	2.017	0.392	2.497	0.335	0.046	1.240	0.587	3181.18297	0.315	3181.17976	
0.920	8.375	27.056	1.867	2.790	2.299	0.375	2.758	0.333	0.045	1.092	0.677	3181.18445	0.311	3181.18064	
0.969	8.525	26.535	2.066	2.776	2.268	0.375	2.867	0.326	0.044	0.106	0.721	3181.18594	0.314	3181.18152	
0.903	8.442	27.305	1.900	2.828	2.068	0.397	2.745	0.335	0.047	1.134	0.692	3181.18742	0.315	3181.18241	
1.017	8.342	27.517	1.531	2.739	2.367	0.405	2.658	0.328	0.049	1.657	0.576	3181.18890	0.319	3181.18329	
1.091	8.425	27.703	1.498	2.753	2.224	0.397	2.584	0.327	0.047	1.584	0.580	3181.19039	0.324	3181.18417	
0.916	8.637	28.277	1.312	2.818	1.921	0.375	2.427	0.326	0.043	1.504	0.541	3181.19187	0.329	3181.18505	
0.877	7.880	26.843	1.977	2.668	2.865	0.388	2.832	0.339	0.049	2.414	0.698	3181.19336	0.333	3181.18594	
0.828	8.726	28.074	1.551	2.992	1.694	0.397	2.532	0.343	0.045	1.024	0.613	3181.19484	0.335	3181.18682	
0.877	8.703	28.499	1.501	3.006	1.383	0.358	2.475	0.345	0.041	1.518	0.607	3181.19632	0.343	3181.18770	
0.872	8.915	29.146	1.123	3.124	1.263	0.362	2.170	0.350	0.041	1.510	0.517	3181.19781	0.341	3181.18858	
0.991	8.948	29.209	0.930	3.114	1.375	0.401	2.082	0.348	0.045	1.470	0.446	3181.19929	0.344	3181.18947	
0.929	8.820	28.590	0.870	3.030	2.192	0.436	2.100	0.343	0.049	1.247	0.414	3181.20077	0.358	3181.19035	
0.991	8.464	27.404	2.126	2.804	1.534	0.362	2.754	0.331	0.043	1.165	0.772	3181.20226	0.371	3181.19123	
0.837	8.425	27.210	1.857	2.875	2.236	0.371	2.649	0.341	0.044	1.091	0.701	3181.20374	0.382	3181.19211	
0.855	8.893	29.164	0.823	3.152	1.610	0.397	2.109	0.354	0.045	1.597	0.391	3181.20523	0.382	3181.19299	
0.912	8.809	28.056	0.747	3.011	2.801	0.427	2.122	0.342	0.048	0.747	0.352	3181.20671	0.391	3181.19388	
0.929	8.898	28.897	0.823	3.039	1.845	0.397	2.117	0.342	0.045	1.313	0.389	3181.20819	0.386	3181.19476	
0.811	9.059	29.182	0.867	3.044	1.542	0.397	2.122	0.336	0.044	1.098	0.408	3181.20968	0.378	3181.19564	
0.798	8.920	29.223	0.923	3.142	1.506	0.418	2.113	0.352	0.047	1.570	0.437	3181.21116	0.361	3181.19652	
1.004	8.854	28.861	0.966	3.063	1.630	0.410	2.161	0.346	0.046	1.415	0.447	3181.21265	0.358	3181.19741	
0.868	8.197	26.210	2.103	2.602	2.937	0.379	2.941	0.317	0.046	0.798	0.715	3181.21413	0.372	3181.19829	
0.736	7.385	23.033	3.701	2.274	3.841	0.332	4.058	0.308	0.045	0.139	0.912	3181.21561	0.362	3181.19917	
0.890	7.318	22.273	4.662	2.264	3.009	0.327	4.467	0.309	0.045	-0.414	1.043	3181.21710	0.370	3181.20005	
0.750	6.879	20.862	5.512	2.156	3.232	0.319	5.030	0.313	0.046	-0.463	1.096	3181.21858	0.434	3181.20094	
0.868	7.630	22.880	4.017	2.396	3.156	0.349	4.123	0.314	0.046	-0.773	0.974	3181.22006	0.410	3181.20182	
0.855	8.798	27.191	1.677	2.809	2.144	0.379	2.710	0.319	0.043	-0.082	0.619	3181.22155	0.396	3181.20270	
0.995	8.436	27.504	0.843	2.762	3.268	0.366	2.353	0.327	0.043	1.351	0.358	3181.22303	0.374	3181.20358	
0.942	8.715	27.893	1.039	2.823	2.419	0.405	2.431	0.324	0.047	0.878	0.428	3181.22452	0.367	3181.20446	
1.030	8.253	26.002	1.212	2.560	4.160	0.414	2.636	0.310	0.050	0.417	0.460	3181.22600	0.367	3181.20535	
0.969	8.737	27.888	1.063	2.978	2.256	0.427	2.471	0.341	0.049	0.804	0.430	3181.22800	0.369	3181.20623	
0.929	8.475	28.029	1.103	3.020	2.252	0.410	2.475	0.356	0.048	1.755	0.446	3181.23005	0.370	3181.20711	
1.012	8.220	26.468	1.810	2.649	2.909	0.384	2.872	0.322	0.047	0.987	0.630	3181.23209	0.371	3181.20799	
0.920	8.242	27.078	1.930	2.668	2.355	0.384	2.819	0.324	0.047	1.529	0.685	3181.23414	0.370	3181.20888	
0.820	8.442	27.477	1.664	2.856	2.176	0.392	2.719	0.338	0.046	1.306	0.612	3181.23619	0.386	3181.20976	
0.951	8.659	27.992	1.372	2.936	1.921	0.410	2.505	0.339	0.047	1.150	0.548	3181.23824	0.396	3181.21064	
0.925	8.498	27.572	1.309	2.847	2.511	0.410	2.510	0.335	0.048	1.229	0.521	3181.24028	0.388	3181.21152	
0.802	8.409	28.133	0.857	2.940	2.933	0.414	2.178	0.350	0.049	2.066	0.393	3181.24233	0.393	3181.21240	
1.034	8.620	28.644	0.960	2.964	2.040	0.414	2.157	0.344	0.048	1.922	0.445	3181.24438	0.386	3181.21329	
0.863	8.709	28.703	0.986	3.105	1.913	0.453	2.165	0.357	0.052	1.705	0.455	3181.24642	0.397	3181.21417	
0.798	8.898	29.237	0.970	3.175	1.379	0.444	2.087	0.357	0.050	1.652	0.465	3181.24847	0.395	3181.21505	
0.877	8.687	29.395	0.960	3.030	1.578	0.405	2.043	0.349	0.047	2.466	0.470	3181.25052	0.394	3181.21593	
0.750	8.030	25.187	3.927	2.574	1.367	0.327	3.648	0.321	0.041	0.293	1.077	3181.25256	0.408	3181.21682	
0.925	8.598	27.264	2.056	2.847	1.690	0.414	2.832	0.331	0.048	0.611	0.726	3181.25461	0.412	3181.21770	
0.793	8.420	27.160	1.648	2.710	2.554	0.405	2.767	0.322	0.048	1.058	0.595	3181.25666	0.415	3181.21858	
0.938	8.576	27.603	1.797	2.926	1.694	0.401	2.723	0.341	0.047	1.019	0.660	3181.25870	0.409	3181.21943	
													0.403	3181.22028	
													0.408	3181.22113	
													0.411	3181.22198	
													0.406	3181.22283	
													0.398	3181.22368	
													0.390	3181.22453	
													0.378	3181.22538	
													0.374	3181.22623	
													0.379	3181.22708	
													0.393	3181.22793	
													0.400	3181.22878	
													0.426	3181.22963	
													0.426	3181.23047	

EDXRF												Hyperspectral Imagery		
Mg	Al	Si	S	K	Ca	Ti	Fe	K/Al	Ti/Al	Si bio	S/Fe	Depth	TOC	Depth
%	%	%	%	%	%	%	%			%		m	%	m
													0.414	3181.23132
													0.404	3181.23217
													0.388	3181.23302
													0.384	3181.23387
													0.387	3181.23472
													0.397	3181.23557
													0.421	3181.23642
													0.421	3181.23727
													0.418	3181.23812
													0.427	3181.23897
													0.401	3181.23982
													0.400	3181.24067
													0.398	3181.24152
													0.420	3181.24237
													0.386	3181.24322
													0.401	3181.24407
													0.394	3181.24492
													0.399	3181.24577
													0.453	3181.24662
													0.457	3181.24747
													0.418	3181.24832
													0.378	3181.24916
													0.323	3181.25001
													0.365	3181.25086
													0.343	3181.25171
													0.355	3181.25256
													0.372	3181.25341
													0.346	3181.25426
													0.393	3181.25511
													0.381	3181.25596
													0.424	3181.25681
													0.467	3181.25766
													0.445	3181.25851
													0.414	3181.25936
													0.412	3181.26021
													0.414	3181.26106

EDXRF												Hyperspectral Imagery			
Mg %	Al %	Si %	S %	K %	Ca %	Ti %	Fe %	K/Al	Ti/Al	Si bio %	S/Fe	Depth m	TOC %	Depth m	
1.258	6.668	22.590	1.883	2.048	7.077	0.371	3.517	0.307	0.056	1.920	0.536	3182.90710	0.456	3182.88202	
													0.462	3182.88273	
													0.464	3182.88343	
													0.477	3182.88414	
													0.478	3182.88484	
													0.476	3182.88554	
													0.475	3182.88625	
													0.473	3182.88695	
													0.464	3182.88766	
													0.457	3182.88836	
													0.460	3182.88907	
													0.461	3182.88977	
													0.459	3182.89048	
													0.466	3182.89118	
													0.472	3182.89189	
													0.475	3182.89259	
													0.474	3182.89330	
													0.472	3182.89400	
													0.471	3182.89471	
													0.468	3182.89541	
													0.465	3182.89612	
													0.459	3182.89682	
													0.453	3182.89753	
													0.450	3182.89823	
													0.451	3182.89894	
													0.455	3182.89964	
													0.456	3182.90035	
													0.462	3182.90105	
													0.462	3182.90176	
													0.466	3182.90246	
													0.469	3182.90316	
													0.469	3182.90387	
													0.459	3182.90457	
													0.447	3182.90528	
													0.440	3182.90598	
													0.442	3182.90669	
													0.448	3182.90739	

EDXRF												Hyperspectral Imagery		
Mg %	Al %	Si %	S %	K %	Ca %	Ti %	Fe %	K/Al	Ti/Al	Si bio %	S/Fe	Depth m	TOC %	Depth m
0.881	7.357	27.522	1.481	2.339	3.841	0.340	2.418	0.318	0.046	4.714	0.613	3183.81545	0.599	3183.79697
0.820	7.152	27.906	1.418	2.339	3.834	0.340	2.340	0.327	0.048	5.737	0.606	3183.81653	0.560	3183.79779
0.885	7.279	27.477	1.202	2.405	3.312	0.362	3.369	0.330	0.050	4.910	0.357	3183.81760	0.533	3183.79862
													0.509	3183.79945
													0.501	3183.80028
													0.492	3183.80111
													0.524	3183.80193
													0.521	3183.80276
													0.547	3183.80359
													0.555	3183.80442
													0.546	3183.80524
													0.555	3183.80607
													0.532	3183.80690
													0.536	3183.80773
													0.531	3183.80856
													0.515	3183.80938
													0.522	3183.81021
													0.507	3183.81104
													0.513	3183.81187
													0.530	3183.81269
													0.524	3183.81352
													0.542	3183.81435
													0.563	3183.81518
													0.578	3183.81601
													0.590	3183.81683
													0.600	3183.81766

EDXRF												Hyperspectral Imagery			
Mg %	Al %	Si %	S %	K %	Ca %	Ti %	Fe %	K/Al	Ti/Al	Si bio %	S/Fe	Depth m	TOC %	Depth m	
0.863	6.095	22.916	3.588	1.809	5.113	0.262	4.372	0.297	0.043	4.022	0.821	3184.77513	0.555	3184.74180	
0.938	6.573	24.567	3.017	2.015	4.312	0.284	3.726	0.307	0.043	4.191	0.810	3184.77637	0.526	3184.74251	
0.938	7.168	27.160	1.830	2.302	3.622	0.349	2.715	0.321	0.049	4.938	0.674	3184.77760	0.540	3184.74322	
0.947	6.606	23.920	2.990	2.114	4.614	0.310	3.883	0.320	0.047	3.440	0.770	3184.77960	0.549	3184.74393	
0.960	6.473	24.011	2.987	2.091	4.591	0.293	3.896	0.323	0.045	3.945	0.767	3184.78068	0.575	3184.74464	
0.859	6.879	26.187	2.179	2.180	4.308	0.306	2.915	0.317	0.044	4.862	0.748	3184.78175	0.573	3184.74535	
0.999	7.013	27.413	1.309	2.236	4.308	0.349	2.475	0.319	0.050	5.674	0.529	3184.78283	0.558	3184.74606	
0.802	6.957	26.685	1.275	2.189	5.204	0.327	2.562	0.315	0.047	5.118	0.498	3184.78391	0.531	3184.74677	
0.855	6.962	26.653	1.222	2.166	5.288	0.323	2.532	0.311	0.046	5.070	0.483	3184.78499	0.521	3184.74748	
0.973	7.168	27.748	1.096	2.349	4.272	0.353	2.300	0.328	0.049	5.526	0.476	3184.78606	0.519	3184.74819	
0.916	6.924	26.970	1.222	2.222	4.921	0.345	2.558	0.321	0.050	5.507	0.478	3184.78714	0.539	3184.74889	
0.916	6.968	27.472	1.196	2.260	4.559	0.353	2.436	0.324	0.051	5.871	0.491	3184.78822	0.527	3184.74960	
0.920	7.101	28.341	1.003	2.391	4.025	0.388	2.196	0.337	0.055	6.326	0.457	3184.78929	0.539	3184.75031	
0.894	7.090	27.997	1.093	2.302	4.232	0.349	2.314	0.325	0.049	6.017	0.472	3184.79037	0.555	3184.75102	
0.859	7.174	28.282	0.996	2.438	3.997	0.319	2.239	0.340	0.044	6.043	0.445	3184.79145	0.552	3184.75173	
0.899	6.873	27.020	1.299	2.264	4.778	0.336	2.532	0.329	0.049	5.712	0.513	3184.79252	0.561	3184.75244	
0.960	6.840	26.630	1.382	2.156	5.061	0.319	2.588	0.315	0.047	5.426	0.534	3184.79360	0.529	3184.75315	
0.920	6.946	27.246	1.269	2.208	4.718	0.306	2.449	0.318	0.044	5.714	0.518	3184.79468	0.533	3184.75386	
1.021	6.890	26.893	1.279	2.189	4.893	0.323	2.558	0.318	0.047	5.533	0.500	3184.79576	0.525	3184.75457	
0.899	6.990	26.979	1.378	2.236	4.694	0.319	2.566	0.320	0.046	5.309	0.537	3184.79683	0.493	3184.75528	
1.148	6.746	26.314	1.495	2.166	5.045	0.332	2.684	0.321	0.049	5.403	0.557	3184.79791	0.504	3184.75599	
0.916	6.996	26.988	1.352	2.241	4.718	0.345	2.518	0.320	0.049	5.301	0.537	3184.79899	0.490	3184.75670	
0.916	7.057	27.567	1.179	2.316	4.391	0.371	2.414	0.328	0.053	5.690	0.488	3184.80006	0.527	3184.75740	
0.912	7.029	27.594	1.089	2.288	4.563	0.345	2.366	0.325	0.049	5.804	0.460	3184.80114	0.585	3184.75811	
0.951	7.152	27.599	1.096	2.335	4.391	0.353	2.348	0.326	0.049	5.429	0.467	3184.80222	0.524	3184.75882	
0.837	7.324	28.562	1.049	2.424	3.650	0.353	2.191	0.331	0.048	5.858	0.479	3184.80329	0.522	3184.75953	
0.785	7.140	28.341	1.069	2.462	3.857	0.336	2.287	0.345	0.047	6.205	0.468	3184.80437	0.529	3184.76024	
1.017	6.651	25.974	1.638	2.109	5.240	0.327	2.880	0.317	0.049	5.356	0.569	3184.80545	0.572	3184.76095	
1.091	6.184	23.436	2.232	1.837	6.710	0.280	3.530	0.297	0.045	4.267	0.632	3184.80653	0.582	3184.76166	
0.912	6.584	24.934	1.970	2.015	5.754	0.301	3.120	0.306	0.046	4.523	0.631	3184.80760	0.568	3184.76237	
0.863	7.135	27.635	1.461	2.344	3.925	0.340	2.492	0.329	0.048	5.517	0.586	3184.80868	0.582	3184.76308	
0.973	6.746	26.513	1.535	2.222	4.881	0.327	2.723	0.329	0.049	5.602	0.563	3184.80976	0.573	3184.76379	
0.920	6.690	25.680	1.727	2.081	5.419	0.297	2.941	0.311	0.044	4.942	0.587	3184.81083	0.507	3184.76450	
0.846	6.568	25.341	1.903	2.053	5.503	0.293	3.072	0.313	0.045	4.982	0.620	3184.81191	0.540	3184.76521	
0.986	6.751	25.780	1.654	2.076	5.296	0.306	2.920	0.308	0.045	4.851	0.567	3184.81300	0.551	3184.76591	
													0.554	3184.76662	
													0.530	3184.76733	
													0.576	3184.76804	
													0.528	3184.76875	
													0.506	3184.76946	
													0.533	3184.77017	
													0.545	3184.77088	
													0.543	3184.77159	
													0.531	3184.77230	
													0.532	3184.77301	
													0.543	3184.77372	
													0.493	3184.77442	
													0.454	3184.77513	
													0.437	3184.77650	
													0.402	3184.77786	
													0.473	3184.77923	
													0.432	3184.78059	
													0.473	3184.78196	
													0.461	3184.78332	
													0.431	3184.78469	
													0.502	3184.78605	
													0.462	3184.78742	
													0.455	3184.78878	
													0.456	3184.79015	
													0.616	3184.79151	
													0.621	3184.79288	

EDXRF												Hyperspectral Imagery		
Mg	Al	Si	S	K	Ca	Ti	Fe	K/Al	Ti/Al	Si bio	S/Fe	Depth	TOC	Depth
%	%	%	%	%	%	%	%			%		m	%	m
													0.554	3184.79424
													0.576	3184.79561
													0.585	3184.79697
													0.650	3184.79834
													0.692	3184.79970
													0.695	3184.80107
													0.661	3184.80243
													0.568	3184.80380
													0.573	3184.80516
													0.535	3184.80652
													0.600	3184.80789
													0.626	3184.80925
													0.580	3184.81062
													0.663	3184.81198
													0.598	3184.81335
													0.584	3184.81471

Slab 3186.8 m

EDXRF													Hyperspectral Imagery		
Mg	Al	Si	S	K	Ca	Ti	Fe	K/Al	Ti/Al	Si bio	S/Fe	Depth	TOC	Depth	
%	%	%	%	%	%	%	%	%	%	%	%	m	%	m	
0.964	4.771	25.983	0.820	1.428	8.998	0.232	2.065	0.299	0.049	11.194	0.397	3186.81387	0.788	3186.81358	
1.021	4.871	25.920	0.863	1.494	8.822	0.262	2.082	0.307	0.054	10.820	0.415	3186.81525	0.695	3186.81422	
1.065	5.127	27.110	0.787	1.583	7.511	0.258	2.109	0.309	0.050	11.217	0.373	3186.81664	0.784	3186.81487	
1.096	4.776	25.771	0.847	1.438	8.954	0.228	2.135	0.301	0.048	10.964	0.397	3186.81803	0.782	3186.81551	
1.126	4.721	25.124	0.893	1.443	9.524	0.228	2.109	0.306	0.048	10.489	0.424	3186.81941	0.812	3186.81616	
1.039	4.621	25.115	0.953	1.396	9.468	0.236	2.287	0.302	0.051	10.791	0.417	3186.82080	0.818	3186.81680	
1.030	4.788	25.517	0.893	1.485	8.998	0.241	2.244	0.310	0.050	10.676	0.398	3186.82219	0.816	3186.81745	
1.039	4.737	25.581	0.903	1.419	9.006	0.245	2.274	0.300	0.052	10.895	0.397	3186.82357	0.815	3186.81809	
1.109	4.843	26.363	0.804	1.494	8.352	0.219	2.157	0.309	0.045	11.350	0.373	3186.82496	0.824	3186.81874	
0.938	4.710	25.825	0.900	1.452	8.866	0.228	2.314	0.308	0.048	11.225	0.389	3186.82635	0.827	3186.81938	
0.859	4.587	25.287	0.990	1.367	9.444	0.228	2.239	0.298	0.050	11.066	0.442	3186.82773	0.833	3186.82003	
0.982	4.509	25.341	0.980	1.410	9.408	0.215	2.187	0.313	0.048	11.362	0.448	3186.82912	0.860	3186.82067	
0.890	4.648	26.259	0.917	1.461	8.683	0.228	2.100	0.314	0.049	11.849	0.436	3186.83051	0.874	3186.82132	
1.026	5.550	28.449	0.877	1.790	5.451	0.271	2.414	0.323	0.049	11.246	0.363	3186.83189	0.875	3186.82196	
1.065	5.244	26.979	0.910	1.644	7.129	0.262	2.348	0.314	0.050	10.723	0.387	3186.83328	0.872	3186.82261	
0.960	4.576	24.807	0.956	1.405	9.902	0.223	2.213	0.307	0.049	10.621	0.432	3186.83467	0.899	3186.82325	
0.969	5.016	26.400	1.146	1.508	7.703	0.249	2.383	0.301	0.050	10.851	0.481	3186.83605	0.906	3186.82390	
0.955	5.538	28.897	0.747	1.729	5.447	0.236	2.287	0.312	0.043	11.728	0.327	3186.83744	0.897	3186.82454	
1.161	4.776	25.124	0.917	1.377	8.986	0.223	2.492	0.288	0.047	10.317	0.368	3186.83883	0.897	3186.82519	
1.161	4.704	24.766	0.887	1.363	9.555	0.206	2.418	0.290	0.044	10.184	0.367	3186.84021	0.894	3186.82583	
0.863	4.921	25.495	0.830	1.522	9.300	0.245	2.035	0.309	0.050	10.240	0.408	3186.84160	0.856	3186.82648	
0.855	4.782	24.952	0.893	1.494	9.755	0.241	2.100	0.312	0.050	10.128	0.425	3186.84299	0.843	3186.82712	
1.034	5.171	26.169	0.740	1.616	8.448	0.275	2.008	0.313	0.053	10.138	0.369	3186.84437	0.842	3186.82777	
1.078	5.099	26.078	0.780	1.583	8.336	0.223	2.117	0.311	0.044	10.271	0.369	3186.84576	0.858	3186.82841	
0.995	5.016	25.793	0.790	1.551	8.906	0.258	1.995	0.309	0.051	10.245	0.396	3186.84715	0.872	3186.82906	
1.135	4.826	25.716	0.863	1.489	8.766	0.262	2.170	0.309	0.054	10.754	0.398	3186.84853	0.872	3186.82970	
0.986	4.760	25.332	0.804	1.508	9.524	0.236	2.021	0.317	0.050	10.577	0.398	3186.84992	0.880	3186.83035	
0.947	4.726	25.445	0.827	1.513	9.436	0.245	2.017	0.320	0.052	10.793	0.410	3186.85131	0.912	3186.83099	
0.986	4.804	25.983	0.830	1.461	8.806	0.219	2.130	0.304	0.046	11.090	0.390	3186.85269	0.925	3186.83164	
1.118	5.138	27.273	0.810	1.597	7.288	0.262	2.104	0.311	0.051	11.345	0.385	3186.85408	0.914	3186.83228	
1.056	4.832	25.929	0.867	1.405	8.519	0.232	2.436	0.291	0.048	10.950	0.356	3186.85547	0.899	3186.83293	
1.240	4.053	23.735	1.003	1.175	10.815	0.197	2.492	0.290	0.049	11.169	0.402	3186.85685	0.920	3186.83357	
1.083	4.037	23.925	1.000	1.170	10.938	0.202	2.375	0.290	0.050	11.411	0.421	3186.85824	0.958	3186.83422	
1.148	3.892	23.540	1.000	1.114	11.313	0.193	2.488	0.286	0.050	11.475	0.402	3186.85963	0.909	3186.83486	
1.153	4.109	24.006	0.923	1.142	10.938	0.202	2.353	0.278	0.049	11.268	0.392	3186.86101	0.878	3186.83551	
1.170	3.964	23.956	0.993	1.100	10.779	0.145	2.497	0.277	0.037	11.667	0.398	3186.86240	0.855	3186.83615	
1.240	3.797	23.640	1.079	1.043	11.018	0.184	2.662	0.275	0.048	11.868	0.405	3186.86379	0.859	3186.83680	
0.903	3.736	23.128	1.156	1.048	11.592	0.158	2.693	0.281	0.042	11.546	0.429	3186.86517	0.880	3186.83744	
0.982	4.109	24.459	1.053	1.189	10.472	0.215	2.353	0.289	0.052	11.721	0.447	3186.86656	0.829	3186.83809	
1.157	4.142	24.974	0.983	1.222	9.787	0.215	2.414	0.295	0.052	12.133	0.407	3186.86795	0.826	3186.83873	
1.122	4.059	24.793	1.046	1.170	9.926	0.215	2.510	0.288	0.053	12.211	0.417	3186.86933	0.807	3186.83938	
1.061	4.265	25.373	0.996	1.302	9.468	0.241	2.287	0.305	0.056	12.152	0.436	3186.87072	0.864	3186.84002	
1.052	4.203	25.024	0.990	1.222	9.727	0.202	2.453	0.291	0.048	11.993	0.403	3186.87211	0.865	3186.84067	
1.061	4.170	24.875	0.990	1.189	9.930	0.184	2.475	0.285	0.044	11.947	0.400	3186.87349	0.864	3186.84131	
1.135	4.209	24.250	1.039	1.231	10.145	0.219	2.619	0.293	0.052	11.202	0.397	3186.87488	0.848	3186.84196	
1.091	4.170	24.250	0.946	1.170	10.412	0.215	2.566	0.281	0.051	11.323	0.369	3186.87627	0.839	3186.84260	
0.920	4.376	25.119	0.940	1.311	9.870	0.219	2.231	0.300	0.050	11.554	0.421	3186.87765	0.814	3186.84325	
0.934	4.443	25.250	0.860	1.386	9.747	0.202	2.170	0.312	0.045	11.478	0.396	3186.87904	0.821	3186.84389	
1.012	4.437	25.097	0.897	1.335	9.834	0.232	2.183	0.301	0.052	11.342	0.411	3186.88043	0.808	3186.84454	
1.078	4.487	24.807	0.993	1.339	9.711	0.232	2.318	0.298	0.052	10.897	0.428	3186.88181	0.840	3186.84518	
0.960	4.571	24.961	0.883	1.372	9.894	0.206	2.161	0.300	0.045	10.792	0.409	3186.88320	0.862	3186.84582	
													0.844	3186.84647	
													0.828	3186.84711	
													0.806	3186.84776	
													0.819	3186.84840	
													0.821	3186.84905	
													0.867	3186.84969	
													0.862	3186.85034	
													0.882	3186.85098	
													0.834	3186.85163	
													0.820	3186.85227	

EDXRF												Hyperspectral Imagery		
Mg	Al	Si	S	K	Ca	Ti	Fe	K/Al	Ti/Al	Si bio	S/Fe	Depth	TOC	Depth
%	%	%	%	%	%	%	%			%		m	%	m
													0.844	3186.85292
													0.866	3186.85356
													0.849	3186.85421
													0.855	3186.85485
													0.837	3186.85550
													0.835	3186.85614
													0.833	3186.85679
													0.858	3186.85743
													0.907	3186.85808
													0.882	3186.85872
													0.854	3186.85937
													0.872	3186.86001
													0.875	3186.86066
													0.860	3186.86130
													0.875	3186.86195
													0.856	3186.86259
													0.860	3186.86324
													0.851	3186.86388
													0.778	3186.86453
													0.748	3186.86517
													0.766	3186.86582
													0.816	3186.86646
													0.849	3186.86711
													0.834	3186.86775
													0.878	3186.86840
													0.854	3186.86904
													0.872	3186.86969
													0.857	3186.87033
													0.881	3186.87098
													0.819	3186.87162
													0.899	3186.87227
													0.794	3186.87291
													0.753	3186.87356
													0.748	3186.87420
													0.773	3186.87485
													0.760	3186.87549
													0.780	3186.87614
													0.771	3186.87678
													0.725	3186.87743
													0.736	3186.87807
													0.767	3186.87872
													0.767	3186.87936
													0.743	3186.88001
													0.746	3186.88065
													0.777	3186.88130
													0.747	3186.88194
													0.764	3186.88259
													0.753	3186.88323
													0.759	3186.88388

EDXRF												Hyperspectral Imagery		
Mg %	Al %	Si %	S %	K %	Ca %	Ti %	Fe %	K/Al	Ti/Al	Si bio %	S/Fe	Depth m	TOC %	Depth m
1.122	5.127	21.635	1.003	1.485	11.739	0.236	2.423	0.290	0.046	5.742	0.414	3187.24300	0.640	3187.21805
1.179	5.088	21.585	1.039	1.527	11.823	0.262	2.318	0.300	0.052	5.813	0.448	3187.24420	0.647	3187.21889
1.017	5.099	21.441	1.136	1.480	11.831	0.262	2.488	0.290	0.051	5.634	0.457	3187.24540	0.618	3187.21974
1.012	4.932	21.196	1.452	1.466	11.731	0.232	2.588	0.297	0.047	5.907	0.561	3187.24660	0.625	3187.22058
1.096	5.171	21.364	1.259	1.522	11.743	0.236	2.379	0.294	0.046	5.333	0.529	3187.24780	0.626	3187.22143
1.004	5.216	21.757	1.026	1.546	11.791	0.275	2.261	0.296	0.053	5.588	0.454	3187.24900	0.623	3187.22228
1.148	5.171	22.011	0.784	1.541	11.974	0.258	2.052	0.298	0.050	5.980	0.382	3187.25020	0.612	3187.22312
0.982	5.132	22.527	0.697	1.593	11.767	0.228	1.956	0.310	0.044	6.616	0.356	3187.25140	0.620	3187.22397
1.223	5.728	23.490	0.857	1.691	9.547	0.267	2.414	0.295	0.047	5.735	0.355	3187.25260	0.629	3187.22481
1.061	5.561	23.165	0.890	1.668	10.125	0.249	2.440	0.300	0.045	5.926	0.365	3187.25380	0.604	3187.22566
1.240	5.277	22.160	0.946	1.555	11.125	0.254	2.383	0.295	0.048	5.801	0.397	3187.25500	0.591	3187.22651
1.052	5.021	21.744	0.900	1.541	12.118	0.245	2.178	0.307	0.049	6.178	0.413	3187.25620	0.609	3187.22735
1.069	4.932	21.504	0.877	1.428	12.572	0.258	2.109	0.290	0.052	6.214	0.416	3187.25740	0.603	3187.22820
1.008	4.826	21.549	0.830	1.452	12.691	0.254	2.130	0.301	0.053	6.587	0.390	3187.25860	0.603	3187.22904
													0.624	3187.22989
													0.662	3187.23073
													0.676	3187.23158
													0.667	3187.23243
													0.619	3187.23327
													0.619	3187.23412
													0.617	3187.23496
													0.609	3187.23581
													0.625	3187.23666
													0.626	3187.23750
													0.619	3187.23835
													0.619	3187.23919
													0.613	3187.24004
													0.608	3187.24089
													0.612	3187.24173
													0.611	3187.24258
													0.605	3187.24342
													0.620	3187.24427
													0.639	3187.24511
													0.619	3187.24596
													0.592	3187.24681
													0.610	3187.24765
													0.601	3187.24850
													0.574	3187.24934
													0.561	3187.25019
													0.585	3187.25104
													0.567	3187.25188
													0.603	3187.25273
													0.612	3187.25357
													0.594	3187.25442
													0.580	3187.25527
													0.608	3187.25611
													0.606	3187.25696
													0.614	3187.25780
													0.634	3187.25865

EDXRF												Hyperspectral Imagery		
Mg	Al	Si	S	K	Ca	Ti	Fe	K/Al	Ti/Al	Si bio	S/Fe	Depth	TOC	Depth
%	%	%	%	%	%	%	%			%		m	%	m
													0.361	3188.19838
													0.378	3188.19927
													0.393	3188.20015
													0.406	3188.20103
													0.417	3188.20191
													0.388	3188.20279
													0.384	3188.20367
													0.391	3188.20456
													0.367	3188.20544
													0.356	3188.20632
													0.351	3188.20720
													0.365	3188.20808
													0.354	3188.20896
													0.352	3188.20985
													0.367	3188.21073
													0.361	3188.21161
													0.365	3188.21249
													0.353	3188.21337
													0.330	3188.21425
													0.331	3188.21514
													0.332	3188.21602
													0.350	3188.21690
													0.348	3188.21778
													0.343	3188.21866
													0.356	3188.21954
													0.385	3188.22043
													0.389	3188.22131
													0.386	3188.22219
													0.386	3188.22307
													0.350	3188.22395
													0.359	3188.22483
													0.329	3188.22571
													0.348	3188.22660

Slab 3188.9 m

EDXRF													Hyperspectral Imagery		
Mg	Al	Si	S	K	Ca	Ti	Fe	K/Al	Ti/Al	Si bio	S/Fe	Depth	TOC	Depth	
%	%	%	%	%	%	%	%			%		m	%	m	
0.697	6.139	30.418	2.714	2.011	0.490	0.319	2.719	0.328	0.052	11.386	0.998	3188.90000	0.414	3188.90023	
0.671	6.089	30.345	2.741	2.044	0.498	0.358	2.715	0.336	0.059	11.469	1.010	3188.90129	0.389	3188.90091	
0.631	5.978	31.123	2.648	2.030	0.212	0.297	2.632	0.340	0.050	12.592	1.006	3188.90258	0.399	3188.90159	
0.526	5.911	31.042	2.824	1.997	0.247	0.293	2.702	0.338	0.049	12.717	1.045	3188.90387	0.387	3188.90228	
0.618	5.789	30.585	3.116	1.865	0.235	0.284	2.915	0.322	0.049	12.640	1.069	3188.90516	0.409	3188.90296	
0.491	5.789	30.481	3.203	1.907	0.215	0.288	3.007	0.330	0.050	12.536	1.065	3188.90645	0.390	3188.90364	
0.517	5.194	26.563	5.785	1.588	0.176	0.232	4.341	0.306	0.045	10.462	1.333	3188.90774	0.359	3188.90433	
0.495	5.205	27.585	5.203	1.635	0.196	0.254	4.010	0.314	0.049	11.450	1.298	3188.90903	0.350	3188.90501	
0.500	5.700	31.675	2.625	1.898	0.219	0.267	2.662	0.333	0.047	14.006	0.986	3188.91032	0.368	3188.90569	
0.548	5.655	31.626	2.694	1.903	0.196	0.293	2.641	0.336	0.052	14.094	1.020	3188.91161	0.365	3188.90638	
0.592	5.750	31.721	2.595	1.903	0.212	0.275	2.558	0.331	0.048	13.896	1.014	3188.91290	0.351	3188.90706	
0.482	5.533	32.499	2.332	1.907	0.223	0.306	2.409	0.345	0.055	15.347	0.968	3188.91419	0.336	3188.90774	
0.557	5.388	32.657	2.389	1.762	0.208	0.284	2.401	0.327	0.053	15.954	0.995	3188.91548	0.361	3188.90842	
0.601	6.228	31.237	2.389	2.114	0.227	0.306	2.532	0.339	0.049	11.929	0.944	3188.91677	0.374	3188.90911	
0.710	7.185	30.644	2.073	2.396	0.247	0.353	2.318	0.333	0.049	8.370	0.894	3188.91806	0.390	3188.90979	
0.815	7.257	30.757	1.920	2.438	0.259	0.340	2.239	0.336	0.047	8.259	0.857	3188.91935	0.365	3188.91047	
0.671	7.363	30.250	2.246	2.504	0.223	0.332	2.348	0.340	0.045	7.425	0.956	3188.92064	0.382	3188.91116	
0.710	7.446	30.259	2.183	2.537	0.200	0.353	2.314	0.341	0.047	7.175	0.943	3188.92194	0.389	3188.91184	
0.706	7.630	30.594	1.850	2.593	0.219	0.401	2.244	0.340	0.053	6.941	0.825	3188.92323	0.425	3188.91252	
0.688	7.307	30.630	1.973	2.518	0.247	0.345	2.309	0.345	0.047	7.978	0.855	3188.92452	0.394	3188.91321	
0.732	7.424	30.974	1.744	2.616	0.204	0.371	2.130	0.352	0.050	7.959	0.819	3188.92581	0.412	3188.91389	
0.736	7.457	31.105	1.714	2.546	0.200	0.349	2.087	0.341	0.047	7.987	0.821	3188.92710	0.381	3188.91457	
0.828	7.502	30.951	1.727	2.523	0.200	0.384	2.135	0.336	0.051	7.695	0.809	3188.92839	0.358	3188.91525	
0.745	7.385	31.114	1.737	2.598	0.176	0.405	2.096	0.352	0.055	8.220	0.829	3188.92968	0.411	3188.91594	
0.828	7.430	31.010	1.697	2.565	0.200	0.358	2.061	0.345	0.048	7.978	0.824	3188.93097	0.447	3188.91662	
0.793	7.496	31.015	1.664	2.574	0.215	0.371	2.087	0.343	0.049	7.776	0.797	3188.93226	0.406	3188.91730	
0.863	7.469	30.961	1.704	2.588	0.192	0.397	2.109	0.347	0.053	7.808	0.808	3188.93355	0.447	3188.91799	
0.776	7.246	30.852	1.930	2.466	0.212	0.366	2.209	0.340	0.051	8.389	0.874	3188.93484	0.437	3188.91867	
0.802	7.363	30.748	1.857	2.499	0.259	0.345	2.191	0.339	0.047	7.923	0.847	3188.93613	0.438	3188.91935	
0.728	7.402	30.621	1.973	2.476	0.231	0.388	2.305	0.334	0.052	7.675	0.856	3188.93742	0.444	3188.92004	
0.714	7.196	30.680	2.086	2.405	0.239	0.353	2.366	0.334	0.049	8.372	0.882	3188.93871	0.457	3188.92072	
0.640	6.768	30.843	2.249	2.302	0.223	0.349	2.475	0.340	0.052	9.863	0.909	3188.94000	0.482	3188.92140	
0.544	5.894	31.313	2.545	1.987	0.351	0.310	2.514	0.337	0.053	13.041	1.012	3188.94200	0.477	3188.92208	
0.548	5.783	31.268	2.581	2.048	0.359	0.275	2.523	0.354	0.048	13.340	1.023	3188.94334	0.477	3188.92277	
0.425	5.550	31.974	2.708	1.832	0.184	0.271	2.597	0.330	0.049	14.770	1.043	3188.94468	0.492	3188.92345	
0.614	5.583	32.852	2.099	1.912	0.196	0.275	2.200	0.342	0.049	15.545	0.954	3188.94602	0.487	3188.92413	
0.609	5.639	33.150	1.950	1.889	0.192	0.280	2.113	0.335	0.050	15.671	0.923	3188.94735	0.409	3188.92482	
0.596	5.683	32.938	2.013	1.931	0.184	0.284	2.174	0.340	0.050	15.320	0.926	3188.94869	0.422	3188.92550	
0.504	5.577	33.092	2.036	1.889	0.200	0.271	2.183	0.339	0.049	15.802	0.933	3188.95003	0.410	3188.92618	
0.535	5.299	33.345	2.109	1.828	0.160	0.262	2.196	0.345	0.049	16.917	0.961	3188.95137	0.411	3188.92687	
0.548	5.333	33.508	2.063	1.767	0.176	0.275	2.148	0.331	0.052	16.977	0.960	3188.95271	0.454	3188.92755	
0.500	4.932	32.703	2.804	1.621	0.156	0.236	2.457	0.329	0.048	17.413	1.141	3188.95405	0.435	3188.92823	
0.364	4.743	33.648	2.498	1.583	0.132	0.219	2.279	0.334	0.046	18.945	1.096	3188.95539	0.410	3188.92891	
0.452	4.760	33.236	2.661	1.597	0.156	0.223	2.357	0.336	0.047	18.481	1.129	3188.95673	0.404	3188.92960	
0.495	4.977	32.680	2.837	1.616	0.160	0.262	2.457	0.325	0.053	17.252	1.155	3188.95806	0.445	3188.93028	
0.566	5.522	31.028	3.156	1.879	0.152	0.280	2.824	0.340	0.051	13.911	1.118	3188.95940	0.426	3188.93096	
0.421	5.210	28.644	4.715	1.668	0.168	0.262	3.670	0.320	0.050	12.492	1.285	3188.96074	0.424	3188.93165	
													0.422	3188.93233	
													0.394	3188.93301	
													0.383	3188.93370	
													0.389	3188.93438	
													0.387	3188.93506	
													0.390	3188.93574	
													0.384	3188.93643	
													0.340	3188.93711	
													0.386	3188.93779	
													0.390	3188.93848	
													0.331	3188.93916	
													0.301	3188.93984	
													0.302	3188.94053	
													0.312	3188.94121	

EDXRF												Hyperspectral Imagery		
Mg	Al	Si	S	K	Ca	Ti	Fe	K/Al	Ti/Al	Si bio	S/Fe	Depth	TOC	Depth
%	%	%	%	%	%	%	%			%		m	%	m
													0.351	3188.94189
													0.356	3188.94257
													0.329	3188.94326
													0.345	3188.94394
													0.342	3188.94462
													0.326	3188.94531
													0.355	3188.94599
													0.377	3188.94667
													0.372	3188.94736
													0.334	3188.94804
													0.344	3188.94872
													0.316	3188.94940
													0.330	3188.95009
													0.328	3188.95077
													0.332	3188.95145
													0.291	3188.95214
													0.396	3188.95282
													0.187	3188.95350
													0.574	3188.95419
													0.379	3188.95487
													0.313	3188.95555
													0.300	3188.95623
													0.335	3188.95692
													0.342	3188.95760
													0.357	3188.95828
													0.354	3188.95897
													0.367	3188.95965

EDXRF												Hyperspectral Imagery		
Mg %	Al %	Si %	S %	K %	Ca %	Ti %	Fe %	K/Al	Ti/Al	Si bio %	S/Fe	Depth m	TOC %	Depth m
2.001	6.082	27.475	0.631	1.033	30.635	0.264	3.162	0.170	0.043	8.620	0.199	3189.94372	0.438	3189.89380
2.060	6.425	27.532	0.671	1.045	30.306	0.323	3.311	0.163	0.050	7.616	0.203	3189.94535	0.486	3189.89459
2.009	6.510	27.235	0.631	1.062	30.590	0.294	3.143	0.163	0.045	7.053	0.201	3189.94700	0.466	3189.89539
													0.482	3189.89618
													0.468	3189.89697
													0.452	3189.89777
													0.513	3189.89856
													0.515	3189.89935
													0.474	3189.90015
													0.451	3189.90094
													0.460	3189.90173
													0.439	3189.90253
													0.429	3189.90332
													0.447	3189.90411
													0.437	3189.90491
													0.419	3189.90570
													0.445	3189.90649
													0.418	3189.90729
													0.427	3189.90808
													0.451	3189.90888
													0.459	3189.90967
													0.442	3189.91046
													0.457	3189.91126
													0.450	3189.91205
													0.423	3189.91284
													0.395	3189.91364
													0.415	3189.91443
													0.436	3189.91522
													0.425	3189.91602
													0.414	3189.91681
													0.427	3189.91760
													0.459	3189.91840
													0.451	3189.91919
													0.458	3189.91998
													0.425	3189.92078
													0.430	3189.92157
													0.421	3189.92236
													0.471	3189.92316
													0.391	3189.92395
													0.396	3189.92474
													0.421	3189.92554
													0.406	3189.92633
													0.405	3189.92712
													0.403	3189.92792
													0.393	3189.92871
													0.395	3189.92950
													0.427	3189.93030
													0.395	3189.93109
													0.434	3189.93188
													0.404	3189.93268
													0.437	3189.93347
													0.433	3189.93426
													0.432	3189.93506
													0.466	3189.93585
													0.454	3189.93664
													0.452	3189.93744
													0.434	3189.93823
													0.443	3189.93903
													0.422	3189.93982
													0.426	3189.94061
													0.414	3189.94141

EDXRF												Hyperspectral Imagery		
Mg	Al	Si	S	K	Ca	Ti	Fe	K/Al	Ti/Al	Si bio	S/Fe	Depth	TOC	Depth
%	%	%	%	%	%	%	%			%		m	%	m
													0.435	3189.94220
													0.433	3189.94299
													0.452	3189.94379
													0.414	3189.94458
													0.410	3189.94537
													0.394	3189.94617
													0.388	3189.94696
													0.382	3189.94775
													0.378	3189.94855

EDXRF												Hyperspectral Imagery		
Mg	Al	Si	S	K	Ca	Ti	Fe	K/Al	Ti/Al	Si bio	S/Fe	Depth	TOC	Depth
%	%	%	%	%	%	%	%			%		m	%	m
1.481	3.375	14.219	0.707	0.879	20.131	0.171	2.405	0.260	0.051	3.758	0.294	3190.94208	0.359	3190.89992
1.529	3.280	13.894	0.661	0.870	20.330	0.162	2.492	0.265	0.050	3.725	0.265	3190.94399	0.351	3190.90074
1.324	3.436	14.473	0.710	0.917	19.939	0.184	2.423	0.267	0.054	3.821	0.293	3190.94590	0.342	3190.90156
													0.355	3190.90238
													0.337	3190.90320
													0.335	3190.90403
													0.336	3190.90485
													0.329	3190.90567
													0.342	3190.90649
													0.337	3190.90731
													0.325	3190.90814
													0.323	3190.90896
													0.327	3190.90978
													0.326	3190.91060
													0.332	3190.91142
													0.328	3190.91225
													0.330	3190.91307
													0.330	3190.91389
													0.317	3190.91471
													0.328	3190.91554
													0.324	3190.91636
													0.319	3190.91718
													0.326	3190.91800
													0.322	3190.91882
													0.326	3190.91965
													0.329	3190.92047
													0.328	3190.92129
													0.337	3190.92211
													0.338	3190.92293
													0.346	3190.92376
													0.339	3190.92458
													0.376	3190.92540
													0.336	3190.92622
													0.337	3190.92704
													0.328	3190.92787
													0.324	3190.92869
													0.321	3190.92951
													0.335	3190.93033
													0.335	3190.93115
													0.329	3190.93198
													0.343	3190.93280
													0.344	3190.93362
													0.334	3190.93444
													0.328	3190.93527
													0.343	3190.93609
													0.353	3190.93691
													0.358	3190.93773
													0.364	3190.93855
													0.358	3190.93938
													0.366	3190.94020
													0.399	3190.94102
													0.390	3190.94184
													0.384	3190.94266
													0.370	3190.94349
													0.364	3190.94431
													0.364	3190.94513
													0.366	3190.94595
													0.360	3190.94677
													0.373	3190.94760
													0.344	3190.94842
													0.338	3190.94924
													0.455	3190.95006

EDXRF												Hyperspectral Imagery		
Mg	Al	Si	S	K	Ca	Ti	Fe	K/Al	Ti/Al	Si bio	S/Fe	Depth	TOC	Depth
%	%	%	%	%	%	%	%			%		m	%	m
													0.366	3191.25871
													0.359	3191.25951
													0.351	3191.26031
													0.357	3191.26111
													0.369	3191.26190
													0.380	3191.26270
													0.382	3191.26350
													0.376	3191.26430
													0.373	3191.26510
													0.367	3191.26589
													0.362	3191.26669
													0.365	3191.26749
													0.359	3191.26829
													0.358	3191.26909
													0.355	3191.26989
													0.351	3191.27068
													0.350	3191.27148
													0.352	3191.27228
													0.347	3191.27308
													0.350	3191.27388
													0.353	3191.27467
													0.353	3191.27547
													0.346	3191.27627
													0.347	3191.27707
													0.363	3191.27787
													0.367	3191.27867
													0.367	3191.27946
													0.373	3191.28026
													0.382	3191.28106
													0.402	3191.28186
													0.407	3191.28266
													0.407	3191.28345
													0.409	3191.28425
													0.421	3191.28505
													0.427	3191.28585
													0.440	3191.28665
													0.442	3191.28745
													0.426	3191.28824
													0.428	3191.28904
													0.431	3191.28984
													0.427	3191.29064
													0.430	3191.29144
													0.431	3191.29224
													0.430	3191.29303
													0.432	3191.29383
													0.429	3191.29463
													0.422	3191.29543
													0.405	3191.29623
													0.398	3191.29702

EDXRF											Hyperspectral Imagery			
Mg	Al	Si	S	K	Ca	Ti	Fe	K/Al	Ti/Al	Si bio	S/Fe	Depth	TOC	Depth
%	%	%	%	%	%	%	%			%		m	%	m
													0.421	3192.25872
													0.422	3192.25945
													0.421	3192.26018
													0.421	3192.26091
													0.426	3192.26164
													0.433	3192.26237
													0.425	3192.26310
													0.429	3192.26383
													0.437	3192.26456
													0.444	3192.26529
													0.442	3192.26602
													0.443	3192.26675
													0.438	3192.26748
													0.432	3192.26821
													0.418	3192.26894
													0.414	3192.26967
													0.411	3192.27040
													0.415	3192.27113
													0.424	3192.27186
													0.425	3192.27259
													0.422	3192.27332
													0.443	3192.27405
													0.441	3192.27478
													0.453	3192.27551
													0.467	3192.27624
													0.454	3192.27697
													0.456	3192.27770
													0.445	3192.27843
													0.439	3192.27916
													0.434	3192.27989
													0.422	3192.28062
													0.421	3192.28135
													0.425	3192.28208
													0.440	3192.28281
													0.437	3192.28354
													0.447	3192.28427
													0.463	3192.28500
													0.474	3192.28573
													0.471	3192.28646
													0.451	3192.28719
													0.402	3192.28792
													0.394	3192.28865
													0.393	3192.28938
													0.386	3192.29011
													0.377	3192.29084
													0.377	3192.29157
													0.390	3192.29230
													0.401	3192.29303
													0.391	3192.29376
													0.383	3192.29449
													0.375	3192.29522
													0.387	3192.29595
													0.405	3192.29668
													0.422	3192.29741
													0.436	3192.29814

EDXRF												Hyperspectral Imagery		
Mg	Al	Si	S	K	Ca	Ti	Fe	K/Al	Ti/Al	Si bio	S/Fe	Depth	TOC	Depth
%	%	%	%	%	%	%	%			%		m	%	m
													1.208	3192.84656
													1.212	3192.84737
													1.214	3192.84819
													1.221	3192.84900
													1.223	3192.84982
													1.216	3192.85063
													1.197	3192.85144
													1.173	3192.85226
													1.154	3192.85307
													1.148	3192.85389
													1.125	3192.85470
													1.097	3192.85552
													1.075	3192.85633
													1.060	3192.85715
													1.058	3192.85796
													1.075	3192.85877
													1.115	3192.85959
													1.178	3192.86040
													1.241	3192.86122
													1.277	3192.86203
													1.281	3192.86285
													1.284	3192.86366
													1.288	3192.86448
													1.321	3192.86529
													1.324	3192.86610
													1.335	3192.86692
													1.332	3192.86773
													1.326	3192.86855
													1.328	3192.86936
													1.320	3192.87018
													1.300	3192.87099
													1.275	3192.87181
													1.244	3192.87262
													1.215	3192.87343
													1.198	3192.87425
													1.191	3192.87506
													1.207	3192.87588
													1.226	3192.87669
													1.247	3192.87751
													1.256	3192.87832
													1.243	3192.87914
													1.241	3192.87995
													1.244	3192.88077
													1.262	3192.88158
													1.292	3192.88239
													1.334	3192.88321
													1.398	3192.88402
													1.475	3192.88484
													1.547	3192.88565
													1.594	3192.88647
													1.581	3192.88728
													1.601	3192.88810
													1.601	3192.88891
													1.590	3192.88972
													1.565	3192.89054
													1.537	3192.89135
													1.506	3192.89217
													1.461	3192.89298
													1.404	3192.89380

Slab 3193.61 m

EDXRF													Hyperspectral Imagery		
Mg %	Al %	Si %	S %	K %	Ca %	Ti %	Fe %	K/Al	Ti/Al	Si bio %	S/Fe	Depth m	TOC %	Depth m	
0.653	5.589	28.558	1.219	1.781	5.766	0.275	1.987	0.319	0.049	11.233	0.614	3193.61764	1.218	3193.61844	
0.640	5.461	28.345	1.239	1.724	5.953	0.280	2.061	0.316	0.051	11.417	0.601	3193.61874	1.099	3193.61903	
0.798	5.538	28.182	1.262	1.738	5.870	0.267	2.048	0.314	0.048	11.013	0.616	3193.61983	1.063	3193.61963	
0.658	5.583	28.662	1.259	1.813	5.527	0.262	1.995	0.325	0.047	11.355	0.631	3193.62092	1.016	3193.62023	
0.741	5.572	28.648	1.236	1.813	5.467	0.258	1.995	0.325	0.046	11.376	0.619	3193.62201	0.965	3193.62082	
0.741	5.739	28.467	1.289	1.846	5.447	0.271	2.035	0.322	0.047	10.677	0.633	3193.62310	0.948	3193.62142	
0.885	5.906	29.368	1.232	1.912	4.527	0.267	1.939	0.324	0.045	11.061	0.636	3193.62420	0.953	3193.62201	
0.758	6.039	29.440	1.216	1.987	4.379	0.293	1.943	0.329	0.048	10.719	0.626	3193.62529	0.967	3193.62261	
0.793	6.100	29.942	1.096	1.997	4.112	0.284	1.843	0.327	0.047	11.032	0.595	3193.62638	0.996	3193.62320	
0.679	6.022	30.155	0.993	2.076	4.140	0.293	1.790	0.345	0.049	11.486	0.555	3193.62747	1.027	3193.62380	
0.881	5.900	29.006	1.066	1.907	5.053	0.275	1.882	0.323	0.047	10.716	0.566	3193.62857	1.079	3193.62439	
0.793	5.878	28.350	1.136	1.879	5.678	0.262	1.912	0.320	0.045	10.129	0.594	3193.62966	1.119	3193.62499	
0.758	5.922	28.413	1.142	1.907	5.527	0.275	1.965	0.322	0.046	10.054	0.581	3193.63075	1.119	3193.62559	
0.793	5.933	28.965	1.219	1.978	4.806	0.310	2.008	0.333	0.052	10.572	0.607	3193.63184	1.108	3193.62618	
0.736	5.922	29.015	1.269	1.983	4.682	0.284	2.017	0.335	0.048	10.656	0.629	3193.63293	1.099	3193.62678	
0.811	6.440	30.304	1.348	2.044	3.025	0.314	2.069	0.317	0.049	10.342	0.652	3193.63403	1.083	3193.62737	
0.868	6.695	30.585	1.757	2.231	1.722	0.293	2.157	0.333	0.044	9.829	0.815	3193.63512	1.053	3193.62797	
0.671	6.506	28.875	2.302	2.217	2.690	0.314	2.427	0.341	0.048	8.705	0.949	3193.63621	1.022	3193.62856	
0.863	6.534	28.997	1.425	2.114	3.869	0.306	2.052	0.324	0.047	8.741	0.694	3193.63730	0.999	3193.62916	
0.728	6.395	28.943	1.335	2.147	4.284	0.306	2.013	0.336	0.048	9.118	0.663	3193.63839	0.983	3193.62976	
0.697	6.111	28.377	1.967	2.015	4.120	0.284	2.296	0.330	0.046	9.432	0.856	3193.63949	1.018	3193.63035	
0.877	6.295	28.775	1.604	2.091	4.045	0.275	2.056	0.332	0.044	9.261	0.780	3193.64058	1.010	3193.63095	
0.776	6.584	30.712	0.903	2.170	3.323	0.297	1.694	0.330	0.045	10.301	0.533	3193.64167	1.004	3193.63154	
0.789	6.200	29.590	1.049	1.983	4.363	0.275	1.886	0.320	0.044	10.368	0.556	3193.64276	1.000	3193.63214	
0.776	5.516	27.314	1.362	1.705	6.336	0.245	2.279	0.309	0.044	10.213	0.598	3193.64385	0.997	3193.63273	
0.807	5.633	26.694	1.491	1.762	6.463	0.280	2.375	0.313	0.050	9.231	0.628	3193.64495	0.992	3193.63333	
0.859	5.794	26.576	1.551	1.776	6.316	0.271	2.375	0.306	0.047	8.614	0.653	3193.64604	0.988	3193.63393	
0.842	5.878	26.490	1.601	1.846	6.244	0.310	2.409	0.314	0.053	8.269	0.664	3193.64713	0.988	3193.63452	
0.833	5.972	27.033	1.568	1.907	5.734	0.275	2.318	0.319	0.046	8.519	0.676	3193.64822	0.978	3193.63512	
0.973	5.972	25.907	1.618	1.879	6.400	0.288	2.457	0.315	0.048	7.392	0.658	3193.64931	0.964	3193.63571	
0.877	6.022	25.038	1.747	1.809	6.969	0.271	2.606	0.300	0.045	6.368	0.671	3193.65041	0.957	3193.63631	
0.807	6.301	26.259	1.641	1.997	5.921	0.297	2.449	0.317	0.047	6.728	0.670	3193.65150	0.945	3193.63690	
0.789	6.128	26.630	1.578	1.940	5.882	0.319	2.431	0.317	0.052	7.633	0.649	3193.65259	0.919	3193.63750	
0.798	5.950	27.015	1.535	1.832	5.925	0.284	2.357	0.308	0.048	8.570	0.651	3193.65368	0.889	3193.63810	
0.767	5.867	28.169	1.232	1.879	5.595	0.293	2.074	0.320	0.050	9.982	0.594	3193.65477	0.870	3193.63869	
0.785	5.906	27.965	1.159	1.922	5.906	0.293	1.978	0.325	0.050	9.658	0.586	3193.65587	0.869	3193.63929	
0.758	5.839	27.775	1.212	1.964	5.993	0.301	2.008	0.336	0.052	9.675	0.604	3193.65696	0.888	3193.63988	
0.798	5.928	27.807	1.249	1.945	5.818	0.284	2.008	0.328	0.048	9.431	0.622	3193.65805	0.928	3193.64048	
0.793	5.972	27.992	1.182	1.931	5.670	0.293	2.004	0.323	0.049	9.478	0.590	3193.65914	0.983	3193.64107	
0.798	6.034	28.540	1.106	2.001	5.236	0.301	1.987	0.332	0.050	9.836	0.557	3193.66023	1.014	3193.64167	
0.789	6.657	30.074	1.252	2.194	2.953	0.310	2.117	0.330	0.047	9.439	0.591	3193.66133	1.023	3193.64227	
0.850	6.273	29.771	1.342	2.138	3.296	0.301	2.196	0.341	0.048	10.325	0.611	3193.66242	1.000	3193.64286	
0.833	6.000	28.381	1.262	1.936	5.049	0.280	2.178	0.323	0.047	9.781	0.579	3193.66351	0.961	3193.64346	
0.907	5.911	28.074	1.239	1.968	5.376	0.284	2.096	0.333	0.048	9.749	0.591	3193.66460	0.922	3193.64405	
0.872	5.906	27.255	1.279	1.823	6.244	0.301	2.130	0.309	0.051	8.948	0.600	3193.66570	0.908	3193.64465	
0.894	5.844	27.110	1.282	1.842	6.336	0.275	2.139	0.315	0.047	8.992	0.599	3193.66679	0.888	3193.64524	
0.863	5.800	27.400	1.229	1.842	6.232	0.284	2.091	0.318	0.049	9.420	0.588	3193.66788	0.894	3193.64584	
													0.911	3193.64643	
													0.935	3193.64703	
													0.948	3193.64763	
													0.945	3193.64822	
													0.908	3193.64882	
													0.854	3193.64941	
													0.830	3193.65001	
													0.836	3193.65060	
													0.868	3193.65120	
													0.900	3193.65180	
													0.922	3193.65239	
													0.913	3193.65299	
													0.902	3193.65358	
													0.902	3193.65418	

EDXRF												Hyperspectral Imagery		
Mg	Al	Si	S	K	Ca	Ti	Fe	K/Al	Ti/Al	Si bio	S/Fe	Depth	TOC	Depth
%	%	%	%	%	%	%	%			%		m	%	m
													0.942	3193.65477
													0.996	3193.65537
													1.084	3193.65597
													1.197	3193.65656
													1.224	3193.65716
													1.248	3193.65775
													1.244	3193.65835
													1.217	3193.65894
													1.162	3193.65954
													1.141	3193.66014
													1.123	3193.66073
													1.108	3193.66133
													1.090	3193.66192
													1.031	3193.66252
													1.019	3193.66311
													1.004	3193.66371
													1.002	3193.66431
													0.989	3193.66490
													0.963	3193.66550
													0.960	3193.66609
													0.995	3193.66669
													1.040	3193.66728
													1.077	3193.66788
													1.121	3193.66848

EDXRF											Hyperspectral Imagery			
Mg %	Al %	Si %	S %	K %	Ca %	Ti %	Fe %	K/Al	Ti/Al	Si bio %	S/Fe	Depth m	TOC %	Depth m
1.131	3.853	19.391	0.913	1.043	15.190	0.210	2.418	0.271	0.055	7.447	0.378	3194.09455	0.537	3194.04344
													0.536	3194.04419
													0.539	3194.04494
													0.575	3194.04570
													0.552	3194.04645
													0.540	3194.04720
													0.533	3194.04796
													0.530	3194.04871
													0.535	3194.04947
													0.541	3194.05022
													0.543	3194.05097
													0.530	3194.05173
													0.529	3194.05248
													0.539	3194.05323
													0.556	3194.05399
													0.554	3194.05474
													0.549	3194.05549
													0.542	3194.05625
													0.564	3194.05700
													0.559	3194.05775
													0.577	3194.05851
													0.572	3194.05926
													0.578	3194.06002
													0.599	3194.06077
													0.607	3194.06152
													0.588	3194.06228
													0.575	3194.06303
													0.567	3194.06378
													0.575	3194.06454
													0.590	3194.06529
													0.586	3194.06604
													0.568	3194.06680
													0.566	3194.06755
													0.563	3194.06830
													0.566	3194.06906
													0.559	3194.06981
													0.542	3194.07057
													0.543	3194.07132
													0.548	3194.07207
													0.573	3194.07283
													0.589	3194.07358
													0.602	3194.07433
													0.607	3194.07509
													0.623	3194.07584
													0.639	3194.07659
													0.646	3194.07735
													0.643	3194.07810
													0.619	3194.07885
													0.610	3194.07961
													0.604	3194.08036
													0.609	3194.08112
													0.598	3194.08187
													0.589	3194.08262
													0.590	3194.08338
													0.614	3194.08413
													0.626	3194.08488
													0.629	3194.08564
													0.623	3194.08639
													0.617	3194.08714
													0.596	3194.08790
													0.587	3194.08865

EDXRF												Hyperspectral Imagery		
Mg	Al	Si	S	K	Ca	Ti	Fe	K/Al	Ti/Al	Si bio	S/Fe	Depth	TOC	Depth
%	%	%	%	%	%	%	%			%		m	%	m
													0.567	3194.08941
													0.581	3194.09016
													0.567	3194.09091
													0.566	3194.09167
													0.565	3194.09242
													0.566	3194.09317
													0.553	3194.09393

EDXRF													Hyperspectral Imagery		
Mg %	Al %	Si %	S %	K %	Ca %	Ti %	Fe %	K/Al	Ti/Al	Si bio %	S/Fe	Depth m	TOC %	Depth m	
1.508	3.792	17.486	1.269	0.884	15.194	0.167	3.530	0.233	0.044	5.731	0.359	3195.06934	0.882	3195.05079	
1.884	4.320	20.491	1.179	1.119	11.763	0.184	3.587	0.259	0.043	7.098	0.329	3195.07031	0.875	3195.05153	
1.880	4.270	20.282	1.146	1.114	11.930	0.193	3.700	0.261	0.045	7.045	0.310	3195.07128	0.874	3195.05228	
1.893	4.404	20.662	1.133	1.142	11.604	0.210	3.604	0.259	0.048	7.011	0.314	3195.07226	0.858	3195.05302	
1.871	4.415	20.880	1.159	1.180	11.356	0.175	3.556	0.267	0.040	7.194	0.326	3195.07323	0.828	3195.05377	
2.020	4.443	20.920	1.109	1.161	11.333	0.197	3.517	0.261	0.044	7.148	0.315	3195.07420	0.800	3195.05451	
1.810	4.426	21.468	1.152	1.250	10.914	0.189	3.460	0.282	0.043	7.747	0.333	3195.07517	0.785	3195.05525	
1.836	4.582	21.477	1.176	1.222	10.787	0.219	3.447	0.267	0.048	7.273	0.341	3195.07614	0.814	3195.05600	
1.696	4.699	22.359	1.166	1.264	10.289	0.202	3.190	0.269	0.043	7.794	0.365	3195.07711	0.895	3195.05674	
1.398	4.832	23.377	1.106	1.433	9.874	0.223	2.798	0.297	0.046	8.398	0.395	3195.07808	0.872	3195.05748	
1.481	5.088	23.649	0.857	1.424	9.695	0.219	2.763	0.280	0.043	7.876	0.310	3195.07905	0.835	3195.05823	
1.608	5.077	23.413	0.907	1.489	9.651	0.228	2.776	0.293	0.045	7.675	0.327	3195.08002	0.828	3195.05897	
1.389	5.049	23.404	1.069	1.508	9.703	0.228	2.745	0.299	0.045	7.753	0.390	3195.08099	0.825	3195.05972	
1.297	5.010	23.504	1.222	1.551	9.488	0.241	2.806	0.309	0.048	7.973	0.436	3195.08197	0.819	3195.06046	
1.380	5.116	23.468	1.086	1.536	9.376	0.223	2.937	0.300	0.044	7.609	0.370	3195.08294	0.794	3195.06120	
1.394	5.299	23.373	0.943	1.551	9.233	0.232	3.138	0.293	0.044	6.945	0.301	3195.08391	0.770	3195.06195	
1.363	5.271	23.395	0.936	1.527	9.607	0.219	2.859	0.290	0.042	7.054	0.328	3195.08488	0.758	3195.06269	
1.424	5.138	23.350	0.996	1.504	9.747	0.232	2.710	0.293	0.045	7.422	0.368	3195.08585	0.699	3195.06343	
1.424	5.227	23.540	0.960	1.494	9.635	0.219	2.671	0.286	0.042	7.336	0.359	3195.08682	0.681	3195.06418	
1.367	5.149	23.608	0.920	1.522	9.727	0.215	2.658	0.296	0.042	7.646	0.346	3195.08779	0.776	3195.06492	
1.473	5.205	23.486	0.883	1.494	9.683	0.223	2.767	0.287	0.043	7.351	0.319	3195.08876	1.123	3195.06567	
1.582	5.266	23.671	0.813	1.457	9.599	0.241	2.702	0.277	0.046	7.347	0.301	3195.08973	1.083	3195.06641	
1.722	5.249	23.698	0.813	1.480	9.340	0.232	2.802	0.282	0.044	7.426	0.290	3195.09070	0.540	3195.06715	
1.937	4.838	21.436	0.887	1.222	11.141	0.206	3.111	0.253	0.043	6.440	0.285	3195.09168	0.590	3195.06790	
1.801	4.298	19.984	1.202	1.086	12.412	0.193	3.391	0.253	0.045	6.660	0.355	3195.09265	0.621	3195.06864	
1.862	4.398	20.984	1.362	1.133	11.157	0.171	3.482	0.258	0.039	7.349	0.391	3195.09362	0.650	3195.06938	
1.740	4.526	21.219	1.176	1.222	11.281	0.184	3.251	0.270	0.041	7.188	0.362	3195.09459	0.649	3195.07013	
1.499	4.915	22.477	1.029	1.363	10.603	0.219	2.806	0.277	0.045	7.239	0.367	3195.09556	0.651	3195.07087	
1.275	5.032	23.386	1.206	1.452	9.723	0.223	2.745	0.289	0.044	7.786	0.439	3195.09653	0.661	3195.07161	
1.451	4.999	23.246	1.136	1.466	9.846	0.223	2.710	0.293	0.045	7.749	0.419	3195.09750	0.676	3195.07236	
													0.686	3195.07310	
													0.699	3195.07385	
													0.726	3195.07459	
													0.764	3195.07533	
													0.790	3195.07608	
													0.811	3195.07682	
													0.830	3195.07756	
													0.844	3195.07831	
													0.852	3195.07905	
													0.845	3195.07980	
													0.809	3195.08054	
													0.761	3195.08128	
													0.736	3195.08203	
													0.762	3195.08277	
													0.779	3195.08351	
													0.770	3195.08426	
													0.749	3195.08500	
													0.740	3195.08575	
													0.739	3195.08649	
													0.733	3195.08723	
													0.713	3195.08798	
													0.690	3195.08872	
													0.683	3195.08946	
													0.680	3195.09021	
													0.692	3195.09095	
													0.708	3195.09170	
													0.742	3195.09244	
													0.753	3195.09318	
													0.736	3195.09393	
													0.706	3195.09467	
													0.677	3195.09541	

EDXRF													Hyperspectral Imagery	
Mg	Al	Si	S	K	Ca	Ti	Fe	K/Al	Ti/Al	Si bio	S/Fe	Depth	TOC	Depth
%	%	%	%	%	%	%	%			%		m	%	m
													0.675	3195.09616
													0.693	3195.09690
													0.686	3195.09765

Slab 3195.17 m

EDXRF												Hyperspectral Imagery		
Mg %	Al %	Si %	S %	K %	Ca %	Ti %	Fe %	K/Al	Ti/Al	Si bio %	S/Fe	Depth m	TOC %	Depth m
1.573	5.210	23.160	1.119	1.489	9.464	0.236	2.815	0.286	0.045	7.008	0.398	3195.18921	0.900	3195.18910
1.402	5.283	23.395	1.083	1.565	9.436	0.232	2.763	0.296	0.044	7.019	0.392	3195.19096	0.876	3195.18974
1.516	5.144	23.386	1.099	1.541	9.412	0.241	2.784	0.300	0.047	7.441	0.395	3195.19271	0.831	3195.19038
1.608	5.055	23.151	1.136	1.504	9.551	0.232	2.872	0.297	0.046	7.482	0.396	3195.19445	0.855	3195.19102
1.319	5.233	23.576	1.053	1.555	9.404	0.228	2.789	0.297	0.043	7.355	0.377	3195.19620	0.818	3195.19166
1.385	5.221	23.156	1.053	1.574	9.508	0.236	2.924	0.301	0.045	6.969	0.360	3195.19820	0.826	3195.19230
1.310	5.271	23.169	1.036	1.588	9.504	0.223	2.941	0.301	0.042	6.828	0.352	3195.20014	0.853	3195.19294
1.402	5.127	23.404	1.099	1.574	9.468	0.254	2.828	0.307	0.049	7.511	0.389	3195.20208	0.838	3195.19358
1.380	5.294	23.617	1.063	1.536	9.364	0.228	2.697	0.290	0.043	7.206	0.394	3195.20403	0.880	3195.19422
1.288	5.288	23.463	1.116	1.574	9.352	0.245	2.819	0.298	0.046	7.070	0.396	3195.20597	0.786	3195.19486
1.416	5.294	23.585	1.109	1.588	9.189	0.241	2.780	0.300	0.045	7.175	0.399	3195.20791	0.851	3195.19550
1.398	5.333	23.712	1.086	1.574	9.157	0.232	2.671	0.295	0.043	7.181	0.407	3195.20985	0.967	3195.19614
1.253	5.310	23.870	1.103	1.621	9.161	0.236	2.662	0.305	0.044	7.408	0.414	3195.21179	0.973	3195.19678
1.354	5.366	23.812	1.089	1.635	9.041	0.236	2.645	0.305	0.044	7.177	0.412	3195.21374	0.978	3195.19742
1.446	5.500	23.712	1.096	1.630	8.982	0.223	2.654	0.296	0.041	6.663	0.413	3195.21568	0.981	3195.19806
1.494	5.271	23.613	1.039	1.565	9.077	0.236	2.885	0.297	0.045	7.271	0.360	3195.21762	0.955	3195.19870
1.293	5.377	23.830	1.099	1.635	9.089	0.245	2.641	0.304	0.046	7.160	0.416	3195.21956	0.968	3195.19934
1.332	5.466	24.635	1.013	1.654	8.376	0.215	2.614	0.303	0.039	7.690	0.387	3195.22150	0.950	3195.19998
1.258	5.466	24.807	0.897	1.630	8.635	0.228	2.431	0.298	0.042	7.862	0.369	3195.22344	0.941	3195.20062
1.288	5.411	24.463	1.116	1.593	8.571	0.219	2.606	0.294	0.040	7.690	0.428	3195.22539	0.971	3195.20126
1.280	5.961	25.965	0.857	1.790	7.228	0.254	2.401	0.300	0.043	7.486	0.357	3195.22733	0.956	3195.20190
1.218	5.538	24.852	0.837	1.654	8.707	0.241	2.383	0.299	0.043	7.683	0.351	3195.22927	0.933	3195.20254
1.547	5.322	23.540	1.083	1.522	9.113	0.236	2.885	0.286	0.044	7.043	0.375	3195.23121	0.961	3195.20318
1.402	5.299	23.427	1.149	1.536	9.193	0.236	2.920	0.290	0.045	6.999	0.394	3195.23315	0.923	3195.20382
1.578	5.277	23.603	1.089	1.532	9.057	0.245	2.859	0.290	0.046	7.245	0.381	3195.23510	0.920	3195.20446
1.437	5.271	23.744	1.152	1.551	9.069	0.254	2.750	0.294	0.048	7.402	0.419	3195.23704	0.945	3195.20510
1.210	5.794	25.703	0.863	1.743	7.627	0.249	2.414	0.301	0.043	7.740	0.358	3195.23898	0.955	3195.20574
1.249	5.661	24.784	0.847	1.705	8.256	0.254	2.706	0.301	0.045	7.236	0.313	3195.24092	0.928	3195.20638
1.486	4.960	22.653	1.285	1.372	9.958	0.236	3.037	0.277	0.048	7.277	0.423	3195.24286	0.921	3195.20702
1.464	4.966	22.771	1.272	1.419	9.779	0.219	3.055	0.286	0.044	7.378	0.416	3195.24481	0.909	3195.20766
1.380	5.110	22.712	1.196	1.391	9.791	0.228	3.159	0.272	0.045	6.871	0.378	3195.24675	0.919	3195.20830
1.578	4.960	22.839	1.229	1.471	9.631	0.245	3.064	0.297	0.049	7.463	0.401	3195.24869	0.915	3195.20894
1.639	4.960	22.839	1.209	1.405	9.639	0.215	3.081	0.283	0.043	7.463	0.392	3195.25063	0.921	3195.20958
1.459	5.216	23.441	1.189	1.508	9.209	0.210	2.928	0.289	0.040	7.271	0.406	3195.25257	0.930	3195.21022
1.503	5.171	22.952	1.156	1.424	9.504	0.223	3.103	0.275	0.043	6.921	0.372	3195.25452	0.930	3195.21086
1.516	5.177	23.445	1.182	1.504	9.121	0.210	2.941	0.290	0.041	7.397	0.402	3195.25646	0.929	3195.21150
1.573	5.055	23.079	1.265	1.461	9.308	0.228	3.085	0.289	0.045	7.410	0.410	3195.25840	0.920	3195.21214
													0.900	3195.21278
													0.914	3195.21342
													0.909	3195.21406
													0.914	3195.21470
													0.914	3195.21534
													0.910	3195.21598
													0.904	3195.21662
													0.908	3195.21726
													0.916	3195.21790
													0.929	3195.21854
													0.860	3195.21918
													0.890	3195.21982
													0.895	3195.22046
													0.904	3195.22110
													0.900	3195.22174
													0.881	3195.22238
													0.871	3195.22302
													0.891	3195.22366
													0.876	3195.22430
													0.854	3195.22494
													0.859	3195.22558
													0.853	3195.22622
													0.842	3195.22686
													0.838	3195.22750

EDXRF											Hyperspectral Imagery			
Mg	Al	Si	S	K	Ca	Ti	Fe	K/Al	Ti/Al	Si bio	S/Fe	Depth	TOC	Depth
%	%	%	%	%	%	%	%			%		m	%	m
													0.848	3195.22814
													0.838	3195.22878
													0.840	3195.22942
													0.842	3195.23006
													0.845	3195.23070
													0.849	3195.23134
													0.843	3195.23198
													0.832	3195.23262
													0.848	3195.23326
													0.858	3195.23390
													0.881	3195.23454
													0.880	3195.23518
													0.875	3195.23582
													0.851	3195.23646
													0.816	3195.23710
													0.798	3195.23774
													0.794	3195.23838
													0.799	3195.23902
													0.786	3195.23966
													0.750	3195.24030
													0.722	3195.24094
													0.717	3195.24158
													0.713	3195.24222
													0.707	3195.24286
													0.696	3195.24367
													0.687	3195.24447
													0.693	3195.24527
													0.723	3195.24608
													0.729	3195.24688
													0.720	3195.24768
													0.730	3195.24848
													0.695	3195.24929
													0.673	3195.25009
													0.670	3195.25089
													0.687	3195.25170
													0.695	3195.25250
													0.695	3195.25330
													0.694	3195.25410
													0.703	3195.25491
													0.709	3195.25571
													0.713	3195.25651
													0.710	3195.25732
													0.708	3195.25812
													0.714	3195.25892
													0.707	3195.25972
													0.705	3195.26053
													0.698	3195.26133
													0.698	3195.26213

EDXRF													Hyperspectral Imagery		
Mg	Al	Si	S	K	Ca	Ti	Fe	K/Al	Ti/Al	Si bio	S/Fe	Depth	TOC	Depth	
%	%	%	%	%	%	%	%			%		m	%	m	
1.201	4.476	22.812	0.950	1.302	11.380	0.241	2.457	0.291	0.054	8.936	0.386	3196.24458	0.917	3196.23033	
1.135	4.504	22.680	0.993	1.335	11.376	0.219	2.575	0.296	0.049	8.718	0.386	3196.24564	0.905	3196.23115	
1.161	4.582	22.780	0.983	1.339	11.165	0.223	2.606	0.292	0.049	8.577	0.377	3196.24670	0.902	3196.23196	
1.297	5.238	23.495	1.016	1.489	9.647	0.249	2.723	0.284	0.048	7.257	0.373	3196.24870	0.899	3196.23277	
1.258	5.105	23.572	0.990	1.518	9.695	0.249	2.737	0.297	0.049	7.748	0.362	3196.25049	0.915	3196.23359	
1.161	4.354	21.350	1.136	1.245	12.452	0.219	2.645	0.286	0.050	7.854	0.429	3196.25227	0.946	3196.23440	
1.249	4.459	21.984	1.199	1.344	11.440	0.223	2.776	0.301	0.050	8.160	0.432	3196.25406	0.959	3196.23522	
1.297	4.548	22.119	1.123	1.320	11.356	0.232	2.763	0.290	0.051	8.019	0.406	3196.25585	0.952	3196.23603	
1.223	4.448	22.088	1.136	1.320	11.572	0.219	2.706	0.297	0.049	8.298	0.420	3196.25764	0.940	3196.23685	
1.153	4.420	22.504	0.933	1.349	11.811	0.219	2.375	0.305	0.050	8.801	0.393	3196.25942	0.948	3196.23766	
1.157	4.559	22.518	1.063	1.316	11.368	0.206	2.627	0.289	0.045	8.383	0.404	3196.26121	0.952	3196.23848	
1.310	4.832	22.929	1.049	1.381	10.587	0.228	2.658	0.286	0.047	7.950	0.395	3196.26300	0.963	3196.23929	
1.249	4.915	23.843	0.833	1.471	10.113	0.228	2.436	0.299	0.046	8.605	0.342	3196.26478	0.984	3196.24010	
1.359	4.966	23.536	1.096	1.480	9.555	0.262	2.889	0.298	0.053	8.142	0.379	3196.26657	1.000	3196.24092	
1.205	4.470	22.613	1.123	1.330	11.070	0.219	2.710	0.297	0.049	8.754	0.414	3196.26836	1.027	3196.24173	
1.324	4.470	22.798	1.036	1.297	11.177	0.202	2.505	0.290	0.045	8.940	0.414	3196.27014	1.037	3196.24255	
1.083	4.648	23.459	1.046	1.391	10.508	0.210	2.593	0.299	0.045	9.048	0.403	3196.27193	1.031	3196.24336	
1.315	4.582	22.852	1.093	1.358	10.775	0.219	2.632	0.296	0.048	8.649	0.415	3196.27372	0.990	3196.24418	
1.275	4.526	23.074	1.049	1.273	10.886	0.202	2.514	0.281	0.045	9.043	0.417	3196.27550	0.980	3196.24499	
													0.969	3196.24581	
													0.983	3196.24662	
													0.975	3196.24743	
													0.966	3196.24825	
													0.949	3196.24906	
													0.972	3196.24988	
													0.953	3196.25069	
													0.930	3196.25151	
													0.953	3196.25232	
													0.944	3196.25314	
													0.947	3196.25395	
													0.937	3196.25476	
													0.939	3196.25558	
													0.941	3196.25639	
													0.933	3196.25721	
													0.952	3196.25802	
													0.981	3196.25884	
													0.990	3196.25965	
													1.003	3196.26047	
													1.003	3196.26128	
													1.031	3196.26209	
													1.024	3196.26291	
													1.020	3196.26372	
													1.017	3196.26454	
													0.976	3196.26535	
													0.943	3196.26617	
													0.935	3196.26698	
													0.949	3196.26780	
													0.923	3196.26861	
													0.904	3196.26942	
													0.932	3196.27024	
													0.977	3196.27105	
													1.017	3196.27187	
													0.987	3196.27268	
													0.937	3196.27350	
													0.927	3196.27431	
													0.911	3196.27513	
													0.886	3196.27594	
													0.868	3196.27675	
													0.807	3196.27757	
													1.031	3196.27838	

Slab 3197.78 m

EDXRF													Hyperspectral Imagery		
Mg %	Al %	Si %	S %	K %	Ca %	Ti %	Fe %	K/Al	Ti/Al	Si bio %	S/Fe	Depth m	TOC %	Depth m	
1.148	5.755	19.169	1.555	1.602	10.432	1.182	3.866	0.278	0.205	1.328	0.402	3197.78000	0.434	3197.77845	
1.196	5.761	18.997	1.581	1.579	10.536	1.169	3.892	0.274	0.203	1.138	0.406	3197.78165	0.428	3197.77925	
1.297	6.951	23.626	1.937	2.058	5.746	0.284	3.674	0.296	0.041	2.077	0.527	3197.78330	0.433	3197.78005	
1.192	6.918	23.332	2.006	2.044	6.069	0.319	3.748	0.295	0.046	1.886	0.535	3197.78495	0.435	3197.78085	
1.196	7.096	23.956	2.508	2.152	4.806	0.340	3.604	0.303	0.048	1.959	0.696	3197.78661	0.429	3197.78165	
1.126	7.474	25.821	1.771	2.372	4.045	0.319	3.129	0.317	0.043	2.651	0.566	3197.78826	0.414	3197.78245	
1.253	7.402	25.400	1.568	2.311	4.583	0.314	3.151	0.312	0.042	2.454	0.498	3197.78991	0.413	3197.78325	
1.223	7.218	24.902	2.080	2.255	4.463	0.345	3.391	0.312	0.048	2.525	0.613	3197.79156	0.422	3197.78405	
1.306	7.591	26.074	1.342	2.377	4.260	0.327	2.915	0.313	0.043	2.542	0.460	3197.79321	0.422	3197.78484	
1.232	7.385	25.404	1.668	2.330	4.435	0.323	3.181	0.316	0.044	2.510	0.524	3197.79486	0.428	3197.78564	
1.275	7.546	25.929	1.332	2.433	4.407	0.358	2.907	0.322	0.047	2.535	0.458	3197.79652	0.455	3197.78644	
1.214	7.552	26.318	1.202	2.382	4.363	0.327	2.771	0.315	0.043	2.907	0.434	3197.79817	0.479	3197.78724	
1.249	7.647	26.685	1.216	2.457	3.901	0.340	2.841	0.321	0.045	2.980	0.428	3197.79982	0.522	3197.78804	
1.183	7.530	26.002	1.591	2.429	4.017	0.345	3.042	0.323	0.046	2.659	0.523	3197.80147	0.494	3197.78884	
1.284	7.780	26.757	1.123	2.476	3.913	0.362	2.758	0.318	0.047	2.639	0.407	3197.80312	0.487	3197.78964	
1.236	7.252	24.821	1.468	2.180	5.423	0.353	3.255	0.301	0.049	2.340	0.451	3197.80477	0.486	3197.79044	
1.310	6.890	23.156	2.159	2.011	5.762	0.293	3.918	0.292	0.042	1.796	0.551	3197.80643	0.494	3197.79124	
1.341	7.591	26.585	1.335	2.339	3.770	0.332	2.959	0.308	0.044	3.053	0.451	3197.80808	0.496	3197.79204	
1.271	7.713	26.268	1.458	2.391	3.794	0.353	3.033	0.310	0.046	2.357	0.481	3197.80973	0.507	3197.79284	
1.205	7.847	27.219	1.152	2.532	3.431	0.345	2.728	0.323	0.044	2.893	0.422	3197.81138	0.483	3197.79364	
1.170	7.786	26.639	2.113	2.574	2.570	0.371	3.094	0.331	0.048	2.504	0.683	3197.81303	0.472	3197.79444	
1.367	7.563	25.029	1.947	2.344	4.236	0.349	3.207	0.310	0.046	1.583	0.607	3197.81468	0.475	3197.79524	
1.210	7.424	25.563	1.571	2.358	4.523	0.327	3.077	0.318	0.044	2.548	0.511	3197.81634	0.472	3197.79603	
1.258	7.741	26.549	1.172	2.457	3.925	0.332	2.867	0.317	0.043	2.551	0.409	3197.81799	0.460	3197.79683	
1.288	7.263	24.495	1.980	2.170	4.965	0.319	3.334	0.299	0.044	1.980	0.594	3197.81964	0.469	3197.79763	
1.192	7.051	24.513	2.186	2.142	4.893	0.297	3.438	0.304	0.042	2.653	0.636	3197.82129	0.461	3197.79843	
1.196	6.962	23.993	2.605	2.091	4.726	0.323	3.718	0.300	0.046	2.409	0.701	3197.82294	0.482	3197.79923	
1.267	7.029	23.961	2.086	2.123	5.491	0.319	3.399	0.302	0.045	2.170	0.614	3197.82459	0.496	3197.80003	
1.100	7.190	24.888	1.903	2.231	4.961	0.340	3.251	0.310	0.047	2.598	0.585	3197.82625	0.482	3197.80083	
1.043	7.218	24.400	1.950	2.227	5.407	0.340	3.203	0.308	0.047	2.023	0.609	3197.82790	0.472	3197.80163	
1.091	7.229	24.775	2.076	2.283	4.686	0.327	3.329	0.316	0.045	2.364	0.624	3197.82955	0.467	3197.80243	
1.188	7.535	25.965	1.398	2.377	4.471	0.327	2.832	0.315	0.043	2.606	0.494	3197.83120	0.464	3197.80323	
1.315	7.291	24.038	1.591	2.217	5.507	0.310	3.517	0.304	0.043	1.437	0.452	3197.83320	0.463	3197.80403	
1.315	7.368	23.952	1.628	2.222	5.495	0.332	3.504	0.302	0.045	1.110	0.465	3197.83454	0.440	3197.80483	
1.240	7.185	24.169	1.963	2.199	5.220	0.319	3.465	0.306	0.044	1.896	0.567	3197.83588	0.430	3197.80563	
1.293	7.185	24.563	1.897	2.180	5.021	0.332	3.360	0.303	0.046	2.289	0.565	3197.83722	0.426	3197.80643	
1.258	7.268	24.916	1.604	2.241	5.121	0.358	3.216	0.308	0.049	2.384	0.499	3197.83856	0.432	3197.80723	
1.315	7.357	24.563	2.003	2.231	4.730	0.336	3.373	0.303	0.046	1.755	0.594	3197.83990	0.441	3197.80802	
1.148	7.419	25.133	1.780	2.302	4.595	0.340	3.242	0.310	0.046	2.135	0.549	3197.84123	0.460	3197.80882	
1.205	7.407	25.603	1.412	2.368	4.770	0.345	2.976	0.320	0.047	2.640	0.474	3197.84257	0.472	3197.80962	
1.218	7.463	25.902	1.342	2.400	4.575	0.353	2.872	0.322	0.047	2.767	0.467	3197.84391	0.496	3197.81042	
0.986	7.546	26.015	1.641	2.419	4.116	0.353	3.037	0.321	0.047	2.621	0.540	3197.84525	0.510	3197.81122	
1.126	7.953	27.386	1.156	2.570	3.371	0.345	2.571	0.323	0.043	2.733	0.450	3197.84659	0.500	3197.81202	
1.188	7.864	26.839	1.249	2.485	3.690	0.327	2.737	0.316	0.042	2.462	0.456	3197.84793	0.480	3197.81282	
1.464	7.013	23.576	1.957	2.048	5.615	0.293	3.617	0.292	0.042	1.838	0.541	3197.84927	0.465	3197.81362	
1.288	7.780	26.255	1.332	2.424	4.017	0.349	2.880	0.312	0.045	2.137	0.462	3197.85061	0.433	3197.81442	
1.302	7.841	26.558	1.162	2.527	3.778	0.323	2.793	0.322	0.041	2.250	0.416	3197.85195	0.444	3197.81522	
1.218	7.624	26.246	1.551	2.443	3.774	0.353	3.002	0.320	0.046	2.610	0.517	3197.85329	0.461	3197.81602	
1.179	7.413	25.988	1.644	2.415	4.041	0.345	3.042	0.326	0.046	3.008	0.541	3197.85462	0.481	3197.81682	
1.148	7.485	26.259	1.531	2.405	4.013	0.314	2.941	0.321	0.042	3.055	0.521	3197.85596	0.460	3197.81762	
1.275	7.647	26.377	1.438	2.382	3.865	0.358	2.972	0.311	0.047	2.673	0.484	3197.85730	0.424	3197.81842	
1.437	7.241	24.545	2.206	2.222	4.355	0.323	3.491	0.307	0.045	2.099	0.632	3197.85864	0.423	3197.81921	
1.319	7.268	23.830	1.797	2.067	5.623	0.310	3.595	0.284	0.043	1.298	0.500	3197.85998	0.428	3197.82001	
1.144	7.140	23.898	1.840	2.100	5.690	0.340	3.630	0.294	0.048	1.762	0.507	3197.86132	0.444	3197.82081	
1.293	7.035	23.694	1.854	2.076	5.866	0.319	3.556	0.295	0.045	1.886	0.521	3197.86266	0.446	3197.82161	
1.337	6.990	23.839	1.917	2.072	5.587	0.310	3.521	0.296	0.044	2.169	0.544	3197.86400	0.445	3197.82241	
1.468	6.962	23.504	1.840	2.039	5.878	0.297	3.530	0.293	0.043	1.920	0.521	3197.86534	0.437	3197.82321	
1.170	7.146	24.346	1.913	2.133	5.093	0.323	3.408	0.298	0.045	2.193	0.561	3197.86668	0.426	3197.82401	
1.394	7.135	24.472	1.807	2.105	5.073	0.353	3.334	0.295	0.050	2.354	0.542	3197.86801	0.418	3197.82481	
1.297	7.079	24.033	1.790	2.072	5.555	0.297	3.425	0.293	0.042	2.088	0.523	3197.86935	0.423	3197.82561	
1.218	6.940	23.979	1.980	2.091	5.487	0.301	3.552	0.301	0.043	2.464	0.557	3197.87069	0.430	3197.82641	

EDXRF													Hyperspectral Imagery	
Mg %	Al %	Si %	S %	K %	Ca %	Ti %	Fe %	K/Al	Ti/Al	Si bio %	S/Fe	Depth m	TOC %	Depth m
1.232	7.013	23.974	1.937	2.048	5.587	0.310	3.543	0.292	0.044	2.236	0.547	3197.87203	0.445	3197.82721
1.284	6.912	23.789	1.943	2.128	5.611	0.301	3.639	0.308	0.044	2.361	0.534	3197.87337	0.420	3197.82801
1.249	7.051	24.296	1.890	2.123	5.320	0.301	3.491	0.301	0.043	2.436	0.541	3197.87470	0.437	3197.82881
													0.451	3197.82961
													0.472	3197.83041
													0.479	3197.83120
													0.502	3197.83200
													0.485	3197.83280
													0.464	3197.83360
													0.453	3197.83440
													0.428	3197.83520
													0.419	3197.83600
													0.426	3197.83680
													0.414	3197.83760
													0.408	3197.83840
													0.401	3197.83920
													0.412	3197.84000
													0.410	3197.84080
													0.413	3197.84160
													0.425	3197.84239
													0.405	3197.84319
													0.430	3197.84399
													0.450	3197.84479
													0.445	3197.84559
													0.460	3197.84639
													0.471	3197.84719
													0.440	3197.84799
													0.414	3197.84879
													0.416	3197.84959
													0.432	3197.85039
													0.444	3197.85119
													0.454	3197.85199
													0.444	3197.85279
													0.438	3197.85359
													0.435	3197.85438
													0.446	3197.85518
													0.427	3197.85598
													0.424	3197.85678
													0.423	3197.85758
													0.399	3197.85838
													0.378	3197.85918
													0.378	3197.85998
													0.380	3197.86078
													0.416	3197.86158
													0.437	3197.86238
													0.456	3197.86318
													0.455	3197.86398
													0.459	3197.86478
													0.453	3197.86557
													0.482	3197.86637
													0.488	3197.86717
													0.498	3197.86797
													0.525	3197.86877
													0.515	3197.86957
													0.514	3197.87037
													0.495	3197.87117
													0.490	3197.87197
													0.481	3197.87277
													0.496	3197.87357
													0.468	3197.87437

Slab 3198.12 m

EDXRF													Hyperspectral Imagery		
Mg %	Al %	Si %	S %	K %	Ca %	Ti %	Fe %	K/Al	Ti/Al	Si bio %	S/Fe	Depth m	TOC %	Depth m	
1.315	7.241	24.784	1.641	2.250	5.041	0.332	3.264	0.311	0.046	2.339	0.503	3198.13116	0.360	3198.13350	
1.367	7.229	23.956	2.000	2.213	5.188	0.332	3.491	0.306	0.046	1.545	0.573	3198.13275	0.372	3198.13416	
1.249	7.263	24.291	1.727	2.222	5.372	0.345	3.408	0.306	0.047	1.777	0.507	3198.13434	0.391	3198.13482	
1.345	7.140	24.291	1.754	2.199	5.284	0.310	3.421	0.308	0.043	2.156	0.513	3198.13594	0.411	3198.13548	
1.359	7.046	23.956	2.129	2.123	5.172	0.306	3.530	0.301	0.043	2.114	0.603	3198.13753	0.421	3198.13614	
1.288	7.268	24.612	1.601	2.283	5.272	0.319	3.207	0.314	0.044	2.081	0.499	3198.13912	0.426	3198.13681	
1.214	7.107	23.495	2.392	2.100	5.296	0.297	3.670	0.295	0.042	1.463	0.652	3198.14072	0.406	3198.13747	
1.310	7.291	24.920	1.551	2.288	5.053	0.336	3.159	0.314	0.046	2.319	0.491	3198.14231	0.400	3198.13813	
1.350	7.457	25.151	1.382	2.283	5.037	0.323	3.042	0.306	0.043	2.033	0.454	3198.14390	0.403	3198.13879	
1.210	7.469	25.128	1.355	2.278	5.192	0.345	3.085	0.305	0.046	1.976	0.439	3198.14550	0.407	3198.13945	
1.267	7.496	26.033	1.206	2.377	4.591	0.336	2.846	0.317	0.045	2.794	0.424	3198.14709	0.413	3198.14012	
1.210	7.597	26.146	1.368	2.410	4.132	0.336	2.989	0.317	0.044	2.597	0.458	3198.14869	0.417	3198.14078	
1.210	7.647	26.278	1.119	2.415	4.415	0.358	2.837	0.316	0.047	2.573	0.395	3198.15028	0.413	3198.14144	
1.253	7.279	25.083	1.412	2.260	5.081	0.353	3.229	0.310	0.049	2.517	0.437	3198.15187	0.412	3198.14210	
1.275	7.480	24.567	1.518	2.278	5.200	0.327	3.299	0.305	0.044	1.380	0.460	3198.15347	0.413	3198.14276	
1.144	7.686	25.481	1.302	2.321	4.846	0.332	3.011	0.302	0.043	1.656	0.432	3198.15506	0.413	3198.14342	
1.271	7.669	26.413	1.079	2.405	4.300	0.310	2.780	0.314	0.040	2.640	0.388	3198.15665	0.406	3198.14409	
1.188	7.357	24.481	2.000	2.199	4.738	0.340	3.547	0.299	0.046	1.673	0.564	3198.15825	0.408	3198.14475	
1.267	7.157	23.916	2.026	2.199	5.180	0.310	3.635	0.307	0.043	1.729	0.558	3198.15984	0.406	3198.14541	
1.280	7.046	23.816	1.996	2.072	5.439	0.306	3.678	0.294	0.043	1.974	0.543	3198.16143	0.407	3198.14607	
1.350	7.430	24.830	1.661	2.288	4.810	0.336	3.260	0.308	0.045	1.798	0.510	3198.16303	0.405	3198.14673	
1.337	7.574	26.359	1.026	2.433	4.483	0.353	2.710	0.321	0.047	2.879	0.379	3198.16462	0.402	3198.14740	
1.367	7.608	25.911	1.229	2.391	4.483	0.319	2.863	0.314	0.042	2.327	0.429	3198.16622	0.402	3198.14806	
1.218	7.374	25.255	1.272	2.269	5.188	0.358	3.111	0.308	0.049	2.395	0.409	3198.16781	0.405	3198.14872	
1.420	7.480	25.658	1.242	2.335	4.754	0.336	2.933	0.312	0.045	2.470	0.424	3198.16940	0.412	3198.14938	
1.275	7.368	24.974	1.551	2.278	5.041	0.345	3.225	0.309	0.047	2.132	0.481	3198.17100	0.421	3198.15004	
1.324	7.446	25.020	1.452	2.288	4.989	0.327	3.133	0.307	0.044	1.936	0.463	3198.17259	0.428	3198.15071	
1.280	7.441	25.436	1.325	2.339	4.949	0.353	2.985	0.314	0.047	2.369	0.444	3198.17418	0.434	3198.15137	
1.140	7.558	25.888	1.481	2.419	4.248	0.345	3.055	0.320	0.046	2.460	0.485	3198.17578	0.435	3198.15203	
1.275	7.791	26.689	1.043	2.466	3.977	0.319	2.789	0.317	0.041	2.536	0.374	3198.17737	0.435	3198.15269	
1.324	7.741	26.653	1.020	2.494	4.081	0.358	2.763	0.322	0.046	2.655	0.369	3198.17897	0.441	3198.15335	
1.380	7.613	26.051	1.099	2.415	4.455	0.353	2.933	0.317	0.046	2.450	0.375	3198.18056	0.454	3198.15401	
1.385	7.374	25.269	1.272	2.269	5.097	0.332	3.033	0.308	0.045	2.409	0.419	3198.18215	0.468	3198.15468	
1.205	7.563	25.535	1.571	2.344	4.371	0.323	3.155	0.310	0.043	2.090	0.498	3198.18375	0.476	3198.15534	
1.210	7.068	24.481	2.030	2.147	4.921	0.327	3.582	0.304	0.046	2.570	0.567	3198.18534	0.482	3198.15600	
1.341	7.179	24.943	1.604	2.217	5.005	0.340	3.251	0.309	0.047	2.687	0.494	3198.18693	0.478	3198.15666	
1.302	7.380	26.250	1.245	2.349	4.443	0.349	2.885	0.318	0.047	3.374	0.432	3198.18853	0.465	3198.15732	
1.284	7.719	26.825	1.179	2.452	3.837	0.353	2.776	0.318	0.046	2.896	0.425	3198.19012	0.444	3198.15799	
1.306	7.513	26.323	1.159	2.396	4.284	0.310	2.893	0.319	0.041	3.032	0.401	3198.19171	0.443	3198.15865	
1.245	7.502	25.802	1.385	2.311	4.543	0.327	3.016	0.308	0.044	2.546	0.459	3198.19331	0.446	3198.15931	
1.267	7.324	25.739	1.408	2.330	4.658	0.323	2.968	0.318	0.044	3.035	0.475	3198.19490	0.448	3198.15997	
1.385	6.974	24.146	1.505	2.048	5.961	0.306	3.404	0.294	0.044	2.528	0.442	3198.19650	0.451	3198.16063	
1.275	6.829	23.395	2.339	2.001	5.547	0.306	3.827	0.293	0.045	2.226	0.611	3198.19809	0.456	3198.16130	
1.494	5.872	20.463	2.435	1.588	8.129	0.254	4.607	0.270	0.043	2.260	0.529	3198.19968	0.452	3198.16196	
1.547	6.568	22.427	1.867	1.818	6.949	0.297	3.927	0.277	0.045	2.068	0.475	3198.20128	0.436	3198.16262	
1.696	6.679	22.803	1.664	1.884	6.766	0.301	3.779	0.282	0.045	2.098	0.440	3198.20287	0.416	3198.16328	
1.451	6.679	23.178	1.744	1.940	6.527	0.284	3.696	0.291	0.043	2.474	0.472	3198.20446	0.398	3198.16394	
1.508	6.846	23.766	1.707	2.025	6.037	0.345	3.473	0.296	0.050	2.545	0.492	3198.20606	0.388	3198.16460	
1.389	7.152	24.739	1.518	2.208	5.376	0.323	3.142	0.309	0.045	2.569	0.483	3198.20765	0.396	3198.16527	
1.214	7.574	25.468	1.382	2.316	4.834	0.345	2.941	0.306	0.046	1.987	0.470	3198.20924	0.405	3198.16593	
1.218	7.452	25.753	1.302	2.321	4.750	0.349	3.011	0.311	0.047	2.652	0.432	3198.21084	0.419	3198.16659	
1.249	7.318	25.422	1.348	2.288	4.945	0.340	3.120	0.313	0.046	2.735	0.432	3198.21243	0.435	3198.16725	
1.372	7.419	25.744	1.405	2.354	4.491	0.345	3.029	0.317	0.046	2.746	0.464	3198.21403	0.444	3198.16791	
1.214	7.274	25.088	2.013	2.246	4.344	0.332	3.377	0.309	0.046	2.538	0.596	3198.21562	0.444	3198.16858	
1.218	7.335	26.087	1.375	2.297	4.535	0.319	2.933	0.313	0.043	3.349	0.469	3198.21721	0.440	3198.16924	
1.569	6.840	23.572	1.724	1.968	6.141	0.314	3.539	0.288	0.046	2.368	0.487	3198.21881	0.438	3198.16990	
1.201	7.129	25.241	1.501	2.152	5.208	0.288	3.177	0.302	0.040	3.141	0.473	3198.22040	0.440	3198.17056	
													0.446	3198.17122	
													0.448	3198.17188	
													0.443	3198.17255	
													0.434	3198.17321	

EDXRF												Hyperspectral Imagery		
Mg	Al	Si	S	K	Ca	Ti	Fe	K/Al	Ti/Al	Si bio	S/Fe	Depth	TOC	Depth
%	%	%	%	%	%	%	%			%		m	%	m
													0.434	3198.17387
													0.434	3198.17453
													0.434	3198.17519
													0.440	3198.17586
													0.451	3198.17652
													0.462	3198.17718
													0.472	3198.17784
													0.483	3198.17850
													0.485	3198.17917
													0.478	3198.17983
													0.463	3198.18049
													0.450	3198.18115
													0.448	3198.18181
													0.447	3198.18247
													0.453	3198.18314
													0.458	3198.18380
													0.460	3198.18446
													0.456	3198.18512
													0.450	3198.18578
													0.448	3198.18645
													0.456	3198.18711
													0.471	3198.18777
													0.477	3198.18843
													0.475	3198.18909
													0.471	3198.18975
													0.481	3198.19042
													0.494	3198.19108
													0.502	3198.19174
													0.502	3198.19240
													0.494	3198.19306
													0.481	3198.19373
													0.467	3198.19439
													0.454	3198.19505
													0.438	3198.19571
													0.429	3198.19637
													0.419	3198.19704
													0.406	3198.19770
													0.406	3198.19836
													0.410	3198.19902
													0.414	3198.19968
													0.412	3198.20034
													0.413	3198.20101
													0.419	3198.20167
													0.436	3198.20233
													0.444	3198.20299
													0.449	3198.20365
													0.459	3198.20432
													0.473	3198.20498
													0.482	3198.20564
													0.482	3198.20630
													0.478	3198.20696
													0.477	3198.20763
													0.479	3198.20829
													0.486	3198.20895
													0.492	3198.20961
													0.492	3198.21027
													0.493	3198.21093
													0.487	3198.21160
													0.474	3198.21226
													0.468	3198.21292
													0.478	3198.21358

EDXRF												Hyperspectral Imagery		
Mg	Al	Si	S	K	Ca	Ti	Fe	K/Al	Ti/Al	Si bio	S/Fe	Depth	TOC	Depth
%	%	%	%	%	%	%	%			%		m	%	m
													0.485	3198.21424
													0.484	3198.21491
													0.483	3198.21557
													0.480	3198.21623
													0.474	3198.21689
													0.452	3198.21755
													0.423	3198.21821
													0.407	3198.21888
													0.405	3198.21954
													0.398	3198.22020
													0.393	3198.22086

Slab 3199.11 m

EDXRF													Hyperspectral Imagery		
Mg %	Al %	Si %	S %	K %	Ca %	Ti %	Fe %	K/Al	Ti/Al	Si bio %	S/Fe	Depth m	TOC %	Depth m	
1.687	6.484	21.477	1.222	1.809	8.934	0.288	3.460	0.279	0.044	1.376	0.353	3199.14733	0.421	3199.14701	
1.639	6.390	21.328	1.259	1.832	8.978	0.288	3.521	0.287	0.045	1.520	0.357	3199.14862	0.410	3199.14755	
1.718	6.823	22.830	0.993	2.015	7.922	0.327	3.042	0.295	0.048	1.677	0.326	3199.14990	0.429	3199.14808	
1.288	6.801	23.160	1.129	2.072	7.802	0.323	3.081	0.305	0.047	2.077	0.367	3199.15119	0.427	3199.14862	
1.126	6.996	23.934	1.312	2.231	6.826	0.319	2.981	0.319	0.046	2.247	0.440	3199.15248	0.414	3199.14915	
1.534	6.061	20.346	1.159	1.630	10.599	0.258	3.277	0.269	0.043	1.556	0.354	3199.15377	0.418	3199.14969	
1.779	5.639	19.088	1.169	1.485	11.604	0.245	3.731	0.263	0.043	1.608	0.313	3199.15505	0.404	3199.15023	
1.657	6.312	21.255	1.106	1.752	9.492	0.280	3.360	0.278	0.044	1.689	0.329	3199.15634	0.398	3199.15076	
1.832	6.056	20.563	1.578	1.710	9.117	0.267	3.892	0.282	0.044	1.790	0.405	3199.15763	0.394	3199.15130	
1.674	6.401	21.500	1.545	1.846	8.392	0.284	3.587	0.288	0.044	1.658	0.431	3199.15892	0.402	3199.15184	
1.459	6.779	22.585	1.206	1.959	8.069	0.262	3.146	0.289	0.039	1.571	0.383	3199.16020	0.415	3199.15237	
1.433	6.523	22.178	1.375	1.964	8.284	0.280	3.360	0.301	0.043	1.957	0.409	3199.16149	0.429	3199.15291	
1.560	6.629	22.626	1.239	1.954	8.069	0.332	3.164	0.295	0.050	2.077	0.392	3199.16278	0.447	3199.15345	
1.481	6.684	22.961	1.226	2.011	7.810	0.297	3.037	0.301	0.044	2.240	0.403	3199.16406	0.433	3199.15398	
1.433	6.940	23.708	1.066	2.091	7.292	0.332	2.863	0.301	0.048	2.193	0.372	3199.16535	0.408	3199.15452	
1.302	7.068	23.857	1.398	2.203	6.686	0.314	2.920	0.312	0.044	1.946	0.479	3199.16664	0.411	3199.15505	
1.411	6.695	22.486	1.116	1.987	8.496	0.297	2.950	0.297	0.044	1.730	0.378	3199.16793	0.411	3199.15559	
1.481	5.878	19.816	1.189	1.569	11.368	0.271	3.268	0.267	0.046	1.595	0.364	3199.16921	0.415	3199.15613	
1.586	6.673	22.269	1.093	1.936	8.432	0.280	3.273	0.290	0.042	1.582	0.334	3199.17050	0.419	3199.15666	
1.788	6.306	21.147	1.209	1.790	9.149	0.280	3.574	0.284	0.044	1.598	0.338	3199.17179	0.421	3199.15720	
1.832	6.356	21.463	1.375	1.757	8.671	0.293	3.556	0.276	0.046	1.759	0.387	3199.17308	0.424	3199.15774	
1.551	6.768	22.594	1.302	1.973	7.870	0.284	3.186	0.292	0.042	1.614	0.409	3199.17436	0.425	3199.15827	
1.490	6.734	23.029	1.096	1.964	7.962	0.336	3.055	0.292	0.050	2.152	0.359	3199.17565	0.430	3199.15881	
1.687	6.462	21.522	1.126	1.795	9.073	0.301	3.438	0.278	0.047	1.490	0.327	3199.17694	0.420	3199.15935	
1.499	6.562	22.789	1.053	1.922	8.244	0.306	3.168	0.293	0.047	2.447	0.332	3199.17822	0.431	3199.15988	
1.525	6.228	20.979	1.049	1.734	9.878	0.271	3.404	0.278	0.043	1.672	0.308	3199.17951	0.451	3199.16042	
1.985	5.550	18.595	1.282	1.438	11.468	0.254	4.079	0.259	0.046	1.391	0.314	3199.18080	0.466	3199.16095	
1.976	5.761	19.794	1.179	1.551	10.540	0.262	3.892	0.269	0.046	1.935	0.303	3199.18209	0.480	3199.16149	
1.849	6.123	20.586	1.129	1.677	9.830	0.267	3.704	0.274	0.044	1.606	0.305	3199.18337	0.483	3199.16203	
1.740	6.295	21.174	1.139	1.752	9.261	0.271	3.600	0.278	0.043	1.659	0.316	3199.18466	0.479	3199.16256	
1.578	6.640	22.196	1.133	1.978	8.412	0.332	3.290	0.298	0.050	1.613	0.344	3199.18595	0.492	3199.16310	
1.372	6.723	23.445	1.103	2.039	7.615	0.319	3.020	0.303	0.047	2.603	0.365	3199.18723	0.478	3199.16364	
1.486	6.762	23.033	0.923	2.034	8.049	0.336	3.046	0.301	0.050	2.071	0.303	3199.18852	0.462	3199.16417	
1.525	6.200	21.477	1.249	1.743	9.356	0.284	3.417	0.281	0.046	2.256	0.366	3199.18981	0.429	3199.16471	
1.411	6.629	22.318	1.069	1.978	8.603	0.297	3.120	0.298	0.045	1.770	0.343	3199.19110	0.418	3199.16524	
1.998	6.006	19.377	1.106	1.579	10.739	0.241	3.861	0.263	0.040	0.760	0.286	3199.19210	0.435	3199.16578	
1.718	5.972	19.368	1.083	1.593	10.978	0.262	3.931	0.267	0.044	0.854	0.275	3199.19318	0.444	3199.16632	
1.766	5.894	19.522	1.083	1.527	11.149	0.245	3.722	0.259	0.042	1.249	0.291	3199.19427	0.468	3199.16685	
1.727	5.744	19.721	1.275	1.546	10.962	0.249	3.626	0.269	0.043	1.914	0.352	3199.19536	0.460	3199.16739	
1.836	5.972	20.649	1.139	1.673	9.962	0.267	3.609	0.280	0.045	2.135	0.316	3199.19644	0.461	3199.16793	
1.705	6.417	21.617	1.126	1.889	8.958	0.301	3.347	0.294	0.047	1.723	0.336	3199.19753	0.461	3199.16846	
1.547	6.729	22.504	1.073	1.973	8.193	0.319	3.173	0.293	0.047	1.645	0.338	3199.19862	0.462	3199.16900	
1.437	6.940	23.183	1.076	2.081	7.667	0.319	2.950	0.300	0.046	1.668	0.365	3199.19970	0.458	3199.16954	
1.372	7.024	23.789	1.020	2.128	7.244	0.288	2.841	0.303	0.041	2.016	0.359	3199.20079	0.474	3199.17007	
1.341	7.101	23.708	1.086	2.166	7.204	0.336	2.846	0.305	0.047	1.693	0.382	3199.20188	0.470	3199.17061	
1.267	7.035	24.269	1.036	2.203	6.938	0.297	2.771	0.313	0.042	2.461	0.374	3199.20296	0.472	3199.17114	
1.372	6.868	23.174	1.046	2.053	7.842	0.306	2.968	0.299	0.044	1.883	0.353	3199.20405	0.468	3199.17168	
1.547	6.267	20.735	0.973	1.715	10.424	0.249	3.151	0.274	0.040	1.307	0.309	3199.20514	0.453	3199.17222	
1.586	5.989	19.703	0.953	1.574	11.615	0.275	3.264	0.263	0.046	1.137	0.292	3199.20622	0.428	3199.17275	
1.692	5.789	19.739	1.066	1.532	11.205	0.258	3.582	0.265	0.045	1.794	0.298	3199.20731	0.432	3199.17329	
1.801	5.978	20.165	1.126	1.621	10.440	0.288	3.683	0.271	0.048	1.633	0.306	3199.20840	0.435	3199.17383	
													0.420	3199.17436	
													0.430	3199.17490	
													0.458	3199.17544	
													0.486	3199.17597	
													0.498	3199.17651	
													0.493	3199.17704	
													0.492	3199.17758	
													0.502	3199.17812	
													0.474	3199.17865	
													0.507	3199.17919	

EDXRF												Hyperspectral Imagery		
Mg	Al	Si	S	K	Ca	Ti	Fe	K/Al	Ti/Al	Si bio	S/Fe	Depth	TOC	Depth
%	%	%	%	%	%	%	%			%		m	%	m
													0.477	3199.17973
													0.455	3199.18026
													0.443	3199.18080
													0.451	3199.18134
													0.426	3199.18187
													0.448	3199.18241
													0.445	3199.18294
													0.474	3199.18348
													0.472	3199.18402
													0.474	3199.18455
													0.476	3199.18509
													0.487	3199.18563
													0.537	3199.18616
													0.503	3199.18670
													0.506	3199.18724
													0.504	3199.18795
													0.499	3199.18867
													0.498	3199.18938
													0.505	3199.19010
													0.478	3199.19081
													0.488	3199.19152
													0.454	3199.19224
													0.448	3199.19295
													0.465	3199.19367
													0.463	3199.19438
													0.478	3199.19510
													0.476	3199.19581
													0.473	3199.19653
													0.452	3199.19724
													0.409	3199.19796
													0.420	3199.19867
													0.438	3199.19939
													0.496	3199.20010
													0.498	3199.20082
													0.515	3199.20153
													0.513	3199.20225
													0.540	3199.20296
													0.533	3199.20368
													0.516	3199.20439
													0.504	3199.20511
													0.511	3199.20582
													0.515	3199.20654
													0.500	3199.20725
													0.496	3199.20797
													0.481	3199.20868
													0.505	3199.20940
													0.486	3199.21011
													0.505	3199.21083
													0.503	3199.21154
													0.493	3199.21226
													0.501	3199.21297
													0.547	3199.21369
													0.532	3199.21440
													0.501	3199.21512

Slab 3200.21 m

EDXRF													Hyperspectral Imagery		
Mg %	Al %	Si %	S %	K %	Ca %	Ti %	Fe %	K/Al	Ti/Al	Si bio %	S/Fe	Depth m	TOC %	Depth m	
1.109	5.733	18.405	1.478	1.710	12.978	0.241	2.802	0.298	0.042	0.632	0.528	3200.21879	0.290	3200.21905	
1.214	5.861	18.595	1.521	1.715	12.636	0.271	2.732	0.293	0.046	0.425	0.557	3200.22025	0.288	3200.21972	
1.012	5.989	19.472	1.139	1.813	12.612	0.297	2.405	0.303	0.050	0.906	0.474	3200.22172	0.277	3200.22039	
1.043	6.078	19.663	1.043	1.870	12.556	0.319	2.279	0.308	0.052	0.821	0.458	3200.22318	0.279	3200.22107	
1.004	5.950	19.699	1.016	1.903	12.584	0.301	2.279	0.320	0.051	1.253	0.446	3200.22465	0.279	3200.22174	
0.942	6.028	19.803	1.136	1.879	12.384	0.249	2.300	0.312	0.041	1.116	0.494	3200.22611	0.277	3200.22242	
0.868	6.173	20.576	0.794	1.950	12.213	0.301	2.065	0.316	0.049	1.441	0.384	3200.22757	0.277	3200.22309	
1.157	5.933	18.495	1.455	1.781	12.480	0.232	2.946	0.300	0.039	0.102	0.494	3200.22904	0.275	3200.22376	
1.240	5.583	17.844	1.844	1.626	12.643	0.249	3.220	0.291	0.045	0.536	0.572	3200.23050	0.274	3200.22444	
1.179	5.867	18.346	1.744	1.734	12.400	0.267	2.963	0.296	0.045	0.159	0.589	3200.23197	0.271	3200.22511	
1.004	5.894	18.667	1.687	1.799	12.305	0.280	2.911	0.305	0.047	0.394	0.580	3200.23343	0.271	3200.22579	
1.078	5.967	18.884	1.731	1.790	12.010	0.306	2.937	0.300	0.051	0.387	0.589	3200.23490	0.270	3200.22646	
1.083	5.928	18.975	1.714	1.818	11.942	0.280	2.907	0.307	0.047	0.598	0.590	3200.23636	0.282	3200.22713	
1.140	5.950	18.739	1.531	1.757	12.396	0.284	2.784	0.295	0.048	0.294	0.550	3200.23783	0.292	3200.22781	
1.083	6.028	18.536	1.345	1.743	12.552	0.267	2.937	0.289	0.044	-0.151	0.458	3200.23929	0.292	3200.22848	
1.293	5.933	18.703	1.319	1.738	12.528	0.262	2.780	0.293	0.044	0.310	0.474	3200.24075	0.295	3200.22916	
0.907	5.995	18.916	1.505	1.762	12.349	0.284	2.872	0.294	0.047	0.333	0.524	3200.24222	0.298	3200.22983	
1.052	6.095	19.142	1.634	1.828	11.862	0.323	2.872	0.300	0.053	0.249	0.569	3200.24368	0.301	3200.23050	
1.135	6.167	19.631	1.302	1.856	11.878	0.275	2.562	0.301	0.045	0.513	0.508	3200.24515	0.299	3200.23118	
1.087	6.239	19.925	1.352	1.893	11.508	0.297	2.562	0.303	0.048	0.583	0.528	3200.24661	0.299	3200.23185	
1.100	6.406	20.794	1.358	2.015	10.520	0.271	2.532	0.315	0.042	0.934	0.537	3200.24808	0.302	3200.23253	
0.877	6.067	19.138	1.920	1.818	11.456	0.267	3.085	0.300	0.044	0.330	0.622	3200.24954	0.301	3200.23320	
0.872	5.733	18.169	2.156	1.720	12.054	0.254	3.329	0.300	0.044	0.397	0.648	3200.25101	0.289	3200.23387	
1.078	5.789	18.595	1.850	1.729	12.082	0.262	3.120	0.299	0.045	0.649	0.593	3200.25247	0.287	3200.23455	
1.087	5.800	18.368	2.040	1.762	11.882	0.236	3.164	0.304	0.041	0.389	0.645	3200.25394	0.287	3200.23522	
0.969	5.917	18.658	2.050	1.851	11.588	0.258	3.190	0.313	0.044	0.316	0.643	3200.25540	0.284	3200.23590	
0.995	6.028	18.807	1.614	1.846	11.922	0.275	3.011	0.306	0.046	0.121	0.536	3200.25740	0.285	3200.23657	
1.153	6.173	18.491	1.601	1.813	11.942	0.275	3.077	0.294	0.045	-0.644	0.520	3200.25890	0.283	3200.23724	
1.201	5.878	17.948	1.751	1.738	12.392	0.327	3.212	0.296	0.056	-0.273	0.545	3200.26039	0.280	3200.23792	
1.175	5.805	17.934	1.601	1.696	12.763	0.254	3.129	0.292	0.044	-0.063	0.512	3200.26189	0.276	3200.23859	
0.793	5.833	17.807	1.830	1.752	12.783	0.284	3.290	0.300	0.049	-0.276	0.556	3200.26339	0.284	3200.23927	
0.325	5.683	17.884	1.564	1.893	13.189	0.332	3.334	0.333	0.058	0.267	0.469	3200.26489	0.281	3200.23994	
1.236	6.034	18.654	1.329	1.795	12.460	0.336	2.872	0.297	0.056	-0.050	0.463	3200.26638	0.293	3200.24061	
1.262	6.111	18.735	1.435	1.828	12.169	0.301	2.828	0.299	0.049	-0.210	0.507	3200.26788	0.289	3200.24129	
1.126	6.006	18.893	1.761	1.856	11.687	0.271	2.989	0.309	0.045	0.276	0.589	3200.26938	0.296	3200.24196	
0.894	5.700	17.853	2.173	1.677	12.153	0.241	3.434	0.294	0.042	0.183	0.633	3200.27087	0.286	3200.24264	
0.925	4.604	15.043	2.458	1.278	14.915	0.219	3.975	0.278	0.048	0.770	0.618	3200.27237	0.293	3200.24331	
1.074	5.155	16.645	1.970	1.438	13.831	0.275	3.539	0.279	0.053	0.665	0.557	3200.27387	0.290	3200.24398	
0.495	4.888	15.839	2.399	1.410	14.249	0.275	4.127	0.288	0.056	0.687	0.581	3200.27536	0.290	3200.24466	
0.653	5.416	17.219	1.618	1.518	14.054	0.306	3.377	0.280	0.056	0.429	0.479	3200.27686	0.291	3200.24533	
0.723	5.711	18.255	1.392	1.691	13.301	0.284	3.037	0.296	0.050	0.552	0.458	3200.27836	0.293	3200.24601	
1.122	5.644	17.690	1.249	1.621	13.775	0.319	3.033	0.287	0.056	0.193	0.412	3200.27986	0.289	3200.24668	
1.332	5.817	17.762	1.179	1.649	13.560	0.297	2.837	0.284	0.051	-0.269	0.416	3200.28135	0.291	3200.24735	
1.534	5.889	17.943	1.126	1.687	13.173	0.293	2.828	0.286	0.050	-0.312	0.398	3200.28285	0.303	3200.24803	
1.078	5.917	18.178	1.206	1.734	13.253	0.297	2.841	0.293	0.050	-0.163	0.424	3200.28435	0.309	3200.24870	
1.258	5.900	18.115	1.189	1.729	13.173	0.327	2.863	0.293	0.055	-0.175	0.415	3200.28584	0.304	3200.24938	
1.061	5.722	18.251	1.219	1.776	13.273	0.275	2.889	0.310	0.048	0.513	0.422	3200.28734	0.297	3200.25005	
1.262	5.883	18.368	1.245	1.715	12.859	0.262	2.898	0.291	0.045	0.130	0.430	3200.28884	0.289	3200.25072	
1.091	5.939	18.577	1.368	1.781	12.687	0.314	2.885	0.300	0.053	0.166	0.474	3200.29033	0.281	3200.25140	
1.236	6.089	18.405	1.342	1.785	12.592	0.249	2.850	0.293	0.041	-0.472	0.471	3200.29183	0.273	3200.25207	
1.214	6.212	18.215	1.395	1.809	12.536	0.297	2.933	0.291	0.048	-1.041	0.476	3200.29333	0.276	3200.25275	
1.188	6.089	18.654	1.458	1.781	12.145	0.301	3.011	0.292	0.049	-0.223	0.484	3200.29483	0.283	3200.25342	
0.916	6.189	18.943	1.734	1.832	11.544	0.301	3.173	0.296	0.049	-0.244	0.547	3200.29632	0.288	3200.25409	
1.131	5.995	18.527	2.020	1.795	11.436	0.310	3.316	0.299	0.052	-0.056	0.609	3200.29782	0.291	3200.25477	
1.170	5.983	17.957	1.867	1.832	11.743	0.301	3.617	0.306	0.050	-0.592	0.516	3200.29932	0.289	3200.25544	
1.144	5.839	18.043	2.475	1.710	11.213	0.245	3.709	0.293	0.042	-0.058	0.667	3200.30081	0.287	3200.25612	
1.275	6.117	19.260	1.348	1.818	11.855	0.297	2.819	0.297	0.049	0.297	0.478	3200.30231	0.289	3200.25679	
0.977	6.161	19.350	1.329	1.865	11.990	0.271	2.750	0.303	0.044	0.250	0.483	3200.30380	0.295	3200.25746	
													0.298	3200.25814	
													0.302	3200.25881	
													0.301	3200.25949	

EDXRF													Hyperspectral Imagery	
Mg	Al	Si	S	K	Ca	Ti	Fe	K/Al	Ti/Al	Si bio	S/Fe	Depth	TOC	Depth
%	%	%	%	%	%	%	%			%		m	%	m
													0.299	3200.26016
													0.295	3200.26083
													0.293	3200.26151
													0.292	3200.26218
													0.293	3200.26286
													0.292	3200.26353
													0.289	3200.26420
													0.279	3200.26488
													0.274	3200.26555
													0.274	3200.26623
													0.276	3200.26690
													0.278	3200.26757
													0.280	3200.26825
													0.284	3200.26892
													0.283	3200.26960
													0.277	3200.27027
													0.271	3200.27094
													0.270	3200.27162
													0.269	3200.27229
													0.270	3200.27297
													0.272	3200.27364
													0.278	3200.27431
													0.279	3200.27499
													0.282	3200.27566
													0.281	3200.27634
													0.274	3200.27701
													0.278	3200.27768
													0.278	3200.27836
													0.282	3200.27903
													0.280	3200.27971
													0.277	3200.28038
													0.266	3200.28105
													0.273	3200.28173
													0.265	3200.28240
													0.266	3200.28308
													0.272	3200.28375
													0.268	3200.28442
													0.262	3200.28510
													0.270	3200.28577
													0.277	3200.28645
													0.277	3200.28712
													0.277	3200.28779
													0.286	3200.28847
													0.269	3200.28914
													0.269	3200.28982
													0.274	3200.29049
													0.266	3200.29116
													0.275	3200.29184
													0.280	3200.29251
													0.282	3200.29319
													0.285	3200.29386
													0.289	3200.29453
													0.289	3200.29521
													0.279	3200.29588
													0.273	3200.29656
													0.277	3200.29723
													0.269	3200.29790
													0.271	3200.29858
													0.275	3200.29925

Slab 3201.03 m

EDXRF												Hyperspectral Imagery		
Mg %	Al %	Si %	S %	K %	Ca %	Ti %	Fe %	K/Al	Ti/Al	Si bio %	S/Fe	Depth m	TOC %	Depth m
0.999	5.666	18.301	1.069	1.743	13.911	0.245	2.536	0.308	0.043	0.735	0.422	3201.06351	0.327	3201.06392
1.104	5.411	16.966	1.850	1.640	13.731	0.232	3.234	0.303	0.043	0.193	0.572	3201.06471	0.328	3201.06478
1.310	5.611	17.563	1.236	1.710	14.050	0.267	2.675	0.305	0.048	0.170	0.462	3201.06590	0.322	3201.06563
1.363	5.661	17.337	1.176	1.720	14.285	0.249	2.614	0.304	0.044	-0.212	0.450	3201.06710	0.319	3201.06649
1.030	5.833	17.984	1.285	1.743	13.739	0.262	2.606	0.299	0.045	-0.099	0.493	3201.06910	0.308	3201.06735
1.056	5.861	17.889	1.312	1.785	13.695	0.241	2.614	0.305	0.041	-0.281	0.502	3201.07049	0.303	3201.06820
0.846	5.132	15.803	2.698	1.499	13.751	0.215	3.896	0.292	0.042	-0.107	0.692	3201.07187	0.303	3201.06906
1.148	5.188	16.174	2.056	1.518	14.452	0.215	3.220	0.293	0.041	0.091	0.639	3201.07326	0.301	3201.06992
1.253	4.999	15.500	1.561	1.457	15.767	0.219	3.125	0.291	0.044	0.003	0.500	3201.07465	0.295	3201.07077
1.280	5.166	15.740	1.415	1.424	15.692	0.197	3.011	0.276	0.038	-0.274	0.470	3201.07604	0.288	3201.07163
1.069	5.004	15.703	1.691	1.461	15.397	0.223	3.321	0.292	0.045	0.190	0.509	3201.07742	0.282	3201.07249
1.341	4.910	15.378	2.016	1.443	15.070	0.249	3.486	0.294	0.051	0.157	0.578	3201.07881	0.295	3201.07334
1.214	5.227	15.360	1.937	1.518	14.556	0.210	3.822	0.290	0.040	-0.844	0.507	3201.08020	0.286	3201.07420
1.227	5.360	15.943	1.508	1.499	15.070	0.236	3.203	0.280	0.044	-0.674	0.471	3201.08158	0.263	3201.07506
1.153	5.266	16.138	1.093	1.551	15.963	0.232	2.706	0.294	0.044	-0.187	0.404	3201.08297	0.269	3201.07591
1.205	5.483	16.355	1.043	1.551	15.704	0.245	2.671	0.283	0.045	-0.642	0.390	3201.08436	0.275	3201.07677
1.332	5.333	16.626	1.020	1.593	15.477	0.258	2.632	0.299	0.048	0.095	0.387	3201.08574	0.276	3201.07763
1.258	5.355	16.640	1.073	1.579	15.457	0.245	2.623	0.295	0.046	0.040	0.409	3201.08713	0.268	3201.07848
1.192	5.288	16.758	1.063	1.630	15.345	0.241	2.619	0.308	0.045	0.364	0.406	3201.08852	0.261	3201.07934
1.236	5.411	16.830	0.980	1.630	15.345	0.275	2.623	0.301	0.051	0.057	0.373	3201.08991	0.255	3201.08020
1.078	5.488	17.142	1.036	1.659	15.090	0.280	2.588	0.302	0.051	0.128	0.400	3201.09129	0.251	3201.08105
1.135	5.511	16.821	1.325	1.630	14.640	0.232	2.898	0.296	0.042	-0.262	0.457	3201.09268	0.255	3201.08191
1.109	5.505	16.961	1.033	1.640	15.114	0.228	2.649	0.298	0.041	-0.104	0.390	3201.09407	0.259	3201.08277
1.183	5.572	17.165	1.033	1.640	14.883	0.267	2.614	0.294	0.048	-0.108	0.395	3201.09545	0.260	3201.08362
1.179	5.683	17.224	1.026	1.682	14.739	0.271	2.606	0.296	0.048	-0.394	0.394	3201.09684	0.266	3201.08448
1.280	5.488	17.350	0.963	1.654	14.799	0.245	2.549	0.301	0.045	0.336	0.378	3201.09823	0.271	3201.08534
1.280	5.661	17.577	0.920	1.710	14.564	0.254	2.457	0.302	0.045	0.028	0.374	3201.09961	0.265	3201.08619
1.232	5.678	17.296	0.923	1.691	14.831	0.232	2.484	0.298	0.041	-0.304	0.372	3201.10100	0.263	3201.08705
1.192	5.633	17.332	0.903	1.677	14.919	0.254	2.444	0.298	0.045	-0.130	0.370	3201.10239	0.265	3201.08791
1.196	5.622	17.563	0.870	1.724	14.807	0.232	2.375	0.307	0.041	0.135	0.366	3201.10378	0.267	3201.08876
1.135	5.633	17.880	0.893	1.781	14.604	0.245	2.287	0.316	0.043	0.417	0.391	3201.10516	0.267	3201.08962
1.113	5.650	17.785	0.917	1.771	14.612	0.241	2.327	0.314	0.043	0.271	0.394	3201.10655	0.268	3201.09048
1.131	5.611	18.147	0.936	1.743	14.333	0.245	2.309	0.311	0.044	0.753	0.406	3201.10794	0.272	3201.09133
0.903	5.705	18.414	0.671	1.767	14.604	0.271	2.209	0.310	0.047	0.727	0.304	3201.10932	0.271	3201.09219
1.341	5.438	16.486	1.634	1.536	14.209	0.254	3.286	0.283	0.047	-0.373	0.497	3201.11071	0.270	3201.09305
1.205	5.422	16.798	1.309	1.621	14.700	0.267	2.937	0.299	0.049	-0.009	0.446	3201.11210	0.268	3201.09390
													0.267	3201.09476
													0.269	3201.09562
													0.265	3201.09647
													0.271	3201.09733
													0.273	3201.09819
													0.278	3201.09904
													0.278	3201.09990
													0.271	3201.10076
													0.264	3201.10161
													0.273	3201.10247
													0.282	3201.10333
													0.287	3201.10418
													0.284	3201.10504
													0.279	3201.10590
													0.275	3201.10675
													0.281	3201.10761
													0.272	3201.10847
													0.268	3201.10932
													0.265	3201.11018
													0.261	3201.11104
													0.259	3201.11189

Slab 3202.4 m

EDXRF													Hyperspectral Imagery	
Mg %	Al %	Si %	S %	K %	Ca %	Ti %	Fe %	K/Al	Ti/Al	Si bio %	S/Fe	Depth m	TOC %	Depth m
1.271	5.093	15.400	1.043	1.536	16.999	0.241	2.440	0.302	0.047	-0.389	0.427	3202.42118	0.292	3202.42118
1.205	5.372	16.210	0.804	1.579	16.437	0.210	2.309	0.294	0.039	-0.442	0.348	3202.42250	0.294	3202.42184
1.157	5.160	15.889	1.063	1.574	16.576	0.232	2.427	0.305	0.045	-0.108	0.438	3202.42383	0.299	3202.42250
1.153	5.266	15.889	1.013	1.569	16.592	0.249	2.409	0.298	0.047	-0.435	0.420	3202.42515	0.289	3202.42317
1.324	5.344	15.762	0.996	1.546	16.524	0.236	2.405	0.289	0.044	-0.803	0.414	3202.42648	0.287	3202.42383
1.223	5.132	15.446	1.093	1.504	16.772	0.249	2.597	0.293	0.049	-0.465	0.421	3202.42780	0.276	3202.42449
1.275	5.043	15.378	1.139	1.485	16.736	0.232	2.671	0.294	0.046	-0.257	0.426	3202.42912	0.277	3202.42515
1.328	5.210	15.269	1.179	1.513	16.584	0.228	2.732	0.290	0.044	-0.883	0.432	3202.43045	0.281	3202.42581
1.157	5.299	15.749	1.049	1.555	16.301	0.249	2.732	0.293	0.047	-0.679	0.384	3202.43177	0.288	3202.42648
1.341	6.000	17.577	0.810	1.752	14.022	0.262	2.854	0.292	0.044	-1.024	0.284	3202.43310	0.280	3202.42714
1.345	5.271	16.360	0.897	1.527	16.210	0.197	2.331	0.290	0.037	0.018	0.385	3202.43442	0.274	3202.42780
1.109	4.910	15.124	1.581	1.471	16.528	0.184	2.885	0.300	0.038	-0.096	0.548	3202.43574	0.284	3202.42846
1.056	4.899	15.201	1.528	1.452	16.660	0.223	2.841	0.296	0.046	0.015	0.538	3202.43707	0.278	3202.42912
1.144	5.066	15.826	1.103	1.541	16.616	0.210	2.510	0.304	0.041	0.122	0.439	3202.43839	0.277	3202.42979
1.284	5.989	18.147	0.674	1.757	14.062	0.241	2.488	0.293	0.040	-0.419	0.271	3202.43971	0.261	3202.43045
1.205	5.522	17.169	0.933	1.626	15.297	0.228	2.366	0.294	0.041	0.052	0.394	3202.44104	0.260	3202.43111
1.030	5.166	16.056	1.312	1.555	16.138	0.206	2.553	0.301	0.040	0.042	0.514	3202.44236	0.265	3202.43177
0.977	5.249	16.007	1.255	1.560	16.198	0.197	2.575	0.297	0.038	-0.266	0.488	3202.44369	0.257	3202.43243
1.131	5.077	15.830	1.332	1.565	16.269	0.193	2.601	0.308	0.038	0.092	0.512	3202.44501	0.253	3202.43310
1.034	5.110	15.468	1.644	1.513	16.046	0.215	2.959	0.296	0.042	-0.373	0.556	3202.44633	0.247	3202.43376
0.964	5.032	15.369	1.551	1.513	16.421	0.193	2.819	0.301	0.038	-0.231	0.550	3202.44766	0.248	3202.43442
1.126	5.016	15.613	1.355	1.527	16.505	0.202	2.606	0.304	0.040	0.065	0.520	3202.44898	0.249	3202.43508
1.262	5.182	15.464	1.292	1.541	16.505	0.223	2.575	0.297	0.043	-0.602	0.502	3202.45030	0.250	3202.43574
1.078	5.149	15.622	1.239	1.574	16.592	0.215	2.510	0.306	0.042	-0.340	0.494	3202.45163	0.256	3202.43640
1.122	5.166	15.464	1.172	1.536	16.748	0.223	2.514	0.297	0.043	-0.550	0.466	3202.45295	0.267	3202.43707
1.008	5.477	15.848	1.106	1.583	15.843	0.236	3.055	0.289	0.043	-1.131	0.362	3202.45428	0.275	3202.43773
1.104	5.110	15.617	1.202	1.560	16.369	0.197	2.824	0.305	0.039	-0.224	0.426	3202.45560	0.283	3202.43839
1.192	5.071	15.522	1.192	1.527	16.700	0.189	2.553	0.301	0.037	-0.198	0.467	3202.45692	0.280	3202.43905
1.236	5.171	15.477	1.106	1.522	16.756	0.206	2.501	0.294	0.040	-0.554	0.442	3202.45825	0.282	3202.43971
1.043	5.171	15.459	1.159	1.541	16.903	0.215	2.518	0.298	0.041	-0.572	0.460	3202.45957	0.283	3202.44038
1.004	5.188	15.346	1.109	1.485	17.086	0.241	2.523	0.286	0.046	-0.737	0.440	3202.46090	0.270	3202.44104
1.310	4.966	15.283	1.269	1.466	16.772	0.215	2.654	0.295	0.043	-0.111	0.478	3202.46222	0.264	3202.44170
1.030	4.960	14.930	1.368	1.485	17.058	0.197	2.763	0.299	0.040	-0.446	0.495	3202.46354	0.259	3202.44236
1.083	5.004	15.075	1.073	1.447	17.485	0.215	2.475	0.289	0.043	-0.439	0.433	3202.46487	0.263	3202.44302
1.157	4.927	15.093	1.079	1.485	17.389	0.219	2.536	0.301	0.044	-0.180	0.426	3202.46619	0.268	3202.44369
1.196	5.055	15.034	1.053	1.475	17.353	0.241	2.518	0.292	0.048	-0.635	0.418	3202.46751	0.270	3202.44435
1.201	4.904	15.093	1.123	1.461	17.429	0.228	2.484	0.298	0.046	-0.111	0.452	3202.46884	0.269	3202.44501
1.140	4.949	15.111	1.029	1.471	17.473	0.215	2.471	0.297	0.043	-0.231	0.417	3202.47016	0.271	3202.44567
1.315	5.010	15.084	1.049	1.447	17.409	0.232	2.418	0.289	0.046	-0.448	0.434	3202.47149	0.268	3202.44633
1.297	4.899	14.844	1.142	1.438	17.457	0.232	2.497	0.294	0.047	-0.342	0.458	3202.47281	0.264	3202.44700
1.376	4.888	14.948	1.089	1.466	17.417	0.223	2.462	0.300	0.046	-0.204	0.442	3202.47413	0.264	3202.44766
1.188	4.943	14.943	1.069	1.447	17.580	0.228	2.488	0.293	0.046	-0.381	0.430	3202.47546	0.274	3202.44832
1.166	4.810	14.731	1.166	1.438	17.684	0.262	2.632	0.299	0.055	-0.180	0.443	3202.47678	0.278	3202.44898
1.091	4.899	14.835	1.179	1.447	17.497	0.180	2.627	0.295	0.037	-0.352	0.449	3202.47810	0.288	3202.44964
1.122	5.004	14.975	1.136	1.461	17.437	0.210	2.527	0.292	0.042	-0.539	0.449	3202.47943	0.294	3202.45031
1.240	4.949	15.025	1.096	1.466	17.337	0.189	2.518	0.296	0.038	-0.317	0.435	3202.48075	0.297	3202.45097
1.319	5.055	15.007	1.079	1.424	17.238	0.249	2.558	0.282	0.049	-0.662	0.422	3202.48208	0.295	3202.45163
1.245	4.932	14.645	1.036	1.438	17.676	0.228	2.562	0.292	0.046	-0.645	0.404	3202.48340	0.296	3202.45229
													0.298	3202.45295
													0.292	3202.45361
													0.292	3202.45428
													0.294	3202.45494
													0.287	3202.45560
													0.287	3202.45626
													0.286	3202.45692
													0.280	3202.45759
													0.278	3202.45825
													0.281	3202.45891
													0.279	3202.45957
													0.277	3202.46023
													0.264	3202.46090

EDXRF												Hyperspectral Imagery		
Mg	Al	Si	S	K	Ca	Ti	Fe	K/Al	Ti/Al	Si bio	S/Fe	Depth	TOC	Depth
%	%	%	%	%	%	%	%			%		m	%	m
													0.262	3202.46156
													0.262	3202.46222
													0.270	3202.46288
													0.283	3202.46354
													0.294	3202.46421
													0.298	3202.46487
													0.297	3202.46553
													0.288	3202.46619
													0.282	3202.46685
													0.281	3202.46751
													0.277	3202.46818
													0.280	3202.46884
													0.276	3202.46950
													0.276	3202.47016
													0.262	3202.47082
													0.273	3202.47149
													0.279	3202.47215
													0.281	3202.47281
													0.285	3202.47347
													0.286	3202.47413
													0.286	3202.47480
													0.286	3202.47546
													0.282	3202.47612
													0.281	3202.47678
													0.276	3202.47744
													0.275	3202.47811
													0.273	3202.47877
													0.265	3202.47943
													0.259	3202.48009
													0.254	3202.48075
													0.248	3202.48141
													0.243	3202.48208
													0.240	3202.48274
													0.238	3202.48340

EDXRF												Hyperspectral Imagery		
Mg %	Al %	Si %	S %	K %	Ca %	Ti %	Fe %	K/Al	Ti/Al	Si bio %	S/Fe	Depth m	TOC %	Depth m
1.451	7.101	25.214	1.259	2.236	5.435	0.327	2.893	0.315	0.046	3.200	0.435	3203.87733	0.465	3203.88207
1.416	7.357	25.721	1.209	2.297	4.969	0.349	2.771	0.312	0.047	2.913	0.436	3203.87927	0.456	3203.88328
1.267	7.279	26.332	1.149	2.339	4.754	0.340	2.645	0.321	0.047	3.765	0.434	3203.88120	0.459	3203.88450
1.288	7.268	25.495	1.737	2.335	4.551	0.349	2.972	0.321	0.048	2.963	0.585	3203.88313	0.470	3203.88572
1.310	7.385	26.074	1.216	2.274	4.838	0.340	2.728	0.308	0.046	3.180	0.446	3203.88507	0.484	3203.88693
1.210	7.374	26.151	1.113	2.321	4.921	0.288	2.649	0.315	0.039	3.291	0.420	3203.88700	0.493	3203.88815
1.363	7.391	26.142	1.106	2.335	4.786	0.345	2.645	0.316	0.047	3.230	0.418	3203.88893	0.484	3203.88937
1.135	7.257	25.943	1.212	2.297	5.129	0.340	2.758	0.317	0.047	3.445	0.439	3203.89087	0.474	3203.89058
1.306	7.363	25.350	1.295	2.236	5.292	0.336	2.819	0.304	0.046	2.525	0.459	3203.89280	0.458	3203.89180
1.161	7.496	26.621	1.056	2.377	4.563	0.340	2.619	0.317	0.045	3.382	0.403	3203.89473	0.441	3203.89302
1.565	6.757	23.255	2.056	1.931	6.133	0.284	3.500	0.286	0.042	2.310	0.588	3203.89667	0.439	3203.89423
1.122	7.018	24.567	2.139	2.133	5.152	0.297	3.277	0.304	0.042	2.811	0.653	3203.89860	0.447	3203.89545
													0.460	3203.89667
													0.474	3203.89788
													0.470	3203.89910
													0.482	3203.90032

EDXRF													Hyperspectral Imagery	
Mg %	Al %	Si %	S %	K %	Ca %	Ti %	Fe %	K/Al	Ti/Al	Si bio %	S/Fe	Depth m	TOC %	Depth m
0.754	6.161	29.666	1.415	2.006	3.539	0.301	2.170	0.326	0.049	10.566	0.652	3204.88152	1.155	3204.86045
0.850	6.362	30.128	1.309	2.015	3.180	0.310	2.035	0.317	0.049	10.407	0.643	3204.88286	1.296	3204.86144
0.802	6.200	29.924	1.375	2.006	3.252	0.306	2.209	0.324	0.049	10.703	0.623	3204.88420	1.302	3204.86243
													1.176	3204.86342
													1.193	3204.86442
													1.191	3204.86541
													1.342	3204.86640
													1.782	3204.86740
													0.800	3204.86839
													0.769	3204.86938
													0.835	3204.87037
													0.868	3204.87137
													0.919	3204.87236
													0.919	3204.87335
													0.917	3204.87435
													1.005	3204.87534
													1.055	3204.87633
													1.108	3204.87732
													1.087	3204.87832
													1.047	3204.87931
													1.013	3204.88030
													1.110	3204.88130
													1.105	3204.88229
													1.063	3204.88328
													1.055	3204.88427

EDXRF												Hyperspectral Imagery		
Mg	Al	Si	S	K	Ca	Ti	Fe	K/Al	Ti/Al	Si bio	S/Fe	Depth	TOC	Depth
%	%	%	%	%	%	%	%			%		m	%	m
													0.918	3205.25934
													0.900	3205.26012
													0.878	3205.26090
													0.882	3205.26168
													0.901	3205.26246
													0.938	3205.26323
													0.927	3205.26401
													0.933	3205.26479
													0.918	3205.26557
													0.902	3205.26635
													0.901	3205.26713
													0.927	3205.26791
													0.932	3205.26869
													0.947	3205.26947
													0.889	3205.27025
													0.875	3205.27103
													0.851	3205.27181
													0.837	3205.27259
													0.841	3205.27337
													0.862	3205.27415
													0.870	3205.27493
													0.887	3205.27571
													0.887	3205.27649
													0.848	3205.27727
													0.789	3205.27805
													0.751	3205.27883
													0.737	3205.27961
													0.739	3205.28025
													0.699	3205.28089
													0.587	3205.28152
													0.524	3205.28216
													0.486	3205.28280
													0.473	3205.28344
													0.477	3205.28407
													0.487	3205.28471
													0.478	3205.28535
													0.467	3205.28599
													0.464	3205.28662
													0.489	3205.28726
													0.561	3205.28790
													0.701	3205.28854
													0.795	3205.28917
													0.828	3205.28981
													0.884	3205.29045
													0.906	3205.29109
													0.889	3205.29172
													0.845	3205.29236
													0.849	3205.29300
													0.840	3205.29364
													0.827	3205.29428
													0.833	3205.29491
													0.832	3205.29555
													0.840	3205.29619
													0.838	3205.29683

EDXRF												Hyperspectral Imagery		
Mg	Al	Si	S	K	Ca	Ti	Fe	K/Al	Ti/Al	Si bio	S/Fe	Depth	TOC	Depth
%	%	%	%	%	%	%	%			%		m	%	m
													0.902	3206.21686
													0.934	3206.21763
													0.936	3206.21840
													0.929	3206.21916
													0.950	3206.21993
													0.948	3206.22070
													0.971	3206.22147
													0.993	3206.22224
													0.990	3206.22300
													0.954	3206.22377
													0.944	3206.22454
													1.019	3206.22531
													1.142	3206.22608
													0.905	3206.22684
													0.830	3206.22761
													0.837	3206.22838
													0.875	3206.22915
													0.879	3206.22992
													0.902	3206.23068
													0.902	3206.23145
													0.900	3206.23222
													0.882	3206.23299
													0.885	3206.23376
													0.905	3206.23452
													0.932	3206.23529
													0.954	3206.23606
													0.952	3206.23683
													0.925	3206.23760
													0.898	3206.23837
													0.873	3206.23913
													0.872	3206.23990
													0.900	3206.24067
													0.912	3206.24144
													0.925	3206.24221
													0.941	3206.24297
													0.959	3206.24374
													0.907	3206.24451
													0.894	3206.24528
													0.868	3206.24605
													0.854	3206.24681
													0.846	3206.24758
													0.852	3206.24835
													0.893	3206.24912
													0.917	3206.24989
													0.889	3206.25065
													0.849	3206.25142
													0.834	3206.25219
													0.828	3206.25296
													0.843	3206.25373
													0.826	3206.25449
													0.812	3206.25526

Slab 3207.2 m

EDXRF												Hyperspectral Imagery			
Mg %	Al %	Si %	S %	K %	Ca %	Ti %	Fe %	K/Al	Ti/Al	Si bio %	S/Fe	Depth m	TOC %	Depth m	
1.043	5.260	24.450	1.701	1.560	7.667	0.362	2.898	0.297	0.069	8.142	0.587	3207.20000	0.818	3207.20050	
0.964	5.338	24.517	1.751	1.569	7.579	0.388	2.889	0.294	0.073	7.969	0.606	3207.20156	0.811	3207.20132	
1.034	5.027	23.223	1.890	1.344	8.990	0.241	3.129	0.267	0.048	7.641	0.604	3207.20311	0.803	3207.20213	
1.223	4.826	22.671	2.222	1.259	8.695	0.219	3.582	0.261	0.045	7.709	0.620	3207.20467	0.803	3207.20295	
1.232	4.537	22.590	2.070	1.231	9.125	0.228	3.604	0.271	0.050	8.524	0.574	3207.20622	0.798	3207.20377	
1.140	4.988	23.929	2.365	1.377	7.324	0.215	3.513	0.276	0.043	8.467	0.673	3207.20778	0.781	3207.20459	
1.175	4.843	23.400	2.458	1.386	7.603	0.228	3.648	0.286	0.047	8.386	0.674	3207.20933	0.756	3207.20540	
1.034	5.322	25.237	1.980	1.522	6.758	0.232	3.077	0.286	0.044	8.740	0.644	3207.21089	0.750	3207.20622	
0.912	5.878	28.065	1.668	1.926	4.447	0.301	2.606	0.328	0.051	9.844	0.640	3207.21244	0.763	3207.20704	
0.960	5.972	27.974	1.704	1.837	4.336	0.280	2.750	0.308	0.047	9.460	0.620	3207.21400	0.786	3207.20786	
1.065	5.533	26.517	1.824	1.687	5.654	0.271	2.968	0.305	0.049	9.365	0.615	3207.21556	0.801	3207.20867	
0.960	5.728	27.449	1.624	1.813	5.053	0.262	2.776	0.317	0.046	9.694	0.585	3207.21711	0.817	3207.20949	
1.104	5.550	26.201	1.681	1.659	6.073	0.262	2.911	0.299	0.047	8.997	0.577	3207.21867	0.841	3207.21031	
0.955	5.828	27.857	1.641	1.907	4.575	0.275	2.693	0.327	0.047	9.791	0.609	3207.22022	0.863	3207.21113	
0.881	5.983	28.368	1.671	1.926	4.164	0.314	2.627	0.322	0.053	9.819	0.636	3207.22178	0.873	3207.21194	
0.890	6.156	28.336	1.614	1.978	4.116	0.301	2.553	0.321	0.049	9.253	0.632	3207.22333	0.866	3207.21276	
0.850	6.362	30.182	1.285	2.175	2.941	0.319	2.144	0.342	0.050	10.461	0.600	3207.22489	0.837	3207.21358	
0.842	6.072	28.191	1.445	1.903	4.650	0.293	2.501	0.313	0.048	9.367	0.578	3207.22645	0.812	3207.21440	
0.885	6.156	28.341	1.339	1.973	4.607	0.314	2.392	0.321	0.051	9.257	0.560	3207.22800	0.817	3207.21521	
0.995	6.089	28.730	1.249	1.922	4.391	0.284	2.300	0.316	0.047	9.854	0.543	3207.22956	0.840	3207.21603	
1.126	5.060	24.640	1.943	1.475	7.324	0.236	3.247	0.292	0.047	8.953	0.599	3207.23111	0.863	3207.21685	
1.004	5.444	25.707	1.668	1.668	6.479	0.301	3.103	0.306	0.055	8.831	0.537	3207.23267	0.882	3207.21766	
1.065	5.945	27.825	1.515	1.832	4.826	0.284	2.558	0.308	0.048	9.397	0.592	3207.23422	0.885	3207.21848	
1.021	5.722	27.440	1.581	1.757	5.208	0.280	2.662	0.307	0.049	9.702	0.594	3207.23578	0.881	3207.21930	
0.999	5.605	27.128	1.707	1.691	5.463	0.275	2.697	0.302	0.049	9.752	0.633	3207.23733	0.876	3207.22012	
0.903	5.978	28.146	1.531	1.846	4.662	0.306	2.497	0.309	0.051	9.615	0.613	3207.23889	0.889	3207.22093	
0.842	6.056	29.092	1.491	2.006	3.841	0.297	2.305	0.331	0.049	10.319	0.647	3207.24045	0.916	3207.22175	
0.920	6.100	28.309	1.927	2.001	3.630	0.293	2.693	0.328	0.048	9.398	0.715	3207.24200	0.938	3207.22257	
0.872	6.134	28.146	2.395	2.030	2.985	0.293	2.968	0.331	0.048	9.132	0.807	3207.24356	0.939	3207.22339	
0.811	6.178	28.372	2.256	2.020	3.076	0.288	2.863	0.327	0.047	9.220	0.788	3207.24511	0.926	3207.22420	
0.837	6.100	29.060	1.478	2.076	3.722	0.323	2.449	0.340	0.053	10.149	0.604	3207.24667	0.903	3207.22502	
0.942	5.016	24.350	2.296	1.438	7.344	0.245	3.356	0.287	0.049	8.802	0.684	3207.24822	0.890	3207.22584	
0.912	5.778	27.440	2.103	1.809	4.312	0.254	3.002	0.313	0.044	9.530	0.700	3207.24978	0.892	3207.22666	
1.109	4.426	22.291	2.678	1.259	8.627	0.202	3.818	0.285	0.046	8.571	0.701	3207.25133	0.916	3207.22747	
1.411	4.142	20.979	2.644	1.043	9.794	0.189	3.966	0.252	0.046	8.138	0.667	3207.25289	0.943	3207.22829	
1.473	4.081	20.536	2.797	1.025	9.910	0.197	4.136	0.251	0.048	7.884	0.676	3207.25445	0.939	3207.22911	
1.367	4.098	20.975	2.907	1.081	9.432	0.175	4.110	0.264	0.043	8.271	0.707	3207.25600	0.907	3207.22993	
1.288	4.415	22.694	2.438	1.165	8.587	0.202	3.770	0.264	0.046	9.008	0.647	3207.25756	0.877	3207.23074	
1.306	4.693	23.070	2.538	1.245	7.878	0.219	3.774	0.265	0.047	8.521	0.672	3207.25911	0.862	3207.23156	
1.183	5.038	24.979	2.199	1.424	6.718	0.236	3.334	0.283	0.047	9.362	0.660	3207.26067	0.849	3207.23238	
1.061	5.789	27.382	1.857	1.757	4.758	0.262	2.798	0.304	0.045	9.436	0.664	3207.26222	0.824	3207.23319	
0.982	5.945	28.246	1.618	1.912	4.304	0.301	2.553	0.322	0.051	9.818	0.634	3207.26378	0.828	3207.23401	
1.074	5.867	27.857	1.601	1.837	4.690	0.297	2.575	0.313	0.051	9.670	0.622	3207.26534	0.835	3207.23483	
1.026	5.711	27.540	1.707	1.799	4.977	0.297	2.654	0.315	0.052	9.836	0.643	3207.26689	0.845	3207.23565	
0.754	6.568	30.069	1.295	2.156	3.013	0.314	2.152	0.328	0.048	9.710	0.602	3207.26845	0.854	3207.23646	
0.802	6.317	27.042	1.545	2.095	3.905	0.340	3.787	0.332	0.054	7.459	0.408	3207.27000	0.859	3207.23728	
0.771	6.434	29.802	1.252	2.119	3.335	0.332	2.178	0.329	0.052	9.857	0.575	3207.27156	0.866	3207.23810	
0.820	6.050	29.219	1.295	1.973	4.049	0.301	2.287	0.326	0.050	10.463	0.566	3207.27311	0.872	3207.23892	
0.960	6.150	28.712	1.332	1.940	4.316	0.297	2.331	0.315	0.048	9.646	0.571	3207.27467	0.888	3207.23973	
0.929	5.867	27.753	1.498	1.846	4.933	0.297	2.619	0.315	0.051	9.566	0.572	3207.27622	0.895	3207.24055	
0.872	6.228	29.323	1.412	2.105	3.551	0.293	2.292	0.338	0.047	10.015	0.616	3207.27778	0.888	3207.24137	
0.877	6.334	29.666	1.611	2.067	2.821	0.314	2.401	0.326	0.050	10.031	0.671	3207.27934	0.874	3207.24219	
													0.868	3207.24300	
													0.860	3207.24382	
													0.876	3207.24464	
													0.897	3207.24545	
													0.913	3207.24627	
													0.912	3207.24709	
													0.876	3207.24791	
													0.838	3207.24872	
													0.802	3207.24954	

EDXRF												Hyperspectral Imagery		
Mg	Al	Si	S	K	Ca	Ti	Fe	K/Al	Ti/Al	Si bio	S/Fe	Depth	TOC	Depth
%	%	%	%	%	%	%	%			%		m	%	m
													0.762	3207.25036
													0.736	3207.25118
													0.733	3207.25199
													0.740	3207.25281
													0.740	3207.25363
													0.736	3207.25445
													0.729	3207.25526
													0.729	3207.25608
													0.746	3207.25690
													0.764	3207.25772
													0.797	3207.25853
													0.842	3207.25935
													0.876	3207.26017
													0.877	3207.26098
													0.871	3207.26180
													0.849	3207.26262
													0.849	3207.26344
													0.868	3207.26425
													0.858	3207.26507
													0.871	3207.26589
													0.899	3207.26671
													0.914	3207.26752
													0.886	3207.26834
													0.872	3207.26916
													0.896	3207.26998
													0.923	3207.27079
													0.909	3207.27161
													0.898	3207.27243
													0.890	3207.27325
													0.868	3207.27406
													0.849	3207.27488
													0.852	3207.27570
													0.875	3207.27651
													0.889	3207.27733
													0.893	3207.27815
													0.901	3207.27897

Slab 3207.79 m

EDXRF												Hyperspectral Imagery		
Mg %	Al %	Si %	S %	K %	Ca %	Ti %	Fe %	K/Al	Ti/Al	Si bio %	S/Fe	Depth m	TOC %	Depth m
0.934	5.772	26.911	1.604	1.776	5.384	0.288	2.710	0.308	0.050	9.017	0.592	3207.79000	0.855	3207.79071
1.087	5.728	26.839	1.677	1.799	5.288	0.306	2.706	0.314	0.053	9.083	0.620	3207.79135	0.758	3207.79154
0.824	6.128	28.784	1.505	2.020	3.921	0.301	2.436	0.330	0.049	9.787	0.618	3207.79270	0.847	3207.79238
0.885	6.406	29.228	1.455	2.123	3.304	0.314	2.292	0.331	0.049	9.368	0.635	3207.79404	0.882	3207.79321
1.113	6.017	28.228	1.172	1.860	4.961	0.306	2.209	0.309	0.051	9.575	0.531	3207.79539	0.915	3207.79404
1.253	4.799	23.784	1.555	1.330	8.934	0.215	2.950	0.277	0.045	8.909	0.527	3207.79674	0.926	3207.79488
1.201	4.932	24.576	1.628	1.367	8.069	0.254	2.976	0.277	0.051	9.287	0.547	3207.79809	0.897	3207.79571
1.205	4.910	23.490	2.329	1.306	7.810	0.236	3.495	0.266	0.048	8.270	0.666	3207.79943	0.862	3207.79654
1.113	5.016	24.255	2.751	1.410	6.495	0.223	3.552	0.281	0.045	8.707	0.774	3207.80078	0.840	3207.79738
0.986	4.754	23.907	1.727	1.330	8.890	0.236	2.950	0.280	0.050	9.169	0.586	3207.80213	0.841	3207.79821
1.113	4.404	22.124	1.817	1.175	10.388	0.202	3.234	0.267	0.046	8.472	0.562	3207.80348	0.864	3207.79904
0.916	5.483	26.612	1.405	1.673	6.527	0.288	2.545	0.305	0.053	9.616	0.552	3207.80482	0.863	3207.79988
1.288	4.643	22.581	1.830	1.212	9.727	0.241	3.151	0.261	0.052	8.188	0.581	3207.80617	0.881	3207.80071
1.376	4.203	20.970	2.186	1.109	10.536	0.180	3.696	0.264	0.043	7.939	0.591	3207.80752	0.868	3207.80154
1.271	3.937	19.970	2.066	1.006	11.667	0.219	3.879	0.256	0.056	7.767	0.533	3207.80887	0.839	3207.80238
1.332	4.782	23.979	1.668	1.339	8.476	0.258	3.094	0.280	0.054	9.155	0.539	3207.81021	0.813	3207.80321
1.135	5.249	25.658	1.508	1.541	7.109	0.301	2.776	0.294	0.057	9.385	0.543	3207.81156	0.805	3207.80404
1.135	5.233	26.164	1.508	1.560	6.706	0.297	2.789	0.298	0.057	9.944	0.541	3207.81291	0.797	3207.80488
0.969	6.173	28.590	1.229	1.973	4.479	0.310	2.248	0.320	0.050	9.455	0.547	3207.81426	0.789	3207.80571
1.004	5.844	27.997	1.305	1.865	5.069	0.297	2.370	0.319	0.051	9.879	0.551	3207.81560	0.781	3207.80654
1.069	5.678	27.169	1.339	1.785	5.742	0.284	2.562	0.314	0.050	9.569	0.522	3207.81695	0.765	3207.80738
1.030	5.789	27.250	1.365	1.781	5.647	0.306	2.566	0.308	0.053	9.305	0.532	3207.81830	0.770	3207.80821
1.030	5.933	27.934	1.385	1.884	5.021	0.306	2.392	0.318	0.052	9.540	0.579	3207.81965	0.789	3207.80904
1.047	6.045	27.771	1.372	1.875	4.985	0.314	2.401	0.310	0.052	9.032	0.571	3207.82099	0.816	3207.80988
0.885	6.161	28.531	1.272	2.015	4.483	0.310	2.261	0.327	0.050	9.430	0.563	3207.82234	0.838	3207.81071
0.938	6.339	29.164	1.216	2.062	3.953	0.345	2.139	0.325	0.054	9.512	0.568	3207.82369	0.841	3207.81154
0.793	6.467	29.721	1.133	2.147	3.515	0.319	2.091	0.332	0.049	9.672	0.542	3207.82504	0.839	3207.81238
0.977	6.250	29.056	1.372	2.053	3.841	0.306	2.253	0.328	0.049	9.679	0.609	3207.82639	0.850	3207.81321
0.969	5.761	26.680	2.203	1.720	4.965	0.271	2.946	0.298	0.047	8.821	0.748	3207.82773	0.868	3207.81404
0.973	5.822	27.734	1.860	1.842	4.547	0.293	2.675	0.316	0.050	9.686	0.695	3207.82908	0.882	3207.81488
0.947	5.772	27.083	1.774	1.738	5.308	0.271	2.702	0.301	0.047	9.189	0.657	3207.83043	0.883	3207.81571
0.999	5.655	26.151	1.960	1.715	5.726	0.245	2.898	0.303	0.043	8.619	0.676	3207.83178	0.864	3207.81654
0.929	5.850	27.730	1.471	1.893	5.049	0.319	2.558	0.324	0.054	9.595	0.575	3207.83312	0.840	3207.81738
0.872	5.705	26.970	1.525	1.729	5.718	0.310	2.614	0.303	0.054	9.283	0.583	3207.83447	0.831	3207.81821
1.043	5.082	24.839	1.721	1.471	7.639	0.262	2.876	0.289	0.052	9.083	0.598	3207.83582	0.846	3207.81904
0.960	5.411	25.730	1.581	1.574	6.957	0.258	2.815	0.291	0.048	8.957	0.562	3207.83717	0.870	3207.81988
1.100	5.316	25.925	1.658	1.569	6.623	0.262	2.832	0.295	0.049	9.445	0.585	3207.83851	0.891	3207.82071
1.074	5.494	26.305	1.694	1.616	6.180	0.254	2.776	0.294	0.046	9.273	0.610	3207.83986	0.913	3207.82155
1.065	5.494	26.296	1.634	1.635	6.204	0.267	2.763	0.298	0.049	9.264	0.592	3207.84121	0.935	3207.82238
1.026	5.566	26.332	1.568	1.649	6.264	0.245	2.750	0.296	0.044	9.076	0.570	3207.84256	0.954	3207.82321
1.039	5.466	26.449	1.528	1.640	6.280	0.288	2.806	0.300	0.053	9.504	0.544	3207.84390	0.970	3207.82405
0.999	5.522	26.621	1.515	1.663	6.180	0.275	2.745	0.301	0.050	9.504	0.552	3207.84525	0.985	3207.82488
1.210	5.416	26.056	1.505	1.602	6.575	0.267	2.798	0.296	0.049	9.266	0.538	3207.84660	0.995	3207.82571
0.991	5.511	25.997	1.571	1.630	6.503	0.275	2.893	0.296	0.050	8.914	0.543	3207.84795	0.992	3207.82655
1.166	5.249	25.255	1.691	1.480	7.109	0.241	2.950	0.282	0.046	8.982	0.573	3207.84929	0.975	3207.82738
0.907	5.850	27.481	1.588	1.856	5.117	0.288	2.601	0.317	0.049	9.346	0.610	3207.85064	0.952	3207.82821
0.850	6.223	29.042	1.348	2.048	3.953	0.301	2.261	0.329	0.048	9.752	0.596	3207.85199	0.942	3207.82905
1.069	5.577	27.535	1.355	1.771	5.607	0.293	2.475	0.318	0.052	10.245	0.548	3207.85334	0.954	3207.82988
0.973	5.694	26.934	1.471	1.715	5.969	0.284	2.566	0.301	0.050	9.282	0.573	3207.85468	0.974	3207.83071
0.815	6.078	28.992	1.295	2.030	4.308	0.319	2.196	0.334	0.052	10.150	0.590	3207.85603	0.983	3207.83155
0.842	6.200	29.522	1.159	2.091	3.885	0.327	2.109	0.337	0.053	10.300	0.550	3207.85738	0.989	3207.83238
1.034	5.844	27.477	1.531	1.828	5.109	0.280	2.553	0.313	0.048	9.359	0.600	3207.85873	0.996	3207.83321
1.240	4.765	23.133	1.960	1.335	8.810	0.219	3.316	0.280	0.046	8.360	0.591	3207.86008	1.000	3207.83405
1.131	5.477	24.631	1.604	1.602	7.356	0.310	3.159	0.293	0.057	7.651	0.508	3207.86142	0.995	3207.83488
0.969	6.100	28.246	1.471	1.950	4.411	0.301	2.457	0.320	0.049	9.335	0.599	3207.86277	0.984	3207.83571
0.758	6.145	28.409	1.996	2.062	3.463	0.306	2.715	0.336	0.050	9.360	0.735	3207.86412	0.961	3207.83655
0.942	5.633	26.558	2.056	1.682	5.411	0.275	2.933	0.299	0.049	9.096	0.701	3207.86547	0.915	3207.83738
1.135	5.160	25.450	2.043	1.513	6.467	0.258	3.168	0.293	0.050	9.453	0.645	3207.86681	0.858	3207.83821
1.083	5.233	25.359	1.950	1.546	6.726	0.241	3.055	0.295	0.046	9.138	0.638	3207.86816	0.833	3207.83905
0.995	5.961	28.182	1.508	1.898	4.527	0.267	2.466	0.318	0.045	9.703	0.611	3207.86951	0.844	3207.83988
0.881	6.028	28.576	1.388	1.907	4.507	0.293	2.322	0.316	0.049	9.889	0.598	3207.87086	0.847	3207.84071

EDXRF													Hyperspectral Imagery	
Mg	Al	Si	S	K	Ca	Ti	Fe	K/Al	Ti/Al	Si bio	S/Fe	Depth	TOC	Depth
%	%	%	%	%	%	%	%			%		m	%	m
1.039	5.755	27.182	1.571	1.795	5.455	0.293	2.545	0.312	0.051	9.341	0.617	3207.87220	0.853	3207.84155
1.056	5.516	26.146	1.681	1.593	6.340	0.254	2.798	0.289	0.046	9.046	0.601	3207.87355	0.858	3207.84238
1.056	5.394	25.282	1.817	1.532	6.874	0.271	3.007	0.284	0.050	8.561	0.604	3207.87490	0.862	3207.84321
													0.863	3207.84405
													0.861	3207.84488
													0.870	3207.84571
													0.892	3207.84655
													0.901	3207.84738
													0.885	3207.84821
													0.863	3207.84905
													0.853	3207.84988
													0.855	3207.85071
													0.876	3207.85155
													0.897	3207.85238
													0.913	3207.85321
													0.931	3207.85405
													0.932	3207.85488
													0.936	3207.85571
													0.945	3207.85655
													0.946	3207.85738
													0.950	3207.85821
													0.942	3207.85905
													0.925	3207.85988
													0.862	3207.86071
													0.801	3207.86155
													0.760	3207.86238
													0.753	3207.86321
													0.762	3207.86405
													0.779	3207.86488
													0.789	3207.86571
													0.806	3207.86655
													0.833	3207.86738
													0.863	3207.86821
													0.905	3207.86905
													0.952	3207.86988
													0.989	3207.87071
													1.006	3207.87155
													1.008	3207.87238
													0.993	3207.87321
													0.972	3207.87405
													0.942	3207.87488
													0.933	3207.87571

Slab 3208.74 m

EDXRF													Hyperspectral Imagery		
Mg %	Al %	Si %	S %	K %	Ca %	Ti %	Fe %	K/Al	Ti/Al	Si bio %	S/Fe	Depth m	TOC %	Depth m	
1.109	7.752	24.780	2.016	2.429	4.352	0.366	3.090	0.313	0.047	0.748	0.653	3208.74385	0.397	3208.74305	
1.078	7.652	24.653	2.399	2.490	3.897	0.358	3.260	0.325	0.047	0.931	0.736	3208.74578	0.406	3208.74383	
1.179	7.635	24.993	1.658	2.391	4.746	0.366	2.950	0.313	0.048	1.323	0.562	3208.74770	0.417	3208.74460	
1.091	7.463	24.771	1.867	2.396	4.866	0.388	2.998	0.321	0.052	1.635	0.623	3208.74963	0.420	3208.74537	
0.969	7.875	25.232	2.232	2.579	3.622	0.332	3.103	0.327	0.042	0.821	0.719	3208.75155	0.426	3208.74614	
1.192	7.680	25.183	1.551	2.386	4.782	0.323	2.798	0.311	0.042	1.375	0.554	3208.75348	0.428	3208.74691	
0.964	7.769	25.630	1.917	2.485	3.877	0.362	2.946	0.320	0.047	1.547	0.651	3208.75541	0.434	3208.74769	
1.258	7.391	24.205	1.860	2.269	5.284	0.336	3.068	0.307	0.045	1.294	0.606	3208.75733	0.437	3208.74846	
1.196	7.574	24.671	1.930	2.363	4.722	0.349	2.985	0.312	0.046	1.191	0.647	3208.75926	0.438	3208.74923	
1.175	7.496	24.857	1.953	2.316	4.539	0.332	3.168	0.309	0.044	1.618	0.617	3208.76118	0.429	3208.75000	
1.253	7.168	23.337	1.837	2.138	6.029	0.293	3.364	0.298	0.041	1.115	0.546	3208.76311	0.434	3208.75077	
1.245	7.630	23.857	1.714	2.386	5.132	0.388	3.513	0.313	0.051	0.204	0.488	3208.76504	0.439	3208.75155	
1.232	7.674	24.481	1.917	2.372	4.618	0.371	3.220	0.309	0.048	0.691	0.595	3208.76696	0.455	3208.75232	
1.389	7.591	23.662	2.362	2.269	4.690	0.362	3.364	0.299	0.048	0.130	0.702	3208.76889	0.469	3208.75309	
1.288	7.864	24.965	1.697	2.447	4.503	0.371	2.889	0.311	0.047	0.588	0.588	3208.77081	0.461	3208.75386	
1.061	7.847	24.839	2.229	2.391	3.989	0.375	3.212	0.305	0.048	0.513	0.694	3208.77274	0.446	3208.75463	
1.245	7.763	25.287	1.661	2.494	4.352	0.379	2.885	0.321	0.049	1.220	0.576	3208.77466	0.441	3208.75541	
1.416	6.912	22.807	1.867	2.081	6.619	0.366	3.404	0.301	0.053	1.379	0.549	3208.77659	0.435	3208.75618	
1.363	7.469	23.658	1.800	2.194	5.782	0.349	3.159	0.294	0.047	0.505	0.570	3208.77852	0.428	3208.75695	
1.175	7.702	24.273	1.721	2.307	5.328	0.384	3.020	0.299	0.050	0.396	0.570	3208.78044	0.422	3208.75772	
1.297	7.875	24.590	1.727	2.424	4.778	0.332	2.955	0.308	0.042	0.178	0.585	3208.78237	0.418	3208.75849	
1.236	7.830	24.689	1.824	2.476	4.587	0.349	2.915	0.316	0.045	0.416	0.626	3208.78429	0.419	3208.75927	
1.140	7.786	25.151	1.790	2.466	4.375	0.375	2.950	0.317	0.048	1.015	0.607	3208.78622	0.433	3208.76004	
1.083	7.852	25.825	1.618	2.532	4.069	0.375	2.789	0.322	0.048	1.483	0.580	3208.78815	0.445	3208.76081	
1.262	7.530	24.481	1.654	2.302	5.252	0.358	2.981	0.306	0.047	1.139	0.555	3208.79007	0.445	3208.76158	
1.240	7.741	24.689	2.422	2.415	3.774	0.379	3.199	0.312	0.049	0.692	0.757	3208.79200	0.430	3208.76235	
1.249	7.641	24.730	1.561	2.405	5.152	0.371	2.859	0.315	0.049	1.043	0.546	3208.79392	0.418	3208.76313	
1.359	7.190	23.726	1.761	2.156	5.933	0.319	3.103	0.300	0.044	1.435	0.567	3208.79585	0.422	3208.76390	
1.367	7.029	22.979	1.923	2.105	6.424	0.332	3.290	0.299	0.047	1.189	0.585	3208.79777	0.435	3208.76467	
1.113	7.469	24.318	1.820	2.382	5.288	0.349	3.064	0.319	0.047	1.166	0.594	3208.79970	0.445	3208.76544	
1.104	7.146	23.088	1.744	2.123	6.551	0.314	3.404	0.297	0.044	0.935	0.512	3208.80170	0.463	3208.76622	
1.275	7.285	22.916	1.751	2.081	6.543	0.332	3.360	0.286	0.046	0.332	0.521	3208.80286	0.462	3208.76699	
1.175	7.413	23.676	1.711	2.217	5.981	0.327	3.094	0.299	0.044	0.696	0.553	3208.80402	0.464	3208.76776	
1.240	7.385	24.065	1.681	2.283	5.666	0.358	3.042	0.309	0.048	1.171	0.553	3208.80518	0.457	3208.76853	
1.096	7.585	24.667	1.684	2.354	5.188	0.388	2.941	0.310	0.051	1.152	0.573	3208.80634	0.449	3208.76930	
1.109	7.630	24.717	2.209	2.447	4.260	0.384	3.168	0.321	0.050	1.064	0.697	3208.80750	0.441	3208.77008	
1.087	7.808	24.898	2.013	2.424	4.240	0.362	3.111	0.310	0.046	0.693	0.647	3208.80866	0.441	3208.77085	
1.043	7.836	25.006	2.173	2.480	3.933	0.358	3.046	0.317	0.046	0.715	0.713	3208.80982	0.444	3208.77162	
1.232	7.958	25.436	1.890	2.546	3.758	0.375	2.928	0.320	0.047	0.766	0.645	3208.81098	0.450	3208.77239	
1.267	7.752	24.042	1.933	2.278	4.981	0.340	3.207	0.294	0.044	0.010	0.603	3208.81214	0.456	3208.77316	
1.328	7.519	23.771	1.943	2.203	5.463	0.345	3.090	0.293	0.046	0.463	0.629	3208.81330	0.446	3208.77394	
1.324	7.597	24.042	1.834	2.236	5.312	0.345	3.042	0.294	0.045	0.493	0.603	3208.81446	0.414	3208.77471	
1.402	7.758	23.825	1.867	2.255	5.121	0.371	3.133	0.291	0.048	-0.224	0.596	3208.81562	0.389	3208.77548	
1.232	7.580	23.965	1.907	2.302	5.280	0.345	3.133	0.304	0.045	0.468	0.609	3208.81678	0.389	3208.77625	
1.183	7.697	24.391	1.923	2.410	4.897	0.353	3.020	0.313	0.046	0.531	0.637	3208.81794	0.391	3208.77702	
1.170	7.908	24.812	1.973	2.466	4.296	0.353	2.972	0.312	0.045	0.297	0.664	3208.81910	0.402	3208.77780	
1.205	8.042	25.364	2.083	2.565	3.539	0.362	2.959	0.319	0.045	0.435	0.704	3208.82026	0.399	3208.77857	
1.284	7.919	24.694	1.771	2.391	4.626	0.349	2.907	0.302	0.044	0.144	0.609	3208.82142	0.396	3208.77934	
1.223	7.724	24.404	1.721	2.325	5.089	0.366	3.016	0.301	0.047	0.458	0.571	3208.82258	0.398	3208.78011	
1.196	8.036	24.649	1.694	2.405	4.718	0.401	2.911	0.299	0.050	-0.263	0.582	3208.82374	0.401	3208.78088	
1.210	7.886	24.689	1.910	2.391	4.427	0.392	2.994	0.303	0.050	0.243	0.638	3208.82490	0.407	3208.78166	
1.232	8.080	24.563	1.983	2.452	4.140	0.414	3.094	0.303	0.051	-0.487	0.641	3208.82606	0.427	3208.78243	
1.240	8.292	24.422	2.033	2.419	3.786	0.392	3.173	0.292	0.047	-1.282	0.641	3208.82722	0.431	3208.78320	
1.223	8.069	24.205	2.551	2.480	3.515	0.349	3.329	0.307	0.043	-0.810	0.766	3208.82838	0.427	3208.78397	
0.811	7.941	24.409	2.664	2.466	3.618	0.340	3.465	0.311	0.043	-0.210	0.769	3208.82954	0.434	3208.78474	
													0.444	3208.78552	
													0.452	3208.78629	
													0.465	3208.78706	
													0.468	3208.78783	
													0.457	3208.78861	
													0.448	3208.78938	

EDXRF												Hyperspectral Imagery		
Mg	Al	Si	S	K	Ca	Ti	Fe	K/Al	Ti/Al	Si bio	S/Fe	Depth	TOC	Depth
%	%	%	%	%	%	%	%			%		m	%	m
													0.442	3208.79015
													0.438	3208.79092
													0.437	3208.79169
													0.436	3208.79247
													0.443	3208.79324
													0.441	3208.79401
													0.423	3208.79478
													0.406	3208.79555
													0.406	3208.79633
													0.410	3208.79710
													0.416	3208.79787
													0.421	3208.79864
													0.427	3208.79941
													0.427	3208.80019
													0.428	3208.80096
													0.425	3208.80173
													0.417	3208.80250
													0.416	3208.80327
													0.416	3208.80405
													0.421	3208.80482
													0.441	3208.80559
													0.437	3208.80636
													0.434	3208.80713
													0.440	3208.80791
													0.447	3208.80868
													0.449	3208.80945
													0.452	3208.81022
													0.446	3208.81100
													0.431	3208.81177
													0.414	3208.81254
													0.401	3208.81331
													0.396	3208.81408
													0.407	3208.81486
													0.407	3208.81563
													0.405	3208.81640
													0.403	3208.81717
													0.407	3208.81794
													0.422	3208.81872
													0.433	3208.81949
													0.435	3208.82026
													0.433	3208.82103
													0.422	3208.82180
													0.418	3208.82258
													0.416	3208.82335
													0.419	3208.82412
													0.425	3208.82489
													0.431	3208.82566
													0.439	3208.82644
													0.448	3208.82721
													0.451	3208.82798
													0.452	3208.82875
													0.447	3208.82952

Slab 3209.06 m

EDXRF												Hyperspectral Imagery		
Mg %	Al %	Si %	S %	K %	Ca %	Ti %	Fe %	K/Al	Ti/Al	Si bio %	S/Fe	Depth m	TOC %	Depth m
1.306	6.406	22.300	1.335	1.968	8.731	0.262	2.880	0.307	0.041	2.441	0.464	3209.06828	0.413	3209.06878
1.324	5.678	20.432	1.395	1.715	11.305	0.219	2.706	0.302	0.039	2.831	0.516	3209.07035	0.399	3209.06964
1.468	6.428	21.916	1.402	1.973	8.830	0.284	2.950	0.307	0.044	1.988	0.475	3209.07242	0.467	3209.07051
1.468	6.017	20.531	1.422	1.767	10.376	0.262	3.098	0.294	0.044	1.879	0.459	3209.07449	0.480	3209.07137
1.363	6.523	21.848	1.618	1.940	8.595	0.271	3.072	0.297	0.042	1.627	0.527	3209.07656	0.416	3209.07223
1.341	6.590	22.115	1.501	2.030	8.432	0.262	3.020	0.308	0.040	1.687	0.497	3209.07863	0.413	3209.07309
1.293	6.606	22.033	1.485	2.039	8.575	0.280	2.959	0.309	0.042	1.553	0.502	3209.08070	0.376	3209.07396
1.354	6.245	21.875	1.299	1.950	9.380	0.271	2.780	0.312	0.043	2.516	0.467	3209.08277	0.368	3209.07482
1.293	6.267	22.070	1.352	1.931	9.213	0.275	2.789	0.308	0.044	2.641	0.485	3209.08484	0.369	3209.07568
1.240	6.473	22.567	1.299	2.053	8.615	0.267	2.771	0.317	0.041	2.501	0.469	3209.08691	0.395	3209.07654
1.442	6.456	21.925	1.325	1.917	9.085	0.232	2.806	0.297	0.036	1.910	0.472	3209.08898	0.358	3209.07741
1.083	3.753	15.934	1.236	1.072	17.768	0.136	2.423	0.286	0.036	4.300	0.510	3209.09100	0.436	3209.07827
1.297	7.074	23.694	1.329	2.147	6.854	0.262	2.976	0.304	0.037	1.766	0.446	3209.09380	0.425	3209.07913
1.354	7.163	23.694	1.319	2.105	6.838	0.271	2.928	0.294	0.038	1.490	0.450	3209.09590	0.364	3209.08000
1.565	6.595	22.151	1.319	1.917	8.587	0.258	2.889	0.291	0.039	1.706	0.456	3209.09801	0.389	3209.08086
1.578	6.634	22.346	1.299	1.917	8.352	0.275	2.994	0.289	0.041	1.779	0.434	3209.10011	0.419	3209.08172
1.240	6.540	22.178	1.232	1.926	9.045	0.280	2.867	0.295	0.043	1.905	0.430	3209.10221	0.392	3209.08258
1.319	6.512	22.160	1.903	1.912	7.938	0.284	3.255	0.294	0.044	1.973	0.585	3209.10432	0.411	3209.08345
1.529	6.479	21.997	1.611	1.936	8.344	0.236	3.103	0.299	0.036	1.914	0.519	3209.10642	0.397	3209.08431
1.451	6.206	21.386	1.285	1.842	9.818	0.271	2.837	0.297	0.044	2.148	0.453	3209.10852	0.445	3209.08517
1.420	6.623	21.871	1.282	2.011	8.655	0.284	3.190	0.304	0.043	1.339	0.402	3209.11062	0.452	3209.08604
1.538	6.234	21.789	1.292	1.809	9.336	0.241	2.907	0.290	0.039	2.464	0.445	3209.11273	0.417	3209.08690
1.451	5.767	20.681	1.425	1.757	10.635	0.241	2.920	0.305	0.042	2.804	0.488	3209.11483	0.423	3209.08776
1.372	5.733	20.807	1.555	1.687	10.324	0.258	2.981	0.294	0.045	3.034	0.522	3209.11693	0.389	3209.08862
1.389	6.384	21.925	1.206	1.846	9.444	0.275	2.763	0.289	0.043	2.135	0.436	3209.11904	0.345	3209.08949
1.332	5.800	21.296	1.302	1.757	10.440	0.254	2.737	0.303	0.044	3.316	0.476	3209.12114	0.357	3209.09035
1.490	5.644	21.024	1.491	1.701	10.328	0.236	2.959	0.301	0.042	3.528	0.504	3209.12324	0.364	3209.09121
1.306	6.173	22.441	1.269	1.912	9.037	0.241	2.784	0.310	0.039	3.306	0.456	3209.12535	0.380	3209.09207
1.814	6.662	23.866	0.980	2.072	7.169	0.262	2.846	0.311	0.039	3.213	0.344	3209.12745	0.387	3209.09294
1.442	6.056	21.803	1.236	1.804	9.771	0.249	2.758	0.298	0.041	3.030	0.448	3209.12955	0.403	3209.09380
1.328	5.861	21.613	1.362	1.771	10.006	0.245	2.806	0.302	0.042	3.443	0.485	3209.13165	0.401	3209.09466
1.565	6.045	22.011	0.990	1.781	9.958	0.267	2.593	0.295	0.044	3.272	0.382	3209.13376	0.393	3209.09553
1.617	5.906	20.938	1.216	1.720	10.372	0.215	2.832	0.291	0.036	2.631	0.429	3209.13586	0.387	3209.09639
1.473	5.822	21.006	1.355	1.715	10.309	0.228	2.976	0.295	0.039	2.958	0.455	3209.13796	0.392	3209.09725
1.473	5.928	21.273	1.116	1.781	10.532	0.275	2.675	0.300	0.046	2.897	0.417	3209.14007	0.393	3209.09811
1.503	5.894	21.540	1.123	1.752	10.348	0.223	2.614	0.297	0.038	3.267	0.429	3209.14217	0.397	3209.09898
1.394	6.006	21.753	1.006	1.795	10.348	0.245	2.562	0.299	0.041	3.135	0.393	3209.14427	0.389	3209.09984
1.324	5.817	21.653	0.980	1.724	10.675	0.232	2.571	0.296	0.040	3.622	0.381	3209.14638	0.376	3209.10070
1.468	5.805	21.079	1.016	1.687	10.830	0.258	2.780	0.291	0.044	3.082	0.366	3209.14848	0.375	3209.10156
1.372	5.583	19.957	1.109	1.518	11.859	0.210	2.719	0.272	0.038	2.649	0.408	3209.15058	0.363	3209.10243
1.621	6.078	21.961	1.046	1.748	9.703	0.245	2.763	0.288	0.040	3.119	0.379	3209.15268	0.366	3209.10329
1.578	5.844	21.355	1.282	1.724	10.101	0.262	2.946	0.295	0.045	3.237	0.435	3209.15479	0.385	3209.10415
1.350	5.121	19.463	1.777	1.494	11.607	0.223	3.334	0.292	0.044	3.587	0.533	3209.15689	0.380	3209.10502
1.271	5.411	20.124	1.442	1.588	11.492	0.219	3.055	0.294	0.040	3.351	0.472	3209.15900	0.369	3209.10588
														0.357 3209.10674
														0.366 3209.10760
														0.369 3209.10847
														0.381 3209.10933
														0.383 3209.11019
														0.392 3209.11106
														0.402 3209.11192
														0.433 3209.11278
														0.431 3209.11364
														0.459 3209.11451
														0.459 3209.11537
														0.467 3209.11623
														0.439 3209.11709
														0.405 3209.11796
														0.395 3209.11882
														0.402 3209.11968
														0.400 3209.12055

EDXRF												Hyperspectral Imagery		
Mg	Al	Si	S	K	Ca	Ti	Fe	K/Al	Ti/Al	Si bio	S/Fe	Depth	TOC	Depth
%	%	%	%	%	%	%	%			%		m	%	m
													0.400	3209.12141
													0.409	3209.12227
													0.415	3209.12313
													0.407	3209.12400
													0.402	3209.12486
													0.396	3209.12572
													0.376	3209.12658
													0.390	3209.12745
													0.391	3209.12831
													0.398	3209.12917
													0.408	3209.13004
													0.410	3209.13090
													0.438	3209.13176
													0.437	3209.13262
													0.438	3209.13349
													0.439	3209.13435
													0.434	3209.13521
													0.397	3209.13608
													0.380	3209.13694
													0.374	3209.13780
													0.386	3209.13866
													0.400	3209.13953
													0.409	3209.14039
													0.396	3209.14125
													0.406	3209.14211
													0.385	3209.14298
													0.378	3209.14384
													0.366	3209.14470
													0.379	3209.14557
													0.364	3209.14643
													0.353	3209.14729
													0.353	3209.14815
													0.354	3209.14902
													0.346	3209.14988
													0.354	3209.15074
													0.369	3209.15160
													0.373	3209.15247
													0.373	3209.15333
													0.374	3209.15419
													0.365	3209.15506
													0.364	3209.15592
													0.363	3209.15678
													0.361	3209.15764
													0.365	3209.15851
													0.364	3209.15937

Slab 3210.6 m

EDXRF													Hyperspectral Imagery		
Mg %	Al %	Si %	S %	K %	Ca %	Ti %	Fe %	K/Al	Ti/Al	Si bio %	S/Fe	Depth m	TOC %	Depth m	
1.315	5.572	25.418	1.445	1.659	6.898	0.271	2.828	0.298	0.049	8.145	0.511	3210.61891	0.813	3210.61776	
1.166	5.778	26.486	1.458	1.813	5.949	0.293	2.632	0.314	0.051	8.575	0.554	3210.62049	0.782	3210.61851	
1.236	6.006	26.983	1.329	1.893	5.483	0.288	2.514	0.315	0.048	8.366	0.528	3210.62207	0.784	3210.61925	
1.065	5.711	26.549	1.212	1.851	6.304	0.275	2.558	0.324	0.048	8.845	0.474	3210.62364	0.791	3210.62000	
1.586	4.760	22.753	1.631	1.311	9.089	0.228	3.360	0.275	0.048	7.998	0.485	3210.62522	0.805	3210.62074	
1.446	5.483	24.830	1.588	1.593	7.193	0.262	2.937	0.291	0.048	7.833	0.541	3210.62680	0.835	3210.62149	
1.153	5.839	26.350	1.528	1.823	5.933	0.297	2.715	0.312	0.051	8.250	0.563	3210.62837	0.866	3210.62224	
1.175	6.123	26.970	1.432	1.931	5.340	0.297	2.497	0.315	0.048	7.990	0.573	3210.62995	0.877	3210.62298	
1.179	5.811	26.400	1.418	1.818	5.981	0.297	2.715	0.313	0.051	8.386	0.522	3210.63152	0.848	3210.62373	
0.982	5.828	26.915	1.471	1.870	5.682	0.288	2.584	0.321	0.049	8.850	0.569	3210.63310	0.854	3210.62447	
1.126	6.217	27.753	1.192	1.903	5.045	0.293	2.383	0.306	0.047	8.480	0.500	3210.63468	0.862	3210.62522	
1.148	6.006	27.115	1.292	1.903	5.491	0.288	2.545	0.317	0.048	8.497	0.508	3210.63625	0.849	3210.62597	
0.977	5.800	27.119	1.368	1.828	5.770	0.293	2.492	0.315	0.050	9.139	0.549	3210.63783	0.881	3210.62671	
1.210	5.355	25.056	2.106	1.654	6.479	0.245	3.055	0.309	0.046	8.456	0.689	3210.63941	0.917	3210.62746	
1.376	4.765	23.056	1.531	1.283	9.579	0.232	3.002	0.269	0.049	8.284	0.510	3210.64098	0.902	3210.62820	
1.267	5.322	25.730	1.428	1.607	6.938	0.249	2.763	0.302	0.047	9.233	0.517	3210.64256	0.907	3210.62895	
1.319	5.822	27.250	1.378	1.870	5.332	0.306	2.492	0.321	0.052	9.202	0.553	3210.64413	0.925	3210.62969	
1.236	5.221	24.916	1.634	1.513	7.460	0.241	2.955	0.290	0.046	8.729	0.553	3210.64571	0.925	3210.63044	
1.140	5.583	25.979	1.584	1.691	6.463	0.280	2.737	0.303	0.050	8.672	0.579	3210.64729	0.920	3210.63119	
1.052	5.310	24.676	2.541	1.607	6.312	0.245	3.290	0.303	0.046	8.214	0.772	3210.64886	0.897	3210.63193	
1.210	5.132	24.612	2.119	1.499	7.013	0.232	3.203	0.292	0.045	8.702	0.662	3210.65044	0.862	3210.63268	
1.372	5.294	25.658	1.505	1.527	6.934	0.258	2.811	0.288	0.049	9.247	0.535	3210.65201	0.852	3210.63342	
1.284	5.650	26.639	1.332	1.743	6.168	0.284	2.518	0.309	0.050	9.125	0.529	3210.65359	0.868	3210.63417	
1.153	5.516	26.463	1.325	1.724	6.475	0.293	2.614	0.313	0.053	9.363	0.507	3210.65517	0.893	3210.63491	
1.188	5.433	26.033	1.408	1.654	6.726	0.245	2.723	0.304	0.045	9.192	0.517	3210.65674	0.889	3210.63566	
1.144	5.616	26.540	1.418	1.762	6.188	0.284	2.645	0.314	0.051	9.129	0.536	3210.65832	0.918	3210.63641	
1.122	5.811	26.689	1.342	1.785	6.029	0.262	2.514	0.307	0.045	8.675	0.534	3210.65990	0.913	3210.63715	
1.315	5.333	25.124	1.481	1.555	7.396	0.254	2.789	0.292	0.048	8.592	0.531	3210.66147	0.906	3210.63790	
1.240	5.233	25.603	1.511	1.560	7.181	0.275	2.758	0.298	0.053	9.382	0.548	3210.66305	0.884	3210.63864	
1.188	5.744	27.096	1.242	1.771	5.814	0.301	2.501	0.308	0.052	9.289	0.497	3210.66462	0.858	3210.63939	
1.179	5.555	25.916	1.491	1.687	6.559	0.258	2.710	0.304	0.046	8.695	0.550	3210.66620	0.839	3210.64013	
1.380	5.472	25.703	1.541	1.644	6.655	0.271	2.758	0.301	0.050	8.741	0.559	3210.66778	0.824	3210.64088	
1.218	5.789	26.974	1.378	1.860	5.682	0.306	2.466	0.321	0.053	9.029	0.559	3210.66935	0.835	3210.64163	
1.065	5.794	26.992	1.329	1.799	5.941	0.314	2.475	0.311	0.054	9.030	0.537	3210.67093	0.919	3210.64237	
1.153	5.716	26.382	1.405	1.799	6.220	0.275	2.593	0.315	0.048	8.661	0.542	3210.67251	0.976	3210.64312	
0.991	5.789	26.934	1.465	1.767	5.814	0.254	2.610	0.305	0.044	8.988	0.561	3210.67408	0.972	3210.64386	
1.109	5.794	27.196	1.292	1.767	5.798	0.306	2.462	0.305	0.053	9.234	0.525	3210.67566	0.979	3210.64461	
1.262	5.322	25.875	1.465	1.588	6.874	0.249	2.719	0.298	0.047	9.378	0.539	3210.67723	0.970	3210.64535	
1.245	5.700	26.811	1.352	1.748	5.945	0.267	2.575	0.307	0.047	9.142	0.525	3210.67881	0.953	3210.64610	
0.991	5.722	27.418	1.458	1.809	5.483	0.293	2.501	0.316	0.051	9.679	0.583	3210.68039	0.959	3210.64685	
1.140	5.844	27.277	1.355	1.846	5.531	0.301	2.409	0.316	0.052	9.160	0.562	3210.68196	0.948	3210.64759	
1.034	6.056	28.146	1.249	1.959	4.901	0.284	2.239	0.324	0.047	9.373	0.558	3210.68354	0.965	3210.64834	
1.157	5.922	27.526	1.255	1.893	5.364	0.275	2.388	0.320	0.046	9.167	0.526	3210.68511	1.009	3210.64908	
1.153	5.794	26.879	1.305	1.799	6.045	0.284	2.436	0.311	0.049	8.917	0.536	3210.68669	1.003	3210.64983	
1.223	5.627	26.744	1.395	1.757	6.017	0.275	2.536	0.312	0.049	9.298	0.550	3210.68827	1.026	3210.65057	
1.078	5.750	26.866	1.362	1.813	5.985	0.275	2.471	0.315	0.048	9.041	0.551	3210.68984	0.944	3210.65132	
1.061	5.817	27.296	1.345	1.870	5.639	0.293	2.392	0.321	0.050	9.264	0.562	3210.69142	0.913	3210.65207	
1.004	6.084	28.250	1.245	1.936	4.738	0.288	2.335	0.318	0.047	9.391	0.533	3210.69300	0.920	3210.65281	
1.345	5.010	24.943	1.452	1.433	7.774	0.236	2.828	0.286	0.047	9.412	0.513	3210.69457	0.913	3210.65356	
1.100	5.577	27.250	1.206	1.748	6.081	0.275	2.370	0.313	0.049	9.960	0.509	3210.69615	0.906	3210.65430	
1.074	5.600	27.232	1.405	1.720	5.882	0.293	2.457	0.307	0.052	9.873	0.572	3210.69772	0.896	3210.65505	
0.991	5.238	26.522	1.495	1.640	6.543	0.258	2.715	0.313	0.049	10.284	0.551	3210.69930	0.922	3210.65579	
													0.964	3210.65654	
													0.975	3210.65729	
													0.982	3210.65803	
													0.981	3210.65878	
													0.959	3210.65952	
													0.929	3210.66027	
													0.935	3210.66101	
													0.968	3210.66176	
													0.983	3210.66251	

EDXRF												Hyperspectral Imagery		
Mg	Al	Si	S	K	Ca	Ti	Fe	K/Al	Ti/Al	Si bio	S/Fe	Depth	TOC	Depth
%	%	%	%	%	%	%	%			%		m	%	m
													1.009	3210.66325
													0.931	3210.66400
													0.920	3210.66474
													0.904	3210.66549
													0.915	3210.66623
													0.873	3210.66698
													0.831	3210.66773
													0.828	3210.66847
													0.837	3210.66922
													0.841	3210.66996
													0.875	3210.67071
													0.870	3210.67145
													0.865	3210.67220
													0.902	3210.67295
													0.904	3210.67369
													0.916	3210.67444
													0.903	3210.67518
													0.910	3210.67593
													0.871	3210.67667
													0.909	3210.67742
													0.856	3210.67817
													0.874	3210.67891
													0.893	3210.67966
													0.877	3210.68040
													0.898	3210.68115
													0.855	3210.68189
													0.876	3210.68264
													0.854	3210.68339
													0.878	3210.68413
													0.866	3210.68488
													0.917	3210.68562
													0.936	3210.68637
													0.984	3210.68711
													1.030	3210.68786
													1.030	3210.68861
													0.983	3210.68935
													0.982	3210.69010
													0.923	3210.69084
													0.988	3210.69159
													0.902	3210.69234
													1.311	3210.69308
													0.965	3210.69383
													0.945	3210.69457
													0.886	3210.69532
													0.930	3210.69606
													0.927	3210.69681
													0.928	3210.69756
													0.919	3210.69830
													0.940	3210.69905
													0.907	3210.69979

EDXRF												Hyperspectral Imagery		
Mg	Al	Si	S	K	Ca	Ti	Fe	K/Al	Ti/Al	Si bio	S/Fe	Depth	TOC	Depth
%	%	%	%	%	%	%	%			%		m	%	m
													0.584	3211.93125
													0.567	3211.93204
													0.570	3211.93284
													0.551	3211.93364
													0.571	3211.93444
													0.563	3211.93524
													0.558	3211.93603
													0.546	3211.93683
													0.546	3211.93763
													0.551	3211.93843
													0.551	3211.93923
													0.554	3211.94002
													0.554	3211.94082
													0.556	3211.94162
													0.555	3211.94242
													0.561	3211.94322
													0.582	3211.94401
													0.597	3211.94481
													0.596	3211.94561
													0.580	3211.94641
													0.573	3211.94721
													0.573	3211.94800
													0.568	3211.94880
													0.570	3211.94960
													0.557	3211.95040
													0.556	3211.95120
													0.525	3211.95199
													0.537	3211.95279
													0.522	3211.95359
													0.528	3211.95439
													0.563	3211.95519
													0.557	3211.95598
													0.538	3211.95678
													0.528	3211.95758
													0.539	3211.95838
													0.554	3211.95918
													0.553	3211.95997
													0.599	3211.96077
													0.580	3211.96157
													0.546	3211.96237
													0.544	3211.96317
													0.536	3211.96396
													0.521	3211.96476
													0.554	3211.96556
													0.571	3211.96636
													0.565	3211.96716
													0.557	3211.96795
													0.533	3211.96875
													0.553	3211.96955

EDXRF												Hyperspectral Imagery		
Mg %	Al %	Si %	S %	K %	Ca %	Ti %	Fe %	K/Al	Ti/Al	Si bio %	S/Fe	Depth m	TOC %	Depth m
1.091	5.127	24.717	1.501	1.583	8.125	0.245	2.641	0.309	0.048	8.823	0.569	3213.43754	1.056	3213.40020
1.166	5.210	25.278	1.571	1.612	7.428	0.241	2.641	0.309	0.046	9.126	0.595	3213.43888	0.989	3213.40101
1.175	5.383	25.576	1.525	1.659	7.169	0.275	2.532	0.308	0.051	8.890	0.602	3213.44022	0.900	3213.40181
1.166	5.566	26.323	1.358	1.705	6.619	0.267	2.457	0.306	0.048	9.067	0.553	3213.44156	0.817	3213.40262
1.069	5.678	26.468	1.358	1.809	6.435	0.293	2.383	0.319	0.052	8.867	0.570	3213.44291	0.810	3213.40342
1.030	5.666	26.097	1.495	1.748	6.647	0.297	2.457	0.308	0.052	8.531	0.608	3213.44425	0.810	3213.40423
1.047	5.500	26.042	1.378	1.776	6.926	0.275	2.379	0.323	0.050	8.994	0.579	3213.44559	0.863	3213.40503
0.942	5.828	26.549	1.149	1.950	5.921	0.323	2.933	0.335	0.055	8.483	0.392	3213.44694	0.838	3213.40584
1.074	5.544	25.418	1.372	1.785	6.607	0.271	3.255	0.322	0.049	8.231	0.421	3213.44828	0.898	3213.40664
1.253	5.199	25.296	1.551	1.583	7.420	0.284	2.606	0.305	0.055	9.178	0.595	3213.44962	0.910	3213.40744
1.271	5.338	24.993	1.624	1.663	7.360	0.271	2.619	0.312	0.051	8.444	0.620	3213.45096	0.871	3213.40825
1.056	5.755	26.056	1.295	1.799	6.866	0.310	2.348	0.313	0.054	8.214	0.552	3213.45231	0.861	3213.40905
1.091	5.550	25.264	1.634	1.654	7.141	0.275	2.584	0.298	0.050	8.060	0.632	3213.45365	0.836	3213.40986
1.008	5.794	26.581	1.392	1.813	6.276	0.306	2.392	0.313	0.053	8.618	0.582	3213.45499	0.864	3213.41066
1.179	5.650	26.142	1.425	1.715	6.567	0.293	2.501	0.304	0.052	8.628	0.570	3213.45634	0.871	3213.41147
													0.865	3213.41227
													0.859	3213.41308
													0.867	3213.41388
													0.838	3213.41469
													0.853	3213.41549
													0.870	3213.41629
													0.887	3213.41710
													0.868	3213.41790
													0.862	3213.41871
													0.863	3213.41951
													0.881	3213.42032
													0.855	3213.42112
													0.882	3213.42193
													0.891	3213.42273
													0.916	3213.42354
													0.871	3213.42434
													0.852	3213.42515
													0.955	3213.42595
													0.883	3213.42675
													0.895	3213.42756
													0.847	3213.42836
													0.859	3213.42917
													0.849	3213.42997
													0.854	3213.43078
													0.850	3213.43158
													0.886	3213.43239
													0.834	3213.43319
													0.886	3213.43400
													0.884	3213.43480
													0.883	3213.43560
													0.909	3213.43641
													0.915	3213.43721
													0.903	3213.43802
													0.899	3213.43882
													0.900	3213.43963
													0.891	3213.44043
													0.923	3213.44124
													0.979	3213.44204
													0.994	3213.44285
													0.992	3213.44365
													0.999	3213.44446
													0.997	3213.44526
													0.931	3213.44606
													0.906	3213.44687
													0.902	3213.44767

EDXRF												Hyperspectral Imagery		
Mg	Al	Si	S	K	Ca	Ti	Fe	K/Al	Ti/Al	Si bio	S/Fe	Depth	TOC	Depth
%	%	%	%	%	%	%	%			%		m	%	m
													0.944	3213.44848
													0.896	3213.44928
													0.928	3213.45009
													0.965	3213.45089
													0.976	3213.45170
													0.970	3213.45250
													0.973	3213.45331
													0.993	3213.45411
													0.956	3213.45491
													0.920	3213.45572
													0.896	3213.45652

Slab 3214.26 m

	EDXRF												Hyperspectral Imagery		
	Mg %	Al %	Si %	S %	K %	Ca %	Ti %	Fe %	K/Al	Ti/Al	Si bio %	S/Fe	Depth m	TOC %	Depth m
1.078	5.822	24.309	1.860	1.757	7.049	0.349	2.972	0.302	0.060		6.261	0.626	3214.26000	0.581	3214.25912
1.166	5.678	24.318	1.857	1.799	7.033	0.362	2.941	0.317	0.064		6.718	0.631	3214.26156	0.494	3214.26007
0.982	6.334	25.413	1.588	1.945	6.396	0.323	2.606	0.307	0.051		5.778	0.609	3214.26312	0.463	3214.26102
0.912	6.540	26.074	1.501	2.119	5.770	0.327	2.497	0.324	0.050		5.801	0.601	3214.26468	0.519	3214.26197
1.104	6.490	25.843	1.571	2.058	5.774	0.288	2.505	0.317	0.044		5.725	0.627	3214.26623	0.532	3214.26292
0.982	6.529	25.712	1.641	2.076	5.818	0.306	2.532	0.318	0.047		5.473	0.648	3214.26779	0.508	3214.26387
1.026	6.373	25.934	1.584	2.076	5.878	0.375	2.501	0.326	0.059		6.178	0.634	3214.26935	0.595	3214.26482
0.951	6.278	25.450	1.661	2.044	6.224	0.310	2.619	0.326	0.049		5.987	0.634	3214.27091	0.478	3214.26577
1.056	6.212	25.214	1.694	1.978	6.332	0.306	2.680	0.318	0.049		5.959	0.632	3214.27247	0.466	3214.26672
1.175	6.056	24.590	1.711	1.898	6.862	0.301	2.784	0.313	0.050		5.817	0.614	3214.27403	0.447	3214.26767
0.938	6.184	24.875	1.950	1.945	6.479	0.310	2.784	0.315	0.050		5.705	0.700	3214.27559	0.455	3214.26862
0.934	6.339	25.282	1.844	1.950	6.212	0.297	2.667	0.308	0.047		5.630	0.691	3214.27715	0.439	3214.26957
1.113	6.167	25.042	1.790	1.945	6.412	0.332	2.689	0.315	0.054		5.925	0.666	3214.27870	0.459	3214.27052
1.069	6.362	25.789	1.634	2.044	5.858	0.301	2.518	0.321	0.047		6.068	0.649	3214.28026	0.455	3214.27147
1.034	6.523	26.173	1.584	2.091	5.623	0.301	2.388	0.320	0.046		5.952	0.664	3214.28182	0.471	3214.27242
1.074	6.245	25.667	1.545	2.006	6.073	0.319	2.667	0.321	0.051		6.308	0.579	3214.28338	0.543	3214.27337
1.126	6.145	24.318	2.080	1.879	6.212	0.275	3.343	0.306	0.045		5.270	0.622	3214.28494	0.458	3214.27432
1.012	6.367	25.839	1.558	2.034	6.085	0.332	2.457	0.319	0.052		6.100	0.634	3214.28650	0.441	3214.27527
1.039	6.412	26.459	1.305	2.081	5.834	0.306	2.261	0.325	0.048		6.582	0.577	3214.28806	0.497	3214.27622
1.026	6.150	25.649	1.624	1.898	6.340	0.319	2.532	0.309	0.052		6.583	0.642	3214.28962	0.505	3214.27717
1.157	6.245	25.830	1.694	1.931	5.790	0.293	2.636	0.309	0.047		6.470	0.643	3214.29117	0.476	3214.27812
1.039	6.289	26.155	1.428	2.015	6.057	0.284	2.335	0.320	0.045		6.658	0.612	3214.29273	0.489	3214.27907
0.942	5.989	25.300	1.794	1.926	6.412	0.310	2.719	0.322	0.052		6.734	0.660	3214.29429	0.479	3214.28002
1.083	5.961	24.707	1.777	1.856	6.854	0.288	2.758	0.311	0.048		6.228	0.644	3214.29585	0.514	3214.28097
0.999	6.173	25.246	1.644	1.926	6.595	0.332	2.575	0.312	0.054		6.111	0.638	3214.29741	0.516	3214.28192
1.065	6.323	26.531	1.392	2.034	5.678	0.323	2.366	0.322	0.051		6.930	0.588	3214.29897	0.500	3214.28287
1.017	6.289	26.264	1.368	2.030	6.013	0.284	2.314	0.323	0.045		6.767	0.591	3214.30053	0.567	3214.28382
1.096	6.134	25.400	1.598	1.922	6.479	0.293	2.549	0.313	0.048		6.385	0.627	3214.30208	0.575	3214.28477
1.087	6.028	25.445	1.588	1.931	6.527	0.301	2.510	0.320	0.050		6.758	0.633	3214.30364	0.558	3214.28572
1.087	6.262	26.124	1.495	2.030	5.921	0.284	2.357	0.324	0.045		6.713	0.634	3214.30520	0.552	3214.28667
0.960	6.250	26.002	1.375	1.978	6.424	0.301	2.266	0.316	0.048		6.625	0.607	3214.30676	0.564	3214.28762
1.004	6.117	25.463	1.485	1.968	6.722	0.293	2.383	0.322	0.048		6.501	0.623	3214.30832	0.538	3214.28857
0.942	6.117	25.567	1.701	1.926	6.384	0.280	2.532	0.315	0.046		6.605	0.672	3214.30988	0.529	3214.28952
0.920	6.089	25.558	1.624	1.917	6.451	0.284	2.571	0.315	0.047		6.682	0.632	3214.31144	0.508	3214.29047
0.960	6.100	25.382	1.977	1.959	6.105	0.288	2.641	0.321	0.047		6.471	0.749	3214.31300	0.526	3214.29142
1.021	6.239	26.427	1.591	2.011	5.682	0.332	2.362	0.322	0.053		7.085	0.674	3214.31455	0.603	3214.29237
1.012	5.939	25.006	1.771	1.804	6.834	0.310	2.623	0.304	0.052		6.595	0.675	3214.31611	0.572	3214.29332
0.938	5.894	25.309	1.624	1.860	6.930	0.275	2.492	0.316	0.047		7.036	0.652	3214.31767	0.569	3214.29427
0.920	5.850	25.051	2.043	1.856	6.467	0.301	2.824	0.317	0.051		6.916	0.724	3214.31923	0.503	3214.29522
1.008	5.967	25.445	1.754	1.879	6.495	0.297	2.597	0.315	0.050		6.948	0.675	3214.32079	0.536	3214.29617
0.929	6.039	25.766	1.714	1.959	6.292	0.306	2.514	0.324	0.051		7.045	0.682	3214.32235	0.513	3214.29712
0.929	6.034	26.015	1.511	1.968	6.435	0.288	2.314	0.326	0.048		7.311	0.653	3214.32391	0.578	3214.29807
0.771	6.284	26.223	1.661	2.086	5.766	0.297	2.444	0.332	0.047		6.743	0.679	3214.32547	0.590	3214.29902
1.113	5.805	24.640	1.874	1.846	6.874	0.314	2.815	0.318	0.054		6.643	0.666	3214.32702	0.615	3214.29997
1.026	6.078	25.748	1.628	1.926	6.324	0.310	2.492	0.317	0.051		6.906	0.653	3214.32858	0.584	3214.30092
0.969	6.022	25.843	1.561	1.926	6.420	0.319	2.466	0.320	0.053		7.174	0.633	3214.33014	0.517	3214.30187
0.947	6.250	26.422	1.415	2.067	5.965	0.267	2.270	0.331	0.043		7.046	0.623	3214.33170	0.488	3214.30283
0.916	6.339	26.608	1.259	2.034	6.141	0.301	2.139	0.321	0.048		6.956	0.588	3214.33326	0.555	3214.30378
0.969	6.139	25.870	1.757	1.940	5.949	0.280	2.571	0.316	0.046		6.839	0.684	3214.33482	0.536	3214.30473
0.881	5.917	24.775	2.173	1.893	6.372	0.288	2.928	0.320	0.049		6.434	0.742	3214.33638	0.554	3214.30568
0.995	6.100	25.658	1.757	1.954	6.212	0.310	2.545	0.320	0.051		6.747	0.691	3214.33793	0.610	3214.30663
0.929	6.367	26.078	1.727	2.076	5.706	0.310	2.436	0.326	0.049		6.340	0.709	3214.33949	0.603	3214.30758
0.824	6.373	26.735	1.564	2.100	5.447	0.310	2.331	0.330	0.049		6.979	0.671	3214.34105	0.550	3214.30853
0.942	6.373	26.839	1.541	2.166	5.284	0.314	2.296	0.340	0.049		7.083	0.671	3214.34261	0.606	3214.30948
0.846	6.529	26.811	1.422	2.138	5.547	0.358	2.248	0.327	0.055		6.573	0.632	3214.34417	0.565	3214.31043
0.951	6.556	27.124	1.461	2.156	5.005	0.319	2.322	0.329	0.049		6.799	0.629	3214.34573	0.549	3214.31138
0.815	6.351	26.757	1.422	2.053	5.770	0.301	2.222	0.323	0.047		7.070	0.640	3214.34729	0.551	3214.31233
0.991	6.423	26.938	1.461	2.048	5.344	0.319	2.270	0.319	0.050		7.027	0.644	3214.34885	0.612	3214.31328
0.955	6.217	25.839	1.661	1.922	6.180	0.319	2.479	0.309	0.051		6.566	0.670	3214.35040	0.575	3214.31423
0.758	6.267	26.336	1.541	2.020	6.045	0.323	2.327	0.322	0.052		6.908	0.662	3214.35196	0.573	3214.31518
0.999	6.273	25.784	1.651	2.034	5.662	0.323	2.806	0.324	0.051		6.339	0.588	3214.35352	0.582	3214.31613

EDXRF													Hyperspectral Imagery	
Mg %	Al %	Si %	S %	K %	Ca %	Ti %	Fe %	K/Al	Ti/Al	Si bio %	S/Fe	Depth m	TOC %	Depth m
0.969	6.467	27.096	1.382	2.142	4.977	0.314	2.418	0.331	0.049	7.048	0.571	3214.35508	0.645	3214.31708
0.934	6.228	25.961	1.611	1.973	6.153	0.314	2.409	0.317	0.050	6.653	0.669	3214.35664	0.584	3214.31803
0.973	6.328	26.585	1.485	2.011	5.758	0.353	2.296	0.318	0.056	6.967	0.647	3214.35820	0.531	3214.31898
													0.574	3214.31993
													0.526	3214.32088
													0.586	3214.32183
													0.527	3214.32278
													0.616	3214.32373
													0.608	3214.32468
													0.653	3214.32563
													0.620	3214.32658
													0.643	3214.32753
													0.728	3214.32848
													0.571	3214.32943
													0.599	3214.33038
													0.563	3214.33133
													0.643	3214.33228
													0.606	3214.33323
													0.641	3214.33418
													0.659	3214.33513
													0.668	3214.33608
													0.689	3214.33703
													0.667	3214.33798
													0.646	3214.33893
													0.685	3214.33988
													0.632	3214.34083
													0.696	3214.34178
													0.625	3214.34273
													0.588	3214.34368
													0.604	3214.34463
													0.621	3214.34558
													0.640	3214.34653
													0.635	3214.34748
													0.707	3214.34843
													0.661	3214.34938
													0.672	3214.35033
													0.658	3214.35128
													0.698	3214.35223
													0.633	3214.35318
													0.661	3214.35413
													0.699	3214.35508
													0.648	3214.35603
													0.623	3214.35698
													0.626	3214.35793
													0.579	3214.35888

Slab 3215.45 m

EDXRF													Hyperspectral Imagery		
Mg %	Al %	Si %	S %	K %	Ca %	Ti %	Fe %	K/Al	Ti/Al	Si bio %	S/Fe	Depth m	TOC %	Depth m	
0.807	4.843	24.603	3.475	1.691	5.459	0.271	3.421	0.349	0.056	9.590	1.016	3215.45000	0.726	3215.45080	
0.697	4.971	24.626	3.429	1.724	5.491	0.258	3.425	0.347	0.052	9.216	1.001	3215.45160	0.804	3215.45160	
0.640	4.682	24.807	3.233	1.640	6.276	0.293	3.173	0.350	0.062	10.293	1.019	3215.45320	0.826	3215.45240	
0.666	4.732	24.508	3.120	1.405	6.918	0.219	3.120	0.297	0.046	9.839	1.000	3215.45479	0.777	3215.45320	
0.697	4.954	26.087	3.239	1.579	5.069	0.258	3.138	0.319	0.052	10.729	1.032	3215.45639	0.755	3215.45400	
0.732	5.216	27.237	3.977	1.710	2.355	0.267	3.670	0.328	0.051	11.068	1.084	3215.45799	0.756	3215.45480	
0.754	5.144	27.305	4.449	1.682	1.746	0.271	3.770	0.327	0.053	11.360	1.180	3215.45959	0.800	3215.45559	
0.579	5.288	28.155	4.210	1.790	1.367	0.262	3.600	0.338	0.050	11.762	1.169	3215.46119	0.822	3215.45639	
0.526	5.438	27.843	4.286	1.813	1.403	0.280	3.678	0.333	0.051	10.984	1.165	3215.46278	0.855	3215.45719	
0.640	5.244	28.033	4.087	1.757	1.586	0.275	3.626	0.335	0.052	11.778	1.127	3215.46438	0.834	3215.45799	
0.622	5.299	27.956	4.389	1.738	1.255	0.288	3.731	0.328	0.054	11.528	1.176	3215.46598	0.917	3215.45879	
0.526	4.932	27.078	5.107	1.654	1.108	0.275	4.175	0.335	0.056	11.789	1.223	3215.46758	0.853	3215.45959	
0.570	5.322	27.653	4.439	1.781	1.331	0.284	3.800	0.335	0.053	11.156	1.168	3215.46918	0.879	3215.46039	
0.614	5.093	26.232	5.452	1.565	1.343	0.232	4.219	0.307	0.046	10.442	1.292	3215.47077	0.887	3215.46119	
0.592	4.960	26.291	5.509	1.630	1.144	0.232	4.428	0.329	0.047	10.915	1.244	3215.47237	0.800	3215.46199	
0.566	4.854	25.653	5.868	1.565	0.865	0.228	4.978	0.322	0.047	10.605	1.179	3215.47397	0.932	3215.46279	
0.544	4.877	26.404	5.615	1.569	0.877	0.241	4.655	0.322	0.049	11.287	1.206	3215.47557	0.748	3215.46358	
0.360	4.409	24.151	6.855	1.288	0.853	0.171	5.488	0.292	0.039	10.482	1.249	3215.47717	0.851	3215.46438	
0.566	4.815	25.278	6.190	1.560	0.929	0.206	4.930	0.324	0.043	10.350	1.256	3215.47876	0.837	3215.46518	
0.530	4.849	25.983	5.825	1.569	0.925	0.228	4.703	0.324	0.047	10.952	1.239	3215.48036	0.875	3215.46598	
0.447	5.099	26.866	5.087	1.640	1.176	0.236	4.350	0.322	0.046	11.059	1.169	3215.48196	0.859	3215.46678	
0.566	4.877	26.314	5.266	1.565	1.415	0.254	4.459	0.321	0.052	11.196	1.181	3215.48356	0.831	3215.46758	
0.658	5.049	26.766	4.745	1.630	1.586	0.267	4.271	0.323	0.053	11.114	1.111	3215.48516	0.836	3215.46838	
0.750	5.055	26.766	4.612	1.673	1.769	0.254	4.106	0.331	0.050	11.097	1.123	3215.48675	0.866	3215.46918	
0.723	4.849	25.436	5.526	1.583	1.578	0.241	4.725	0.327	0.050	10.405	1.169	3215.48835	0.858	3215.46998	
0.649	4.938	25.522	5.469	1.607	1.586	0.215	4.668	0.325	0.043	10.215	1.172	3215.48995	0.846	3215.47078	
0.732	4.932	25.074	5.725	1.485	1.546	0.232	4.882	0.301	0.047	9.784	1.173	3215.49155	0.906	3215.47157	
0.679	5.110	25.988	5.167	1.593	1.439	0.236	4.572	0.312	0.046	10.146	1.130	3215.49315	0.833	3215.47237	
0.671	5.021	25.911	4.984	1.635	1.614	0.245	4.638	0.326	0.049	10.345	1.075	3215.49474	0.862	3215.47317	
0.631	4.949	26.983	4.878	1.607	1.299	0.228	4.267	0.325	0.046	11.642	1.143	3215.49634	0.891	3215.47397	
0.583	4.932	26.318	5.326	1.579	1.204	0.223	4.481	0.320	0.045	11.029	1.189	3215.49794	0.908	3215.47477	
0.587	4.999	27.051	4.974	1.579	1.168	0.254	4.232	0.316	0.051	11.555	1.175	3215.49954	0.898	3215.47557	
0.482	4.760	25.097	6.061	1.466	1.152	0.228	4.842	0.308	0.048	10.341	1.252	3215.50114	0.913	3215.47637	
0.561	5.238	27.567	4.442	1.668	1.259	0.293	3.962	0.318	0.056	11.329	1.121	3215.50273	0.942	3215.47717	
0.767	5.355	28.169	4.020	1.762	1.204	0.262	3.622	0.329	0.049	11.569	1.110	3215.50433	0.941	3215.47797	
0.754	5.483	28.544	3.645	1.832	1.435	0.262	3.377	0.334	0.048	11.548	1.079	3215.50593	0.922	3215.47876	
0.745	5.466	28.979	3.449	1.879	1.427	0.314	3.194	0.344	0.057	12.034	1.080	3215.50753	0.882	3215.47956	
0.535	5.533	29.341	3.322	1.828	1.391	0.275	3.190	0.330	0.050	12.189	1.042	3215.50913	0.878	3215.48036	
0.820	5.644	29.372	3.179	1.907	1.323	0.288	2.994	0.338	0.051	11.875	1.062	3215.51072	0.822	3215.48116	
0.614	5.605	29.698	2.954	2.001	1.451	0.297	2.955	0.357	0.053	12.322	1.000	3215.51232	0.817	3215.48196	
0.745	5.900	30.015	2.801	1.922	1.343	0.310	2.697	0.326	0.053	11.725	1.038	3215.51392	0.828	3215.48276	
0.728	5.817	29.540	3.136	1.992	1.172	0.319	2.885	0.342	0.055	11.508	1.087	3215.51552	0.800	3215.48356	
0.728	5.989	30.775	2.438	2.072	1.152	0.288	2.536	0.346	0.048	12.209	0.962	3215.51712	0.778	3215.48436	
0.706	6.017	30.911	2.488	2.109	0.921	0.314	2.536	0.351	0.052	12.259	0.981	3215.51871	0.801	3215.48516	
0.666	6.123	30.965	2.528	2.138	0.805	0.293	2.527	0.349	0.048	11.985	1.000	3215.52031	0.825	3215.48596	
0.644	5.989	30.834	2.691	2.128	0.737	0.293	2.571	0.355	0.049	12.268	1.047	3215.52191	0.824	3215.48675	
0.601	6.056	31.173	2.508	2.170	0.765	0.306	2.518	0.358	0.050	12.400	0.996	3215.52351	0.811	3215.48755	
0.631	5.956	31.951	2.249	2.166	0.618	0.258	2.309	0.364	0.043	13.489	0.974	3215.52511	0.830	3215.48835	
0.728	6.028	32.526	1.963	2.180	0.522	0.262	2.117	0.362	0.044	13.839	0.927	3215.52670	0.826	3215.48915	
0.644	6.173	32.517	1.907	2.292	0.510	0.262	2.087	0.371	0.042	13.382	0.914	3215.52830	0.878	3215.48995	
0.609	6.022	31.146	2.488	2.152	0.885	0.280	2.510	0.357	0.046	12.477	0.991	3215.52990	0.913	3215.49075	
0.693	6.084	30.531	2.618	2.133	1.016	0.267	2.641	0.351	0.044	11.672	0.991	3215.53150	0.886	3215.49155	
0.671	6.072	31.286	2.415	2.180	0.702	0.301	2.566	0.359	0.050	12.462	0.941	3215.53310	0.928	3215.49235	
0.644	6.167	32.291	2.063	2.250	0.455	0.275	2.231	0.365	0.045	13.173	0.925	3215.53469	0.913	3215.49315	
0.522	6.045	31.363	2.538	2.175	0.534	0.258	2.601	0.360	0.043	12.625	0.976	3215.53629	0.861	3215.49395	
0.609	6.078	31.490	2.531	2.166	0.518	0.258	2.484	0.356	0.042	12.648	1.019	3215.53789	1.014	3215.49474	
0.750	5.983	31.015	2.538	2.095	0.797	0.288	2.606	0.350	0.048	12.466	0.974	3215.53949	1.123	3215.49554	
0.741	6.339	31.300	2.226	2.288	0.650	0.297	2.436	0.361	0.047	11.648	0.914	3215.54109	0.856	3215.49634	
0.614	6.217	32.626	1.910	2.302	0.371	0.254	2.148	0.370	0.041	13.353	0.889	3215.54268	0.889	3215.49714	
0.627	6.100	32.214	2.166	2.231	0.431	0.249	2.261	0.366	0.041	13.303	0.958	3215.54428	0.865	3215.49794	
0.530	6.123	32.354	2.189	2.213	0.355	0.262	2.314	0.361	0.043	13.374	0.946	3215.54588	0.798	3215.49874	

EDXRF												Hyperspectral Imagery		
Mg %	Al %	Si %	S %	K %	Ca %	Ti %	Fe %	K/Al	Ti/Al	Si bio %	S/Fe	Depth m	TOC %	Depth m
0.662	6.212	31.865	2.226	2.311	0.399	0.262	2.340	0.372	0.042	12.610	0.951	3215.54748	0.802	3215.49954
0.596	6.100	31.671	2.332	2.222	0.490	0.262	2.492	0.364	0.043	12.760	0.936	3215.54908	0.778	3215.50034
0.684	6.128	31.332	2.492	2.208	0.538	0.275	2.532	0.360	0.045	12.334	0.984	3215.55067	0.717	3215.50114
													0.795	3215.50206
													0.876	3215.50298
													0.899	3215.50390
													0.924	3215.50482
													0.940	3215.50574
													0.985	3215.50666
													1.020	3215.50758
													1.017	3215.50850
													1.013	3215.50942
													1.064	3215.51034
													1.083	3215.51126
													1.083	3215.51218
													1.079	3215.51310
													1.108	3215.51402
													1.126	3215.51494
													1.104	3215.51586
													0.995	3215.51678
													0.947	3215.51770
													0.933	3215.51862
													0.958	3215.51954
													1.018	3215.52046
													0.964	3215.52138
													1.019	3215.52230
													1.084	3215.52322
													1.148	3215.52414
													1.187	3215.52506
													1.150	3215.52598
													1.158	3215.52690
													1.206	3215.52782
													1.052	3215.52874
													1.059	3215.52966
													1.005	3215.53058
													0.925	3215.53150
													0.981	3215.53242
													1.041	3215.53334
													1.033	3215.53426
													1.223	3215.53518
													1.100	3215.53610
													1.085	3215.53702
													1.136	3215.53794
													1.181	3215.53886
													1.113	3215.53978
													1.093	3215.54070
													1.124	3215.54162
													1.082	3215.54254
													1.087	3215.54346
													1.114	3215.54438
													1.050	3215.54530
													1.084	3215.54622
													1.036	3215.54714
													1.033	3215.54806
													1.132	3215.54898
													1.122	3215.54990
													1.180	3215.55082
													1.153	3215.55174
													1.164	3215.55266
													1.052	3215.55358

Slab 3218.55 m

EDXRF												Hyperspectral Imagery			
Mg %	Al %	Si %	S %	K %	Ca %	Ti %	Fe %	K/Al	Ti/Al	Si bio %	S/Fe	Depth m	TOC %	Depth m	
0.877	8.559	29.974	1.594	3.128	0.215	0.306	2.030	0.366	0.036	3.442	0.785	3218.55734	0.378	3218.55734	
0.942	8.692	30.060	1.498	3.124	0.196	0.327	1.973	0.359	0.038	3.114	0.759	3218.55881	0.522	3218.55844	
0.820	8.609	29.716	1.794	3.100	0.204	0.340	2.148	0.360	0.040	3.029	0.835	3218.56028	0.518	3218.55954	
0.793	8.765	29.757	1.737	3.048	0.200	0.336	2.104	0.348	0.038	2.587	0.826	3218.56174	0.551	3218.56064	
0.820	8.681	29.752	1.797	3.114	0.200	0.358	2.043	0.359	0.041	2.841	0.880	3218.56321	0.607	3218.56174	
0.798	8.520	29.309	2.143	3.091	0.188	0.349	2.200	0.363	0.041	2.897	0.974	3218.56468	0.573	3218.56285	
0.877	8.520	29.725	1.870	3.077	0.180	0.319	2.091	0.361	0.037	3.314	0.894	3218.56615	0.647	3218.56395	
0.820	8.626	30.010	1.638	3.100	0.215	0.353	2.061	0.359	0.041	3.271	0.795	3218.56762	0.635	3218.56505	
0.868	8.620	29.721	1.877	3.006	0.196	0.332	2.061	0.349	0.038	2.999	0.911	3218.56908	0.612	3218.56615	
0.820	8.359	29.517	2.126	3.063	0.180	0.314	2.174	0.366	0.038	3.606	0.978	3218.57055	0.566	3218.56725	
0.758	8.392	30.223	1.724	3.072	0.188	0.323	2.013	0.366	0.038	4.208	0.857	3218.57202	0.554	3218.56835	
0.771	8.336	29.409	2.232	3.063	0.188	0.297	2.196	0.367	0.036	3.566	1.017	3218.57349	0.639	3218.56945	
0.785	8.464	30.083	1.757	3.077	0.192	0.336	2.113	0.363	0.040	3.843	0.832	3218.57496	0.598	3218.57055	
0.763	8.386	30.160	1.724	3.114	0.196	0.327	2.069	0.371	0.039	4.162	0.833	3218.57642	0.554	3218.57165	
0.872	8.364	29.748	1.987	3.067	0.192	0.323	2.104	0.367	0.039	3.819	0.944	3218.57789	0.540	3218.57275	
0.723	8.309	28.621	2.847	3.030	0.172	0.310	2.327	0.365	0.037	2.865	1.224	3218.57936	0.598	3218.57386	
0.767	8.431	29.400	2.209	3.020	0.204	0.319	2.200	0.358	0.038	3.264	1.004	3218.58083	0.575	3218.57496	
0.894	8.525	29.662	1.973	3.067	0.184	0.310	2.043	0.360	0.036	3.233	0.966	3218.58230	0.556	3218.57606	
0.780	8.492	30.083	1.767	3.095	0.176	0.319	2.026	0.365	0.038	3.757	0.872	3218.58376	0.613	3218.57716	
0.820	8.531	30.218	1.618	3.091	0.200	0.332	1.991	0.362	0.039	3.772	0.813	3218.58523	0.573	3218.57826	
0.907	8.503	29.915	1.731	3.128	0.196	0.327	2.030	0.368	0.038	3.555	0.852	3218.58670	0.586	3218.57936	
0.824	8.487	30.042	1.687	3.124	0.180	0.310	2.026	0.368	0.037	3.734	0.833	3218.58817	0.660	3218.58046	
0.785	8.453	29.888	1.857	3.152	0.180	0.332	2.056	0.373	0.039	3.683	0.903	3218.58964	0.666	3218.58156	
0.776	8.603	29.834	1.837	3.105	0.196	0.340	2.052	0.361	0.040	3.164	0.895	3218.59110	0.664	3218.58266	
0.828	8.487	30.350	1.498	3.189	0.184	0.353	1.965	0.376	0.042	4.041	0.762	3218.59257	0.643	3218.58376	
0.942	8.525	29.838	1.787	3.044	0.192	0.323	2.061	0.357	0.038	3.409	0.867	3218.59404	0.633	3218.58487	
0.934	8.576	29.952	1.687	3.110	0.192	0.319	1.987	0.363	0.037	3.367	0.849	3218.59551	0.577	3218.58597	
0.877	8.598	30.173	1.601	3.138	0.176	0.323	1.947	0.365	0.038	3.520	0.822	3218.59698	0.585	3218.58707	
0.745	8.626	30.259	1.485	3.208	0.172	0.345	1.973	0.372	0.040	3.520	0.752	3218.59844	0.551	3218.58817	
0.763	8.559	29.784	1.830	3.175	0.172	0.306	2.087	0.371	0.036	3.252	0.877	3218.59991	0.572	3218.58927	
0.934	8.509	29.757	1.860	3.114	0.180	0.340	2.030	0.366	0.040	3.380	0.916	3218.60138	0.603	3218.59037	
0.723	8.581	30.164	1.677	3.128	0.184	0.349	1.995	0.365	0.041	3.563	0.841	3218.60285	0.622	3218.59147	
0.728	8.609	30.137	1.661	3.142	0.180	0.332	1.982	0.365	0.039	3.449	0.838	3218.60432	0.518	3218.59257	
0.964	8.531	30.056	1.654	3.119	0.180	0.288	1.947	0.366	0.034	3.609	0.849	3218.60578	0.554	3218.59367	
0.750	8.503	30.472	1.438	3.199	0.184	0.349	1.960	0.376	0.041	4.112	0.734	3218.60725	0.570	3218.59477	
0.885	8.531	29.825	1.814	3.114	0.184	0.327	2.061	0.365	0.038	3.379	0.880	3218.60872	0.614	3218.59588	
0.828	8.392	29.051	2.409	3.058	0.184	0.301	2.209	0.364	0.036	3.036	1.090	3218.61019	0.573	3218.59698	
0.750	8.648	29.476	2.066	3.067	0.204	0.353	2.122	0.355	0.041	2.668	0.974	3218.61166	0.568	3218.59808	
0.780	8.648	30.024	1.588	3.142	0.212	0.310	2.013	0.363	0.036	3.216	0.789	3218.61312	0.554	3218.59918	
0.837	8.570	30.096	1.651	3.138	0.192	0.340	1.973	0.366	0.040	3.529	0.837	3218.61459	0.529	3218.60028	
0.754	8.548	29.974	1.780	3.119	0.208	0.319	2.008	0.365	0.037	3.476	0.887	3218.61606	0.646	3218.60138	
0.863	8.703	30.096	1.578	3.180	0.176	0.323	1.921	0.365	0.037	3.116	0.821	3218.61753	0.645	3218.60248	
0.859	8.698	30.187	1.521	3.133	0.200	0.327	1.926	0.360	0.038	3.223	0.790	3218.61900	0.661	3218.60358	
0.815	8.631	30.128	1.618	3.119	0.180	0.314	1.995	0.361	0.036	3.371	0.811	3218.62046	0.559	3218.60468	
0.780	8.559	30.336	1.538	3.156	0.180	0.353	1.930	0.369	0.041	3.804	0.797	3218.62193	0.554	3218.60578	
0.894	8.609	30.065	1.604	3.105	0.223	0.349	1.956	0.361	0.041	3.377	0.820	3218.62340	0.573	3218.60689	
0.837	8.425	29.789	1.767	3.208	0.212	0.345	2.078	0.381	0.041	3.670	0.850	3218.62487	0.615	3218.60799	
0.842	8.464	30.074	1.641	3.189	0.180	0.345	2.043	0.377	0.041	3.834	0.803	3218.62634	0.659	3218.60909	
0.723	8.481	30.028	1.757	3.105	0.188	0.301	2.074	0.366	0.036	3.737	0.847	3218.62780	0.567	3218.61019	
0.811	8.436	30.101	1.734	3.133	0.192	0.332	2.021	0.371	0.039	3.948	0.858	3218.62927	0.531	3218.61129	
0.877	8.487	30.214	1.601	3.119	0.192	0.319	2.004	0.368	0.038	3.906	0.799	3218.63074	0.532	3218.61239	
0.798	8.603	30.617	1.378	3.124	0.192	0.319	1.878	0.363	0.037	3.946	0.734	3218.63221	0.603	3218.61349	
0.798	8.514	30.228	1.618	3.152	0.180	0.301	1.969	0.370	0.035	3.833	0.822	3218.63368	0.574	3218.61459	
0.745	8.431	30.304	1.651	3.124	0.200	0.319	2.013	0.370	0.038	4.169	0.820	3218.63514	0.673	3218.61569	
0.881	8.492	30.268	1.604	3.048	0.188	0.314	2.000	0.359	0.037	3.943	0.802	3218.63661	0.507	3218.61679	
0.815	8.592	30.028	1.658	3.128	0.160	0.297	2.030	0.364	0.035	3.393	0.816	3218.63808	0.535	3218.61790	
0.802	8.436	30.010	1.761	3.100	0.192	0.306	2.052	0.367	0.036	3.857	0.858	3218.63955	0.534	3218.61900	
0.723	8.525	30.051	1.827	3.114	0.176	0.297	2.004	0.365	0.035	3.622	0.912	3218.64102	0.614	3218.62010	
0.815	8.409	29.879	1.937	3.039	0.192	0.327	2.074	0.361	0.039	3.812	0.934	3218.64250	0.556	3218.62120	
													0.669	3218.62230	
													0.648	3218.62340	

EDXRF												Hyperspectral Imagery		
Mg	Al	Si	S	K	Ca	Ti	Fe	K/Al	Ti/Al	Si bio	S/Fe	Depth	TOC	Depth
%	%	%	%	%	%	%	%			%		m	%	m
													0.671	3218.62450
													0.579	3218.62560
													0.548	3218.62670
													0.571	3218.62780
													0.580	3218.62891
													0.511	3218.63001
													0.504	3218.63111
													0.691	3218.63221
													0.571	3218.63331
													0.529	3218.63441
													0.654	3218.63551
													0.640	3218.63661
													0.657	3218.63771
													0.603	3218.63881
													0.549	3218.63992
													0.569	3218.64102
													0.611	3218.64212
													0.578	3218.64322

Slab 3221.17 m

EDXRF													Hyperspectral Imagery			
Mg %	Al %	Si %	S %	K %	Ca %	Ti %	Fe %	K/Al	Ti/Al	Si bio %	S/Fe	Depth m	TOC %	Depth m		
0.982	8.475	26.721	1.990	3.077	1.981	0.453	2.566	0.363	0.053	0.447	0.775	3221.17000	0.629	3221.17000		
0.960	8.453	26.902	1.993	3.114	1.925	0.479	2.545	0.368	0.057	0.697	0.783	3221.17157	0.768	3221.17134		
0.842	8.598	28.160	2.196	3.161	0.698	0.340	2.536	0.368	0.040	1.507	0.866	3221.17314	0.925	3221.17268		
0.951	8.754	28.332	2.046	3.218	0.662	0.327	2.388	0.368	0.037	1.196	0.857	3221.17470	1.028	3221.17401		
0.960	8.776	28.146	2.136	3.199	0.614	0.345	2.436	0.364	0.039	0.941	0.877	3221.17627	1.053	3221.17535		
0.916	8.932	28.730	1.717	3.241	0.630	0.327	2.266	0.363	0.037	1.042	0.758	3221.17784	1.155	3221.17669		
0.899	8.759	28.476	2.040	3.171	0.642	0.336	2.353	0.362	0.038	1.323	0.867	3221.17941	1.103	3221.17802		
1.047	8.881	28.386	1.854	3.208	0.714	0.340	2.335	0.361	0.038	0.853	0.794	3221.18098	1.057	3221.17936		
1.030	8.904	28.834	1.618	3.218	0.674	0.340	2.239	0.361	0.038	1.232	0.722	3221.18254	0.996	3221.18070		
0.991	8.815	28.698	1.644	3.208	0.845	0.319	2.257	0.364	0.036	1.373	0.729	3221.18411	0.964	3221.18204		
1.004	8.820	28.377	1.827	3.180	0.865	0.336	2.322	0.361	0.038	1.034	0.787	3221.18568	0.953	3221.18337		
0.916	8.826	28.427	1.790	3.213	0.861	0.340	2.331	0.364	0.039	1.067	0.768	3221.18725	1.032	3221.18471		
0.881	8.726	28.486	1.864	3.180	0.909	0.340	2.331	0.364	0.039	1.436	0.799	3221.18882	1.058	3221.18605		
1.017	8.865	28.662	1.601	3.194	0.845	0.327	2.213	0.360	0.037	1.181	0.723	3221.19038	1.094	3221.18739		
1.126	8.809	28.210	1.854	3.194	0.837	0.332	2.331	0.363	0.038	0.901	0.795	3221.19195	1.140	3221.18872		
0.859	8.781	28.730	1.754	3.255	0.769	0.366	2.274	0.371	0.042	1.508	0.771	3221.19352	1.181	3221.19006		
0.995	8.865	27.870	2.302	3.095	0.678	0.319	2.453	0.349	0.036	0.389	0.938	3221.19509	1.146	3221.19140		
0.947	8.703	27.888	2.329	3.119	0.730	0.297	2.505	0.358	0.034	0.908	0.929	3221.19666	1.148	3221.19274		
0.934	8.826	28.612	1.754	3.203	0.781	0.349	2.279	0.363	0.040	1.252	0.770	3221.19822	1.074	3221.19407		
1.034	8.759	28.490	1.834	3.171	0.737	0.349	2.344	0.362	0.040	1.337	0.782	3221.19979	1.165	3221.19541		
1.026	8.820	28.476	1.887	3.100	0.674	0.336	2.305	0.351	0.038	1.134	0.819	3221.20136	1.066	3221.19675		
0.999	8.670	28.282	2.106	3.147	0.737	0.336	2.344	0.363	0.039	1.405	0.898	3221.20293	1.134	3221.19809		
1.074	8.809	28.237	1.963	3.138	0.753	0.310	2.344	0.356	0.035	0.928	0.838	3221.20450	1.123	3221.19942		
1.039	8.848	27.934	2.040	3.166	0.845	0.332	2.457	0.358	0.037	0.504	0.830	3221.20606	1.116	3221.20076		
0.934	8.854	28.291	1.761	3.124	0.945	0.327	2.392	0.353	0.037	0.845	0.736	3221.20763	1.299	3221.20210		
1.052	8.792	28.549	1.684	3.180	0.837	0.310	2.314	0.362	0.035	1.292	0.728	3221.20920	1.318	3221.20344		
1.004	8.748	28.273	1.874	3.142	0.873	0.323	2.414	0.359	0.037	1.154	0.776	3221.21077	1.293	3221.20477		
0.846	8.831	28.345	2.033	3.189	0.682	0.349	2.431	0.361	0.040	0.968	0.836	3221.21234	1.160	3221.20611		
1.004	8.564	27.336	2.086	3.335	0.857	0.401	2.784	0.389	0.047	0.787	0.749	3221.21390	1.177	3221.20745		
1.017	8.776	26.766	1.814	3.448	0.889	0.405	2.889	0.393	0.046	-0.439	0.628	3221.21547	1.153	3221.20878		
0.999	8.614	27.164	2.292	3.034	0.845	0.366	2.697	0.352	0.043	0.460	0.850	3221.21704	1.172	3221.21012		
0.999	8.754	28.105	1.761	3.119	1.008	0.397	2.431	0.356	0.045	0.970	0.724	3221.21861	1.317	3221.21146		
0.991	8.792	28.160	1.807	3.142	0.953	0.345	2.388	0.357	0.039	0.903	0.757	3221.22018	1.322	3221.21280		
1.030	8.642	28.286	1.787	3.185	0.996	0.371	2.405	0.368	0.043	1.495	0.743	3221.22174	1.325	3221.21413		
0.899	8.676	28.359	1.890	3.147	0.929	0.345	2.401	0.363	0.040	1.464	0.787	3221.22331	1.387	3221.21547		
1.069	8.592	28.214	1.734	3.114	1.176	0.353	2.375	0.362	0.041	1.578	0.730	3221.22488	1.353	3221.21681		
1.126	8.631	27.811	1.947	3.081	1.176	0.353	2.475	0.357	0.041	1.055	0.787	3221.22645	1.289	3221.21815		
1.017	8.665	27.870	1.943	3.048	1.236	0.336	2.444	0.352	0.039	1.010	0.795	3221.22802	1.384	3221.21948		
1.258	8.442	27.694	1.850	2.992	1.339	0.314	2.527	0.354	0.037	1.523	0.732	3221.22958	1.441	3221.22082		
1.052	8.514	28.105	1.913	3.133	1.108	0.358	2.444	0.368	0.042	1.711	0.783	3221.23115	1.565	3221.22216		
1.153	8.442	27.744	2.010	3.048	1.240	0.310	2.518	0.361	0.037	1.573	0.798	3221.23272	1.475	3221.22350		
1.056	8.487	27.920	1.950	3.072	1.216	0.319	2.488	0.362	0.038	1.612	0.784	3221.23429	1.371	3221.22483		
1.170	8.403	27.780	2.030	2.997	1.240	0.358	2.501	0.357	0.043	1.730	0.812	3221.23586	1.399	3221.22617		
1.140	8.609	27.621	2.056	3.077	1.240	0.323	2.484	0.357	0.038	0.934	0.828	3221.23742	1.503	3221.22751		
1.153	8.520	27.572	1.887	3.114	1.363	0.358	2.527	0.366	0.042	1.160	0.747	3221.23899	1.538	3221.22885		
1.188	8.464	27.440	2.113	3.053	1.287	0.358	2.566	0.361	0.042	1.201	0.823	3221.24056	1.395	3221.23018		
1.192	8.453	27.676	1.840	3.081	1.399	0.345	2.514	0.365	0.041	1.471	0.732	3221.24213	1.504	3221.23152		
0.951	8.659	28.128	1.897	3.161	1.048	0.366	2.457	0.365	0.042	1.285	0.772	3221.24370	1.327	3221.23286		
1.148	8.537	27.879	2.060	3.091	0.853	0.332	2.497	0.362	0.039	1.416	0.825	3221.24526	1.414	3221.23420		
1.065	8.481	27.929	2.090	3.091	0.989	0.336	2.536	0.364	0.040	1.638	0.824	3221.24683	1.407	3221.23553		
1.061	8.498	27.739	2.070	3.110	1.172	0.319	2.514	0.366	0.037	1.396	0.823	3221.24840	1.457	3221.23687		
1.161	8.520	27.639	1.950	3.025	1.375	0.314	2.518	0.355	0.037	1.228	0.774	3221.24997	1.661	3221.23821		
0.934	8.125	25.730	3.778	2.908	1.052	0.306	3.064	0.358	0.038	0.543	1.233	3221.25154	1.509	3221.23955		
1.047	8.548	27.490	2.186	3.011	1.228	0.332	2.597	0.352	0.039	0.992	0.842	3221.25310	1.485	3221.24088		
0.977	8.498	27.766	2.166	2.983	1.116	0.332	2.571	0.351	0.039	1.423	0.843	3221.25467	1.482	3221.24222		
0.960	8.492	27.495	2.322	3.058	1.108	0.336	2.632	0.360	0.040	1.169	0.882	3221.25624	1.379	3221.24356		
0.999	8.403	28.020	1.927	3.011	1.287	0.340	2.540	0.358	0.040	1.970	0.758	3221.25781	1.368	3221.24489		
1.175	8.542	27.703	1.907	3.058	1.347	0.323	2.488	0.358	0.038	1.222	0.766	3221.25938	1.442	3221.24623		
1.153	8.403	27.327	2.292	3.025	1.244	0.327	2.614	0.360	0.039	1.278	0.877	3221.26094	1.479	3221.24757		
1.096	8.448	27.712	1.953	3.077	1.224	0.314	2.566	0.364	0.037	1.524	0.761	3221.26251	1.463	3221.24891		
1.061	8.370	27.829	2.143	3.053	1.068	0.340	2.571	0.365	0.041	1.883	0.833	3221.26408	1.537	3221.25024		

EDXRF												Hyperspectral Imagery		
Mg %	Al %	Si %	S %	K %	Ca %	Ti %	Fe %	K/Al	Ti/Al	Si bio %	S/Fe	Depth m	TOC %	Depth m
1.179	8.370	27.630	2.199	2.973	1.212	0.327	2.584	0.355	0.039	1.684	0.851	3221.26565	1.636	3221.25158
1.183	8.381	27.250	2.043	2.908	1.503	0.323	2.627	0.347	0.039	1.270	0.778	3221.26722	1.665	3221.25292
													1.598	3221.25426
													1.528	3221.25559
													1.797	3221.25693
													1.594	3221.25827
													1.814	3221.25961
													1.864	3221.26094
													1.699	3221.26228
													1.768	3221.26362
													1.741	3221.26496
													1.731	3221.26629
													1.674	3221.26763
													1.652	3221.26897

Slab 3223.28 m

EDXRF												Hyperspectral Imagery		
Mg	Al	Si	S	K	Ca	Ti	Fe	K/Al	Ti/Al	Si bio	S/Fe	Depth	TOC	Depth
%	%	%	%	%	%	%	%			%		m	%	m
0.557	2.852	35.422	1.691	0.959	1.793	0.206	1.498	0.336	0.072	26.581	1.129	3223.28000	2.966	3223.27484
0.491	2.907	35.336	1.764	0.945	1.825	0.236	1.503	0.325	0.081	26.323	1.174	3223.28172	3.045	3223.27557
0.346	2.357	38.023	1.265	0.809	1.283	0.110	1.171	0.343	0.047	30.717	1.080	3223.28344	3.165	3223.27630
0.434	2.346	38.404	1.179	0.729	1.148	0.071	1.049	0.311	0.030	31.132	1.124	3223.28516	3.284	3223.27703
0.338	2.179	38.440	1.159	0.691	1.323	0.097	1.045	0.317	0.045	31.685	1.109	3223.28688	3.389	3223.27776
0.294	2.112	38.716	1.079	0.677	1.323	0.063	1.023	0.321	0.030	32.168	1.055	3223.28860	3.442	3223.27848
0.403	2.112	38.422	1.226	0.668	1.323	0.076	1.062	0.316	0.036	31.874	1.154	3223.29031	3.458	3223.27921
0.360	2.118	38.607	1.179	0.705	1.311	0.102	1.088	0.333	0.048	32.043	1.083	3223.29203	3.474	3223.27994
0.237	2.106	38.716	1.109	0.658	1.435	0.084	1.023	0.313	0.040	32.186	1.084	3223.29375	3.559	3223.28067
0.395	2.090	38.241	1.166	0.691	1.566	0.080	1.053	0.331	0.038	31.762	1.107	3223.29547	3.630	3223.28140
0.329	2.034	38.214	1.089	0.625	1.881	0.089	1.019	0.307	0.044	31.908	1.069	3223.29719	3.650	3223.28213
0.351	2.084	38.476	1.139	0.630	1.506	0.084	1.058	0.302	0.040	32.015	1.077	3223.29891	3.694	3223.28285
0.250	2.746	36.820	1.049	0.574	1.399	0.097	1.088	0.209	0.035	28.307	0.964	3223.30063	3.769	3223.28358
0.544	2.485	36.698	1.764	0.804	1.347	0.136	1.415	0.324	0.055	28.995	1.246	3223.30235	3.838	3223.28431
0.360	2.351	37.684	1.355	0.738	1.550	0.136	1.193	0.314	0.058	30.395	1.136	3223.30407	3.833	3223.28504
0.338	2.435	37.109	1.481	0.832	1.538	0.110	1.346	0.342	0.045	29.562	1.101	3223.30579	3.797	3223.28577
0.382	2.763	36.472	1.531	0.766	1.522	0.128	1.372	0.277	0.046	27.907	1.116	3223.30750	3.782	3223.28650
0.346	2.446	37.195	1.471	0.785	1.499	0.128	1.285	0.321	0.052	29.614	1.145	3223.30922	3.783	3223.28722
0.368	2.557	37.526	1.392	0.790	1.291	0.115	1.254	0.309	0.045	29.599	1.110	3223.31094	3.773	3223.28795
0.233	2.368	38.408	1.229	0.682	1.196	0.089	1.097	0.288	0.037	31.068	1.120	3223.31266	3.735	3223.28868
0.268	2.613	36.517	1.913	0.884	1.156	0.193	1.546	0.338	0.074	28.418	1.237	3223.31438	3.718	3223.28941
0.320	3.453	32.852	2.791	1.264	1.156	0.301	2.366	0.366	0.087	22.149	1.180	3223.31610	3.674	3223.29014
0.320	4.254	31.553	2.684	1.330	1.192	0.310	2.571	0.313	0.073	18.367	1.044	3223.31782	3.650	3223.29087
0.316	2.234	38.408	1.129	0.649	1.530	0.093	1.040	0.290	0.042	31.481	1.085	3223.31954	3.672	3223.29160
0.189	2.479	37.571	1.026	0.583	1.487	0.132	1.040	0.235	0.053	29.886	0.986	3223.32126	3.697	3223.29232
0.233	2.201	37.938	1.039	0.593	1.722	0.132	1.023	0.269	0.060	31.114	1.016	3223.32298	3.722	3223.29305
0.303	2.079	37.766	1.119	0.621	1.905	0.071	0.997	0.299	0.034	31.322	1.123	3223.32469	3.724	3223.29378
0.219	2.151	38.340	1.056	0.611	1.598	0.089	0.997	0.284	0.041	31.672	1.059	3223.32641	3.726	3223.29451
0.482	2.073	38.168	1.166	0.630	1.518	0.084	1.106	0.304	0.041	31.742	1.054	3223.32813	3.701	3223.29524
0.329	2.056	38.345	1.139	0.625	1.606	0.093	1.040	0.304	0.045	31.970	1.095	3223.32985	3.693	3223.29597
0.368	3.247	35.616	0.933	0.532	1.467	0.089	0.979	0.164	0.027	25.551	0.953	3223.33157	3.656	3223.29669
0.351	2.991	36.331	0.820	0.522	1.283	0.136	0.975	0.175	0.046	27.059	0.841	3223.33330	3.598	3223.29742
0.360	3.597	30.911	3.532	1.438	1.375	0.496	2.776	0.400	0.138	19.759	1.272	3223.33530	3.480	3223.29815
0.434	3.586	30.897	3.462	1.461	1.363	0.401	2.802	0.407	0.112	19.780	1.236	3223.33709	3.236	3223.29888
0.452	1.995	38.440	1.096	0.635	1.658	0.097	1.019	0.318	0.049	32.255	1.076	3223.33887	2.997	3223.29961
0.382	2.029	38.512	1.126	0.611	1.562	0.071	1.075	0.301	0.035	32.223	1.047	3223.34066	2.883	3223.30034
0.307	1.873	38.711	1.103	0.616	1.706	0.080	0.984	0.329	0.043	32.905	1.121	3223.34245	2.834	3223.30106
0.355	1.867	38.571	1.099	0.522	1.877	0.063	0.962	0.280	0.034	32.782	1.143	3223.34424	2.938	3223.30179
0.395	1.967	38.693	1.029	0.616	1.686	0.054	0.975	0.313	0.027	32.594	1.056	3223.34602	3.247	3223.30252
0.377	1.778	38.996	1.069	0.593	1.467	0.058	0.984	0.333	0.033	33.484	1.087	3223.34781	3.453	3223.30325
0.364	1.739	38.924	1.129	0.499	1.666	0.054	0.997	0.287	0.031	33.532	1.133	3223.34960	3.517	3223.30398
0.403	1.884	38.268	1.109	0.607	1.969	0.084	0.997	0.322	0.045	32.427	1.113	3223.35138	3.513	3223.30471
0.399	1.878	38.539	1.139	0.640	1.714	0.097	1.036	0.340	0.052	32.716	1.100	3223.35317	3.517	3223.30543
0.421	1.823	38.408	1.162	0.574	1.909	0.071	0.984	0.315	0.039	32.757	1.182	3223.35496	3.491	3223.30616
0.338	1.739	38.675	1.113	0.513	1.985	0.063	0.944	0.295	0.036	33.283	1.178	3223.35674	3.416	3223.30689
0.382	1.750	38.639	1.013	0.485	2.152	0.058	0.923	0.277	0.033	33.212	1.098	3223.35853	3.348	3223.30762
0.325	1.884	38.417	1.083	0.508	2.036	0.089	0.940	0.270	0.047	32.577	1.152	3223.36032	3.297	3223.30835
0.360	2.101	38.042	1.249	0.579	1.630	0.115	1.067	0.275	0.055	31.529	1.171	3223.36211	3.223	3223.30908
													3.178	3223.30981
													3.118	3223.31053
													3.109	3223.31126
													3.124	3223.31199
													3.040	3223.31272
													2.808	3223.31345
													2.458	3223.31418
													2.140	3223.31490
													1.830	3223.31563
													1.576	3223.31636
													1.411	3223.31709
													1.381	3223.31782
													1.452	3223.31855

EDXRF													Hyperspectral Imagery	
Mg %	Al %	Si %	S %	K %	Ca %	Ti %	Fe %	K/Al	Ti/Al	Si bio %	S/Fe	Depth m	TOC %	Depth m
													1.650	3223.31927
													2.054	3223.32000
													2.584	3223.32073
													2.918	3223.32146
													3.039	3223.32219
													3.035	3223.32292
													2.914	3223.32364
													2.763	3223.32437
													2.624	3223.32510
													2.547	3223.32583
													2.575	3223.32656
													2.705	3223.32729
													2.862	3223.32802
													3.019	3223.32874
													3.194	3223.32947
													3.294	3223.33020
													3.180	3223.33093
													2.938	3223.33166
													2.392	3223.33239
													1.445	3223.33311
													0.974	3223.33384
													0.723	3223.33457
													0.546	3223.33530
													0.570	3223.33603
													1.166	3223.33676
													1.768	3223.33748
													2.271	3223.33821
													2.561	3223.33894
													2.719	3223.33967
													2.829	3223.34040
													2.865	3223.34113
													2.826	3223.34185
													2.672	3223.34258
													2.559	3223.34331
													2.602	3223.34404
													2.656	3223.34477
													2.730	3223.34550
													2.687	3223.34623
													2.611	3223.34695
													3.038	3223.34768
													2.983	3223.34841
													2.976	3223.34914
													2.976	3223.34987
													3.098	3223.35060
													3.065	3223.35132
													3.011	3223.35205
													2.933	3223.35278
													2.858	3223.35351
													2.799	3223.35424
													2.822	3223.35497
													2.905	3223.35569
													2.931	3223.35642
													2.816	3223.35715
													2.770	3223.35788
													2.663	3223.35861
													2.586	3223.35934
													2.403	3223.36006
													2.236	3223.36079

Slab 3224.1 m

EDXRF													Hyperspectral Imagery			
Mg	Al	Si	S	K	Ca	Ti	Fe	K/Al	Ti/Al	Si bio	S/Fe	Depth	TOC	Depth		
%	%	%	%	%	%	%	%			%		m	%	m		
0.982	4.760	28.264	2.897	1.635	2.479	0.362	2.920	0.344	0.076	13.509	0.992	3224.10000	1.167	3224.10000		
0.894	4.804	28.259	2.787	1.813	2.546	0.353	2.946	0.377	0.074	13.366	0.946	3224.10125	1.075	3224.10067		
1.144	5.839	25.024	4.067	2.062	1.873	0.527	3.922	0.353	0.090	6.924	1.037	3224.10250	1.014	3224.10134		
1.061	6.111	24.445	4.329	2.166	1.698	0.557	4.110	0.354	0.091	5.500	1.053	3224.10375	0.937	3224.10200		
1.052	5.277	26.526	3.881	1.842	1.857	0.410	3.561	0.349	0.078	10.168	1.090	3224.10500	0.789	3224.10267		
0.934	4.788	28.422	3.356	1.626	2.028	0.349	3.072	0.340	0.073	13.581	1.092	3224.10625	0.661	3224.10334		
0.842	4.181	30.472	2.658	1.513	2.260	0.275	2.492	0.362	0.066	17.510	1.066	3224.10750	0.638	3224.10401		
0.842	4.103	31.345	2.186	1.466	2.220	0.254	2.218	0.357	0.062	18.625	0.986	3224.10875	0.685	3224.10467		
0.644	3.397	34.245	1.731	1.180	2.096	0.180	1.542	0.347	0.053	23.715	1.122	3224.11000	0.890	3224.10534		
0.789	3.236	34.413	1.555	1.086	2.291	0.132	1.481	0.336	0.041	24.382	1.050	3224.11125	1.149	3224.10601		
0.684	3.047	35.205	1.375	1.015	2.264	0.162	1.337	0.333	0.053	25.760	1.029	3224.11250	1.444	3224.10668		
0.745	2.974	34.874	1.584	0.987	2.232	0.149	1.472	0.332	0.050	25.654	1.076	3224.11375	1.531	3224.10734		
0.728	3.019	35.200	1.345	0.982	2.252	0.123	1.350	0.325	0.041	25.842	0.996	3224.11500	1.521	3224.10801		
0.679	3.035	34.820	1.701	0.954	2.200	0.149	1.472	0.314	0.049	25.410	1.155	3224.11625	1.523	3224.10868		
0.649	2.685	33.951	2.252	0.926	2.471	0.141	1.681	0.345	0.052	25.628	1.340	3224.11750	1.502	3224.10935		
0.653	2.780	34.263	2.046	0.945	2.447	0.106	1.559	0.340	0.038	25.647	1.312	3224.11875	1.524	3224.11001		
0.750	2.958	34.879	1.541	0.940	2.363	0.102	1.411	0.318	0.034	25.711	1.092	3224.12000	1.549	3224.11068		
0.697	2.802	35.173	1.418	0.978	2.411	0.115	1.367	0.349	0.041	26.487	1.037	3224.12125	1.561	3224.11135		
0.697	2.746	35.426	1.398	0.940	2.387	0.110	1.346	0.342	0.040	26.913	1.039	3224.12250	1.599	3224.11202		
0.605	2.835	35.707	1.302	0.907	2.379	0.132	1.289	0.320	0.047	26.918	1.010	3224.12375	1.607	3224.11268		
0.622	2.863	35.585	1.309	0.949	2.371	0.123	1.302	0.332	0.043	26.709	1.005	3224.12500	1.616	3224.11335		
0.671	3.002	34.413	1.830	0.978	2.359	0.154	1.594	0.326	0.051	25.107	1.148	3224.12625	1.661	3224.11402		
0.846	2.996	33.644	2.109	1.053	2.244	0.162	1.725	0.351	0.054	24.355	1.223	3224.12750	1.679	3224.11469		
0.592	3.069	35.092	1.515	1.076	2.136	0.149	1.446	0.351	0.049	25.578	1.048	3224.12875	1.712	3224.11535		
0.622	2.969	34.901	1.704	0.992	2.156	0.158	1.620	0.334	0.053	25.699	1.052	3224.13000	1.736	3224.11602		
0.618	2.557	36.494	1.299	0.888	2.013	0.132	1.250	0.347	0.052	28.567	1.039	3224.13125	1.773	3224.11669		
0.399	2.212	37.734	1.079	0.752	2.024	0.089	1.088	0.340	0.040	30.876	0.992	3224.13250	1.776	3224.11736		
0.666	2.101	37.417	1.309	0.654	1.897	0.093	1.184	0.311	0.044	30.904	1.105	3224.13375	1.748	3224.11802		
0.408	1.906	38.259	1.245	0.630	1.765	0.084	1.132	0.331	0.044	32.349	1.100	3224.13500	1.742	3224.11869		
0.382	1.750	39.146	1.039	0.503	1.638	0.058	0.971	0.288	0.033	33.719	1.071	3224.13625	1.753	3224.11936		
0.596	1.945	38.064	1.073	0.593	1.993	0.080	1.040	0.305	0.041	32.034	1.031	3224.13750	1.770	3224.12003		
0.478	1.823	38.919	0.917	0.527	1.857	0.076	0.936	0.289	0.042	33.269	0.979	3224.13880	1.735	3224.12069		
0.885	4.037	28.929	2.259	1.424	2.475	0.288	4.533	0.353	0.071	16.415	0.498	3224.14180	1.691	3224.12136		
0.995	4.103	28.943	2.189	1.381	2.435	0.215	4.533	0.337	0.052	16.222	0.483	3224.14301	1.657	3224.12203		
0.850	2.785	33.562	1.661	0.912	2.168	0.141	2.837	0.327	0.051	24.928	0.585	3224.14422	1.660	3224.12270		
0.951	2.379	36.784	1.159	0.710	2.036	0.067	1.119	0.298	0.028	29.409	1.036	3224.14543	1.743	3224.12336		
0.793	2.373	36.286	1.129	0.743	2.359	0.093	1.328	0.313	0.039	28.928	0.850	3224.14664	1.891	3224.12403		
0.701	2.296	35.630	1.229	0.733	2.574	0.097	1.712	0.320	0.042	28.514	0.718	3224.14785	2.089	3224.12470		
0.701	2.173	37.227	1.023	0.607	2.363	0.076	1.053	0.279	0.035	30.490	0.971	3224.14906	2.225	3224.12537		
0.728	2.090	37.824	0.950	0.640	2.112	0.084	0.958	0.306	0.040	31.346	0.992	3224.15027	2.323	3224.12603		
0.587	2.040	37.919	1.126	0.564	1.989	0.058	1.014	0.277	0.029	31.596	1.110	3224.15148	2.421	3224.12670		
0.548	1.878	38.236	0.983	0.564	2.136	0.054	0.949	0.300	0.029	32.413	1.036	3224.15269	2.556	3224.12737		
0.535	1.823	38.263	0.960	0.555	2.240	0.084	0.931	0.304	0.046	32.613	1.030	3224.15390	2.474	3224.12804		
0.592	1.789	37.906	1.109	0.532	2.287	0.041	1.014	0.297	0.023	32.359	1.094	3224.15511	2.504	3224.12870		
0.609	1.767	38.195	1.079	0.494	2.140	0.050	1.006	0.280	0.028	32.717	1.073	3224.15632	2.437	3224.12937		
0.535	1.873	38.585	0.996	0.466	1.997	0.037	0.905	0.249	0.020	32.779	1.101	3224.15753	2.490	3224.13004		
0.513	1.812	38.417	1.043	0.513	2.100	0.084	0.958	0.283	0.047	32.801	1.089	3224.15874	2.536	3224.13071		
0.644	1.784	38.182	0.943	0.480	2.244	0.050	0.931	0.269	0.028	32.652	1.013	3224.15995	2.607	3224.13137		
0.640	1.712	38.087	1.066	0.503	2.232	0.037	0.931	0.294	0.021	32.781	1.145	3224.16116	2.608	3224.13204		
0.491	1.778	38.521	0.996	0.494	2.132	0.050	0.931	0.278	0.028	33.008	1.070	3224.16237	2.558	3224.13271		
0.544	1.762	38.594	0.966	0.489	2.036	0.045	0.914	0.278	0.026	33.133	1.057	3224.16358	2.528	3224.13338		
0.609	1.767	37.870	1.269	0.503	2.092	0.097	1.149	0.285	0.055	32.391	1.104	3224.16479	2.585	3224.13404		
													2.760	3224.13471		
													2.654	3224.13538		
													2.747	3224.13605		
													2.784	3224.13671		
													2.804	3224.13738		
													2.748	3224.13805		
													2.613	3224.13872		
													2.419	3224.13939		
													2.255	3224.14005		

EDXRF												Hyperspectral Imagery		
Mg	Al	Si	S	K	Ca	Ti	Fe	K/Al	Ti/Al	Si bio	S/Fe	Depth	TOC	Depth
%	%	%	%	%	%	%	%			%		m	%	m
													2.235	3224.14072
													2.300	3224.14139
													2.296	3224.14206
													2.304	3224.14272
													2.429	3224.14339
													2.532	3224.14406
													2.474	3224.14473
													2.472	3224.14539
													2.539	3224.14606
													2.519	3224.14673
													2.510	3224.14740
													2.471	3224.14806
													2.319	3224.14873
													2.361	3224.14940
													2.394	3224.15007
													2.435	3224.15073
													2.408	3224.15140
													2.306	3224.15207
													2.263	3224.15274
													2.197	3224.15340
													2.222	3224.15407
													2.239	3224.15474
													2.231	3224.15541
													2.217	3224.15607
													2.249	3224.15674
													2.053	3224.15741
													2.116	3224.15808
													2.084	3224.15874
													2.021	3224.15941
													1.931	3224.16008
													1.865	3224.16075
													1.875	3224.16141
													1.844	3224.16208
													1.885	3224.16275
													1.830	3224.16342
													1.765	3224.16408
													1.698	3224.16475

Slab 3225 m

EDXRF													Hyperspectral Imagery		
Mg	Al	Si	S	K	Ca	Ti	Fe	K/Al	Ti/Al	Si bio	S/Fe	Depth	TOC	Depth	
%	%	%	%	%	%	%	%			%		m	%	m	
1.376	5.750	26.775	3.023	1.865	2.686	0.414	2.863	0.324	0.072	8.951	1.056	3225.00000	2.002	3224.99546	
1.521	5.655	26.603	2.990	1.889	2.738	0.401	2.876	0.334	0.071	9.072	1.040	3225.00159	1.975	3224.99624	
1.538	5.839	26.992	2.910	1.912	2.455	0.397	2.863	0.327	0.068	8.892	1.017	3225.00317	1.969	3224.99703	
1.608	6.562	26.160	3.066	2.156	2.092	0.466	2.955	0.329	0.071	5.818	1.038	3225.00476	1.931	3224.99781	
1.516	7.057	25.169	3.329	2.316	2.124	0.427	3.186	0.328	0.061	3.292	1.045	3225.00635	1.884	3224.99859	
1.218	5.805	29.124	2.545	1.903	1.813	0.353	2.418	0.328	0.061	11.127	1.052	3225.00794	1.811	3224.99938	
1.065	5.177	30.295	2.508	1.799	1.670	0.297	2.266	0.348	0.057	14.247	1.107	3225.00952	1.747	3225.00016	
1.148	6.334	28.481	2.804	2.194	1.311	0.371	2.641	0.346	0.059	8.846	1.062	3225.01111	1.690	3225.00094	
1.052	7.435	26.572	3.289	2.541	0.973	0.475	3.068	0.342	0.064	3.522	1.072	3225.01270	1.294	3225.00173	
0.767	6.367	28.431	3.302	2.227	0.710	0.423	2.941	0.350	0.066	8.693	1.123	3225.01429	0.833	3225.00251	
0.491	3.959	34.684	2.053	1.372	0.785	0.223	1.769	0.347	0.056	22.412	1.161	3225.01587	0.576	3225.00329	
0.535	3.497	35.137	1.864	1.217	0.913	0.189	1.956	0.348	0.054	24.296	0.953	3225.01746	0.639	3225.00408	
0.552	3.692	33.336	2.292	1.292	0.969	0.193	2.667	0.350	0.052	21.891	0.860	3225.01905	0.561	3225.00486	
0.566	3.742	34.929	1.993	1.259	0.909	0.215	1.712	0.337	0.057	23.329	1.164	3225.02063	0.524	3225.00565	
0.609	4.381	32.386	2.644	1.518	1.032	0.258	2.270	0.346	0.059	18.803	1.165	3225.02222	0.551	3225.00643	
0.561	3.430	34.992	2.086	1.198	1.048	0.175	1.703	0.349	0.051	24.358	1.225	3225.02381	0.792	3225.00721	
0.522	2.824	37.005	1.508	0.898	1.116	0.136	1.263	0.318	0.048	28.251	1.194	3225.02540	1.058	3225.00800	
0.478	2.774	37.164	1.468	0.860	1.188	0.106	1.180	0.310	0.038	28.564	1.244	3225.02698	1.172	3225.00878	
0.500	2.546	37.503	1.445	0.804	1.128	0.089	1.176	0.316	0.035	29.611	1.229	3225.02857	1.147	3225.00956	
0.412	2.524	37.671	1.352	0.837	1.152	0.102	1.171	0.332	0.040	29.847	1.154	3225.03016	1.051	3225.01035	
0.491	2.535	36.938	1.687	0.799	1.196	0.102	1.367	0.315	0.040	29.080	1.234	3225.03175	0.845	3225.01113	
0.596	2.462	37.014	1.611	0.752	1.331	0.102	1.224	0.305	0.041	29.381	1.317	3225.03333	0.694	3225.01191	
0.377	2.446	37.132	1.677	0.752	1.295	0.097	1.337	0.308	0.040	29.550	1.255	3225.03492	0.620	3225.01270	
0.469	2.462	37.354	1.438	0.799	1.339	0.110	1.171	0.325	0.045	29.720	1.228	3225.03651	0.674	3225.01348	
0.653	2.396	36.956	1.508	0.804	1.491	0.080	1.245	0.336	0.033	29.529	1.211	3225.03809	0.976	3225.01426	
0.535	2.468	36.784	1.704	0.762	1.411	0.106	1.319	0.309	0.043	29.133	1.291	3225.03968	1.371	3225.01505	
0.671	2.490	36.585	1.668	0.762	1.530	0.115	1.289	0.306	0.046	28.865	1.294	3225.04127	1.780	3225.01583	
0.596	2.457	36.978	1.458	0.771	1.590	0.119	1.228	0.314	0.048	29.362	1.188	3225.04286	2.015	3225.01662	
0.684	2.440	36.562	1.558	0.762	1.678	0.115	1.311	0.312	0.047	28.997	1.189	3225.04444	2.115	3225.01740	
0.513	2.474	36.675	1.498	0.813	1.658	0.110	1.298	0.329	0.045	29.007	1.154	3225.04603	2.104	3225.01818	
0.587	2.646	36.693	1.491	0.870	1.503	0.106	1.280	0.329	0.040	28.491	1.165	3225.04762	2.067	3225.01897	
0.820	2.985	34.603	1.784	0.926	1.598	0.154	2.178	0.310	0.052	25.348	0.819	3225.04920	1.958	3225.01975	
0.798	2.741	35.621	1.578	0.884	1.738	0.110	1.490	0.322	0.040	27.125	1.059	3225.05079	1.876	3225.02053	
0.636	2.713	35.933	1.601	0.879	1.742	0.110	1.376	0.324	0.041	27.523	1.163	3225.05238	1.869	3225.02132	
0.644	2.802	35.634	1.614	0.912	1.881	0.141	1.415	0.325	0.050	26.949	1.141	3225.05397	1.930	3225.02210	
0.793	2.785	35.634	1.598	0.931	1.773	0.119	1.428	0.334	0.043	27.001	1.118	3225.05555	2.129	3225.02288	
0.807	3.019	35.245	1.631	0.992	1.789	0.141	1.433	0.329	0.047	25.887	1.138	3225.05714	2.340	3225.02367	
0.693	3.113	34.449	1.910	0.978	1.905	0.106	1.681	0.314	0.034	24.798	1.136	3225.05873	2.553	3225.02445	
0.679	3.130	33.902	2.212	1.015	1.881	0.154	1.847	0.324	0.049	24.199	1.198	3225.06032	2.653	3225.02523	
0.947	3.458	32.662	2.289	1.137	2.024	0.158	2.035	0.329	0.046	21.942	1.125	3225.06190	2.708	3225.02602	
0.693	3.419	33.178	2.312	1.142	1.873	0.171	2.008	0.334	0.050	22.578	1.151	3225.06349	2.801	3225.02680	
0.947	3.430	32.893	2.183	1.100	2.184	0.175	1.864	0.321	0.051	22.259	1.171	3225.06508	2.927	3225.02759	
0.846	3.408	32.381	2.515	1.081	2.072	0.136	2.096	0.317	0.040	21.816	1.200	3225.06666	2.822	3225.02837	
0.863	3.430	31.078	3.063	1.109	2.264	0.189	2.471	0.323	0.055	20.444	1.240	3225.06825	2.791	3225.02915	
0.934	3.658	30.761	2.950	1.208	2.331	0.171	2.475	0.330	0.047	19.420	1.192	3225.06984	2.746	3225.02994	
0.929	3.925	31.178	2.581	1.269	2.295	0.189	2.331	0.323	0.048	19.009	1.107	3225.07143	2.770	3225.03072	
0.881	3.925	30.499	3.116	1.302	2.080	0.162	2.588	0.332	0.041	18.330	1.204	3225.07301	2.786	3225.03150	
0.640	3.152	22.070	8.858	0.978	1.251	0.149	5.632	0.310	0.047	12.298	1.573	3225.07460	2.815	3225.03229	
0.714	3.386	24.323	7.426	1.090	1.403	0.167	4.633	0.322	0.049	13.827	1.603	3225.07619	2.897	3225.03307	
0.828	4.031	31.205	2.764	1.386	1.949	0.219	2.344	0.344	0.054	18.709	1.179	3225.07778	2.913	3225.03385	
0.925	3.975	30.793	3.103	1.311	1.909	0.189	2.457	0.330	0.047	18.469	1.263	3225.07936	2.878	3225.03464	
0.842	3.786	31.336	2.897	1.245	1.913	0.197	2.418	0.329	0.052	19.598	1.198	3225.08095	2.790	3225.03542	
0.850	3.981	32.019	2.302	1.349	2.068	0.180	2.056	0.339	0.045	19.678	1.120	3225.08254	2.694	3225.03620	
0.951	4.176	30.205	3.176	1.433	1.945	0.241	2.558	0.343	0.058	17.260	1.242	3225.08412	2.670	3225.03699	
1.074	4.721	30.178	2.585	1.640	1.849	0.271	2.492	0.347	0.057	15.543	1.037	3225.08571	2.659	3225.03777	
0.942	4.754	30.295	2.678	1.654	1.805	0.262	2.440	0.348	0.055	15.557	1.097	3225.08730	2.621	3225.03856	
1.122	4.865	29.703	2.874	1.626	1.893	0.288	2.497	0.334	0.059	14.620	1.151	3225.08889	2.591	3225.03934	
0.977	5.099	30.318	2.525	1.752	1.626	0.314	2.418	0.344	0.062	14.511	1.044	3225.09047	2.583	3225.04012	
0.991	4.960	30.033	2.611	1.724	1.857	0.336	2.457	0.348	0.068	14.657	1.063	3225.09206	2.627	3225.04091	
0.916	4.487	31.218	2.355	1.588	1.993	0.262	2.161	0.354	0.058	17.308	1.090	3225.09365	2.785	3225.04169	

EDXRF												Hyperspectral Imagery		
Mg	Al	Si	S	K	Ca	Ti	Fe	K/Al	Ti/Al	Si bio	S/Fe	Depth	TOC	Depth
%	%	%	%	%	%	%	%			%		m	%	m
													2.623	3225.04326
													2.657	3225.04404
													2.612	3225.04482
													2.633	3225.04561
													2.610	3225.04639
													2.568	3225.04717
													2.505	3225.04796
													2.592	3225.04874
													2.599	3225.04953
													2.607	3225.05031
													2.509	3225.05109
													2.430	3225.05188
													2.443	3225.05266
													2.525	3225.05344
													2.487	3225.05423
													2.448	3225.05501
													2.301	3225.05579
													2.202	3225.05658
													2.133	3225.05736
													2.048	3225.05814
													1.995	3225.05893
													1.854	3225.05971
													1.815	3225.06050
													1.805	3225.06128
													1.821	3225.06206
													1.826	3225.06285
													1.842	3225.06363
													1.816	3225.06441
													1.832	3225.06520
													1.797	3225.06598
													1.763	3225.06676
													1.762	3225.06755
													1.748	3225.06833
													1.672	3225.06911
													1.545	3225.06990
													1.484	3225.07068
													1.471	3225.07147
													1.443	3225.07225
													1.436	3225.07303
													1.447	3225.07382
													1.414	3225.07460
													1.393	3225.07538
													1.425	3225.07617
													1.437	3225.07695
													1.475	3225.07773
													1.470	3225.07852
													1.491	3225.07930
													1.466	3225.08008
													1.463	3225.08087
													1.432	3225.08165
													1.387	3225.08244
													1.353	3225.08322
													1.314	3225.08400
													1.224	3225.08479
													1.248	3225.08557
													1.206	3225.08635
													1.210	3225.08714
													1.193	3225.08792
													1.175	3225.08870
													1.183	3225.08949
													1.203	3225.09027

EDXRF												Hyperspectral Imagery		
Mg	Al	Si	S	K	Ca	Ti	Fe	K/Al	Ti/Al	Si bio	S/Fe	Depth	TOC	Depth
%	%	%	%	%	%	%	%			%		m	%	m
													1.283	3225.09105
													1.341	3225.09184
													1.387	3225.09262
													1.367	3225.09341
													1.271	3225.09419

Slab 3225.9 m

EDXRF													Hyperspectral Imagery		
Mg %	Al %	Si %	S %	K %	Ca %	Ti %	Fe %	K/Al	Ti/Al	Si bio %	S/Fe	Depth m	TOC %	Depth m	
0.991	2.774	31.617	1.681	0.893	4.614	0.128	1.625	0.322	0.046	23.017	1.035	3225.92354	2.657	3225.92255	
0.951	2.791	31.598	1.402	0.856	5.204	0.167	1.437	0.307	0.060	22.947	0.975	3225.92461	2.494	3225.92332	
1.012	2.768	31.187	1.767	0.832	4.985	0.145	1.651	0.301	0.052	22.605	1.070	3225.92568	2.409	3225.92408	
0.763	2.752	32.607	1.551	0.888	4.196	0.119	1.407	0.323	0.043	24.077	1.103	3225.92675	2.353	3225.92485	
0.785	2.785	33.037	1.628	0.884	3.778	0.145	1.402	0.317	0.052	24.404	1.161	3225.92782	2.272	3225.92561	
0.815	2.830	33.508	1.362	0.917	3.738	0.132	1.267	0.324	0.047	24.736	1.075	3225.92889	2.235	3225.92638	
0.767	2.830	34.318	1.192	0.926	3.292	0.119	1.193	0.327	0.042	25.546	0.999	3225.92996	2.242	3225.92714	
0.903	2.818	33.490	1.581	0.874	3.331	0.115	1.354	0.310	0.041	24.753	1.167	3225.93103	2.226	3225.92791	
0.951	2.796	32.562	1.628	0.818	4.065	0.119	1.346	0.293	0.043	23.894	1.210	3225.93210	2.236	3225.92867	
0.745	2.724	32.743	1.073	0.841	5.065	0.132	1.145	0.309	0.049	24.299	0.937	3225.93317	2.255	3225.92944	
0.820	2.785	32.567	1.295	0.851	4.750	0.158	1.324	0.306	0.057	23.933	0.978	3225.93423	2.321	3225.93020	
0.789	2.724	32.141	1.432	0.860	4.917	0.141	1.381	0.316	0.052	23.697	1.037	3225.93530	2.404	3225.93097	
0.802	2.846	33.028	1.142	0.884	4.455	0.128	1.193	0.310	0.045	24.205	0.958	3225.93637	2.471	3225.93173	
0.842	2.846	33.657	1.335	0.949	3.594	0.145	1.293	0.334	0.051	24.834	1.032	3225.93744	2.502	3225.93250	
0.859	2.830	31.531	1.262	0.846	5.567	0.128	1.341	0.299	0.045	22.759	0.941	3225.93851	2.522	3225.93326	
0.837	2.941	32.960	1.242	0.884	4.316	0.128	1.285	0.301	0.043	23.844	0.967	3225.93958	2.551	3225.93403	
0.912	2.991	33.811	1.525	0.940	2.909	0.145	1.376	0.314	0.049	24.539	1.108	3225.94065	2.514	3225.93479	
0.960	2.930	34.019	1.385	0.987	2.925	0.154	1.337	0.337	0.052	24.937	1.036	3225.94172	2.486	3225.93556	
0.912	3.024	34.060	1.438	0.959	2.833	0.141	1.315	0.317	0.047	24.685	1.094	3225.94279	2.413	3225.93632	
0.947	2.985	33.445	1.574	0.940	3.088	0.145	1.394	0.315	0.049	24.190	1.130	3225.94386	2.449	3225.93709	
0.986	2.952	33.802	1.475	0.954	2.913	0.141	1.381	0.323	0.048	24.651	1.068	3225.94493	2.478	3225.93785	
1.043	3.074	33.825	1.398	0.964	2.917	0.158	1.376	0.313	0.051	24.294	1.016	3225.94600	2.549	3225.93862	
0.885	3.186	33.426	1.538	1.025	3.068	0.162	1.472	0.322	0.051	23.551	1.045	3225.94707	2.595	3225.93938	
1.192	3.097	32.861	1.581	0.978	3.216	0.158	1.503	0.316	0.051	23.261	1.052	3225.94814	2.623	3225.94015	
1.104	3.108	32.304	1.917	1.006	3.184	0.171	1.725	0.324	0.055	22.670	1.111	3225.94921	2.613	3225.94091	
0.951	3.269	32.988	1.661	1.043	3.021	0.154	1.594	0.319	0.047	22.854	1.042	3225.95028	2.566	3225.94168	
1.047	3.186	33.331	1.548	1.020	2.905	0.197	1.516	0.320	0.062	23.456	1.021	3225.95135	2.529	3225.94245	
0.991	3.308	32.960	1.731	1.034	2.921	0.171	1.590	0.313	0.052	22.706	1.089	3225.95242	2.552	3225.94321	
0.912	3.408	32.472	1.947	1.029	2.981	0.158	1.703	0.302	0.046	21.907	1.143	3225.95349	2.558	3225.94398	
0.964	3.369	32.345	1.913	1.057	3.057	0.171	1.734	0.314	0.051	21.901	1.104	3225.95456	2.564	3225.94474	
0.938	3.269	33.467	1.531	0.982	2.913	0.184	1.490	0.301	0.056	23.333	1.028	3225.95563	2.550	3225.94551	
0.929	3.225	33.508	1.578	1.020	2.833	0.171	1.468	0.316	0.053	23.512	1.075	3225.95670	2.550	3225.94627	
0.964	3.174	33.426	1.591	0.968	2.901	0.149	1.468	0.305	0.047	23.586	1.084	3225.95777	2.563	3225.94704	
0.934	3.258	33.101	1.674	1.001	2.945	0.132	1.559	0.307	0.041	23.001	1.074	3225.95884	2.528	3225.94780	
1.069	3.369	32.264	1.923	1.034	3.057	0.162	1.708	0.307	0.048	21.819	1.126	3225.95991	2.488	3225.94857	
0.995	3.286	33.241	1.621	1.006	2.957	0.167	1.503	0.306	0.051	23.055	1.079	3225.96098	2.393	3225.94933	
0.855	3.230	33.286	1.634	1.039	2.929	0.154	1.564	0.322	0.048	23.273	1.045	3225.96205	2.305	3225.95010	
0.828	3.174	34.010	1.558	0.982	2.654	0.171	1.442	0.309	0.054	24.169	1.081	3225.96312	2.272	3225.95086	
0.728	3.208	34.915	1.385	0.996	2.287	0.141	1.263	0.311	0.044	24.971	1.097	3225.96419	2.280	3225.95163	
0.736	3.141	34.752	1.432	1.015	2.347	0.145	1.319	0.323	0.046	25.015	1.085	3225.96526	2.282	3225.95239	
0.991	3.236	33.820	1.528	1.015	2.682	0.197	1.381	0.314	0.061	23.790	1.107	3225.96633	2.251	3225.95316	
1.144	3.425	32.992	1.515	1.048	2.989	0.180	1.472	0.306	0.053	22.375	1.029	3225.96740	2.196	3225.95392	
1.109	3.875	31.218	1.927	1.316	2.686	0.223	2.309	0.340	0.058	19.205	0.834	3225.96940	2.143	3225.95469	
1.004	3.875	31.350	1.930	1.292	2.666	0.249	2.327	0.333	0.064	19.336	0.830	3225.97108	2.213	3225.95545	
1.253	4.687	28.762	2.651	1.518	2.881	0.310	2.471	0.324	0.066	14.231	1.073	3225.97275	2.285	3225.95622	
1.464	6.223	24.486	3.927	1.893	2.491	0.466	3.569	0.304	0.075	5.196	1.100	3225.97443	2.344	3225.95698	
1.332	6.356	24.667	3.897	2.072	2.212	0.501	3.582	0.326	0.079	4.963	1.088	3225.97611	2.350	3225.95775	
1.166	4.454	29.599	2.595	1.475	2.698	0.310	2.348	0.331	0.070	15.792	1.105	3225.97779	2.326	3225.95851	
0.785	3.530	33.051	1.800	1.156	2.682	0.189	1.607	0.327	0.053	22.106	1.120	3225.97946	2.316	3225.95928	
0.868	3.291	34.236	1.385	1.048	2.626	0.145	1.306	0.318	0.044	24.033	1.060	3225.98114	2.289	3225.96004	
0.811	3.291	33.879	1.435	1.034	2.933	0.162	1.350	0.314	0.049	23.676	1.063	3225.98282	2.267	3225.96081	
0.714	3.263	34.761	1.305	1.076	2.451	0.158	1.258	0.330	0.048	24.644	1.037	3225.98450	2.272	3225.96157	
0.697	3.291	34.363	1.322	1.062	2.817	0.158	1.254	0.323	0.048	24.160	1.054	3225.98617	2.290	3225.96234	
0.807	3.197	33.983	1.521	1.057	2.790	0.158	1.389	0.331	0.049	24.073	1.095	3225.98785	2.344	3225.96310	
0.745	3.202	34.748	1.382	1.053	2.455	0.167	1.289	0.329	0.052	24.821	1.072	3225.98953	2.404	3225.96387	
0.776	3.113	34.942	1.521	1.067	2.036	0.149	1.376	0.343	0.048	25.291	1.105	3225.99121	2.474	3225.96463	
0.658	3.258	35.467	1.372	1.119	1.857	0.158	1.267	0.343	0.049	25.368	1.083	3225.99288	2.498	3225.96540	
0.719	3.163	35.508	1.348	1.072	1.905	0.149	1.258	0.339	0.047	25.701	1.072	3225.99456	2.413	3225.96616	
0.767	3.197	35.485	1.299	1.053	2.044	0.141	1.202	0.329	0.044	25.575	1.081	3225.99624	2.275	3225.96693	
0.693	3.152	35.585	1.345	1.029	1.909	0.136	1.224	0.327	0.043	25.813	1.099	3225.99792	2.149	3225.96769	
0.789	3.286	35.671	1.259	1.020	1.845	0.154	1.189	0.310	0.047	25.485	1.059	3225.99959	2.087	3225.96846	

EDXRF													Hyperspectral Imagery	
Mg %	Al %	Si %	S %	K %	Ca %	Ti %	Fe %	K/Al	Ti/Al	Si bio %	S/Fe	Depth m	TOC %	Depth m
0.754	3.152	35.105	1.531	1.015	1.953	0.136	1.381	0.322	0.043	25.333	1.109	3226.00127	2.032	3225.96922
0.693	3.163	35.092	1.538	1.043	1.945	0.141	1.385	0.330	0.045	25.285	1.111	3226.00295	1.990	3225.96999
0.631	3.208	35.562	1.265	1.020	2.005	0.141	1.263	0.318	0.044	25.618	1.002	3226.00463	1.890	3225.97075
0.780	3.186	35.404	1.329	1.006	1.981	0.128	1.197	0.316	0.040	25.528	1.110	3226.00630	1.613	3225.97152
0.842	3.225	35.114	1.358	1.001	2.124	0.149	1.245	0.310	0.046	25.118	1.091	3226.00798	1.180	3225.97228
0.736	3.275	34.046	1.874	1.048	2.084	0.145	1.655	0.320	0.044	23.895	1.132	3226.00966	0.860	3225.97305
0.982	3.536	33.987	1.531	1.165	2.228	0.175	1.402	0.330	0.050	23.026	1.092	3226.01134	0.628	3225.97382
0.964	3.753	33.503	1.658	1.194	2.220	0.197	1.533	0.318	0.053	21.869	1.081	3226.01301	0.547	3225.97458
0.938	3.959	32.512	2.056	1.316	2.064	0.206	1.860	0.332	0.052	20.240	1.105	3226.01469	0.534	3225.97535
0.960	4.237	31.888	2.123	1.400	2.080	0.232	1.908	0.330	0.055	18.754	1.113	3226.01637	0.577	3225.97611
1.188	6.367	26.590	3.439	2.128	1.598	0.449	3.037	0.334	0.070	6.851	1.132	3226.01804	0.832	3225.97688
1.275	7.986	23.993	3.778	2.673	1.411	0.566	3.486	0.335	0.071	-0.764	1.084	3226.01972	1.297	3225.97764
0.929	5.650	29.314	2.827	1.968	1.475	0.362	2.475	0.348	0.064	11.799	1.142	3226.02140	1.707	3225.97841
													1.928	3225.97917
													2.061	3225.97994
													2.203	3225.98070
													2.278	3225.98147
													2.307	3225.98223
													2.319	3225.98300
													2.402	3225.98376
													2.513	3225.98453
													2.629	3225.98529
													2.648	3225.98606
													2.644	3225.98682
													2.604	3225.98759
													2.545	3225.98835
													2.571	3225.98912
													2.565	3225.98988
													2.547	3225.99065
													2.581	3225.99141
													2.440	3225.99218
													2.439	3225.99294
													2.489	3225.99371
													2.602	3225.99447
													2.670	3225.99524
													2.630	3225.99600
													2.615	3225.99677
													2.631	3225.99753
													2.643	3225.99830
													2.601	3225.99906
													2.530	3225.99983
													2.455	3226.00059
													2.378	3226.00136
													2.352	3226.00212
													2.386	3226.00289
													2.410	3226.00365
													2.415	3226.00442
													2.410	3226.00518
													2.376	3226.00595
													2.291	3226.00672
													2.286	3226.00748
													2.232	3226.00825
													2.163	3226.00901
													2.036	3226.00978
													1.997	3226.01054
													1.943	3226.01131
													1.911	3226.01207
													1.815	3226.01284
													1.703	3226.01360
													1.641	3226.01437
													1.612	3226.01513

EDXRF												Hyperspectral Imagery		
Mg	Al	Si	S	K	Ca	Ti	Fe	K/Al	Ti/Al	Si bio	S/Fe	Depth	TOC	Depth
%	%	%	%	%	%	%	%			%		m	%	m
													1.490	3226.01590
													1.313	3226.01666
													0.896	3226.01743
													0.529	3226.01819
													0.411	3226.01896
													0.371	3226.01972
													0.550	3226.02049
													1.027	3226.02125

EDXRF													Hyperspectral Imagery	
Mg %	Al %	Si %	S %	K %	Ca %	Ti %	Fe %	K/Al	Ti/Al	Si bio %	S/Fe	Depth m	TOC %	Depth m
0.881	0.688	9.640	0.445	0.081	29.152	0.024	0.726	0.117	0.034	7.507	0.612	3266.97400	1.029	3226.96023
0.999	0.616	9.437	0.491	0.081	29.196	0.054	0.770	0.131	0.088	7.528	0.638	3266.97504	0.999	3226.96118
0.938	0.677	9.464	0.481	0.067	29.243	0.032	0.753	0.098	0.048	7.365	0.639	3266.97607	0.922	3226.96214
													0.927	3226.96310
													0.897	3226.96405
													0.847	3226.96501
													0.838	3226.96596
													0.788	3226.96692
													0.754	3226.96788
													0.736	3226.96883
													0.714	3226.96979
													0.655	3226.97075
													0.644	3226.97170
													0.601	3226.97266
													0.596	3226.97361
													0.593	3226.97457
													0.605	3226.97553

EDXRF													Hyperspectral Imagery		
Mg %	Al %	Si %	S %	K %	Ca %	Ti %	Fe %	K/Al	Ti/Al	Si bio %	S/Fe	Depth m	TOC %	Depth m	
0.504	2.618	24.241	1.053	0.762	13.249	0.102	1.206	0.291	0.039	16.125	0.873	3231.03114	1.429	3231.00829	
0.517	2.513	25.250	0.993	0.719	12.755	0.115	1.062	0.286	0.046	17.462	0.935	3231.03274	1.458	3231.00907	
0.504	2.440	25.183	1.106	0.738	12.663	0.106	1.215	0.302	0.043	17.618	0.910	3231.03435	1.369	3231.00986	
0.500	2.501	25.585	1.106	0.757	12.217	0.119	1.197	0.303	0.048	17.831	0.924	3231.03595	1.345	3231.01065	
0.487	2.563	26.567	1.252	0.766	11.042	0.115	1.376	0.299	0.045	18.623	0.910	3231.03755	1.309	3231.01144	
0.614	2.830	27.020	1.418	0.785	10.026	0.106	1.450	0.277	0.037	18.248	0.978	3231.03915	1.267	3231.01222	
0.574	2.835	28.056	1.116	0.846	9.607	0.136	1.206	0.298	0.048	19.267	0.925	3231.04076	1.225	3231.01301	
0.526	2.774	25.735	1.123	0.738	11.767	0.106	1.228	0.266	0.038	17.135	0.914	3231.04236	1.139	3231.01380	
0.517	2.946	27.042	1.139	0.813	10.324	0.110	1.285	0.276	0.037	17.908	0.887	3231.04396	1.131	3231.01458	
0.526	2.780	25.861	1.299	0.785	11.293	0.128	1.398	0.282	0.046	17.245	0.929	3231.04557	1.122	3231.01537	
0.701	4.459	27.839	2.874	1.560	4.459	0.293	2.702	0.350	0.066	14.014	1.064	3231.04717	1.099	3231.01616	
0.750	4.999	28.051	2.625	1.687	4.204	0.293	2.505	0.337	0.059	12.555	1.048	3231.04877	1.172	3231.01694	
0.859	5.883	28.096	3.681	2.194	1.172	0.414	3.216	0.373	0.070	9.858	1.145	3231.05038	1.276	3231.01773	
0.688	3.636	27.820	1.711	1.142	7.635	0.180	1.834	0.314	0.049	16.548	0.933	3231.05198	1.318	3231.01852	
0.679	3.241	27.124	1.574	0.884	9.065	0.175	1.699	0.273	0.054	17.076	0.927	3231.05358	1.310	3231.01931	
0.618	3.063	27.897	1.275	0.949	9.141	0.171	1.372	0.310	0.056	18.401	0.930	3231.05518	1.298	3231.02009	
0.767	3.052	27.250	1.375	0.917	9.436	0.154	1.433	0.300	0.050	17.789	0.960	3231.05679	1.257	3231.02088	
0.714	2.874	27.182	1.116	0.856	10.161	0.141	1.263	0.298	0.049	18.273	0.884	3231.05839	1.154	3231.02167	
0.618	2.924	27.811	1.259	0.903	9.448	0.145	1.381	0.309	0.050	18.747	0.912	3231.06000	0.980	3231.02245	
													0.945	3231.02324	
													1.116	3231.02403	
													1.234	3231.02481	
													1.326	3231.02560	
													1.428	3231.02639	
													1.409	3231.02718	
													1.389	3231.02796	
													1.433	3231.02875	
													1.425	3231.02954	
													1.444	3231.03032	
													1.449	3231.03111	
													1.502	3231.03190	
													1.407	3231.03268	
													1.443	3231.03347	
													1.538	3231.03426	
													1.390	3231.03505	
													1.364	3231.03583	
													1.455	3231.03662	
													1.435	3231.03741	
													1.445	3231.03819	
													1.461	3231.03898	
													1.537	3231.03977	
													1.465	3231.04055	
													1.561	3231.04134	
													1.567	3231.04213	
													1.611	3231.04292	
													1.639	3231.04370	
													1.741	3231.04449	
													1.692	3231.04528	
													1.704	3231.04606	
													1.594	3231.04685	
													1.557	3231.04764	
													1.509	3231.04842	
													1.678	3231.04921	
													1.811	3231.05000	
													1.760	3231.05079	
													1.666	3231.05157	
													1.664	3231.05236	
													1.581	3231.05315	
													1.670	3231.05393	
													1.673	3231.05472	
													1.558	3231.05551	

EDXRF												Hyperspectral Imagery		
Mg	Al	Si	S	K	Ca	Ti	Fe	K/Al	Ti/Al	Si bio	S/Fe	Depth	TOC	Depth
%	%	%	%	%	%	%	%			%		m	%	m
													1.651	3231.05708
													1.544	3231.05787
													1.490	3231.05866
													1.505	3231.05944
													1.566	3231.06023
													1.626	3231.06102
													1.534	3231.06180
													1.567	3231.06259

EDXRF												Hyperspectral Imagery		
Mg %	Al %	Si %	S %	K %	Ca %	Ti %	Fe %	K/Al	Ti/Al	Si bio %	S/Fe	Depth m	TOC %	Depth m
													5.178	3234.07756
													5.235	3234.07828
													5.324	3234.07900
													5.445	3234.07971
													5.500	3234.08043
													5.494	3234.08115
													5.511	3234.08186
													5.579	3234.08258
													5.642	3234.08330
													5.608	3234.08401
													5.524	3234.08473
													5.487	3234.08545
													5.481	3234.08617
													5.393	3234.08688
													5.219	3234.08760
													5.002	3234.08832
													4.747	3234.08903
													4.387	3234.08975
													3.848	3234.09047
													3.443	3234.09118
													3.864	3234.09190
													4.226	3234.09262
													4.477	3234.09333
													4.540	3234.09405
													4.503	3234.09477
													4.453	3234.09548
													4.473	3234.09620
													4.584	3234.09692
													4.616	3234.09763
													4.592	3234.09835
													4.612	3234.09907
													4.684	3234.09978
													4.780	3234.10050
													4.816	3234.10122
													4.777	3234.10193
													4.757	3234.10265
													4.767	3234.10337
													4.776	3234.10408
													4.745	3234.10480
													4.639	3234.10552
													4.448	3234.10623
													4.189	3234.10695
													4.001	3234.10767
													3.991	3234.10838
													4.117	3234.10910
													4.276	3234.10982
													4.431	3234.11054
													4.588	3234.11125
													4.680	3234.11197
													4.734	3234.11269
													4.802	3234.11340
													4.893	3234.11412
													4.896	3234.11484
													4.827	3234.11555
													4.725	3234.11627
													4.589	3234.11699
													4.532	3234.11770
													4.412	3234.11842
													4.201	3234.11914
													4.117	3234.11985
													4.152	3234.12057
													4.311	3234.12129

EDXRF													Hyperspectral Imagery	
Mg %	Al %	Si %	S %	K %	Ca %	Ti %	Fe %	K/Al	Ti/Al	Si bio %	S/Fe	Depth m	TOC %	Depth m
0.566	3.536	33.549	1.588	1.320	2.937	0.136	1.372	0.373	0.039	22.587	1.157	3236.15716	2.894	3236.13016
0.644	3.608	31.200	1.332	1.273	5.284	0.149	1.267	0.353	0.041	20.015	1.051	3236.15854	2.974	3236.13092
0.614	3.325	27.888	1.179	1.133	8.599	0.123	1.154	0.341	0.037	17.582	1.022	3236.15992	2.952	3236.13167
0.587	3.608	30.313	1.342	1.250	5.969	0.154	1.280	0.346	0.043	19.128	1.048	3236.16130	2.980	3236.13242
0.780	3.753	29.789	1.634	1.283	5.650	0.154	1.472	0.342	0.041	18.155	1.110	3236.16268	2.902	3236.13318
0.627	4.092	31.540	1.594	1.565	3.798	0.189	1.485	0.382	0.046	18.854	1.074	3236.16406	3.036	3236.13393
0.728	5.561	29.983	2.462	2.161	1.841	0.332	2.235	0.389	0.060	12.745	1.101	3236.16544	3.071	3236.13468
0.754	7.113	27.386	3.276	2.748	0.909	0.436	2.928	0.386	0.061	5.337	1.119	3236.16682	3.087	3236.13544
0.789	7.508	27.210	3.140	2.879	0.861	0.423	2.867	0.384	0.056	3.936	1.095	3236.16820	2.855	3236.13619
0.828	7.836	27.187	2.997	3.002	0.686	0.410	2.798	0.383	0.052	2.896	1.071	3236.16958	2.795	3236.13694
0.846	8.225	26.639	3.053	3.110	0.646	0.457	2.885	0.378	0.056	1.142	1.058	3236.17097	2.965	3236.13770
0.837	7.808	27.160	3.126	2.959	0.618	0.401	2.793	0.379	0.051	2.955	1.119	3236.17235	3.088	3236.13845
0.710	7.802	27.458	2.993	2.978	0.634	0.423	2.767	0.382	0.054	3.271	1.082	3236.17373	3.050	3236.13920
0.798	7.580	27.201	3.223	2.894	0.630	0.427	2.941	0.382	0.056	3.703	1.096	3236.17511	2.968	3236.13996
0.701	6.178	29.870	2.728	2.288	1.080	0.353	2.322	0.370	0.057	10.718	1.175	3236.17649	3.049	3236.14071
0.535	4.776	32.386	2.196	1.762	1.614	0.228	1.821	0.369	0.048	17.579	1.206	3236.17787	3.231	3236.14146
0.491	4.287	33.517	1.867	1.574	1.897	0.206	1.564	0.367	0.048	20.227	1.194	3236.17925	3.311	3236.14222
0.351	3.742	34.576	1.551	1.414	2.192	0.154	1.363	0.378	0.041	22.976	1.138	3236.18063	3.349	3236.14297
0.408	3.937	34.241	1.697	1.489	2.068	0.162	1.433	0.378	0.041	22.038	1.185	3236.18201	3.307	3236.14372
													3.130	3236.14448
													2.998	3236.14523
													2.931	3236.14598
													2.946	3236.14674
													3.152	3236.14749
													3.082	3236.14824
													2.960	3236.14900
													2.907	3236.14975
													2.903	3236.15050
													2.911	3236.15125
													2.970	3236.15201
													3.024	3236.15276
													3.116	3236.15351
													3.103	3236.15427
													3.113	3236.15502
													3.161	3236.15577
													3.229	3236.15653
													3.202	3236.15728
													3.242	3236.15803
													3.220	3236.15879
													3.216	3236.15954
													3.197	3236.16029
													3.174	3236.16105
													3.131	3236.16180
													3.065	3236.16255
													3.001	3236.16331
													2.952	3236.16406
													2.377	3236.16481
													2.087	3236.16557
													2.342	3236.16632
													2.425	3236.16707
													2.517	3236.16783
													2.613	3236.16858
													2.511	3236.16933
													2.421	3236.17009
													2.378	3236.17084
													2.356	3236.17159
													2.255	3236.17235
													2.238	3236.17310
													2.201	3236.17385
													2.223	3236.17461
													2.204	3236.17536

EDXRF												Hyperspectral Imagery		
Mg	Al	Si	S	K	Ca	Ti	Fe	K/Al	Ti/Al	Si bio	S/Fe	Depth	TOC	Depth
%	%	%	%	%	%	%	%			%		m	%	m
													2.136	3236.17611
													2.098	3236.17687
													1.981	3236.17762
													1.924	3236.17837
													1.994	3236.17913
													1.900	3236.17988

EDXRF													Hyperspectral Imagery		
Mg %	Al %	Si %	S %	K %	Ca %	Ti %	Fe %	K/Al	Ti/Al	Si bio %	S/Fe	Depth m	TOC %	Depth m	
0.294	2.474	37.100	1.123	0.841	2.435	0.106	1.006	0.340	0.043	29.432	1.116	3237.09018	3.930	3237.06376	
0.364	2.574	36.942	1.216	0.856	2.351	0.102	1.019	0.332	0.040	28.964	1.193	3237.09122	4.007	3237.06447	
0.360	2.524	37.417	1.209	0.865	1.941	0.119	1.032	0.343	0.047	29.594	1.172	3237.09226	4.063	3237.06518	
0.460	3.508	32.784	2.681	1.391	1.889	0.288	2.039	0.396	0.082	21.909	1.315	3237.09331	4.084	3237.06589	
0.443	3.414	33.028	2.502	1.363	2.072	0.258	1.943	0.399	0.076	22.446	1.288	3237.09435	4.005	3237.06660	
0.425	2.780	36.200	1.528	0.978	1.989	0.141	1.324	0.352	0.051	27.583	1.154	3237.09540	3.766	3237.06731	
0.574	4.459	29.056	3.924	1.889	1.232	0.505	3.055	0.424	0.113	15.232	1.284	3237.09644	3.573	3237.06802	
0.399	4.031	31.309	3.322	1.602	1.479	0.388	2.466	0.397	0.096	18.813	1.347	3237.09748	3.472	3237.06874	
0.443	2.579	36.924	1.262	0.870	2.132	0.110	1.097	0.337	0.043	28.928	1.150	3237.09853	3.528	3237.06945	
0.377	2.457	37.046	1.169	0.870	2.268	0.097	1.045	0.354	0.040	29.430	1.119	3237.09957	3.721	3237.07016	
0.342	2.485	37.046	1.169	0.841	2.375	0.115	1.019	0.339	0.046	29.344	1.148	3237.10062	3.870	3237.07087	
0.259	2.385	37.385	1.169	0.827	2.248	0.093	0.992	0.347	0.039	29.993	1.178	3237.10166	3.930	3237.07158	
0.307	2.335	37.272	1.196	0.804	2.283	0.080	1.023	0.344	0.034	30.035	1.169	3237.10270	3.966	3237.07229	
0.417	2.396	37.028	1.196	0.809	2.383	0.093	1.036	0.338	0.039	29.601	1.154	3237.10375	3.879	3237.07300	
0.233	2.412	37.137	1.129	0.823	2.487	0.097	1.006	0.341	0.040	29.658	1.123	3237.10479	3.724	3237.07371	
0.307	2.323	37.155	1.116	0.780	2.566	0.080	0.979	0.336	0.034	29.952	1.139	3237.10584	3.714	3237.07442	
0.325	2.407	36.978	1.083	0.766	2.686	0.084	0.962	0.318	0.035	29.517	1.126	3237.10688	3.779	3237.07513	
0.338	2.351	37.078	1.129	0.799	2.546	0.084	0.997	0.340	0.036	29.789	1.133	3237.10792	3.733	3237.07584	
0.289	2.284	37.241	1.109	0.799	2.487	0.097	1.014	0.350	0.043	30.159	1.094	3237.10897	3.662	3237.07655	
0.272	2.457	36.892	1.249	0.851	2.467	0.110	1.067	0.346	0.045	29.276	1.171	3237.11001	3.606	3237.07726	
0.338	2.474	36.797	1.289	0.841	2.391	0.102	1.106	0.340	0.041	29.129	1.165	3237.11106	3.596	3237.07797	
0.307	2.451	37.132	1.226	0.846	2.264	0.115	1.045	0.345	0.047	29.533	1.173	3237.11210	3.400	3237.07868	
0.268	2.368	37.404	1.123	0.790	2.295	0.102	1.010	0.334	0.043	30.063	1.112	3237.11314	3.252	3237.07939	
0.246	2.357	36.856	1.192	0.832	2.467	0.093	1.045	0.353	0.039	29.550	1.141	3237.11419	3.192	3237.08010	
0.259	2.373	36.852	1.216	0.809	2.367	0.110	1.045	0.341	0.047	29.494	1.163	3237.11523	3.055	3237.08081	
0.206	2.435	37.354	1.182	0.823	2.244	0.102	1.010	0.338	0.042	29.806	1.171	3237.11628	3.010	3237.08152	
0.219	2.407	37.494	1.123	0.827	2.216	0.106	0.988	0.344	0.044	30.033	1.136	3237.11732	3.003	3237.08223	
0.276	2.312	37.485	1.172	0.813	2.136	0.084	1.014	0.352	0.037	30.317	1.156	3237.11836	2.889	3237.08294	
0.303	2.401	37.557	1.162	0.827	2.036	0.089	1.010	0.345	0.037	30.113	1.151	3237.11941	3.056	3237.08365	
0.298	2.396	37.318	1.162	0.799	2.315	0.106	1.006	0.334	0.044	29.891	1.156	3237.12045	3.075	3237.08436	
0.276	2.490	37.132	1.206	0.827	2.260	0.084	1.058	0.332	0.034	29.412	1.140	3237.12150	3.130	3237.08507	
0.311	2.529	36.983	1.279	0.846	2.307	0.115	1.088	0.335	0.045	29.142	1.175	3237.12254	3.344	3237.08578	
0.303	2.635	36.996	1.275	0.879	2.192	0.110	1.088	0.334	0.042	28.828	1.172	3237.12358	3.182	3237.08649	
0.268	2.540	37.186	1.252	0.884	2.092	0.097	1.110	0.348	0.038	29.311	1.128	3237.12463	3.127	3237.08720	
0.360	2.629	36.806	1.302	0.888	2.232	0.115	1.093	0.338	0.044	28.655	1.191	3237.12570	3.100	3237.08792	
													3.121	3237.08863	
													3.134	3237.08934	
													3.093	3237.09005	
													2.980	3237.09076	
													2.887	3237.09147	
													2.860	3237.09218	
													2.814	3237.09289	
													2.781	3237.09360	
													2.714	3237.09431	
													2.713	3237.09502	
													2.662	3237.09573	
													1.417	3237.09644	
													2.094	3237.09715	
													2.189	3237.09786	
													2.187	3237.09857	
													2.186	3237.09928	
													2.188	3237.09999	
													2.232	3237.10070	
													2.264	3237.10141	
													2.251	3237.10212	
													2.200	3237.10283	
													2.148	3237.10354	
													2.118	3237.10425	
													2.056	3237.10496	
													1.907	3237.10567	
													1.813	3237.10638	

EDXRF												Hyperspectral Imagery		
Mg	Al	Si	S	K	Ca	Ti	Fe	K/Al	Ti/Al	Si bio	S/Fe	Depth	TOC	Depth
%	%	%	%	%	%	%	%			%		m	%	m
													1.798	3237.10710
													2.017	3237.10781
													2.146	3237.10852
													2.065	3237.10923
													1.730	3237.10994
													0.713	3237.11065
													0.517	3237.11136
													0.573	3237.11207
													0.816	3237.11278
													1.163	3237.11349
													1.476	3237.11420
													1.705	3237.11491
													2.032	3237.11562
													2.175	3237.11633
													2.232	3237.11704
													2.311	3237.11775
													2.322	3237.11846
													2.279	3237.11917
													2.275	3237.11988

EDXRF												Hyperspectral Imagery		
Mg	Al	Si	S	K	Ca	Ti	Fe	K/Al	Ti/Al	Si bio	S/Fe	Depth	TOC	Depth
%	%	%	%	%	%	%	%			%		m	%	m
1.906	4.704	25.866	2.485	1.597	5.344	0.267	2.423	0.340	0.057	11.283	1.026	3237.82807	2.322	3237.81044
1.898	4.960	26.069	2.246	1.715	5.228	0.319	2.357	0.346	0.064	10.693	0.953	3237.82907	2.309	3237.81141
1.792	5.082	26.264	2.246	1.729	5.136	0.306	2.257	0.340	0.060	10.509	0.995	3237.83006	2.192	3237.81238
2.003	5.188	25.983	2.206	1.781	5.085	0.327	2.287	0.343	0.063	9.900	0.964	3237.83106	2.210	3237.81334
1.854	5.366	25.988	2.276	1.851	4.917	0.349	2.357	0.345	0.065	9.353	0.965	3237.83205	2.253	3237.81431
1.867	5.377	25.834	2.472	1.912	4.611	0.323	2.497	0.356	0.060	9.165	0.990	3237.83305	2.238	3237.81528
1.801	5.483	25.771	2.674	1.922	4.324	0.358	2.632	0.350	0.065	8.774	1.016	3237.83404	2.108	3237.81625
1.727	5.322	25.323	2.950	1.865	4.551	0.332	2.710	0.350	0.062	8.826	1.088	3237.83504	2.039	3237.81721
1.946	5.383	25.128	2.811	1.846	4.662	0.301	2.654	0.343	0.056	8.442	1.059	3237.83603	2.042	3237.81818
1.753	5.283	25.183	2.980	1.870	4.539	0.349	2.885	0.354	0.066	8.806	1.033	3237.83703	1.966	3237.81915
1.819	5.249	24.780	3.249	1.771	4.511	0.327	3.007	0.337	0.062	8.507	1.081	3237.83802	1.843	3237.82011
1.700	5.372	25.427	2.781	1.809	4.746	0.314	2.667	0.337	0.059	8.775	1.043	3237.83902	1.962	3237.82108
1.565	5.333	25.807	2.585	1.907	4.734	0.310	2.566	0.358	0.058	9.276	1.007	3237.84001	1.977	3237.82205
1.740	5.171	24.956	3.120	1.828	4.678	0.288	2.750	0.353	0.056	8.925	1.135	3237.84101	1.973	3237.82302
1.630	5.132	25.083	3.249	1.776	4.483	0.301	2.841	0.346	0.059	9.173	1.144	3237.84200	1.969	3237.82398
1.512	5.188	25.992	2.754	1.870	4.539	0.301	2.649	0.360	0.058	9.910	1.040	3237.84300	1.955	3237.82495
1.692	5.171	26.124	2.518	1.804	4.654	0.280	2.523	0.349	0.054	10.092	0.998	3237.84399	1.898	3237.82592
1.713	5.221	26.531	2.329	1.781	4.722	0.301	2.362	0.341	0.058	10.345	0.986	3237.84499	2.006	3237.82689
1.591	5.021	26.970	2.226	1.767	4.830	0.310	2.222	0.352	0.062	11.404	1.002	3237.84600	2.229	3237.82785
													2.331	3237.82882
													2.311	3237.82979
													2.538	3237.83076
													2.565	3237.83172
													2.585	3237.83269
													2.558	3237.83366
													2.609	3237.83463
													2.390	3237.83559
													2.429	3237.83656
													2.666	3237.83753
													2.386	3237.83849
													2.453	3237.83946
													2.588	3237.84043
													2.720	3237.84140
													2.771	3237.84236
													2.846	3237.84333
													2.997	3237.84430
													2.965	3237.84527
													2.945	3237.84623

EDXRF													Hyperspectral Imagery		
Mg %	Al %	Si %	S %	K %	Ca %	Ti %	Fe %	K/Al	Ti/Al	Si bio %	S/Fe	Depth m	TOC %	Depth m	
0.346	2.101	36.404	1.109	0.672	3.590	0.089	0.953	0.320	0.042	29.891	1.164	3238.11462	2.362	3238.09765	
0.325	2.112	36.580	1.129	0.701	3.379	0.102	0.975	0.332	0.048	30.033	1.158	3238.11588	2.328	3238.09865	
0.338	2.051	36.490	1.069	0.701	3.571	0.089	0.936	0.342	0.043	30.132	1.143	3238.11713	2.444	3238.09965	
0.382	2.034	36.073	1.182	0.672	3.694	0.080	1.019	0.331	0.039	29.767	1.161	3238.11838	2.433	3238.10065	
0.316	2.084	36.634	1.206	0.672	3.176	0.067	1.014	0.323	0.032	30.173	1.189	3238.11964	2.379	3238.10165	
0.325	2.079	36.096	1.149	0.668	3.818	0.084	0.953	0.321	0.041	29.652	1.206	3238.12089	2.433	3238.10265	
0.338	1.917	35.680	1.126	0.668	4.260	0.067	0.975	0.348	0.035	29.736	1.155	3238.12215	2.421	3238.10365	
0.421	2.017	35.861	1.103	0.687	3.993	0.071	0.984	0.340	0.035	29.606	1.121	3238.12340	2.423	3238.10465	
0.386	2.112	35.453	1.222	0.719	4.081	0.080	1.014	0.341	0.038	28.906	1.205	3238.12465	2.311	3238.10564	
0.289	1.917	35.616	1.521	0.658	3.734	0.063	1.202	0.343	0.033	29.673	1.266	3238.12591	2.376	3238.10664	
0.246	1.934	35.598	1.555	0.611	3.762	0.093	1.193	0.316	0.048	29.603	1.303	3238.12716	2.327	3238.10764	
0.259	1.956	36.186	1.202	0.635	3.722	0.071	1.014	0.325	0.036	30.122	1.185	3238.12842	2.339	3238.10864	
0.316	1.934	35.512	1.146	0.635	4.128	0.084	1.001	0.328	0.044	29.517	1.144	3238.12967	2.399	3238.10964	
0.303	1.928	35.512	1.139	0.640	4.220	0.097	0.984	0.332	0.051	29.534	1.158	3238.13092	2.455	3238.11064	
0.254	1.901	35.883	1.166	0.658	3.949	0.067	1.014	0.346	0.035	29.991	1.149	3238.13218	2.581	3238.11164	
0.329	1.940	35.924	1.159	0.630	3.961	0.067	0.979	0.325	0.035	29.911	1.183	3238.13343	2.631	3238.11264	
0.289	2.023	35.571	1.202	0.644	4.212	0.089	0.988	0.318	0.044	29.300	1.217	3238.13469	2.650	3238.11363	
0.408	1.995	35.580	1.192	0.616	4.136	0.054	0.988	0.309	0.027	29.395	1.207	3238.13594	2.679	3238.11463	
0.495	1.862	33.906	1.744	0.597	4.666	0.071	1.407	0.321	0.038	28.135	1.240	3238.13719	2.670	3238.11563	
0.360	1.956	34.227	1.099	0.630	5.511	0.071	0.979	0.322	0.036	28.163	1.122	3238.13845	2.772	3238.11663	
0.395	1.973	34.191	1.073	0.597	5.627	0.071	0.971	0.303	0.036	28.075	1.105	3238.13970	2.805	3238.11763	
													2.791	3238.11863	
													2.850	3238.11963	
													2.717	3238.12063	
													2.685	3238.12163	
													2.498	3238.12262	
													2.384	3238.12362	
													2.397	3238.12462	
													2.303	3238.12562	
													2.338	3238.12662	
													2.271	3238.12762	
													2.313	3238.12862	
													2.231	3238.12962	
													2.216	3238.13061	
													2.337	3238.13161	
													2.388	3238.13261	
													2.319	3238.13361	
													2.250	3238.13461	
													2.249	3238.13561	
													2.306	3238.13661	
													2.226	3238.13761	
													2.282	3238.13860	
													2.240	3238.13960	

EDXRF												Hyperspectral Imagery		
Mg %	Al %	Si %	S %	K %	Ca %	Ti %	Fe %	K/Al	Ti/Al	Si bio %	S/Fe	Depth m	TOC %	Depth m
0.447	3.063	33.458	1.777	1.142	3.594	0.141	1.511	0.373	0.046	23.962	1.176	3240.94054	3.316	3240.90978
0.403	3.163	33.105	1.827	1.161	3.714	0.136	1.516	0.367	0.043	23.299	1.205	3240.94161	3.292	3240.91044
0.526	3.174	32.843	1.780	1.086	4.021	0.175	1.468	0.342	0.055	23.002	1.213	3240.94268	3.194	3240.91109
0.447	3.163	32.689	1.724	1.161	4.176	0.141	1.463	0.367	0.045	22.883	1.178	3240.94376	3.134	3240.91175
0.478	3.141	32.499	1.797	1.147	4.236	0.162	1.503	0.365	0.052	22.762	1.196	3240.94483	3.105	3240.91240
													3.132	3240.91306
													3.238	3240.91372
													3.316	3240.91437
													3.284	3240.91503
													3.149	3240.91569
													2.978	3240.91634
													2.795	3240.91700
													2.584	3240.91765
													2.351	3240.91831
													1.995	3240.91897
													1.590	3240.91962
													1.477	3240.92028
													1.559	3240.92094
													1.729	3240.92159
													1.913	3240.92225
													2.047	3240.92290
													2.075	3240.92356
													2.099	3240.92422
													2.020	3240.92487
													1.911	3240.92553
													1.865	3240.92619
													1.829	3240.92684
													1.808	3240.92750
													1.810	3240.92815
													1.759	3240.92881
													1.758	3240.92947
													1.786	3240.93012
													1.826	3240.93078
													1.899	3240.93143
													1.937	3240.93209
													1.906	3240.93275
													1.806	3240.93340
													1.729	3240.93406
													1.718	3240.93472
													1.770	3240.93537
													1.828	3240.93603
													1.901	3240.93668
													1.974	3240.93734
													2.034	3240.93800
													2.124	3240.93865
													2.199	3240.93931
													2.234	3240.93997
													2.266	3240.94062
													2.166	3240.94128
													2.189	3240.94193
													2.024	3240.94259
													2.020	3240.94325
													1.930	3240.94390
													1.902	3240.94456
													1.519	3240.94521

EDXRF													Hyperspectral Imagery	
Mg %	Al %	Si %	S %	K %	Ca %	Ti %	Fe %	K/Al	Ti/Al	Si bio %	S/Fe	Depth m	TOC %	Depth m
0.539	2.557	20.115	0.946	0.649	16.174	0.119	1.058	0.254	0.047	12.188	0.895	3241.87116	0.643	3241.83075
0.447	1.217	17.613	0.687	0.203	20.916	0.032	0.574	0.167	0.027	13.842	1.197	3241.87302	0.964	3241.83157
0.233	0.977	15.907	0.551	0.151	23.298	0.058	0.552	0.155	0.060	12.877	0.998	3241.87489	1.317	3241.83239
0.307	1.077	15.129	0.511	0.203	23.717	0.041	0.548	0.188	0.038	11.789	0.933	3241.87675	1.862	3241.83321
0.583	2.713	18.463	0.946	0.762	17.537	0.136	1.228	0.281	0.050	10.054	0.771	3241.87861	2.738	3241.83404
1.161	5.149	29.047	2.219	1.945	3.347	0.306	2.091	0.378	0.059	13.084	1.061	3241.88047	3.380	3241.83486
0.942	5.266	28.911	2.641	1.992	2.794	0.297	2.266	0.378	0.056	12.587	1.166	3241.88233	3.648	3241.83568
0.859	5.561	29.128	2.578	2.105	2.459	0.332	2.270	0.378	0.060	11.890	1.136	3241.88420	3.631	3241.83650
													3.263	3241.83732
													2.488	3241.83814
													1.349	3241.83896
													0.692	3241.83979
													0.663	3241.84061
													0.670	3241.84143
													0.729	3241.84225
													0.751	3241.84307
													0.776	3241.84389
													0.745	3241.84471
													1.001	3241.84554
													1.027	3241.84636
													1.001	3241.84718
													0.747	3241.84800
													0.744	3241.84882
													0.771	3241.84964
													0.806	3241.85046
													0.754	3241.85128
													0.780	3241.85211
													0.803	3241.85293
													0.777	3241.85375
													0.823	3241.85457
													0.880	3241.85539
													0.839	3241.85621
													0.780	3241.85703
													0.788	3241.85786
													0.782	3241.85868
													0.758	3241.85950
													0.781	3241.86032
													0.850	3241.86114
													0.818	3241.86196
													0.850	3241.86278
													0.765	3241.86361
													0.782	3241.86443
													0.799	3241.86525
													0.803	3241.86607
													0.815	3241.86689
													0.793	3241.86771
													0.784	3241.86853
													0.800	3241.86936
													0.855	3241.87018
													0.809	3241.87100
													0.812	3241.87182
													0.841	3241.87264
													0.770	3241.87346
													0.748	3241.87428
													0.704	3241.87511
													0.521	3241.87593
													0.452	3241.87675
													0.458	3241.87757
													0.509	3241.87839
													0.546	3241.87921
													0.597	3241.88003

EDXRF													Hyperspectral Imagery	
Mg	Al	Si	S	K	Ca	Ti	Fe	K/Al	Ti/Al	Si bio	S/Fe	Depth	TOC	Depth
%	%	%	%	%	%	%	%			%		m	%	m
													0.701	3241.88086
													0.751	3241.88168
													0.767	3241.88250
													0.726	3241.88332
													0.660	3241.88414

EDXRF												Hyperspectral Imagery			
Mg %	Al %	Si %	S %	K %	Ca %	Ti %	Fe %	K/Al	Ti/Al	Si bio %	S/Fe	Depth m	TOC %	Depth m	
0.425	3.675	31.698	1.737	1.396	3.981	0.154	1.529	0.380	0.042	20.305	1.136	3244.58293	7.990	3244.57770	
0.390	3.625	31.965	1.691	1.400	4.033	0.167	1.494	0.386	0.046	20.727	1.132	3244.58397	7.055	3244.57865	
0.500	3.681	32.368	1.711	1.396	3.555	0.162	1.503	0.379	0.044	20.958	1.139	3244.58500	6.853	3244.57960	
0.500	3.742	30.689	1.973	1.532	3.284	0.206	2.859	0.409	0.055	19.089	0.690	3244.58700	5.966	3244.58055	
0.548	3.636	30.780	1.947	1.513	3.296	0.210	2.854	0.416	0.058	19.508	0.682	3244.58883	6.153	3244.58151	
0.544	3.681	32.725	1.820	1.443	3.045	0.175	1.642	0.392	0.048	21.315	1.109	3244.59067	6.311	3244.58246	
0.417	3.636	32.748	1.774	1.410	3.312	0.162	1.533	0.388	0.045	21.476	1.157	3244.59250	6.136	3244.58341	
0.438	3.519	33.010	1.757	1.353	3.248	0.162	1.507	0.385	0.046	22.100	1.166	3244.59433	5.736	3244.58436	
0.504	3.631	32.693	1.780	1.381	3.327	0.171	1.581	0.381	0.047	21.439	1.126	3244.59617	6.473	3244.58532	
0.434	3.697	31.644	1.767	1.452	4.160	0.180	1.642	0.393	0.049	20.182	1.076	3244.59800	2.325	3244.58627	
0.412	3.497	31.408	1.990	1.339	4.316	0.167	1.725	0.383	0.048	20.568	1.154	3244.59983	2.012	3244.58722	
0.386	3.386	31.653	1.744	1.278	4.642	0.136	1.503	0.378	0.040	21.157	1.161	3244.60166	4.052	3244.58817	
0.355	3.352	31.970	1.960	1.288	4.164	0.154	1.581	0.384	0.046	21.577	1.240	3244.60350	3.488	3244.58913	
0.417	3.419	32.200	1.761	1.320	4.108	0.158	1.533	0.386	0.046	21.601	1.148	3244.60533	5.129	3244.59008	
0.447	3.553	32.377	1.797	1.335	3.794	0.180	1.568	0.376	0.051	21.363	1.146	3244.60716	4.662	3244.59103	
0.460	3.647	32.119	2.053	1.424	3.423	0.154	1.734	0.390	0.042	20.812	1.184	3244.60900	3.353	3244.59198	
0.452	3.803	32.255	2.046	1.433	3.244	0.184	1.716	0.377	0.048	20.465	1.192	3244.61083	3.132	3244.59294	
0.447	4.031	31.825	2.212	1.588	2.957	0.215	1.917	0.394	0.053	19.328	1.154	3244.61266	3.051	3244.59389	
0.447	4.220	30.820	2.319	1.696	3.196	0.241	2.113	0.402	0.057	17.738	1.097	3244.61450	1.516	3244.59484	
													1.137	3244.59579	
													1.173	3244.59674	
													1.562	3244.59770	
													1.503	3244.59865	
													1.142	3244.59960	
													0.000	3244.60055	
													0.432	3244.60151	
													0.800	3244.60246	
													0.861	3244.60341	
													1.098	3244.60436	
													1.108	3244.60532	
													1.144	3244.60627	
													1.223	3244.60722	
													0.856	3244.60817	
													0.815	3244.60913	
													1.198	3244.61008	
													1.058	3244.61103	
													1.523	3244.61198	
													1.452	3244.61294	
													1.469	3244.61389	
													1.816	3244.61484	

EDXRF													Hyperspectral Imagery	
Mg %	Al %	Si %	S %	K %	Ca %	Ti %	Fe %	K/Al	Ti/Al	Si bio %	S/Fe	Depth m	TOC %	Depth m
0.272	2.062	31.657	1.604	0.771	6.890	0.110	1.149	0.374	0.054	25.265	1.396	3249.57976	4.503	3249.54611
0.211	2.023	30.214	2.292	0.738	6.945	0.106	1.725	0.365	0.052	23.943	1.329	3249.58138	5.008	3249.54717
0.294	1.984	30.617	1.515	0.691	8.133	0.076	1.027	0.348	0.038	24.466	1.474	3249.58299	3.897	3249.54823
0.250	1.917	29.893	1.382	0.687	9.045	0.106	0.966	0.358	0.055	23.949	1.430	3249.58460	1.688	3249.54928
													0.000	3249.55034
													4.587	3249.55140
													3.083	3249.55245
													1.477	3249.55351
													0.732	3249.55457
													0.860	3249.55563
													1.105	3249.55668
													1.452	3249.55774
													7.909	3249.55880
													7.253	3249.55985
													6.900	3249.56091
													4.065	3249.56197
													1.884	3249.56302
													0.494	3249.56408
													0.000	3249.56514
													0.000	3249.56619
													0.000	3249.56725
													0.497	3249.56831
													1.473	3249.56936
													1.931	3249.57042
													2.729	3249.57148
													3.016	3249.57253
													2.903	3249.57359
													2.930	3249.57465
													2.566	3249.57570
													2.216	3249.57676
													2.291	3249.57782
													1.866	3249.57887
													1.473	3249.57993
													0.000	3249.58099
													0.000	3249.58204
													0.000	3249.58310
													0.000	3249.58416
													0.000	3249.58521

EDXRF												Hyperspectral Imagery		
Mg %	Al %	Si %	S %	K %	Ca %	Ti %	Fe %	K/Al	Ti/Al	Si bio %	S/Fe	Depth m	TOC %	Depth m
9.346	1.011	4.342	0.631	0.236	25.319	0.045	0.844	0.233	0.045	1.209	0.747	3250.55153	0.333	3250.52508
9.407	1.116	4.455	0.581	0.222	25.239	0.050	0.792	0.199	0.045	0.994	0.734	3250.55275	0.292	3250.52584
8.956	0.994	4.387	0.601	0.217	25.729	0.050	0.814	0.218	0.050	1.306	0.738	3250.55396	0.303	3250.52660
8.829	0.988	4.360	0.584	0.226	25.964	0.045	0.801	0.229	0.046	1.296	0.730	3250.55518	0.294	3250.52737
8.969	0.933	4.410	0.661	0.212	25.649	0.054	0.888	0.228	0.058	1.518	0.744	3250.55640	0.326	3250.52813
													0.321	3250.52890
													0.306	3250.52966
													0.255	3250.53042
													0.269	3250.53119
													0.289	3250.53195
													0.336	3250.53272
													0.321	3250.53348
													0.334	3250.53424
													0.322	3250.53501
													0.277	3250.53577
													0.288	3250.53654
													0.274	3250.53730
													0.283	3250.53806
													0.265	3250.53883
													0.295	3250.53959
													0.290	3250.54036
													0.291	3250.54112
													0.281	3250.54188
													0.300	3250.54265
													0.260	3250.54341
													0.262	3250.54418
													0.306	3250.54494
													0.340	3250.54570
													0.292	3250.54647
													0.271	3250.54723
													0.293	3250.54800
													0.302	3250.54876
													0.263	3250.54952
													0.255	3250.55029
													0.299	3250.55105
													0.261	3250.55182
													0.271	3250.55258
													0.262	3250.55334
													0.279	3250.55411
													0.267	3250.55487
													0.284	3250.55564
													0.279	3250.55640

EDXRF												Hyperspectral Imagery		
Mg	Al	Si	S	K	Ca	Ti	Fe	K/Al	Ti/Al	Si bio	S/Fe	Depth	TOC	Depth
%	%	%	%	%	%	%	%			%		m	%	m
													87.491	3251.53235
													88.234	3251.53303
													87.291	3251.53371
													86.629	3251.52624
													87.326	3251.52692
													88.872	3251.5276
													90.255	3251.52828
													90.527	3251.52896
													89.360	3251.52964
													88.069	3251.53031
													87.164	3251.53099
													86.859	3251.53167
													88.389	3251.53439
													88.629	3251.53507
													88.064	3251.53575
													87.284	3251.53643
													85.926	3251.5371
													84.623	3251.53778
													84.714	3251.53846
													85.197	3251.53914
													86.143	3251.53982
													87.510	3251.5405
													89.072	3251.54118
													90.258	3251.54186
													90.950	3251.54254
													91.264	3251.54322
													90.938	3251.54389
													89.842	3251.54457
													88.690	3251.54525
													88.921	3251.54593
													89.481	3251.54661
													89.754	3251.54729
													89.364	3251.54797
													88.220	3251.54865
													86.943	3251.54933
													85.560	3251.55001
													87.152	3251.55068
													89.424	3251.55136
													91.006	3251.55204
													92.186	3251.55272
													92.144	3251.5534
													91.538	3251.55408
													77.355	3251.55476
													65.414	3251.55544
													65.287	3251.55612
													70.970	3251.55679
													78.911	3251.55747
													80.120	3251.55815
													80.837	3251.55883
													79.683	3251.55951
													76.186	3251.56019
													75.331	3251.56087
													74.644	3251.56155
													74.780	3251.56223
													74.178	3251.56291

EDXRF												Hyperspectral Imagery		
Mg	Al	Si	S	K	Ca	Ti	Fe	K/Al	Ti/Al	Si bio	S/Fe	Depth	TOC	Depth
%	%	%	%	%	%	%	%			%		m	%	m
0.281	1.917	34.825	1.518	0.719	4.555	0.093	1.045	0.375	0.049	28.881	1.453	3252.52777	5.420	3252.48045
0.237	1.912	34.571	1.598	0.785	4.611	0.089	1.088	0.411	0.046	28.645	1.468	3252.52936	5.557	3252.48125
													5.413	3252.48206
													5.819	3252.48286
													5.719	3252.48366
													5.534	3252.48446
													5.139	3252.48526
													4.723	3252.48606
													5.235	3252.48686
													5.706	3252.48766
													5.788	3252.48847
													5.403	3252.48927
													5.526	3252.49007
													5.724	3252.49087
													6.312	3252.49167
													6.293	3252.49247
													3.576	3252.49327
													4.329	3252.49407
													4.259	3252.49488
													2.978	3252.49568
													2.533	3252.49648
													2.011	3252.49728
													2.100	3252.49808
													1.801	3252.49888
													2.493	3252.49968
													1.459	3252.50048
													1.214	3252.50129
													3.226	3252.50209
													4.424	3252.50289
													5.039	3252.50369
													3.256	3252.50449
													2.977	3252.50529
													1.802	3252.50609
													2.493	3252.50689
													2.055	3252.50770
													1.673	3252.50850
													1.598	3252.50930
													1.946	3252.51010
													3.545	3252.51090
													6.160	3252.51170
													5.828	3252.51250
													5.426	3252.51330
													5.685	3252.51411
													5.909	3252.51491
													6.019	3252.51571
													5.902	3252.51651
													5.810	3252.51731
													5.777	3252.51811
													6.171	3252.51891
													6.581	3252.51971
													7.000	3252.52052
													7.006	3252.52132
													6.547	3252.52212
													5.698	3252.52292
													6.115	3252.52372
													5.367	3252.52452
													5.514	3252.52532
													6.145	3252.52612
													6.093	3252.52693
													6.505	3252.52773
													7.253	3252.52853
													6.580	3252.52933

EDXRF												Hyperspectral Imagery		
Mg	Al	Si	S	K	Ca	Ti	Fe	K/Al	Ti/Al	Si bio	S/Fe	Depth	TOC	Depth
%	%	%	%	%	%	%	%			%		m	%	m
													4.627	3253.55575
													4.427	3253.55651
													4.752	3253.55728
													4.577	3253.55804
													5.627	3253.55880
													5.743	3253.55957
													5.285	3253.56033
													5.022	3253.56110
													4.557	3253.56186
													3.900	3253.56263
													3.772	3253.56339
													3.774	3253.56416
													4.009	3253.56492
													3.692	3253.56569
													4.120	3253.56645
													3.936	3253.56722
													3.479	3253.56798
													2.995	3253.56875
													2.173	3253.56951
													2.045	3253.57027
													2.500	3253.57104
													2.861	3253.57180
													3.271	3253.57257
													3.529	3253.57333
													3.473	3253.57410
													3.263	3253.57486
													2.871	3253.57563
													2.342	3253.57639
													2.706	3253.57716
													2.951	3253.57792
													3.415	3253.57869
													3.313	3253.57945
													3.062	3253.58021
													2.404	3253.58098
													1.275	3253.58174
													1.094	3253.58251
													1.901	3253.58327
													2.730	3253.58404
													3.646	3253.58480
													3.945	3253.58557
													4.013	3253.58633
													4.043	3253.58710
													4.229	3253.58786
													4.152	3253.58863
													4.156	3253.58939
													4.132	3253.59016
													4.183	3253.59092
													4.278	3253.59168
													4.375	3253.59245
													4.416	3253.59321
													4.503	3253.59398
													4.739	3253.59474
													4.569	3253.59551
													4.627	3253.59627

EDXRF											Hyperspectral Imagery		
Mg %	Al %	Si %	S %	K %	Ca %	Ti %	Fe %	K/Al	Ti/Al	Si bio %	S/Fe	Depth m	Depth m
0.504	2.974	26.300	2.279	1.184	8.814	0.167	1.655	0.398	0.056	17.080	1.377	3255.60917	3255.57111
0.368	3.030	26.789	2.163	1.222	8.647	0.167	1.529	0.403	0.055	17.396	1.415	3255.61060	3255.57192
0.425	3.024	26.906	2.272	1.264	8.157	0.167	1.642	0.418	0.055	17.531	1.384	3255.61200	3255.57273
													3255.57354
													3255.57435
													3255.57516
													3255.57597
													3255.57678
													3255.57759
													3255.57840
													3255.57921
													3255.58002
													3255.58083
													3255.58164
													3255.58245
													3255.58326
													3255.58407
													3255.58488
													3255.58569
													3255.58650
													3255.58730
													3255.58811
													3255.58892
													3255.58973
													3255.59054
													3255.59135
													3255.59216
													3255.59297
													3255.59378
													3255.59459
													3255.59540
													3255.59621
													3255.59702
													3255.59783
													3255.59864
													3255.59945
													3255.60026
													3255.60107
													3255.60188
													3255.60269
													3255.60349
													3255.60430
													3255.60511
													3255.60592
													3255.60673
													3255.60754
													3255.60835
													3255.60916
													3255.60997
													3255.61078
													3255.61159
													3255.61240

Slab 3257.43 m

EDXRF													Hyperspectral Imagery	
Mg %	Al %	Si %	S %	K %	Ca %	Ti %	Fe %	K/Al	Ti/Al	Si bio %	S/Fe	Depth m	TOC %	Depth m
0.807	2.919	28.544	2.163	1.241	7.069	0.136	1.734	0.425	0.047	19.497	1.247	3257.43000	1.493	3257.43029
0.763	2.896	28.413	2.222	1.231	7.041	0.158	1.721	0.425	0.055	19.434	1.292	3257.43218	1.680	3257.43108
0.710	3.024	28.178	2.086	1.259	7.507	0.149	1.699	0.416	0.049	18.803	1.228	3257.43435	1.687	3257.43187
0.723	3.464	28.924	2.541	1.527	5.423	0.167	2.004	0.441	0.048	18.187	1.268	3257.43653	1.728	3257.43266
0.916	3.753	28.725	2.728	1.724	4.611	0.202	2.239	0.459	0.054	17.091	1.218	3257.43871	1.817	3257.43345
1.161	3.920	27.029	2.674	1.705	5.690	0.175	2.318	0.435	0.045	14.877	1.154	3257.44089	1.735	3257.43424
1.065	3.853	26.590	2.784	1.738	6.017	0.206	2.348	0.451	0.053	14.645	1.185	3257.44306	1.773	3257.43503
1.161	3.870	26.359	3.120	1.682	5.443	0.267	2.750	0.435	0.069	14.363	1.135	3257.44524	1.774	3257.43582
1.004	3.736	27.083	2.930	1.635	5.551	0.215	2.501	0.438	0.057	15.501	1.172	3257.44742	1.755	3257.43661
1.026	3.447	27.635	2.784	1.518	5.714	0.193	2.379	0.440	0.056	16.949	1.170	3257.44959	1.731	3257.43740
0.925	3.180	29.870	2.399	1.349	4.989	0.171	2.026	0.424	0.054	20.012	1.184	3257.45177	1.668	3257.43819
0.732	3.002	31.101	2.345	1.302	4.539	0.180	1.873	0.434	0.060	21.795	1.252	3257.45395	1.429	3257.43898
0.776	2.796	31.861	2.216	1.180	4.439	0.145	1.703	0.422	0.052	23.193	1.301	3257.45612	1.375	3257.43977
0.601	2.462	31.992	2.006	1.034	5.228	0.128	1.537	0.420	0.052	24.358	1.305	3257.45830	1.321	3257.44056
0.478	2.229	30.761	1.721	0.949	7.045	0.119	1.476	0.426	0.053	23.852	1.165	3257.46048	1.222	3257.44135
0.443	2.296	29.630	1.674	0.945	8.033	0.145	1.516	0.412	0.063	22.514	1.105	3257.46266	1.107	3257.44214
0.530	2.273	31.458	1.930	0.912	6.117	0.089	1.490	0.401	0.039	24.411	1.296	3257.46483	1.097	3257.44293
0.399	2.006	32.246	1.681	0.804	6.316	0.076	1.319	0.401	0.038	26.026	1.274	3257.46701	1.046	3257.44372
0.342	1.962	31.983	1.621	0.799	6.778	0.102	1.272	0.407	0.052	25.901	1.275	3257.46919	1.056	3257.44451
0.504	1.912	32.612	1.754	0.795	5.977	0.097	1.311	0.416	0.051	26.685	1.338	3257.47136	0.979	3257.44530
0.307	1.728	33.123	1.711	0.710	6.109	0.084	1.123	0.411	0.049	27.766	1.523	3257.47354	1.118	3257.44609
0.289	1.511	30.427	1.285	0.546	9.424	0.054	0.979	0.361	0.036	25.742	1.312	3257.47572	1.008	3257.44688
0.351	1.495	30.418	1.219	0.508	9.583	0.071	0.901	0.340	0.048	25.784	1.353	3257.47789	1.151	3257.44767
0.294	1.489	28.531	1.229	0.489	11.261	0.080	0.923	0.329	0.054	23.915	1.332	3257.48007	1.266	3257.44846
0.193	1.628	33.182	1.465	0.602	6.754	0.076	1.006	0.370	0.047	28.135	1.457	3257.48225	1.255	3257.44925
0.224	1.634	33.942	1.594	0.597	5.846	0.063	1.075	0.366	0.038	28.878	1.483	3257.48443	1.271	3257.45004
0.351	2.490	32.255	2.698	1.015	4.061	0.158	1.825	0.408	0.064	24.535	1.478	3257.48660	1.356	3257.45083
0.443	3.174	32.273	2.495	1.344	3.112	0.189	2.013	0.423	0.059	22.432	1.240	3257.48878	1.452	3257.45162
0.215	2.062	35.168	1.960	0.827	3.571	0.093	1.189	0.401	0.045	28.776	1.649	3257.49096	1.616	3257.45241
0.276	1.611	35.693	1.681	0.640	4.224	0.063	1.019	0.397	0.039	30.698	1.650	3257.49313	1.769	3257.45320
0.206	1.561	36.037	1.827	0.602	3.889	0.054	0.975	0.386	0.035	31.197	1.874	3257.49531	2.109	3257.45399
0.259	1.712	34.929	1.661	0.658	4.826	0.063	0.971	0.385	0.037	29.623	1.711	3257.49750	2.095	3257.45479
0.649	1.528	32.065	1.568	0.532	7.101	0.071	1.115	0.348	0.047	27.328	1.407	3257.50000	2.320	3257.45558
0.614	1.495	32.055	1.525	0.527	7.204	0.071	1.128	0.352	0.048	27.422	1.352	3257.50165	1.958	3257.45637
0.894	1.033	31.992	1.182	0.301	8.488	0.024	0.713	0.292	0.023	28.790	1.657	3257.50329	1.959	3257.45716
0.478	1.500	31.571	1.790	0.508	7.432	0.063	1.106	0.339	0.042	26.921	1.619	3257.50494	2.062	3257.45795
0.329	1.344	33.757	1.501	0.461	6.503	0.028	0.875	0.343	0.021	29.589	1.716	3257.50659	1.977	3257.45874
0.491	1.200	34.635	1.405	0.367	6.033	0.015	0.788	0.306	0.013	30.915	1.784	3257.50824	2.195	3257.45953
0.552	1.044	36.037	1.358	0.330	4.977	-0.011	0.744	0.316	-0.011	32.801	1.826	3257.50988	2.154	3257.46032
													2.261	3257.46111
													2.249	3257.46190
													2.289	3257.46269
													2.291	3257.46348
													2.370	3257.46427
													2.300	3257.46506
													2.346	3257.46585
													2.613	3257.46664
													2.646	3257.46743
													2.815	3257.46822
													2.867	3257.46901
													2.861	3257.46980
													2.722	3257.47059
													2.922	3257.47138
													2.739	3257.47217
													2.974	3257.47296
													3.195	3257.47375
													3.192	3257.47454
													3.104	3257.47533
													3.176	3257.47612
													3.013	3257.47691
													2.838	3257.47770

EDXRF												Hyperspectral Imagery		
Mg	Al	Si	S	K	Ca	Ti	Fe	K/Al	Ti/Al	Si bio	S/Fe	Depth	TOC	Depth
%	%	%	%	%	%	%	%			%		m	%	m
													2.627	3257.47849
													2.460	3257.47928
													2.426	3257.48007
													2.241	3257.48074
													2.246	3257.48140
													2.173	3257.48206
													2.650	3257.48273
													2.853	3257.48339
													2.957	3257.48406
													3.168	3257.48472
													3.175	3257.48539
													3.042	3257.48605
													2.800	3257.48671
													2.338	3257.48738
													2.346	3257.48804
													2.538	3257.48871
													2.950	3257.48937
													3.094	3257.49004
													3.129	3257.49070
													3.401	3257.49136
													3.439	3257.49203
													3.415	3257.49269
													3.345	3257.49336
													3.370	3257.49402
													3.262	3257.49469
													3.319	3257.49535
													3.333	3257.49601
													3.279	3257.49668
													3.168	3257.49734
													3.049	3257.49801
													2.292	3257.49867
													2.158	3257.49934
													2.040	3257.50000
													2.113	3257.50066
													2.135	3257.50133
													2.090	3257.50199
													1.969	3257.50266
													2.054	3257.50332
													2.556	3257.50399
													2.828	3257.50465
													3.039	3257.50531
													3.268	3257.50598
													3.416	3257.50664
													3.410	3257.50731
													3.217	3257.50797
													3.501	3257.50864
													3.527	3257.50930
													4.032	3257.50996
													4.498	3257.51063

EDXRF													Hyperspectral Imagery	
Mg %	Al %	Si %	S %	K %	Ca %	Ti %	Fe %	K/Al	Ti/Al	Si bio %	S/Fe	Depth m	TOC %	Depth m
8.877	1.717	9.767	0.983	0.405	19.895	0.054	1.219	0.236	0.031	4.444	0.806	3258.59707	1.066	3258.54899
6.836	1.667	12.912	1.099	0.447	18.883	0.063	1.232	0.268	0.038	7.744	0.892	3258.59874	1.009	3258.54980
4.535	1.606	15.966	1.325	0.527	17.859	0.080	1.385	0.328	0.050	10.988	0.957	3258.60040	0.903	3258.55060
													0.957	3258.55140
													0.920	3258.55221
													0.901	3258.55301
													0.903	3258.55381
													0.778	3258.55462
													0.801	3258.55542
													0.775	3258.55622
													0.763	3258.55703
													0.786	3258.55783
													0.690	3258.55863
													0.717	3258.55944
													0.619	3258.56024
													0.592	3258.56104
													0.595	3258.56184
													0.570	3258.56265
													0.521	3258.56345
													0.498	3258.56425
													0.522	3258.56506
													0.420	3258.56586
													0.445	3258.56666
													0.428	3258.56747
													0.434	3258.56827
													0.373	3258.56907
													0.410	3258.56988
													0.389	3258.57068
													0.379	3258.57148
													0.335	3258.57229
													0.340	3258.57309
													0.350	3258.57389
													0.339	3258.57470
													0.329	3258.57550
													0.333	3258.57630
													0.324	3258.57710
													0.320	3258.57791
													0.325	3258.57871
													0.312	3258.57951
													0.302	3258.58032
													0.313	3258.58112
													0.296	3258.58192
													0.311	3258.58273
													0.319	3258.58353
													0.289	3258.58433
													0.287	3258.58514
													0.284	3258.58594
													0.319	3258.58674
													0.332	3258.58755
													0.307	3258.58835
													0.288	3258.58915
													0.304	3258.58996
													0.302	3258.59076
													0.314	3258.59156
													0.323	3258.59237
													0.312	3258.59317
													0.306	3258.59397
													0.316	3258.59477
													0.316	3258.59558
													0.355	3258.59638
													0.334	3258.59718

EDXRF												Hyperspectral Imagery		
Mg	Al	Si	S	K	Ca	Ti	Fe	K/Al	Ti/Al	Si bio	S/Fe	Depth	TOC	Depth
%	%	%	%	%	%	%	%			%		m	%	m
													0.357	3258.59799
													0.430	3258.59879
													0.420	3258.59959
													0.549	3258.60040

EDXRF												Hyperspectral Imagery		
Mg %	Al %	Si %	S %	K %	Ca %	Ti %	Fe %	K/Al	Ti/Al	Si bio %	S/Fe	Depth m	TOC %	Depth m
0.390	3.369	30.589	3.033	1.616	3.304	0.301	2.226	0.480	0.089	20.145	1.362	3259.59241	4.509	3259.57140
0.513	3.403	30.513	3.013	1.475	3.475	0.271	2.187	0.434	0.080	19.965	1.378	3259.59359	4.512	3259.57223
0.184	2.162	35.544	1.428	0.879	4.037	0.084	1.067	0.407	0.039	28.841	1.339	3259.59480	4.294	3259.57306
													3.963	3259.57389
													4.168	3259.57473
													4.146	3259.57556
													3.925	3259.57639
													3.966	3259.57722
													4.102	3259.57805
													4.168	3259.57888
													4.065	3259.57971
													4.325	3259.58054
													4.362	3259.58137
													4.232	3259.58220
													4.421	3259.58304
													4.582	3259.58387
													4.380	3259.58470
													4.522	3259.58553
													4.339	3259.58636
													4.390	3259.58719
													4.449	3259.58802
													4.362	3259.58885
													4.256	3259.58968
													4.244	3259.59051
													4.004	3259.59135
													3.353	3259.59218
													3.077	3259.59301
													3.336	3259.59384
													3.531	3259.59467
													3.637	3259.59551

EDXRF													Hyperspectral Imagery	
Mg %	Al %	Si %	S %	K %	Ca %	Ti %	Fe %	K/Al	Ti/Al	Si bio %	S/Fe	Depth m	TOC %	Depth m
0.316	2.212	34.150	1.661	0.921	4.710	0.080	1.250	0.416	0.036	27.293	1.329	3260.61748	1.790	3260.56395
0.294	2.179	34.381	1.588	0.898	4.722	0.071	1.162	0.412	0.033	27.627	1.366	3260.61908	2.750	3260.56475
0.351	2.184	33.698	1.638	0.921	5.121	0.063	1.237	0.422	0.029	26.926	1.324	3260.62070	3.863	3260.56565
													3.996	3260.56655
													4.028	3260.56744
													4.198	3260.56834
													4.550	3260.56924
													4.613	3260.57013
													4.162	3260.57103
													3.963	3260.57193
													3.954	3260.57282
													3.863	3260.57372
													4.140	3260.57462
													4.053	3260.57552
													4.288	3260.57641
													4.142	3260.57731
													4.154	3260.57821
													3.651	3260.57910
													3.609	3260.58000
													3.499	3260.58090
													3.235	3260.58179
													3.344	3260.58269
													3.375	3260.58359
													3.354	3260.58449
													3.367	3260.58538
													3.082	3260.58628
													2.971	3260.58718
													2.835	3260.58807
													2.691	3260.58897
													2.597	3260.58987
													2.371	3260.59076
													2.340	3260.59166
													2.159	3260.59256
													1.995	3260.59346
													2.030	3260.59435
													1.507	3260.59525
													1.767	3260.59615
													2.327	3260.59704
													2.059	3260.59794
													2.126	3260.59884
													2.146	3260.59973
													2.425	3260.60063
													2.502	3260.60153
													2.601	3260.60243
													2.693	3260.60332
													2.635	3260.60422
													2.666	3260.60512
													2.569	3260.60601
													2.411	3260.60691
													2.464	3260.60781
													2.611	3260.60870
													2.756	3260.60960
													2.990	3260.61050
													2.940	3260.61140
													3.005	3260.61229
													2.938	3260.61319
													2.730	3260.61409
													2.451	3260.61498
													1.873	3260.61588
													2.288	3260.61678
													2.908	3260.61767

EDXRF													Hyperspectral Imagery	
Mg	Al	Si	S	K	Ca	Ti	Fe	K/Al	Ti/Al	Si bio	S/Fe	Depth	TOC	Depth
%	%	%	%	%	%	%	%			%		m	%	m
													3.035	3260.61857
													3.005	3260.61947
													2.987	3260.62037

EDXRF												Hyperspectral Imagery		
Mg	Al	Si	S	K	Ca	Ti	Fe	K/Al	Ti/Al	Si bio	S/Fe	Depth	TOC	Depth
%	%	%	%	%	%	%	%			%		m	%	m
													4.626	3262.60485
													4.713	3262.60561
													5.031	3262.60637
													4.871	3262.60713
													5.030	3262.60788
													5.019	3262.60864
													4.192	3262.60940
													4.489	3262.61016
													4.705	3262.61092
													4.217	3262.61168
													4.451	3262.61244
													4.319	3262.61319
													3.892	3262.61395
													3.829	3262.61471
													3.960	3262.61547
													3.612	3262.61623
													3.331	3262.61699
													3.012	3262.61775
													2.824	3262.61851
													2.921	3262.61926
													2.891	3262.62002
													2.939	3262.62078
													3.051	3262.62154
													2.878	3262.62230
													2.740	3262.62306
													2.616	3262.62382
													2.711	3262.62457
													2.764	3262.62533
													2.766	3262.62609
													2.734	3262.62685
													3.062	3262.62761
													3.273	3262.62837
													3.167	3262.62913
													3.335	3262.62989
													3.796	3262.63064
													4.028	3262.63140
													4.084	3262.63216
													4.287	3262.63292
													4.604	3262.63368
													4.678	3262.63444
													4.688	3262.63520
													4.685	3262.63596
													4.355	3262.63671
													4.219	3262.63747
													3.916	3262.63823
													4.051	3262.63899
													4.225	3262.63975
													3.550	3262.64051
													3.634	3262.64127
													3.901	3262.64202
													3.447	3262.64278
													3.088	3262.64354
													2.538	3262.64430

EDXRF												Hyperspectral Imagery		
Mg %	Al %	Si %	S %	K %	Ca %	Ti %	Fe %	K/Al	Ti/Al	Si bio %	S/Fe	Depth m	TOC %	Depth m
0.289	2.173	34.911	1.478	0.874	4.427	0.067	1.080	0.402	0.031	28.174	1.369	3263.62760	2.455	3263.58926
0.228	2.162	35.123	1.521	0.870	4.244	0.071	1.106	0.402	0.033	28.421	1.376	3263.62920	2.613	3263.59023
0.268	2.145	35.336	1.538	0.884	4.017	0.054	1.123	0.412	0.025	28.685	1.369	3263.63005	2.263	3263.59119
													2.419	3263.59216
													2.438	3263.59313
													2.442	3263.59410
													2.382	3263.59507
													2.327	3263.59603
													2.352	3263.59700
													2.237	3263.59797
													2.270	3263.59894
													2.316	3263.59991
													2.499	3263.60087
													2.356	3263.60184
													2.376	3263.60281
													2.274	3263.60378
													2.218	3263.60475
													2.407	3263.60571
													2.352	3263.60668
													2.278	3263.60765
													2.080	3263.60862
													2.053	3263.60959
													1.956	3263.61055
													1.991	3263.61152
													2.013	3263.61249
													2.061	3263.61346
													2.107	3263.61442
													2.019	3263.61539
													2.190	3263.61636
													2.460	3263.61733
													2.403	3263.61830
													2.399	3263.61926
													2.019	3263.62023
													1.829	3263.62120
													2.072	3263.62217
													2.367	3263.62314
													2.453	3263.62410
													2.689	3263.62507
													2.541	3263.62604
													2.582	3263.62701
													2.598	3263.62798
													2.762	3263.62894
													2.796	3263.62991
													2.804	3263.63088

EDXRF												Hyperspectral Imagery		
Mg	Al	Si	S	K	Ca	Ti	Fe	K/Al	Ti/Al	Si bio	S/Fe	Depth	TOC	Depth
%	%	%	%	%	%	%	%			%		m	%	m
													4.239	3264.31806
													4.315	3264.31878
													4.347	3264.31950
													4.371	3264.32022
													4.381	3264.32094
													4.310	3264.32166
													4.169	3264.32238
													4.030	3264.32310
													3.982	3264.32382
													4.058	3264.32455
													4.203	3264.32527
													4.288	3264.32599
													4.330	3264.32671
													4.366	3264.32743
													4.423	3264.32815
													4.465	3264.32887
													4.456	3264.32959
													4.371	3264.33031
													4.234	3264.33103
													4.145	3264.33176
													4.162	3264.33248
													4.223	3264.33320
													4.248	3264.33392
													4.234	3264.33464
													4.235	3264.33536
													4.288	3264.33608
													4.380	3264.33680
													4.478	3264.33752
													4.561	3264.33825
													4.583	3264.33897
													4.514	3264.33969
													4.404	3264.34041
													4.302	3264.34113
													4.180	3264.34185
													4.034	3264.34257
													3.938	3264.34329
													3.923	3264.34401
													3.964	3264.34474
													3.994	3264.34546
													3.931	3264.34618
													3.767	3264.34690
													3.463	3264.34762
													3.004	3264.34834
													2.345	3264.34906
													1.681	3264.34978
													1.584	3264.35050
													2.052	3264.35122
													2.385	3264.35195
													3.759	3264.35267
													3.768	3264.35339
													3.752	3264.35411
													3.698	3264.35483
													3.609	3264.35555

EDXRF												Hyperspectral Imagery		
Mg	Al	Si	S	K	Ca	Ti	Fe	K/Al	Ti/Al	Si bio	S/Fe	Depth	TOC	Depth
%	%	%	%	%	%	%	%			%		m	%	m
													2.465	3265.29428
													2.510	3265.29501
													2.562	3265.29575
													2.578	3265.29649
													2.563	3265.29722
													2.526	3265.29796
													2.483	3265.29870
													2.439	3265.29943
													2.423	3265.30017
													2.419	3265.30091
													2.441	3265.30164
													2.490	3265.30238
													2.542	3265.30312
													2.575	3265.30385
													2.598	3265.30459
													2.597	3265.30533
													2.562	3265.30606
													2.519	3265.30680
													2.443	3265.30754
													2.254	3265.30827
													1.909	3265.30901
													1.079	3265.30975
													0.824	3265.31048
													1.252	3265.31095
													1.847	3265.31142
													2.227	3265.31188
													2.499	3265.31235
													2.609	3265.31282
													2.602	3265.31328
													2.533	3265.31375
													2.449	3265.31421
													2.365	3265.31468
													2.270	3265.31515
													2.173	3265.31561
													2.137	3265.31608
													2.221	3265.31655
													2.391	3265.31701
													2.604	3265.31748
													2.736	3265.31795
													2.784	3265.31841
													2.780	3265.31888
													2.743	3265.31935
													2.679	3265.31981
													2.607	3265.32028
													2.527	3265.32074
													2.461	3265.32121
													2.403	3265.32168
													2.357	3265.32214
													2.296	3265.32261
													2.211	3265.32308
													2.113	3265.32354
													1.962	3265.32401
													1.809	3265.32448
													1.655	3265.32494
													1.529	3265.32541
													1.475	3265.32588
													0.978	3265.32634
													0.916	3265.32681
													0.819	3265.32728
													0.766	3265.32774
													0.750	3265.32821
													0.782	3265.32867
													0.855	3265.32914

EDXRF													Hyperspectral Imagery	
Mg	Al	Si	S	K	Ca	Ti	Fe	K/Al	Ti/Al	Si bio	S/Fe	Depth	TOC	Depth
%	%	%	%	%	%	%	%			%		m	%	m
													0.947	3265.32961
													1.027	3265.33007
													1.082	3265.33054
													1.114	3265.33101
													1.129	3265.33147
													1.137	3265.33194
													1.151	3265.33241
													1.183	3265.33287
													1.251	3265.33334
													1.324	3265.33381

EDXRF													Hyperspectral Imagery	
Mg	Al	Si	S	K	Ca	Ti	Fe	K/Al	Ti/Al	Si bio	S/Fe	Depth	TOC	Depth
%	%	%	%	%	%	%	%			%		m	%	m
													2.639	3265.94846
													2.615	3265.94918
													2.578	3265.94990
													2.523	3265.95061
													2.450	3265.95133
													2.375	3265.95205
													2.312	3265.95277
													2.280	3265.95348
													2.275	3265.95420
													2.317	3265.95492
													2.401	3265.95564
													2.486	3265.95635
													2.546	3265.95707
													2.589	3265.95779
													2.634	3265.95851
													2.657	3265.95923
													2.603	3265.95994
													2.467	3265.96066
													2.316	3265.96138
													2.126	3265.96210
													1.987	3265.96281
													1.893	3265.96353
													1.805	3265.96425
													1.689	3265.96497
													1.565	3265.96568
													1.501	3265.96640
													1.481	3265.96712
													1.479	3265.96784
													1.455	3265.96855
													1.390	3265.96927
													1.320	3265.96999
													1.265	3265.97071
													1.225	3265.97142
													1.195	3265.97214
													1.170	3265.97286
													1.149	3265.97358
													1.138	3265.97429
													1.133	3265.97501
													1.129	3265.97573
													1.126	3265.97645
													1.126	3265.97717
													1.138	3265.97788
													1.157	3265.97860
													1.176	3265.97932
													1.201	3265.98004
													1.208	3265.98075
													1.217	3265.98147
													1.246	3265.98219
													1.316	3265.98291
													1.371	3265.98362
													1.427	3265.98434
													1.481	3265.98506
													1.518	3265.98578
													1.544	3265.98649
													1.571	3265.98721
													1.621	3265.98793
													1.743	3265.98865

EDXRF											Hyperspectral Imagery			
Mg %	Al %	Si %	S %	K %	Ca %	Ti %	Fe %	K/Al	Ti/Al	Si bio %	S/Fe	Depth m	TOC %	Depth m
1.578	2.223	24.563	1.641	0.870	11.687	0.123	1.472	0.391	0.056	17.670	1.115	3267.01199	0.973	3266.98899
1.521	2.151	24.264	1.558	0.785	12.341	0.102	1.437	0.365	0.047	17.596	1.084	3267.01350	1.016	3266.99012
													0.971	3266.99125
													0.960	3266.99238
													1.009	3266.99352
													1.052	3266.99465
													1.099	3266.99578
													1.150	3266.99691
													1.198	3266.99804
													1.232	3266.99917
													1.235	3267.00030
													1.211	3267.00143
													1.154	3267.00256
													1.075	3267.00369
													0.989	3267.00483
													0.938	3267.00596
													0.925	3267.00709
													0.944	3267.00822
													0.983	3267.00935
													1.031	3267.01048
													1.065	3267.01161
													1.086	3267.01274
													1.119	3267.01387
													1.161	3267.01500

EDXRF												Hyperspectral Imagery		
Mg %	Al %	Si %	S %	K %	Ca %	Ti %	Fe %	K/Al	Ti/Al	Si bio %	S/Fe	Depth m	TOC %	Depth m
													1.499	3267.96249
													1.621	3267.96319
													1.706	3267.96389
													1.734	3267.96458
													1.735	3267.96528
													1.736	3267.96598
													1.754	3267.96668
													1.789	3267.96737
													1.807	3267.96807
													1.802	3267.96877
													1.770	3267.96946
													1.723	3267.97016
													1.677	3267.97086
													1.646	3267.97156
													1.642	3267.97225
													1.666	3267.97295
													1.709	3267.97365
													1.755	3267.97434
													1.792	3267.97504
													1.825	3267.97574
													1.868	3267.97643
													1.930	3267.97713
													1.986	3267.97783
													2.024	3267.97853
													2.057	3267.97922
													2.087	3267.97992

EDXRF												Hyperspectral Imagery		
Mg	Al	Si	S	K	Ca	Ti	Fe	K/Al	Ti/Al	Si bio	S/Fe	Depth	TOC	Depth
%	%	%	%	%	%	%	%			%		m	%	m
													1.205	3269.19867
													1.181	3269.19942
													1.161	3269.20018
													1.118	3269.20093
													1.016	3269.20168
													0.868	3269.20243
													0.736	3269.20318
													0.705	3269.20393
													0.797	3269.20468
													1.035	3269.20543
													1.279	3269.20618
													1.446	3269.20693
													1.555	3269.20769
													1.618	3269.20844
													1.633	3269.20919
													1.601	3269.20994
													1.568	3269.21069
													1.562	3269.21144
													1.581	3269.21219
													1.610	3269.21294
													1.644	3269.21369
													1.682	3269.21444
													1.722	3269.21520
													1.761	3269.21595
													1.778	3269.21670
													1.762	3269.21745
													1.738	3269.21820
													1.736	3269.21895
													1.761	3269.21970
													1.785	3269.22045
													1.783	3269.22120
													1.760	3269.22195
													1.721	3269.22271
													1.673	3269.22346
													1.629	3269.22421
													1.608	3269.22496
													1.613	3269.22571
													1.634	3269.22646

EDXRF													Hyperspectral Imagery	
Mg %	Al %	Si %	S %	K %	Ca %	Ti %	Fe %	K/Al	Ti/Al	Si bio %	S/Fe	Depth m	TOC %	Depth m
0.420	2.526	30.772	1.325	1.063	5.524	0.097	1.347	0.421	0.038	22.941	0.983	3269.75082	1.350	3269.70951
0.615	2.601	30.037	1.456	1.031	5.980	0.101	1.364	0.397	0.039	21.974	1.068	3269.75244	1.369	3269.71044
0.484	2.611	29.629	1.523	1.108	6.137	0.114	1.418	0.424	0.043	21.533	1.074	3269.75381	1.393	3269.71137
													1.416	3269.71231
													1.420	3269.71324
													1.411	3269.71417
													1.416	3269.71510
													1.443	3269.71604
													1.478	3269.71697
													1.491	3269.71790
													1.487	3269.71883
													1.471	3269.71977
													1.442	3269.72070
													1.430	3269.72163
													1.446	3269.72257
													1.483	3269.72350
													1.511	3269.72443
													1.518	3269.72536
													1.502	3269.72630
													1.474	3269.72723
													1.444	3269.72816
													1.415	3269.72909
													1.380	3269.73003
													1.355	3269.73096
													1.358	3269.73189
													1.405	3269.73283
													1.488	3269.73376
													1.559	3269.73469
													1.586	3269.73562
													1.586	3269.73656
													1.597	3269.73749
													1.636	3269.73842
													1.698	3269.73935
													1.760	3269.74029
													1.804	3269.74122
													1.825	3269.74215
													1.833	3269.74309
													1.832	3269.74402
													1.830	3269.74495
													1.830	3269.74588
													1.832	3269.74682
													1.845	3269.74775
													1.879	3269.74868
													1.934	3269.74961
													1.990	3269.75055
													2.008	3269.75148
													1.980	3269.75241
													1.928	3269.75335

EDXRF												Hyperspectral Imagery		
Mg %	Al %	Si %	S %	K %	Ca %	Ti %	Fe %	K/Al	Ti/Al	Si bio %	S/Fe	Depth m	TOC %	Depth m
													1.450	3270.72516
													1.441	3270.72589
													1.421	3270.72661
													1.395	3270.72734
													1.378	3270.72806
													1.381	3270.72879
													1.393	3270.72952
													1.410	3270.73024
													1.417	3270.73097
													1.429	3270.73170
													1.446	3270.73242
													1.456	3270.73315
													1.452	3270.73388
													1.436	3270.73460
													1.405	3270.73533
													1.381	3270.73606
													1.370	3270.73678
													1.356	3270.73751
													1.361	3270.73824
													1.381	3270.73896
													1.399	3270.73969
													1.411	3270.74042
													1.430	3270.74114
													1.424	3270.74187
													1.427	3270.74259
													1.443	3270.74332
													1.447	3270.74405
													1.423	3270.74477

Slab 3271.61 m

EDXRF													Hyperspectral Imagery		
Mg %	Al %	Si %	S %	K %	Ca %	Ti %	Fe %	K/Al	Ti/Al	Si bio %	S/Fe	Depth m	TOC %	Depth m	
0.871	3.535	23.627	1.780	1.410	10.401	0.183	1.968	0.399	0.052	12.667	0.905	3271.61000	0.906	3271.60961	
0.919	3.463	23.593	1.816	1.405	10.424	0.183	1.967	0.406	0.053	12.857	0.923	3271.61162	0.885	3271.61010	
0.731	3.767	23.213	2.377	1.568	9.453	0.217	2.426	0.416	0.058	11.536	0.980	3271.61324	0.898	3271.61059	
0.709	4.369	23.634	2.747	1.829	7.671	0.260	2.643	0.419	0.060	10.091	1.039	3271.61486	0.892	3271.61108	
0.596	3.435	19.106	1.687	1.260	14.806	0.200	1.989	0.367	0.058	8.459	0.848	3271.61648	0.885	3271.61157	
0.753	4.186	21.868	1.977	1.642	10.756	0.234	2.218	0.392	0.056	8.893	0.892	3271.61810	0.896	3271.61206	
0.718	4.511	23.088	2.347	1.875	8.622	0.256	2.473	0.416	0.057	9.104	0.949	3271.61972	0.928	3271.61255	
0.922	4.555	23.894	2.126	1.810	8.147	0.247	2.317	0.397	0.054	9.775	0.917	3271.62134	0.962	3271.61304	
1.005	3.450	21.821	1.812	1.367	11.829	0.204	2.109	0.396	0.059	11.127	0.859	3271.62296	0.989	3271.61353	
1.379	2.687	22.169	1.475	1.068	13.078	0.165	1.611	0.398	0.062	13.839	0.916	3271.62458	1.016	3271.61403	
2.949	2.080	18.341	1.093	0.691	16.633	0.105	1.152	0.332	0.051	11.893	0.948	3271.62620	1.033	3271.61452	
4.340	1.919	17.063	0.993	0.569	16.817	0.079	1.100	0.297	0.041	11.113	0.903	3271.62782	1.031	3271.61501	
3.666	2.079	19.478	1.158	0.677	14.913	0.101	1.260	0.325	0.048	13.032	0.919	3271.62944	1.015	3271.61550	
3.144	2.112	19.189	1.359	0.704	14.852	0.088	1.459	0.334	0.042	12.641	0.932	3271.63106	0.987	3271.61599	
3.208	1.737	16.098	1.165	0.513	18.287	0.092	1.364	0.296	0.053	10.714	0.854	3271.63268	0.963	3271.61648	
3.521	1.897	17.017	0.960	0.574	17.411	0.083	1.169	0.303	0.044	11.137	0.821	3271.63430	0.955	3271.61697	
2.943	2.387	22.352	1.306	0.830	12.172	0.135	1.372	0.348	0.057	14.951	0.952	3271.63592	0.947	3271.61746	
2.334	2.382	22.925	1.319	0.830	12.309	0.118	1.351	0.348	0.049	15.541	0.977	3271.63754	0.937	3271.61795	
2.260	2.260	22.720	1.787	0.839	11.604	0.096	1.735	0.371	0.043	15.714	1.030	3271.63916	0.929	3271.61844	
2.112	2.392	22.588	1.494	0.802	12.619	0.122	1.463	0.335	0.051	15.172	1.021	3271.64078	0.922	3271.61893	
1.959	2.546	23.066	1.227	0.932	12.353	0.148	1.342	0.366	0.058	15.172	0.914	3271.64240	0.916	3271.61943	
2.268	2.447	23.418	1.213	0.951	11.834	0.131	1.285	0.388	0.053	15.833	0.944	3271.64402	0.913	3271.61992	
2.354	2.535	22.977	1.138	0.904	12.366	0.118	1.242	0.357	0.046	15.118	0.916	3271.64564	0.926	3271.62041	
2.767	2.375	22.616	1.111	0.829	12.507	0.113	1.164	0.349	0.048	15.254	0.954	3271.64726	0.950	3271.62090	
2.788	2.408	22.470	1.062	0.834	12.589	0.105	1.181	0.346	0.044	15.006	0.899	3271.64888	0.965	3271.62139	
2.193	2.462	22.916	1.829	0.885	11.367	0.126	1.760	0.359	0.051	15.283	1.039	3271.65050	0.972	3271.62188	
2.297	2.407	22.914	2.086	0.885	10.809	0.113	1.985	0.368	0.047	15.452	1.051	3271.65212	0.967	3271.62237	
2.375	2.368	21.800	1.193	0.829	13.454	0.135	1.246	0.350	0.057	14.458	0.958	3271.65374	0.948	3271.62286	
2.470	2.423	22.914	1.549	0.838	11.450	0.096	1.617	0.346	0.040	15.402	0.957	3271.65536	0.922	3271.62335	
3.112	2.462	22.778	1.249	0.852	11.868	0.105	1.267	0.346	0.043	15.147	0.985	3271.65698	0.902	3271.62384	
3.095	2.472	23.089	1.143	0.880	11.424	0.122	1.272	0.356	0.049	15.425	0.899	3271.65860	0.887	3271.62433	
2.799	2.411	22.944	1.199	0.866	12.035	0.135	1.228	0.359	0.056	15.468	0.976	3271.66022	0.869	3271.62483	
2.842	2.604	24.134	1.186	0.931	10.771	0.135	1.211	0.358	0.052	16.061	0.979	3271.66184	0.844	3271.62532	
2.512	2.565	23.558	1.288	0.912	11.476	0.126	1.284	0.356	0.049	15.606	1.003	3271.66346	0.820	3271.62581	
2.330	2.267	21.898	1.153	0.828	13.551	0.113	1.254	0.365	0.050	14.868	0.919	3271.66508	0.808	3271.62630	
2.716	2.339	22.111	1.275	0.796	12.764	0.135	1.297	0.340	0.058	14.860	0.983	3271.66670	0.814	3271.62679	
													0.838	3271.62728	
													0.864	3271.62777	
													0.877	3271.62826	
													0.879	3271.62875	
													0.878	3271.62924	
													0.835	3271.62973	
													0.823	3271.63023	
													0.803	3271.63072	
													0.786	3271.63121	
													0.789	3271.63170	
													0.785	3271.63219	
													0.778	3271.63268	
													0.768	3271.63317	
													0.767	3271.63366	
													0.776	3271.63415	
													0.792	3271.63464	
													0.810	3271.63513	
													0.828	3271.63563	
													0.842	3271.63612	
													0.856	3271.63661	
													0.863	3271.63710	
													0.859	3271.63759	
													0.853	3271.63808	
													0.847	3271.63857	
													0.841	3271.63906	

EDXRF												Hyperspectral Imagery		
Mg %	Al %	Si %	S %	K %	Ca %	Ti %	Fe %	K/Al	Ti/Al	Si bio %	S/Fe	Depth m	TOC %	Depth m
													0.834	3271.63955
													0.830	3271.64004
													0.828	3271.64053
													0.831	3271.64103
													0.831	3271.64152
													0.826	3271.64201
													0.811	3271.64250
													0.797	3271.64299
													0.797	3271.64348
													0.810	3271.64397
													0.824	3271.64446
													0.821	3271.64495
													0.802	3271.64544
													0.817	3271.64594
													0.786	3271.64643
													0.787	3271.64692
													0.794	3271.64741
													0.805	3271.64790
													0.814	3271.64839
													0.817	3271.64888
													0.812	3271.64937
													0.821	3271.64986
													0.829	3271.65035
													0.843	3271.65084
													0.856	3271.65134
													0.862	3271.65183
													0.860	3271.65232
													0.854	3271.65281
													0.849	3271.65330
													0.837	3271.65379
													0.806	3271.65428
													0.778	3271.65477
													0.743	3271.65526
													0.723	3271.65575
													0.717	3271.65624
													0.720	3271.65674
													0.725	3271.65723
													0.728	3271.65772
													0.731	3271.65821
													0.732	3271.65870
													0.731	3271.65919
													0.730	3271.65968
													0.734	3271.66017
													0.741	3271.66066
													0.739	3271.66115
													0.722	3271.66164
													0.684	3271.66214
													0.645	3271.66263
													0.618	3271.66312
													0.597	3271.66361
													0.577	3271.66410
													0.559	3271.66459
													0.551	3271.66508
													0.553	3271.66557
													0.559	3271.66606
													0.567	3271.66655
													0.576	3271.66704

EDXRF												Hyperspectral Imagery		
Mg %	Al %	Si %	S %	K %	Ca %	Ti %	Fe %	K/Al	Ti/Al	Si bio %	S/Fe	Depth m	TOC %	Depth m
													1.490	3272.81556
													1.423	3272.81631
													1.372	3272.81705
													1.348	3272.81779
													1.339	3272.81854
													1.322	3272.81928
													1.300	3272.82002
													1.237	3272.82077
													1.151	3272.82151
													1.164	3272.82226
													1.181	3272.82300
													1.162	3272.82374
													1.145	3272.82449
													1.130	3272.82523
													1.115	3272.82597
													1.103	3272.82672
													1.089	3272.82746
													1.077	3272.82821
													1.052	3272.82895
													1.016	3272.82969
													0.965	3272.83044
													0.921	3272.83118
													0.901	3272.83192
													0.895	3272.83267
													0.888	3272.83341
													0.878	3272.83416
													0.872	3272.83490
													0.882	3272.83564
													0.899	3272.83639
													0.916	3272.83713
													0.926	3272.83787
													0.936	3272.83862
													0.949	3272.83936
													0.958	3272.84011
													0.961	3272.84085
													0.953	3272.84159
													0.921	3272.84234
													0.877	3272.84308
													0.873	3272.84382
													0.887	3272.84457
													0.915	3272.84531
													0.936	3272.84606
													0.940	3272.84680
													0.929	3272.84754
													0.900	3272.84829
													0.887	3272.84903
													0.885	3272.84977
													0.891	3272.85052
													0.887	3272.85126
													0.885	3272.85201
													0.879	3272.85275
													0.873	3272.85349
													0.921	3272.85424
													0.912	3272.85498

EDXRF												Hyperspectral Imagery		
Mg	Al	Si	S	K	Ca	Ti	Fe	K/Al	Ti/Al	Si bio	S/Fe	Depth	TOC	Depth
%	%	%	%	%	%	%	%			%		m	%	m
													2.112	3273.94110
													2.159	3273.94161
													2.186	3273.94211
													2.191	3273.94262
													2.136	3273.94312
													1.988	3273.94363
													1.762	3273.94413
													1.490	3273.94463
													1.256	3273.94514
													1.211	3273.94564
													1.441	3273.94615
													1.693	3273.94665
													2.026	3273.94716
													2.263	3273.94766
													2.449	3273.94817
													2.605	3273.94867
													2.685	3273.94918
													2.881	3273.94968
													2.874	3273.95019
													2.869	3273.95069
													2.856	3273.95120
													2.831	3273.95170
													2.796	3273.95221
													2.753	3273.95271
													2.705	3273.95322
													2.639	3273.95372
													2.537	3273.95423
													2.388	3273.95473
													2.243	3273.95524
													2.062	3273.95574
													2.112	3273.95625
													2.246	3273.95675
													2.306	3273.95726
													2.367	3273.95776
													2.443	3273.95827
													2.522	3273.95877
													2.574	3273.95928
													2.598	3273.95978
													2.578	3273.96029
													2.567	3273.96079
													2.555	3273.96130
													2.703	3273.96180
													2.844	3273.96231
													2.859	3273.96281
													2.831	3273.96332
													2.814	3273.96382
													2.813	3273.96433
													2.817	3273.96483
													2.793	3273.96533
													2.673	3273.96584
													2.460	3273.96634
													2.276	3273.96685
													2.327	3273.96735
													2.547	3273.96786
													2.754	3273.96836
													2.875	3273.96887
													2.919	3273.96937
													2.947	3273.96988
													2.980	3273.97038
													2.998	3273.97089
													2.995	3273.97139

EDXRF												Hyperspectral Imagery		
Mg	Al	Si	S	K	Ca	Ti	Fe	K/Al	Ti/Al	Si bio	S/Fe	Depth	TOC	Depth
%	%	%	%	%	%	%	%			%		m	%	m
													2.984	3273.97190
													2.958	3273.97240
													2.902	3273.97291
													2.829	3273.97341
													2.769	3273.97392
													2.752	3273.97442
													2.785	3273.97493
													2.853	3273.97543
													2.906	3273.97594
													2.899	3273.97644
													2.816	3273.97695
													2.695	3273.97745
													2.597	3273.97796
													2.542	3273.97846
													2.543	3273.97897
													2.588	3273.97947

EDXRF													Hyperspectral Imagery	
Mg %	Al %	Si %	S %	K %	Ca %	Ti %	Fe %	K/Al	Ti/Al	Si bio %	S/Fe	Depth m	TOC %	Depth m
0.552	4.081	27.497	2.591	1.701	5.271	0.254	2.344	0.417	0.062	14.846	1.105	3274.88784	1.461	3274.84467
0.552	4.755	24.728	2.901	2.011	6.133	0.336	2.793	0.423	0.071	9.989	1.038	3274.88928	1.444	3274.84540
0.281	1.912	16.550	1.063	0.569	20.920	0.106	1.197	0.298	0.055	10.623	0.888	3274.89080	1.448	3274.84613
													1.435	3274.84687
													1.437	3274.84760
													1.440	3274.84833
													1.431	3274.84906
													1.402	3274.84980
													1.375	3274.85053
													1.350	3274.85126
													1.235	3274.85200
													1.206	3274.85273
													1.151	3274.85346
													1.083	3274.85420
													1.007	3274.85493
													0.937	3274.85566
													0.898	3274.85640
													0.932	3274.85713
													0.917	3274.85786
													0.695	3274.85859
													0.667	3274.85933
													0.856	3274.86006
													0.785	3274.86079
													0.821	3274.86153
													0.845	3274.86226
													0.872	3274.86299
													0.897	3274.86373
													0.928	3274.86446
													0.974	3274.86519
													1.033	3274.86593
													1.070	3274.86666
													1.115	3274.86739
													1.138	3274.86812
													1.144	3274.86886
													1.142	3274.86959
													1.134	3274.87032
													1.128	3274.87106
													1.117	3274.87179
													1.128	3274.87252
													1.137	3274.87326
													1.154	3274.87399
													1.196	3274.87472
													1.184	3274.87546
													1.193	3274.87619
													1.233	3274.87692
													1.225	3274.87766
													1.246	3274.87839
													1.293	3274.87912
													1.308	3274.87985
													1.354	3274.88059
													1.349	3274.88132
													1.337	3274.88205
													1.330	3274.88279
													1.328	3274.88352
													1.303	3274.88425
													1.292	3274.88499
													1.266	3274.88572
													1.257	3274.88645
													1.218	3274.88719
													1.168	3274.88792

EDXRF													Hyperspectral Imagery	
Mg %	Al %	Si %	S %	K %	Ca %	Ti %	Fe %	K/Al	Ti/Al	Si bio %	S/Fe	Depth m	TOC %	Depth m
0.383	3.083	27.330	1.859	1.355	7.051	0.156	2.499	0.439	0.050	17.773	0.744	3275.84445	0.819	3275.79912
0.387	3.190	27.886	1.907	1.341	6.531	0.139	2.415	0.420	0.044	17.997	0.790	3275.84597	0.829	3275.79987
0.392	2.959	26.770	1.820	1.196	7.907	0.130	2.343	0.404	0.044	17.598	0.777	3275.84737	0.829	3275.80063
													0.840	3275.80138
													0.827	3275.80213
													0.817	3275.80288
													0.799	3275.80364
													0.787	3275.80439
													0.793	3275.80514
													0.814	3275.80589
													0.840	3275.80665
													0.869	3275.80740
													0.904	3275.80815
													0.935	3275.80890
													0.949	3275.80966
													0.957	3275.81041
													0.980	3275.81116
													1.020	3275.81191
													1.047	3275.81266
													1.052	3275.81342
													1.046	3275.81417
													1.043	3275.81492
													1.046	3275.81567
													1.056	3275.81643
													1.078	3275.81718
													1.102	3275.81793
													1.128	3275.81868
													1.159	3275.81944
													1.190	3275.82019
													1.220	3275.82094
													1.248	3275.82169
													1.269	3275.82244
													1.276	3275.82320
													1.271	3275.82395
													1.258	3275.82470
													1.243	3275.82545
													1.222	3275.82621
													1.197	3275.82696
													1.184	3275.82771
													1.174	3275.82846
													1.166	3275.82922
													1.158	3275.82997
													1.159	3275.83072
													1.170	3275.83147
													1.214	3275.83222
													1.299	3275.83298
													1.364	3275.83373
													1.381	3275.83448
													1.367	3275.83523
													1.355	3275.83599
													1.354	3275.83674
													1.350	3275.83749
													1.326	3275.83824
													1.293	3275.83900
													1.282	3275.83975
													1.310	3275.84050
													1.369	3275.84125
													1.429	3275.84200
													1.470	3275.84276
													1.492	3275.84351
													1.507	3275.84426

EDXRF												Hyperspectral Imagery		
Mg	Al	Si	S	K	Ca	Ti	Fe	K/Al	Ti/Al	Si bio	S/Fe	Depth	TOC	Depth
%	%	%	%	%	%	%	%			%		m	%	m
													1.518	3275.84501
													1.523	3275.84577
													1.522	3275.84652
													1.510	3275.84727
													1.484	3275.84802
													1.444	3275.84878
													1.394	3275.84953
													1.333	3275.85028
													1.261	3275.85103

APPENDIX C: WHOLE-ROCK GEOCHEMICAL DATA

Appendix C presents the whole-rock geochemical dataset of all core slabs. This dataset is composed of major oxides and some trace elements by ICP-MS analysis, and organic carbon content by LECO combustion.

Depth m	SiO ₂ %	Al ₂ O ₃ %	Fe ₂ O ₃ %	MgO %	CaO %	K ₂ O %	TiO ₂ %	S %	TOC %	Ba PPM	Mo PPM
3083.1	77.47	8.26	2.7	0.73	0.34	1.54	0.35	1.1	3.4	3370	34.9
3084.1	70.34	11.93	3.18	1.02	0.64	2.35	0.5	1.44	2.82	4430	33.5
3085.17	72.43	8.82	2.77	1.41	1.81	1.73	0.44	1.19	3.73	3708	42.5
3087.39	87.36	4.25	1.78	0.45	0.26	0.71	0.16	0.75	1.94	2531	24
3087.8	81.17	6.16	2.73	0.4	0.28	1.14	0.26	1.39	6.72	3517	49.5
3088.41	86.41	4.24	1.79	0.45	0.53	0.74	0.2	0.86	1.99	2515	22.1
3089.74	83.9	5.87	2.03	0.4	0.22	1.05	0.24	1.06	4.18	3143	29.8
3090.6	79.97	7.05	3.42	0.45	0.32	1.28	0.27	1.54	2.17	3657	35.7
3091.35	79.79	5.5	3.83	0.66	0.86	1.01	0.24	1.21	2.12	2901	37.6
3092.7	18.69	4.81	5.07	13.28	21.26	0.93	0.25	0.58	1.09	3030	4.4
3093.75	85.97	4.04	2.67	0.49	0.64	0.73	0.16	0.53	1.98	2453	30.8
3094.9	84.24	5.02	2.86	0.52	0.6	0.91	0.23	0.75	1.7	2841	27.5
3096	84.75	4.89	2.56	0.54	0.68	0.87	0.2	0.83	1.8	2651	27.9
3097.13	82.04	5.78	2.55	0.62	0.83	1.03	0.23	0.99	3.04	2897	35.6
3097.95	86.35	4.19	2.42	0.46	0.57	0.72	0.18	0.78	2.15	2467	23.7
3098.7	86.54	3.88	2.56	0.35	0.38	0.66	0.17	0.66	2.54	2483	23.3
3099.77	83.77	4.92	2.73	0.64	0.83	0.91	0.18	0.91	1.85	2587	23.1
3101.08	84.53	5.04	3	0.4	0.37	0.88	0.17	0.79	2.06	2814	26
3101.93	87.91	4.02	1.53	0.42	0.47	0.68	0.14	0.52	1.92	2538	17.7
3103.03	88.21	3.44	1.82	0.47	0.61	0.6	0.12	0.45	2.01	2353	18.4
3104.05	85.35	4.36	2.99	0.43	0.52	0.72	0.18	0.87	1.48	3979	27
3105.05	67.75	6.67	11.02	0.39	0.3	1.19	0.27	8.26	2.47	5503	43.4
3105.95	86.2	4.18	1.93	0.46	0.61	0.68	0.13	0.69	2.15	3667	26.6
3106.95	85.79	4.18	2.35	0.27	0.24	0.72	0.15	0.84	2.08	3287	47.6
3107.15	87.73	3.49	2.28	0.46	0.63	0.54	0.12	0.66	1.8	3202	18
3108.2	81.55	4.68	3.48	0.58	0.79	0.77	0.2	1.97	1.92	5558	42.8
3109.52	80.53	5.56	2.45	0.37	0.34	0.98	0.25	1.22	3.76	7111	49.4
3110.27	77.24	6.9	3.42	0.4	0.24	1.25	0.29	1.89	8	6823	62.7
3111.35	82.34	4.18	2.59	0.5	0.62	0.71	0.17	1.05	8.03	4875	58.4
3112.29	42.66	5.6	3.2	8.73	12.78	0.91	0.3	1.37	5.3	6757	19.1
3113.14	77.86	6.31	4.43	0.32	0.19	1.09	0.27	2.89	6.4	7001	36.8
3113.42	73.42	8.61	4.05	0.65	0.51	1.61	0.4	2.69	3.86	7110	45.4
3114.42	71.63	10.71	3.21	0.73	0.33	2.08	0.46	1.71	4.16	7038	45.2
3115.75	85.6	3.26	1.99	0.6	1	0.54	0.13	0.54	2.55	4449	25.1
3116.78	26.59	6.77	4.5	11.49	18.16	1.31	0.28	0.98	1.06	4703	5.2
3117.77	73.18	11.3	2.8	0.75	0.3	2.24	0.47	1.41	2.07	7630	19.6
3120	73.24	8.29	3.84	0.46	0.2	1.5	0.38	2.36	5.21	12771	44.5
3121.25	78.63	7.17	2.61	0.35	0.09	1.29	0.27	0.96	4.35	7126	48.9
3122.23	73.72	9.8	3.11	0.61	0.15	1.96	0.41	1.75	4.45	5410	20.9
3122.88	54.14	9.81	3.76	2.37	10.66	2	0.45	1.63	2.43	3678	7.9
3122.95	70.51	12.34	3.73	0.86	0.26	2.55	0.55	1.82	2.76	5303	17.5
3124.15	42.65	9.82	4.35	7.21	11.22	2.04	0.43	1.14	3.01	4303	8.1
3124.92	55.22	14.54	4.14	3.32	4.45	3.09	0.62	1.47	1.98	5315	10.7
3125.8	75.99	8.03	2.95	0.74	0.5	1.54	0.34	1.01	4	6764	48.5
3126.95	74.43	9.34	2.75	0.73	0.2	1.9	0.37	1.07	4.39	5262	48.7
3128.05	69.36	12.5	2.47	0.86	0.35	2.58	0.54	1.11	4.65	6247	41.5
3128.55	71.09	11.04	2.96	0.97	0.83	2.22	0.52	1.47	3.47	5510	22.9
3129.54	66.1	11.4	3.46	1.86	2.44	2.33	0.56	1.43	3.05	5089	20.8
3129.85	65.26	12.03	3.47	1.75	2.06	2.48	0.59	1.46	3.3	5381	24.9
3131.05	70.63	11.33	2.69	0.82	0.39	2.3	0.51	1.24	4.6	6593	37.4
3131.8	69.75	9.41	4.11	0.68	0.42	1.84	0.41	1.97	6.14	6988	23.5
3133.1	54.92	10.83	13.68	0.98	0.82	2.23	0.53	10.23	2.15	7889	30.4

Depth m	SiO ₂ %	Al ₂ O ₃ %	Fe ₂ O ₃ %	MgO %	CaO %	K ₂ O %	TiO ₂ %	S %	TOC %	Ba PPM	Mo PPM
3133.85	67.27	7.51	4.98	1.07	1.27	1.35	0.39	3.08	7.41	5214	11.5
3134.95	59.66	11.44	6.01	1.75	2.07	2.15	0.59	3.75	5.33	6112	12.6
3135.9	81.15	6.09	2.33	0.44	0.33	1.18	0.24	0.71	3.39	8426	29.6
3136.65	68.58	8.29	7.93	0.53	0.31	1.68	0.35	5.89	4.34	6872	37
3137.75	81.82	6.07	2.13	0.43	0.28	1.18	0.23	0.7	5.51	5618	29.9
3138.9	78.72	5.91	2.14	1.06	1.55	1.09	0.24	0.71	2.96	5904	30.8
3140	85.41	4.56	1.51	0.41	0.4	0.87	0.18	0.54	3.2	5112	28.2
3141	84.08	4.92	1.85	0.49	0.5	0.93	0.19	0.57	2.81	5726	29.7
3142	84.08	5.03	1.79	0.56	0.64	0.95	0.19	0.54	2.76	6124	24.8
3143.15	61.36	10.9	9.82	0.63	0.34	2.21	0.46	7.08	5.03	6634	59.9
3144	85.43	4.44	2.15	0.34	0.3	0.82	0.15	0.51	3.26	4656	30.8
3144.9	69.64	11.56	3.14	0.85	0.57	2.33	0.44	1.83	4.25	6565	48.8
3146.05	71.44	10.96	2.96	0.7	0.34	2.21	0.41	1.56	4.32	6384	52
3147.15	79.42	7.41	2.26	0.51	0.3	1.47	0.25	1.08	3.85	4932	34.9
3148.25	76.24	8.09	2.34	0.58	0.44	1.57	0.29	1.1	4.77	5190	58.7
3149.18	68.06	11.7	4.94	0.9	0.39	2.45	0.49	3.33	3.53	5498	23.1
3150.4	74.71	8.67	2.49	0.57	0.27	1.81	0.33	1.34	5.54	5218	61.8
3152.51	72.02	10.6	2.63	0.66	0.3	2.16	0.39	1.5	4.97	5126	47.4
3153.93	58.56	11.44	4.17	2.33	5.29	2.28	0.54	2.44	3.03	5560	23.5
3154.7	52.9	7.48	3.24	3.51	10.29	1.31	0.39	1.56	4.67	3896	10.2
3155.5	64.55	7.88	5.09	2	2.94	1.57	0.36	3.09	6.66	4441	14.3
3155.9	59.4	12.93	6.5	1.46	1.8	2.33	0.69	4.36	4.54	4140	6.9
3156.9	73.86	9.43	3.01	0.93	1.26	1.89	0.37	1.35	2.72	3947	22.3
3158	68.3	12.56	3.36	0.96	0.89	2.55	0.53	1.67	3.76	3935	32.9
3158.75	75.04	8.8	3.3	0.76	0.93	1.73	0.36	1.65	3.55	3476	25.2
3159.77	75.47	8.31	3.52	0.73	0.95	1.63	0.33	1.91	3.53	3532	27.9
3160.8	77.6	8.04	2.34	0.65	0.76	1.57	0.35	1	3.43	2952	38
3161.6	40.7	9.2	6.69	5.96	12.93	1.85	0.45	1.73	0.384	3736	2.2
3163	47.77	14.07	5.9	3.99	7.77	2.98	0.62	1.68	0.418	4320	7.2
3164	53.25	15.04	5.28	2.95	5.66	3.18	0.66	1.64	0.455	4192	4.8
3165	54.06	12.98	5.54	2.99	6.54	2.71	0.63	1.4	0.419	3889	4.5
3165.8	49.63	12.35	5.92	3.71	8.44	2.53	0.6	1.24	0.724	3617	3.1
3166.81	50.61	13.9	5	3.39	7.63	2.91	0.63	0.52	0.423	4030	2
3167.81	57.74	15.17	5.13	2.16	3.79	3.21	0.71	0.75	0.547	4201	4.3
3168.8	56.8	15.24	6.45	2.12	3.35	3.2	0.68	0.85	0.38	4940	1.8
3169.8	47.56	11.16	7.43	3.58	9.39	2.25	0.52	1.15	0.85	3798	6.3
3170.77	54.76	13.17	5.78	2.6	6.02	2.74	0.61	1.1	0.967	4211	7.3
3171.8	57.23	15.6	6.3	2.01	2.85	3.25	0.66	0.74	0.588	4338	4.8
3172.85	56.38	12.69	5.51	2.53	5.78	2.65	0.55	1.69	0.996	3986	8.3
3173.8	69.09	13.38	3	1.05	1.03	2.76	0.57	1.45	1.77	3875	17
3174.81	67.92	9.24	8.12	0.69	0.75	1.82	0.37	6.24	3	3025	28.3
3175.2	44.36	11.7	6.19	4.44	10.59	2.44	0.51	1.01	1.02	3878	5
3176.3	55.22	13.23	4.73	2.71	5.78	2.78	0.56	1.31	2.01	3865	11.8
3176.83	65.83	13.98	3.6	1.12	1.4	2.91	0.57	1.94	2.67	3793	18.5
3177.74	50.01	13.43	5.48	2.32	8.72	2.8	0.64	2.16	1.61	3582	10.4
3177.9	51.8	14.58	4.95	2.33	7.4	3.07	0.67	1.77	1.71	3964	9.9
3178.9	51.28	13.49	4.95	2.5	8.53	2.79	0.63	1.59	1.34	3762	5.1
3179.45	49.98	12.93	5.3	2.45	9.39	2.69	0.63	1.82	1.45	3851	6.4
3180.45	49.89	12.79	5.31	2.32	9.3	2.65	0.63	1.91	1.87	3561	7.4
3181.18	59.25	16.2	4.48	1.38	2.96	3.45	0.69	2.41	1.95	4289	11.5
3181.83	47.13	12.33	5.06	2.39	12.05	2.54	0.53	2.02	1.06	3992	1.6
3182.81	50.8	13.13	4.2	2.09	10.19	2.74	0.56	1.59	1.18	4438	1.7

Depth m	SiO ₂ %	Al ₂ O ₃ %	Fe ₂ O ₃ %	MgO %	CaO %	K ₂ O %	TiO ₂ %	S %	TOC %	Ba PPM	Mo PPM
3183.75	59.35	13.66	4.4	1.42	5.29	2.84	0.58	2.4	1.42	4068	8.5
3184.7	57.72	13.11	4.08	1.6	6.5	2.73	0.56	2	1.84	3944	12
3185.8	57.15	13.78	4.25	1.7	6.54	2.83	0.61	2.14	1.26	4346	5
3186.8	53.95	8.79	2.65	1.85	13.26	1.76	0.39	0.91	1.78	3225	3.6
3187.16	45.57	8.81	3.08	2.03	17.79	1.75	0.37	1.14	1.48	3336	1.9
3188.14	30.41	6.28	2.82	2.14	28.72	1.2	0.26	0.96	0.937	3376	1.2
3188.29	30.85	6.56	2.41	2.1	28.44	1.23	0.26	0.71	0.99	3038	1
3188.9	69.08	11.01	4.24	0.75	0.46	2.15	0.46	2.93	3.63	7988	32.6
3189.04	27.2	5.64	2.06	1.85	31.91	1.02	0.23	0.59	0.967	2793	0.8
3189.85	27.42	5.82	2.17	2	31.33	1.08	0.24	0.61	0.97	3144	1.2
3190.85	30.04	6.06	2.46	2.17	29.35	1.12	0.24	0.65	1.14	2966	1.2
3191.21	29.56	5.22	1.95	1.8	30.96	0.95	0.21	0.55	0.866	3660	1
3192.2	38.7	6.89	2.55	2.24	23	1.29	0.28	0.78	0.971	2969	2.8
3192.79	57.34	8.53	2.37	1.44	11.6	1.68	0.36	1.04	2.21	3033	5.8
3193.61	60.24	11.49	2.62	1.3	7.24	2.33	0.48	1.27	2.77	3445	7.8
3194	35.87	5.74	2.73	1.95	26.19	1.07	0.25	1.04	1.69	2566	3.5
3195	47.86	8.92	3.64	2.83	14.87	1.75	0.35	1.11	1.39	2904	4.5
3195.17	50.04	9.6	3.51	2.61	12.94	1.93	0.38	1.15	1.77	3033	3.9
3196.18	48.79	8.58	3.15	2.16	15.3	1.68	0.35	1.11	2.3	2838	5.8
3196.78	59.85	11.14	3.4	1.53	7.16	2.29	0.47	1.68	2.33	3425	11
3197.78	54.23	14.13	4.64	2.26	6.84	2.91	0.58	2.02	1.3	4301	5.5
3198.12	53.9	13.76	4.61	2.4	7.17	2.83	0.57	1.83	1.3	3953	5
3199.11	44.7	11.09	4.46	2.86	14.21	2.24	0.45	1.49	1.33	4819	4.8
3199.32	44.99	11.42	4.07	2.81	14.02	2.35	0.47	1.26	1.13	3616	2.6
3200.21	41.44	11.24	4.22	1.9	17.84	2.31	0.44	2.39	1.09	3979	1.4
3201.03	37.39	10.4	3.45	2.09	21.11	2.12	0.4	1.57	0.862	3501	1.2
3202.1	33.91	9.69	3.05	2.04	24.1	1.97	0.36	1.35	0.956	3495	1.1
3202.4	33.89	9.61	3.1	1.93	24.27	1.95	0.35	1.57	0.773	3425	0.6
3203.39	36.39	9.77	3.84	2.88	20.92	1.99	0.37	1.3	0.642	3336	1.1
3203.8	51.62	13.17	4.41	2.61	8.67	2.66	0.55	1.75	1.6	3867	8.5
3204.35	1.08	0.27	0.19	0.54	54.55	0.07	0.01	0.09	0.135	281	0.8
3204.8	63.87	11	3.18	1.27	5.6	2.24	0.48	1.77	2.66	3525	18.4
3205.21	63.03	12.16	3.47	1.43	5.04	2.43	0.52	1.88	2.13	3705	10.2
3205.24	8.47	0.24	0.18	1.41	49.28	0.06	0.01	0.1	0.282	240	1.2
3206.17	60.48	12.19	4.43	1.5	5.6	2.46	0.51	2.74	1.79	3856	9.1
3207.2	58.18	11.15	4.2	1.8	7.71	2.28	0.49	2.04	2.22	3455	8.6
3207.79	58.17	10.7	3.87	1.87	8.31	2.15	0.47	1.74	1.96	3421	9.3
3208.74	53.79	14.54	4.71	2.13	7.03	2.99	0.6	2.27	1.2	4440	1.9
3209.06	45.89	11.67	4.08	2.54	14.16	2.38	0.44	1.67	0.76	4083	2.7
3210.07	52.08	10.83	3.93	2.67	10.7	2.18	0.46	1.49	1.97	3632	5.6
3210.6	56.32	10.83	3.75	2.13	8.9	2.19	0.48	1.56	1.97	3491	7.4
3211.73	50.43	10.79	3.99	2.76	11.72	2.17	0.48	1.48	1.66	3928	3.8
3211.87	49.48	9.78	4.13	3.06	12.63	1.95	0.44	1.65	1.91	3816	4.7
3213.35	54.28	10.28	3.7	2.14	10.35	2.09	0.46	1.68	2.33	4052	8.3
3214.26	55.36	12.15	3.54	1.7	8.8	2.51	0.55	1.78	2.27	3906	7.5
3215.45	60.9	10.68	6.26	0.93	1.65	2.16	0.47	4.47	7.56	3555	49.3
3216.55	53.71	12.42	8.23	1.8	2.49	2.67	0.61	5.7	6.17	4385	63
3217.35	65.94	14.74	4.01	0.98	0.36	3.18	0.55	2.58	2.74	5355	36.9
3218.55	63.32	17.27	3.8	1.15	0.28	3.74	0.6	2.1	1.8	5416	23.1
3219.26	29.61	7	6.6	9.35	17.46	1.37	0.29	2.12	1.47	3630	11.1
3220.05	64.92	10.98	4.96	1.18	1.71	2.39	0.44	3.55	4.23	5428	65.1
3220.4	75.69	5.05	2.05	0.94	2.46	1.02	0.24	1.13	5.37	5711	98.3

Depth m	SiO ₂ %	Al ₂ O ₃ %	Fe ₂ O ₃ %	MgO %	CaO %	K ₂ O %	TiO ₂ %	S %	TOC %	Ba PPM	Mo PPM
3221.17	57.38	16.55	6.1	1.63	1.41	3.72	0.6	3.98	2.47	4842	26
3223.28	78.81	3.75	1.66	0.49	2.64	0.72	0.16	0.88	5.49	5444	96.3
3224.1	75.28	4.92	2.1	1.11	3.05	1	0.25	1.38	4.14	6064	75.2
3225	70.05	7.51	3.12	1.3	2.3	1.54	0.35	2.21	4.41	7857	149.3
3225.9	69.88	6.61	2.6	1.47	3.7	1.35	0.3	1.5	5.22	9330	88.2
3226.9	37.32	4.26	1.69	1.24	27.02	0.8	0.21	1.12	3.52	6054	93.9
3228.1	82.24	3.02	1.09	0.73	3.37	0.61	0.13	0.61	3.21	4487	41.4
3229	73.58	6.2	1.91	1.16	4.14	1.34	0.25	1.14	2.94	7569	46.6
3230.05	57.85	2.2	0.8	1.16	18.4	0.41	0.1	0.51	2.75	2788	25.8
3230.95	63.58	7.54	3	0.94	7.92	1.63	0.31	2.12	3.24	5039	54.5
3232	72.33	7.76	2.24	1.1	2.97	1.76	0.34	1.6	4.85	5808	66.9
3232.95	72.85	7.47	2.28	0.76	2.58	1.62	0.32	1.65	3.7	5405	95.2
3234	65.35	6.59	2.72	2.29	6.23	1.49	0.29	2.01	4.53	5544	62.2
3235.1	67.78	8.79	2.9	1.08	3.14	2	0.39	2.03	5.36	5729	99
3236.08	71.09	7.22	2.04	0.68	3.9	1.63	0.29	1.52	5.87	5826	76.2
3237.02	77.98	4.75	1.8	0.41	3.15	1.02	0.19	1.06	3.79	4967	56.9
3238.02	72.87	5.84	1.72	0.68	4.4	1.27	0.25	1.4	4.96	5735	78
3238.75	66.16	5.55	2.05	1.42	7.73	1.23	0.25	1.28	4.26	5468	59.1
3239.75	72.6	5.46	1.71	0.51	5	1.21	0.23	1.28	4.84	4434	58.3
3240.48	68.84	7.21	3.28	0.5	4.66	1.62	0.3	2.51	4.22	6260	47.6
3240.86	69.79	5.75	2.02	0.61	5.43	1.26	0.24	1.64	5.77	4690	73.6
3241.77	49.31	7.85	2.92	1.55	14.81	1.81	0.38	2.15	1.17	5626	60.6
3242.75	5.76	1.55	1.17	16.55	30.55	0.23	0.08	0.85	1.41	2004	6.1
3243.5	62.25	12.81	4.35	1.1	2.53	2.84	0.48	3.38	3.6	5778	65.1
3244.52	60.92	7.37	2.7	0.78	10.02	1.69	0.32	2.02	4.78	6622	66.6
3247.54	10.37	2.37	1.09	14.45	29.96	0.37	0.11	0.73	0.822	2974	7.2
3248.53	70.34	4.84	1.78	0.46	6.29	1.07	0.21	1.26	5.23	4886	49.9
3249.48	53.71	3.3	1.47	0.63	17.03	0.78	0.17	1.3	5.72	2728	130.3
3250.48	11.35	2.24	1.31	12.44	31.52	0.47	0.12	0.79	1.89	2595	10.4
3251.48	64.69	4.66	1.71	0.69	8.45	1.11	0.25	1.45	7.07	3172	124.2
3252.43	69.37	3.33	1.43	0.43	7.89	0.8	0.16	1.04	6.6	2565	78.6
3253.5	64.15	3.26	1.14	0.51	10.89	0.78	0.17	1.14	9.49	1928	75.9
3254.51	65.57	4.8	2.64	0.82	5.65	1.26	0.26	2.32	9.27	1919	177.5
3255.51	55.14	6.02	2.3	0.76	10.84	1.56	0.31	2.14	8.92	2166	134.9
3256.55	56.47	4.13	1.67	0.77	14.09	1.08	0.2	1.52	8.16	1884	132.6
3257.43	66.92	3.93	2	0.88	7.35	0.99	0.19	1.55	8.2	2015	170.8
3258.5	38.25	2.56	1.19	4.84	22.85	0.62	0.13	1.03	6.71	1036	43.6
3259.52	69.94	4.6	1.85	0.51	6.1	1.16	0.21	1.54	6.38	1678	83.7
3260.52	73.58	3.2	1.48	0.34	6.06	0.82	0.14	1.15	7.64	1273	102.7
3261.57	74.68	4.23	1.77	0.36	3.69	1.06	0.19	1.42	6.97	1306	85.6
3262.55	71.19	4.87	2.05	0.44	3.53	1.21	0.23	1.75	8.84	2224	107.4
3263.55	71.99	4.63	1.84	0.52	5.16	1.2	0.19	1.44	7.02	1220	73.8
3264.25	61.72	4.14	1.64	0.57	12.02	1.07	0.18	1.41	7.1	1062	104.8
3265.25	51.56	3.79	1.53	0.69	18.94	0.98	0.16	1.27	6.45	1057	97.3
3265.9	46.04	3.15	1.36	1.57	22.44	0.82	0.15	1.12	5.23	1058	64.9
3266.92	45.31	3.41	1.81	3.68	19.04	0.85	0.17	1.29	5.09	898	146.7
3267.92	69.22	4.27	2.1	0.55	7.01	1.12	0.2	1.5	7.44	1028	92.7
3269.15	66.58	5.62	2.27	0.65	7.29	1.43	0.25	1.81	5.75	1098	96.2
3269.65	59.85	4.81	1.85	1.85	12.45	1.22	0.21	1.37	4.43	1244	55
3270.66	63.84	5.32	2.12	0.62	8.91	1.38	0.25	1.68	5.67	1088	86.4
3271.61	45.52	4.19	1.8	4.45	17.52	1.08	0.2	1.45	5.87	1364	42.4
3272.77	59.53	6.15	2.42	1.41	10.48	1.59	0.28	1.98	5.12	1377	130.1

Depth m	SiO ₂ %	Al ₂ O ₃ %	Fe ₂ O ₃ %	MgO %	CaO %	K ₂ O %	TiO ₂ %	S %	TOC %	Ba PPM	Mo PPM
3273.9	72.59	5.13	2.09	0.54	4.51	1.26	0.24	1.61	6.7	972	89.7
3274.8	50.81	3.34	1.41	0.51	20.31	0.84	0.15	1.17	5.31	926	91.4
3275.75	54.76	7.54	2.85	0.87	11.79	2.03	0.34	2.31	6.29	1843	153.3
3276.75	9.17	2.16	0.94	1.13	46.41	0.56	0.11	0.77	3.07	1057	19.9
3278.47	11.89	2.89	1.11	0.93	44.8	0.81	0.15	0.87	1.89	1838	7
3279	10.14	2.22	0.88	0.84	46.8	0.62	0.12	0.68	1.65	1826	7.4
3280.02	8.63	2.23	0.92	2.52	45.99	0.56	0.12	0.67	1.65	710	1.1
3280.47	8.26	1.66	0.59	0.82	49.11	0.48	0.09	0.42	0.455	491	0.6
3281.38	3.89	0.92	0.54	0.81	52.34	0.23	0.05	0.43	0.15	585	1.6
3282.32	1.48	0.18	0.12	0.61	54.43	0.05	0.01	0.1	0.104	254	0.6
3283.34	1	0.35	0.21	0.65	54.42	0.08	0.02	0.19	0.447	404	0.9
3284.3	1.91	0.14	0.08	0.58	54.22	0.03	<0.01	0.08	0.2	325	0.7
3285.5	1.59	0.29	0.16	0.76	53.95	0.07	0.02	0.12	0.308	420	0.5
3286.38	2.37	0.38	0.15	1.76	52.48	0.09	0.02	0.11	0.317	209	0.5
3287.3	3.04	0.68	0.3	6.17	46.67	0.17	0.03	0.23	0.128	476	0.2
3288.28	3.14	0.23	0.19	0.59	53.22	0.06	0.02	0.14	0.206	840	1.2
3289.38	3.82	0.27	0.11	0.62	52.84	0.07	0.01	0.09	0.325	316	0.9
3289.65	2.27	0.3	0.16	0.58	53.64	0.08	0.01	0.15	0.141	1987	1
3290.65	0.94	0.25	0.12	12.22	40.74	0.05	0.01	0.09	0.239	459	0.4
3291.3	2.98	0.23	0.16	0.79	53.11	0.06	0.01	0.12	0.288	563	1
3292.35	2.85	0.16	0.06	0.61	53.69	0.04	<0.01	0.06	0.153	383	0.7
3293.35	5.65	0.71	0.3	0.95	51.22	0.19	0.04	0.22	0.29	395	1.5
3294.32	0.81	0.11	0.09	0.52	54.79	0.02	<0.01	0.05	0.104	820	0.6
3295.31	1.32	0.13	0.07	0.76	54.2	0.03	<0.01	0.06	0.169	785	0.6
3296.32	0.79	0.1	0.11	0.42	54.69	0.03	<0.01	0.16	0.243	4266	0.8
3297.31	0.84	0.09	0.07	0.56	54.61	0.02	<0.01	0.13	0.1	4279	0.6
3298.34	1.14	0.21	0.09	0.55	54.44	0.06	0.01	0.09	0.173	258	1.5
3299.37	2.11	0.09	0.1	0.48	48.47	0.03	<0.01	0.06	0.117	430	0.9
3300.37	1.67	0.18	0.09	0.41	54.39	0.05	<0.01	0.09	0.216	724	0.8
3301.38	0.88	0.11	0.09	0.37	54.95	0.03	<0.01	0.05	0.101	407	0.5
3302.33	0.76	0.06	0.11	4.04	50.72	0.01	<0.01	0.03	0.092	187	0.4
3303.34	0.71	0.09	0.05	7.18	47.17	0.01	<0.01	0.03	0.0953	209	0.4
3306.34	0.82	0.07	0.12	0.6	54.6	0.02	<0.01	0.06	0.116	550	0.6
3307.17	0.55	0.04	0.07	0.47	55.13	0.01	<0.01	0.03	0.121	224	0.4
3308.29	0.97	0.2	0.09	1.79	53.13	0.05	0.01	0.09	0.182	441	1.8
3309.32	0.86	0.12	0.08	1.3	53.82	0.04	<0.01	0.05	0.148	321	0.5
3310.31	1.32	0.16	0.13	0.83	54.1	0.04	0.01	0.08	0.134	251	0.6
3311.35	1.02	0.28	0.24	12.39	40.56	0.06	0.01	0.16	0.247	230	0.4
3312.34	0.54	0.05	0.1	0.56	54.85	<0.01	<0.01	0.04	0.166	351	0.4
3313.35	0.69	0.15	0.11	1.14	53.96	0.04	<0.01	0.09	0.176	244	1.5
3314.29	0.35	0.08	0.09	0.79	54.67	0.03	<0.01	0.04	0.0952	236	0.8
3315.34	0.7	0.05	0.12	2.24	52.79	0.01	<0.01	0.03	0.141	240	0.5
3316.35	0.59	0.09	0.1	4.38	50.09	0.02	<0.01	0.04	0.0886	113	0.5

**APPENDIX D: COMPLEMENTARY TABLES AND PLOTS BASED ON
GEOCHEMICAL ANALYSIS FOR CHAPTER 2**

Appendix D presents the analytical charts based on millimeter-resolution geochemical data and whole-slab geochemical data.

Table D.1. Si/Al background ratio tested for slab of 3128.05 m. Si/Al_{original} is 3.1. Si/Al₁₋₃ are the ratios varying randomly in the range from 3 to 4. Si/Al₄ is varying from 3 to 4 evenly.

Depth (m)	Si-Al _{original} %	Si-Al ₁ %	Si-Al ₂ %	Si-Al ₃ %	Si-Al ₄ %
3128.05	3.1	3.211792	3.913575	3.155013	3
3128.052	3.1	3.576542	3.961618	3.132878	3.0213
3128.054	3.1	3.409991	3.615151	3.602348	3.0426
3128.055	3.1	3.263725	3.793074	3.519177	3.0639
3128.057	3.1	3.791434	3.875582	3.683609	3.0852
3128.059	3.1	3.045831	3.033709	3.566284	3.1065
3128.061	3.1	3.134724	3.609477	3.462573	3.1278
3128.063	3.1	3.71581	3.094808	3.873895	3.1491
3128.065	3.1	3.574334	3.831639	3.137431	3.1704
3128.066	3.1	3.548903	3.616674	3.250768	3.1917
3128.068	3.1	3.11617	3.738089	3.681593	3.213
3128.07	3.1	3.896645	3.844355	3.597009	3.2343
3128.072	3.1	3.632801	3.810415	3.078745	3.2556
3128.074	3.1	3.139744	3.053934	3.413992	3.2769
3128.076	3.1	3.609029	3.513277	3.514397	3.2982
3128.077	3.1	3.473843	3.421645	3.117202	3.3195
3128.079	3.1	3.754554	3.638024	3.7646	3.3408
3128.081	3.1	3.041387	3.878203	3.987643	3.3621
3128.083	3.1	3.078374	3.577243	3.384792	3.3834
3128.085	3.1	3.786522	3.996173	3.852807	3.4047
3128.087	3.1	3.469522	3.874978	3.850875	3.426
3128.088	3.1	3.894418	3.779251	3.268906	3.4473
3128.09	3.1	3.628022	3.970054	3.174623	3.4686
3128.092	3.1	3.547311	3.316813	3.200209	3.4899
3128.094	3.1	3.561528	3.766819	3.591618	3.5112
3128.096	3.1	3.530153	3.992792	3.92322	3.5325
3128.098	3.1	3.050071	3.994012	3.675733	3.5538
3128.099	3.1	3.512177	3.156586	3.64799	3.5751
3128.101	3.1	3.887826	3.379228	3.233278	3.5964
3128.103	3.1	3.759618	3.20179	3.297366	3.6177
3128.105	3.1	3.616508	3.537964	3.261922	3.639
3128.107	3.1	3.481203	3.931901	3.945881	3.6603
3128.109	3.1	3.449666	3.525887	3.143166	3.6816
3128.111	3.1	3.433245	3.568507	3.475936	3.7029
3128.113	3.1	3.563413	3.366533	3.500688	3.7242
3128.115	3.1	3.853947	3.674821	3.842662	3.7455
3128.117	3.1	3.802694	3.614183	3.754108	3.7668
3128.119	3.1	3.387581	3.656213	3.570477	3.7881
3128.121	3.1	3.861062	3.884982	3.07952	3.8094
3128.123	3.1	3.761428	3.893342	3.299417	3.8307
3128.125	3.1	3.397629	3.32019	3.036813	3.852
3128.127	3.1	3.239389	3.560989	3.147752	3.8733
3128.129	3.1	3.395234	3.768036	3.706484	3.8946
3128.131	3.1	3.780015	3.634964	3.166319	3.9159
3128.133	3.1	3.013513	3.216878	3.308751	3.9372
3128.135	3.1	3.822631	3.375939	3.663909	3.9585
3128.137	3.1	3.870519	3.926283	3.250396	3.9798
3128.139	3.1	3.626646	3.707497	3.232644	4

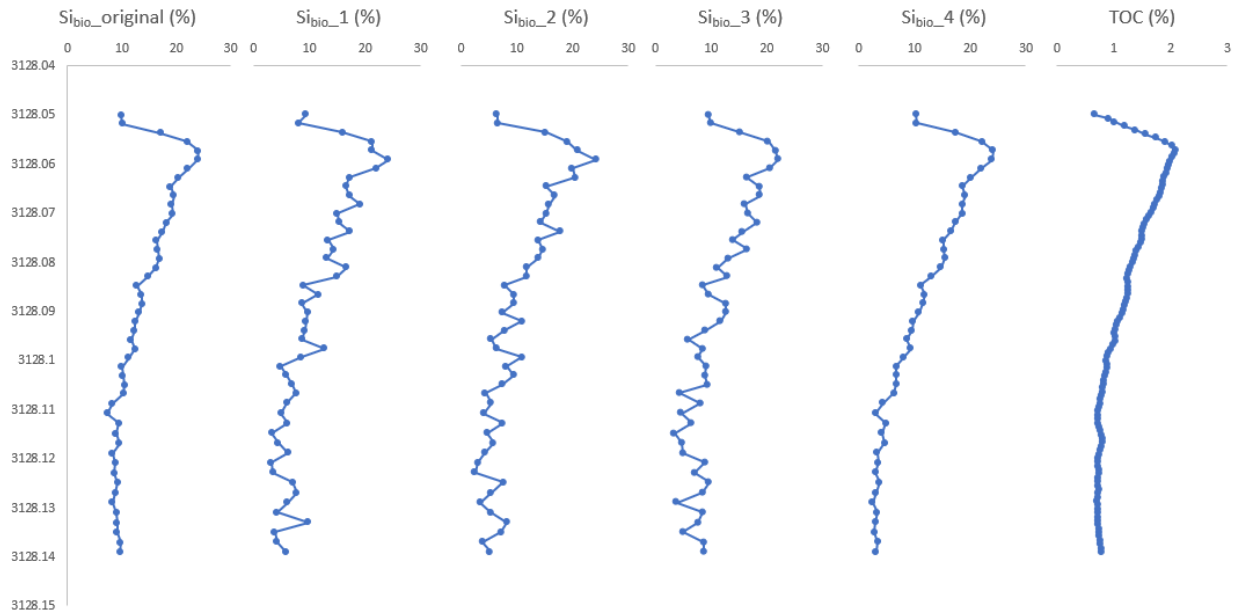


Figure D.1. Si_{bio} profiles calculated from Si/Al background ratios in Table D.1. and related measured TOC profile of the interval of 3128.05 m. All Si_{bio} profiles show similar trends with TOC profile.

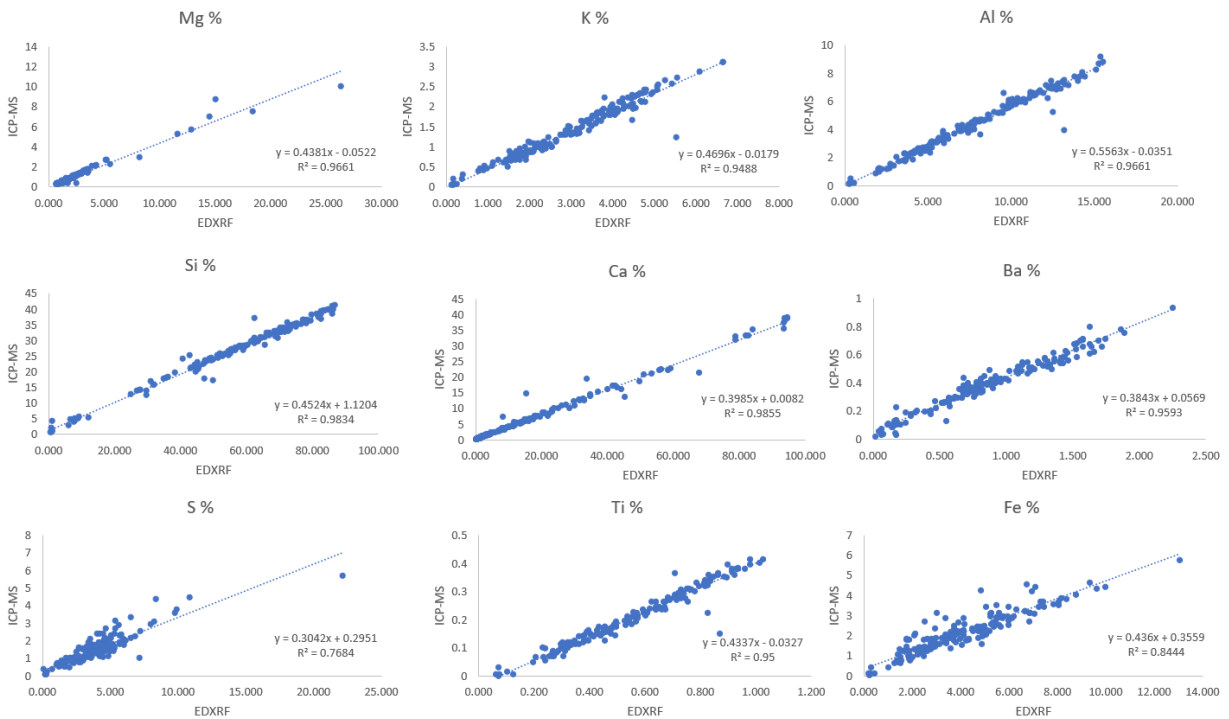


Figure D.2. Elemental proxies' calibration between ICP-MS and EDXRF data.

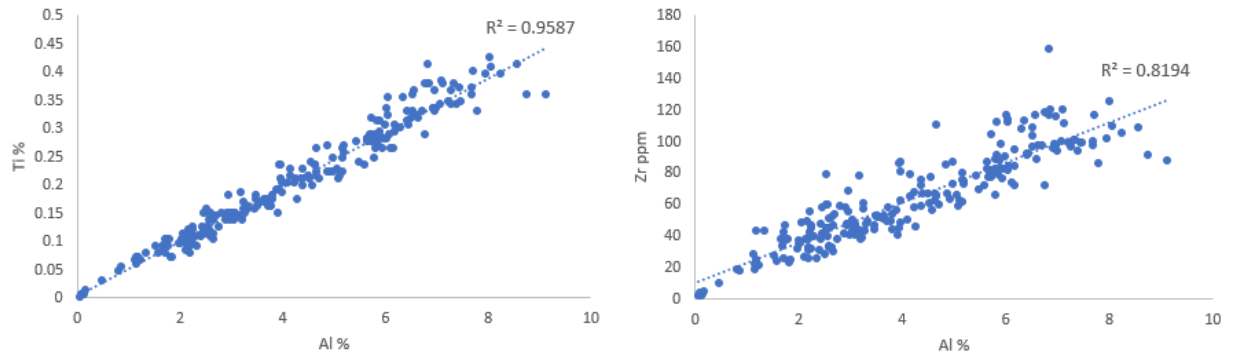


Figure D.3. Ti-Al and Zr-Al correlation based on ICP-MS data in the entire shale.

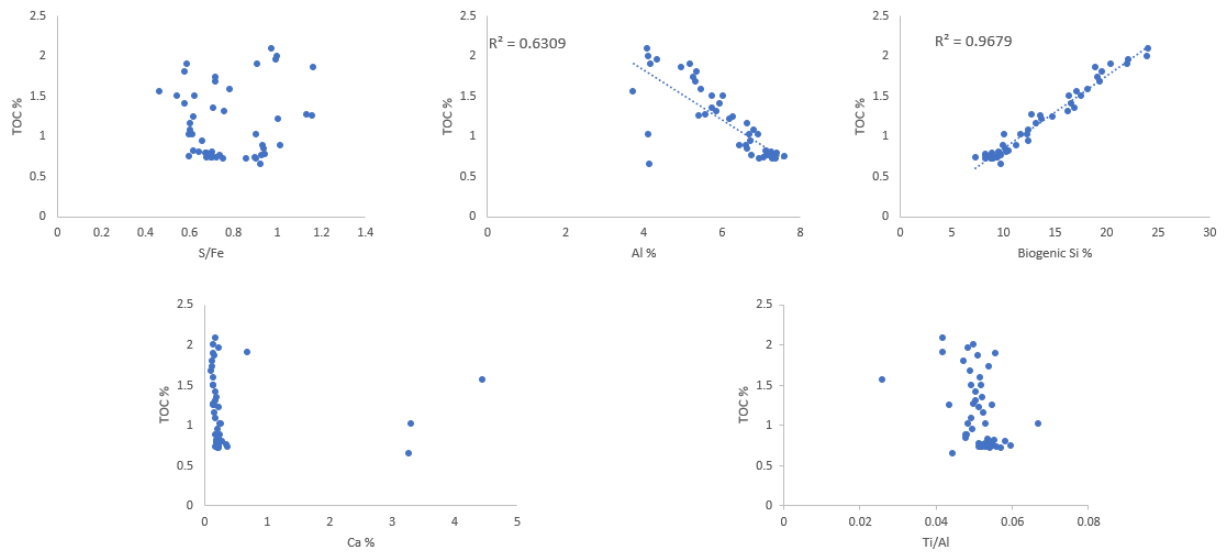


Figure D.4. TOC-proxies plots for the interval of 3128.05 m.

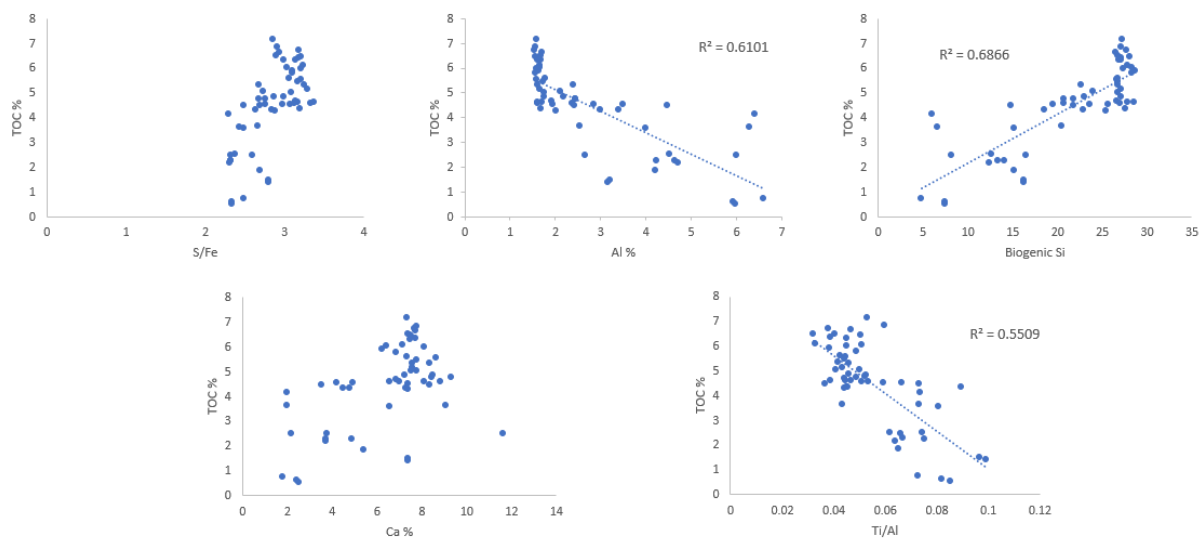


Figure D.5. TOC-proxies plots for the interval of 3251.48 m.

APPENDIX E: ORGANIC PETROGRAPHIC ANALYSIS

Appendix E comprises a report of organic petrographic analysis by USGS for the Horn River Group. Since the petrography of the samples is consistent with the petrography of all the North American shale gas plays, e.g., Woodford, Duvernay, Marcellus, Eagle Ford, Utica, etc., which are all marine rocks containing a Type II kerogen at low maturity, the presence of the solid bitumen network as residual evidence of the thermal conversion of original Type II kerogen.

E200205 Tattoo summary

Lab ID	Field ID	Ro	STD	n	Comments
E200205-001	Tattoo 3128.05'	2.76	0.127	20	Solid bitumen present, mostly in void-filling texture. Pyrite, abundant mineral content.
E200205-002	Tattoo 3146.05'	2.842	0.102	20	Solid bitumen present, mostly in void-filling texture. Pyrite, abundant mineral content.
E200205-003	Tattoo 3182.81'	3.22	0.219	20	Solid bitumen present, mostly in void-filling texture. Abundant pyrite, abundant mineral content.
E200205-004	Tattoo 3218.55'	3.35	0.297	20	Solid bitumen present, mostly in void-filling texture. Pyrite, abundant mineral content.
E200205-005	Tattoo 3251.48'	3.25	0.268	21	Solid bitumen present, mostly in void-filling texture. Abundant pyrite, abundant mineral content.

Figure E.1. Summary of five samples for organic petrography.

Sample : E200205_001_Tattoo_3128_05_shale_VR1

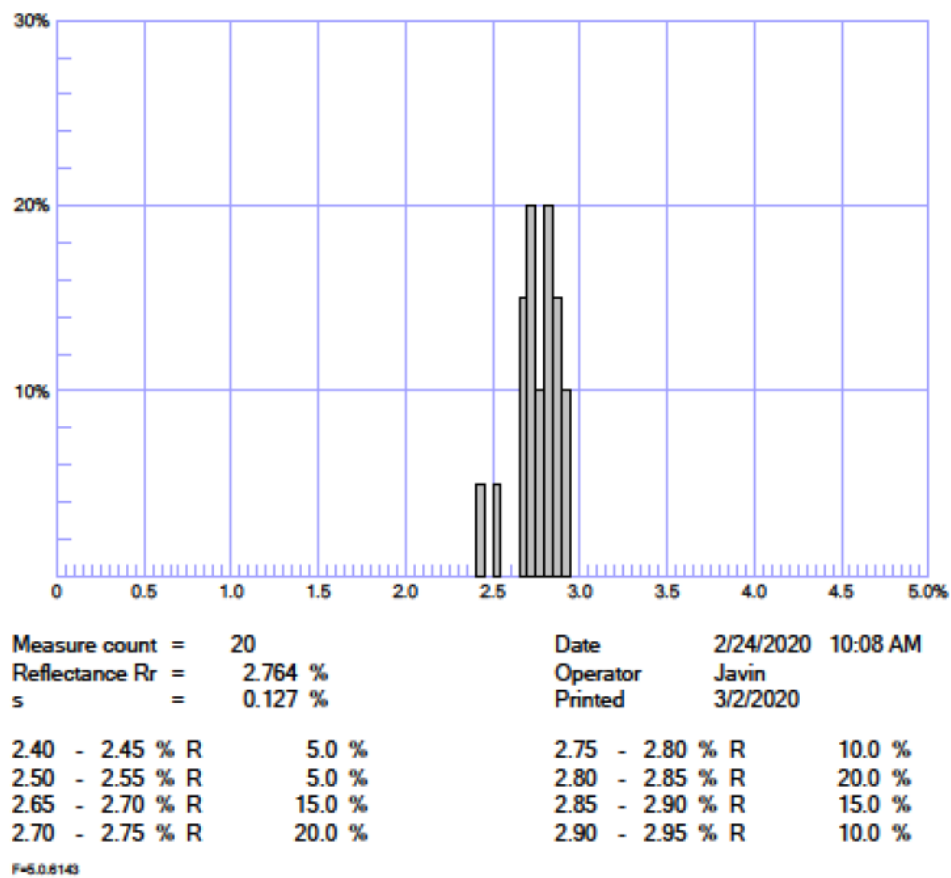


Figure E.2. Thermal maturity of 3128.05 m core slab.

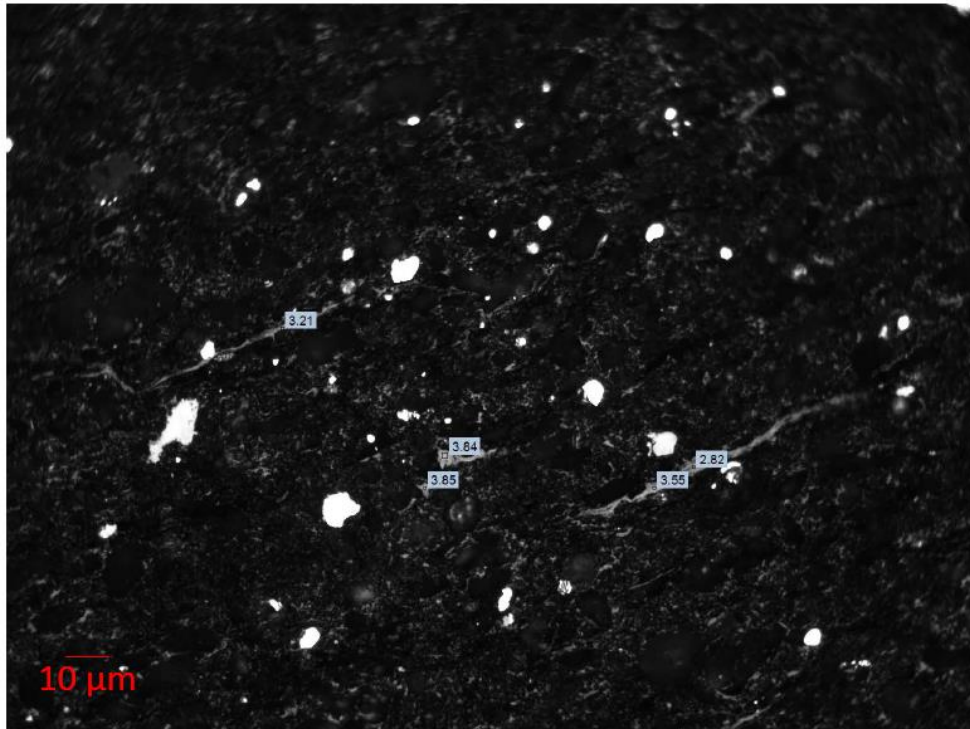


Figure E.3. Micrograph of thermal maturity analysis for organic matter of 3128.05 m core slab.

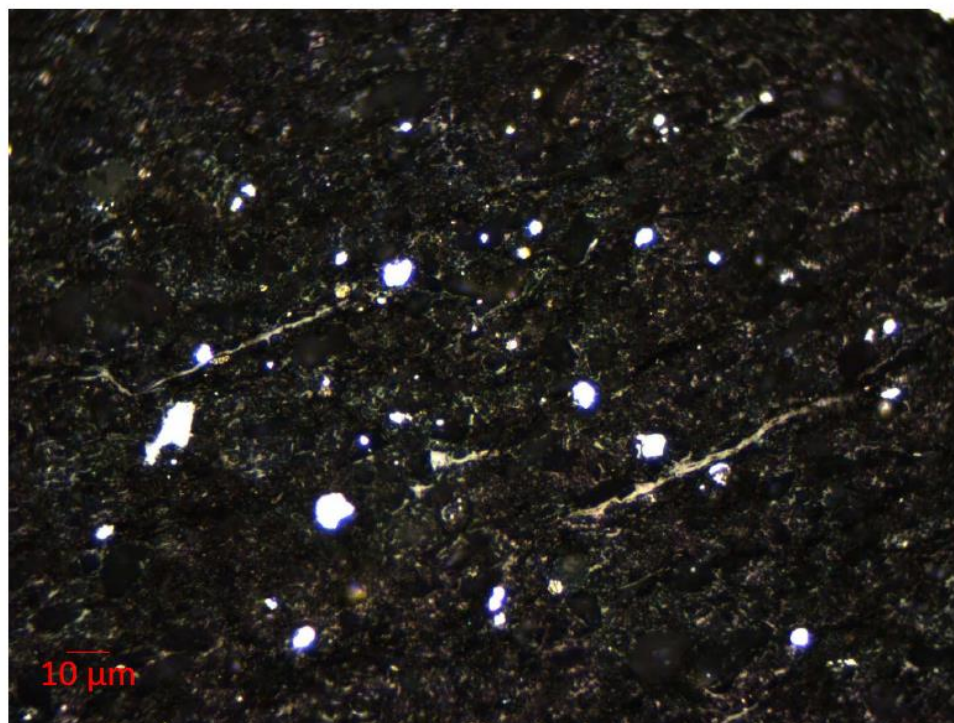


Figure E.4. Micrograph under reflected white light of Figure E.3.

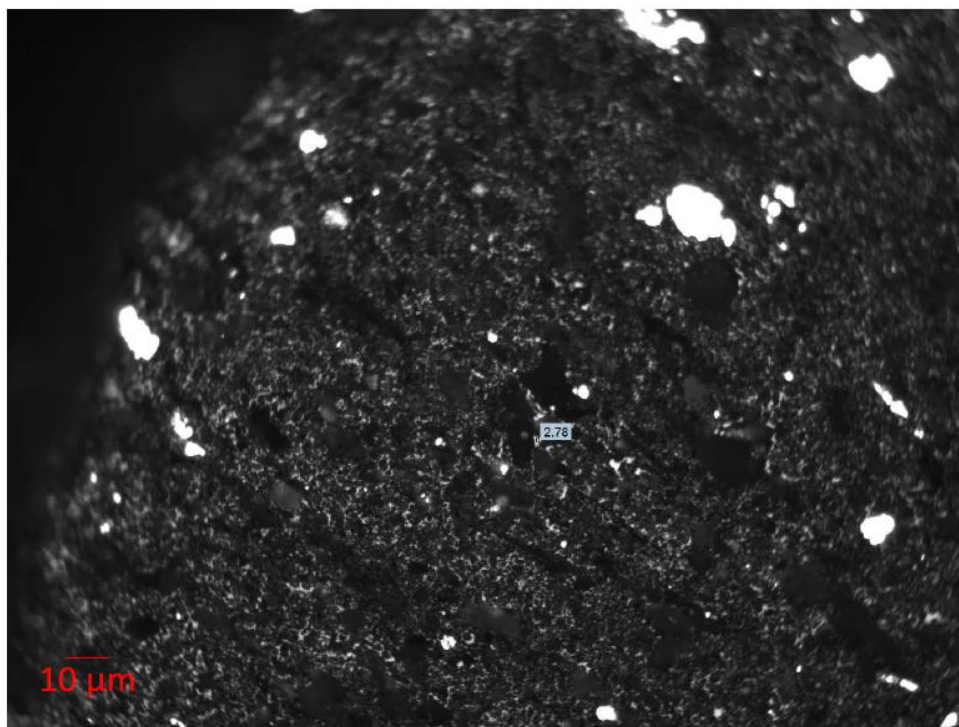


Figure E.5. Micrograph of thermal maturity analysis for organic matter of 3128.05 m core slab.

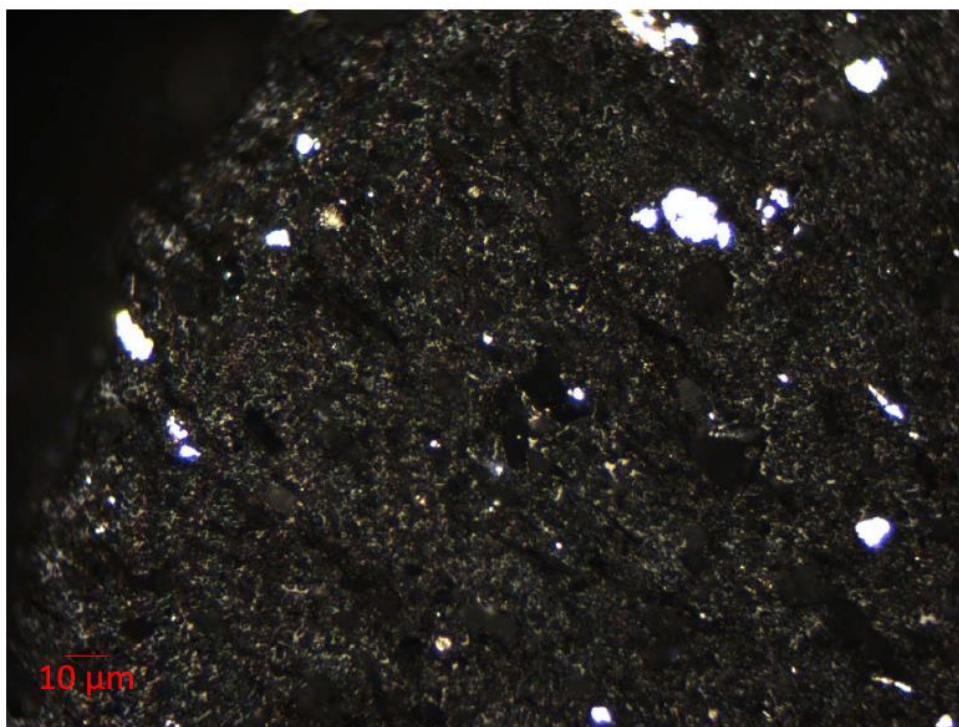


Figure E.6. Micrograph under reflected white light of Figure E.5.

Sample : E200205_002_Tattoo_3146_05_VR1

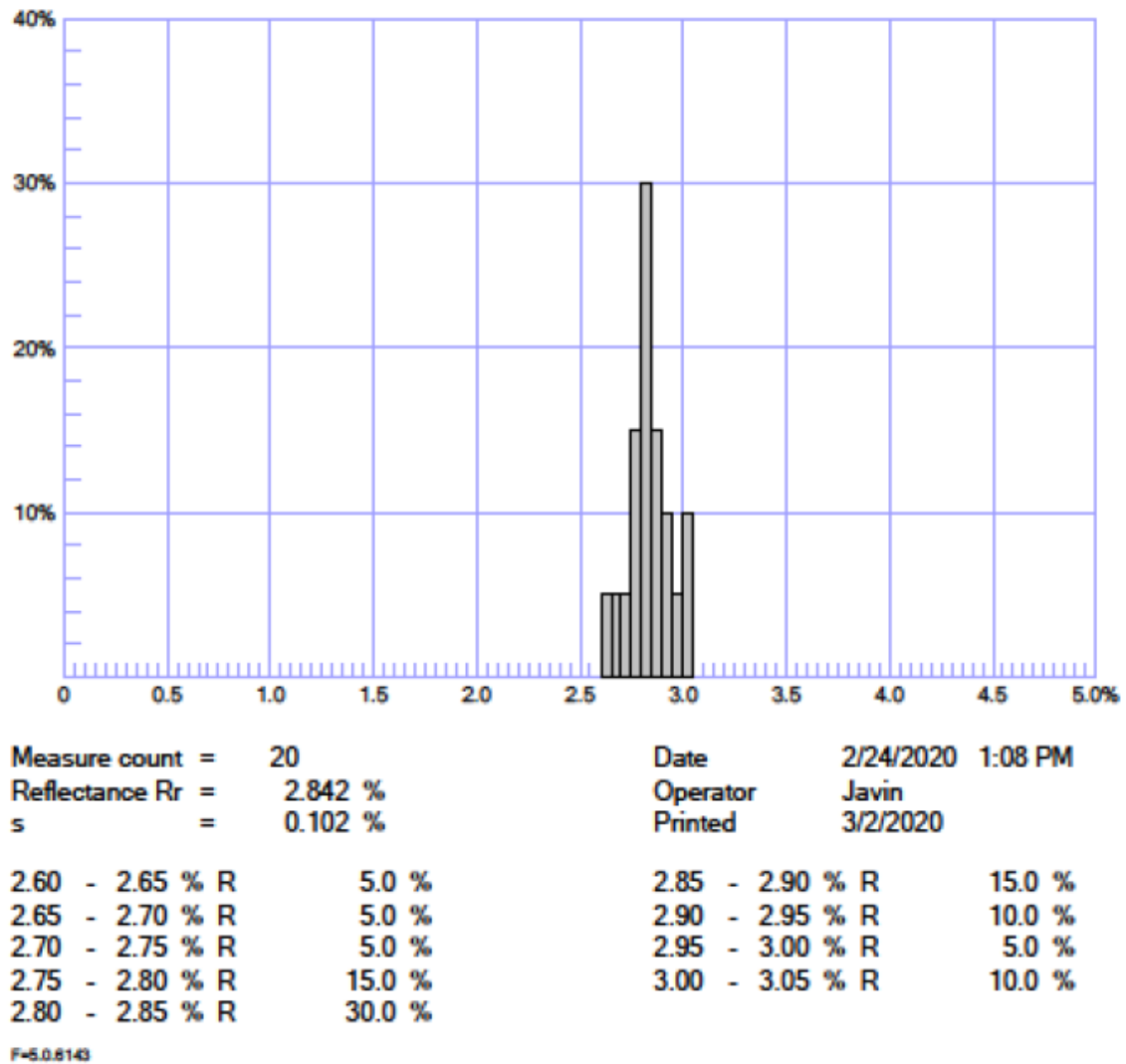


Figure E.7. Thermal maturity of 3146.05 m core slab.

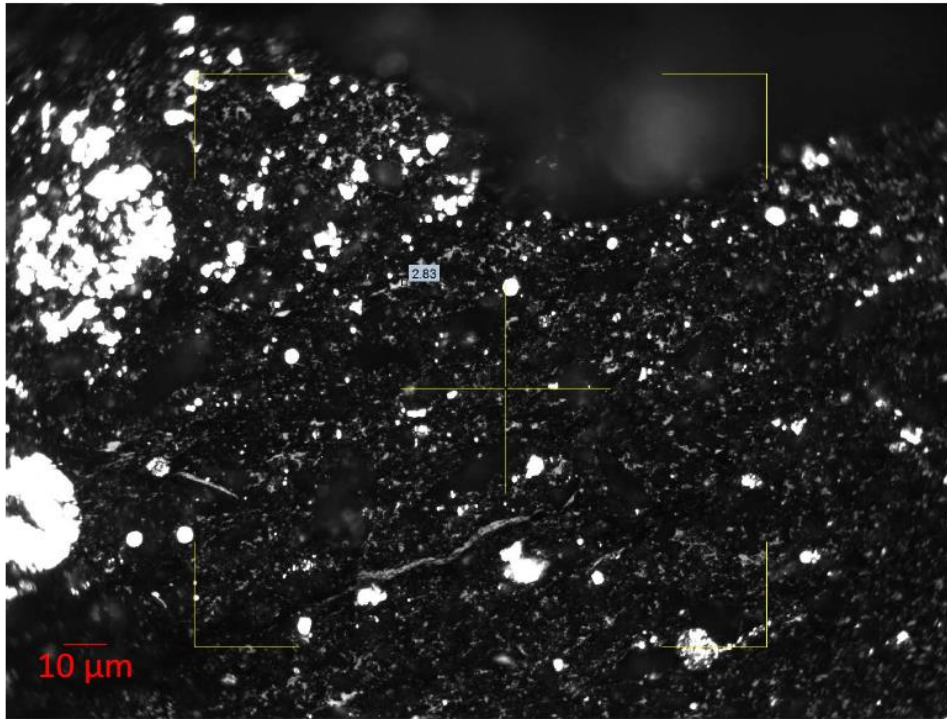


Figure E.8. Micrograph of thermal maturity analysis for organic matter of 3146.05 m core slab.

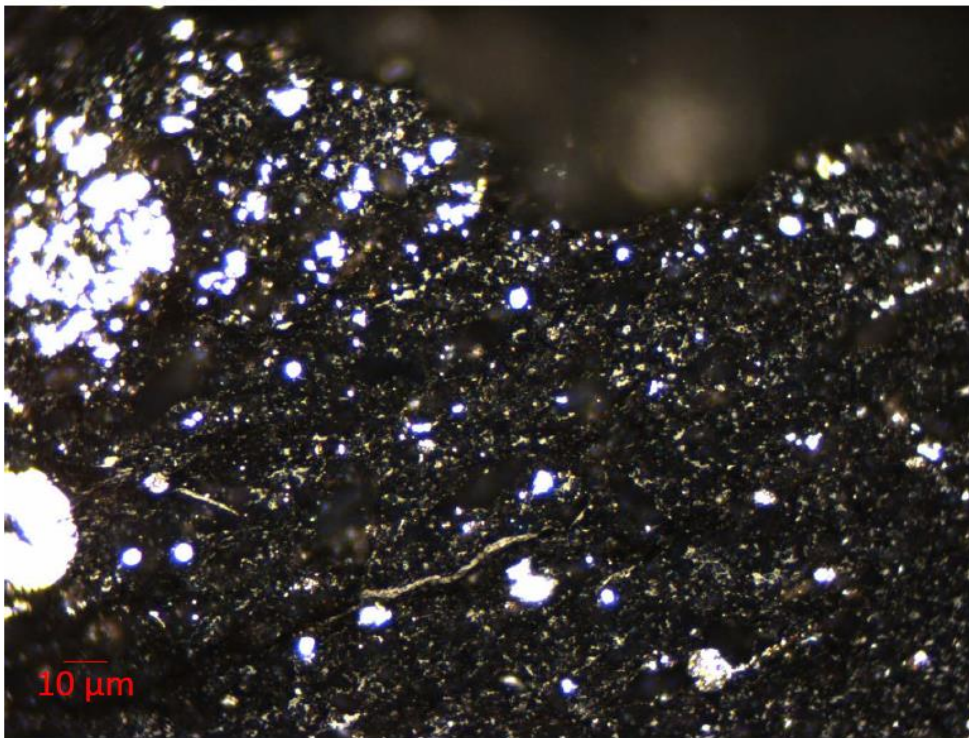
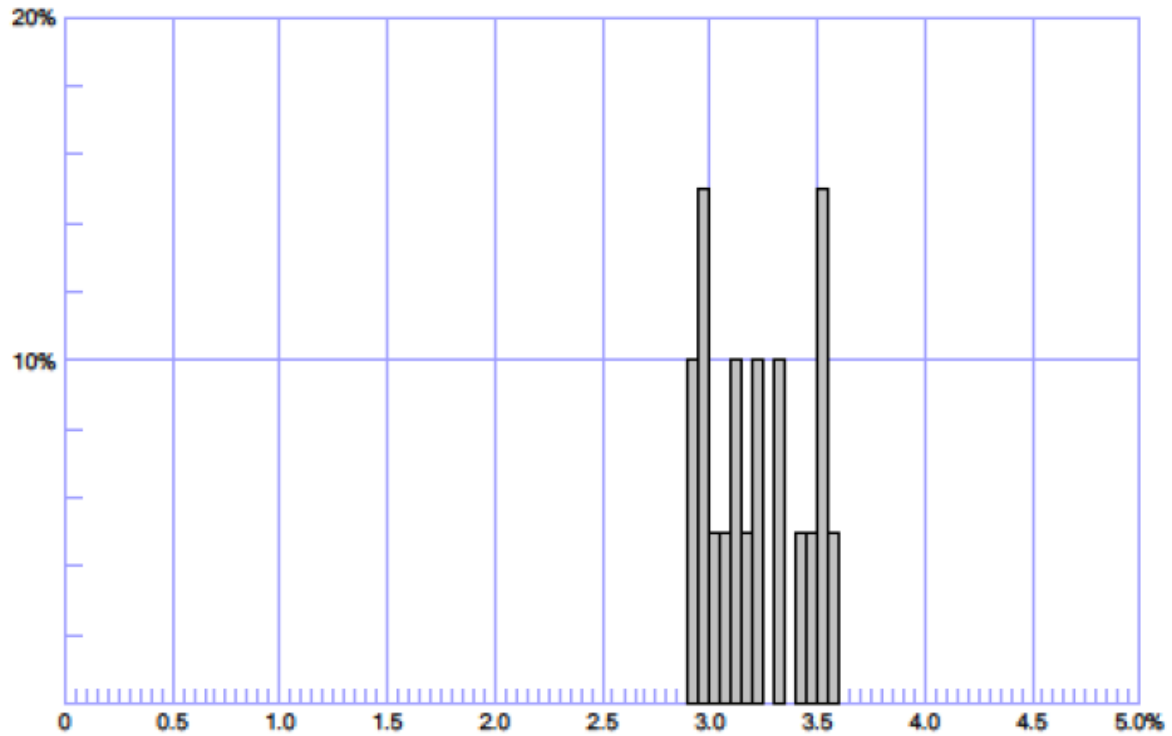


Figure E.9. Micrograph under reflected white light of Figure E.8.

Sample : E200205_003_Tattoo_3182_81_VR1



Measure count =	20	Date	2/24/2020 3:58 PM
Reflectance Rr =	3.221 %	Operator	Javin
s =	0.219 %	Printed	3/2/2020

2.90 - 2.95 % R	10.0 %	3.20 - 3.25 % R	10.0 %
2.95 - 3.00 % R	15.0 %	3.30 - 3.35 % R	10.0 %
3.00 - 3.05 % R	5.0 %	3.40 - 3.45 % R	5.0 %
3.05 - 3.10 % R	5.0 %	3.45 - 3.50 % R	5.0 %
3.10 - 3.15 % R	10.0 %	3.50 - 3.55 % R	15.0 %
3.15 - 3.20 % R	5.0 %	3.55 - 3.60 % R	5.0 %

F=6.06143

Figure E.10. Thermal maturity of 3182.81 m core slab.

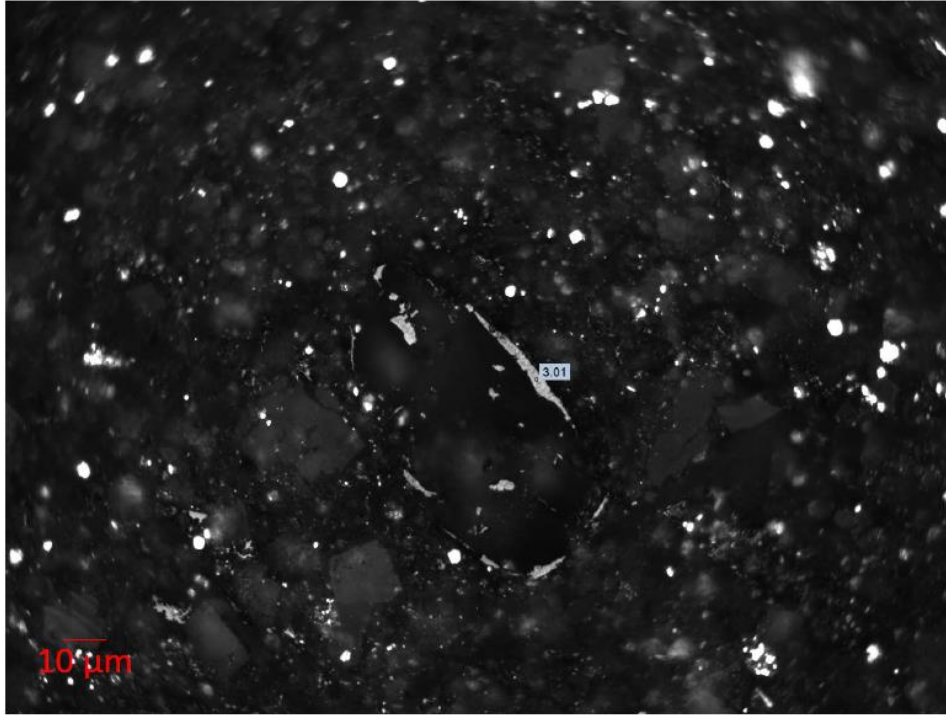


Figure E.11. Micrograph of thermal maturity analysis for organic matter of 3182.81 m core slab.

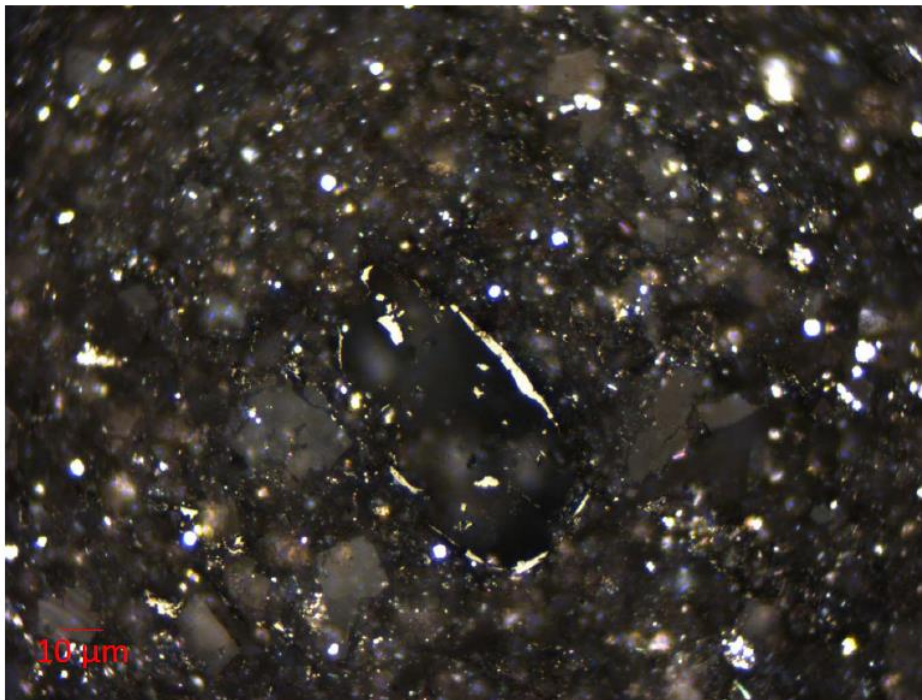


Figure E.12. Micrograph under reflected white light of Figure E.11.

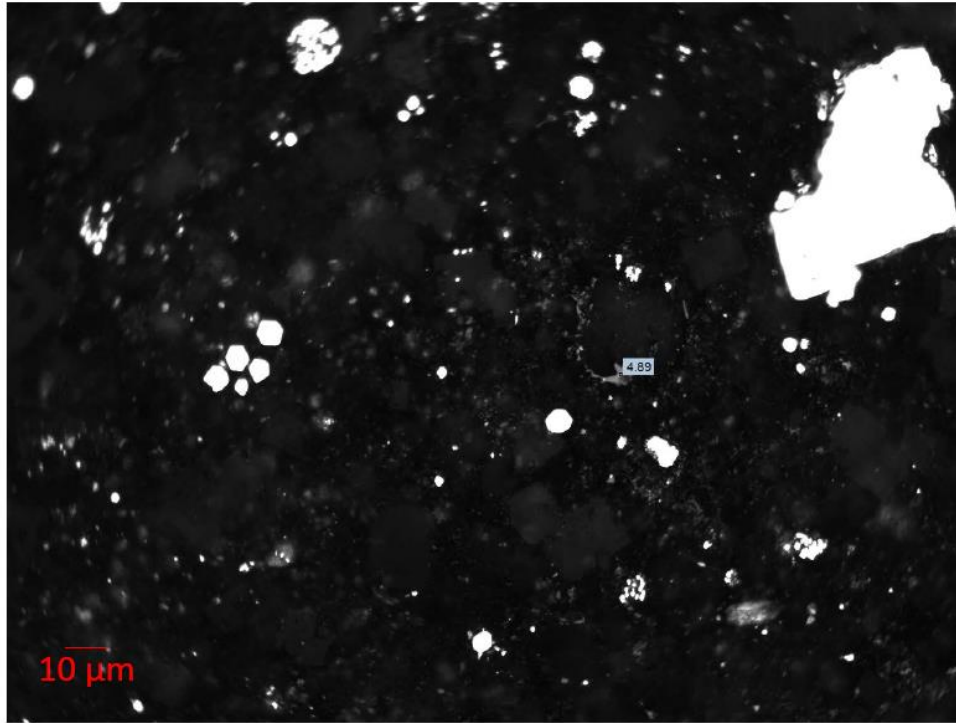


Figure E.13. Micrograph of thermal maturity analysis for organic matter of 3182.81 m core slab.

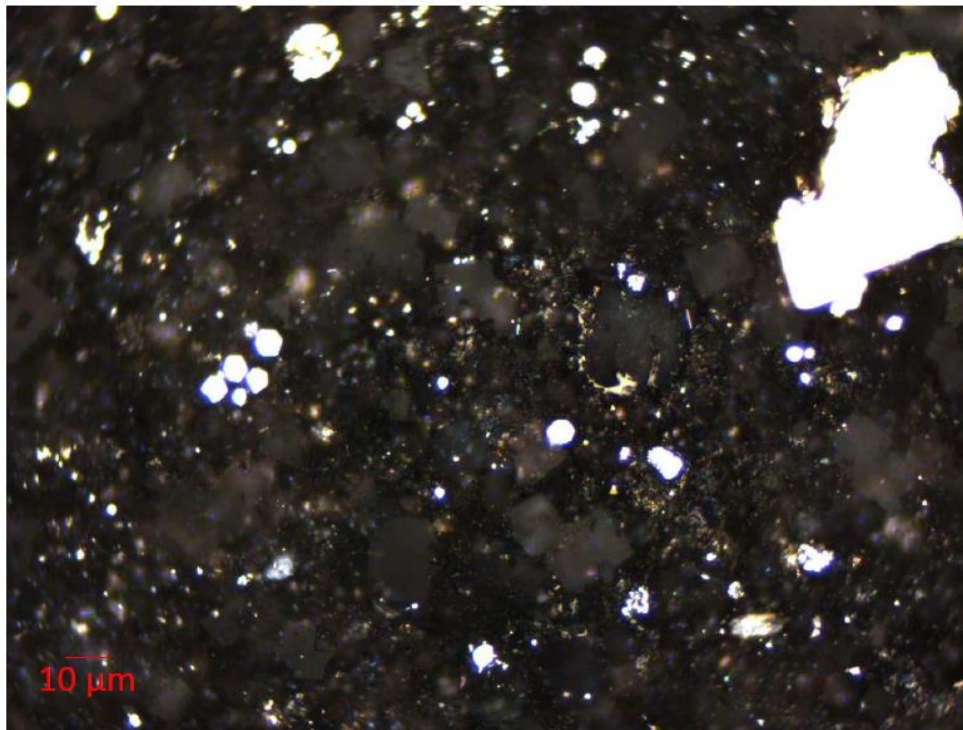


Figure E.14. Micrograph under reflected white light of Figure E.13.

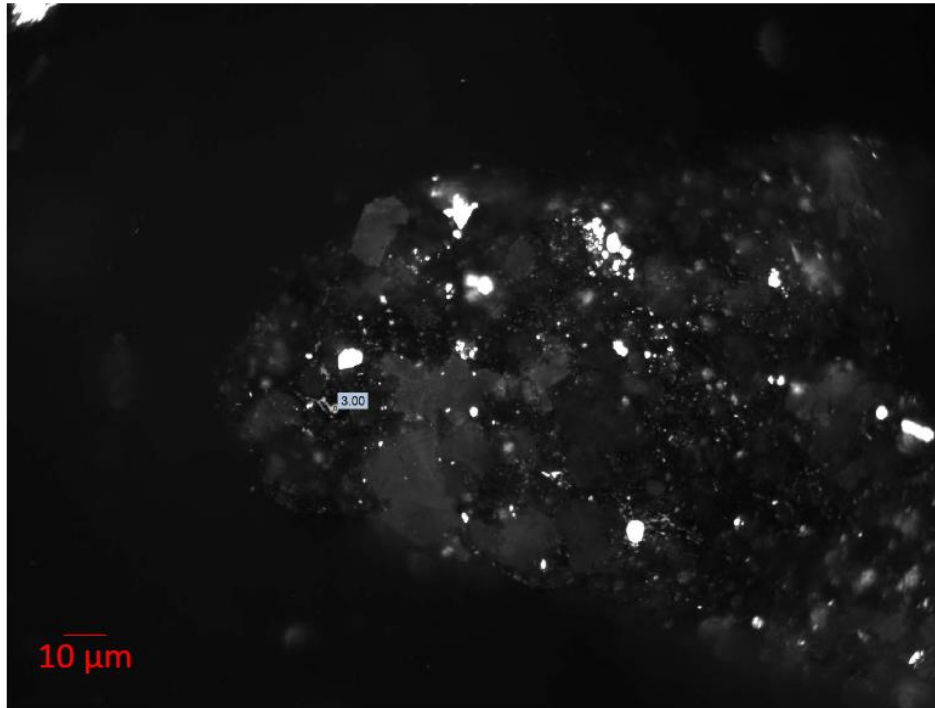


Figure E.15. Micrograph of thermal maturity analysis for organic matter of 3182.81 m core slab.

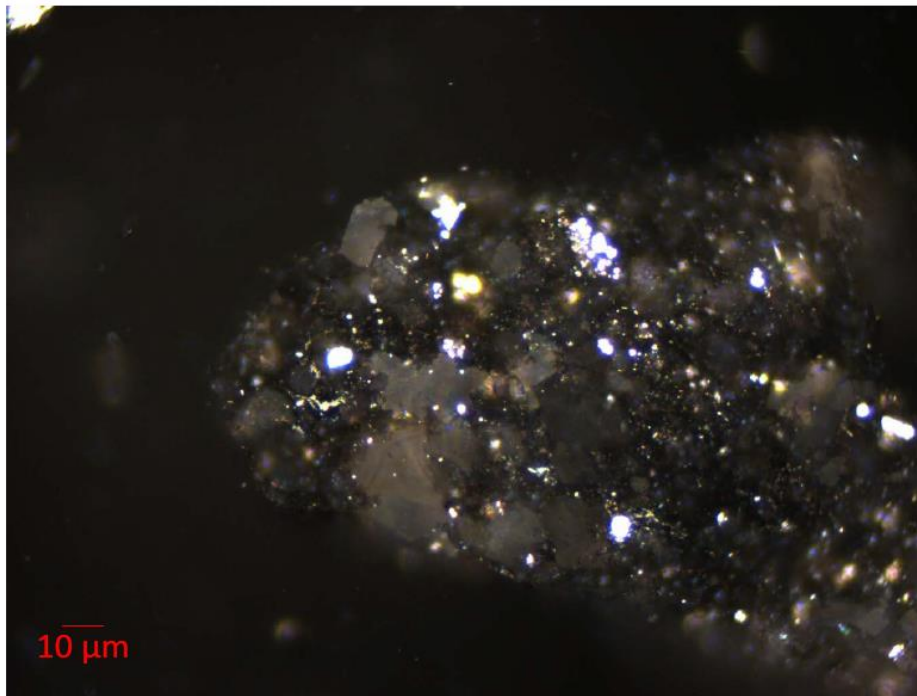


Figure E.16. Micrograph under reflected white light of Figure E.15.

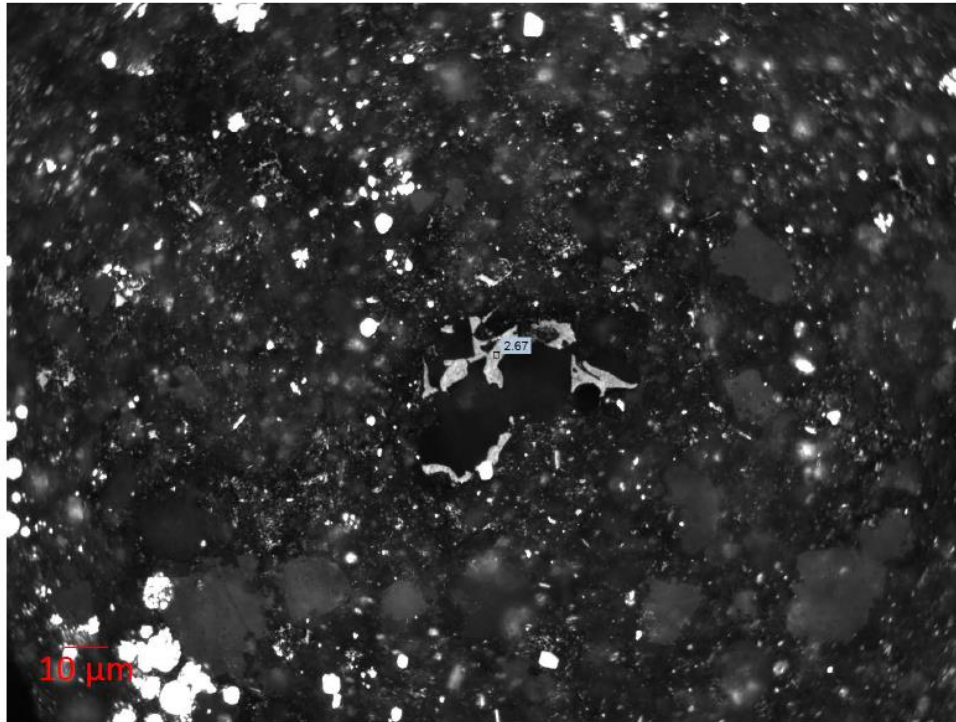


Figure E.17. Micrograph of thermal maturity analysis for organic matter of 3182.81 m core slab.

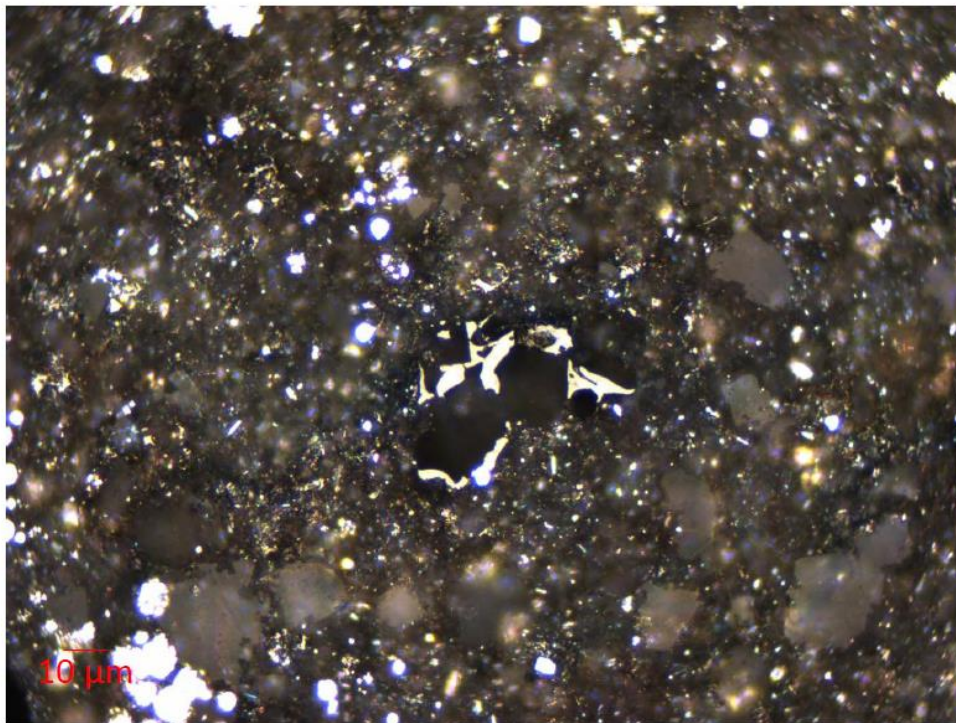


Figure E.18. Micrograph under reflected white light of Figure E.17.

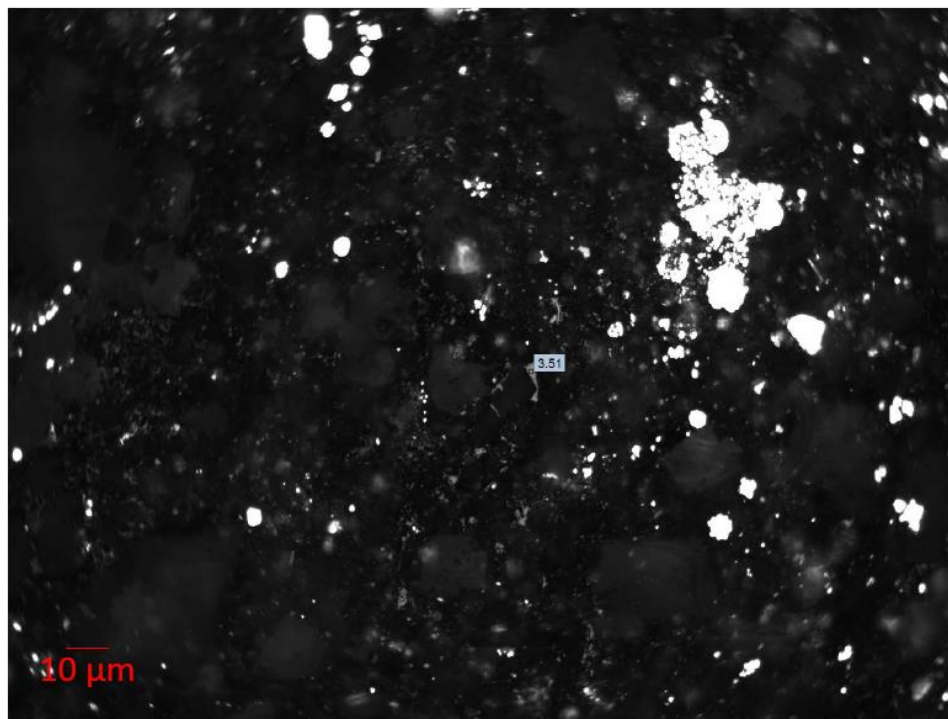


Figure E.19. Micrograph of thermal maturity analysis for organic matter of 3182.81 m core slab.

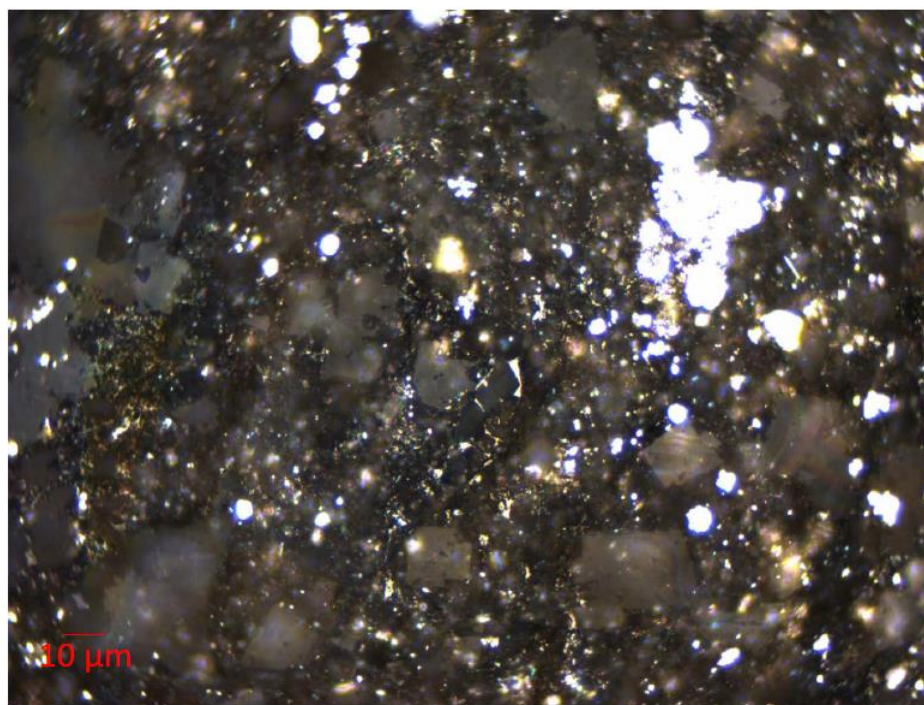
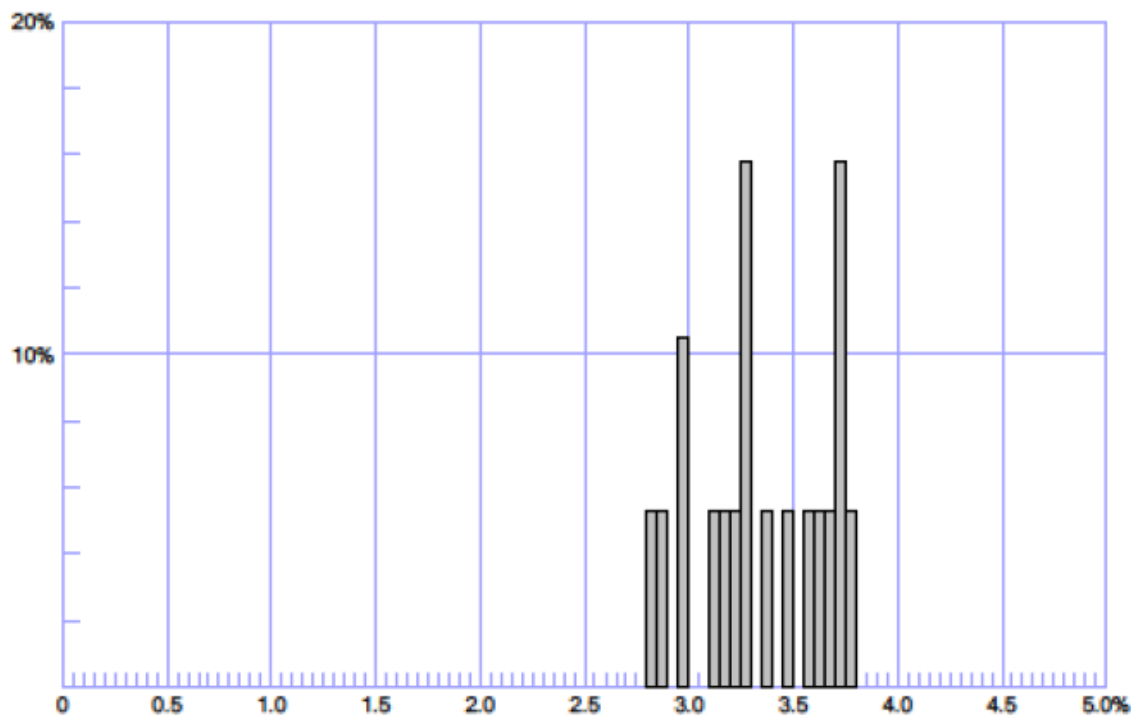


Figure E.20. Micrograph under reflected white light of Figure E.19.

Sample : E200205_004_Tattoo_3218_55_VR1



Measure count =	19	Date	2/26/2020 10:06 AM
Reflectance Rr =	3.349 %	Operator	Javin
s	0.297 %	Printed	3/2/2020

2.80 - 2.85 % R	5.3 %	3.35 - 3.40 % R	5.3 %
2.85 - 2.90 % R	5.3 %	3.45 - 3.50 % R	5.3 %
2.95 - 3.00 % R	10.5 %	3.55 - 3.60 % R	5.3 %
3.10 - 3.15 % R	5.3 %	3.60 - 3.65 % R	5.3 %
3.15 - 3.20 % R	5.3 %	3.65 - 3.70 % R	5.3 %
3.20 - 3.25 % R	5.3 %	3.70 - 3.75 % R	15.8 %
3.25 - 3.30 % R	15.8 %	3.75 - 3.80 % R	5.3 %

F=5.0.8143

Figure E.21. Thermal maturity of 3218.55 m core slab.

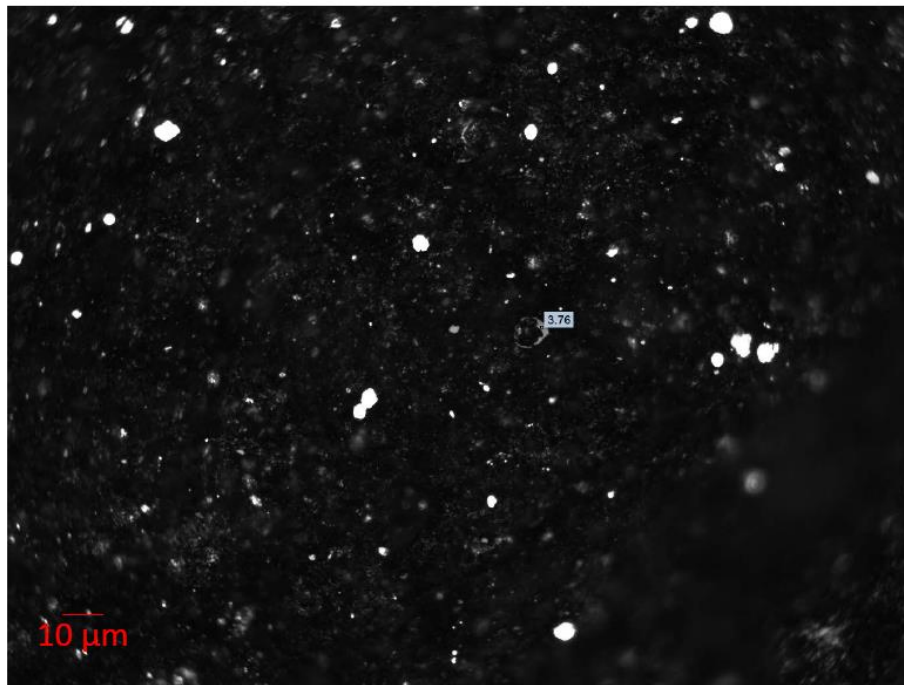


Figure E.22. Micrograph of thermal maturity analysis for organic matter of 3218.55 m core slab.

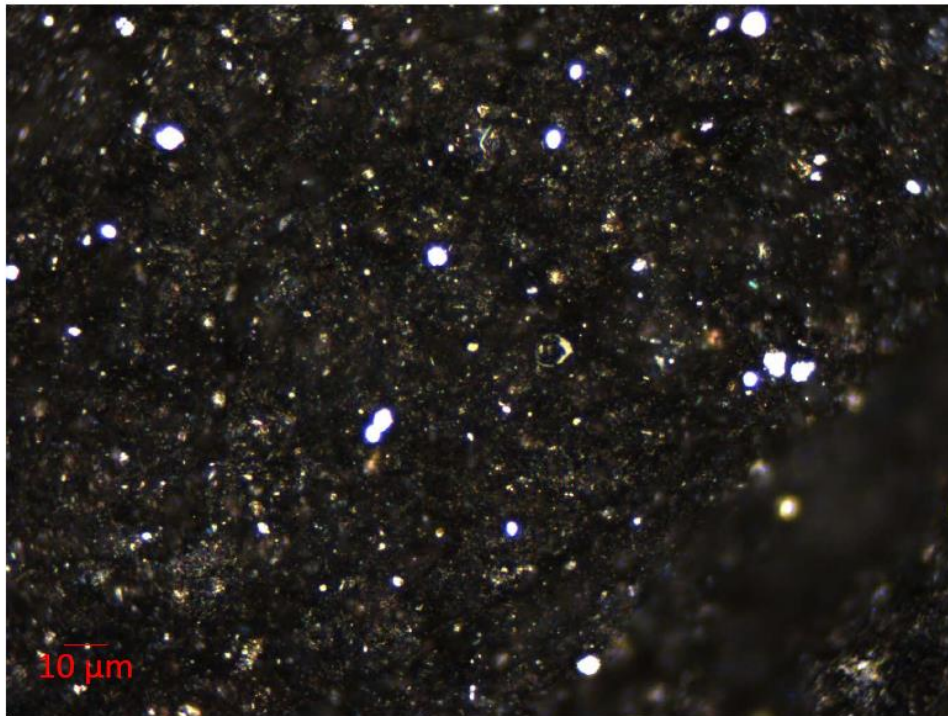


Figure E.23. Micrograph under reflected white light of Figure E.22.

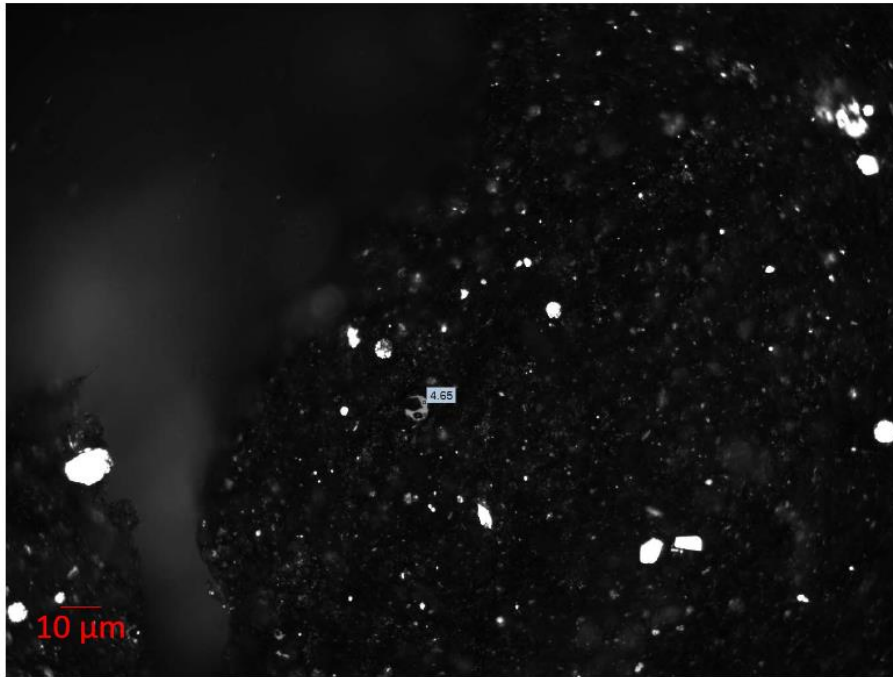


Figure E.24. Micrograph of thermal maturity analysis for organic matter of 3218.55 m core slab.

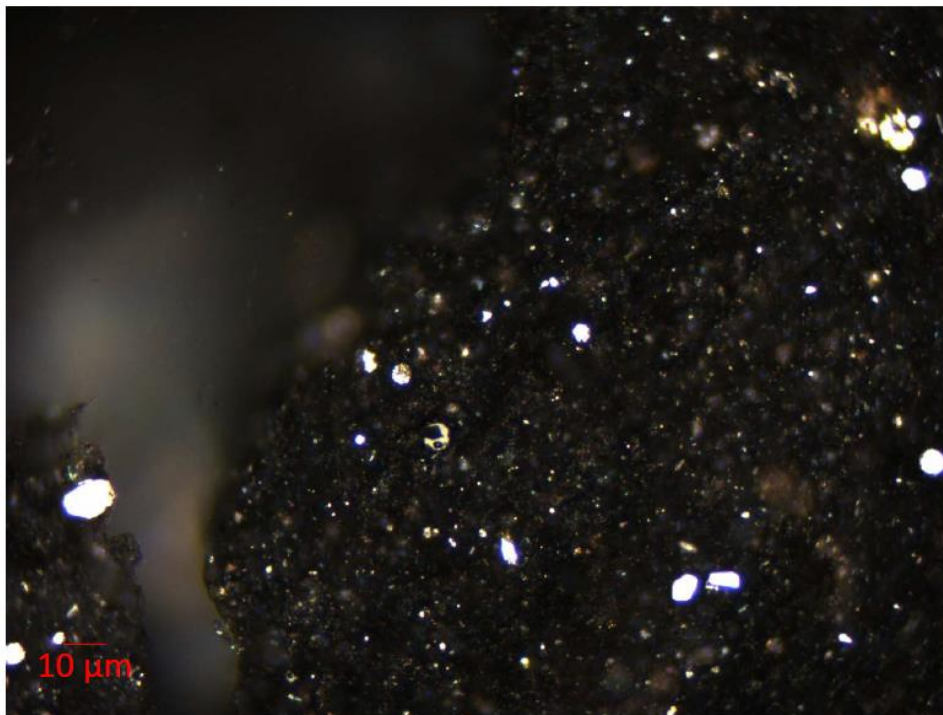


Figure E.25. Micrograph under reflected white light of Figure E.24.

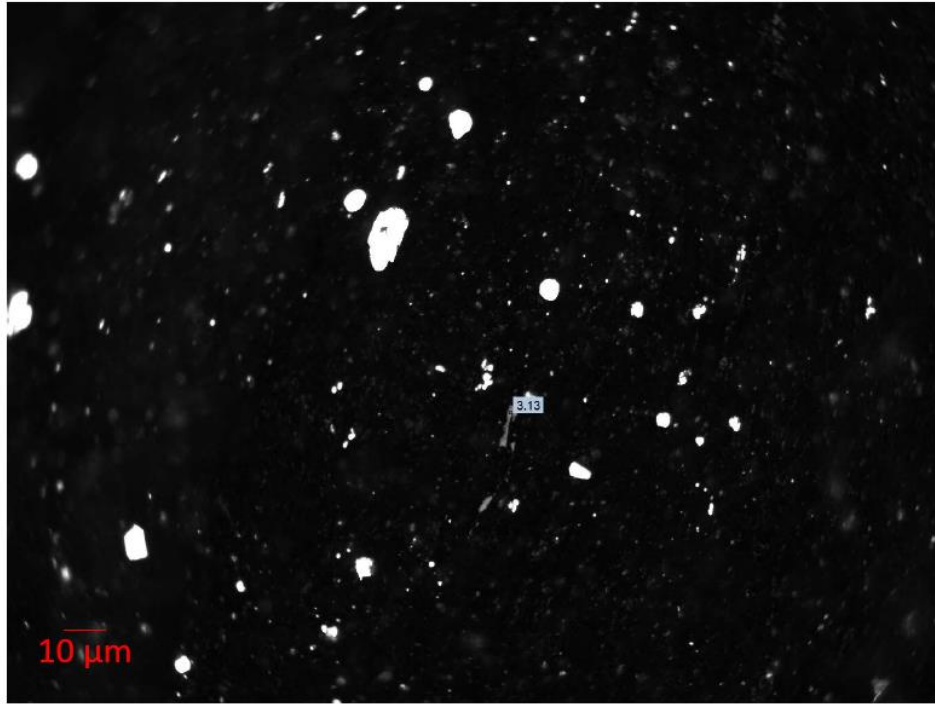


Figure E.26. Micrograph of thermal maturity analysis for organic matter of 3218.55 m core slab.

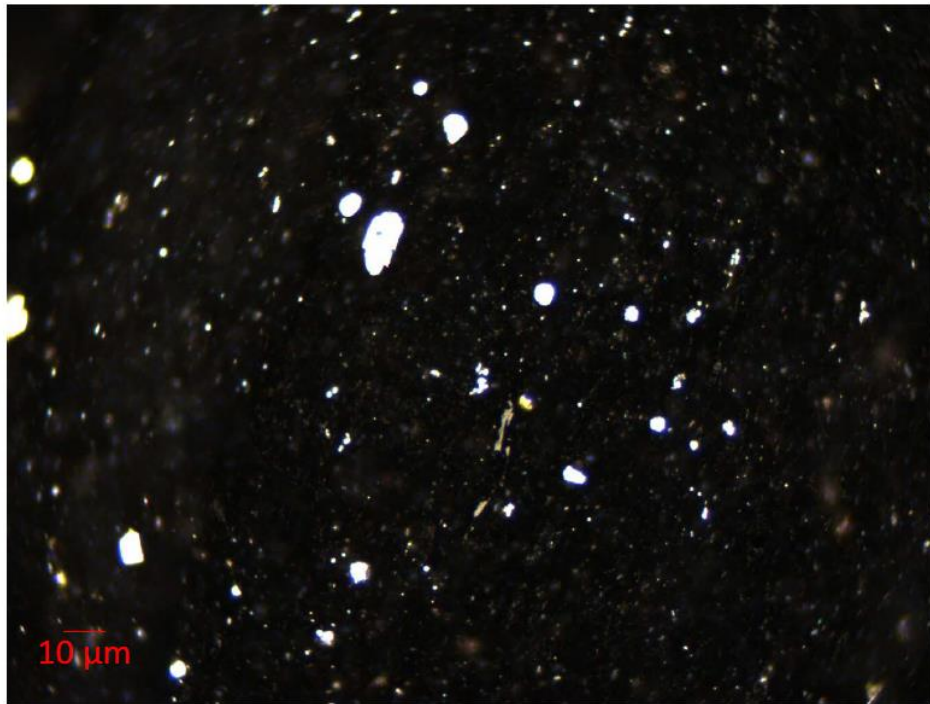
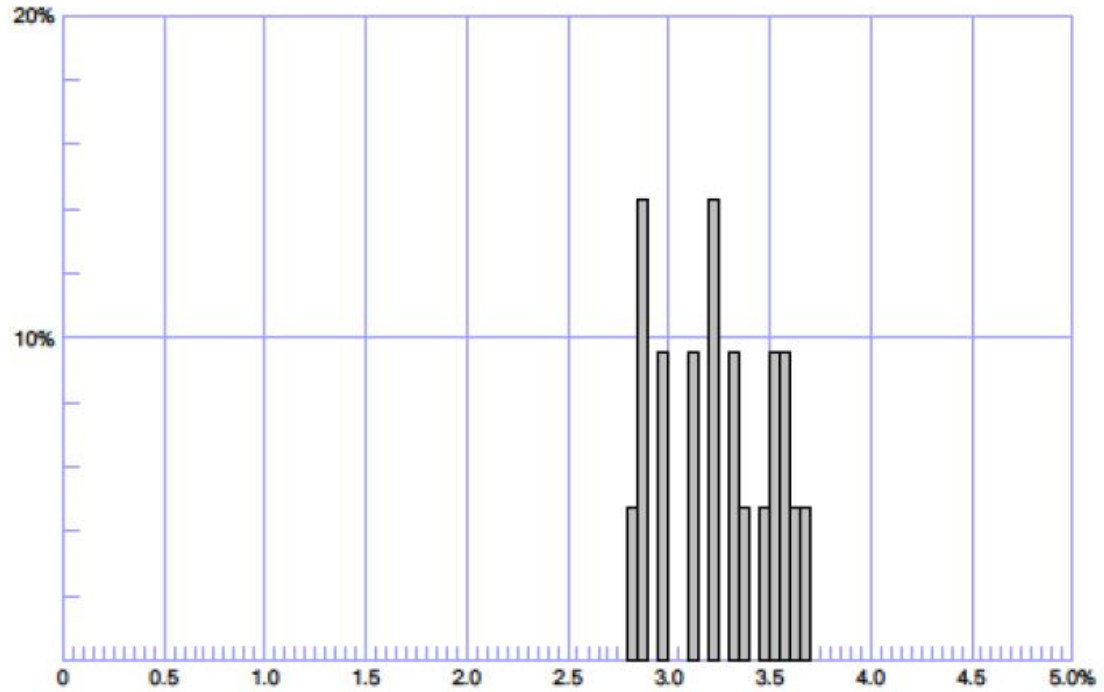


Figure E.27. Micrograph under reflected white light of Figure E.26.

Sample : E200205_005_Tattoo_3251_48_VR1



Measure count =	21	Date	2/26/2020 12:01 PM
Reflectance Rr =	3.253 %	Operator	Javin
s =	0.268 %	Printed	3/2/2020

2.80 - 2.85 % R	4.8 %	3.35 - 3.40 % R	4.8 %
2.85 - 2.90 % R	14.3 %	3.45 - 3.50 % R	4.8 %
2.95 - 3.00 % R	9.5 %	3.50 - 3.55 % R	9.5 %
3.10 - 3.15 % R	9.5 %	3.55 - 3.60 % R	9.5 %
3.20 - 3.25 % R	14.3 %	3.60 - 3.65 % R	4.8 %
3.30 - 3.35 % R	9.5 %	3.65 - 3.70 % R	4.8 %

F-5.0.8143

Figure E.28. Thermal maturity of 3251.48 m core slab.

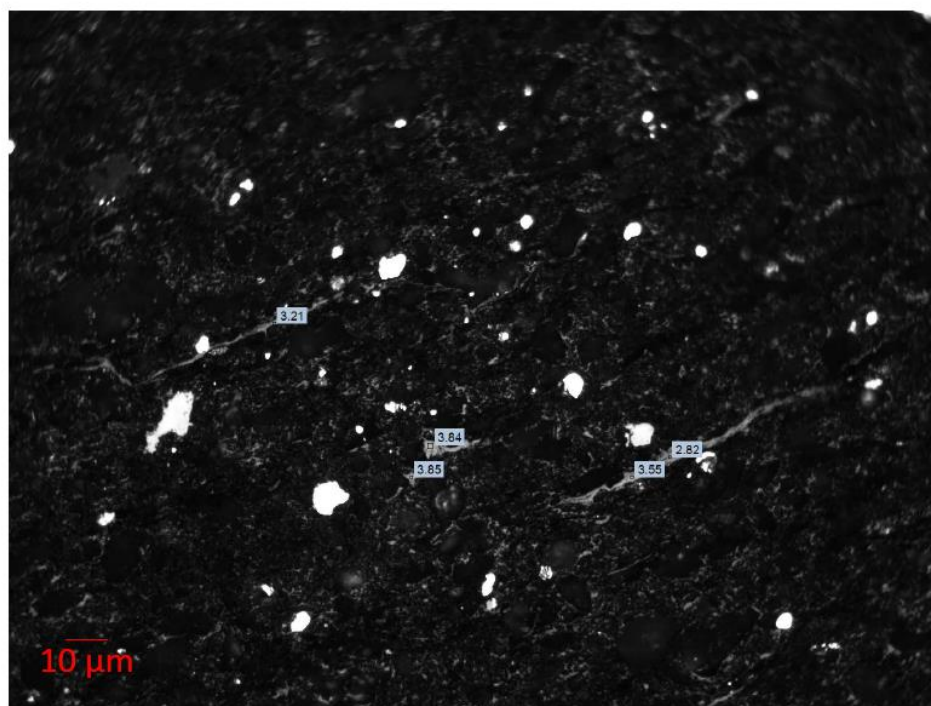


Figure E.29. Micrograph of thermal maturity analysis for organic matter of 3251.48 m core slab.

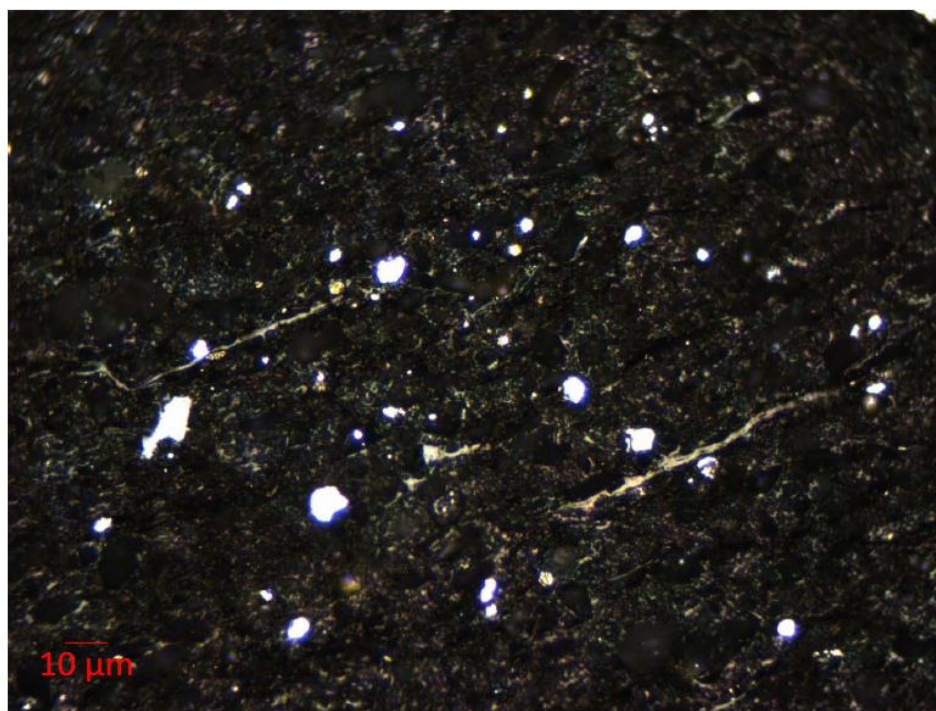


Figure E.30. Micrograph under reflected white light of Figure E.29.

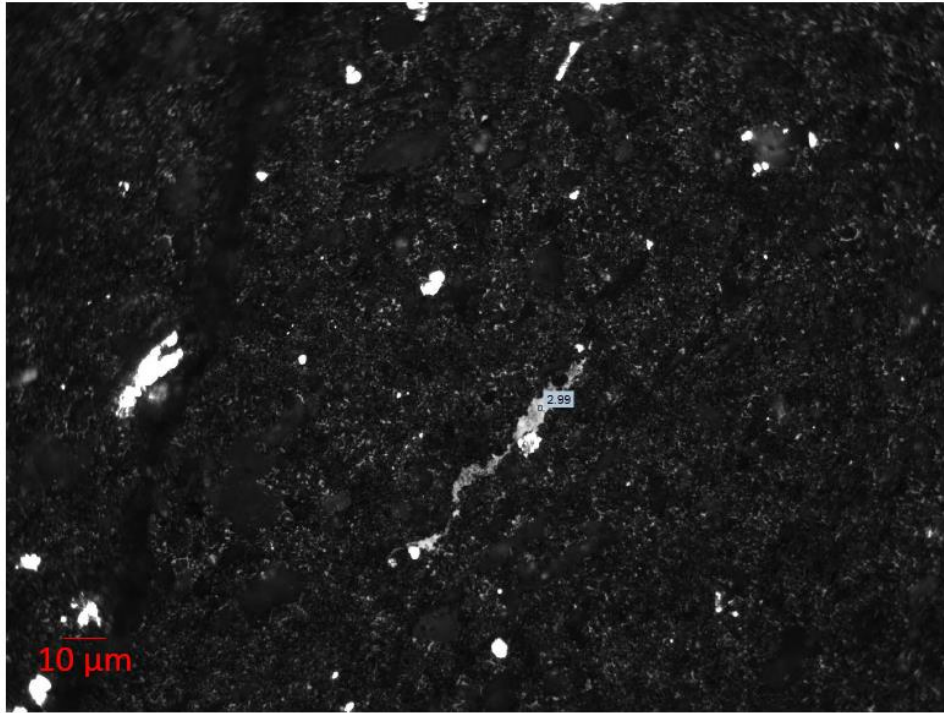


Figure E.31. Micrograph of thermal maturity analysis for organic matter of 3251.48 m core slab.

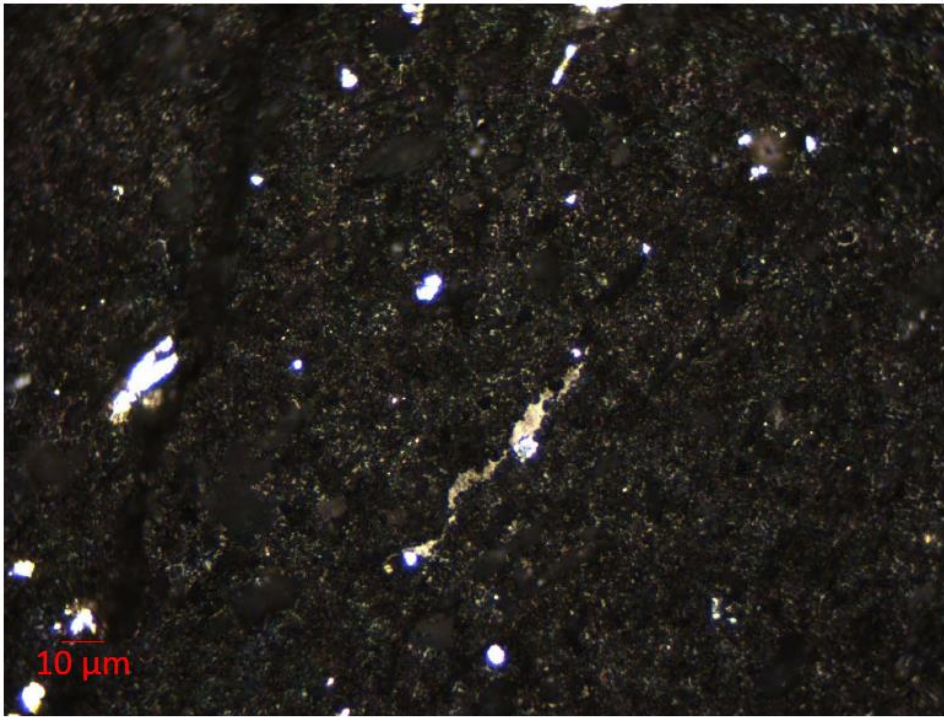


Figure E.32. Micrograph under reflected white light of Figure E.31.

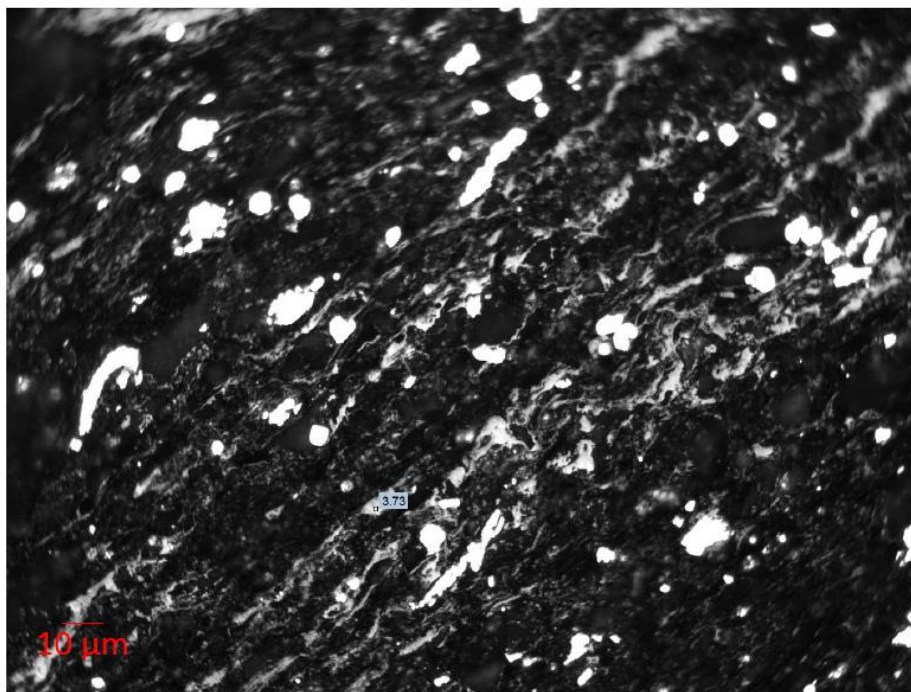


Figure E.33. Micrograph of thermal maturity analysis for organic matter of 3251.48 m core slab.

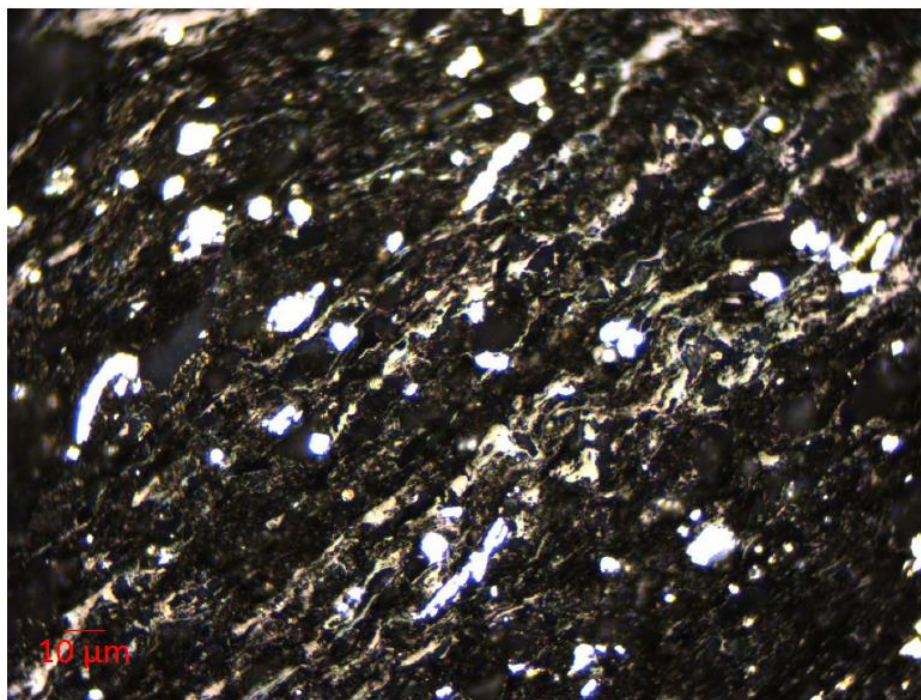


Figure E.34. Micrograph under reflected white light of Figure E.33.